JOSEPH VAN SCHELTEMA 764715

Mineralisation of the northern limb: Harriet's Wish farm

MSc. dissertation

Supervisors: Prof. J.A. Kinnaird and Dr. M. Yudovskaya

School of Geosciences, University of the Witwatersrand, Johannesburg

A Dissertation submitted to the Faculty of Science, University of the Witwatersrand in the Fulfillment of the requirement for the degree of Master of Science.

Declaration:

I declare that this dissertation is my own, unaided work. It is being submitted for the Degree of Master in Science to the University of the Witwatersrand, Johannesburg, South Africa. It has not been submitted before for any degree or examination in any other University.

(Signature of Candidate)

29 day of May 2019

Abstract:
The Bushveld Complex is the largest known layered igneous intrusion on Earth and is vital for its Ni-Cu-PGEs resources. Recent geophysical studies indicate that the total areal extent of the Bushveld is more than 90 000 km^2 (Finn *et al.,* 2015). The northern limb of the Bushveld Complex in the Limpopo province has a sinuous N-S oriented outcrop with an exposed width of around 15 km and an exposed strike length of approximately 110 km. The northern truncation of the northern limb has been believed to be at the Hout River shear zone, however, exploration to the north of the northern limb, led by Platinum Group Metals (PTM) since 2011, revealed the presence of mineralised rocks of a Bushveld affinity, beneath the Waterberg Group sediments (Huthmann *et al.,* 2016; Kinnaird *et al.,* 2017). The Waterberg Project succession hosts world class mineralisation and McDonald *et al.,* (2017) suggested that this succession continues southwards to the Aurora Project area, for up to 40 km. Sylvania Resources Limited, (2012) initiated drilling on the Harriet's Wish farm located between the Waterberg Project to the north, and the Aurora Project to the south, with the Hout River shear zone cross-cutting the farm. The location of this study site is therefore, important in establishing the suggested continuation of the Waterberg Project mineralisation. Three drillcores looked at in this study are located to the north-, and one drillcore is located within the Hout River shear zone.

To understand the Harriet's Wish sequence, the following approaches were used: core logging to establish the lithologies; magnetic susceptibility profiles were obtained to define a boundary between the lower and upper lithologic units; petrographic study was undertaken to confirm lithologies and to identify the mineral assemblages; an ore mineralogical study was carried out to understand mineralisation distribution and controls; major and trace element geochemical study, CIPW norms and PGE tenor calculations were done to confirm stratigraphic subdivision and more fully understand the processes involved in the formation of the sequence. The results were compared to the known characteristics of the Waterberg Project and the Aurora Project successions as well as certain Platreef localities.

Two lithologic units and two mineralised zones occur on Harriet's Wish. The lower lithologic unit is composed of gabbronorite, gabbro, troctolite, olivine gabbronorite, pyroxenite and anorthosite, similar to the TGA sequence on the Waterberg Project. The upper lithologic unit is analogous to the Upper Zone on the Waterberg Project and comprises gabbronorite, gabbro, anorthosite, minor olivine-rich varieties as well as magnetite-bearing varieties and magnetitites. There is no equivalent to the Ultramafic Sequence found on Harriet's Wish as harzburgite is absent on Harriet's Wish. However, this unit may be present deeper in the sequence, or it may have been reworked during the emplacement of later gabbroic melts. The scarce chromite grains within the basal

part of the lower lithologic unit, the relic olivine chadacrysts and the semi-dissolved olivine-rich fragments within troctolite and olivine gabbronorite could be remnants of earlier ultramafic cumulates.

The lower mineralised zone is found within the lower lithologic unit of the Harriet's Wish succession and shows some similarities to the F Zone of the Waterberg Project in terms of ore mineralisation style and base metal concentrations, although the petrographic and chemical compositions of host rock are different. The upper mineralised zone on Harriet's Wish is geochemically analogous to the T Zone on the Waterberg Project, and the mineralisation on the Aurora Project. However, the Harriet's Wish upper mineralised zone is distinguished by notably higher Au proportions than the Waterberg Project T Zone and the Aurora Project succession and carries the indicative quartz-chlorite-amphibole-pyrite assemblage, which is common in the T Zone on the Waterberg Project, but absent on the Aurora Project.

It is, therefore, suggested that the T Zone does indeed continue southwards from the proximal Waterberg facies to Harriet Wish and finally to the distal Aurora facies as suggested by Kinnaird *et al.,* (2017) and McDonald *et al.,* (2017). Furthermore, the lithology, geochemistry, ore mineralisation and petrography suggest that there are definitive differences in the magmatic stratigraphy across the Hout River shear zone. The idea that a separate magmatic basin or sub-chamber exists north of the Hout River shear zone is, therefore, supported by this study.

It is envisaged that different processes related to the proximity to the footwall may have triggered the deposition of the lower mineralised zone. These processes include magma mixing and mingling, assimilation of xenoliths and hydrothermal fluid circulation that involves sediment-derived volatiles. The upper mineralised zone is suggested to be formed due to mixing of the resident S- and PGE-poor Main Zone-type magmas with the later influxes of the PGE- and S-rich fertile Upper Zone magma entering the chamber.

Acknowledgements:

I would like to thank Professor Judith Kinnaird for the constant supervision and guidance throughout the course of this project. For all the food on the field trips and for the informative discussions. I would like to thank Dr. Marina Yudovskaya for the immense help and guidance throughout the course of this project. The informative discussions, fieldwork we did together and the constant question and answer sessions we had made the world of difference. Not only did Marina assist with the work, but she also showed me around Mokopane and helped me to enjoy the town for its beauty. I would also like to thank Judith and Marina for the patience with me during the correction and submission process. It is much appreciated and it made me a better person. The last few months must have been the toughest period that I have faced in my life (and my life has been difficult), on a personal basis, and on an academic basis.

I would like to thank Sylvania Resources Limited for the use of the drillcore and for allowing us to use their facilities at Grasvally. Also thank you to Rob Steen for sending the assay data that was much needed for this thesis and for the help you offered while on our stays on your property.

I would like to thank Rosalind Crossley for the help and assistance during this project, and for being always helpful, personable and friendly.

I would like to thank my wife, Caitlin van Scheltema for the absolute patience that she has had with me, for never complaining and for always being a support during our 6 years of ‘student-married’ life. She ran everything at home during the last parts of the write-up process. Without her this would not have been possible. In addition, I would like to thank my two boys, Jesse and Aiden van Scheltema for the patience that you have had with me while I did my masters. I hope this achievement will make you proud one day.

I would also like to thank my Heavenly Father for the blessing and the trial this has been. It has made me a better person. I have more patience, endurance, empathy and understanding for it.

Lastly, I would like to thank my dad and mom for instilling in me the ethic to never give up. Also for the wisdom that my dad displayed, the confidence he had in me to help me feel that I can achieve anything. For the encouragement to be a scientist, I would like to thank my mom, who always instilled the importance of science in me and whose example of faith I look up to daily.

Table of Figures

Table of tables

Chapter 1
Geology of the Bushveld Complex

1.1 Introduction to the Bushveld Complex

The Palaeoproterozoic Bushveld Complex is the largest known layered igneous intrusion on Earth (Hatch and Corstorphine, 1905; SACS 1980; Kinnaird *et al.,* 2002; Scoates and Friedman 2008) and is considered to have formed from multiple injections of magma (Kruger, 1990; Barnes *et al.,* 2017). According to Armitage, (2011), the most widely accepted description of the Bushveld Complex is a concentric set of 7-8 km thick mafic and ultramafic cumulate units that intruded mostly through the Transvaal Supergroup lithologies (Buchanan, 1988; Kinnaird *et al.,* 2002). The Chuniespoort Group and the Pretoria Group sedimentary successions occur at the base and share unconformable boundaries with the Bushveld Complex (Cheney and Twist, 1991; Kinnaird, 2005). The felsic volcanics of the Rooiberg Group are the predominant roof-rocks of the complex (Hall, 1932; Kinnaird, 2005). Until recently, the complex was thought to cover an area of 65 000 km^2 with approximate dimensions of 240 km x 300 km (Figure 1.1; Tankard *et al.,* 1982; Eales *et al.,* 1993; Eales and Cawthorn, 1996; Kinnaird *et al.,* 2005), and a total volume of >370 000 km^3 (Zeh *et al.,* 2015). However, intersected mafic-ultramafic rocks to the north of the northern limb (Huthmann *et al.,* 2016) and recent geophysical studies reveal that the total areal extent is more than 90 000 km^2 (Finn *et al.,* 2015; Kinnaird *et al.,* 2017). The Bushveld Complex has been dated multiple times (e.g. Walraven *et al.,* 1990; Harmer and Armstrong, 2000; Buick *et al.,* 2001; Dorland *et al.,* 2006; Scoates and Friedman, 2008). However, more recently, a zircon in quenched Marginal Zone rocks shows an age date of 2055.91 ± 0.26 Ma (Zeh *et al.,* 2015). The emplacement and cooling of Bushveld magma occurred in less than 1 million years with the Bushveld magma chamber being accreted with a flux of > 5 km^3/ year (Zeh *et al.,* 2015).

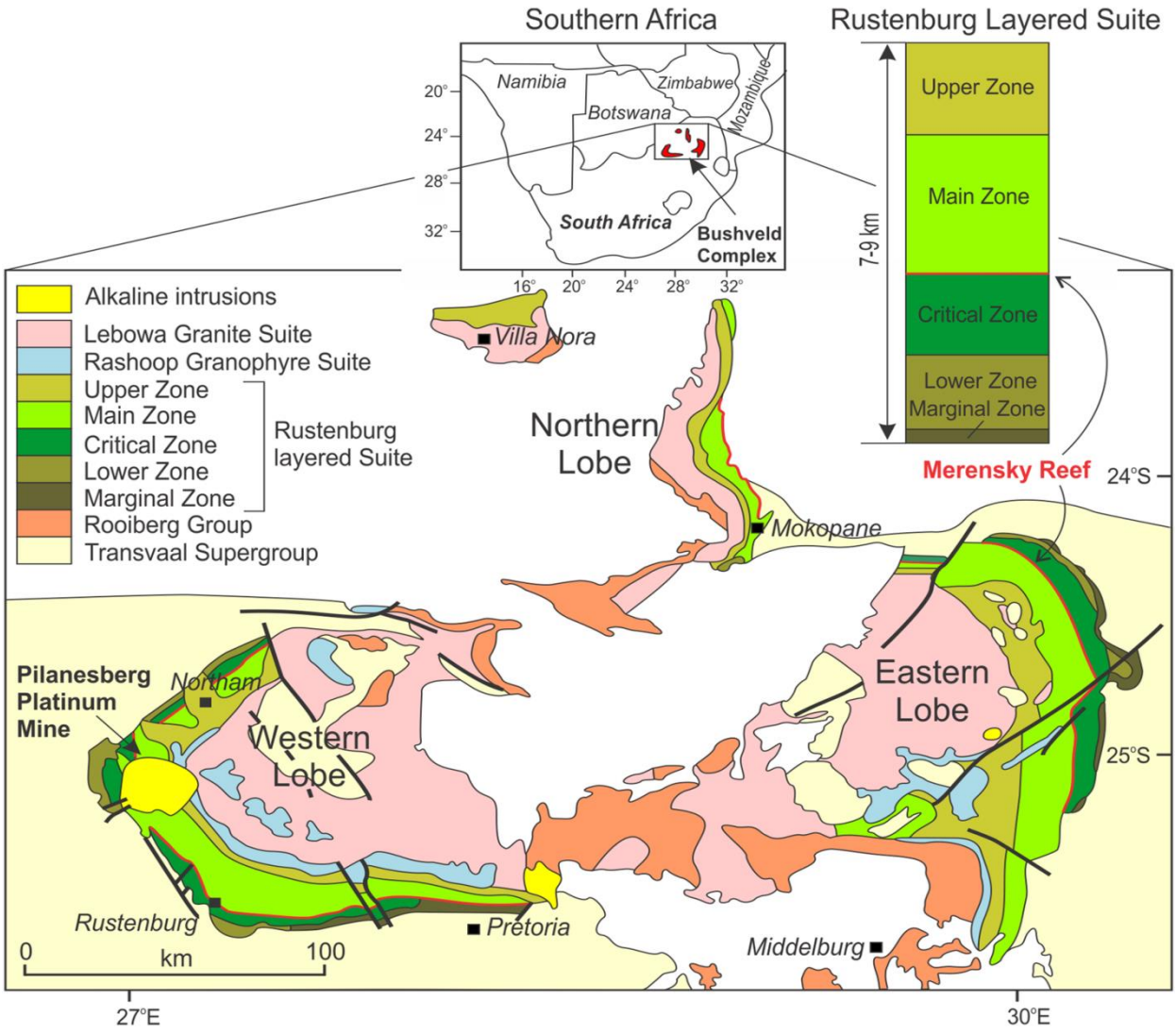

Figure 1.1: Generalised geology and stratigraphy of the Bushveld Igneous Complex (from Webb *et al,* 2006).

The Bushveld Complex is hosted in the northern portion of the Kaapvaal Craton (de Wit *et al.,* 1992), which is an assembly of crustal blocks that joined together around 3700-2700 Ma (de Wit *et al.,* 1992). Between 3700-3100 Ma, continental lithosphere separated from the mantle during intraoceanic obduction and the amalgamation of the Kaapvaal Craton then commenced due to within-shield melting, granite formation and chemical differentiation of the upper lithosphere (de Wit *et al.,* 1992). A possible unknown orogeny involving the Zimbabwean Craton occurred prior to 2900 Ma, as seismic anisotropy reveal a mantle fabric consistent with this age on the Zimbabwean Craton (Silver *et al.,* 2004). Around 2900 Ma the collision of the Pietersburg and

Kimberley blocks with the Kaapvaal shield occurred, which resulted in the formation of the Thabazimbi-Murchison Lineament (Silver *et al.,* 2004). At ~2700-2600 Ma, the Limpopo orogeny started, which resulted in the formation of the Limpopo Belt between the Kaapvaal Craton and the Zimbabwean Craton (de Wit *et al.,* 1992; Silver *et al.,* 2004). This occurred roughly at around the same time as the intrusion of the Great Dyke and the Ventersdorp Supergroup (de Wit *et al.,* 1992; Silver *et al.,* 2004). At ~2000 Ma, during the Magondi orogeny, the reactivation of shear zones in the Limpopo Belt occurred and the Bushveld Complex was intruded along the Thabazimbi-Murchison Lineament. The last major rift in the area, known as the Soutpansberg rift, occurred between 1900-1800 Ma in the Kheis orogeny (Cornel *et al.,* 1998).

During the Late Archaean to early Proterozoic, after the Kaapvaal Craton stabilised, large volcano-sedimentary intracratonic basins, such as the Witwatersrand basin (3074± 6 Ma), developed on this stable cratonic platform (Armstrong *et al.,* 1991; Kinnaird, 2005). The Witwatersrand sequence was deposited either on the granite-greenstone basement or on older sediments and lavas of the Dominion Group, which intruded 3047 Ma (Armstrong *et al.,* 1991; Kinnaird, 2005). The intercalated volcanics were intruded next at ~2917-2780 Ma, followed by the intrusion of Ventersdorp lavas at ~2714 ± 8 Ma, which overlie the Witwatersrand sequence (Armstrong *et al.,* 1991). The nearly 2 km thick, 160 000 km^2 Klipriviersberg Group flood basalts then poured out into the Witwatersrand Basin at ~2718 ± 8 (Armstrong *et al.,* 1991; Stanistreet and McCarthy 1991). The deposition of the Transvaal Supergroup then started towards the end of the Ventersdorp rifting (2670-2100 Ma; Walraven and Martini, 1995; Eriksson *et al.,* 2001). The Transvaal Supergroup comprises a >15 km thick supracrustal volcanosedimentary sequence and includes the protobasinal Wolkberg Group and the Buffelsfontein Group, the carbonaceous Chuniespoort Group, and the predominantly pelitic Pretoria Group (SACS 1980). The Transvaal Supergroup and Archean granite basement lithology form the footwall to the Large Igneous Province of the Bushveld Complex, which was then deposited (2055.91 ± 0.26 Ma; Zeh *et al.,* 2015). The Bushveld Complex is almost completely bound by rocks of the Transvaal sedimentary Basin (SACS 1980).

1.2 **Geology of the Bushveld Complex**

There are five major limbs or lobes in the Large Igneous Province of the Bushveld Complex namely: 1) the eastern limb, 2) the western limb, 3) the far western limb, 4) the northern limb and 5) the south-eastern Bethal limb, which is covered by younger sediments (Figure 1.1; Von Gruenewaldt, 1970; Van der Merwe, 1976; Kruger 1990; Cawthorn *et al.,* 2002; Kinnaird *et al.,* 2005). The overall shape and the interrelations between the various limbs of the Bushveld Complex are still debated, with some authors suggesting that the limbs represent separate intrusions (Cousins, 1959; Sharpe *et al.,* 1981), or dipping sheets (Biesheuvel, 1970; Van der Merwe, 1976; Meyer and De Beer 1987). Hall (1932) and du Toit (1954), however, suggested that the Bushveld western and eastern limbs are connected and suggested it to be a lopolith. Cawthorn and Webb, (2001), with the aid of gravity data, also suggested that eastern and western limbs have been connected throughout much of the evolution of the complex, with similar magmas forming both limbs and that mineral processes operated contemporaneously to produce the mineralised horizons that broadly correlate across these limbs (Lee, 1996; Barnes and Maier, 2002). To support this idea, Webb *et al.,* (2004) present geophysical gravity modelling to illustrate a downwarp in the Moho below the Bushveld Complex in order to achieve isostatic balance.

The Bushveld Complex is divided into the following stratigraphic subdivisions as suggested by the South African Committee on Stratigraphy, or SACS (1980) and revised by Hatton and Schweitzer (1995): 1) the Rooiberg Group, 2) the Rustenburg Layered Suite, 3) the Lebowa Granite Suite, and 4) the Rashoop Granophyre Suite (Figure 1.2).

The stratigraphic units that are associated with the Bushveld Complex are outlined and described in more detail below:

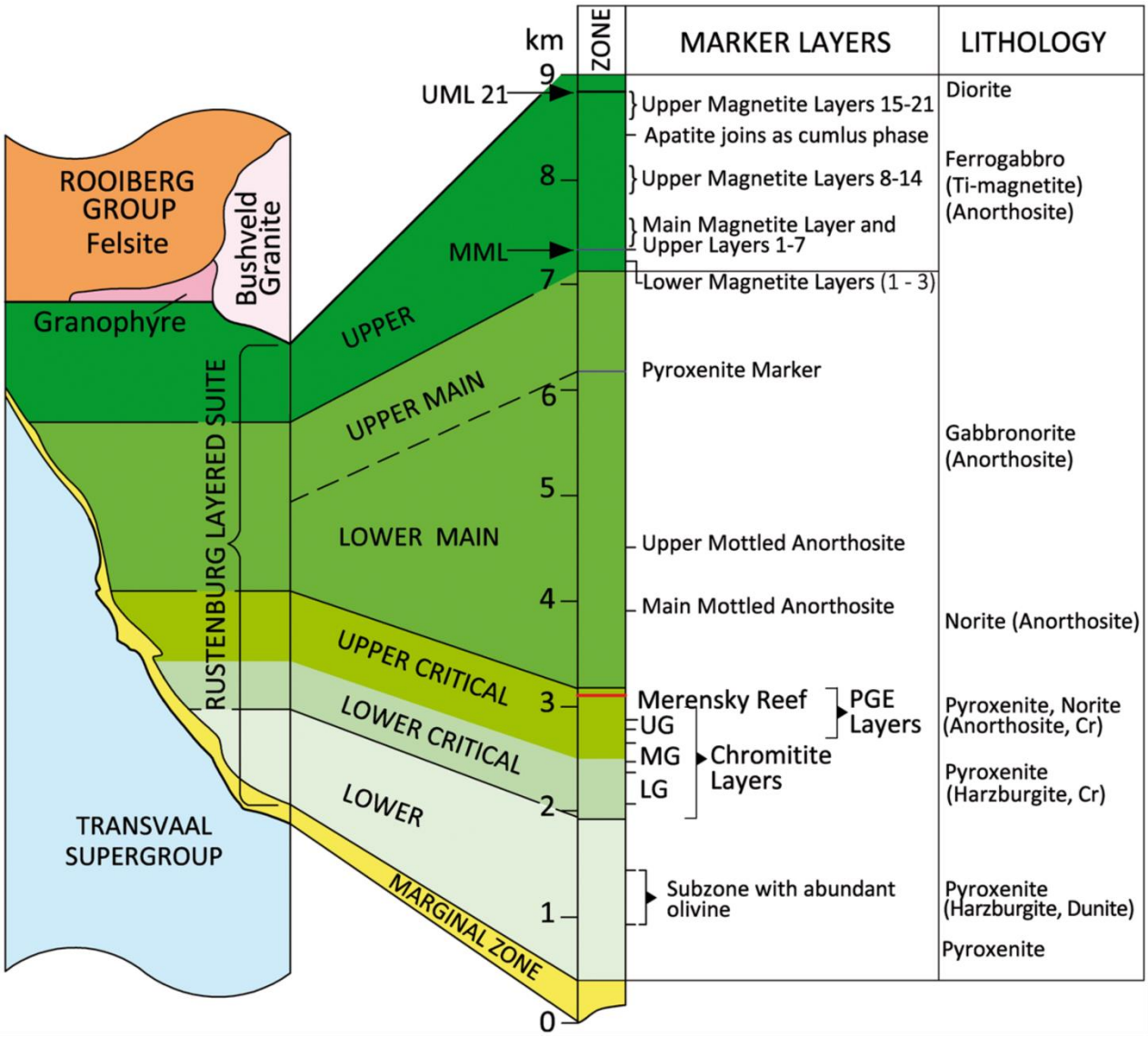

Figure 1.2: Stratigraphic column depicting the broad components of the Bushveld Complex (from Scoon *et al.,* 2018, simplified from Von Gruenewaldt *et al.,* 1985).

1.3 **Rooiberg Group**

The Rooiberg Group is a sequence of volcanic rocks, which represent the first phase of magmatic activity associated with the Bushveld Complex (Buchanan *et al.,* 2004). The Rooiberg group is ~6 km thick and consists of more than 50 000 km^2 of preserved volcanics (Schweitzer *et al.,* 1995; Buchanan *et al.,* 2004). These volcanic rocks unconformably overly the Transvaal Supergroup (Figure 1.2; Cheney and Twist, 1991) and comprises extrusive rhyolitic pyroclastics that are approximately the same age as the Bushveld (Harmer and Armstrong, 2000; Buchanan *et al.,* 2004). Many areas show

significant thinning and erosion (Buchanan *et al.,* 2002), which suggests that it may even have exceeded a volume of 300 000 km^3 (Twist and French, 1983; Schweitzer *et al.,* 1995).

The Rooiberg Group felsites are encountered predominantly above the Upper Zone in the Bushveld stratigraphy and are comprised of several formations, distinguished on the basis of colour, texture, phenocryst content and chemistry (Figure 1.3; Hatton and Schweitzer, 1995; Schweitzer *et al.,* 1995; Buchanan *et al.,* 2002). These formations include the Dullstroom, Damwal, Kwaggasnek and Schrikkloof Formations (Hatton and Schweitzer, 1995; Schweitzer *et al.,* 1995).

The oldest of these formations is the Dullstrom Formation, which consists of basaltic andesite, basalt and basalt rhyolite (Hatton and Schweitzer, 1995; Schweitzer *et al.,* 1995; Buchanan *et al.,* 1999). The lower parts of the Dullstroom Formation occur mostly as the footwall of the Rustenburg Layered Suite whereas the upper part may locally comprise the hanging wall of the mafic-ultramafic intrusion (Schweitzer *et al.,* 1995; Buchanan *et al.,* 1999). The Damwal Formation overlies the Dullstroom Formation and is comprised predominantly of massive dacites and rhyolite (Schweitzer *et al.,* 1995; Buchanan *et al.,* 1999). This is followed by the Kwaggasnek Formation, which consists of shale/tuff, agglomerate and massive rhyolite, and finally the Schrikkloof Formation, which includes flow-banded rhyolite, rare quartzite lenses and occasional quartzite xenoliths towards the base (Schweitzer *et al.,* 1995). The approximate age of the Rooiberg Group taken from zircons of the Kwaggasnek Formation which yielded a crystallisation age of 2057.3 ± 2.8 Ma (Harmer and Armstrong, 2000), whereas Rb-Sr isotopic data for units of the Dullstroom and Damwal Formations suggest a crystallisation age of 2071± 94/-65 Ma (Buchanan *et al.,* 2004).

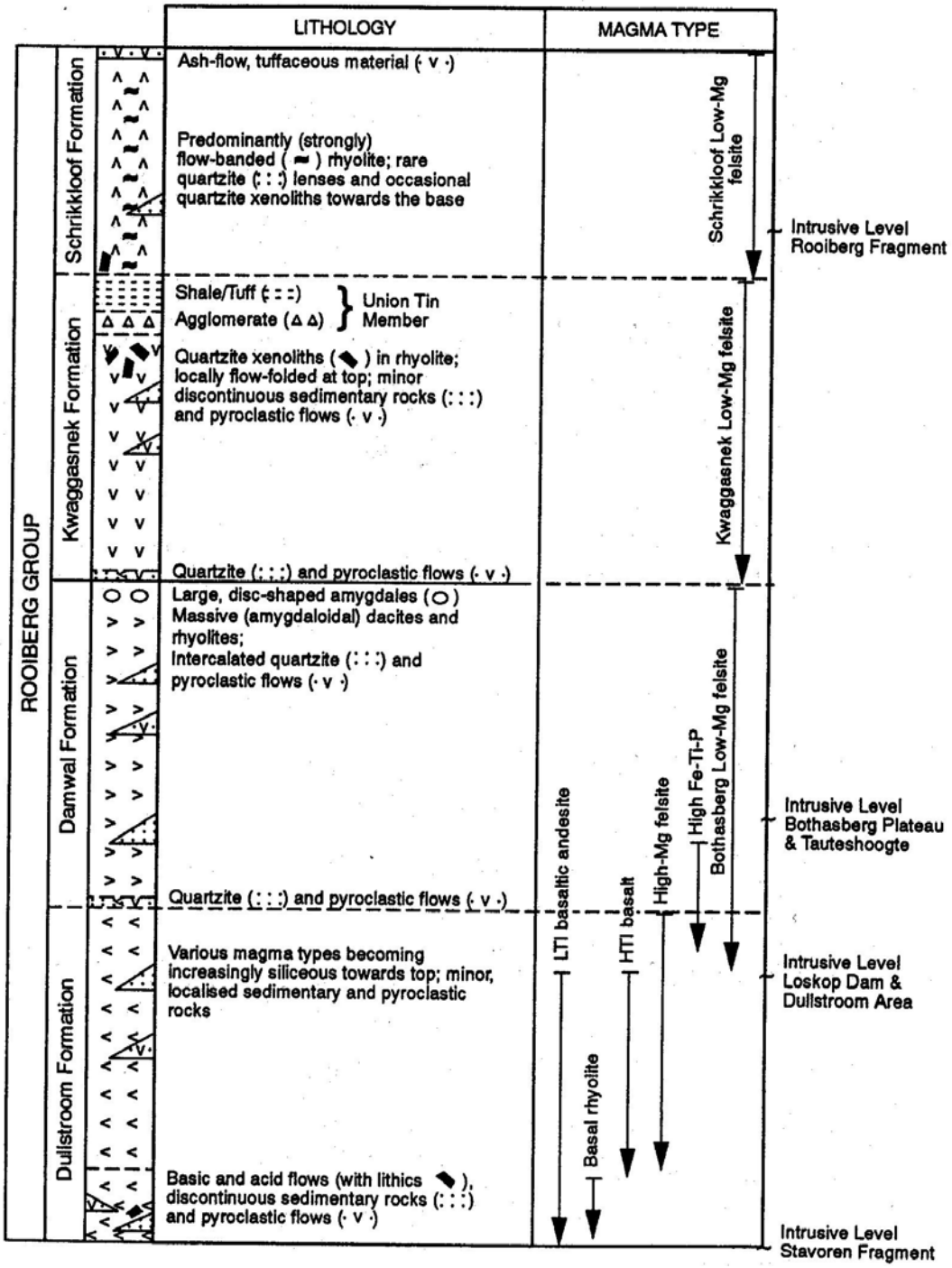

Figure 1.3: Regional stratigraphic subdivision of the Rooiberg Group (from Schweitzer and Hatton, 1995).

1.4 **Rustenburg Layered Suite**

The conventional, approximately 7-8 km thick (Cameron, 1978; Eales and Cawthorn, 1996) stratigraphy of the Rustenburg Layered Suite of the Bushveld Complex is divided into the following layers or zones: 1) a Marginal Zone that is largely fine- to medium grained, 2) an ultramafic Basal Ultramafic Sequence (Wilson 2012) and Lower Zone, 3) an Ultramafic to mafic Critical Zone displaying significant pyroxenite layering, 4) a predominantly gabbronoritic Main Zone, and 5) a gabbroic to ferrodioritic Upper Zone (Figure 1.1 and 1.2; SACS 1980; Cawthorn *et al.,* 2006). Over its entirety, the composition of the Rustenburg Layered Suite ranges from ultramafic rocks of the Lower Zone to felsic rocks of the Upper Zone (Kruger, 1990; Cawthorn *et al.,* 2006). The full Rustenburg Layered Suite stratigraphic suite occurs only in the northern sectors of the eastern and western limbs of the complex, with the southern parts of the eastern and western limbs showing terminations of the Lower Critical Zone and the Main Zone against the sedimentary footwall (Van der Merwe, 1976; Armitage, 2012; Cawthorn *et al.,* 2002). The northern limb shows a similar trend with the Lower Zone not being extensively developed and the stratigraphic correlation of the Critical Zone showing various differences (Kinnaird *et al.,* 2005; McDonald *et al.,* 2012). The properties of the stratigraphic zones are summarised below (ranging in stratigraphy from bottom to top; outlined in Figure 1.2):

1.4.1 **Marginal Zone**

The Marginal Zone is sporadically present in the Bushveld Complex and varies vastly in thickness and mineralogy (Eales and Cawthorn, 1996). Eales and Costin, (2012) suggest that the Marginal Zone formed from a crustally contaminated komatiite magma from the high SiO_2 cap of the staging chamber beneath the complex injected into the Transvaal Supergroup sedimentary rocks. However, according to Cawthorn *et al.,* (1981), this zone may signify the distal facies of evolved magmas or composite sills. The rocks in this zone are genetically related to the immediate adjacent cumulate rocks, however, disruptions in the lithology suggests partial digestion by later injections of magma (Eales, 2003). The Marginal Zone consists mainly of up to 880 m heterogeneous noritic rocks with accessory clinopyroxene, quartz, biotite and

hornblende that display contamination signatures from the underlying sediments (Cawthorn *et al.,* 1981; Eales and Cawthorn, 1996; Kruger, 2004).

1.4.2 **Lower Zone**

The Lower Zone is formed by the lowermost cumulates at the base of the Bushveld magma chamber and is 880-1700 m thick (Cameron, 1978; Kinnaird *et al.,* 2005). The thickest sections of this zone are present in the Oliphants River Trough in the eastern limb of the complex (Cameron, 1978) and in the northern limb on the Grasvally farm (Hulbert and Von Gruenewaldt, 1983). The Lower Zone comprises ultramafic dunites, harzburgites and pyroxenites (bronzitites; Van der Merwe, 1976; Eales and Cawthorn, 1996; Cawthorn *et al.,* 2006). There are three subdivisions of the Lower Zone. These include 1) a Lower Pyroxenite, 2) a middle unit of Harzburgite, and 3) an Upper Pyroxenite (Cameron, 1978; Kinnaird *et al.,* 2002; Cawthorn *et al.,* 2006). In the far western limb, nine cyclic units comprised of dunite, harzburgite and pyroxenite have been recognised (Cawthorn *et al.,* 2006) and in the northern limb, 37 cyclic units comprised of olivine-bearing, chromite-bearing and orthopyroxenite-bearing cumulus packages (Hulbert and Von Gruenewaldt, 1985). The Lower Zone is not continuous throughout the complex and shows limited lateral extent (de Villiers, 1970; Van der Merwe, 1976; Kinnaird, 2005). The Lower Zone is best developed in the northern parts of the eastern and western limbs and in the southern and central parts of the northern limb (Eales and Cawthorn, 1996; Cawthorn *et al.,* 2006; Clarke *et al.,* 2009). The distribution and thickness of the Lower Zone is controlled by the basement topography and structure (Eales and Cawthorn 1996; Cawthorn *et al.,* 2002). The Lower Zone cumulates overlie sills and intrusive feeders to the Complex (Cameron, 1978; Eales and Cawthorn, 1996 Naldrett, 2004; Ashwal *et al.,* 2005; Kinnaird *et al.,* 2005). Recently, an unexposed kilometre-thick ultramafic sequence that forms part of the Lower Zone on Clapham was discovered (Wilson 2012). This has been termed the Basal Ultramafic Sequence and have olivine compositions of Mg# <92 (Wilson, 2012).

1.4.3 **Lower Zone- Critical Zone boundary**

The boundary between the Lower Zone and the Critical Zone is a laterally extensive transition across the Bushveld Complex from ultramafic harzburgite and pyroxenite in the Lower Zone to increasingly plagioclase-rich pyroxenites and norites in the Critical Zone (Boorman *et al.,* 2004). Cameron, (1978) suggested that there is no break between the Lower and Critical zones. However, in the northern limb, a sedimentary interlayer <300 m thick separates the Lower Zone and overlying magmatic sequences (Kinnaird *et al.,* 2005).

1.4.4 **Critical Zone**

The Critical Zone is approximately 1200 m thick and contains world class PGE (platinum group elements) layers including the Merensky Reef and the UG2 chromitite layer (Wagner, 1929; Cameron, 1978; White, 1994; Cawthorn *et al.,* 2010; Scoon and Costin, 2018). Along with the PGE-bearing Merensky Reef and the UG2 chromitites the Critical Zone hosts ~13 other stratiform chromitite layers, which are grouped into the Lower Group (LG), Middle Group (MG) and Upper Group (UG) chromitites (Figure 1.4; Eales and Cawthorn, 1996; Cawthorn *et al.,* 2010).

The boundary between the Critical Zone and the Main Zone is still debated. Some have suggested that the boundary is not distinct (Mitchell and Manthree, 2002), whereas SACS (1980) defined the boundary due to petrographic studies, immediately above the Giant Mottle Anorthosite. Furthermore, Kruger, (1992) suggested that the boundary should be placed at the base of the Merensky Reef based on Rb-Sr isotopic data and a major unconformity at the base of the Merensky Reef, therefore placing the Merensky Reef in the Main Zone (Von Gruenewaldt, 1973; Kinnaird, 2005; Cawthorn *et al.,* 2006). This idea however is not universally accepted (Wagner, 1929; Eales *et al.,* 1986; Viljoen, *et al.,* 1986). The Critical Zone is sub-divided into two compositionally contrasting zones namely the lower (lCZ) and the upper Critical Zone (uCZ; Figure 1.4; Cameron, 1980; Cameron, 1982; Kruger, 1992; White, 1994). These are outlined below:

1.4.4.1 *Lower Critical Zone*

The lower Critical Zone is ~800 m thick and is marked by the onset of cumulus chromite and comprises bronzitite layers interrupted by layers of chromitite, chromitic bronzitite, and minor harzburgite (Cameron, 1978, 1980; Cawthorn *et al.,* 2010). The Critical Zone chromitites are grouped in the Lower Group (LG), Middle Group (MG) and Upper Group (UG) chromitites (Cawthorn *et al.,* 2006; Scoon *et al.,* 2014). The chromitite layers LG1-7 occur in the Lower Critical Zone, with the thickest being the LG6 layer, also known as the Steelpoort seam, with a thickness of ~1 m (Cawthorn *et al.,* 2006; Scoon *et al.,* 2014).

The contact between the lower Critical Zone and the upper Critical Zone is at the first appearance of cumulus plagioclase at the base of the first anorthositic layer, which is between the MG2 and MG3 chromitite layers (Eales and Cawthorn, 1996; Naldrett, 2004; Kinnaird *et al.,* 2005; Cawthorn *et al.,* 2010).

1.4.4.2 *Upper Critical Zone*

The Upper Critical Zone consists of eight cyclic units, which consist of basal ultramafic cumulates (chromitite, harzburgite, pyroxenite); and dominant norites and anorthosites towards the top (Cameron 1982; Cawthorn and Spies 2003; Cawthorn *et al.,* 2006). The top two cyclic units are known as the Bastard Unit and the Merensky Unit and these define the transition in to the Main Zone (Figure 1.4; Wagner, 1929; Cameron, 1978; White, 1994; Cawthorn *et al.,* 2006). These two stratiform units host the largest known PGE reserves in the Bushveld Complex (Eales and Cawthorn, 1996; Naldrett, 2004; Mungal and Naldrett, 2008; Cawthorn *et al.,* 2010). Recently, Hunt *et al.,* (2018) contested the validity of the term “cyclic unit” and suggest that this term is misleading due to various proofs presented for *in-situ* formation of the units in the upper Critical Zone.

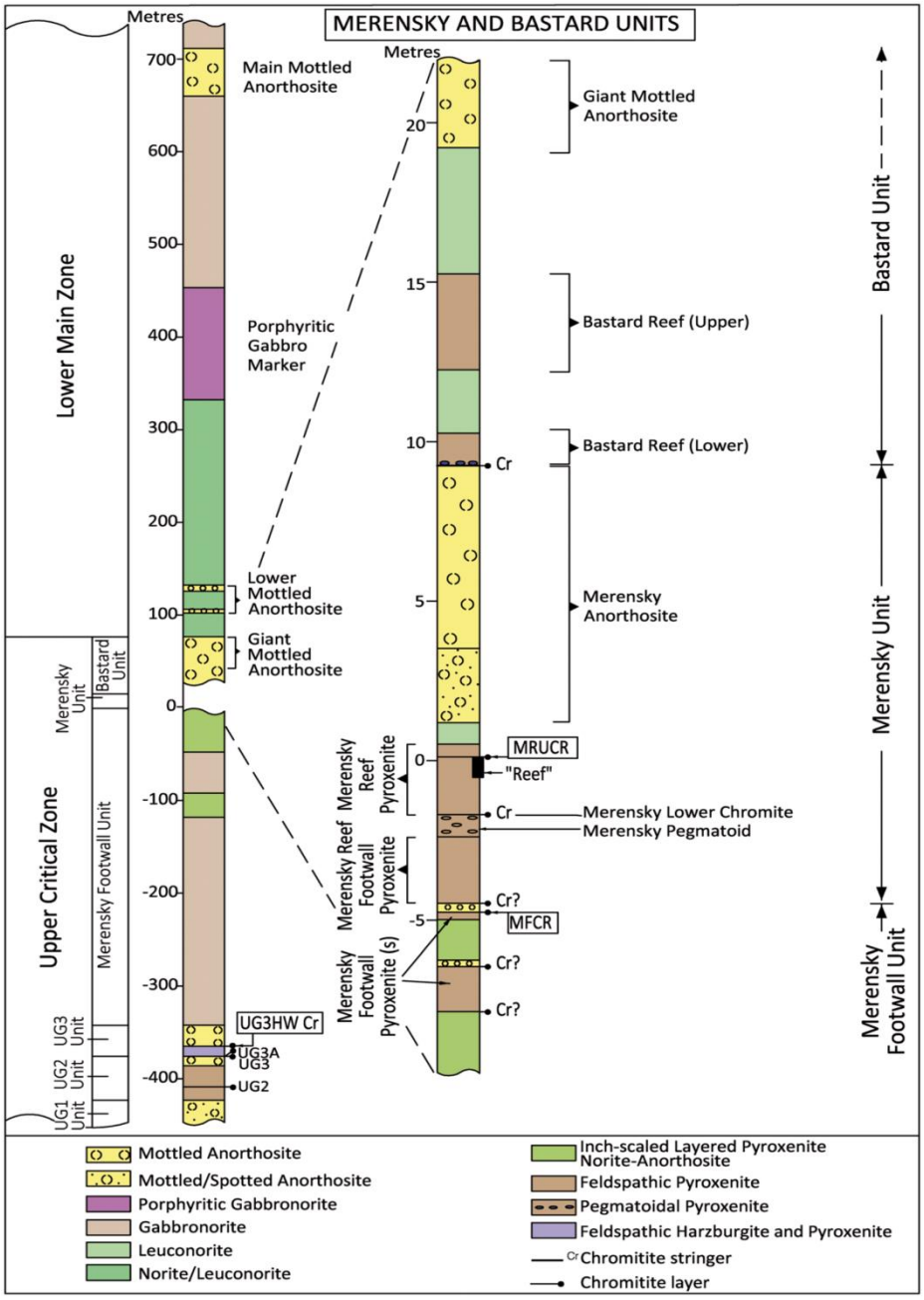

Figure 1.4: Stratigraphic column for part of the Upper Critical Zone and Lower Main Zone at Winnaarshoek based on borehole WH-1 (Scoon *et al.,* 2018, modified from Mitchell and Scoon 2007).

1.4.5 **Main Zone**

The Main Zone ranges from 1200-3500 m in thickness and is the thickest lithologic unit in the Rustenburg Layered Suite (Kruger, 1990; Eales and Cawthorn, 1996; Nex *et al.,* 1998; Cawthorn *et al.,* 2006). The Main Zone is comprised of gabbronorites, gabbros,

norites, and anorthosites (Eales and Cawthorn, 1996; Barnes *et al.,* 2004). Discrete packages of modally layered rocks can be identified in the Main Zone, although the layering is not as distinct as that of the Critical Zone (Molyneux, 1974; Mitchell, 1990; Nex *et al.,* 2002). These layers alternate in colour and are sharp at the base and planar at the top and are composed of orthopyroxene, clinopyroxene, plagioclase and inverted pigeonite (Mitchell, 1986; Kinnaird, 2005). The lighter layers (leucogabbronorite) contain ~70% plagioclase and the darker layers (melagabbronorite) contain 30-40% plagioclase and vary from 2-10 cm in thickness (Mitchell, 1986). The layering is suggested to occur due to mechanical re-distribution of crystals (Kinnaird, 2005; Cawthorn *et al.,* 2006). The Main Zone of the western and eastern limbs does not contain olivine and Cr-spinel, which contrasts with the Main Zone of the northern limb, where olivine is present (Von Gruenewaldt, 1970; Kruger *et al.,* 1987; Kinnaird *et al.,* 2005). The Main Zone is economically important for various quarries of dimension stone, quarrying the dark-coloured inverted-pigeonite-bearing gabbronorite known as coloured Pyramid Gabbronorite (Kinnaird, 2005).

Von Gruenewaldt, (1973) subdivided the eastern limb Main Zone into three subzones; 1) Subzone A comprised of low Ca pyroxene, 2) Subzone B comprising inverted pigeonite bearing lithologies and 3) Subzone C comprising primary orthopyroxene bearing lithologies (Nex *et al.,* 1998). Von Gruenewaldt, (1973) placed the boundary between Subzones B and C at the Pyroxenite Marker, which demarcates the injection of a new magma into the Bushveld magma chamber (Kruger *et al.,* 1987; Cawthorn *et al.,* 1991; Kruger, 1994; Eales and Cawthorn, 1996; Naldrett, 2004). SACS, (1980) then accepted this classification for the western limb of the Bushveld Complex. Mitchell, (1990) suggested that Subzones A and B of the western limb should be termed the Lower Main Zone, collectively, and Subzone C should be termed the Upper Main Zone. However, Nex *et al.,* (1998) divided the Main Zone in the Marikana area into five subzones based on the presence of certain indicator minerals, textures and field characteristics. Subzone A occurs at the base and comprises cumulus plagioclase and primary orthopyroxene (Nex *et al.,* 1998). Subzone B comprises cumulus plagioclase, augite, and discrete primary orthopyroxene (Nex *et al.,* 1998). Subzone C consists of

three units namely the Zebra Unit, Springbok Unit and the Hexrivier Unit (Nex *et al.,* 1998; Nex *et al.,* 2002). The Zebra unit comprises rhythmically layered cumulus clinopyroxene, orthopyroxene and augite, whereas the Springbok and Hexrivier units contain no cumulus orthopyroxene but contains oikocrysts of inverted pigeonite (Nex *et al.,* 1998). Subzone D comprises cumulus plagioclase, orthopyroxene and augite, with no inverted pigeonite (Nex *et al.,* 1998). Subzone E occurs at the top and comprises cumulus plagioclase, augite and inverted pigeonite, with no primary orthopyroxene being present (Nex *et al.,* 1998). Occasional interstitial magnetite is also present in Subzone C (Nex *et al.,* 1998).

1.4.6 **Upper Zone**

The Upper Zone is approximately 1000-2000 m thick and is marked by the first appearance of cumulus magnetite (Cawthorn and McCarthy, 1980). The Upper Zone is the most laterally extensive lithologic unit in the Bushveld Complex (Molyneux, 1974). The most impressive feature of the Upper Zone is the presence of ~25 magnetite layers that are divided into four groups (Molyneux, 1974; Cawthorn and McCarthy, 1980). These magnetite layers generally have sharp bases and gradational tops and get up to 6 m in thickness (Molyneux, 1974; Kinnaird, 2005). The main magnetite layer is up to 2 m thick and occurs near the base (Molyneux, 1974; Cawthorn and McCarthy, 1980). The Upper Zone consists of ~8 % magnetite in total volume and towards the top; ilmenite may surpass magnetite abundance (Reynolds, 1985). Overall, the magnetite layers comprise almost half of the vanadium reserves on Earth (Kinnaird, 2005). The main rock types present in the Upper Zone are gabbros, anorthosites and gabbrodiorites (Molyneux, 1974). Xenoliths and crosscutting intrusions are common near the top (Wagner and Brown, 1968; Kruger *et al.,* 1987).

Conventionally, the base of the Upper Zone has been defined by the Main Magnetite Layer (Willemse, 1969) or the appearance of cumulus magnetite (Von Gruenewaldt 1973; Ashwal *et al.,* 2005). However, petrological and Sr isotopic data places the base of the combined Upper Zone at the Pyroxenite Marker (Von Gruenewaldt, 1970; Kruger *et al.,* 1987; Kruger, 1990; Cawthorn *et al.,* 1991; Nex *et al.,* 1998; Scoon *et al.,* 2012),

which occurs below this level. The Pyroxenite Marker is a massive orthopyroxenite cumulate that is approximately 2-3 m thick and is present in both the eastern and western limbs of the Bushveld Complex (Eales, 2002; Vantongeren and Mathez, 2013).

Scoon, (2012) observed that the Upper Zone is transgressive in relation to the Critical Zone and the Main Zone, and may have formed by a completely new intrusive phase, that differentiated in situ without any further addition of magma (Cawthorn *et al.,* 1991). Scoon *et al.,* (2012) argued against a closed system and suggest five subdivisions of the Upper Zone on the basis of the cumulus mineralogy and whole-rock geochemistry. These units are said to be formed by various processes including separate pulses of magma (Scoon *et al.,* 2012).

1.5 **Rashoop Granophyre Suite**

The Rashoop Granophyre Suite occurs above the Rustenburg Layered Suite and below the Rooiberg volcanic rocks and comprises metamorphosed sediments and intrusive acidic rocks (Harmer and Armstrong, 2000). These include: 1) the Stavoren and Diepkloof Granophyres, 2) the Rooikop Porphyritic Granite and 3) the Zwartbank Pseudogranophyre (Walraven, 1987; Harmer and Armstrong, 2000). The age of the Rashoop Granophyre Suite was determined at ~2061.8 ± 5.5 Ma, taken from the Rooikoppies porphyry, which coincides with the age of the mafic sequences within uncertainty (Harmer and Armstrong, 2000).

1.6 **Lebowa Granite Suite**

The Lebowa Granite suite is one of the largest (60 000 km^2) of A-type granite provinces on Earth (Harmer and Von Gruenewaldt, 1991). The Lebowa Granite Suite comprises sheet-like bodies that are 1.5-3.5 km thick and cover an area of approximately 30 000 km^2 (Molyneux and Klinkert, 1978; Harmer and Von Gruenewaldt, 1991; Kinnaird, 2005). These granites intruded close to the top contact of the Rustenburg Layered Suite and are overlain by the felsic volcanic rocks of the Rooiberg Group and Rashoop Granophyre Suite (Lenthall, 1973; Hatton and Schweitzer, 1995; McNaughton *et al.,*

1993; Kinnaird, 2005) and post-date the mafic Bushveld rocks with intrusion ages of 2061-2054 Ma (Walraven, 1988; Walraven and Hattingh, 1993). The Lebowa Granite Suite comprises seven types of granite, which include the following: 1) the Nebo Granite, 2) the Lease Granite, 3) the Makhutso Granite, 4) the Klipkloof Granite, 5) the Bobbejaankop Granite, 6) the Balmoral Granite and 7) the Verena Granite (SACS, 1980; Eales and Cawthorn, 1996; Cawthorn *et al.,* 2006). The age of the Lebowa Granite Suite is within 2053.4-2057.5 ± 4, taken from Makhutso, Nebo and Steelpoort Park granites (Walraven, 1988; Walraven and Hattingh, 1993; Harmer and Armstrong, 2000).

1.7 **Discordant bodies and Satellite Intrusions**

A number of discordant and satellite bodies occur in the Bushveld Complex. These include the Uitkomst (Nkomati) Complex (Gauert, 2001); the Molopo Farms Igneous Complex (MFIC; Cawthorn and Walraven, 1998) as well as the Mashaneng Complex (Eales and Cawthorn, 1996; Kinnaird, 2005), which falls in the same age range as the Bushveld Complex (Eales and Cawthorn, 1996). Some satellite bodies may be of economic importance, with significant mineralisation being present in the Uitkomst (Nkomati) Complex (Gauert, 2001).

Discordant pipe-like bodies of <1.5 km wide cross-cut the layers of the Bushveld Complex and are generally comprised of magnesium-rich dunites and iron-rich pegmatites and may have been formed due to hydrothermal processes (Eales and Cawthorn 1996).

1.8 **Bushveld mineralisation**

The Bushveld Complex hosts approximately 75% of the platinum group elements (PGE) resources on Earth (Kendall, 2006), as well as one of the largest known deposits of Cr and V on Earth (Kruger, 2005; Naldrett *et al.,* 2009). Accessory minerals of Cu, Ni, Au, Sn, fluorite, Fe as well as andalusite and dimension stone are also prominent in the

complex (Wilson and Anhaeusser, 1998; Oosterhuis, 1998) with the Bushveld felsics hosting noteworthy Sn and F deposits (Bailie and Robb, 2004).

Most of the PGE mineralisation in the eastern and western limbs occurs in three main deposits namely, the Upper Group 2 (UG2) chromitite, the Merensky Reef, and the deposits of the Platreef in the northern limb (Hall and Humphrey, 1908; Wagner, 1929; Van der Merwe 1976; Von Gruenewaldt 1979; Cawthorn 1999; Kinnaird *et al.,* 2005; Barnes *et al.,* 2017). Generally, all the chromitites in the Bushveld Complex are enriched in PGE's, relative to the host rocks; however, the UG2 chromitites show the highest concentration of PGE's (Naldrett *et al.,* 2012). The UG2 chromitites and the Merensky Reef rocks are conventional stratiform reef deposits, with PGE-rich sulphides associated with the chromite (Hall and Humphrey, 1908, Von Gruenewaldt, 1979).

Furthermore, at the base of the northern limb, the lithologically variable, broadly pyroxenitic Platreef (Kinnaird *et al.,* 2005; McDonald and Holwell, 2011), has become increasingly important as a mineral resource over the last few decades (McDonald *et al.,* 2005; Barnes *et al.,* 2017). Ivanhoe's Platreef Project, which focusses on mining in the "Flatreef", is one of these recent and exciting projects (www.Ivanhoemines.com). Further north, just south of the Hout River shear zone, possible economic mineralisation was discovered in the upper Main Zone as part of the Aurora Project (McDonald *et al.,* 2017). In addition to this, in 2011 Platinum Group Metals (PTM) discovered mineralised Bushveld rocks (T- and F-mineralised zones) north of the northern limb, which is overlain by the thick succession of Waterberg Group sedimentary rocks (Lomberg, 2012; Kinnaird *et al.,* 2017).

1.9 **Location and research area**

The study site for this project is north of the exposed northern limb of the Bushveld Complex, on the Sylvania Resources Limited-owned Harriet's Wish farm located in the Capricorn District Municipality, Limpopo Province, South Africa (Figure 1.5; Sylvania Resources Limited, 2012). The study site is ~70 km north of the town of Mokopane (Potgietersrus). The Harriet's Wish Farm was chosen for this study due to the setting

between the Waterberg Project to the north and the Aurora Project to the south (Figure 1.5). The drillcores in this study lie to the north of the Hout River shear zone. And the coordinates to the farm is 23°25'25.21" south latitude and 28°52'26.58" east longitude.

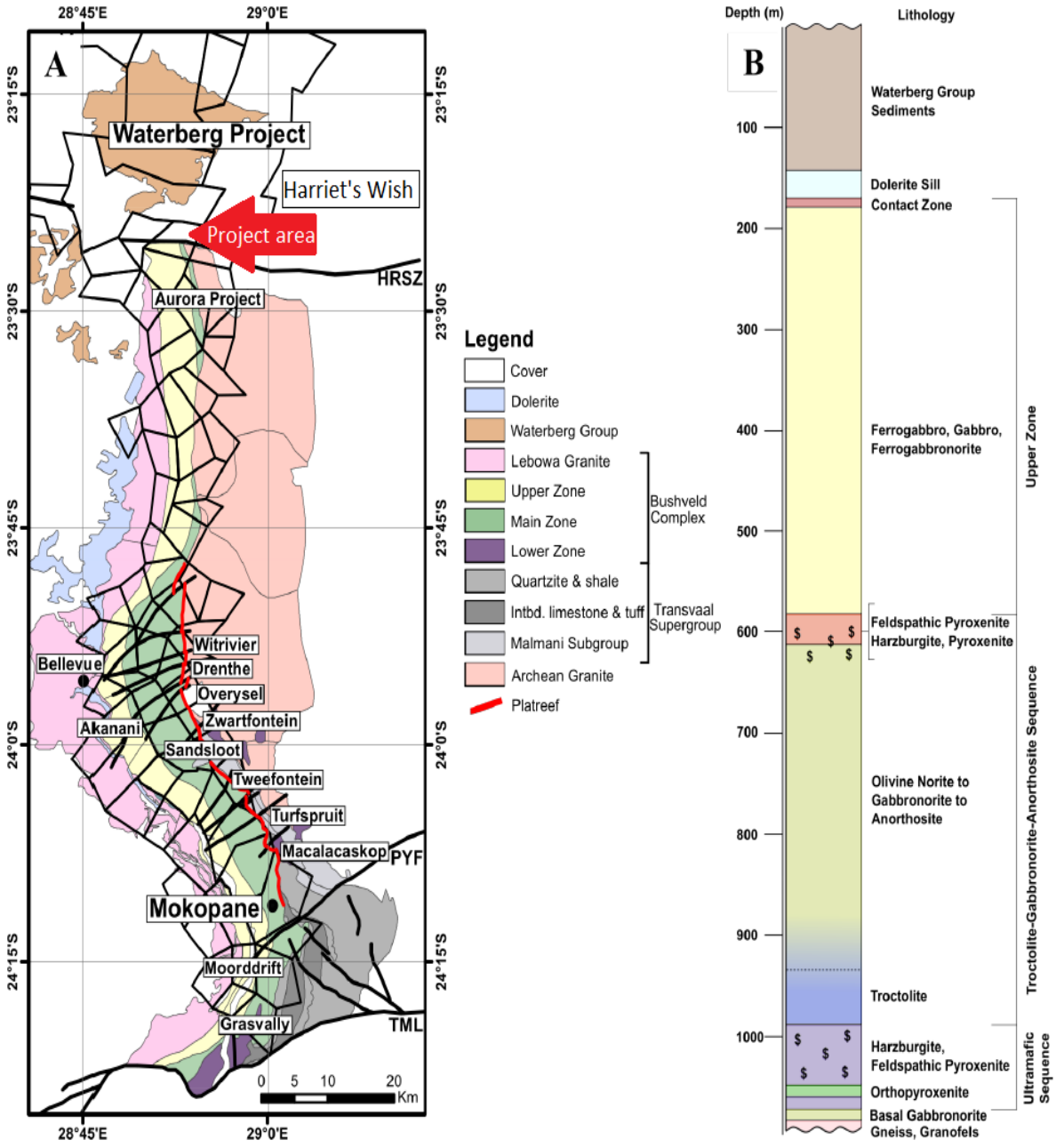

Figure 1.5: Geology of the northern limb of the Bushveld Complex. A) A map showing locations of the Waterberg Project, Aurora Project and Harriet's Wish. HRSZ = Hout River shear zone; PYF = Planknek-Ysterberg Fault, TML = Thabazimbi-Murchison Lineament. B) The stratigraphy of the Waterberg Project area (from Kinnaird *et al.,* 2017).

1.10 **Aims and objectives**

According to the exploration results published by Sylvania Resources Limited, (2012), the study site of Harriet's Wish farm has economic potential due to its promising concentrations of platinum group elements and Au. McDonald *et al.,* (2017) suggests that PGE-sulphide mineralisation encountered on the Waterberg Project could extend up to 40 km south through to the Aurora Project area, just south of the Hout River shear zone. Kinnaird *et al.,* (2017) and McCreesh *et al.,* (2018) suggest that the Waterberg Project forms part of a new basin that exists north of the Hout River shear zone. The Harriet's Wish drillcores are located just to the north of the Hout River shear zone between the Waterberg and Aurora projects.

Therefore, this project has the following aims:

- To understanding the magmatic stratigraphy, petrography, ore mineralogy of host sequences and geochemistry on the Harriet's Wish farm.
- To establish possible connectivity with the surrounding areas such as the Waterberg Project to the north of the Hout River shear zone, the Aurora Project and certain Platreef localities to the south of the Hout River shear zone.
- To provide evidence for or against the idea that a separate basin exists to the north of the northern limb of the Bushveld Complex.

This study investigates the mineralisation and stratigraphy on the Harriet's Wish farm, using the research objectives outlined below:

- Field observations and detailed core logs are used to determine the general stratigraphy and to understand the host rocks of the mineralisation on Harriet's Wish.
- Magnetic susceptibility surveys of the drillcore are used to determine the boundary between the lower and upper lithologic units, similar to the Upper Zone and troctolite-gabbronorite-anorthosite (TGA) sequence on the Waterberg

Project to the north (Kinnaird *et al.,* 2017). This is important because the T Zone mineralisation on the Waterberg Project is confined to the Main Zone-Upper Zone boundary (Kinnaird *et al.,* 2017).

- Sampling was carried out on drillcores HW024, HW025 and HW029 stored on the Sylvania Resources Limited core yard outside Mokopane. A total of 117 samples were collected for petrologic and whole rock major and trace geochemical studies to assist in characterising and distinguishing between geological units and also to establish variation within individual units. These data are compared with the data from the Waterberg and Aurora projects to test whether the lithologic units from the studied area correlate with the northern limb and the areas north of the Hout River shear zone (Kinnaird *et al.,* 2017; McDonald *et al.,* 2017; McDonald and Holwell, 2011).
- Assay data from Sylvania Platinum Limited were obtained to determine the nature of the ore mineralisation and to establish possible links between Harriet's Wish mineralisation and the mineralisation on the Waterberg and Aurora projects, and the Platreef (Kinnaird *et al.,* 2017; McDonald *et al.,* 2017; McDonald and Holwell, 2011). Tenor calculations were also made and plots were drawn to identify individual magmatic sills or pulses in the mineralised zones.

The fundamental research questions, therefore, are: 1) is the Harriet's Wish geology a southward extension of the Waterberg Project geology to the north?, 2) does Harriet's Wish serve as a link between the Waterberg and Aurora projects?, 3) does a basin, separate to the northern limb occur to the north of the Hout River shear zone?

1.11 **Methodology**

Several geological techniques were used to achieve the aims and objectives of this study. These include core logging, sampling for mineralogical studies, magnetic susceptibility, polished thin section for mineralogical studies and whole rock major and trace geochemical analyses (XRF). The methods for each of these techniques are outlined in the relevant chapters.

Chapter 2
Geology of the northern limb

2.1 Introduction

The northern limb of the Bushveld Complex is situated in the province of Limpopo. It has a sinuous outcrop that is N-S oriented (Figure 2.1). The exposed width of the northern limb is around 15 km and the exposed strike length is approximately 110 km (Wagner, 1929; Van der Merwe, 1976; Gain and Mostert, 1982). This extends from the Zebediela Fault in the south, to the Hout River shear zone in the north (Figure 1.5; Van der Merwe, 1976; Gain and Mostert, 1982; Kinnaird *et al.,* 2017). The Zebediela Fault in the south forms a branch of the Thabazimbi-Murchison Lineament, which separates and compartmentalises the northern limb from the eastern and western limbs (Good and de Wit, 1997). The Thabazimbi-Murchison Lineament is approximately 500 km in length and 25 km in width (Good and de Wit, 1997). The Thabazimbi-Murchison Lineament is an ENE-WSW striking (Good and de Wit, 1997) large, old tectonic boundary that was formed when the Pietersburg and Kaapvaal terranes collided at around 2.7 Ga (Truter, 1947; de Wit *et al.,* 1992; Good and de Wit, 1997; Griffin *et al.,* 2004). The Thabazimbi-Murchison Lineament also serves as the marker between significant differences in stratigraphy between the northern limb and the eastern and western limbs of the Bushveld Complex, in particular, the occurrence of the unique Platreef and an unusual Lower Zone (Kinnaird *et al.,* 2005; Armitage *et al.,* 2007). According to Kinnaird *et al.,* (2005) it is still not clear whether there was any connection between the northern limb and the main Bushveld Complex during its emplacement.

2.1.1 Aims

The aim of this chapter is to provide detail on, and to outline the stratigraphic units of, the northern limb of the Bushveld Complex and to elaborate on the structures and controls that influence the mineralisation in the northern limb. This chapter will also provide a backdrop for comparing the stratigraphy and geology of Harriet's Wish to the northern limb, south of the Hout River shear zone.

2.2 **Geology of the northern limb**

Previous work describes the northern limb geology on the farms on which it occurs. These farm localities are outlined in Figure 2.1. Note that the geology described in this section is south of the Hout River shear zone.

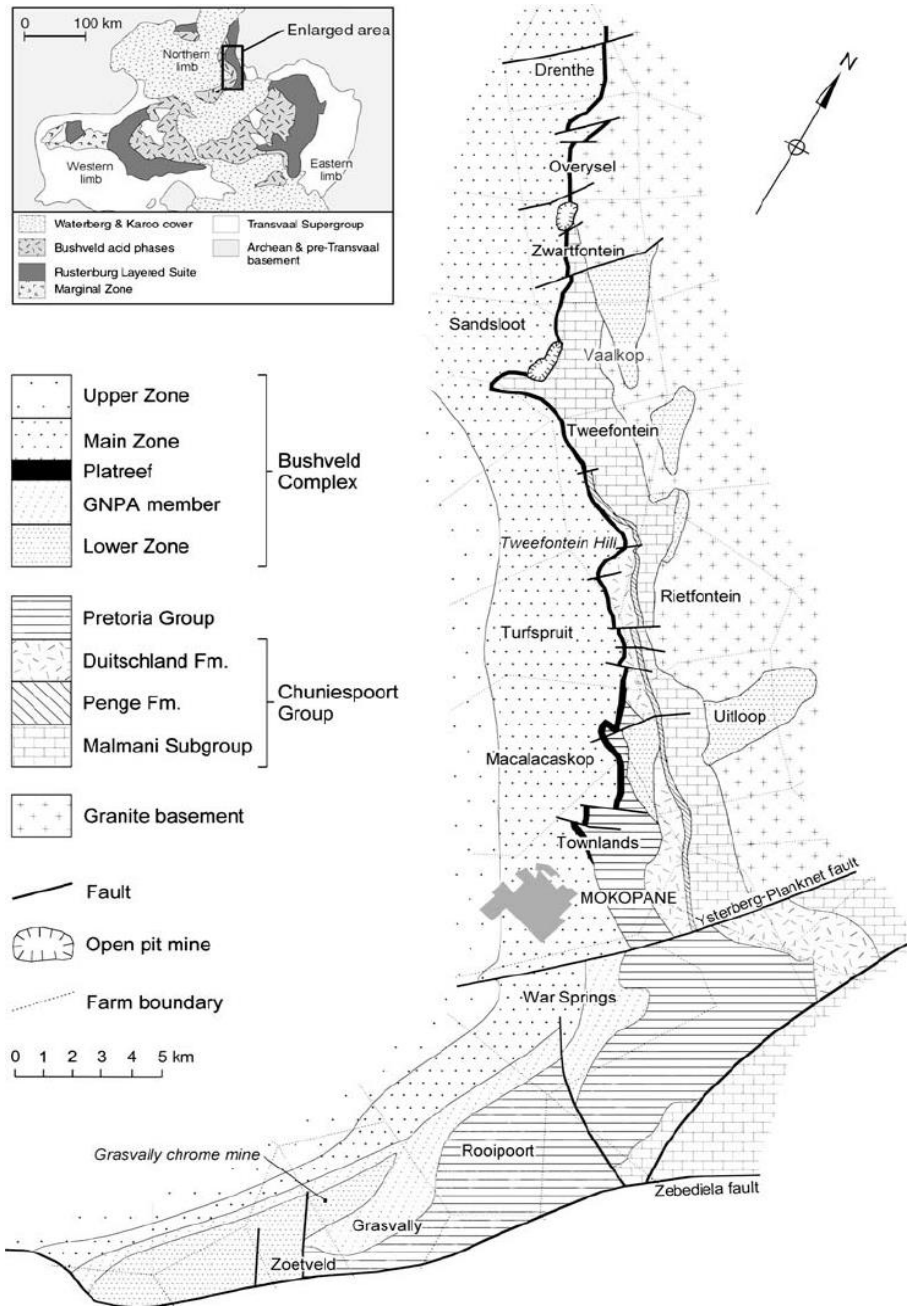

Figure 2.1: Geological map of the northern limb of the Bushveld Complex south of the Hout River shear zone showing the localities and faults described in the text (McDonald *et al.,* 2005).

2.2.1 **Footwall Lithologies**

The footwall rocks vary along the northern limb N-S strike (Figure 2.1; Van der Merwe, 2008). The footwall is composed of progressively older sedimentary units of the Transvaal Supergroup from south to north with eventually Archean granite-gneisses serving as a footwall of the northern lime magmatic sequence north of farm Zwartfontein. The rocks of the Transvaal Supergroup that occur in the northern limb beneath the Platreef are synthesised in Figure 2.2

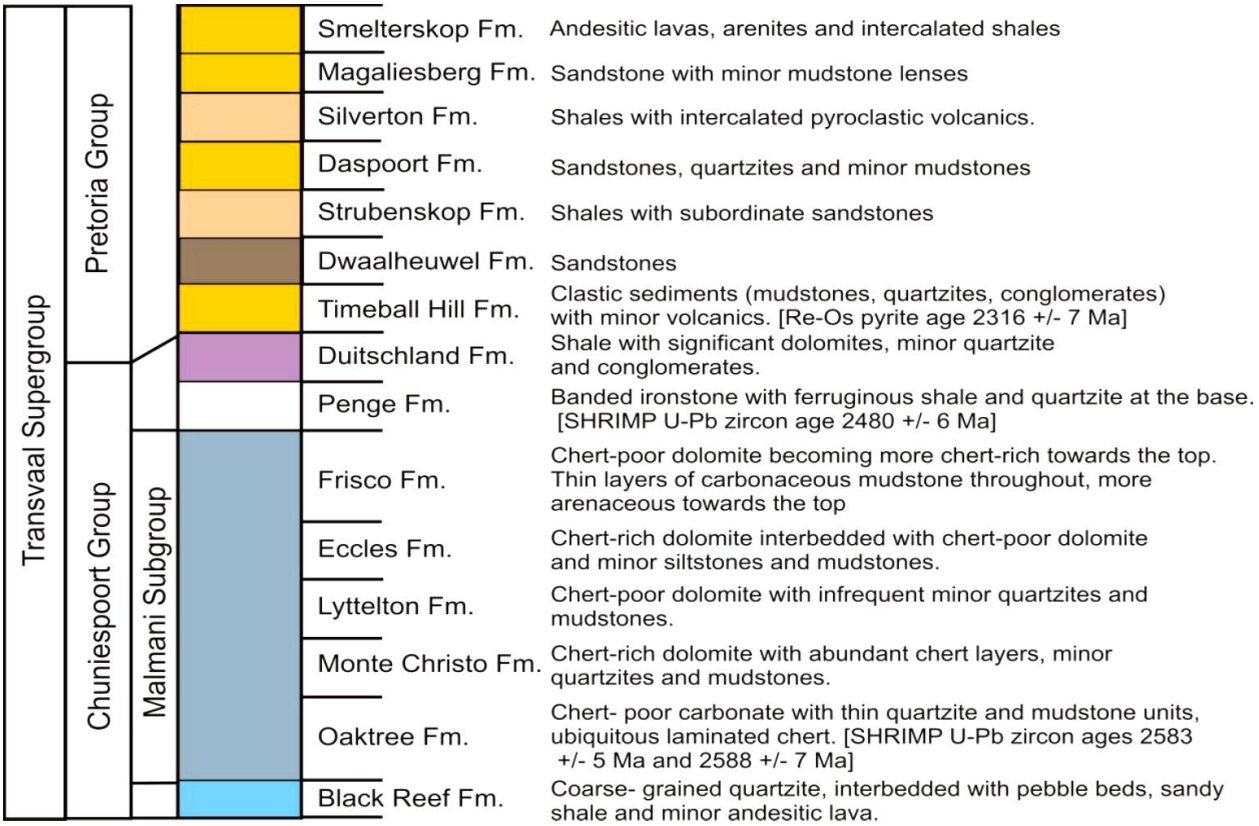

Figure 2.2: Lithostratigraphy of Transvaal Supergroup floor rocks underneath the northern limb (from Kinnaird and Nex, 2012, with data from Button, 1973; Martini, 1979; Catuneanu and Eriksson, 1999; Bekker *et al.,* 2001).

In the southern parts of the northern limb, on the Grasvally farm, the Platreef is underlain by the Lower Zone (Hulbert, 1983; Maier *et al.,* 2007). On Townlands and Macalacaskop the footwall comprises shales of the Timeball Hill Formation (Manyeruke *et al.,* 2005; Kinnaird *et al.,* 2005). On Turfspruit and Tweefontein, sulphidic shales and limestones of Duitschland Formation form the footwall to the thick Lower Zone, which is separated from the overlying Platreef by the same Duitschland metamorphosed shales

(Kinnaird *et al.,* 2005). The footwall in the northern parts of Tweefontein consists of Penge Iron Formation lithology (Buchanan *et al.,* 1981; Kinnaird and Nex, 2012). Between Rooipoort and Zwartfontein it is underlain by progressively older Transvaal Supergroup rocks such as Silverton- and Timeball Hill Formation quartzites and shales, Duitschland Formation shales; Penge Banded Iron Formation (BIF's) and Malmani Subgroup dolomites (Maier, 2002; Kinnaird *et al.,* 2005; Manyeruke *et al.,* 2005; Manyeruke, 2007; Yudovskaya and Kinnaird, 2010; McDonald and Holwell, 2011). The Platreef is a basal unit and underlain by Archaean granite gneiss from Zwartfontein (including Drenthe and Overysel) to the northern edge of the limb (Figure 2.1; Cawthorn *et al.,* 1985; White, 1994; Kinnaird *et al.,* 2005; Holwell and McDonald, 2006; McDonald and Holwell, 2011). The hanging wall of the Platreef comprises Main Zone norites gabbronorites (Figure 2.1; Kinnaird *et al.,* 2005; McDonald and Holwell, 2011).

2.2.1.1 *Footwall mineralisation*

Mineralisation is present in some of the contact-metamorphosed wallrocks in the northern limb (Viljoen and Schürmann, 1998; Kinnaird *et al.,* 2005; Maier *et al.,* 2008; Nex *et al.,* 2008; McDonald and Holwell, 2011). This is highlighted in the immediate footwall to the Platreef north of Turfspruit, on Tweefontein Hill, which comprises aluminous argillaceous shales of the Duitschland Formation and contains xenoliths of ironstone and shale (Wagner 1929; Bekker *et al.,* 2001). The Banded Ironstone of the Penge Formation on Tweefontein Hill shows contact metamorphism to magnetite-bearing hornfels (White, 1994), which contains hydrothermal veins with Cu and PGE (platinum group element) mineralisation (Wagner, 1929; Nex *et al.,* 2008).

2.2.2 **Northern limb magmatic stratigraphy**

In Figure 2.3 the magmatic Rustenburg Layered Suite stratigraphy of the northern limb, south of the Hout River shear zone is outlined. The northern limb, similar to the eastern and western limbs, comprises a Lower Zone, a unit known as the Platreef, a Main Zone and an Upper Zone (Figure 2.3; Van der Merwe, 1976).

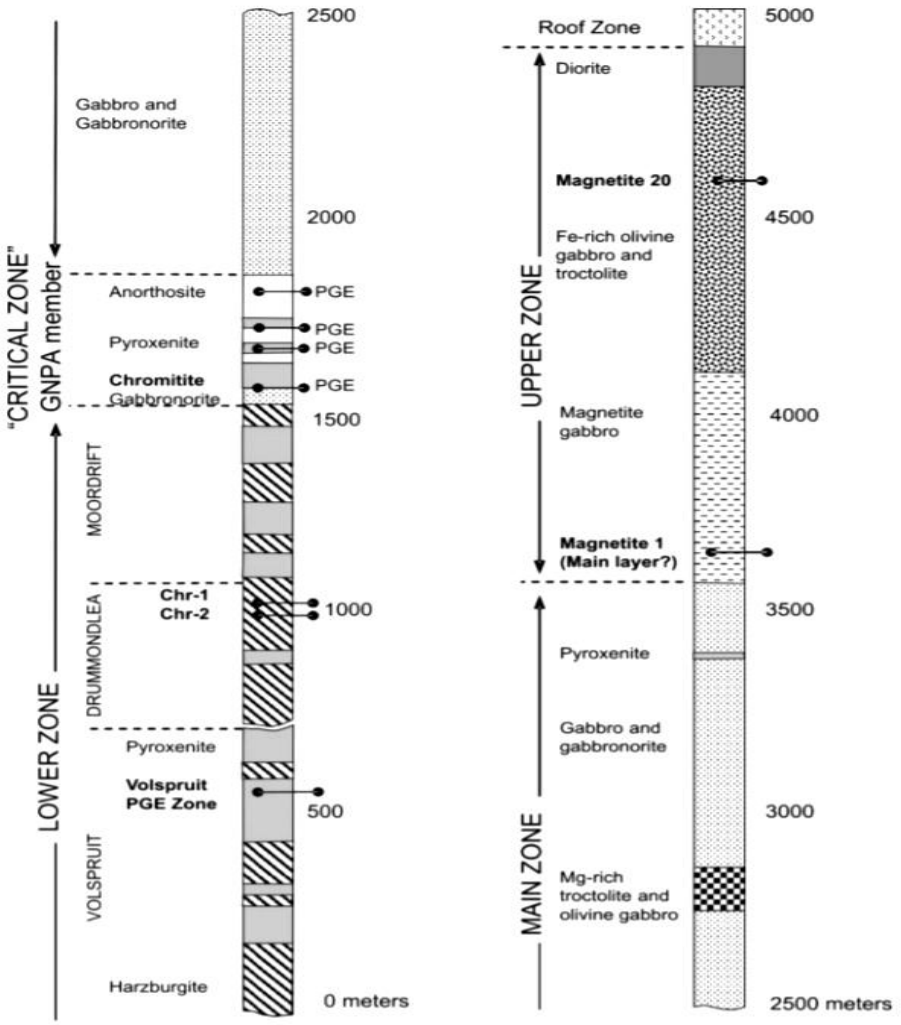

Figure 2.3: Generalised stratigraphy of the northern limb on Grasvally showing the positions of the principal mineral deposits (from Kinnaird and McDonald, 2005, modified after Von Gruenewaldt *et al.,* 1989, and McDonald *et al.,* 2005).

However, there are some differences in the northern limb stratigraphy. This includes the presence of the Platreef instead of the Critical Zone (Figure 2.4; Wagner 1929; Van der Merwe, 1976; White, 1994; Kinnaird *et al.,* 2005; McDonald *et al.,* 2005; Pronost *et al.,* 2008; McDonald and Holwell, 2011). The northern limb Rustenburg Layered Suite stratigraphy is described in more detail below:

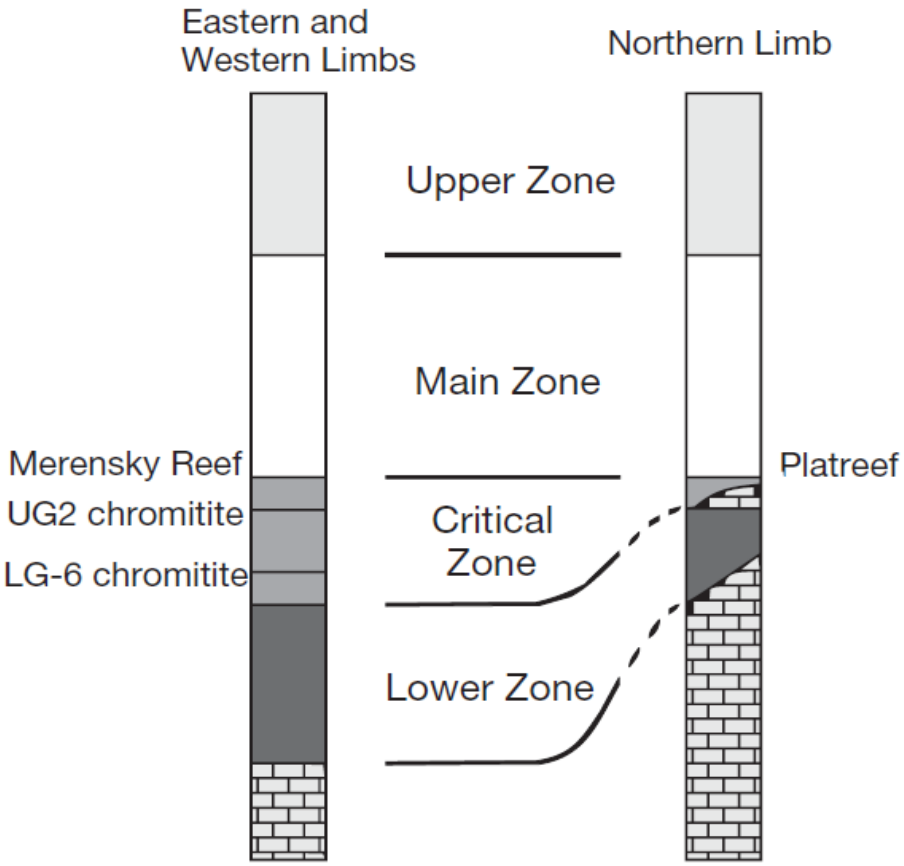

Figure 2.4: Correlation of the stratigraphy of the eastern and western limbs of the Bushveld Complex, with the northern limb stratigraphy (from McDonald and Holwell, 2011).

2.2.2.1 *Marginal Zone*

The exposure of the Marginal Zone in the northern limb is generally poorer than in the eastern and western limbs, however, when it is visible in outcrops; it ranges from a few centimetres to tens of metres in thickness and displays intrusive characteristics (Van der Merwe, 1976). It comprises noritic to gabbroic rocks, which occur sporadically within the succession (Van der Merwe, 1976; Eales and Cawthorn, 1996). Inclusions of calcsilicate, hornfels, quartzite, and granite are also found in this zone (Van der Merwe 1976; Kinnaird *et al.,* 2005; Kinnaird and McDonald 2018). An olivine-bearing chilled margin can be seen along the contact with the Lower Zone at the base of the Uitloop satellite, close to Mokopane (Van der Merwe, 1976).

2.2.2.2 *Lower Zone*

The Lower Zone also differs from the traditional Lower Zone in the eastern and western limbs, and occurs as satellite bodies within the footwall (de Villiers, 1970; Van der Merwe, 1976) as well as a thick package locally underlying the Platreef The Lower Zone also occurs as a thick package locally underlying the Platreef (Figure 2.4; Yudovskaya and Kinnaird, 2010; McDonald and Holwell, 2011) and the Grasvally Norite–Pyroxenite–Anorthosite (GNPA) member (Hulbert and Von Gruenewaldt, 1983). Thick and chemically primitive accumulations of the Lower Zone known are found on Grasvally close to the major fault array of the Thabazimbi-Murchison Lineament (Figure 2.1, Hulbert and Von Gruenewaldt, 1983). The Grasvally Lower Zone mainly consists of bronzitites and harzburgites with a magnesium-rich lower section, due to the presence of fractionated orthopyroxene and olivine, and an iron-rich upper section (de Villiers, 1970; Hulbert and Von Gruenewaldt, 1983). South of Mokopane, the Lower and Critical zones of the northern limb are heavily faulted (Barrett *et al.,* 1978). South of the Planknek-Ysterberg fault, stratigraphic relationships of the Lower Zone are unclear, but to the north of this fault, the Lower Zone occurs as an approximately 1 km thick sequence beneath the Platreef, or as bodies or offshoots at the base of the intrusion (De Villiers, 1970; Van der Merwe, 1976; McDonald and Holwell, 2011). The Grasvally Lower Zone lithology to the north of Thabazimbi-Murchison Lineament contain two well-developed chromitite layers that outcrop over an approximately 5 km strike length on Grasvally, with high Cr/(Cr+Al) ratios (Hulbert and Von Gruenewaldt, 1983), whereas chromitites are not developed in the Lower Zone elsewhere in the eastern or western limbs of the Bushveld Complex (Hulbert and Von Gruenewaldt, 1983). The Grasvally succession of the Lower Zone in the northern limb can be correlated with the Basal Ultramafic sequence on Clapham in the western Bushveld based on mineralogy and geochemistry (Wilson, 2012; Yudovskaya *et al.,* 2013; Maier and Barnes, 2016). On Turfspruit, the Lower Zone is at least 800 m thick and comprises layers of high-Mg cumulates (Smart, 2013; Mayer, 2018). PGE sulphide mineralisation is established in the Lower Zone on Grasvally and on Turfspruit (Hulbert and Von Gruenewaldt, 1983, 1985; Yudovskaya *et al.,* 2013) which is not present in the eastern and western limbs.

2.2.2.3 *Platreef*

The Lower Critical Zone appears to be completely missing from the northern limb (Van der Merwe, 1976; Ashwal *et al.,* 2005) and instead of the traditional Critical Zone, the unique Platreef exists (Figure 2.4; Van der Merwe, 1976; Kinnaird *et al.,* 2005; McDonald and Holwell, 2011; Kinnaird and McDonald, 2018). More details on the Platreef are given in a later section.

2.2.2.4 *Main Zone*

The Main Zone in the northern limb is ~2000 m thick and is comprised of gabbro, anorthosite, pyroxenite, a prominent layer of troctolite to olivine norite, harzburgite and lherzolite in a layered sequence (Van der Merwe, 1976; Van der Merwe 1978; Barton *et al.,* 1986; Eales and Cawthorn, 1996; Ashwal *et al.,* 2005; Kruger, 2005). The troctolite to olivine norite unit, which is approximately 200 m thick, occurs at about 1100 m above the top of the Platreef (Van der Merwe, 1976; Ashwal *et al.,* 2005). This contrasts with the Main Zone in rest of the Bushveld Complex, which reaches a thickness of up to 4000 m and does not contain Ol-bearing lithologies (Van der Merwe, 1976; Ashwal *et al.,* 2005; Kinnaird *et al.,* 2017).

The Main Zone and the Platreef of the northern limb seem to be absent for about 10 km between the farms Elberfeld and Altona, just to the south of Nonnenwerth, and instead, the Archean basement footwall in this area is directly overlain by Upper Zone rocks (Kinnaird *et al.,* 2005; McDonald and Holwell, 2011). In the northern limb there has also been no equivalent found to the extensively developed orthopyroxene-rich Pyroxenite Marker (Van der Merwe, 1976; Ashwal *et al.,* 2005; Kruger, 2005; Tanner *et al.,* 2014), which is met in the Main Zone in the eastern and western limbs (Ashwal *et al.,* 2005; Kruger 2005). The boundary between the Main- and Upper Zone has been distinguished by the presence of cumulus magnetite (SACS 1980). However, Ashwal *et al.,* (2005) suggested that magnetic susceptibility readings reveal unseen magnetite considerably below the visible cumulus magnetite, and proposed this method to be used to distinguish the boundary.

2.2.2.5 *Upper Zone-Main Zone boundary*

As noted in Chapter 1, the Pyroxenite Marker (Von Gruenewaldt, 1973; Cawthorn *et al.,* 1991; Nex *et al.,* 2002; Ashwal *et al.,* 2005) has been suggested as the base of the Upper Zone, therefore forming the boundary between the Main- and Upper Zone (Kruger, 1990, 1994) although this suggestion was not approved by SACS, (1980). In the Bellevue drillcore, in the northern limb, there are two distinct pyroxenite horizons present (Ashwal *et al.,* 2005). The lower horizon is 2.3 m thick and occurs at a depth of 2,806.80 m and the upper horizon is 1.88 m thick and occurs at a depth of 1,971.80 m (Ashwal *et al.,* 2005). Although the lower pyroxenite horizon occurs at the same stratigraphic position as the Pyroxenite Marker elsewhere in the Bushveld Complex (Von Gruenewaldt, 1973; Cawthorn *et al.,* 1991: Nex *et al.,* 2002), Ashwal *et al.,* (2005) did not equate this to the Pyroxenite Marker in the eastern and western limbs due to it being clinopyroxene-rich rather than orthopyroxene-rich. SACS, (1980) suggest the Upper Zone-Main Zone boundary is marked by the appearance of cumulus magnetite, and Ashwal *et al.,* (2005) suggests magnetic susceptibility readings should be used to define this boundary, as magnetic susceptibility indicate the presence of magnetite well below the visible magnetite in the Bellevue drillcore.

2.2.2.6 *Upper Zone*

This Upper Zone overlies the Main Zone and is ~1400 m thick in the Bellevue core (Ashwal *et al.,* 2005; McDonald *et al.,* 2005) and is characterised by cyclic units with magnetitite layers at the base, followed by magnetite gabbro, gabbro, olivine diorite and anorthosite (Eales and Cawthorn 1996; Ashwal *et al.,* 2005; Kinnaird *et al.,* 2005; Kruger 2005). There are 20 distinct magnetitite seams with different titanium and vanadium contents, which are comparable to the Upper Zone magnetitites in the eastern and western limbs (Van der Merwe, 1976).

2.3 **The Platreef**

2.3.1 **Platreef definition**

The Platreef has been defined as a “lithologically variable unit, dominated by pyroxenite, which is irregularly mineralised with PGE, Cu and Ni, between the Transvaal metasedimentary footwall or Archaean basement and the overlying Main Zone gabbronorite” (Kinnaird, 2005). Kinnaird and McDonald, (2005) added boundary constraints to this and defined the Platreef (*sensu stricto*) as “Mafic units enriched in Ni-Cu-PGE that occur between the Archaean granite-gneiss basement or the Transvaal Supergroup and the gabbros and gabbronorites of the Main Zone, north of the Planknek Fault.” However, the new exploration projects showed that the Platreef and its equivalent on Grasvally are underlain by the thick Lower Zone and the Marginal Zone (Yudovskaya *et al.,* 2013).

The Platreef definition does not include the mineralisation on the Aurora Project (Harmer *et al.,* 2004; McDonald and Harmer, 2010; McDonald *et al.,* 2017) or any mineralisation north of the Hout River shear zone (Kinnaird *et al.,* 2017; McCreesh *et al.,* 2018), or any Ni-Cu-PGE mineralisation to the south of Mokopane (Hulbert 1983; Von Gruenewaldt *et al.,* 1989; de Klerk, 2005). This revised definition by Kinnaird and McDonald, (2005) will be followed in this study.

2.3.2 **Platreef geology**

The Platreef is unique to the northern limb of the Bushveld Complex (Figure 1.1; Kinnaird *et al.,* 2005). Kinnaird *et al.,* (2005) divided the Platreef into sectors, assigning farms to each of these sectors based on shared characteristics. These sectors include: 1) the Southern Sector which extends from Townlands 44KS in the south to Tweefontein 238KR, 2) the Central Sector includes the farms Zwartfontein 818LR, Sandsloot 236KR, Vaalkop 819LR and Tweefontein 238KR and 3) the Northern Sector includes the farms Overysel 815LR, Drenthe 778LR, Witrivier 777LR and northwards. A summary of the geological and stratigraphic aspects related to each farm locality is outlined in Figure 2.5 (McDonald and Holwell 2011).

Figure 2.5: A summary of the key aspects of the geology and mineralogy of the Platreef developed on the various farms north of Mokopane, from Townlands to Drenthe (from McDonald and Holwell, 2011).

The footwall of the Platreef, where it comprises the base of the northern limb, is outlined in section 2.2.1 and illustrated in Figure 2.6. The Platreef footwall comprises Transvaal Supergroup sedimentary rocks in the south and Archean granite basement in the north (Figure 2.6; Kinnaird *et al.,* 2005).

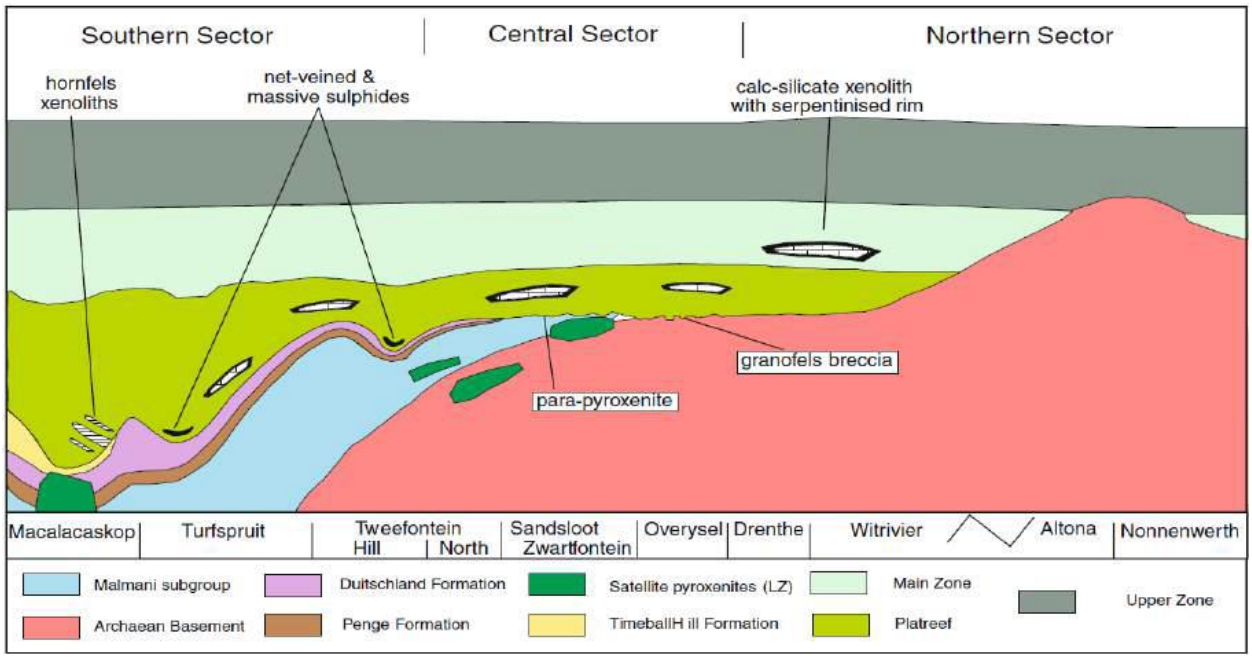

Figure 2.6: Schematic cross-section through the Platreef showing the different lithologies of the footwall and the variations of the thickness of the Platreef from the south to the north of the northern limb of the Bushveld Complex (from Kinnaird *et al.,* 2005).

According to McDonald and Holwell, (2011), the Platreef is a very complex zone of igneous and hybrid lithologic units that vary along strike. The overall Platreef consists mainly of medium- to coarse-grained pyroxenites and feldspathic pyroxenites, peridotites and norite cycles with anorthosite present in the Central-Northern sectors of the Platreef in the south (Gain and Mostert, 1982; White, 1994; Kinnaird *et al.,* 2005). The Platreef contains floor rock xenoliths such as quartzites, hornfelsed banded ironstones, shales, mudstones or siltstones in the Southern Sector, and calcsilicates and dolomites in the Northern Sector (Gain and Mostert, 1982; Kinnaird *et al.,* 2005; Manyeruke 2007). The xenoliths are variable in size and range from a few centimetres to ~1500 m in length (Gain and Mostert, 1982; Kinnaird *et al.,* 2005).

The Platreef orientation changes from south to north with an overall strike of N-NW (Kinnaird *et al.,* 2005). In the south, the Platreef strikes NW with an approximate dip of 15º-27º NW and in the north the Platreef strikes N with an approximate dip of 45º W which flattens with depth to approximately 20º (White, 1994; Bullen *et al.,* 1995; Kinnaird *et al.,* 2005). The average surface dip across the Platreef is 40-45º W; however, this becomes gentler down-dip (Viljoen and Schürmann, 1998; Kinnaird *et al.,* 2005; Barnes *et al.,* 2017) and the strike extent is approximately 30 km (Kinnaird *et al.,* 2005).

The Platreef differs significantly in thickness from the Critical Zone, which is an approved equivalent, with a thickness that ranges from ~10−400 m over its strike length (Van der Merwe, 1976; White, 1994; Kinnaird *et al.,* 2005; McDonald and Holwell, 2011). The thickness and geometry of the Platreef seems to have been controlled by irregular floor topography from south to north (Kinnaird *et al.,* 2005; Yudovskaya and Kinnaird, 2010; Armitage *et al.,* 2011). Various episodes of pre- and syn-Bushveld regional and local folding and faulting within the Archean basement, Transvaal Supergroup and the Rustenburg Layered Suite have been identified (Friese, 2004), which may have had a profound impact on the formation and morphology of the Platreef and the northern limb as a whole. This is evident as the thickest parts of the Platreef coincide with sinusoidal troughs in the basement on the southern farms of Turfspruit and Macalacaskop (Figure 2.6; Kinnaird *et al.,* 2005; Hutchinson and McDonald, 2008; Yudovskaya and Kinnaird, 2010). Basement highs also occur to the south of Macalacaskop and on the southern Turfspruit farm areas with thinned sections of Platreef on the flanks (Figure 1.5; Kinnaird *et al.,* 2005). On Turfspruit, the Platreef is up to 400 m thick and dips 40° inwards (Kinnaird *et al.,* 2005; Hutchinson and McDonald, 2008; Yudovskaya and Kinnaird, 2010) and on Macalacaskop, the Platreef is up to 300 m thick (Kinnaird *et al.,* 2005; Hutchinson *et al.,* 2004; Yudovskaya and Kinnaird, 2010). In the Central Sector, on the farm Sandsloot, the Platreef is up to 300 m thick (Armitage *et al.,* 2002; Kinnaird *et al.,* 2005; McDonald and Holwell, 2011).

On Townlands, in the south, Manyeruke and Maier, (2004) describe a lower, a middle and an upper subdivision of the Platreef based on geochemical data. These layers consist of gabbronorite and feldspathic pyroxenites and are interlayered by hornfelses (Manyeruke *et al.,* 2005). Kinnaird *et al.,* (2005) suggested that the Platreef comprises a sequence of sills that intruded through the Transvaal Supergroup. These sills can be distinguished based on geochemical variations, such as Pt/Pd and Ni/Cu ratios, Mg# and Pt+Pd concentrations (Kinnaird *et al.,* 2005; Manyeruke *et al.,* 2005; Maier *et al.,* 2008; Yudovskaya and Kinnaird, 2010) as well as certain mineralogical and lithological variations.

2.3.3 **Platreef mineralisation**

Although the strike extent of the Platreef (*sensu stricto*) is approximately 30 km long, what is referred to as “Platreef-style” mineralisation occurs up to 110 km in strike length between the Zebediela Fault in the south to the Melinda Fault in the north (Kinnaird *et al.,* 2005). No Platreef mineralisation occurs between Elberfeld and Altona, just to the south of Nonnenwerth (Figure 2.6). This ~10 km portion of the Platreef is suggested to be barren due to the footwall being Archean granite basement, rather than rocks of the Transvaal Supergroup, which may prevent the development of basal contact-style PGE mineralisation (Kinnaird *et al.,* 2005; McDonald and Holwell, 2011). It is also suggested that this section could be barren due the parental magma being too PGE depleted to form this mineralisation (Barnes *et al.,* 2004).

The Platreef hosts the largest primary deposits of PGE in the world (Von Gruenewaldt *et al.,* 1989; Kinnaird *et al.,* 2005; Kinnaird and McDonald, 2005; McDonald and Holwell, 2011), and it has substantial economic reserves of Ni and Cu associated with it (Kinnaird *et al.,* 2005; Naldrett, 2010). The mineralisation in the Platreef is hosted in both base metal sulphides (Kinnaird *et al.,* 2005; McDonald and Holwell, 2011) and PGMs (Yudovskaya *et al.,* 2011; Klemd *et al.,* 2016). A majority of the Platreef mineralisation may be amenable to open-pit mining (Bye, 2001; Bye and Bell, 2001), which reduces mining costs when compared to underground mining operations. In addition to ongoing exploration and various potential sites that have been identified for

possible production over the next 25 years (McDonald and Holwell, 2011), one of the world's largest open-pit mines on the farms of Sandsloot, Zwartfontein and Overysel, together known as Anglo owned Mogalakwena platinum mine is currently operational (McDonald and Holwell, 2011; Klemd *et al.,* 2016).

The whole Platreef sequence is non-uniformly mineralised and carries three types of PGE mineralisation: reef style sulphide ores, as well as massive and disseminated contact style PGE-rich sulphide mineralisation (McDonald and Holwell *et al.,* 2011; Yudovskaya *et al.,* 2017). Concentrations of PGE may be bottom loaded (e.g. at Tweefontein; Nex, 2005), middle loaded (Kinnaird *et al.,* 2005), top loaded (e.g. at Drenthe; Gain and Mostert, 1982), or dispersed evenly throughout (e.g. at Overysel; Holwell and McDonald, 2006). The mineralisation styles include the following:

The contact style mineralisation of the Platreef has lower overall PGE grades than that of the reef-style mineralisation in the Merensky Reef and UG-2 chromitite layer (~7 g/t, Ivanhoe mines, 2018). The overall Pt:Pd ratio of the Platreef is ~1 (Kinnaird *et al.,* 2005; Naldrett *et al.,* 2009). Kinnaird, (2005) demonstrated that the highest Pt+Pd concentration and lowest Pt/Pd ratio occur in the basal pyroxenites (association with sulphides), with the Platreef showing an overall upward increase of Pt/Pd and Ni/Cu ratios with the basal Pt/Pd ratios being ~2 and Ni/Cu being >3 and upper Pt/Pd being ~1 and Ni/Cu being <2. Modal abundances of sulphides commonly range between 0.5-18%, but can reach up to 30% in some pyroxenites (Kinnaird *et al.,* 2005). Mineralisation mainly occurs as disseminated and net-textured ores, but sub-massive or massive ores may also be present at the footwall metasedimentary rocks, and less commonly present elsewhere (Kinnaird *et al.,* 2005). PGEs may be associated with base metal sulphides, more so at lower grades (Kinnaird *et al.,* 2005). The major base metal sulphide minerals in the Platreef, in order of abundance, are pyrrhotite, pentlandite, and chalcopyrite, with accessory pyrite, galena, bornite, gersdorffite, tetrahedrite, marcasite, stibnite and molybdenite (Kinnaird *et al.,* 2005; McDonald and Holwell, 2011). PGEs may also be associated with various platinum group minerals (PGM) such as Pd or Pt-tellurides, bismuthides, arsenides, antimonides,

bismuthoantimonides and complex bismuthotellurides, which occur as micron-sized "satellite grains" around composite sulphides or dispersed within the primary silicate (Hutchinson and Kinnaird, 2005; Kinnaird *et al.,* 2005; Holwell *et al.,* 2006; Klemd *et al.,* 2016).

Deep drilling on two recent exploration projects on Akanani and Turfspruit indicates that with increasing depth in a favourable structural setting, contamination is much less, such that the Platreef sequence becomes a more typical Critical Zone cyclic sequence with PGE reefs at the top (Grobler *et al.,* 2012; Yudovskaya *et al.,* 2017). These discoveries open new Merensky-style horizons for the further exploration in the Central Platreef down dip, westward of the shallow contaminated margins.

The following exploration drilling for the underground mine project by Ivanhoe Mines discovered a sub-horizontal portion of the Platreef below 700 m vertical depth that was termed the "Flatreef". The Flatreef is named after its gentle, or "flat" dip, of between 10° to 15° SW (Grobler *et al.,* 2012) and is characterised by fundamental changes in geology and contains a spectacular regular PGE-bearing layer with the average thickness of 19 m along with other reserves that comprises a world-class PGE deposit. The strike length of the Flatreef is approximately 6 km and it occurs between approximately 700-1100 m depth (Grobler *et al.,* 2012, 2018). The Flatreef structure has much more in common with the Critical Zone than with the Platreef structure up dip although the PGE reefs at the boundary with the Main Zone are much thicker than any known Merensky Reef facies. A key feature that marks the conversion of the Platreef style mineralization into the Merensky style is the regular appearance of chromite seams, which become more persistent with decreasing contamination westward and down dip (Grobler *et al.,* 2018; Yudovskaya *et al.,* 2017). The typical Merensky style ore assemblages of predominant Pt sulphides and alloys are developed within ~1-m thick intervals, which correspond to the highest-temperature mixing zones between two magmas, whereas the rest of the reefs host Pt-Pd bismuthotellurides and arsenides. PGE content and tenor, as well as Cu/Pd in major base metal sulphides in the Turfspruit reefs are within the range of the typical high-grade Merensky values of 4.5 g/t Pt+ Pd+

Rh+ Au over 90 m in drill core suggesting the same enrichment process (Yudovskaya *et al.,* 2017; Grobler et al., 2018).

2.3.4 **Correlations between the Platreef and the correlative units in the eastern and western limbs**

There have been varying thoughts about the interrelations of the Platreef and the Main Zone and the Platreef and the Critical Zone. It has been suggested that the Platreef shows a Main Zone affinity (Wagner, 1929; Van der Merwe, 1976; Kruger, 2005) and a Critical Zone affinity (Buchanan *et al.,* 1981; Von Gruenewaldt *et al.,* 1989; White, 1994; Kruger, 2005). It has also been suggested that a combination of Lower- and Main Zone magmas formed the Platreef (McDonald *et al.,* 2005). Some these thoughts are outlined below.

2.3.4.1 *Platreef and the Main Zone*

Initially the gabbronorites of the Main Zone were thought to be younger, but comagmatic to the Platreef (Wagner, 1929; Van der Merwe, 1976; Kruger, 2005). Friese, (2004) suggested that a separate magma formed the Platreef, proposing that the Platreef represents a syntectonic sheet-like intrusion that intruded along a thrust zone that developed between the Main Zone and the floor rocks, after the deposition of the Main and Lower Zones. Holwell *et al.,* (2005), however, suggested that the Platreef was deposited prior to the Main Zone. Holwell and Jordaan, (2006) built on this idea, using 3D relationships between the Platreef and the Main Zone and showed that the Platreef is clearly intruded by fingers of Main Zone gabbronorites, therefore refuting the idea that the Platreef is of Main Zone affinity.

2.3.4.2 *Platreef and the Critical Zone*

Most of the earlier correlations between the Critical Zone, (including the Merensky Reef and the UG2 chromitites) and the Platreef have been made based on mineralisation grade and lithology. However, the recent studies provide sufficient independent

petrographic data, mineral chemistry, or isotopic data to confirm the proposed correlations. Some of these correlations are outlined below.

The Platreef occupies the stratigraphic position of the Critical Zone between the Lower and Main zones in the northern limb north of Ysterberg-Planknek major fault (Maier *et al.,* 2008). The Platreef internal structure and lithologies are highly variable and its morphology and characteristics greatly depend on changing footwall composition and the degree of contamination. However, with depth and decreasing contamination the Platreef becomes very similar to the Critical Zone (Yudovskaya *et al.,* 2017; Grobler *et al.,* 2018). The recognizable Bastard, Merensky and UG2 cyclic units are reported to be intersected by the deep boreholes on Turfspruit. The PGE reefs of the Platreef shows a pristine magmatic character strongly resembling the Merensky Reef by silicate composition, PGE grade, PGE ratios and S isotope characteristics (Holwell *et al.,* 2007; Maier *et al.,* 2008; Sharman *et al.,* 2013; Mayer *et al.,* 2018) as well as by stratigraphic position near the boundary with the Main Zone.

Mayer, (2018) used strontium isotope stratigraphy across drillcore from Turfspruit and upheld the correlation between Turfspruit reefs and the Merensky Reef. This study documented an isotopic shift in the Platreef reef horizons correlative with the isotopic shift in the Merensky and Bastard Cyclic units in the eastern and western limbs of the Bushveld Complex (Kruger, 2005).

The southern extension of the Platreef, beyond Mokopane, that does not form part of the Platreef (*sensu stricto*), and that is controlled by the Grasvally fault, has been divided into a Lower Mafic Unit and a Mottled Anorthosite Unit (Hulbert and Von Gruenewaldt, 1986; de Klerk, 2005). The pyroxenitic and chromitite-gabbronorite Lower Mafic Unit has been equated with the UG2 chromitite in the rest of the Bushveld Complex on the basis of Pt/Pd and Cr/Fe ratios (Hulbert, 1983; de Klerk, 2005; Maier *et al.,* 2008; Van der Merwe, 2008), although some differences in Mg/Fe ratios, and Ti and sulphide concentrations have been noted (Maier *et al.,* 2008; McDonald and Holwell, 2011). PGE mineralisation that occurs in the Mottled Anorthosite Unit and a sulphide-

enriched pyroxenite in the Lower Mafic Unit, south of Grasvally, have also been equated with the Merensky Reef based on similar geochemistry (Van der Merwe, 2008; Maier *et al.,* 2008). In addition to this, a mafic-ultramafic sequence that was intersected to the west of the Grasvally Fault that hosts a PGE-bearing chromitite and an overlying PGE rich pyroxenite has also been equated with the UG2 chromitite and the Merensky Reef, respectively, based on stratigraphic correlation, lithologic similarity and grade (Maier *et al.,* 2008).

Furthermore, McDonald and Holwell, (2011) state that correlating the Platreef and the Critical Zone has served as a keystone of the inferred relationship between the stratigraphy of the eastern and western limbs with the northern limb (Figure 2.4).

Despite the similarities between Platreef and the Critical Zone, correlation across the Thabazimbi-Murchison Lineament has been shown to be problematic (Cameron, 1982; Hulbert and Von Gruenewaldt, 1985; Maier and Barnes, 1998; Ashwal *et al.,* 2005; McDonald *et al.,* 2005). Some important stratigraphic horizons that correlate across the eastern and western limbs of the Bushveld Complex are not present in the northern limb (e.g. Van der Merwe, 1976; Buchanan *et al.,* 1981; Eales and Cawthorn, 1996). The Platreef differs from the Critical Zone in many aspects, among which the most important is a high degree of contamination with Transvaal footwall rocks (Kinnaird *et al.,* 2005). The digestion of sedimentary material led to changes in the conditions of magmatic crystallisation and the formation of various hybrid rocks, endo- and exo-skarns, hornfelses and metasomatites (Armitage *et al.,* 2002; Appiah-Nimoh, 2004), Kinnaird *et al.,* 2005).

The structure of this complex intrusion differs from the conventional Critical Zone in the following important features (from Yudovskaya *et al.,* 2017): 1) It lacks the typical Critical Zone cyclicity and contains fewer chromitites and anorthosites, 2) the Platreef thickness increases because of physical incorporation as well as chemical assimilation and melting of sedimentary material resulting in formation of hybrid rocks along with skarns and metasomatites, 3) the whole Platreef sequence is non-uniformly mineralised

and carries three types of PGE mineralisation: reef style sulphide ores, massive, and disseminated PGE-rich sulphides. The two latter types of mineralisation are not found anywhere in the Critical Zone.

2.4 **Structural events in the northern limb**

Structural information is important because it can assist in the interpretation of the mineralisation and ore deposition and elucidate on possible hydrothermal pathways that may have assisted in the formation of zones in the northern limb, and north of the northern limb of the Bushveld Complex. The exposed northern limb displays numerous structural features (Figure 2.7; Van der Merwe, 1976) such as the Thabazimbi-Murchison Lineament, which separates the northern limb from the eastern and western limbs of the Bushveld Complex (Good and de Wit, 1997) and the Hout River shear zone, which occurs at the north of the northern limb (Van der Merwe, 1976; Gain and Mostert, 1982). The exposed Transvaal sedimentary rocks also seem to be structurally controlled and are faulted by the Zebediela fault in the south, the Ysterberg-Planknek fault northward, the Rooisloot fault in the north, the transcurrent fault and various other smaller faults (Figure 2.7; Van der Merwe, 2008).

Truter, (1947), Van Rooyen, (1954) and de Villiers, (1967) identified three sets of major faults in the northern limb. These include (from oldest to youngest): 1) N and NNW striking faults, 2) NE to ENE striking faults and 3) NW trending faults. Hulbert, (1983) identified four major sets of faults. These include (from oldest to youngest): 1) N-S trending reverse faulting, 2) WNW to west trending extensional fractures and joints, 3) NE striking faults, assumed to be post-Waterberg Group and 4) Post-Karoo faulting, such as the near EW striking Zebediela fault. The NE to ENE faults are most prominent (White, 1994), and are responsible for the displacement of major lithological units, and setting of the northern limb (Kinnaird *et al.,* 2005). Most of the faults towards the north strike in a NE direction with normal displacement and a downthrow to the south (White, 1994). Two phases of ductile deformation that pre-dates the Bushveld intrusion have been noted on Tweefontein Hill (Nex, 2005).

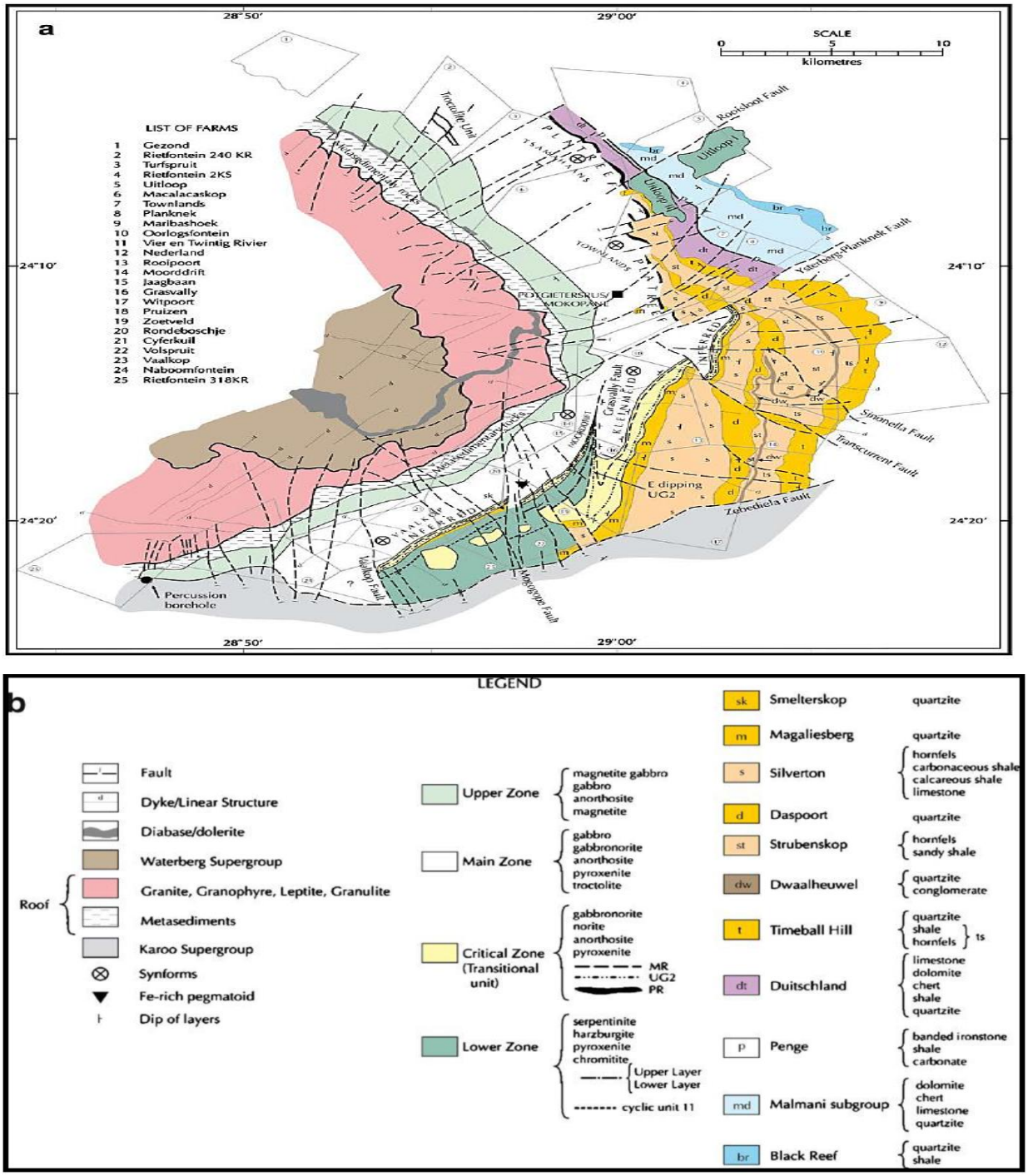

Figure 2.7: A map and legend of the geology and structure of the northern limb at Mokopane, Van der Merwe, (2008). Note the change in thickness in Transvaal Sediments south of the Ysterberg-Planknek fault.

Friese, (2004) also identified structures in the northern limb; this study was extensive and included the Villa Nora section. These include (from oldest to youngest): 1) Shallow NW dipping, SE verging thrusts, and associated ENE trending, subhorizontal, low

amplitude regional folds within the Archean basement, Transvaal Supergroup and the Rustenburg Layered Suite. 2) Moderate to steeply dipping extensional faults, trending NW to WNW, within the Transvaal Supergroup which was formed by the reactivation of structures that were similarly oriented, which formed during the Murchison Orogeny in the Archean basement. 3) Steep to subvertical, often SE dipping and ENE to NNE trending, dextral strike-slip shear zones with associated NE verging, layer-parallel thrusts. The ENE dipping shear zone is interpreted as a lateral ramp and the ENE to NNE trending shear zone is interpreted as an oblique/frontal ramp. The reactivation of the upper section of a Neoarchean sinistral strike-slip system caused these shears to develop in the Transvaal Supergroup. 4) Moderately W dipping, N to S striking, extensional faults with imbricate, normal dip-slip and sinistral strike-slip duplexes in their adjacent hanging wall. These faults are present in the Archaean basement, Transvaal Supergroup and the Rustenburg Layered Suite. 5) NW dipping, SE-verging thrust faults with associated ENE trending, subhorizontal, low-amplitude regional folds. These are of pre- to syn-Rustenburg Layered Suite age and were formed by mild SE directed stress within the northern Kaapvaal craton at an early stage of the Magondi Orogeny at around 2.1 to 2.058 Ga. 6) WNW to WSW trending extensional fractures and joints with minor displacement that cut all other structural features.

2.5 **Conclusion**

This chapter provided detail on- and outlined the stratigraphic units of the northern limb of the Bushveld Complex. The structures and controls that influenced the mineralisation in the northern limb were also outlined. The northern limb of the Bushveld Complex north of the Zebediela fault and south of the Hout River shear zone contains the Rustenburg Layered Suite, similar to the eastern and western limbs; however, there are key differences to consider. The setting and the structure of the northern limb, including the footwall composition, the floor topography and the faulting and folding associated with the northern limb structure all assist in making the northern limb unique. This chapter also provided detail on the world class mineralised horizons of the Platreef, which will assist in comparing Harriet's Wish mineralisation in the far northern limb, south of the Hout River shear zone to the Platreef mineralisation.

Chapter 3
Local geology

3.1 Introduction

The Hout River shear zone has been considered to be responsible for the northern truncation of the northern limb (Grobler and Whitfield, 1970). However, a possible extension of the northern limb beneath cover rocks and a possible linkage to the Villa Nora section (Figure 1.1) have been suggested (Van der Merwe, 1976; Kinnaird *et al.,* 2005; Armitage, 2011). Aeromagnetic and gravity data suggest the dimensions of the northern limb to be <160 x 125 km in size (Finn *et al.,* 2015; Kinnaird, *et al.,* 2017).

Some exploration projects have focussed on the northern end- and northern extension of the northern limb, and these include the Aurora Project (Figure 1.5; McDonald *et al.,* 2017) and the Platinum Group Metals (PTM) owned Waterberg Platinum Project (Figure 1.5; Huthmann *et al.,* 2016; Kinnaird *et al.,* 2017; Huthmann *et al.,* 2018; McCreesh *et al.,* 2018). The Aurora project was originally operated by Pan Palladium and included exploration on the Harriet's Wish farm, but since 2012 it has been owned by Sylvania Resources Limited.

3.1.1 Aims

The aim of this chapter is to provide detail on the Waterberg Project and the Aurora Project, which occur to the north and south of the Hout River shear zone, and to place into context the geology immediately north and south of the study site of Harriet's Wish.

3.2 Waterberg Project

The Waterberg Platinum Project is located 85 km north of Mokopane in the Limpopo Province of South Africa (Figure 2.3), and lies north of the Hout River shear zone (Kinnaird *et al.,* 2017). Huthmann *et al.,* (2016) presented geochronological data on the igneous intrusion of the Waterberg Project area. These data were obtained using U/Pb

dating on zircons that were extracted from both mineralised reefs as well as on detrital zircons of the Waterberg Group which overlie the mafic rocks (Huthmann *et al.,* 2016). An excellent correlation was found between the ages of the 2055 Ma old Bushveld rocks (Zeh *et al.,* 2015) and the Waterberg Project mafic rocks with the U-Pb isotope ages of 2059 ± 3 to 2053 ± 5 Ma (Huthmann *et al.,* 2016). It was also found that these isotope ages are only slightly older than the ages of the Waterberg Group rocks, which has a maximum depositional age of 2045 Ma, based on the age of the youngest detrital zircon (Huthmann *et al.,* 2016). Huthmann *et al.,* (2016) used the combination of these new age dates, local geology and existing literature to argue the following:

- The ultramafic–mafic succession intersected by drilling on the Waterberg Project area is related to the Bushveld Complex.
- A significant unconformity is present between igneous rocks and the overlying Waterberg Group sediments.
- The area was exposed to a level of Paleoproterozoic tectonism not previously observed in the Bushveld Complex.

3.2.1 **Geology of the Waterberg Project Area**

The results of the recent studies on the Waterberg Project geology have been reported in Huthmann *et al.,* (2016, 2017, 2018), Kinnaird *et al.,* (2017) and McCreesh *et al.,* (2013, 2016, 2018). Due to the lack of other published information on this area, these papers, and citations therein were the main sources for the geological description of the Waterberg Project.

3.2.2 **Waterberg stratigraphy**

The general stratigraphy of the drill cores on the Waterberg Project is outlined in Figure 3.1, and includes, the following above the footwall: 1) a harzburgitic and pyroxenitic Ultramafic Sequence, 2) a putative Main Zone, or a troctolite-gabbronorite-anorthosite (TGA) succession, 3) an Upper Zone and 4) Waterberg Group sediments (Figure 3.1; McCreesh, 2016).

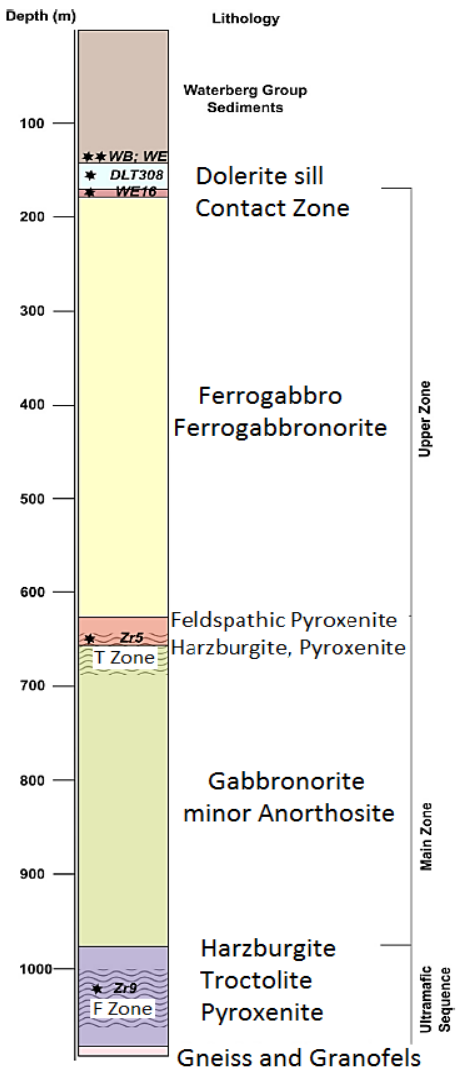

Figure 3.1: Schematic stratigraphic column for the southern part of the mafic succession on the Waterberg Project area. Stars represent sample locations in the stratigraphy with sample IDs in italic font (McCreesh 2016 in Huthmann *et al.,* 2016).

There are notable differences seen in the thicknesses of the stratigraphy between the Waterberg Project igneous succession and that of the northern limb of the Bushveld Complex (Figures 2.2 and 2.3; McCreesh, 2016; Kinnaird *et al.,* 2017). This observation especially holds true for the Main Zone and the Upper Zone, where the thicknesses in the northern limb south of the Hout River Shear Zone are 1000-2000 m for the Upper Zone and 1200-2200 m for the Main Zone (Van der Merwe, 1976; Ashwal *et al.,* 2005 McDonald and Holwell, 2011). The dip of the succession is generally 34^0-38^0 W, however, some blocks, depending on structural and / or tectonic controls may be tilted

away from this dip (McCreesh 2016; Kinnaird *et al.,* 2017). The Waterberg Project stratigraphy is outlined in detail below:

3.2.2.1 *Footwall*

Archaean granite or granite gneiss forms the majority of the footwall to the igneous sequence (McCreesh, 2013; Kinnaird *et al.,* 2017; McCreesh *et al.,* 2018). Interfingered between the igneous succession and the footwall, a banded agmatite is encountered, which formed in response to the interaction between the mafic-ultramafic magmas and floor rocks (Huthmann *et al.,* 2016; Kinnaird *et al.,* 2017). This agmatite commonly shows distinct banding of alternating felsic-rich layers and pyroxenitic layers (McCreesh, 2016; Kinnaird *et al.,* 2017). Within the granite gneiss footwall and the agmatite, chalcopyrite and pyrrhotite may be present (Kinnaird *et al.,* 2017). Calcsilicate xenoliths, similar to the Northern Sector of the Platreef (Gain and Mostert, 1982; Kinnaird *et al.,* 2005; Manyeruke, 2007) are encountered in the pyroxenite at the base of the intrusive package and sporadically throughout the rest of the succession, which suggests a possible local dolomitic footwall (Kinnaird *et al.,* 2017).

3.2.2.2 *Ultramafic Sequences*

The Ultramafic Sequence is unique to the Waterberg Project geology and occurs at the base of the Waterberg Project igneous succession (Kinnaird *et al.,* 2017). The Ultramafic Sequence was separated from the overlying units by PTM geologists and academics working on the Waterberg Project due to its distinct lithology and mineralogy (Huthmann *et al.,* 2016; McCreesh, 2016; Kinnaird *et al.,* 2017). The succession has a maximum thickness of 100 m thick and trends northeast from the Hout River shear zone with a moderate NW dip (Huthmann *et al.,* 2016; Kinnaird *et al.,* 2017). The Ultramafic Sequences comprises troctolite, harzburgite, feldspathic harzburgite, feldspathic pyroxenite and pyroxenite (Woods, 2012; McCreesh, 2013; Kinnaird *et al.,* 2017). This basal unit consists of two parts, 1) a ~60 m thick lower feldspathic orthopyroxenite unit, and 2) an overlying harzburgite unit (Huthmann *et al.,* 2016; Kinnaird *et al.,* 2017).

The texture of the pyroxenites is generally ophitic to equigranular, with a medium grain size overall (McCreesh, 2016). The pyroxenites comprise <90 % cumulus orthopyroxene with a high Mg# (>84), 10-15 % clinopyroxene and 2-5 % sulphides (in the upper section; chalcopyrite, pentlandite and pyrrhotite) with <15 % of the upper section containing semi-massive sulphides (McCreesh, 2016; Kinnaird *et al.,* 2017; Huthmann *et al.,* 2018; McCreesh *et al.,* 2018). Chromitite stringers have been identified in some of the cores, but these are rare (McCreesh, 2016; Kinnaird *et al.,* 2017). The pyroxenites are inter-fingered with Marginal Zone fine-grained equigranular gabbronorite sills, interpreted to have been the first magma to have intruded in the area (McCreesh, 2016; Kinnaird *et al.,* 2017). This inter-fingering in some cores resulted in gabbronorite being the basal lithology (Kinnaird *et al.,* 2017).

The 80-100 m thick harzburgite package in the Ultramafic Sequences is locally pegmatoidal closer towards the base, with lesser olivine-bearing gabbronorite, olivine-bearing norite, pyroxenite, feldspathic pyroxenite, and altered units that have been chloritised and serpentinised extensively (Huthmann *et al.,* 2016; Kinnaird *et al.,* 2017). The harzburgites have <65 % olivine with orthopyroxene and minor interstitial plagioclase and clinopyroxene, with a general high degree of alteration showing fractures in olivine filled with secondary magnetite and serpentine (McCreesh, 2016; Kinnaird *et al.,* 2017). Small intercumulus grains of clinopyroxene occur in this zone and the orthopyroxene often forms large oikocrysts (McCreesh, 2016; Kinnaird *et al.,* 2017). In some samples the rims or the edges of orthopyroxene surround olivine crystals completely (McCreesh, 2016). The medium-grained feldspathic pyroxenites have <30 % interstitial plagioclase and <45 % cumulus orthopyroxene, although some samples contain up to 50 % clinopyroxene that vary from 1 mm to 5 mm in size (McCreesh, 2016; Kinnaird *et al.,* 2017). About 2-5 % of chalcopyrite, pentlandite and pyrrhotite are found within this unit, and are associated with PGE mineralisation (Huthmann *et al.,* 2018; Kinnaird *et al.,* 2017).

3.2.2.3 *Troctolite-gabbronorite-anorthosite (TGA) sequence*

The TGA is up to 850 m in thickness, and varies in lithology throughout the unit (Figure 3.1; McCreesh, 2016; Kinnaird *et al.,* 2017). At the base of this unit a 40-100 m thick troctolite layer exists, which varies in composition from melatroctolite to olivine norite and leucotroctolite (McCreesh, 2016; Kinnaird *et al.,* 2017). This troctolite unit is medium-coarse grained and has an equigranular texture (McCreesh, 2016; Kinnaird *et al.,* 2017). Lenses of pyroxenite up to one metre thick are also found in the troctolite layer (Kinnaird *et al.,* 2017). The troctolite comprises 50-80 % olivine with <40 % sericitised plagioclase and <10 % orthopyroxene with chromite crystals often present in both olivine and pyroxene grains (McCreesh, 2016; Kinnaird *et al.,* 2017). The upper troctolite is heterogeneous and grades upward into olivine-bearing gabbros (McCreesh, 2016; Kinnaird *et al.,* 2017). The gabbronorites are medium-coarse grained melanocratic to leucocratic rocks that are locally altered and are composed of variable proportions of orthopyroxene, plagioclase, subordinate clinopyroxene and inverted pigeonite (McCreesh, 2016; Kinnaird *et al.,* 2017). The anorthosite is generally medium-grained and may be pegmatitic and the anorthosite is often a light greenish-grey in colour due to the alteration of the plagioclase (McCreesh, 2016; Kinnaird *et al.,* 2017).

3.2.2.4 *TGA sequence- Upper Zone boundary*

SACS, (1980) and Ashwal *et al.,* (2005) suggested that the presence of primary cumulus magnetite is a distinguishing feature of the Upper Zone. The boundary between the Upper Zone and the TGA sequence is defined by magnetic susceptibility readings (McCreesh, 2016; Kinnaird *et al.,* 2017) that identify the presence of magnetite well below the visible cumulus magnetite grains.

3.2.2.5 *Upper Zone*

This Upper Zone is ~350 m thick in the SW of the Waterberg Project, close to the Hout River shear zone (Kinnaird *et al.,* 2017). This zone comprises magnetite-gabbronorite and gabbronorite with a ferrogabbro at the top (Kinnaird *et al.,* McCreesh, 2013); however, the ferrogabbro does not occur in all drillcores (McCreesh, 2016). Magnetitite

layers are not present, as seen in the rest of the northern limb (Eales and Cawthorn, 1996), except in one borehole, south of the Hout River shear zone (McCreesh, 2016). The Upper Zone may dissipate northward, or even be completely absent, due to erosion prior to the deposition of the Waterberg Group sedimentary rocks (Kinnaird *et al.,* 2017). The Upper Zone reappears even further north and can be 70-500 m thick (McCreesh, 2016). The gabbros show an inequigranular texture with coarse-grained plagioclases in a finer-grained groundmass of orthopyroxene, clinopyroxene and magnetite (McCreesh, 2016). The magnetite is also intergrown with some pyroxene crystals (McCreesh, 2016; Kinnaird *et al.,* 2017). The olivine-bearing gabbronorite and the magnetite-bearing gabbronorite are similar in composition, with the exception of additional olivine and magnetite, and the olivine bearing gabbronorite being more altered than the magnetite-bearing gabbronorite (McCreesh, 2016; Kinnaird *et al.,* 2017). Brick red alteration and a highly sheared contact zone are seen in the uppermost sections of the Upper Zone and is composed of the Paleoproterozoic paleosol (Engela, 2014; McCreesh, 2016). Waterberg Group sedimentary rocks overlie the Upper Zone with a dip of 20-50°, with these packages varying in thickness from 120-760 m (Kinnaird *et al.,* 2017).

The upper contact of the Waterberg Project igneous succession is often very sharp and mylonitised (Engela, 2014; Kinnaird *et al.,* 2017). This contact is distinguished by red siltstone or by a prominent fine-grained white-grey tuffaceous layer (Engela, 2014; McCreesh *et al.,* 2016; Huthmann *et al.,* 2016; Kinnaird *et al.,* 2017). Dolerite sills or dykes are often present at the contact between the Bushveld- and Waterberg Group rocks, with an average thickness of 80-200 m (McCreesh, 2016; Huthmann *et al.,* 2016).

3.2.3 **Mineralisation of the Waterberg Project**

The mineralisation is concentrated in two zones, namely the F-Zone of the Ultramafic Sequences and the T-Zone, confined to the contact between the TGA sequence and the Upper Zone (Lomberg, 2012; Huthmann *et al.,* 2016; McDonald *et al.,* 2017). These are outlined below:

3.2.3.1 *F-Zone mineralisation*

The F-Zone mineralisation is hosted by troctolites, harzburgites and pyroxenites of the Ultramafic Sequences (Figure 3.1; McCreesh, 2016; Kinnaird *et al.,* 2017). The major sulphides include pyrrhotite, chalcopyrite and pentlandite, which are associated with platinum group minerals (Huthmann *et al.,* 2016; Kinnaird *et al.,* 2017). McCreesh *et al.,* (2018) presented a detailed platinum group element study asserting that F-Zone comprises mainly sperrylite (up to 82 area %) with minor Pt-Pd bismuthotellurides, Pd-Ni arsenides, Au-Ag alloy, Rh-Pt sulpharsenides and rare Pt-Fe alloys. The F-Zone inferred resource has a Ni/Cu ratio of >1, a Pt/Pd ratio of ~0.5, being Pd dominated and a (Pt+Pd)/Au ratio of >20 (Table 3.1; Lomberg, 2012; Kinnaird *et al.,* 2017). These characteristics are similar to some Platreef localities (Kinnaird *et al.,* 2005; Naldrett, 2010; Kinnaird *et al.,* 2017), although it is not clear how much of the total Ni reported for the F-Zone is hosted by olivine as opposed to sulphides (Kinnaird *et al.,* 2017).

3.2.3.2 *T-Zone Mineralisation*

The T-Zone occurs at the Upper-Main Zone boundary of the Waterberg Project, with some mineralisation being present in the Upper Zone and some in the TGA sequence (Kinnaird *et al.,* 2017). The T-Zone occurs mainly towards the south of the Waterberg Project, being either poorly developed or missing in the northern parts of the area (Kinnaird *et al.,* 2017). The mineralisation is divided into a lower and an upper component, namely the T2- and T1 zones, respectively (McCreesh, 2016; Kinnaird *et al.,* 2017). The T2 Zone mineralisation is predominantly hosted in gabbros and gabbronorites and occurs as disseminated and blebby pyrrhotite, pentlandite, chalcopyrite, and pyrite with minor millerite, sphalerite, and bornite (McCreesh *et al.,* 2018; Kinnaird *et al.,* 2017). The T1 zone is predominantly hosted in pyroxenite, feldspathic pyroxenite, troctolite, harzburgite and gabbronorites (McCreesh, 2016; Kinnaird *et al.,* 2017). The T1 Zone has sulphides commonly occurring as blebby to net-textured chalcopyrite and pentlandite, with minor disseminated pyrrhotite, as flame-textured pentlandite in pyrrhotite, as pyrite replacing magnetite and pyrrhotite, or rimming earlier sulphides (Kinnaird *et al.,* 2017; McCreesh *et al.,* 2018). The platinum group elements in the T-Zone are dominated by Pt–Pd bismuthotellurides (> 90 area

%), Pd tellurides and Au–Ag alloy and include rare sperrylite, braggite, Pd stannides and antimonides (McCreesh *et al.,* 2018). Overall, the T-Zone is Pd-dominated and shows an unusually high concentration of Au (Lomberg, 2012; Huthmann *et al.,* 2016). The T-Zone inferred resource has Ni/Cu <1, a higher Pt/Pd ratio of ~0.6, is richer in Au ((Pt+Pd)/Au~4) and falls in the same range as the Aurora Project mineralisation (Lomberg, 2012; Kinnaird *et al.,* 2017; McCreesh *et al.,* 2018).

Table 3.1: Mineral resource estimate of the Waterberg Project (Lomberg, 2012; Lomberg, 2013).

Table 1 Waterberg Project- Mineral Resource Estimate 2 September 2013										
	Strati-graphic Thick-ness	Tonnage Mt	Pt (g/t)	Pd (g/t)	Au (g/t)	2PGE+ Au (g/t)	Pt:Pd:Au	2PGE+ Au (koz)	Cu (%)	Ni (%)
T1 (Cut-off=2g/t)	2.30	8.5	1.04	1.55	0.47	3.06	34:51:15	842	0.17	0.10
T2	3.77	39.2	1.16	2.04	0.84	4.04	29:51:21	5,107	0.18	0.10
T Total	3.38	47.7	1.14	1.95	0.77	3.86	30:51:20	5,948	0.18	0.10
F (Cut-off=2g/t)		119.0	0.91	1.98	0.13	3.02	30:65:4	11,575	0.07	0.17
Total		166.7	0.98	1.97	0.32	3.26	30:60:10	17,523	0.10	0.15
		Content (koz)	5,252	10,558	1,715					

The combined (T- and F- Zone) resource on the Waterberg Project comprise 246 Mt at 3.25 g/t 3E (Pt+Pd+Au) inferred and 121 M/t at 3.24 g/t indicated (Lomberg, 2012; Lomberg, 2013). High-grade zones with <14 g/t 3E over >10 m may occur (Lomberg, 2012; Lomberg, 2013; Huthmann *et al.,* 2016). The inferred mineral resources for the T- and F- zones are based on samples taken from the properties of Ketting 368LR and Goedetrouw 366LR farms on the Waterberg Project (Lomberg, 2012). These data are presented in Table 3.1. The data used to estimate the resources are comprised of PTM's drill cores, company geological logs, borehole collars, downhole surveys and assay data taken from intersections of 111 boreholes (Lomberg, 2012). The drillcores were analysed for Pt, Pd, Au, Cu and Ni concentrations (Lomberg, 2012 and Lomberg, 2013).

3.2.3.3 *Cover rocks*

The sedimentary rocks that unconformably overlie the igneous succession of the Waterberg Project have been identified as belonging to the Setlaole (at the base) and Makgabeng (gradationally overlying the Setlaole Formation) Formations (Table 3.2; Callaghan *et al.,* 1991; Engela, 2014; Roberts *et al.,* 2014; McCreesh, 2016). In the north and northeastern parts of the Waterberg basin, these Formations also unconformably overlie the Limpopo Metamorphic Province and the Kaapvaal Craton (Callaghan *et al.,* 1991). The age of the Waterberg Group sedimentary rocks has been under debate (e.g. Von Gruenewaldt *et al.,* 1985; Cheney *et al.,* 1991; Dorland *et al.,* 2006); however, detrital zircons with a U-Pb isotope age of ~2045 Ma have been found in the basal layer of the Setlaole Formation (Huthmann *et al.,* 2016). This suggests that the roof and the upper parts of the Bushveld sequence were removed within a short space of time before the Waterberg Group sedimentary rocks were deposited (Huthmann *et al.,* 2016).

Table 3.2: Stratigraphy of the Waterberg Group. Green= Waterberg Group sedimentary rocks that are encountered on the Waterberg Project (from McCreesh, 2016, modified from Callaghan *et al.,* 1991 and Woods, 2012).

<table>
<tr><th>Group</th><th>Subgroup</th><th>South/Southwest & central parts</th><th>Southeast & Central parts</th><th>Northern & Central parts</th><th>Nylstroom Area</th><th>Middleburg Area</th></tr>
<tr><td rowspan="7">Waterberg Group</td><td rowspan="3">Kransberg</td><td colspan="3">Vaalwater Formation (475 m)</td><td rowspan="4" colspan="2"></td></tr>
<tr><td colspan="3">Cleremont Formation (125 m)</td></tr>
<tr><td>Sanriviersberg Fm (1250 m)</td><td>Sanriviersberg/ Mogalakwena Fm</td><td>Magalakwena Fm (1250 - 1500 m)</td></tr>
<tr><td rowspan="2">Matlabas</td><td>Aasvoelkop Fm (300-600 m)</td><td>Aasvoelkop/ Makgabeng Fm</td><td>Makgabeng Fm (360 - 1000 m)</td></tr>
<tr><td>Skilpadkop Fm (450-600 m)</td><td>Skilpadkop Fm (450-600 m)</td><td>Setlaole Fm (450 m)</td></tr>
<tr><td rowspan="2">Nylstroom</td><td>Alma Fm (3000 m)</td><td rowspan="2">Sterk River Fm (500-1500 m)</td><td rowspan="2"></td><td>Alma Fm</td><td></td></tr>
<tr><td>Swarshoek Fm</td><td>Swarshoek Fm</td><td>Wilge River Fm</td></tr>
</table>

The Setlaole Formation is mainly comprised of coarse-grained siliciclastic rocks, with evident upward fining sequences and channel flow structures (0.5-2 m thick; Jansen, 1982; Callaghan, 1987; Callaghan *et al.,* 1991). The Makgabeng Formation comprises gritty sandstone and banded arkose, with evident cross-trough bedding, ripple marks and dune structures (Jansen, 1982; Callaghan *et al.,* 1991; Dorland, 2006).

3.3 **Aurora Project**

The Aurora Project is situated immediately south of the Harriet's Wish project area (Figure 2.3). The Aurora Project is located on the area of a group of 7 farms namely: Altona 696LR, Kransplaats 422LR, La Pucella 69LR, Luge 697LR, Nonnenwerth 421LR, Non-Plus Ultra 683LR and Schaffhausen 698LR (McDonald *et al.,* 2017). On the Aurora Project the mineralisation occurs in a narrow zone of mineralisation near the major transgression where Upper Zone cumulates cross-cut the Main Zone, and where these are in contact with the granite-gneiss basement (Van der Merwe, 1976; McDonald *et al.,* 2017). The detection of Cu and Ni anomalies in soil initiated the exploration on the Aurora Project area between 1974 and 1992, which was later confirmed by drilling on Nonnenwerth by Union Corporation and Genmin (Venmyn-Rand, 2010; McDonald *et al.,* 2017). Between 2002 and 2010, Pan Palladium Limited furthered the drilling operations on the project by targeting the farms Kransplaats, Nonnenwerth, Altona and La Pucella (McDonald *et al.,* 2017). Sylvania Resources Limited took over this Project and added it as part of their northern Bushveld PGE projects (Venmyn-Rand, 2010).

3.3.1 **Aurora Geology**

Regional geological maps suggest that gabbronorites of the Main Zone dominate the Aurora Project area (Van der Merwe, 1976; McDonald *et al.,* 2017). Harmer *et al.,* (2004) described the mineralisation to be hosted by anorthosites and leucogabbronorites. Manyeruke, (2007) divided the Nonnenwerth stratigraphy into Platreef and Main Zone, separated by a calcsilicate xenolith. Maier *et al.,* (2008) also suggested that the Aurora Project geology forms part of the Platreef (sensu-stricto; Kinnaird and McDonald, 2005). McDonald and Harmer, (2010), however, suggested

that this mineralisation is hosted in the Main Zone. McDonald *et al.,* (2017), also suggests that this mineralisation is hosted in the Main Zone, more specifically the upper Main Zone, and divided the Aurora Project geology into three major units. Unit 1, which comprises olivine-bearing clinopyroxenite to olivine free orthopyroxenite, Unit 2, which comprises gabbronorites and leucogabbronorites with rare troctolites and magnetite gabbros, and Unit 3, which comprises pigeonite gabbronorite (Figure 3.2; McDonald *et al.,* 2017). The mineral assemblages and lithologies found on the Aurora Project can be encountered both within the Main Zone and the Upper Zone of the Waterberg Project (McDonald *et al.,* 2017; Kinnaird *et al.,* 2017).

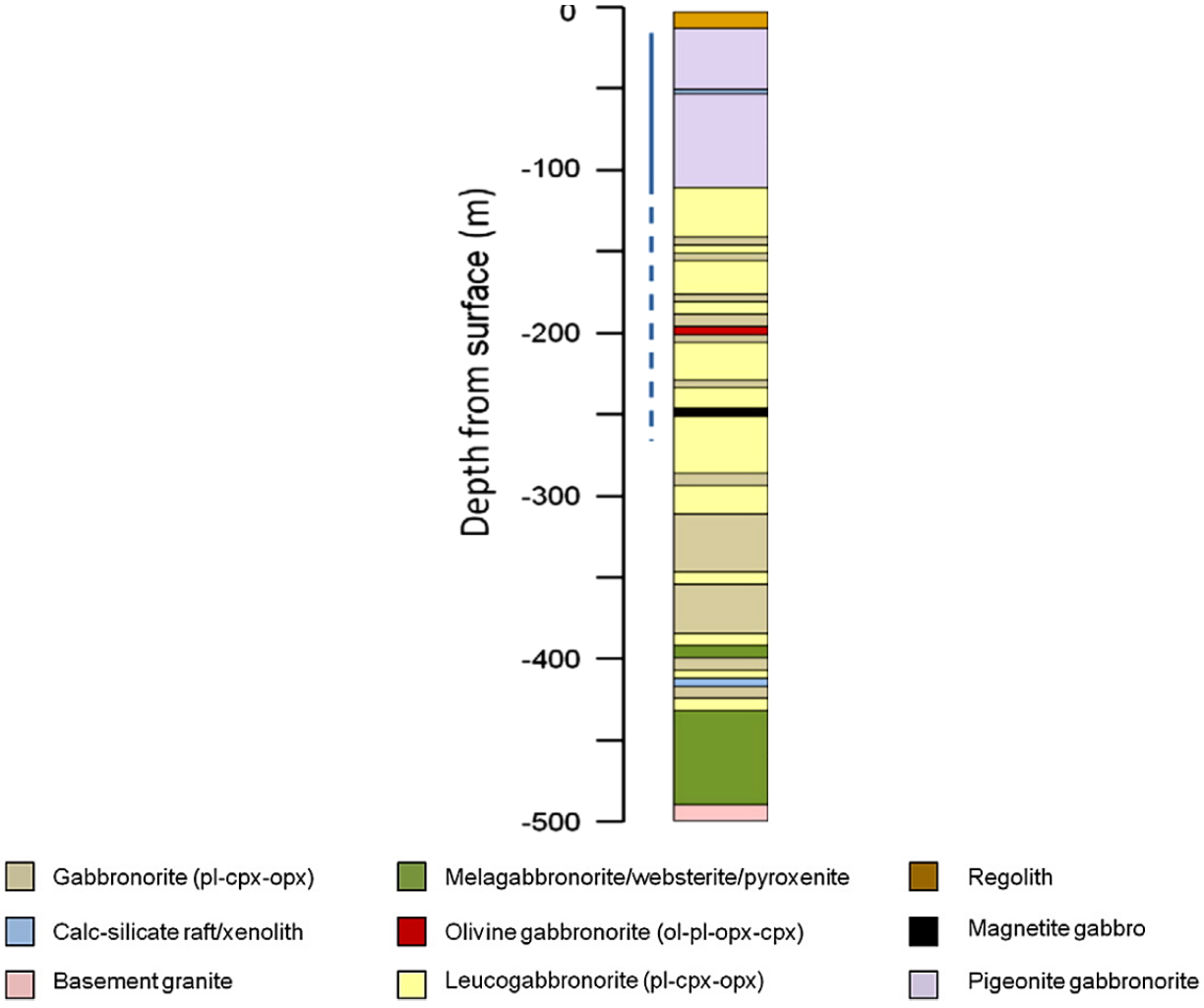

Figure 3.2: Stratigraphy of the Aurora Project of the LAP-29 drillcore plotted against depth (m; from McDonald *et al.,* 2017).

3.3.2 **Aurora Mineralisation**

The major host rocks of the mineralisation on the Aurora Project are gabbronorites and leucogabbronorites (McDonald *et al.,* 2017). The mineralisation is present as interstitial aggregates, irregular inclusions and small stringers of base metal sulphides (pyrrhotite, pentlandite and chalcopyrite) and range between 0.1-5 % in modal abundance (Venmyn-Rand, 2010; McDonald *et al.,* 2017). The base metal sulphide mineralisation is confined to the ultramafic rocks of Unit 1 and gabbronorites and leucogabbronorites of Unit 2, and no mineralisation is found in unit 3 (McDonald *et al.,* 2017). The Aurora Project is suggested to contain an inferred resource of 125 Mt of sulphide ore at 1.34 g/t Pt+Pd+Au, 0.08 % Cu and 0.05 % Ni (Venmyn-Rand, 2010). Target zones were identified within this resource where higher grades were found (McDonald *et al.,* 2017). The Target zone with the highest average PGE grade, and that has the most likely mining potential is Target zone 1 which is found in the northern part of the farm of La Pucella, with local enrichments of up to 4 g/t sporadically present in drillcores LAP 29 and LAP 31 (McDonald *et al.,* 2017). This zone unites three sub-zones of mineralisation that can be traced along strike and down-dip, and is broadly stratiform (Venmyn-Rand, 2010; McDonald *et al.,* 2017).

3.3.3 **Linkages between the Aurora Project and Adjacent Areas**

McDonald *et al.,* (2017) disagrees with the notion that the Aurora Project forms part of the Platreef (Maier *et al.,* 2008), and suggests that there could be a link between the Aurora Project mineralisation and the T-Zone mineralisation on the Waterberg Project (Figure 3.3; Kinnaird *et al.,* 2017). This is argued based on geochemical signatures of the mineralisation, which is Cu-rich (Ni/Cu <1) and Au-rich in contrast to the Platreef (Kinnaird *et al.,* 2005; Lomberg, 2012; McDonald and Holwell, 2010; McDonald *et al.,* 2017). In addition to this, McDonald and Harmer, (2010) noted that the Aurora Project is overall Cu-rich and Au-rich which significantly contrasts with the Platreef mineralisation (Chapter 2.3.3; McDonald and Harmer, 2010; McDonald and Holwell, 2010).

There may also be linkages between the Aurora Project's style of mineralisation and the upper Main Zone of the northern limb of the Bushveld Complex (McDonald *et al.,* 2017).

This was suggested as the pigeonite gabbronorites above the Aurora Project mineralisation, which are characterised by high Cu/Pd ratios (>50,000), show removal of Pd over Cu from the sulphides beneath (Kinnaird *et al.,* 2017), are similar to the high Cu/Pd ratios that characterises the Upper Main Zone above the pigeonite- and orthopyroxene-bearing interval (Cawthorn *et al.,* 1991; Scoon *et al.,* 2012; McDonald *et al.,* 2017).

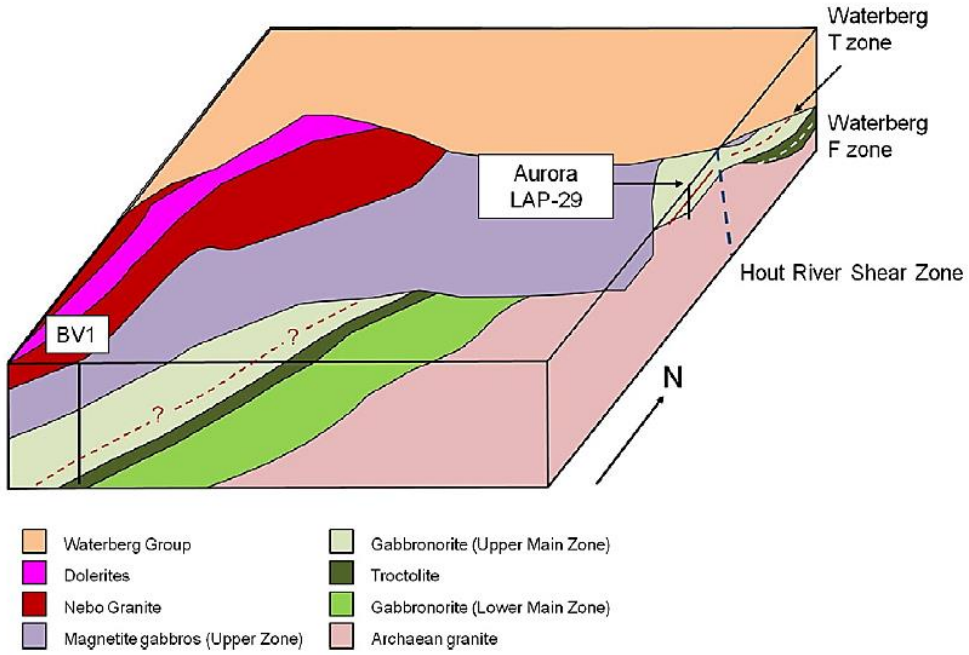

Figure 3.3: Schematic model showing the potential connectivity between the T-Zone on the Waterberg Project and the Aurora Project (McDonald *et al.,* 2017).

McDonald *et al.,* (2017) states that if the links between the Waterberg (Kinnaird *et al.,* 2017) and Aurora (McDonald *et al.,* 2017) projects are proved, a potential for a previously unsuspected zone of Cu-Ni-PGE mineralisation extending for over 40 km may exist.

3.4 **Conclusion**

This chapter provided detail on the Waterberg and the Aurora projects that show promising mineralisation grades, with mining potential. This chapter also provided a backdrop for a comparison to Harriet's Wish geology and mineralisation, as Harriet's Wish provides a possible link between these two areas.

Chapter 4
Stratigraphy and core logging

4.1 Introduction

The Harriet's Wish farm is located in the northern part of the northern limb of the Bushveld Complex and lies between the Waterberg Project to the north, and the Aurora Project to the south and immediately east of the Cracouw farm (Figure 4.1). The east-west Hout River shear zone cross-cuts the Harriet's Wish farm area and the boreholes that are utilised in this study lie to the north of, or within, the Hout River shear zone (Figure 4.1). Although there are some correlations to the northern limb, the overall stratigraphy to the north of the Hout River shear zone is unique, with noteworthy variations from the traditional Rustenburg Layered Suite (Kinnaird *et al.,* 2017). Kinnaird *et al.,* (2017) and Huthmann *et al.,* (2018) suggest that a separate igneous basin exists to the north of the Hout River shear zone. A shear zone, however, is not confined to a singular line, but rather to a zone of at least one km wide with lateral extension (Fossen and Cavalcante, 2017). According to Fossen and Cavalcante, (2017), mature shear zones are heterogeneous, and they are composite zones characterised by anastomosing patterns and local variations in thickness and finite strain. Therefore, the Hout River Shear Zone can affect the expected regularity of the Harriet's Wish stratigraphy when comparing it to adjacent areas, especially in drillcores that are located within closer proximity to the shear zone.

From the studies that have been done on the Waterberg Project, no cumulus magnetite layers are found in the Upper Zone, except for in a single borehole, the location of which is described as being south of the Hout River shear zone (McCreesh, 2016; Kinnaird *et al.,* 2017). McDonald *et al.,* (2017) describes the presence of cumulus and disseminated magnetite throughout the drillcores in the Aurora Project drillcores and suggests that this magnetite gabbro layers belong to the upper Main Zone. However, no magnetitite layering is found in these drillcores because they are collared at the lower levels of the magmatic stratigraphy (McDonald *et al.,* 2017). Massive magnetitites are exposed on

the surface through the entire Aurora Project area. On the Harriet's Wish farm, the drillcores are all located to the north of the Hout River shear zone (HW024, HW025 and HW029); however, one drillcore (HW030) is located within the shear zone. It is therefore expected that this particular drillcore may display differences to the drillcores further north.

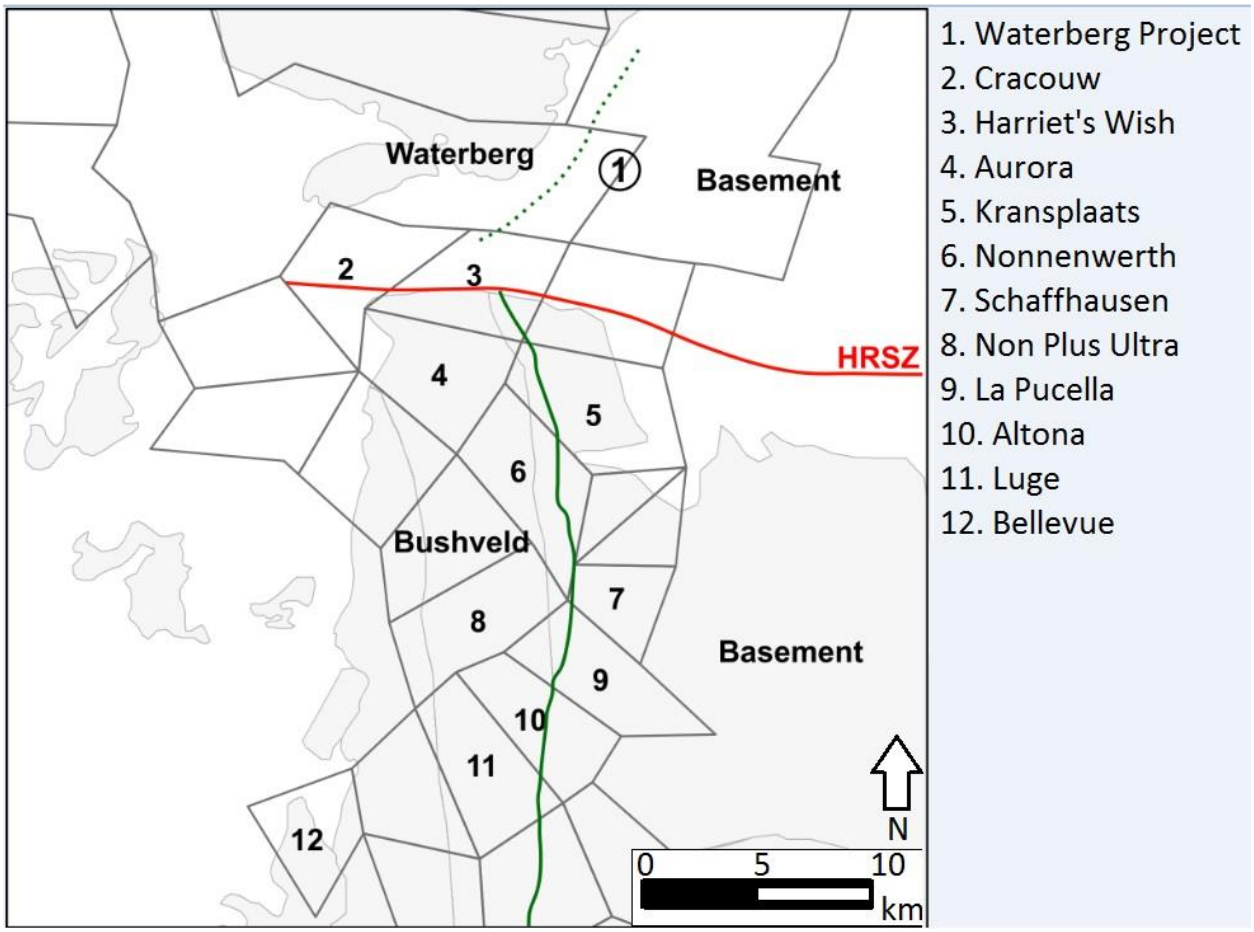

Figure 4.1: Map showing the location of the Project area of Harriet's Wish and other surrounding farms. The red line indicates the HRSZ (Hout River Shear Zone). The green line represents the Aurora mineralisation. The names of the farms are labelled 1-12 on the right-hand side of the map (unpublished figure from F. Huthmann).

The Aurora Project to the south of the study site failed to maintain interest with investors; however, recently Sylvania Resources Limited, (2012-2016) has discovered mineralisation on the farm of Harriet's Wish. It is hypothesised, based on the observations made by Sylvania, and due to the location of the area, that the succession

on Harriet's Wish could serve as the continuation of the Waterberg Project mineralisation southwards (Kinnaird *et al.,* 2017), with possible linkages to the Aurora Project (McDonald *et al.,* 2017). The lithologic units, the mineralised zones and rock types on Harriet's Wish are expected, therefore, to be similar to the Waterberg and Aurora successions.

4.1.1 **Aims**

This chapter is aimed at outlining the stratigraphic units (including lithologic units and mineralised zones) and to provide detail on the rock types and various geological features of the Harriet's Wish farm area. This has been done through core logging and field observations, including the determining of the visual boundary between the upper and lower lithologic units by the first visual appearance of cumulus magnetite (SACS, 1980). This chapter is also aimed at providing a broad lithologic correlation between Harriet's Wish and the Waterberg Project, the Aurora Project and certain northern limb localities.

4.2 **Methodology**

Little has been known about the geology and economic potential of the farm of Harriet's Wish. In 2012, however, Sylvania Resources Limited announced exploration results from this area, conducted by the Hacra Mining and Exploration (Pty) Ltd, a Sylvania Group Company. The exploration method used was diamond drilling and resultant core. The drill holes are located to the north of the Hout River shear zone, immediately south of the Waterberg Project area (Figure 4.1; Figure 4.2).

Sylvania implemented core logging, and based on their observations, it was suggested that this area shows similar characteristics to that of the Waterberg Project area (data from Sylvania Resources Limited, 2012; Kinnaird *et al.,* 2017). Two main lithologic units and two mineralised zones were described (data from Sylvania Resources Limited, 2012). The upper lithologic unit was described as being similar to the Upper Zone extension of the Bushveld Complex, found on the Waterberg Project, and the lower

lithologic unit was described as being similar to the Main Zone of the Bushveld Complex (Kinnaird *et al.,* 2017; Sylvania Resources Limited, 2012). The upper and lower mineralised zones that were intercepted were described as being similar to the Waterberg Project T Zone and the F Zone, respectively (Sylvania Resources Limited, 2012; Kinnaird *et al.,* 2017).

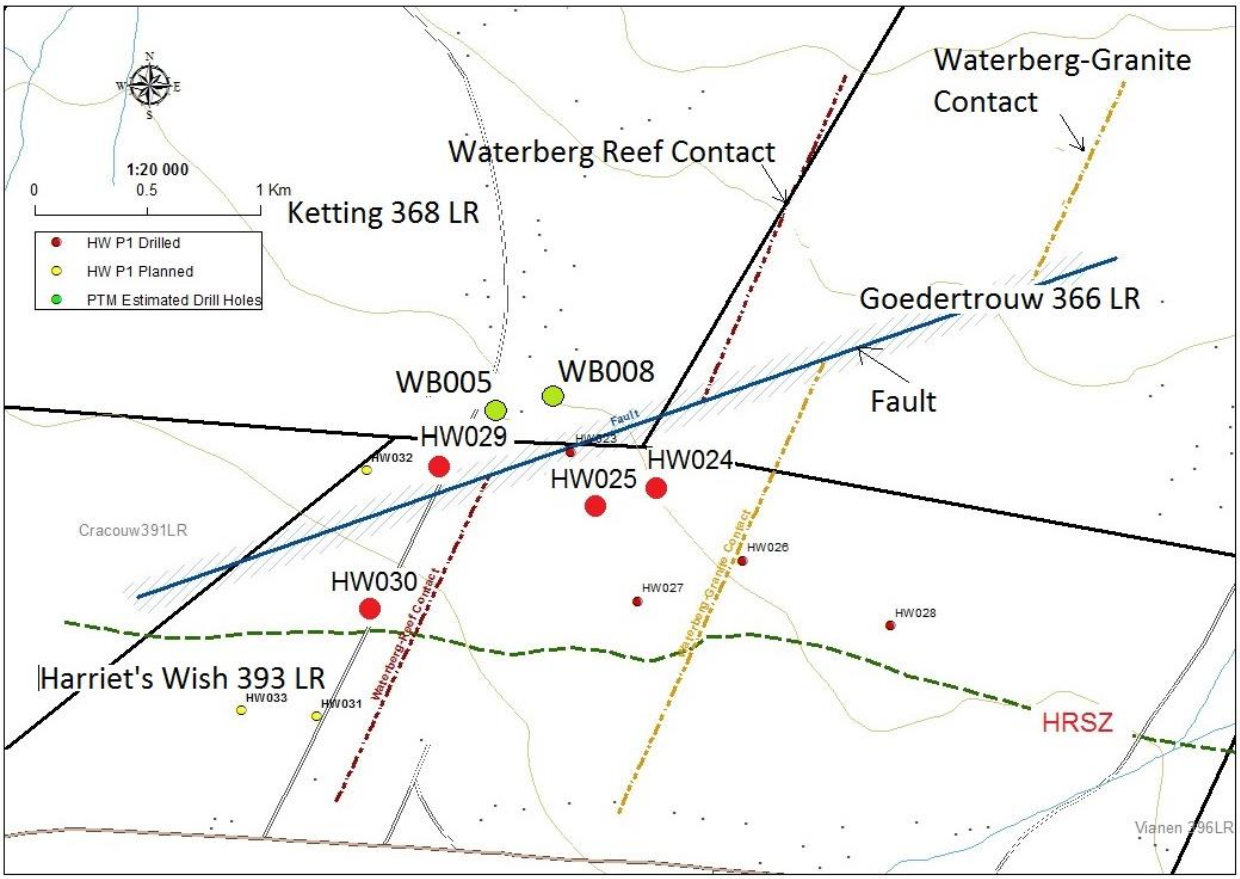

Figure 4.2: Location of drill holes relative to the Hout River Shear Zone. The black dotted line represents the Hout River Shear Zone, black solid lines represent farm boundaries and a fault, and the other dotted lines represent Waterberg-reef and granite contacts (unpublished Figure provided by R. Steen).

The drill cores of Harriet's Wish are housed at Sylvania's core shed just outside the town of Mokopane, Limpopo, South Africa. The boreholes of interest for this Project are: HW024, HW025, HW029, HW030. The boreholes were selected based on the exploration results by Sylvania Resources Limited, (2012). These all lie to the north of the Hout River shear zone, with drillcore HW030 being immediately adjacent to the Hout

River shear zone (Figure 4.2). The core was analysed and described, and detailed logs of drill cores HW024, HW025 and HW029 were made using these observations (Appendix A). Observations used in this study on drill core HW030 were made and provided by Sylvania Resources Limited (2012). The general textures, grain sizes, visible mineralogy, visible mineral associations, mineral proportions, rock types and contacts were recorded in a field note book and these were used to create a digital core log using Golden Software's Strata® version 5 software package. Smaller, less significant rock units were amalgamated with larger units to avoid over cluttering of core logs. Smaller important features that are not visible on the core logs are outlined in the detailed descriptions of this chapter.

4.2.1 **Rock nomenclature**

The nomenclature used to describe rocks on Harriet's Wish generally follows the IUGS standard for igneous rock classification (Figure 4.3; Le Bas and Streckeisen, 1991). The naming of rocks in this classification scheme relies on modal percentage of minerals. There are, however, certain local Bushveld rock names as used by mining geologists, that might differ from the conventional rock names and some of these are included in the rock classification. Some of these rock names are used in Kinnaird *et al.,* (2005), such as the term "feldspathic pyroxenite", which describes a rock comprising cumulus orthopyroxene with significant intercumulus feldspar. Certain prefixes for rocks are also used to more accurately describe the rock in terms of its modal mineralogy. These include the prefixes:

- "mela- ": which indicates that a rock contains "darker" or melanocratic minerals (such as pyroxenes) than their average proportion.
- "leuco- ": which indicates that a rock contains more "light" or leucocratic minerals (such as plagioclase) than the average proportion.
- "Olivine bearing- ": which indicates that a rock contains less than 10 % of olivine.
- "Olivine- ": which indicates that a rock contains more than 10 % of olivine.

- “Mottled- “: which indicates a texture that shows irregular spots, blotches or patches of different shades or colours as well as interstitial to poikilitic and dendritic crystals such as pyroxene’s mottles in mottled anorthosite.

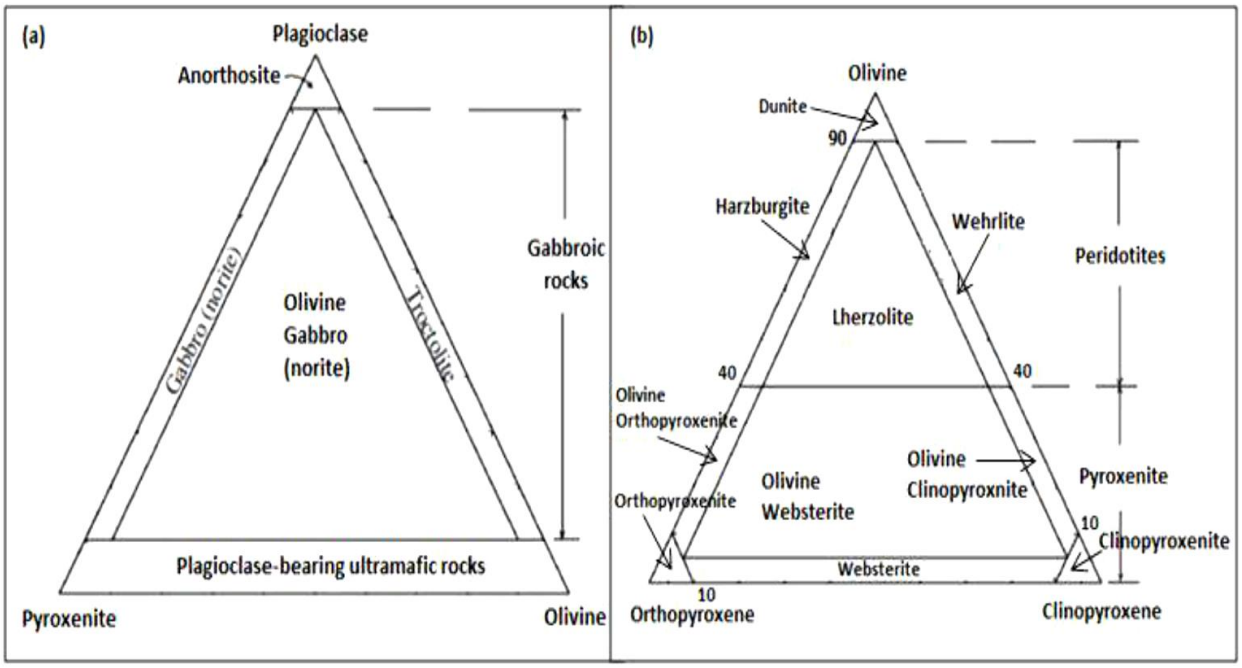

Figure 4.3: Streckeisen diagram (IUGS classification) of (a) Gabbroic rocks, (b) Ultramafic rocks (Le Bas and Streckeisen, 1991).

The above classification including the described prefixes is used in the entire thesis. This classification scheme including the prefixes is also used in the Waterberg Project described in McCreesh, (2016) and Kinnaird *et al.,* (2017).

4.3 **Results**

The stratigraphic units of the Harriet’s Wish succession are presented below, starting from the base to the top as presented in the HW024, HW025, HW029, and HW030 drillcores (Figure 4.4).

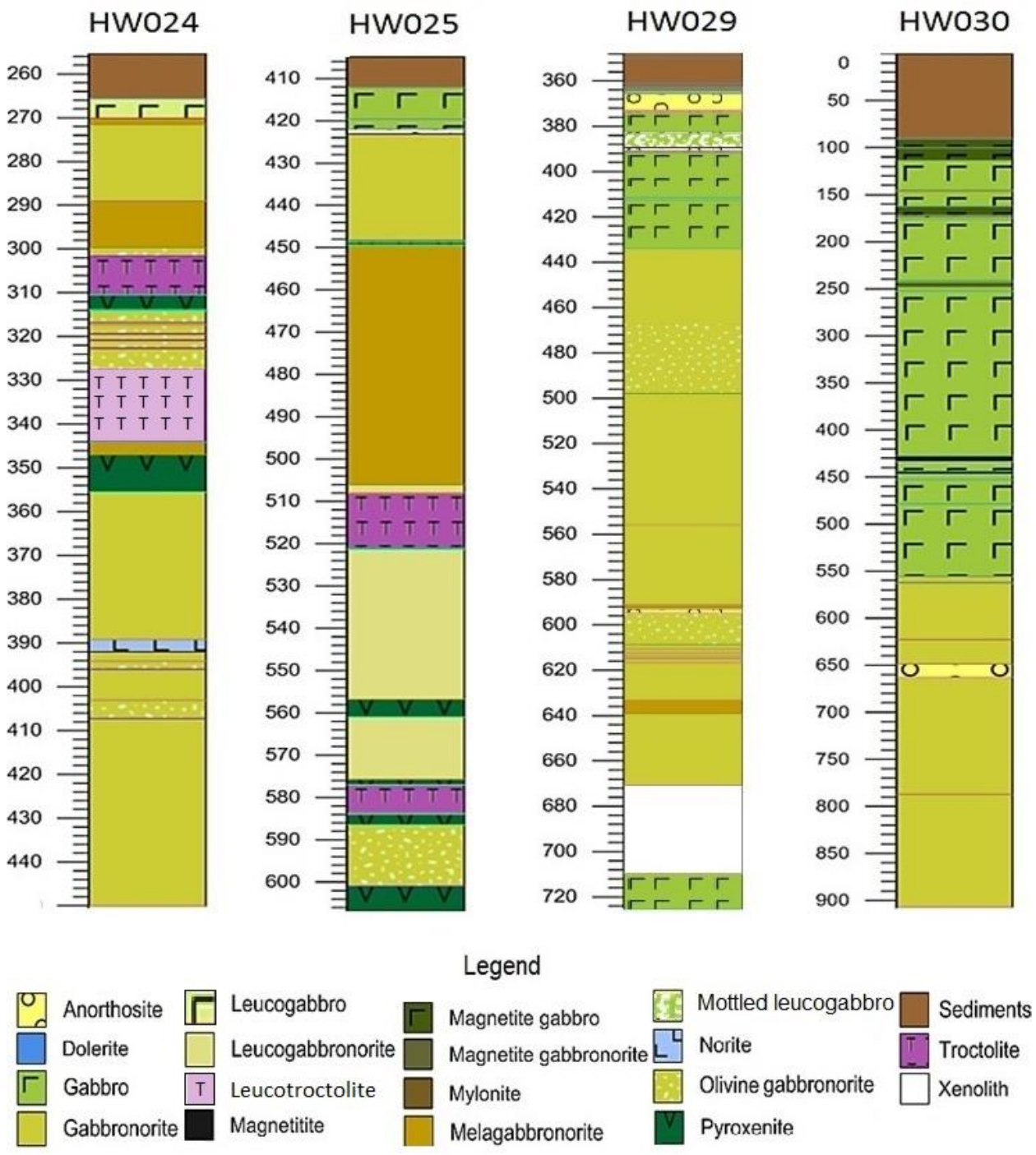

Figure 4.4: Logged stratigraphic drillcores of HW024, HW025, HW029 and HW030 drilled on Harriet's Wish. Rock types are identified based on visual estimations. HW030 data were provided by Sylvania Resources Limited, (2012).

4.3.1 **Basement**

The basement is not intersected in the studied drillcores on the Harriet's Wish farm.

4.3.2 **Lower lithologic unit**

The entire drillcores of HW024, HW025 and the lower portion of HW029 contain lithologies of the lower lithologic unit (Figure 4.4). The thickness of this unit is > 200 m; however, it is incomplete, due to the shallow depth of the drillcores. The lower lithologic unit comprises the following rock types: gabbronorites (including gabbronorite, melagabbronorite, leucogabbronorite, olivine- and olivine bearing gabbronorite and pegmatoidal gabbronorite), troctolite, pyroxenite and gabbro, olivine norite, minor anorthosite and a calcsilicate xenolith. These lithologies are detailed below:

4.3.2.1 *Gabbronorites*

The different varieties of gabbronorite are the major rock type throughout the lower lithologic unit and occur in HW024, HW025 and HW029. The total thickness of gabbronorite is approximately 76 m, with intervals ranging from approximately 1-43 m. Melanocratic and leucocratic varieties of gabbronorite are also present. Sporadic intervals of olivine rich gabbronorites, including olivine gabbronorite and olivine-bearing melagabbronorite are also present in the lower lithologic unit (Figure 4.5 a and b).

Overall, the amount of plagioclase increases upward with the gabbronorite towards the base being more melanocratic than the top. Orthopyroxene increases and clinopyroxene decreases from the base to the top of HW029, thus becoming more noritic at the top. Darker, or melanocratic gabbronorite is more common towards the base of this lithologic unit. The different varieties of gabbronorite area outlined below.

4.3.2.2 *Gabbronorite*

Gabbronorite colour varies from greenish-grey to brownish-grey. Orthopyroxene shows a brown to grey colour, clinopyroxene shows a greenish yellow colour and plagioclase shows milky white colour. The overall texture is equigranular, with some intervals being

inequigranular in texture. Gabbronorites are generally medium-grained (3-5 mm; Figure 4.5 c). Gabbronorites comprise ~50 % plagioclase, ~45 % pyroxenes, and variable concentrations of sulphides (<2 %), mainly as interstitial and sometimes pinhead sized disseminated grains. Pigeonite is also present sporadically throughout the gabbronorite, with a total concentration of ~2 %, and some intervals being locally enriched with concentrations of <10 %. Plagioclase, clinopyroxene and orthopyroxene may be cumulus or interstitial.

4.3.2.3 *Melagabbronorite*

Melagabbronorite is similar to the gabbronorites described above; however, some differences are outlined. Melagabbronorite is dark green/brownish to blackish in colour. Pyroxenes are generally dark green to black when finer grained. The overall texture is equigranular. Melagabbronorites are generally medium-grained (3-5 mm). Melagabbronorites comprise ~20 % plagioclase, ~50 % clinopyroxene and 25 % orthopyroxene.

4.3.2.4 *Leucogabbronorite*

Leucogabbronorite is also the same as the gabbronorite described above; however, the colour is light-green or light-brown, with some intervals appearing light grey. Plagioclase concentration increased to <70 % and clinopyroxene and orthopyroxene is decreased to <30 % and 20 %, respectively. Leucogabbro is largely present in drillcore HW025 in between the upper and lower troctolite horizons.

4.3.2.5 *Olivine-bearing to olivine gabbronorite*

Olivine and olivine-bearing gabbronorites occur sporadically throughout the lower lithologic unit in drillcores HW024 and HW025 and at the base of HW029 and the thickness ranges from a few cm to 35 m (Figure 4.4). This lithology occurs in leucocratic and melanocratic varieties in all three drillcores. The colour ranges from dark green to brownish green overall, with greenish black melanocratic varieties also being present. The texture of olivine-bearing and olivine gabbronorites is generally equigranular.

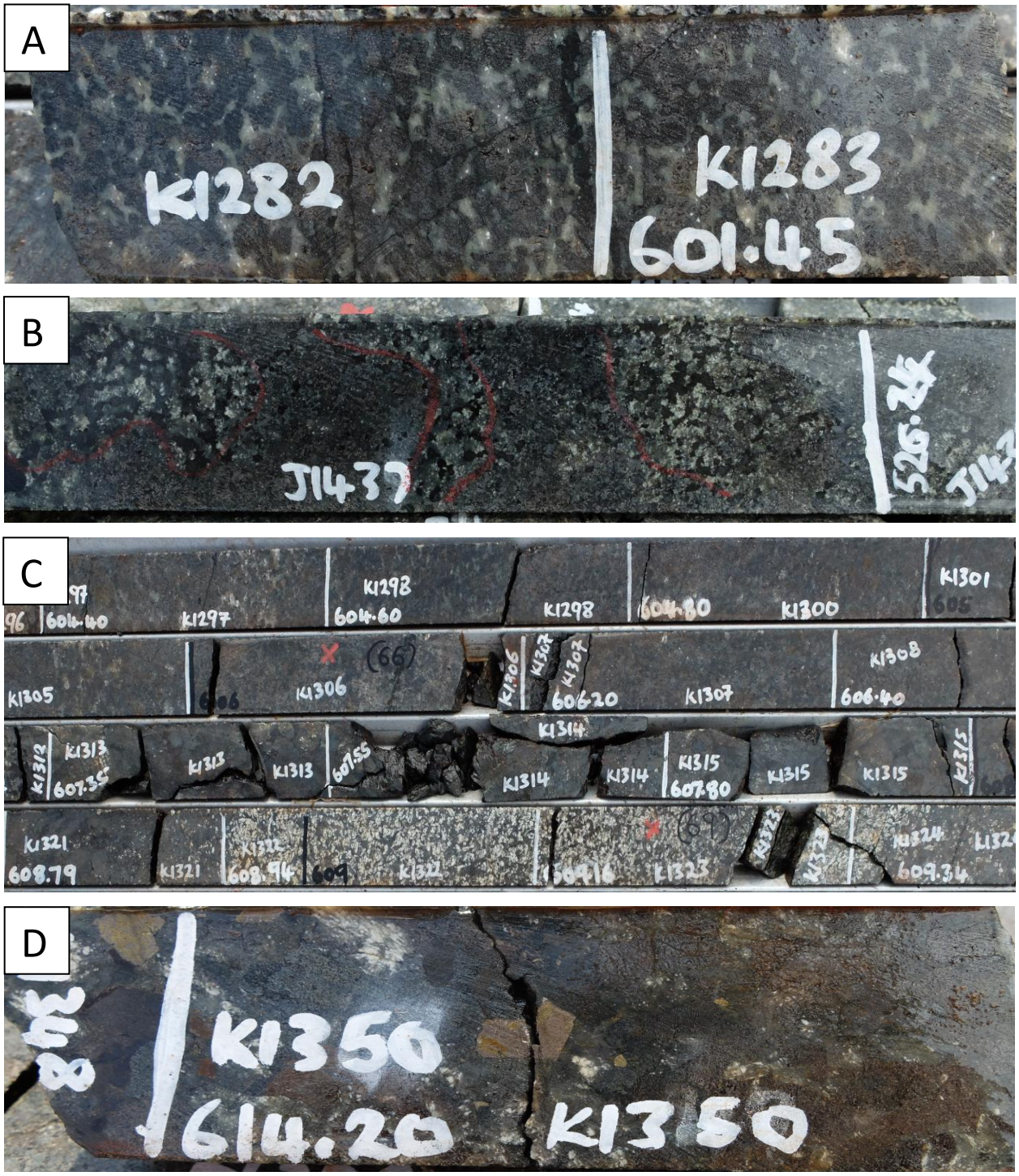

Figure 4.5: Gabbronorites of the lower lithologic unit. A) Olivine gabbronorite from HW029 at a depth of 601.45 m. B) Patches of olivine norite among olivine-bearing melagabbronorite from HW025 at a depth of 525.24. C) Pegmatoidal gabbronorite and leucogabbronorite from HW029 at a depth of 604.4-609.4 m. D) Pegmatoidal gabbronorite with chalcopyrite and pentlandite from HW029 at a depth of 614.25 m.

The overall grain size of olivine- and olivine bearing gabbronorites is medium grained (3-5 mm), with minor fine-grained (0.5-3 mm) intervals present sporadically. These rocks comprise 15-70 % clinopyroxene, 10-40 % orthopyroxene (although pyroxenes can be hard to distinguish from each another in certain intervals), 2-20 % olivine and >5 % pigeonite seen throughout these rocks. A 15 m thick package of olivine melagabbronorite that alternates with vein-like olivine-bearing leucogabbronorite is seen in HW024. Olivine proportion is often higher at the top of the olivine lithologies and olivine relics are sometimes present in altered rocks. Olivine is often seen inside orthopyroxene grains and inverted pigeonite often displays lamellae. Oikocrysts of pigeonite are also visible, and sometimes envelop grains of olivine. Pigeonite oikocrysts show an adamantine lustre when tilted in the sun. Overall, grains of olivine are slightly serpentinised, and the overall rock is locally magnetic. Poikilitic feldspathic harzburgite of <5 cm is present in the large interval of olivine leucogabbronorite in HW025. Certain intervals of this rock type are highly brecciated. Sulphides appear reduced in altered varieties of this rock type.

4.3.2.6 *Pegmatoidal Gabbronorite*

Pegmatoidal gabbronorites occur as vein-like bodies locally alternating with gabbronorite mainly at the possible boundaries between the two lithologic units in drillcore HW029 (Figure 4.4) and is <2 m thick. The colour is overall dark green to blackish grey. The texture is inequigranular to equigranular. The grain sizes of minerals vary from 0.5 mm (interstitial sulphides and other mineral grains) up to 4 cm (pyroxenes and plagioclase). The sulphide blebs can get up to 3 cm in length in pegmatoidal gabbronorite (Figure 4.5 d). This rock type comprises 65-80 % pyroxenes, <30 % plagioclase, ~2 % sulphides (<10 % locally), ~2 % magnetite locally, ~1 % phlogopite, <1 % olivine (<3 % locally). The amount of sulphides decrease upward from <10 % between 613.5-615 m in HW029, to <8 % between 612.5-612.6 m in HW029, and then to <0.2 % in the upper pegmatoidal gabbronorite. Olivine proportion shows an upward decrease through vein-like pegmatoidal gabbronorite, from 3 % olivine at the base, to ~0 % in the upper pegmatoidal gabbronorite package. The proportion of magnetite increases upward, with the rock being magnetic even with a small proportion of

magnetite. Saussuritised plagioclase is seen as sugar-white grains enclosed by other minerals such as pyroxenes and olivine.

4.3.2.7 *Troctolite*

There are two major packages of medium-grained troctolite in the lower lithologic unit, both of which occur in HW024 and HW025. The upper package ranges from 10.5-13 m in total thickness and the lower troctolite ranges from approximately 6.5-16.5 m in total thickness. Troctolite is represented by leucotroctolite and occurs adjacent to other olivine- and olivine bearing lithologies (Figure 4.4). The colour ranges from milky green and black to white and black. The texture is equigranular. The overall grain size is medium- (3-5 mm) to coarse-grained (<1.2 cm) with olivine crystals ranging from 1-8 mm in size and plagioclase <1.2 cm. Plagioclase and olivine proportions are generally proportionate, with a range of 35-45 %. Pyroxenes proportions range between 5-15 %. The lower troctolite package in HW024 has <55 % plagioclase, ~40 % olivine and ~5 % pyroxenes, and is referred to as leucotroctolite in this study (Figure 4.6 a). Only the lower troctolite package hosts visible mineralisation with <1 % sulphides. The upper troctolite interval transitions from a true troctolite at the base (Figure 4.6 b) into an altered olivine-bearing lithology at the top. Overall troctolite packages are more leucocratic towards the base. On a small scale, troctolite can sometimes be heterogeneous, with localised patches of olivine norite and leucocratic rock varieties seen in some places (Figure 4.6 a).

4.3.2.8 *Pyroxenite*

Pyroxenite in the lower lithologic unit only occurs in HW024 and HW025. Pyroxenite ranges from ~0.2-15 m in thickness. The colour is dark green to greyish green. The overall grain size is medium (2-6 mm). Olivine is sometimes present in pyroxenites and proportions of pyroxenes and plagioclase vary considerably throughout the lower lithologic unit. Pyroxenite comprises 40-80 % orthopyroxene, 30-60 % clinopyroxene, and 5-40 % plagioclase with up to 15 % interstitial plagioclase present in feldspathic pyroxenites (towards the base of HW024).

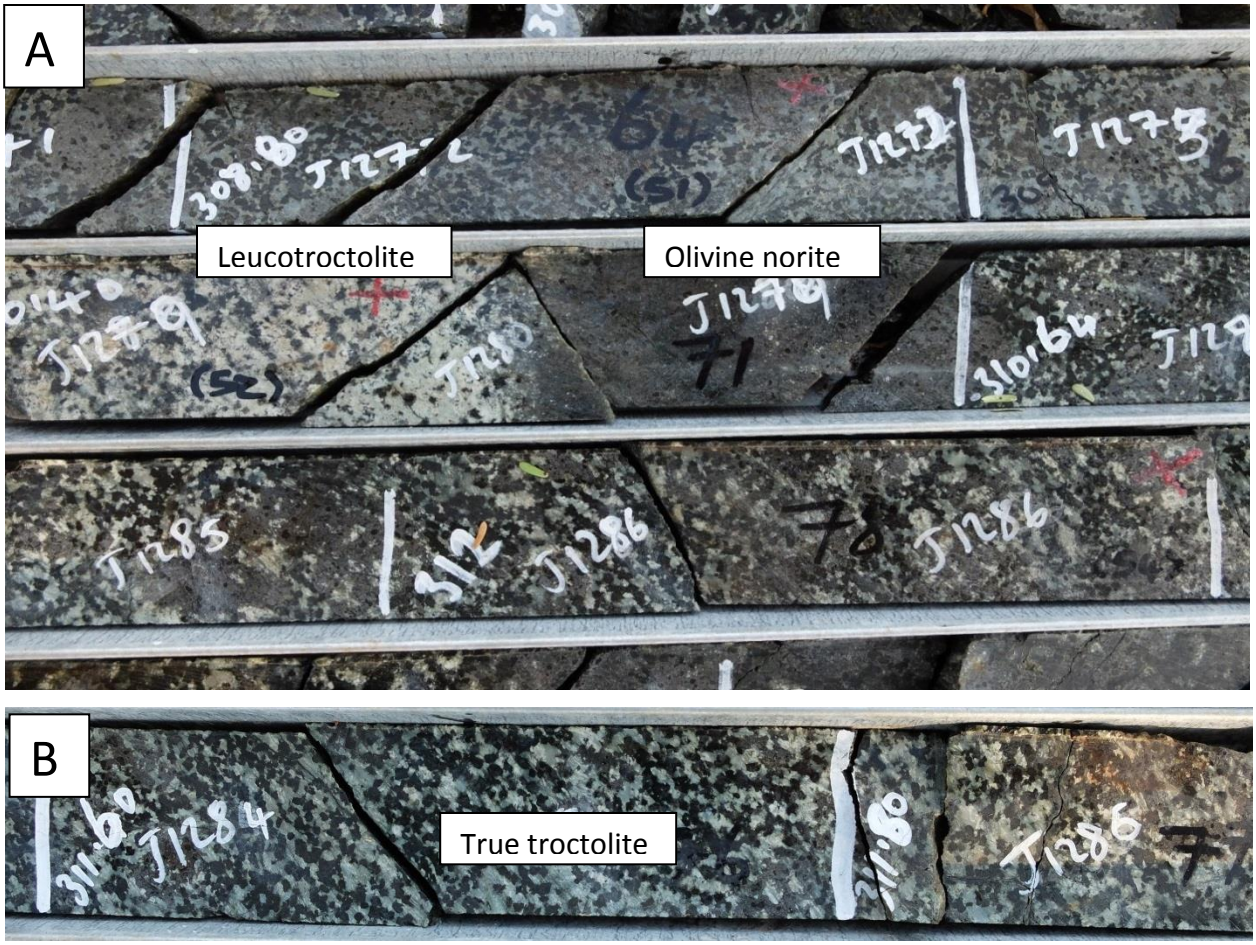

Figure 4.6: Troctolites of the lower lithologic unit. A) Leucotroctolite and olivine norite in troctolite from HW024 at a depth of approximately 308-312 m. B) True troctolite from HW24 at a depth of 311.80 m.

Sulphide contents are <5 % (mainly pyrite, with chalcopyrite and possibly bornite), <1 % of magnetite specks present in mineralised intervals. The different varieties of pyroxenite in the lower lithologic unit include feldspathic pyroxenite, olivine pyroxenite and olivine-bearing feldspathic pyroxenite. Pyroxenites are situated in close proximity, or adjacent to olivine-rich lithologies such as troctolite and olivine-bearing gabbronorites. Orthopyroxene is generally the cumulus mineral, with clinopyroxene only occasionally being the cumulus mineral. Plagioclase grains are found interstially throughout the pyroxenites. Overall, sulphides occur in most pyroxenites; however, sulphides are more prominent in olivine pyroxenites (Figure 4.7). The overall alteration intensity is low, with some olivine grains showing serpentinisation.

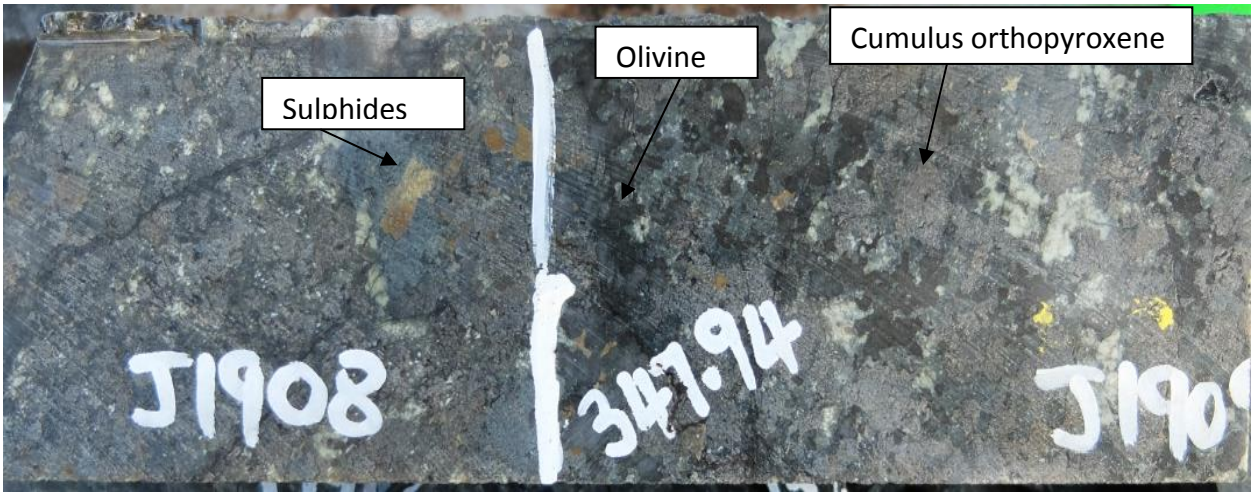

Figure 4.7: Olivine feldspathic pyroxenite of the lower lithologic unit, showing sulphides from HW024 at a depth of 347.94.

4.3.2.9 *Gabbro*

Gabbro is not as widespread as gabbronorite in the lower lithologic unit and occurs in HW024, HW025 and HW029. The thickest occurrence of 15 m occurs at the base of HW029 (Figures 4.4 and 4.8 a). In HW024 and HW025, gabbro is found at, or close to the contact between Bushveld rocks and Waterberg Group sedimentary rocks. In HW024, a 4.5 m interval of leucogabbro occurs *close to* this contact (Figure 4.8 b) and in HW025 a 7 m altered gabbro interval occurs *at* the contact. The colour is greenish grey to light greenish grey. The overall texture is equigranular. The overall grain size is medium (1-6 mm). Gabbro comprises 35-85 % plagioclase (<85 % in leucogabbro), 15-55 % clinopyroxene and <10 % orthopyroxene. This gabbro is altered more intensely at the contact between the Bushveld rocks and the Waterberg sedimentary rocks, and is less altered downward. Clinopyroxene is often replaced by chlorite in gabbros of the lower lithologic unit.

Figure 4.8: Gabbros of the lower lithologic unit. A) Gabbro from HW029 at a depth of 709.2-716 m. B) Leucogabbro from HW029 at a depth of approximately 265-271 m.

4.3.2.10 *Norite*

Norite occurs in small packages of between 0.2-2.8 m thick and is present only in drillcore HW024. The colour ranges from brownish grey to grey. Norite varieties present include norite and olivine norite. The texture is equigranular. The grain size is medium (1-4 mm), with a fine grained (0.1-2mm) interval present in HW029 at a depth of at 371 m. Norite comprises 30-40% orthopyroxene, 30-40% plagioclase and <10% clinopyroxene. Semi-dissolved fragments of olivine norite with up to 30% olivine are found in olivine-bearing melagabbronorite and troctolite (Figures 4.5 b and 4.6 a).

4.3.2.11 *Anorthosite*

Anorthosite is not prominent in the lower lithologic unit and occurs only in the HW025 drillcore of this sequence. Anorthosite packages are <1.5 m thick and appear as vein-like intrusions or veins with sharp contacts with the host lithologies. The colour ranges from milky white to milky green. Anorthosite normally shows an equigranular texture. The grain size is medium-grained (4-5 mm) but pegmatoidal (>3 cm) close to the top contact of the lower lithologic unit (Figure 4.9). Anorthosite comprises ~90% plagioclase and <10% pyroxenes and <5% magnetite locally.

Figure 4.9: Anorthosite of the lower lithologic unit of HW029 at a depth of 592.4. Note the interstitial magnetite and coarse-grained plagioclase grains.

4.3.2.12 *Calcsilicate xenolith*

A xenolith occurs in HW029 at the base of the succession only and has a thickness of ~40 m (Figure 4.10). The colour is greenish-yellow with white quartz-feldspar veins cross-cutting the xenolith. The texture is equigranular to inequigranular. The grain size is medium overall (2-6 mm), with some larger grains (1 cm) of quartz and calcite seen sporadically throughout the drillcore. The contact between the host rock and the xenolith is sharp, with the thin veins of xenolithic material being present in the host rocks. The composition of the xenolith is predominantly calcsilicate, with calcite, quartz and feldspar crystals visible in some sections. Quartz and quartz-feldspar veins are also seen in drillcore close to contact with hornfels being prominent at the top contact.

Figure 4.10: Calcsilicate xenolith of the lower lithologic unit from HW029 at depth of 686-696 m. Note quartz-feldspar veins.

4.3.3 **Boundary between the upper and lower lithologic units**

The boundary between the lower and upper lithologic unit is ambiguous when visually analysing the core. There were two possible boundaries that were visually identified. The first is at 590.2 m and the second is at 592 m in the drillcore HW029. These boundaries were identified based on the first appearance of magnetite cumulates (SACS, 1980) and the lack of magnetism picked up by a magnetic pen in the lithology (Ashwal *et al.,* 2005). Certain sulphides also exert a magnetic field, so using the magnetic pen may have skewed the placement of these possible boundaries. The occurrence of the upper mineralised zone also served as a reference in defining the location of this boundary due to the similarity of the upper mineralised zone on Harriet's Wish to the T Zone on the Waterberg Project (Sylvania Resources Limited, 2012), as the T Zone occurs at the contact between the Upper Zone and the troctolite-gabbronorite-anorthosite (TGA) sequence on the Waterberg Project (Kinnaird *et al.,* 2017).

4.3.4 **Upper lithologic unit**

This unit is ~220 m thick in the HW029 drillcore and ~800 m thick in the HW030 drillcore (Figure 4.4); however, the drill core HW030 was found very close to the Hout River Shear Zone, and it can be expected that results of this drill core may vary from what is expected of the other drillcores further north (HW024, HW025, HW029; McCreesh, 2016; Fossen and Cavalcante, 2017). The upper lithologic unit is identified by the

appearance of cumulus magnetite crystals. The upper lithologic unit comprises gabbronorites (including melagabbronorite and olivine and olivine bearing gabbronorite), gabbros (including magnetite gabbro) and minor anorthosites. These lithologies are detailed below:

4.3.4.1 *Gabbronorite*

Gabbronorite is the dominant rock type in the upper lithologic unit on Harriet's Wish and occurs in drillcore HW029. The thickness ranges from 1-58 m (Figure 4.4). A small (1 m) package of melagabbronorite is seen towards the base of the upper lithologic unit and no leucogabbro is present in the upper lithologic unit. A 58 m package of lineated gabbronorite is present between 497 m to 555 m in HW029 with orthopyroxene and clinopyroxene showing a preferred lineation of ~30° and plagioclase showing slightly more uniform orientation than other gabbronorite layers. The colour is greenish grey to brownish grey, with some intervals being dark green-grey. The texture is equigranular to lineated. The overall grain size is fine (0.5-3 mm; melagabbronorite) to medium (3-5 mm). Gabbronorites comprise 40-70 % plagioclase, 30-40 % clinopyroxene, 20-30 % orthopyroxene, <5 % phlogopite, <4 % chlorite and 1-2 % magnetite overall, with concentrations of <10 % magnetite locally. Magnetite may occur as seen and unseen interstitial specks (Figure 4.11 a; which may be identified using a magnetic pen) or as mottles. Towards the base of, sugar textured, fine grained plagioclase is common.

4.3.4.2 *Olivine-bearing and olivine gabbronorite*

Olivine-bearing gabbronorite and minor olivine gabbronorite (Figure 4.11 c) can be seen in HW029 towards the base of the upper lithologic unit (Figure 4.11 b). The colour is deep green to dark greyish green. The texture varies from being cumulate with equigranular grains in some sections, to inequigranular in other sections. The grain size is medium-coarse grained (3-9 mm) with olivine grains <7 mm in size. Olivine gabbronorite comprises 40-60% plagioclase, 25-40% clinopyroxene, 20-30% orthopyroxene, 15% olivine, <2% magnetite and <0.2% fine-grained sulphides (Figure 4.11 a). Olivine dissipates gradually upward until only rare relics of olivine are present,

with a reappearance of olivine seen between 470 and 500 m (Figure 4.4). The upper gabbronorites show a sudden disappearance of olivine crystals. A lot of olivine grains are serpentinised.

Figure 4.11: Gabbronorites of the upper lithologic unit. A) Fine grained melagabbronorite with interstitial magnetite and sulphides from HW029 at a depth of 590 m. B) Olivine-bearing gabbronorite from HW029 at a depth of 474 m. C) Olivine gabbronorite from HW029 at a depth of 578.8 m.

4.3.4.3 *Gabbro*

Gabbros in the upper lithologic unit occur at the top of the sequence in HW029 and HW030 and vary in thickness from a few cm to ~43 m in HW029 and <200 m in HW030. Lineated gabbro, with ~30° oriented plagioclase grains, occurs in packages from 9 m to 20 m in HW029. Lineated gabbro is separated by thin interlayers of gabbronorite or mottled leucogabbro (Figure 4.4). Mottled leucogabbro is also present in HW029 with a thickness of ~5 m (Figure 4.4) and shows <3 cm mottles consisting of mostly clinopyroxene, magnetite and minor pigeonite oikocrysts (Figure 4.12 c). Gabbro may also occur as leucogabbro or melagabbro sporadically. The colour of the gabbro is greenish grey to dark green and grey. The overall texture varies from equigranular to lineated-equigranular to inequigranular. The grain size overall is medium (2-6 mm). Oikocrysts of pigeonite with adamantine lustre (<3 cm) are visible in mottled leucogabbro over an interval of ~9 m (HW029). Magnetite occurs as interstitial grains and mottles (<2 cm), as well as cumulus magnetite crystals (<0.5 cm; Figure 4.12 c). Gabbro comprises 40-60% plagioclase, 20-35% clinopyroxene, <10% orthopyroxene with <3% pigeonite and <2% magnetite. Overall gabbro is relatively fresh (Figure 4.12 a), although it can be epidotised or chloritised at the Bushveld-Waterberg contact in all four drillcores. Plagioclase in the upper portions of HW029 is chloritised and shows a greenish colour.

4.3.4.4 *Magnetitite and magnetite-rich gabbro*

Magnetite gabbro <10 m thick and massive magnetitite is seen in HW030 (Figure 4.4). Magnetite ranges from massive (0.1-0.4 m) to disseminated specks (Figure 4.11 a). Magnetitite seems to form layering in HW030 at a depth of ~440 m.

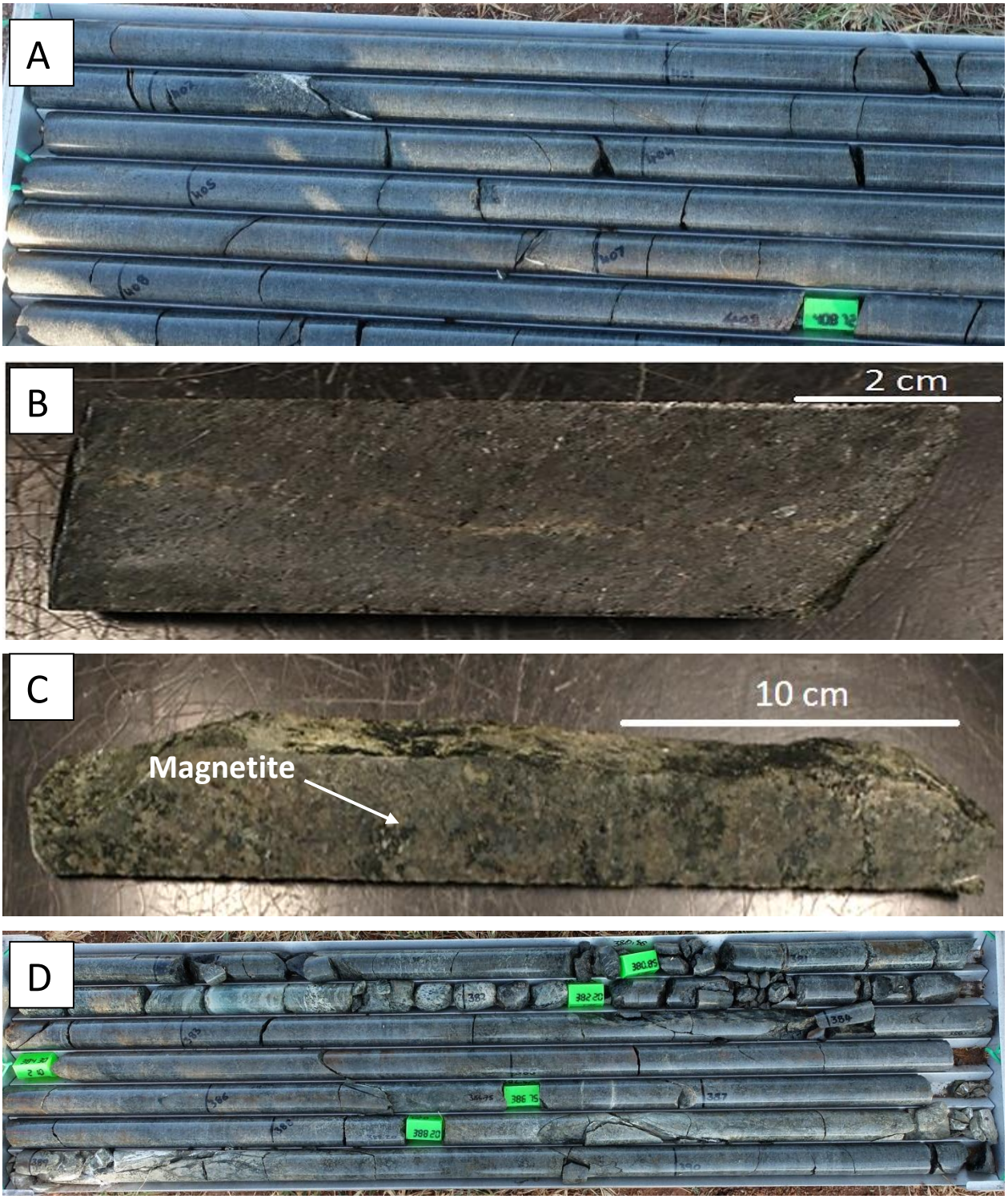

Figure 4.12: Gabbros of the upper lithologic unit on Harriet's Wish. A) Lineated gabbro from HW029 at a depth of 402-410 m, lineation of gabbro is typical of the Upper Zone of the Bushveld Complex (Eales and Cawthorn *et al.,* 1996). B) Lineated gabbro from HW029 at a depth of 421.45 m. C) Mottled leucogabbro from HW029 at a depth of 389.4 m. Mottles that are <3 cm comprise dominant clinopyroxene, magnetite, minor olivine and rare pigeonite oikocrysts. D) Mottled leucogabbro from HW029 at a depth of approximately 380- 389 m.

4.3.4.5 *Anorthosite*

Anorthosite occurs in HW029 and ranges in thickness from 0.2-6.5 m in thickness. A 1.6 m interval of anorthosite is present at the Bushveld-Waterberg contact which can be seen in HW029 at a depth of 370 m, and at a depth of 593 m at the boundary between the upper and lower lithologic units (Figure 4.4). A 12 m thick anorthosite layer is present in HW030 at a depth of 650 m. The colour ranges from milky white to milky green with some portions being dark green. The texture varies from equigranular to cumulate to massive pegmatoidal (Figure 4.13). Anorthosite comprises 70-90% plagioclase, 5-10% clinopyroxene, and 3-8% orthopyroxene, >5% chlorite, >1% interstitial clinopyroxene and >1% sulphides are seen within pegmatoidal anorthosite. The contact between anorthosite packages and surrounding lithology is generally sharp (i.e. anorthosite appears to be vein-like). Anorthosites can be strongly chloritised (showing a green to dark green appearance; Figure 4.13).

Figure 4.13: Pegmatoidal anorthosite of the upper lithologic unit on Harriet's Wish from HW029 at a depth of 593.2 m. Note the discrete sulphides and interstitial clinopyroxene.

4.3.5 **Cover rocks/ sediments**

Sedimentary rocks of the Waterberg Group overlie the magmatic sequence. The thickness of this package differs from drillcore to drillcore. In HW029 the sedimentary rocks have a thickness of 364 m, in HW025 these have a thickness of 412 m and in HW024 these have a thickness of 261 m. There is an erosional unconformity between the sedimentary rocks and igneous rocks below (Figure 4.14).

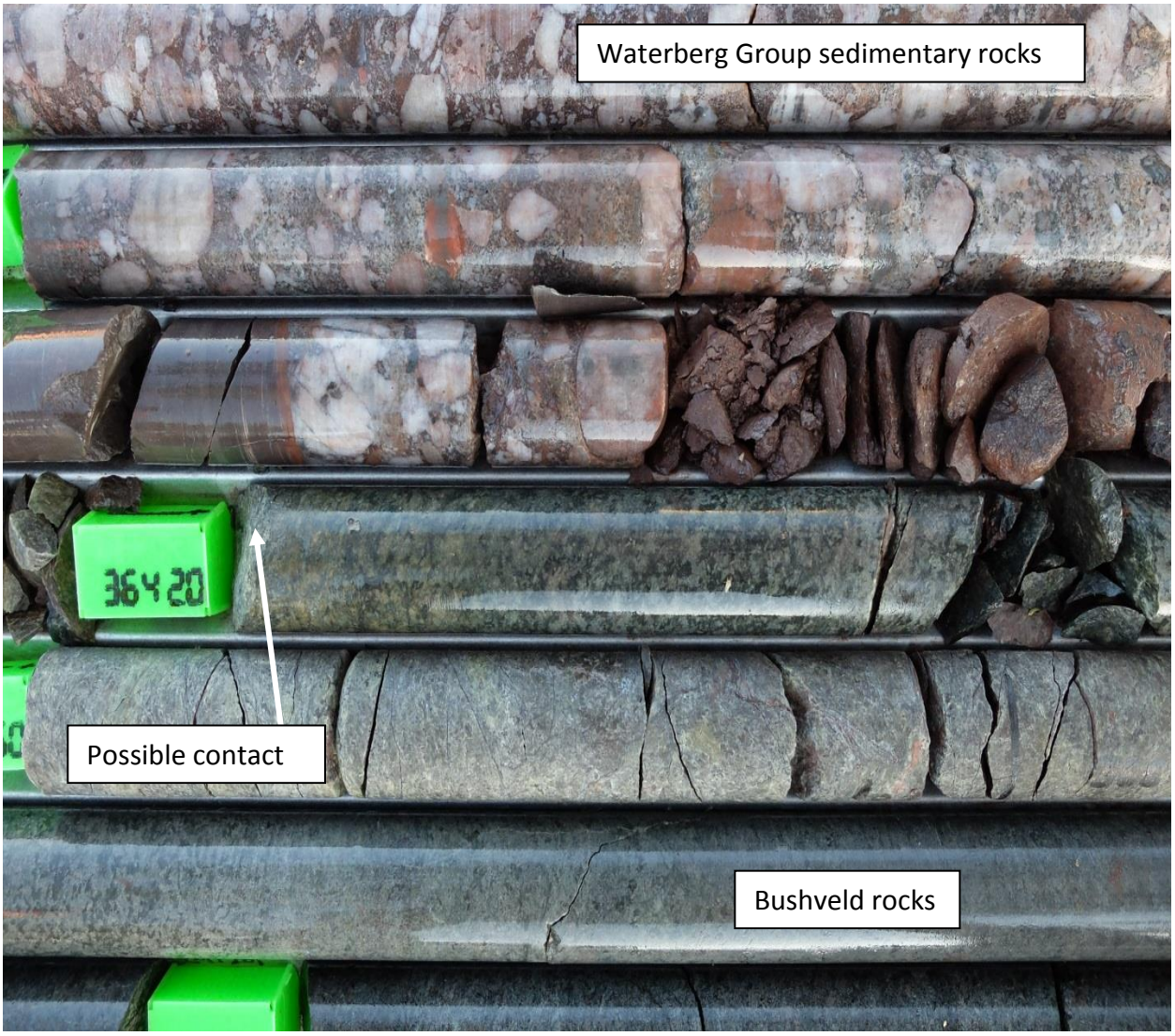

Figure 4.14: Contact between the Bushveld rocks and the overlying Waterberg Group sedimentary rocks on Harriet's Wish from HW029 at a depth of 364.2 m. Note the epidotisation (green) of Bushveld rocks and hematisation (reddish brown) of the Waterberg Group sediments.

The sedimentary rocks above the magmatic succession on Harriet's Wish consist of medium- to coarse-grained red-bed arenites showing hematisation, chloritisation and epidotisation close to the contact (Figure 4.14). Dark brown arkose and very fine grained, dark brown mudstones are also present. Sandstones and mudstones display trough-cross bedding. Towards the sedimentary-igneous contact (Figure 4.14), conglomerate and clay are present and are outlined in more detail below:

4.3.5.1 *Conglomerate*

Conglomerate occurs at the base of the Waterberg Group sedimentary sequence in the HW024, HW025, HW029 and HW030 drillcores. The thickness can vary from a few cm (interlayered with sandstone), up to 3 m. The conglomerate varies from the bottom to the top, being clast-supported towards the base and generally matrix-supported towards the top, with pebble conglomerates being present at the base (Figure 4.14). The conglomerate is overall poorly sorted (Figure 4.15 a) and has an upward fining sequence. The conglomerate varies in colour from brownish-red (vitreous) to brownish-pink to red to greenish brown. The matrix generally consists of a medium-grained (2-5 mm) sandstone (Figure 4.15 a), with minor fine-grained clay also present in some sections. The clasts vary from being well-rounded to angular with well-rounded clasts ranging from 1-8 cm and angular clasts ranging from 0.1-3 cm in size. Quartz pebbles are the largest and most dominant clasts. In some samples, all the clasts are composed of quartz, and in others the clasts are composed of hematitised massive magnetite (Figure 4.15 b). There are no visible Bushveld fragments seen in the lithic clasts. Minor hematite and mica can also be seen in the matrix.

4.3.5.2 *Clay*

Clay can be found close to the Bushveld-Waterberg contact. It is difficult to determine whether the clay is altered Bushveld rocks or Waterberg siltstone. In some cases, the clay appears to be a mixture of Waterberg Group sediments and Bushveld rocks and can be interpreted as paleosol after weathered Bushveld rocks (Engela, 2014). The colour ranges from red to reddish brown to green. The clay can be hematitised, brecciated and/ or semi-lithified.

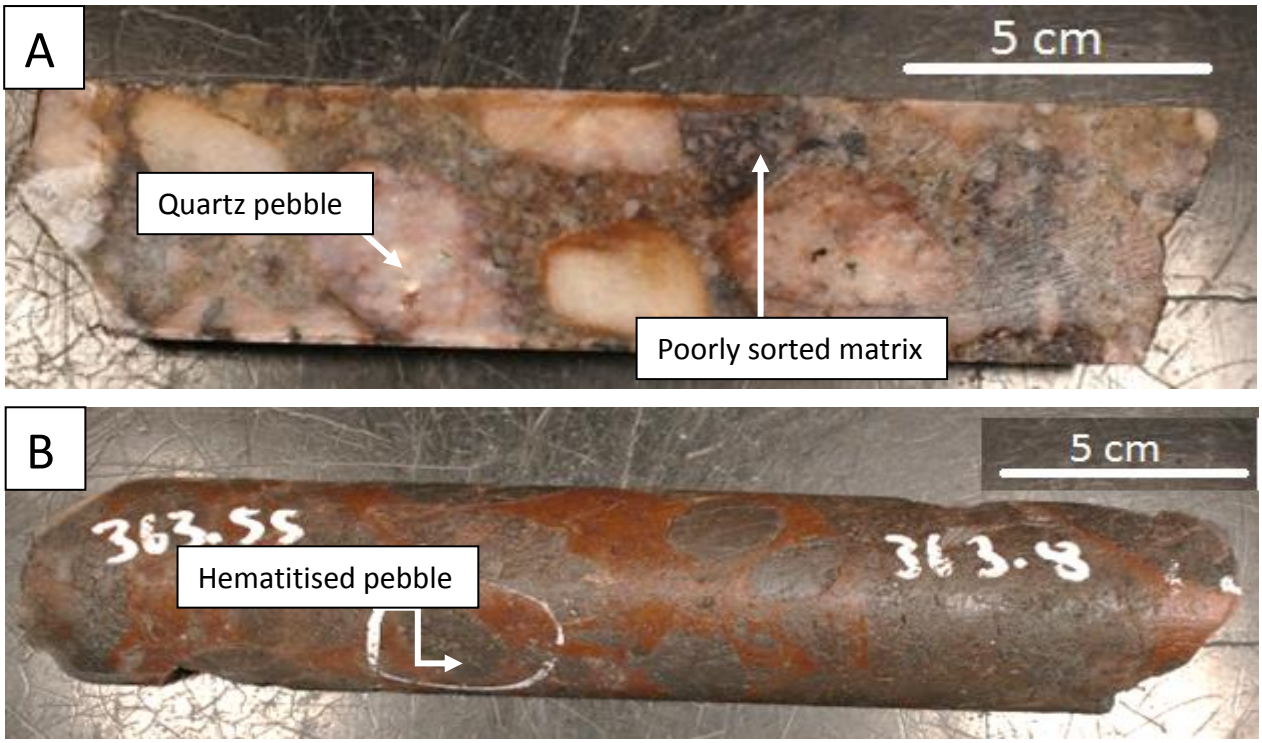

Figure 4.15: Waterberg Group conglomerates of Harriet's Wish: A) Quartz conglomerate of HW029 at a depth of 362.1 m. Note the poorly sorted matrix and the clasts of quartz pebbles. B) Hematitised conglomerate of HW029 at a depth of 363.55 m. Note the hematitised clasts and matrix.

4.3.6 **Mineralised zones**

A lower and an upper mineralised zone have been identified in Harriet's Wish drillcores. These have been identified only based on visual observation of base metal sulphides including chalcopyrite, pentlandite and pyrite. These are detailed below and outlined in Figure 4.16:

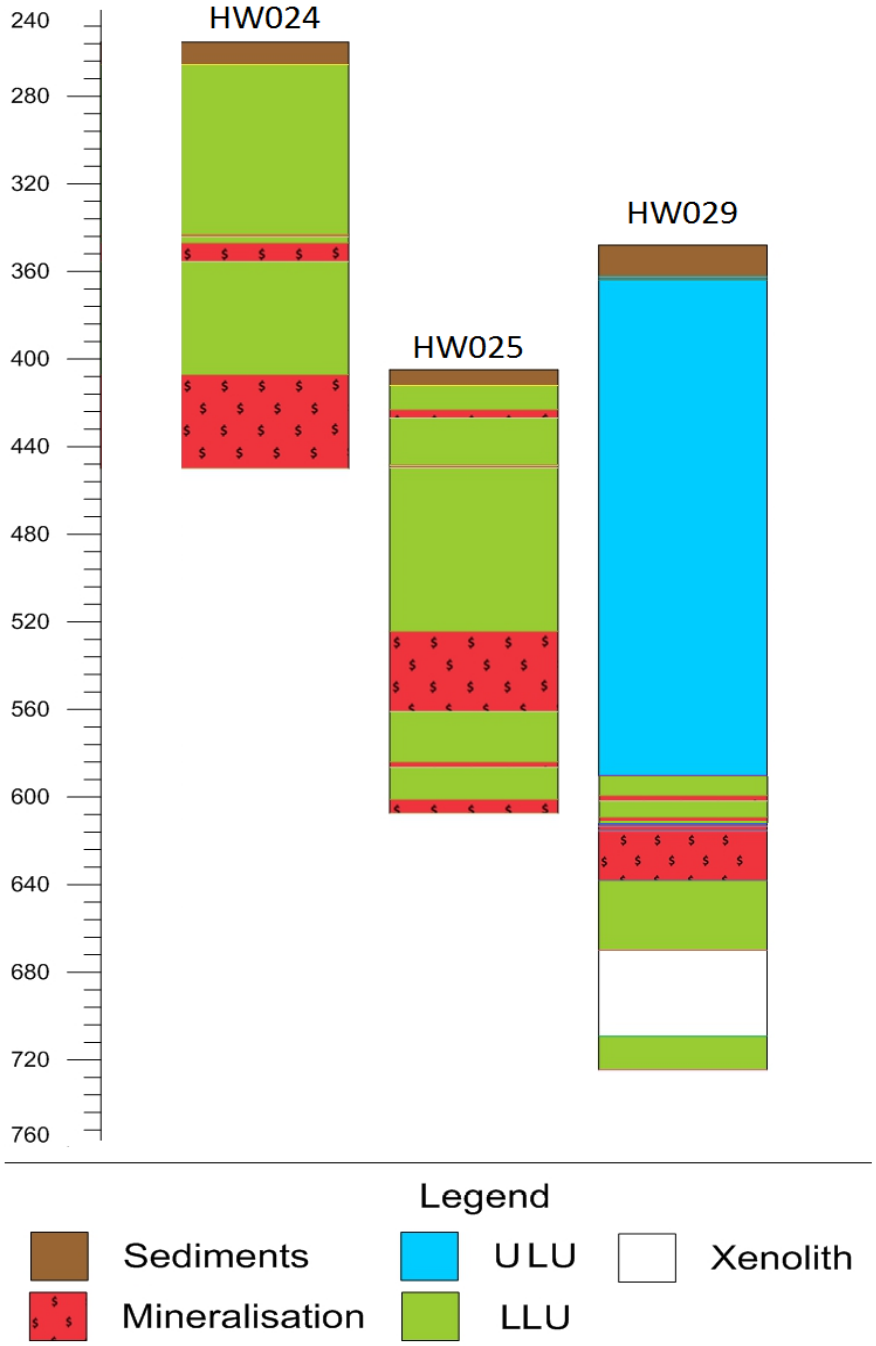

Figure 4.16: Lithologic units and mineralised zones observed in Harriet's Wish drillcores. The boundary between the upper and lower lithologic unit is defined by the visual observation of magnetite cumulates and by use of a magnetic pen. Mineralised zones are defined based on visual observation of sulphides such as pentlandite, pyrite and chalcopyrite. LLU=lower lithologic unit, ULU=upper lithologic unit.

4.3.6.1 *Lower mineralised zone*

This mineralised zone occurs within the lower lithologic unit and has a maximum thickness of ~50 m (HW024; Figure 4.16). Host rock types include pyroxenite, gabbronorite and troctolite. This mineralised zone is well defined in the drillcores HW024 and HW025. Some examples are seen in Figure 4.17 b, c, and d.

4.3.6.2 *Upper mineralised zone*

The mineralised zone occurs at the interface between the lower and upper lithologic units, just below the boundary, as outlined in Figure 4.16. This zone has a total thickness of ~20 m. Rock types in which it occurs include gabbro, gabbronorite (including melagabbronorite and pegmatoidal gabbronorite) and anorthosite. Base metal sulphides observed in this zone include chalcopyrite, pentlandite and pyrrhotite. This mineralised zone occurs only in HW029 among the studied boreholes. Examples are seen in Figure 4.17 a.

4.4 **Discussion**

4.4.1 **Basement lithologies**

The basement lithologies in the northern limb of the Bushveld Complex comprise rocks of the Transvaal Supergroup as well as Archean Granite basement rocks (Chapter 2.2.1; Eales and Cawthorn, 1996; Kinnaird *et al.,* 2005; Kinnaird and Nex, 2012). On the Waterberg Project, Archean Basement forms the footwall of the igneous succession (McCreesh, 2016; Kinnaird *et al.,* 2017). On the Aurora Project, mainly Archean granite-gneiss rocks form the basement (McDonald *et al.,* 2017). On the Harriet's Wish farm, it is not resolved whether the intersected calcsilicate represents the actual floor or a detached fragment due to the boreholes not being drilled to the basement rocks. Nevertheless, the nature and composition of xenoliths in the northern limb are commonly controlled by the nature of the immediate floor rocks (Manyeruke, 2007; Kinnaird *et al.,* 2017). It is therefore suggested that both granite-gneiss and dolomitic footwalls may locally underlie the magmatic sequence on Harriet's Wish (Figure 4.10).

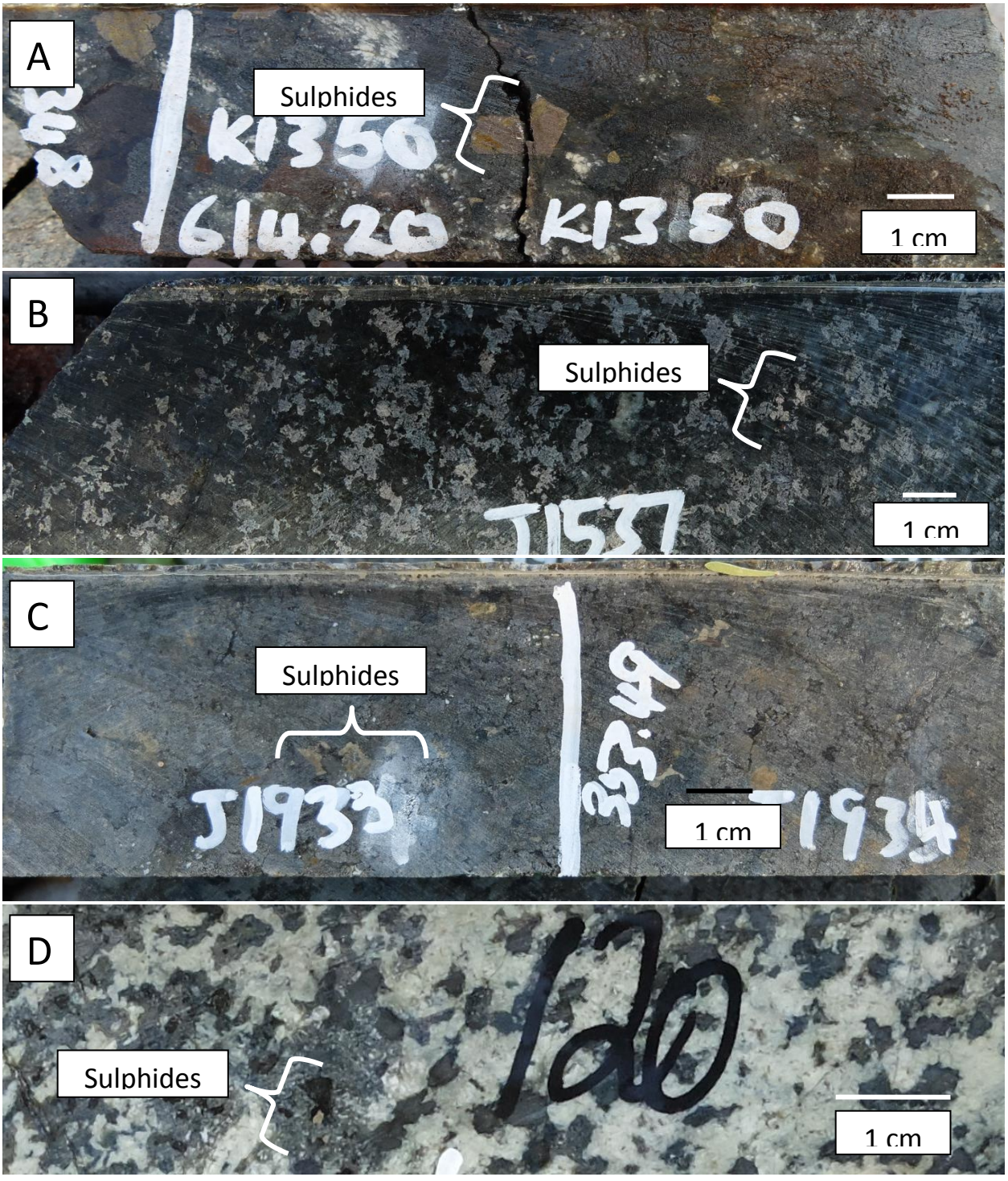

Figure 4.17: Mineralised rocks on Harriet's Wish. A) Pegmatoidal gabbronorite with chalcopyrite and pentlandite of HW029 at a depth of 614.25 m. B) Olivine gabbronorite with sulphides of HW024 at a depth of 4.5 m. C) Olivine pyroxenite with sulphides of HW024 at a depth of 353.49. D) Leucotroctolite with sulphides of HW024 at a depth of 328.5 m.

4.4.2 **Igneous sequence**

The igneous succession on the Waterberg Project to the north comprises an Upper Zone that shows some similarities to the Upper Zone in the northern limb of the Bushveld Complex (Van der Merwe, 1976; SACS, 1980; McCreesh, 2016; Kinnaird *et al.,* 2017; Huthmann *et al.,* 2018; McCreesh *et al.,* 2018). However, correlations with the Ultramafic Sequence at the base of the Waterberg Project igneous succession with the northern limb (Van der Merwe, 1976; Ashwal *et al.,* 2005) has been problematic (Kinnaird and McDonald, 2014; McCreesh, 2016; Kinnaird *et al.,* 2017) and it was suggested that this sequence was formed by a separate ultramafic sulphide-bearing magma which was emplaced on the agmatite above the Archean floor rocks (Kinnaird *et al.,* 2017).

According to field observations and core logging, there are two major lithologic units on Harriet's Wish; a lower and an upper lithologic unit. Similar to the igneous succession on the Waterberg Project, these units can be correlated to the Upper and Main Zones of the northern limb of the Bushveld Complex when broadly comparing stratigraphy and lithology (Van der Merwe *et al.,* 1976; SACS, 1980; Kinnaird *et al.,* 2005; Kinnaird *et al.,* 2017). These units are also broadly similar to the TGA sequence and Upper Zone on the Waterberg Project (McCreesh, 2016; Kinnaird *et al.,* 2017); however, the Ultramafic Sequence found on the Waterberg Project seems to be absent from the Harriet's Wish drillcore (Figure 4.4). The Harriet's Wish lithologic units are discussed below:

The Ultramafic Sequence on the Waterberg Project comprises troctolite, harzburgite, feldspathic harzburgite, feldspathic pyroxenite and pyroxenite and occurs at the base of the Waterberg sequence (Woods, 2012; McCreesh, 2013; Kinnaird *et al.,* 2017). The Ultramafic Sequence also hosts the F Zone mineralisation (Lomberg, 2012; Kinnaird *et al.,* 2017; Huthmann *et al.,* 2018; McCreesh *et al.,* 2018). On the Aurora Project, an ultramafic-mafic unit (Unit 1) has also been identified above the basement rocks of about 80-100m in thickness, and it comprises generally medium-grained olivine-bearing clinopyroxenite, olivine-orthopyroxenite and melagabbronorites (McDonald *et al.,* 2017), and sometimes a thin zone of fine-grained norite or gabbronorite (Manyeruke, 2007).

Olivine is only found in olivine-free orthopyroxenites. Thin medium to coarse-grained gabbronorites and leucogabbronorite sharply cross cut the ultramafic rocks which may be enriched in base metal sulphides (McDonald *et al.,* 2017).

On Harriet's Wish, there is no lithologically equivalent lithologic unit to the Ultramafic Sequence on the Waterberg Project and Unit 1 ultramafics on the Aurora Project (Figures 3.1, 3.2 and 4.4; Kinnaird *et al.,* 2017; McDonald *et al.,* 2017). The major differences include the lack of ultramafic host lithologies including harzburgite, dominant pyroxenite or intensely altered olivine-enriched ultramafic lithologies confined to the base of the succession. There are a few possible reasons for this 1) this unit could be deeper in the sequence, as the boreholes on Harriet's Wish were not drilled all the way to the basement (Figure 4.4), 2) this unit may not have formed altogether, or 3) this unit was reworked or digested by later intrusions. Possible evidence for this layer being reworked is seen at the base of the lower lithologic unit. Figures 4.5 b and 4.6 a show that olivine norite in olivine-bearing melagabbronorite occurs as semi-dissolved fragments that could possibly be remnants of digestion of earlier cumulates or resulted from mingling of two crystal-rich magmas. It can be envisaged that the earlier cumulates of the Ultramafic Sequence have been re-worked and consumed during the emplacement of mafic magmas, which eventually crystallised the lower lithologic unit.

The <2000 m thick Main Zone in the northern limb overlies the Platreef and is dominated by gabbronorites, with pyroxenites, anorthosites and lesser norites (especially towards the base; Kruger *et al.,* 1987; Kinnaird *et al.,* 2005). The Main Zone observed in the Bellevue drillcore comprises olivine norite, gabbro and gabbronorite with minor leucocratic rocks with distinctive pyroxenite horizons (Ashwal *et al.,* 2005). The stratigraphic correlate of the Main Zone on the Waterberg Project is referred to as the TGA sequence to emphasise the significant differences to the Main Zone south of the Hout River shear zone (Kinnaird *et al.,* 2017). The TGA sequence is a cyclically varied unit that is <850 m in thickness, which is significantly thinner than the Main Zone of the northern limb (Van der Merwe, 1976; Ashwal *et al.,* 2005; Kinnaird *et al.,* 2017). The TGA sequence comprises gabbronorite, troctolite, anorthosite with mela- and

leucotroctolite to olivine norite and leucotroctolite (Kinnaird *et al.,* 2017). The upper Main Zone on the Aurora Project comprises the following rocks: Unit 1 comprising of olivine-free to olivine-poor ultramafic rocks, Unit 2 comprising of gabbronorites and leucogabbronorites with rare troctolites and magnetite gabbros and Unit 3 comprising of pigeonite gabbronorite (Figure 3.2; McDonald *et al.,* 2017).

The lower lithologic unit on Harriet's Wish comprises leuco- and melagabbronorite, troctolite and leucotroctolite, pyroxenite, olivine gabbronorite and minor anorthosite and norite (Figure 4.4). Based on stratigraphic position and lithologic similarity, the lower lithologic unit on Harriet's wish equates broadly with the TGA sequence on the Waterberg Project. The observed Unit 2 lithology on the Aurora Project is also similar to Harriet's Wish; however, on the Aurora Project, gabbronorites and gabbros dominate over troctolitic lithologies, which occurs rarely, and feldspathic harzburgite is absent (McDonald *et al.,* 2017; Kinnaird *et al.,* 2017). Stratigraphically, this Unit 2 also coincides with the Waterberg Project TGA sequence (Kinnaird *et al.,* 2017) and the lower lithologic unit on Harriet's Wish. The Unit 1 and Unit 3 are dissimilar to the TGA sequence on the Waterberg Project and the lower lithologic unit on Harriet's Wish.

Unique to the northern limb, at approximately 1100 m from the base is a distinctive >100 m thick package of olivine-bearing lithologies referred to as troctolite (Van der Merwe, 1978; Ashwal *et al.,* 2005). The troctolite on the Waterberg Project was first believed to correlate with the troctolite in the Main Zone seen in Bellevue drillcore (Ashwal *et al.,* 2005; Kinnaird *et al.,* 2017) and in the rest of northern limb (Van der Merwe, 1976). However, the troctolite package in the northern limb comprises mainly olivine-norite, gabbro, and gabbronorite with minor leucocratic varieties and pyroxenite horizons, instead of true troctolite (Ashwal *et al.,* 2005) as observed on the Waterberg Project (Kinnaird *et al.,* 2017). In the Bellevue drillcore the modal abundance of the said troctolite consists of 21.1 % olivine, which decreases up-sequence (Ashwal *et al.,* 2005). On the Waterberg project the modal abundance of the olivine in the troctolite ranges between 25-65 % (Kinnaird *et al.,* 2017). In the Harriet's Wish drillcores the modal abundances of olivine and cumulus plagioclase in troctolite both range between

35-45 %. The overall higher modal abundance of olivine in the troctolite on the Waterberg Project and in Harriet's Wish drillcore suggests that these troctolite packages correlate with each other, rather than with the said troctolite south of the Hout River shear zone. Furthermore, the Waterberg Project troctolite package varies in composition from feldspathic harzburgite to melatroctolite to olivine norite and leucotroctolite and displays an overall equigranular texture with medium- to coarse grain sizes (McCreesh, 2016; Kinnaird *et al.,* 2017). Pegmatoidal anorthosite lenses are also regularly found below and above the troctolite-bearing package at the top of the TGA sequence (Kinnaird *et al.,* 2017; McCreesh *et al.*, 2018). Except for slight variations in lithology (such as the absence of feldspathic harzburgite and melatroctolite), the Harriet's Wish troctolite package can be equated with the troctolite package on the Waterberg Project in terms of lithology modal mineralogy, texture and stratigraphic position. There are no equivalent troctolite packages observed in the Main Zone on the Aurora Project (McDonald *et al.,* 2017).

The base of the Upper Zone is generally taken at the appearance of cumulus magnetite (SACS, 1980; Eales and Cawthorn, 1996), however, some suggest that the Pyroxenite Marker, which occurs <700 m below the cumulus magnetite, defines this boundary (Von Gruenewaldt, 1973; Cawthorn *et al.,* 1991: Kruger, 1994; Nex *et al.,* 2002). There are two pyroxenite horizons in the Main Zone on Bellevue (Ashwal *et al.,* 2005). The lower pyroxenite horizon occurs at the same stratigraphic position as the Pyroxenite Marker elsewhere in the Bushveld Complex (Von Gruenewaldt, 1973; Cawthorn *et al.,* 1991; Nex *et al.,* 2002); but this was not equated to the Pyroxenite Marker in the rest of the Bushveld Complex due it being clinopyroxene-rich rather than orthopyroxene-rich pyroxenite (Ashwal *et al.,* 2005). Ashwal *et al.,* (2005) conclude that the northern limb is devoid of the traditional Pyroxenite Marker in the eastern and western limbs (Ashwal *et al.,* 2005). The upper pyroxenite horizon on Bellevue coincides with the stratigraphic position of the pyroxenite horizon associated with the T1 Zone on the Waterberg Project, and both are clinopyroxene-rich, which is dissimilar to the Pyroxenite Marker (McCreesh, 2013, 2016; Kinnaird *et al.,* 2017). On Harriet's Wish, however, there are no pyroxenite horizons that coincide with the upper mineralised zone, or with the

pyroxenite marker in eastern and western limbs (Figure 4.4; Ashwal *et al.,* 2005; McCreesh, 2016).

Ashwal *et al.,* (2005), however, suggested that an increase in magnetic susceptibility readings defines the boundary between the Main and Upper Zones due to unseen magnetite occurring in the rocks below the visible magnetite. This practice was adopted on the Waterberg Project and aided in the exploration of the T Zone mineralisation that occurs at this boundary (McCreesh, 2016; Kinnaird *et al.,* 2017). The possible boundary between the lower and upper lithologic units on Harriet's Wish, while core logging, therefore, was suggested based on visual observations, including the use of a magnetic pen, with the aim of doing magnetic susceptibility readings at a later stage. The visual boundary was pinpointed at depths of approximately 590.2 m or 592 m (Figure 4.16). However, Ashwal *et al.,* (2005) suggested the use of magnetic susceptibility readings to more clearly define this boundary, as unseen specks of magnetite occur below the visible magnetite cumulates.

On the Waterberg Project, an equivalent of the Upper Zone in the northern limb is found (McCreesh, 2016; Kinnaird *et al.,* 2017), displaying a similar stratigraphic position, similar rock types and the presence of cumulus magnetite (SACS, 1980; Ashwal *et al.,* 2005). However, the overall thickness of the Upper Zone on the Waterberg Project is thinner than the northern limb Upper Zone because of the later erosion (Kinnaird *et al.,* 2017) and characteristic magnetitite layering common in the northern limb, south of the Hout River shear zone, is absent (e.g. on Bellevue; Figure 4.18; Eales and Cawthorn, 1996; Ashwal *et al.,* 2005; Cawthorn *et al.,* 2006). On the Aurora Project, no Upper Zone is noted, however, Unit 3 and some of Unit 2 shows some similarities to the Upper Zone as observed in the northern limb (e.g. in Bellevue; Eales and Cawthorn, 1996; Ashwal *et al.,* 2005; Kinnaird *et al.,* 2005; Cawthorn *et al.,* 2006), especially due to the correlation of the stratigraphic position and the occurrence of magnetite gabbro, pigeonite and magnetite (Nex *et al.,* 1998; Ashwal *et al.,* 2005). However, McDonald *et al.,* (2017) suggest that the magnetite is not of cumulus origin and should be assigned to the upper Main Zone.

Harriet's Wish drillcore also shows similarities to the Upper Zone of the northern limb (Eales and Cawthorn, 1996; Ashwal *et al.,* 2005; Cawthorn *et al.,* 2006). Similarities include a correlation in the stratigraphic position (Figures 3.1 and 4.4), the widespread occurrence of fine-grained cumulus- and disseminated magnetite in drillcore samples (e.g. in Figures 4.11 a and 4.12 c). However, some differences are noted between the northern limb Upper Zone and upper lithologic unit of Harriet's Wish, and the upper lithologic unit more closely resembles the Upper Zone on the Waterberg Project (Kinnaird *et al.,* 2017). These are discussed below.

Firstly, magnetitite layering that is common in the Upper Zone of the northern limb, south of the Hout River shear zone (e.g. on Bellevue; Figure 4.18; Eales and Cawthorn, 1996; Ashwal *et al.,* 2005; Cawthorn *et al.,* 2006), is absent in the Harriet's Wish drillcores, except in drillcore HW030 (Figure 4.4), where magnetitite layering of <1 m thick is seen (Figure 4.4). The position of this borehole, however, is in the Hout River shear zone (Figure 4.2), which may have an influenced the stratigraphy (Fossen and Cavalcante, 2017). This is also observed on the Waterberg Project as drillcores north of the Hout River shear zone contain no magnetitite layers, except for one southernmost drillcore (WB001), which is located within the Hout River shear zone (McCreesh, 2016; Kinnaird *et al.,* 2017). The Aurora Project drill cores are also located to the south of the Hout River shear zone (Figure 4.1) and also show magnetitite layering in geophysical maps (Figure 4.18). These magnetitite layers are not seen in the Aurora Project drillcore as they are collared deeper in the sequence.

Secondly, the upper lithologic unit on Harriet's Wish, north of the Hout River shear zone is thinner (~220 m) than the Upper Zone in the northern limb (e.g. at Bellevue ~1188 m; Ashwal *et al.,* 2005) due to later erosion (Kinnaird *et al.,* 2017).

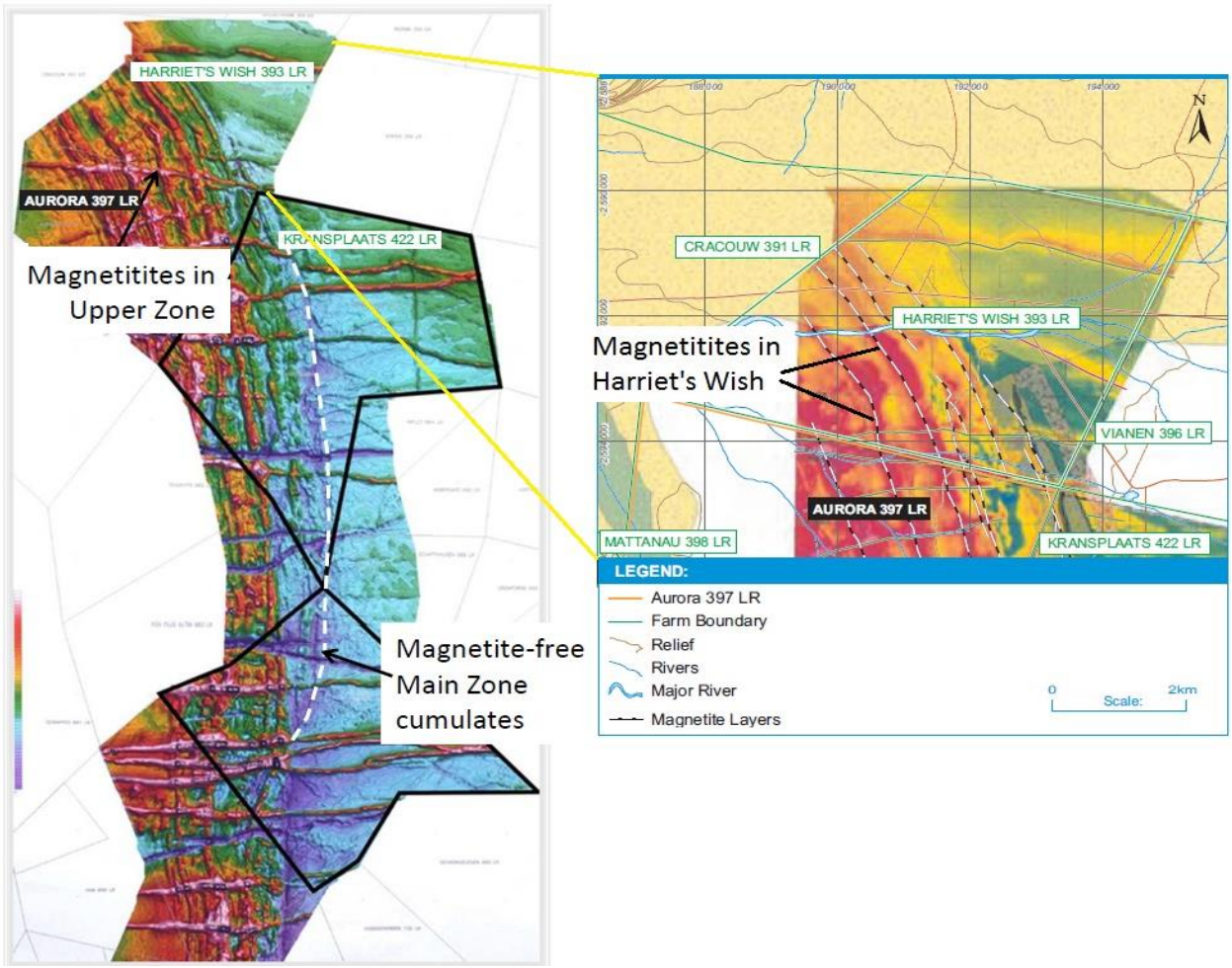

Figure 4.18: Magnetitite layers in the Upper Zone of the northern limb of the Bushveld Complex (left) and on Aurora Project and Harriet's Wish farm (right). Map to the left from Gap geophysics, (2008), map to the right from Sylvania Resources Limited, (2012).

Thirdly, the upper lithologic unit rock types in drillcore HW029 (dominant gabbronorite and gabbro with minor anorthosites) more closely represents the Upper Zone on the Waterberg Project north of the Hout River shear zone (Figure 3.1; Kinnaird *et al.,* 2017), whereas the upper lithologic unit rock types in HW030 (dominant gabbro and magnetite gabbro with minor gabbronorite) more closely represents the Upper Zone, south of the Hout River shear zone (e.g. in the Bellevue drillcore in Ashwal *et al.,* 2005; Eales and Cawthorn, 1996; Kinnaird *et al.,* 2017).

4.4.3 **Cover rocks**

Granites or volcanic rocks overlie the northern limb of the Bushveld Complex (SACS, 1980; Eales and Cawthorn, 1996; Kinnaird *et al.,* 2002; McCreesh, 2013). The hanging wall of the Harriet's Wish igneous succession is not present as it has been tectonised, and the putative Upper Zone correlate (the upper lithologic unit) has an unconformable boundary with the Waterberg Group sediments (Figure 4.14). A similar thick succession of sedimentary rocks also overlies the Bushveld rocks on the Waterberg Project, and these were identified as rocks of Waterberg Group belonging to the Setlaole and Makgabeng Formations (Lomberg, 2013; Jones, 2014; McCreesh, 2016; Kinnaird *et al.,* 2017). These sedimentary rocks were found to be just slightly younger than the Bushveld rocks suggesting that the area north of the Hout River shear zone was uplifted and the Bushveld roof along with the top of the mafic-ultramafic body were eroded shortly after its emplacement (Huthmann *et al.,* 2017; Kinnaird *et al.,* 2017). In this study, it is suggested that sedimentary rocks in the Harriet's Wish drillcores belong to the Waterberg Group, provisionally to the Setlaole Formation, as it is laterally continuous with the sedimentary sequence on the Waterberg Project to the north. Other reasons for this identification include similar rock types, such as arkose, conglomerates and mudstones, similar upward fining and downward coarsening of conglomerates, similar pebble sizes (< 5cm), similar composition of pebbles (mainly quartz and some hematite) and evidence of trough cross bedding in the sandstones, as in the Setlaole Formation. The overall thickness of the sedimentary rocks on Harriet's Wish also falls in the thickness range of the Setlaole Formation (<450 m) and similar to the Setlaole Formation, there also seems to be no visible lithic fragments of Bushveld rocks in the overlying sedimentary rocks on Harriet's Wish (Jansen, 1976, 1982; Callaghan *et al.,* 1991). The observed unconformity between the sedimentary and the igneous rocks on Harriet's Wish and the alteration of rocks close to this contact, that are similar in style to the alteration on the Waterberg Project (Engela, 2014; Kinnaird *et al.,* 20170, suggests that the altered zone represents the Waterberg Group paleosol.

4.4.4 **Harriet's Wish mineralisation**

The Platreef mineralisation is complex and includes reef-style mineralisation hosted in mainly feldspathic pyroxenites and harzburgite (Harris and Chaumba, 2001; Armitage *et al.,* 2002; Kinnaird *et al.,* 2005; McDonald and Holwell, 2011) and contact style mineralisation hosted in highly lithologically diverse packages, which comprise mafic magmatic rocks, hybrid rocks such as parapyroxenite and paraperidotites, and metamorphosed wallrocks transformed into hornfels and calcsilicate (Viljoen and Schürmann, 1998; Kinnaird *et al.,* 2005; Maier *et al.,* 2008; Nex *et al.,* 2008; McDonald and Holwell, 2011). The entire Platreef is not uniformly mineralised and the highest grade can be found at the base (bottom-loaded) and at the top (top-loaded) as well as somewhere in the middle of the Platreef section (middle loaded; Kinnaird *et al.,* 2005). Therefore, the lithology and stratigraphic features of the Platreef hosts are highly variable.

McCreesh, (2016) suggested that the F Zone on the Waterberg Project displays striking lithologic and stratigraphic similarities to the down-dip Platreef on the Akanani Project as outlined in Mitchell and Scoon, (2012). Firstly, a similarity in the thickness of mineralised units is noted, with the Waterberg F Zone ranging from 10-60 m (Kinnaird *et al.,* 2017) and the main ore body on Akanani ranging from 4-30 m (Mitchell and Scoon, 2012), although the entire Platreef on Akanani is >300 m thick (Yudovskaya *et al.,* 2011). Secondly, a similarity in rock type in which the mineralisation occurs, is noted, with the F Zone on the Waterberg Project being hosted in pyroxenite and harzburgite (Kinnaird *et al.,* 2017), and the Platreef mineralisation on Akanani being hosted mainly in feldspathic harzburgite and pyroxenite (Mitchell and Scoon, 2012). Lastly, McCreesh, (2016) notes that both on the Waterberg Project (McCreesh, 2016) and on the Akanani Project (Mitchell and Scoon, 2012), chromitite stringers have been found, although these are rare and inconspicuous on the Waterberg Project (Kinnaird *et al.,* 2017). Yudovskaya *et al.,* (2011), however, reports that these chromite stringers are rather chromitite layers of <1 m thick, which are not similar to the Waterberg Project.

There are some similarities between the F Zone on the Waterberg Project and the mafic-ultramafic mineralised lithology at the base of the magmatic succession on the Aurora Project (McCreesh, 2016; McDonald *et al.,* 2017). Similarities include a correlation in the stratigraphic position above the basement rocks and similarities in some host lithology, such as gabbronorites and leucogabbronorites that cross-cut this mafic-ultramafic unit (McDonald *et al.,* 2017). However, peridotite is absent in this unit on the Aurora Project, which makes these sequences unrelated.

Although stratigraphic and lithologic correlations have been made between the Platreef and the Waterberg Project (McCreesh, 2016), the Platreef and the Aurora projects (Manyeruke *et al.,* 2007; Maier *et al.,* 2008) and between the Aurora Project and Waterberg Project (McDonald *et al.,* 2017), McDonald *et al.,* (2017) asserts that the Aurora Project mineralisation is atypical of the Platreef due to sulphides being hosted predominantly in leucocratic rocks (gabbronorites and leucogabbronorites), rather than mafic-ultramafic rocks, among other geochemical differences noted in Chapter 8. This assertion coincides with the suggestion by Kinnaird *et al.,* (2017) that the characteristics of the stratigraphy on the Waterberg Project, and the igneous sequence north of Hout River shear zone, may be controlled by the unique structure, basement topography and partial magmatic erosion of a separate basin.

When comparing the lower mineralised zone on Harriet's Wish with the mineralisation of the Platreef, some similarities can be seen. Firstly, the mineralisation hosts in both the lower mineralised zone and the Platreef overall are highly variable (Kinnaird *et al.,* 2005). Secondly, the Platreef contains all studied lithologies and mineralisation, which is reported in the lower mineralised zone on Harriet's Wish (Figure 4.4; Kinnaird *et al.,* 2005; McDonald and Holwell, 2011). Thirdly, the stratigraphic position of the Platreef between the Lower Zone (or footwall) and the Main Zone (Kinnaird *et al.,* 2005) agrees well with the position of Waterberg's F Zone and the Harriet's Wish lower mineralised zone (Figure 4.19; Kinnaird *et al.,* 2005; Kinnaird *et al.,* 2017). However, if this correlation holds true for Harriet's Wish, then the upper lithologic unit would be very thin and undeveloped when compared to the northern limb Main Zone and the Waterberg

Project TGA sequence (Eales and Cawthorn, 1996; Ashwal *et al.,* 2005; Kinnaird *et al.,* 2017). Differences between the Platreef and the lower mineralised zone on Harriet's Wish are also pronounced and include the absence of harzburgite and serpentinite as mineralisation host rocks (e.g. at Akanani; Mitchell and Scoon, 2012) and the absence of chromitite stringers on Harriet's Wish (e.g. at Akanani; Mitchell and Scoon, 2012).

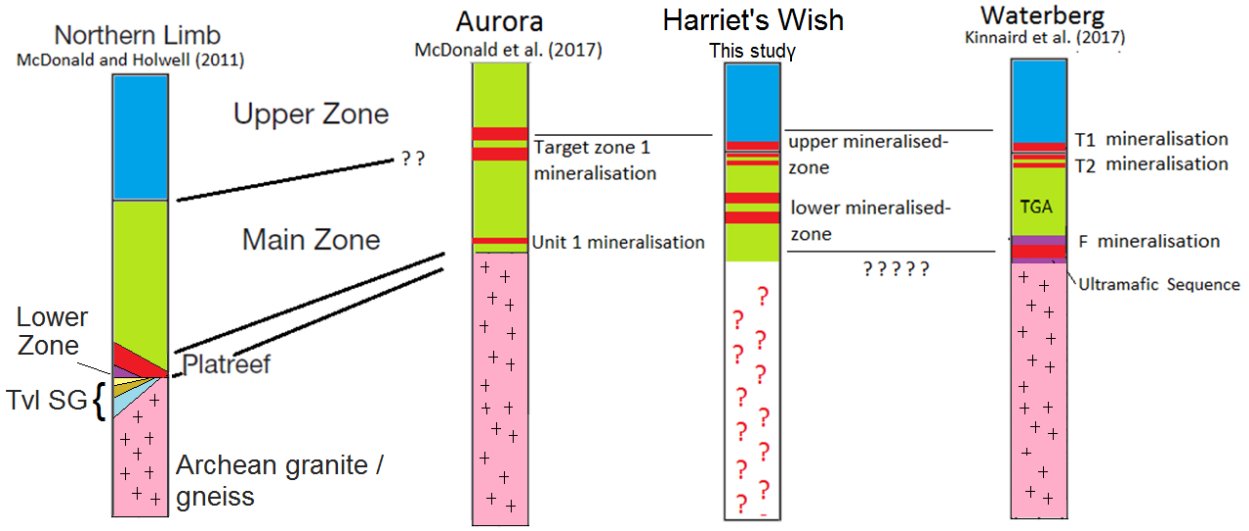

Figure 4.19: Schematic comparison of the positions of stratigraphic units of the northern limb (left), the Aurora succession (middle left), Harriet's Wish (middle right) and the Waterberg succession (right; Figure modified after McDonald and Holwell, 2011). TGA=Troctolite-gabbronorite-anorthosite sequence.

In the exploration report by Sylvania Resources Limited, (2012), a correlation is drawn between the F Zone on the Waterberg Project (Kinnaird *et al.,* 2017), and the lower mineralised zone on Harriet's Wish. Similarities between these areas include 1) a correlation in the stratigraphic position relative to the upper mineralised zone (Figure 4.19), 2) a thickness that falls in the range of the T Zone on the Waterberg Project (~10-60 m; Kinnaird *et al.,* 2017), 3) similarities in some lithology (mainly pyroxenite) and 4) similarities in grade (Sylvania Resources Limited, 2012). According to core logging and visual observations, however, it can be seen that there are some critical differences between these mineralised zones. Firstly, the mineralisation on Harriet's Wish occurs within the lower lithologic unit (or TGA sequence), rather than the Ultramafic Sequence as on the Waterberg Project (Figure 4.19; Kinnaird *et al.,* 2017) and visually it seems to be associated with the more mafic rocks such as leucogabbronorite, leucotroctolite,

olivine pyroxenite, pyroxenite and in minor gabbronorite and olivine bearing leucogabbronorite (e.g. Figures 4.4, 4.5 and 4.6). Secondly, the stratigraphic position of the Harriet's Wish lower mineralised zone is overall higher up, and not at the base of the igneous sequence (Kinnaird *et al.,* 2017). There is, however, a zone of minor sulphides at the base of the HW024 drillcore, over an approximately 40 m interval (Figure 4.16), however, it seems to be unrelated to the main lower mineralised zone due to its stratigraphic position and the lack of host rocks similar to the mineralised zones host rocks in boreholes HW024 and HW025. Thirdly, no harzburgite or serpentinite is seen in the Harriet's Wish drillcores, as with the F Zone (Kinnaird *et al.,* 2017). Lastly, unlike the F Zone (and the Platreef e.g. on Akanani; Mitchell and Scoon, 2012; Kinnaird *et al.,* 2017), no chromite stringers (Mitchell and Scoon, 2012) or chromitite layers (Yudovskaya *et al.,* 2011) were found in the lower mineralised zone in the Harriet's Wish drillcore. It should be added, however, that some Platreef sections in the contaminated sequences are characterised by an absence or paucity of chromitite seams, stringers and dissemination. The absence of chromitites is reported in some intersections at Macalacaskop, Turfspruit and Sandsloot (Kinnaird *et al.,* 2005).

The Harriet's Wish lower mineralised zone also shows similarities to the mineralised Unit 1 gabbronorites and leucogabbronorites on the Aurora Project that cross-cut the pyroxenite (Figure 4.19; McDonald *et al.,* 2017), due to similar host rock types. It is noted that this mineralisation in Unit 1 is not hosted in ultramafic rocks, but rather veins of mafic rocks, cross-cutting olivine-free ultramafic rocks (McDonald *et al.,* 2017). It is possible, therefore, that these gabbronorites and leucogabbronorites are related to the lower mineralised zone on Harriet's Wish. Although, the stratigraphic position of the lower mineralised zone on Harriet's Wish is higher up in the sequence than this.

According to Manyeruke *et al.,* (2007), the xenoliths along strike in the Platreef seem to be controlled by the nature of the floor rocks immediately underlying the Platreef at different localities or the hanging wall as at Drenthe (Gain and Mostert, 1982). It is therefore expected that the floor rocks, at least locally, on Harriet's Wish are dolomitic, due to the calcsilicate xenolith found in drillcore HW029 (Figure 4.10) and may

represent Malmani dolomite, the lowermost unit of the Transvaal sedimentary formations (Buchanan, 1988). According to Ripley, (1999) the incorporation of xenoliths can also allow for sulphide saturation to take place. The ore mineralogy and geochemistry will therefore aim to confirm this assertion, and to see if the xenolith played a part in the formation of the mineralised zones on Harriet's Wish.

Although the Aurora Project mineralisation occurs in the Upper Main Zone (McDonald and Harmer, 2010; McCreesh, 2013; McDonald *et al.,* 2017) and although mineralisation has been found in the Main Zone, e.g. associated with the pyroxenite marker, on the Moordrift farm in the northern limb (Maier and Barnes, 2010), the T Zone on the Waterberg is unique in that it bears such high concentrations of PGE (McCreesh, 2016; Kinnaird *et al.,* 2017). The T Zone on the Waterberg Project occurs at the boundary between the Upper Zone and the TGA sequence and is hosted in a lithologically variable unit of pyroxenite, feldspathic pyroxenites, troctolite to harzburgite and norite to pegmatoidal anorthosite (Lomberg, 2012; McCreesh, 2016; Kinnaird *et al.,* 2017). This mineralised zone sometimes overlaps the boundary and may belong to either the Upper Zone or the TGA sequence (McCreesh, 2016; Kinnaird *et al.,* 2017). The T Zone is divided into a lower- (T2) and an upper (T1) mineralised unit and visible net textured, disseminated and blebby pentlandite, chalcopyrite and pyrite can be seen in this zone (Lomberg and Goldschmidt, 2014; Kinnaird *et al.,* 2017). The T2 mineralisation ranges from 2-15 m in thickness and is hosted in homogeneous gabbronorite or gabbro that is locally pegmatoidal (Kinnaird *et al.,* 2017). Unique features of this unit include the presence of distinctive, elongated milky-white plagioclase <1 cm in size and 5-15% modal abundance of sulphides (McCreesh, 2016). Between the T2 and T1, a 0.2-35 m middling comprised of pegmatoidal leucogabbro or varitextured pegmatoidal anorthosite, however, this middling may be absent (McCreesh, 2016; Kinnaird *et al.,* 2017). In addition to this, pegmatoidal anorthosite commonly overlies the T1 zone (Kinnaird *et al.,* 2017).

The upper mineralised zone on Harriet's Wish correlates well with the T Zone on the Waterberg Project in that it occurs in the same stratigraphic position between the upper

and lower lithologic units, and the overall stratigraphic thickness of the upper mineralised zone (25-45 m) coincides with the T Zone (30-50 m; Kinnaird *et al.,* 2017). The modal abundance of sulphides on Harriet's Wish also coincides with the Waterberg Project (5-15%; McCreesh, 2016), as Harriet's Wish's modal mineralisation ranges from 5-10% in some pegmatoidal gabbronorites. Both the mineralised zones are hosted in a variety of lithologies, such as gabbronorite, melagabbronorite, pegmatoidal gabbronorite and anorthosite (Kinnaird *et al.,* 2017); however, it is seen that the upper lithologic unit on Harriet's Wish contains lithologies more similar to that of the T2 Zone, as there is no troctolite or harzburgite present, and there is no pegmatoidal anorthosite overlying this mineralisation (Kinnaird *et al.,* 2017).

Differences between the upper mineralised zone on Harriet's Wish and the T Zone on the Waterberg Project include the absence of elongated milky white plagioclase in the upper mineralised zone on Harriet's Wish, although some sugar-textured plagioclase is present throughout the upper lithologic unit but is not confined to the upper mineralised zone as with the Waterberg Project (Kinnaird *et al.,* 2017). The upper mineralised zone on Harriet's Wish does not have two well defined divisions such as the T2- and T1 units on the Waterberg Project (Kinnaird *et al.,* 2017); however, Kinnaird *et al.,* (2017) do state that the middling is not always present, so T1 an T2 may be joined. The upper mineralised zone on Harriet's Wish also does not occur both in the upper and lower lithologic units when considering the boundary drawn by field observations, as on the Waterberg Project (Kinnaird *et al.,* 2017); however, the presence of sulphides does not always represent favourable grade (Holwell *et al.,* 2017), furthermore, unseen specks of PGE-bearing sulphides may be present in rock packages that are not incorporated into the visually observed mineralisation zones on Harriet's Wish. The upper mineralised zone is also not hosted in pyroxenites, feldspathic harzburgites or troctolites, whereas the T Zone does contain these host lithologies (Kinnaird *et al.,* 2017); however, as suggested above, the upper mineralised zone on Harriet's Wish more closely represents lithologies of the T2 Zone, which does not contain these ultramafic rocks (Kinnaird *et al.,* 2017). Comparing the mineralisation of only one drillcore to the entire

Waterberg Project also holds obvious challenges, and it is possible that representative features in the may be anomalously absent in the Harriet's Wish drillcore.

The boundary between the TGA and the Upper Zone on the Waterberg project is drawn above the mineralisation, therefore placing the T Zone in the TGA or the lower lithologic unit (Kinnaird *et al.,* 2017), although McCreesh *et al.,* (2018) places the boundary in between the T Zone, with mineralisation straddling the boundary, suggesting that mineralisation was formed during the interaction of Upper Zone melts with the TGA cumulate mush in the resident chamber. On Harriet's Wish, the visual boundary is placed above the upper mineralised zone (Figure 4.16), therefore placing the mineralisation in the upper parts of the lower lithologic unit.

4.5 **Conclusions**

Harriet's Wish does not contain an Ultramafic Sequence as in the Waterberg Project stratigraphy (Kinnaird *et al.,* 2017). This may be deeper in the sequence as boreholes were not drilled to the basement, or this sequence may have been reworked, and possible remnants of olivine-bearing lithologies are found in some of the lower mafic lithologies.

Like the TGA sequence on the Waterberg Project (Kinnaird *et al.,* 2017), the lower lithologic unit can be stratigraphically equated with the Main Zone in the northern limb (e.g. Ashwal *et al.,* 2005), with some mineralogical and lithologic similarities, including the presence of troctolite horizons, however, key differences that are outlined include the lower lithologic unit being thinner overall and the occurrence of a "true troctolite", rather than the olivine-bearing lithologies outlined above. The lower lithologic unit on Harriet's Wish therefore compares better with the TGA unit on the Waterberg Project based on stratigraphy and lithology as observed in the field and in core logging (Kinnaird *et al.,* 2017).

Unlike in the northern limb, there is no pyroxenite marker (Ashwal *et al.,* 2005), or equivalent, whether orthopyroxene-rich or clinopyroxene-rich on Harriet's Wish. The

boundary between the upper and lower lithologic units is more similar to the boundary between the Upper Zone and TGA unit at the Waterberg project (Kinnaird *et al.,* 2017). On Harriet's Wish, there is also associated mineralisation confined to the contact zone between these two units similar to the Waterberg project.

The upper lithologic unit on Harriet's Wish can be compared to the Upper Zone in the northern limb of the Bushveld Complex (Eales and Cawthorn, 1996; Ashwal *et al.,* 2005). This is based on stratigraphic correlation, and lithologic similarity. The upper lithologic unit on Harriet's Wish is significantly thinner than the Upper Zone everywhere else (Eales and Cawthorn, 1996). However, this reduced thickness is not a primary feature, but rather as a result of later erosion during the early Proterozoic, shortly after the emplacement as was shown for the Waterberg section (Kinnaird *et al.,* 2017). There are also no magnetitite layers in the Upper Zone on the Waterberg project, except for one drillcore which was drilled south of the Hout River shear zone. Similarly, magnetitite layering is absent in the studied intersections on Harriet's Wish, north of the Hout River shear zone, except for in the HW030 drillcore, which occurs in the Hout River shear zone. This borehole intersected massive and disseminated magnetites and the prominent magnetitite layers are exposed on the surface and traced on the aeromagnetic maps within the property (Sylvania Resources Limited, 2012). Therefore, magnetite layering seems to be absent north of the Hout River shear zone.

The lower mineralised zone on Harriet's Wish differs from the F Zone on the Waterberg project due to the mineralisation occurring in more leucocratic rocks than the F Zone (McCreesh, 2016; Kinnaird *et al.,* 2017). A thick Ultramafic Sequence containing harzburgitic and orthopyroxenitic bodies host the F Zone on the Waterberg Project (Kinnaird *et al.,* 2017) and according to field observations and core logging, there are no thick ultramafic layers on Harriet's Wish, therefore, the lower mineralised zone does not appear in the same lithologic unit as the F Zone (McCreesh, 2016; Kinnaird *et al.,* 2017). Although the visual observations and core logging places the lower mineralised zone on Harriet's Wish in the TGA sequence, it is important to confirm this through CIPW normative mineralogy and petrography to see whether the host rocks of this

mineralisation could have perhaps been hybridised towards more gabbroic compositions. The upper mineralised zone on Harriet's Wish and the T Zone on the Waterberg Project show important correlations, such as similarities in thickness, stratigraphic position and lithologies, therefore it is suggested based on visual observations that these equate with one another.

The sedimentary succession overlying the Harriet's Wish igneous succession visually correlates with the Setlaole Formation rocks that overlie the Waterberg Project igneous succession.

Therefore, although the stratigraphic units on Harriet's Wish can be broadly correlated with the stratigraphy in the northern limb of the Bushveld Complex, there are distinct differences in overall lithology and mineralogy. There are notable similarities between the Harriet's Wish stratigraphic units, lithology and mineralogy, and the Waterberg Project stratigraphy, and therefore, these areas provisionally represent a separate basin to the north of the Hout River shear zone. However, petrographic, geophysical, geochemical and ore mineralogical study will assist in confirming these observations.

Chapter 5
Magnetic Susceptibility

5.1 Introduction

The base of the Upper Zone of the Bushveld Complex has been commonly taken at the first visible appearance of cumulus magnetite (SACS, 1980; Knoper and Von Gruenewaldt, 1996). In addition to this, the Pyroxenite Marker horizon, at ~600-700 m below this, has also been used to define the Main Zone-Upper Zone boundary, on the basis of significant changes in petrology and isotopic signatures, such as a shift in the Sr isotope signatures (e.g. Kruger *et al.,* 1987; Kruger, 1990). Ashwal *et al.,* (2005), however, states that the Pyroxenite Marker is absent in the northern limb, and proposed that a shift in magnetic susceptibility values, rather than visual observations, should be used to determine the base of the Upper Zone, as small disseminated specks of magnetite is present well below the visible magnetite.

The magnetic susceptibility of a material indicates whether a material is attracted into or repelled out of a magnetic field (IUPAC, 1997). According to IUPAC, (1997) magnetic susceptibility is a dimensionless proportionality constant that indicates the degree of magnetisation of a material in response to an applied magnetic field. The magnetic susceptibility meter, therefore, applies a magnetic field, and picks up on the magnetisation of seen and unseen (due to small size) material in the core logs, such as magnetite (Ashwal *et al.,* 2005). The measured magnetic susceptibility values for titanomagnetite ranges from 1 to 50 SI units, depending on the grain size (Clark and Emerson, 1991). The magnetite throughout the Upper Zone has varying Ti and V contents (Molyneux, 1972; Reynolds, 1985); however, Ashwal *et al.,* (2005) states that this has little or no effect on the magnetic susceptibility values. Secondary magnetite, that are forms due to the alteration of olivine-rich units, and sulphides, such as pyrite- FeS_2, chalcopyrite- $CuFeS_2$, pyrrhotite- $Fe_{(x-1)}S$ and pentlandite- $(Fe, Ni)_9$ S_8, may also be responsible for high magnetic susceptibility readings (McCreesh, 2016).

Ashwal *et al.,* (2005) used a large database of geophysical, petrological and mineralogical evidence of approximately 3000 m of Bellevue drill core to support this concept. This drill core spans through about half of the Main Zone and the entire Upper Zone of the northern limb of the Bushveld Complex. In their study, Ashwal *et al.,* (2005) suggest that magnetic susceptibility data clearly reveal the Main Zone-Upper Zone boundary. Main Zone cumulates showed susceptibility values of <0.05 SI units but was generally <0.02 SI units. Above the Main Zone/Upper Zone boundary, susceptibility varied immensely, from anorthosite (<0.1 SI units) to magnetite (~5 SI units). There was also an excellent correlation found between susceptibility values and lithology, in many cases to a resolution of ≥5 up to 10 cm (Ashwal *et al.,* 2005).

This work has been monumental for the exploration industry, as PTM now uses the magnetic susceptibility technique to correlate the Main Zone/Upper Zone boundary to aid in its exploration for T Zone mineralisation on the Waterberg Project (Kinnaird *et al.,* 2017). This technique is utilised as it is reliable, cost effective method, and correlation of the boundary can be made reliably across all boreholes (McCreesh, 2016).

In Figure 5.1, the magnetic susceptibility profiles through drillcore on the Waterberg project, north of the Hout River shear zone and north of Harriet's Wish are outlined. These profiles reveal that the highest magnetic susceptibility values occur in the Ultramafic Sequence where it is composed of harzburgite (Kinnaird *et al.,* 2017). This is due to pyrrhotite that occurs in the mineralised zones and secondary magnetite, which formed during serpentinisation of olivine (McCreesh, 2016; Kinnaird *et al.,* 2017).

The magnetic susceptibility values decrease upward throughout the TGA sequence as olivine decreases upwards from the troctolite to the gabbronorite-dominated lithology which become olivine-free (McCreesh, 2016; Kinnaird *et al.,* 2017). The overall values in the TGA sequence are very low (Figure 5.1). In the T2 Zone, magnetic susceptibility values range from 0.01 to 3.00 SI units (McCreesh, 2016; Kinnaird *et al.,* 2017). In the T1 zone, values are from 0.01 to 5.00 with maximum values of <12.00 SI units, which are associated with olivine-rich intervals (Kinnaird *et al.,* 2017). Towards the top of this

succession, the magnetic susceptibility becomes consistently higher as primary crystallised magnetite is introduced due to the influx of the Upper Zone magma (Kinnaird *et al.,* 2017). Distinct chemical changes support this rationale (McCreesh, 2016; Kinnaird *et al.,* 2017). The boundary between the TGA sequence and Upper Zone intersects the T Zone; placing the T Zone in the both the Upper Zone and the TGA zone (Kinnaird *et al.,* 2017). This can be seen in drillcore WB027 (Figure 5.1)

There is no available magnetic susceptibility data for the Aurora Project.

5.1.1 **Aims**

The primary aim in doing a magnetic susceptibility survey is to determine the presence of the exact boundary between the lower and upper lithologic units. This will assist in clarifying whether the upper mineralised zone occurs in the lower, upper or both the lower and upper lithologic units as on the Waterberg Project (Kinnaird *et al.,* 2017; McCreesh *et al.,* 2018). This will therefore aid in the interpretation of whether the upper mineralised zone is of upper or lower magmatic origin.

5.2 **Methods**

Magnetic susceptibility values of the HW024, HW025 and HW029 drillcores were acquired during August of 2017. A Kappa-Meter KM-7 pocket magnetic susceptibility meter was used to obtain these readings. A total of 772 metres over the three cores were measured with one metre spacing between readings. For accuracy, at each depth, three readings were taken from which the average values were calculated. Readings were recorded digitally onto an Excel spreadsheet. Magnetic susceptibility values were plotted against lithology intervals using the Golden-Software's Strater ® 5 Software package.

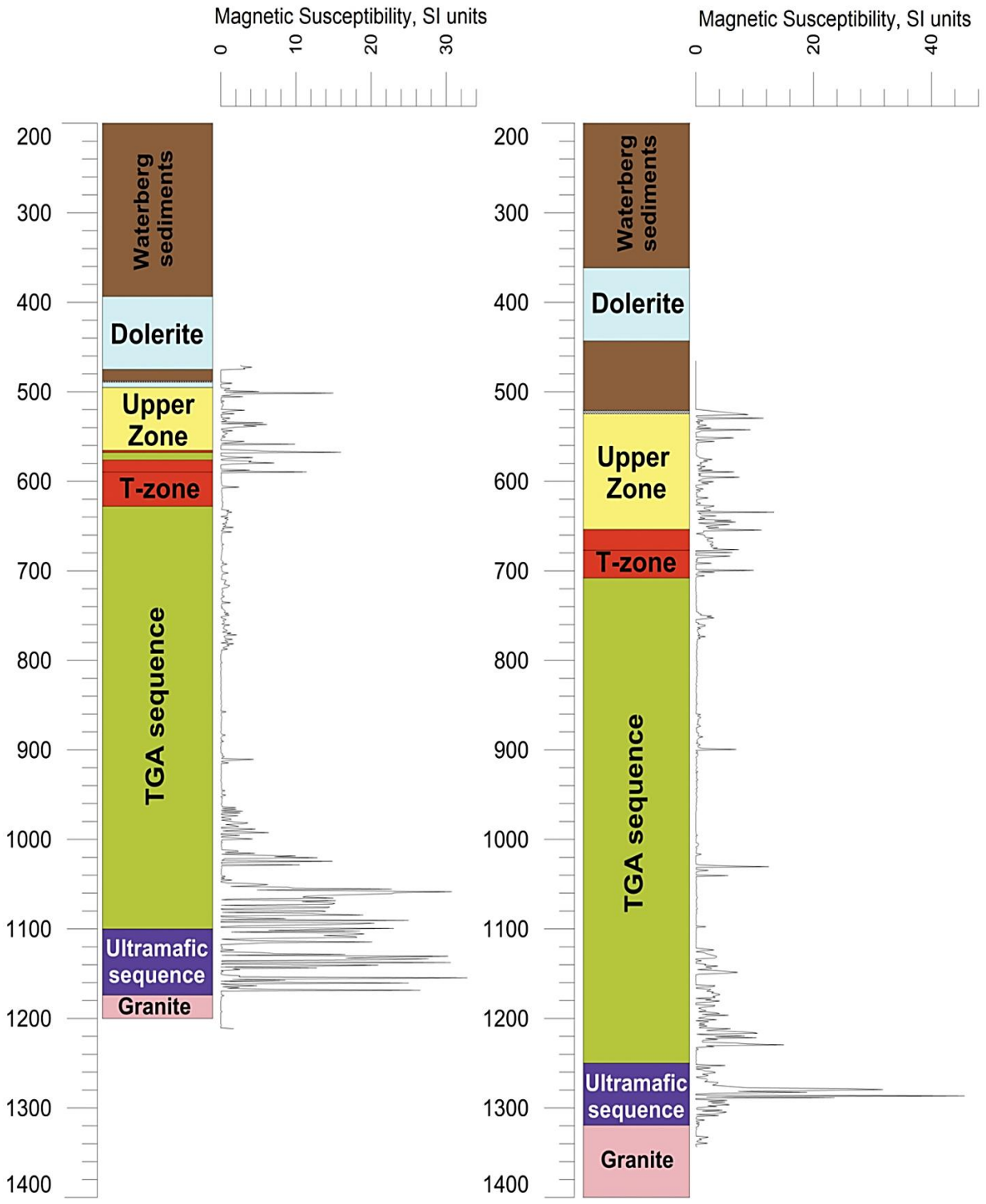

Figure 5.1: Magnetic susceptibility values (SI units) plotted against the depth of the WB027 (left) and WB099 (right) drillcores on the Waterberg Project (Kinnaird *et al.,* 2017). The thin black line through the T Zone represents the boundary between the T1 and T2 zones.

This was done to aid in the interpretation of rock type, distinguishing the upper lithologic unit from the lower lithologic unit and to correlate mineralised zones between boreholes on Harriet's Wish and between Harriet's Wish and the Waterberg Project (Kinnaird *et al.,* 2017). This method is preferred to maintain uniformity with the way in which boundaries on the Waterberg Project (Kinnaird *et al.,* 2017) and on Bellevue (Ashwal *et al.,* 2005) were determined.

Magnetic susceptibility values were sometimes difficult to take due to missing, or broken core, in which case, readings were taken closest to the 1 m interval mark. All the raw data from the magnetic susceptibility readings is present in Appendix E. The mineralisation displayed in core logs in Chapter 4, is identified based on visual observation of sulphide minerals (Figure 4.16). Assay data is not used in this chapter to identify mineralised zones as visually observed iron in sulphides, that may not contain significant PGE grade, may show an increase in magnetic susceptibility values.

5.3 Results

Based on the magnetic susceptibility readings, profiles through the HW024, HW025 and HW029 drillcores were created. Each is presented below:

5.3.1 Magnetic susceptibility readings for the HW024 drillcore

The magnetic susceptibility profile the HW024 drillcore is presented in Figure 5.2. Overall, the magnetic susceptibility values through this drillcore is close to 0, however, some spikes in these values are observed which correspond to change in lithology or mineralogy.

At 450 m depth, the magnetic susceptibility values spike to >8 (SI units). This is probably due to the presence of sulphides that are seen in the lower gabbronorite. At 422 m depth, close to the boundary between Bushveld rocks and the Waterberg Group sedimentary rocks the magnetic susceptibility values reach <17 (SI units). This is due to the alteration of the paleosol to hematite (Figures 4.14 and 4.15 b). From 447-392 m

depth the magnetic susceptibility values are ~0 (SI units), with slight elevations seen over olivine bearing packages. At 390 m depth, the magnetic susceptibility values spike to >20 (SI units). This spike correlates with a ~2 m olivine-bearing norite, which contains secondary magnetite. From 390-272 m depth the magnetic susceptibility values are ~0 (SI units), with slight elevations seen over the troctolite and olivine-rich packages. At 272 m depth there is another spike in magnetic susceptibility values of <20 (SI units). This spike is due to a locally observed secondary magnetite (Appendix A). At ~266 m depth, there is a spike in magnetic susceptibility values of <16 (SI units). This spike is correlated with the contact between the Bushveld rocks and the Waterberg Group sedimentary rocks. At 255 m depth, in the Waterberg Group sedimentary rocks, the magnetic susceptibility values are 0-1.5 (SI units) due to these Waterberg Group sedimentary rocks being mainly siliceous (Figure 4.14).

5.3.2 **Magnetic susceptibility readings for the HW025 drillcore**

The magnetic susceptibility profile of the HW025 drillcore is presented in Figure 5.3. Overall, the magnetic susceptibility values through this drillcore is close to 0, however, some spikes in the magnetic susceptibility values are observed that correspond to change in lithology or mineralogy.

From 610-577 m depth, the magnetic susceptibility values spike irregularly >60 (SI units) over the troctolite, pyroxenite and olivine rich packages. This interval also contains visible sulphide mineralisation in addition to secondary magnetite. From 576-450 m depth the magnetic susceptibility values are ~0-5 (SI units), with slight elevations seen locally over gabbronorite and olivine bearing gabbronorite, due to secondary magnetite. At 449 m depth, the magnetic susceptibility values spike to >20 (SI units). This spike correlates with a ~1 m olivine rich pyroxenite, which contains secondary magnetite as well as visible sulphide specks (Appendix A). From 449-423 m depth, the magnetic susceptibility values are ~0 (SI units) over a gabbronorite package that contains no visible sulphides or magnetite. At 422 m depth, there is spike in magnetic susceptibility values of <20 (SI units). This spike occurs over a 1 m package of pegmatoidal gabbronorite that has secondary grains of magnetite (<3 cm). There are no

spikes seen in magnetic susceptibility values over contact between the Waterberg Group sedimentary rocks and Bushveld rocks. At 410 m depth within the Waterberg Group sedimentary rocks (Figure 5.3), the magnetic susceptibility values are 0 (SI units) due to these being mainly siliceous (Figure 4.14).

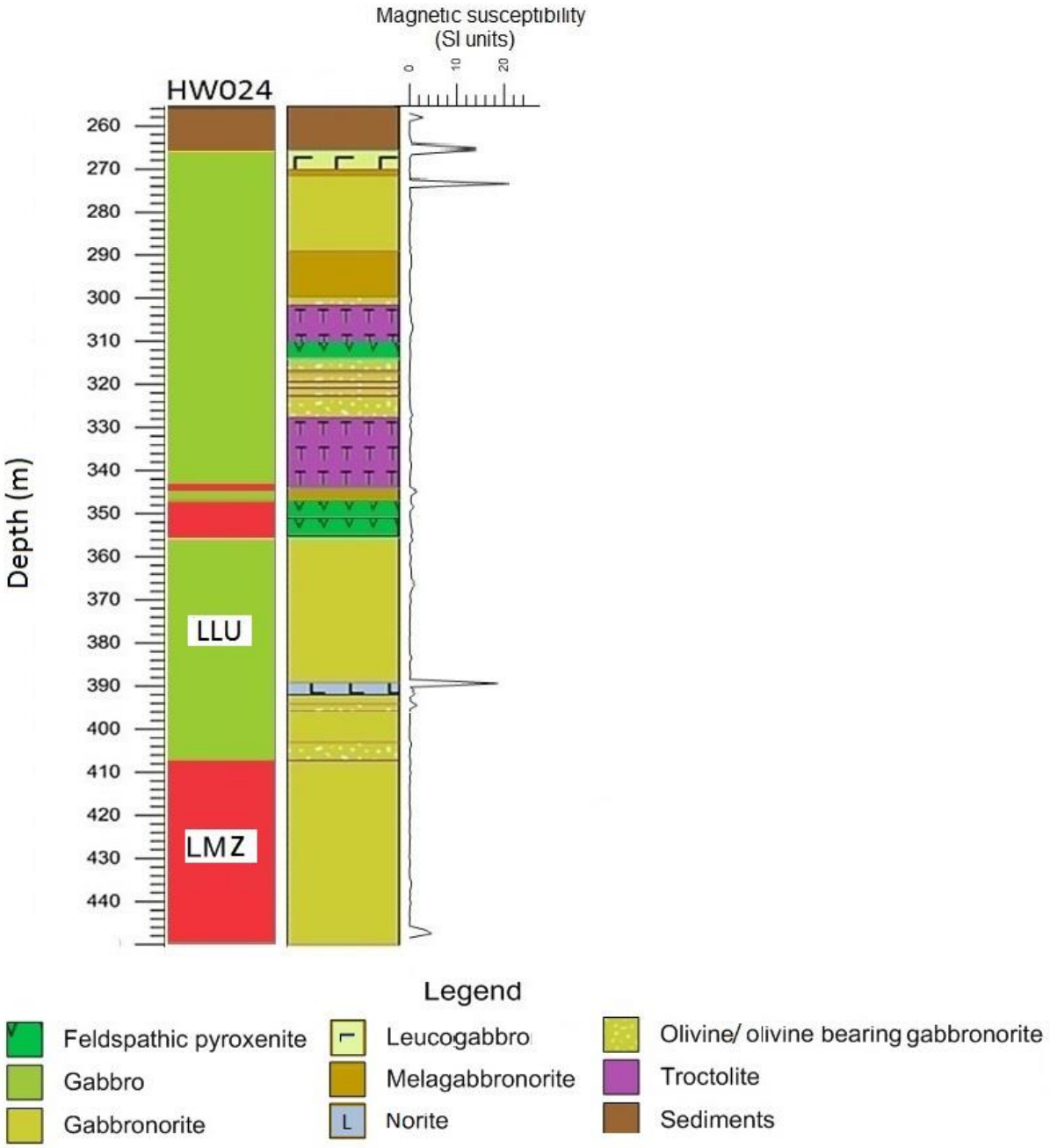

Figure 5.2: Magnetic susceptibility (SI units) profile of the HW024 drillcore on Harriet's Wish. The log on the left shows the lower lithologic unit and the lower mineralised zone based on visual observation of sulphides and the log on the right shows lithologies as logged in Chapter 4. LLU=lower lithologic unit, LMZ=lower mineralised zone.

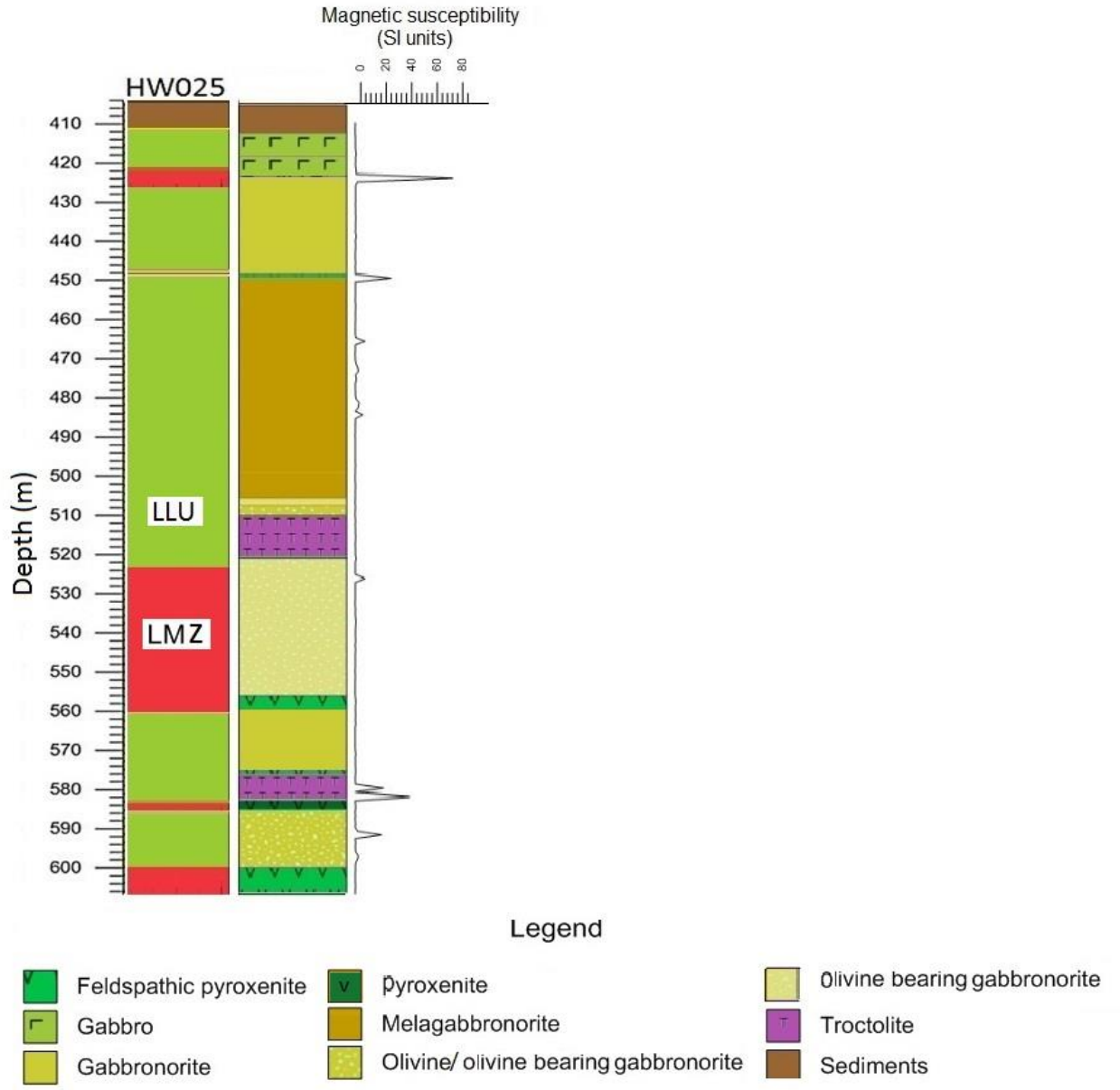

Figure 5.3: Magnetic susceptibility (SI units) profile of the HW025 drillcore on Harriet's Wish. The log on the left shows the lower lithologic unit and the lower mineralised zone based on visual observation of sulphides, the log on the right shows lithologies as logged in Chapter 4. LLU=lower lithologic unit, LMZ=lower mineralised zone.

5.3.3 **Magnetic susceptibility readings the HW029 drillcore**

The magnetic susceptibility profile of the HW029 drillcore is presented in Figure 5.4.

From 722-610 m depth, the magnetic susceptibility values are ~0 (SI units). There are no magnetite grains or sulphides seen in this interval (Appendix A). There are also no olivine-enriched lithologies in this interval. From 609-362 m depth in the HW029 drillcore, magnetic susceptibility values consistently vary between 0-20 (SI units) with an average of 6 (SI units), reaching a maximum of >60 (SI units). This is due to abundant seen and unseen primary/cumulus magnetite, secondary magnetite in altered intervals, and iron rich sulphides (Figures 4.11 and 4.13). There are no spikes seen in magnetic susceptibility values across the contact between the Waterberg Group sedimentary rocks and Bushveld rocks. At 360 m depth within the Waterberg Group sedimentary rocks, the magnetic susceptibility values are ~0 (SI units) due to the Waterberg Group sedimentary rocks being mainly siliceous (Figure 4.15 a).

5.4 **Discussion**

Although iron sulphides and secondary magnetite also emit a magnetic field (Sagnotti, 2007), and although the Ti and V content of magnetite varies throughout the Upper Zone in the northern limb (Cawthorn and Molyneux, 1986; Ashwal *et al.,* 2005), the use of magnetic susceptibility is considered to be a reliable method in determining the boundary between the Main and Upper Zones in, and to the north of the northern limb, as well as the position of the T Zone on the Waterberg Project (Ashwal *et al.,* 2005; Kinnaird *et al.,* 2017). It is also important to note that sulphides on Harriet's Wish are only present in small proportions and are confined to certain zones (Figures 5.2, 5.3 and 5.4) and the variation of Ti and V content of magnetite does not affect the magnetic susceptibility values throughout the drillcore (Cawthorn and Molyneux, 1986; Clark and Emerson, 1991; Clark, 1997; Ashwal *et al.,* 2005).

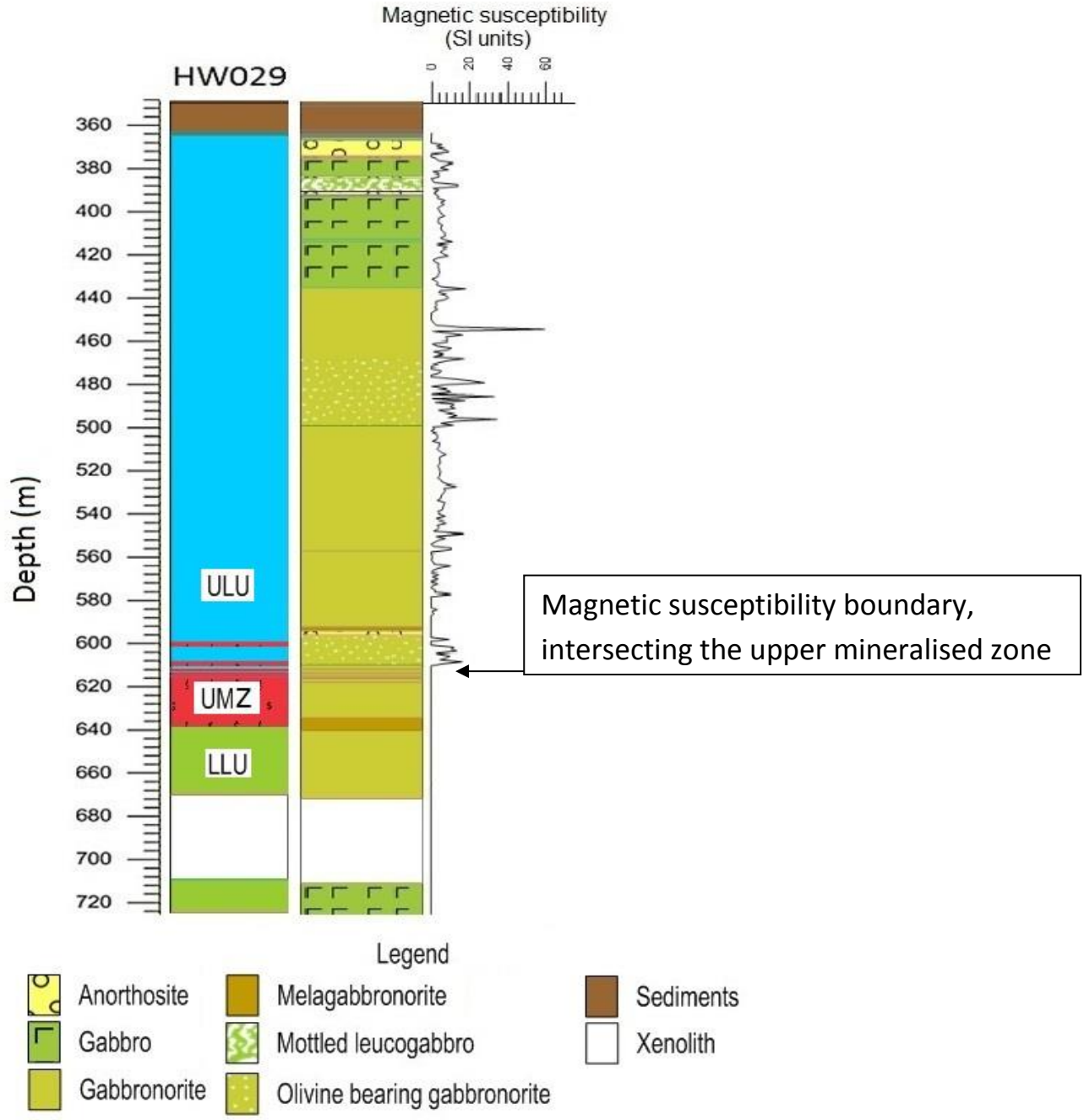

Figure 5.4: Magnetic susceptibility (SI units) profile of the HW029 drillcore on Harriet's Wish. The log on the left shows lower and upper lithologic units and the upper mineralised zone based on visual observation of sulphides, the log on the right shows lithologies as logged in Chapter 4. LLU=lower lithologic unit, ULU=upper lithologic unit, UMZ=upper mineralised zone.

According to the practice of using magnetic susceptibility values to define the boundary between the Main and Upper Zones (Ashwal *et al.,* 2005; Kinnaird *et al.,* 2017), Harriet's Wish drillcores reveal the existence of a lower and an upper lithological unit (Figures 5.2, 5.3 and 5.4). The HW024 and HW025 drillcores represent lithologies of the lower lithologic unit only, due to the generally lower magnetic susceptibility values (~0 SI units; Figures 5.2 and 5.3), and due to the lack of observed primary/cumulus magnetite in the drillcore (Chapter 4). The HW029 drillcore represents lithologies of the lower and upper lithologic units as a shift in magnetic susceptibility values from ~0 to ~20 (SI units) occurs at 610 m depth (Figure 5.4). This shift at ~610 m depth is interpreted to be the boundary between these two lithologic units.

In terms of magnetic susceptibility results, these lithologic units are comparable to the Main and Upper Zones in the northern limb (Ashwal *et al.,* 2005) as well as the TGA sequence and the Upper Zone on the Waterberg Project (Kinnaird *et al.,* 2017; McCreesh *et al.,* 2018). These lithologic units are discussed below:

On the Waterberg Project there is a pronounced increase in magnetic susceptibility values over the Ultramafic Sequence (<50 SI units), which hosts the F Zone mineralisation (Figure 5.1; Kinnaird *et al.,* 2017). Core logging on Harriet's Wish did not reveal the presence of an Ultramafic Sequence as seen in the Waterberg stratigraphy (Kinnaird *et al.,* 2017), however, there is a zone of increased magnetic susceptibility (<60 SI units) seen in the lower lithologic unit in the HW024 drillcore (Figure 5.3). On the Waterberg Project these elevations occur at the base of the succession (Kinnaird *et al.*, 2017), whereas on Harriet's Wish, these values occur towards the base of the drillcore, which may extend deeper, and seem to be associated with olivine- and olivine-bearing lithologies such as olivine gabbronorites, pyroxenites and troctolites. This elevation in magnetic susceptibility readings, however, is not seen in the HW025 drillcore (Figure 5.2) and the mineralisation in the lower lithologic unit is not confined to this zone of increase in magnetic susceptibility, as is seen on the Waterberg Project (Figure 5.1).

The magnetic susceptibility values through the Waterberg Project TGA sequence (0-3 SI units: Kinnaird *et al.,* 2017) and through Bellevue Main Zone (0-0.05 SI units; Ashwal *et al.,* 2005) are generally very low. In the lower lithologic unit on Harriet's Wish the magnetic susceptibility values are also very low (0-5 SI units, >60 maximum) but are generally higher than the TGA sequence on Waterberg and the Main Zone on Bellevue. This could also be due to sample biasing, the increased presence of iron sulphides (Figure 4.5 d) or secondary magnetite as Harriet's Wish drillcores show significant alteration.

The T Zone mineralisation on the Waterberg Project occurs above and below the boundary between the TGA sequence and the Upper Zone (Figure 5.1; Kinnaird *et al.,* 2017). In Chapter 4, the visual boundary on Harriet's Wish was not fully consistent with the boundary on the Waterberg Project, as the upper mineralised zone on Harriet's Wish occurred below the boundary (Figure 4.16). However, magnetic susceptibility values, reveal a boundary on Harriet's Wish at 610 m depth that is ~20 m lower than the visual boundary (Figure 5.4), placing the upper mineralised zone in both the upper and lower lithologic units, which is consistent with the boundary on the Waterberg Project (Figure 5.1; Kinnaird *et al.,* 2017).

The magnetic susceptibility values through the Waterberg Project Upper Zone (0-15, max. 40 SI units; Kinnaird *et al.,* 2017) and through Bellevue Main Zone (0-5 SI units; Ashwal *et al.,* 2005) are consistently higher than the TGA sequence and the Main Zone, respectively. Cumulus or primary magnetite is primarily responsible for this overall increase (Ashwal *et al.,* 2005; Kinnaird *et al.,* 2017). Similarly, the magnetic susceptibility values through the Harriet's Wish upper lithologic unit (0-20, max. 60) are also consistently higher than the lower lithologic unit (Figure 5.4). Disseminated magnetite is primarily responsible for the significant increase in magnetic susceptibility values. Magnetite is especially prominent in gabbronorite and gabbro (e.g. in Figures 4.11 a and 4.12 c). However, the maximum values on Harriet's Wish tend to be higher than the TGA sequence and the Main Zone. This could also be due to sample biasing,

the presence of iron sulphides, secondary magnetite or differences in instrument calibration.

It is therefore interpreted that a separate, magnetite-enriched magma formed the upper lithologic unit on the Harriet's Wish farm. This magma is provisionally hypothesised to be analogous to the Upper Zone magma on the Waterberg Project (Kinnaird *et al.,* 2017; McCreesh *et al.,* 2018). Due to the upper mineralised zone occurring in both the upper and lower lithologic units, it is suggested that an S-rich Upper Zone magma intruded a crystal mush lower lithologic unit, after which some sulphides leached into the upper parts of the lower unit, together forming the upper mineralised zone. To confirm this; however, careful ore mineralogical and geochemical analyses need to be performed.

Furthermore, correlations have been drawn between the T Zone mineralisation on the Waterberg Project (Kinnaird *et al.,* 2017) and the upper mineralisation on the Aurora Project (McDonald *et al.,* 2017). If these correlations hold true, it is suggested that magnetic susceptibility values may place the Aurora upper mineralisation at the boundary between the Upper and Main Zones, rather than in the Upper Main Zone (McDonald *et al.,* 2017), as is observed on the Waterberg Project (Kinnaird *et al.,* 2017) and on Harriet's Wish.

5.5 **Conclusions**

Magnetic susceptibility aids in the identification of a boundary that separates the lower and upper lithologic unit at 610 m depth, based on drillcore HW029. The upper mineralised zone correlates, in terms of stratigraphic position and magnetic susceptibility profiles, to the T Zone on the Waterberg Project, whereas the lower mineralised zone does not correlate with the F Zone on the Waterberg Project in terms of stratigraphic position and magnetic profile (Kinnaird *et al.,* 2017). It is possible that an Ultramafic Sequence may occur beneath the lower lithologic Unit because all the boreholes did not extend into the footwall rocks.

5.6 **Recommendations**

It is recommended that a magnetic susceptibility survey should be done on the Aurora Project drillcores in order to better compare with the Harriet's Wish and the Waterberg Project sequences.

Chapter 6
Petrography

6.1 Introduction

Petrographic microscopy is used to define textures, to identify minerals, to determine modal abundances of minerals and to classify rock types in detail (www.zeiss.com). In this chapter, representative samples from the lower and upper lithologic units and mineralised zones were used for petrographic studies.

6.1.1 Aims

This chapter is aimed at confirming classifications of rock types and identifications of minerals outlined in Chapter 4, and to describe in detail the textures, modal mineralogical abundances, mineral associations, PGE mineralisation and alteration intensity of various samples throughout the stratigraphy on Harriet's Wish. This chapter also aims at comparing the petrography and mineralisation of Harriet's Wish samples to samples of the Waterberg and Aurora Projects (Kinnaird *et al.,* 2017; McDonald *et al.,* 2017; Huthmann *et al.,* 2018; McCreesh *et al.,* 2018).

6.2 Methods

The petrography of the lower and upper lithologic units as well as the lower and upper mineralised zones was described using 32 of the 117 samples from the HW024, HW025 and HW029 boreholes. The set of slabs for petrographic analyses comprised typical lithologies, mineralised samples and rocks with interesting or special features, which would be indicative of specific lithologic units and zone. A target area on each selected sample was identified for the making of polished thin sections in the laboratory of the University of the Witwatersrand. Thin sections were described using a petrographic microscope at the University of the Witwatersrand. The mineralised intervals are best observed in reflected light, therefore, descriptions were both under transmitted- and reflected light, depending on what was being analysed. The modal mineralogical

abundances were estimated by using the percentage of area that each mineral occupies within each sample.

6.2.1 **Rock classification**

The classification scheme in this chapter will be the same classification scheme that is used in Chapter 4 (the IUGS standard for igneous rock classification; Le Bas and Streckeisen, 1991). The rock nomenclature that will be used in this chapter will also be the same nomenclature as outlined in Chapter 4.

6.3 **Results**

For a comprehensive table describing each thin section see Appendix B. Petrographic images of concern of the rock types that are found on Harriet's Wish are shown in Figures 6.1 and 6.2 and descriptions are presented below:

6.3.1.1 *Gabbronorite*

Gabbronorite is the most common rock type of the lower lithologic unit and it occurs in the following varieties: gabbronorite, leucogabbronorite, melagabbronorite olivine gabbronorite and olivine-bearing gabbronorite. The varieties of gabbronorite alternate irregularly throughout the lower lithologic unit. The rock texture is inequigranular to equigranular and the various crystals show an interlocking texture. The grain size overall is medium ranging between 1-6 mm in diameter except for pegmatoidal melagabbronorite, in which case the grains are <4 cm in size. Gabbronorite in the lower lithologic unit is more melanocratic than gabbronorite in the upper lithologic unit and comprises 35-65% plagioclase, 10-50% clinopyroxene, 15-40% orthopyroxene and <10% pigeonite in thin section samples. Plagioclase inclusions are seen in poikilitic orthopyroxene and clinopyroxene. Abundant carlsbad and albite twinning is seen in plagioclase. Some twins are deformed showing tapered polysynthetic twinning. Clinopyroxene forms euhedral grains as well as exsolutions and smaller grains inside orthopyroxene grains. Sulphide grains are present as small disseminated specks to pegmatoidal grains and range from 0.02-2 cm in size.

6.3.2 **Lower lithologic unit**

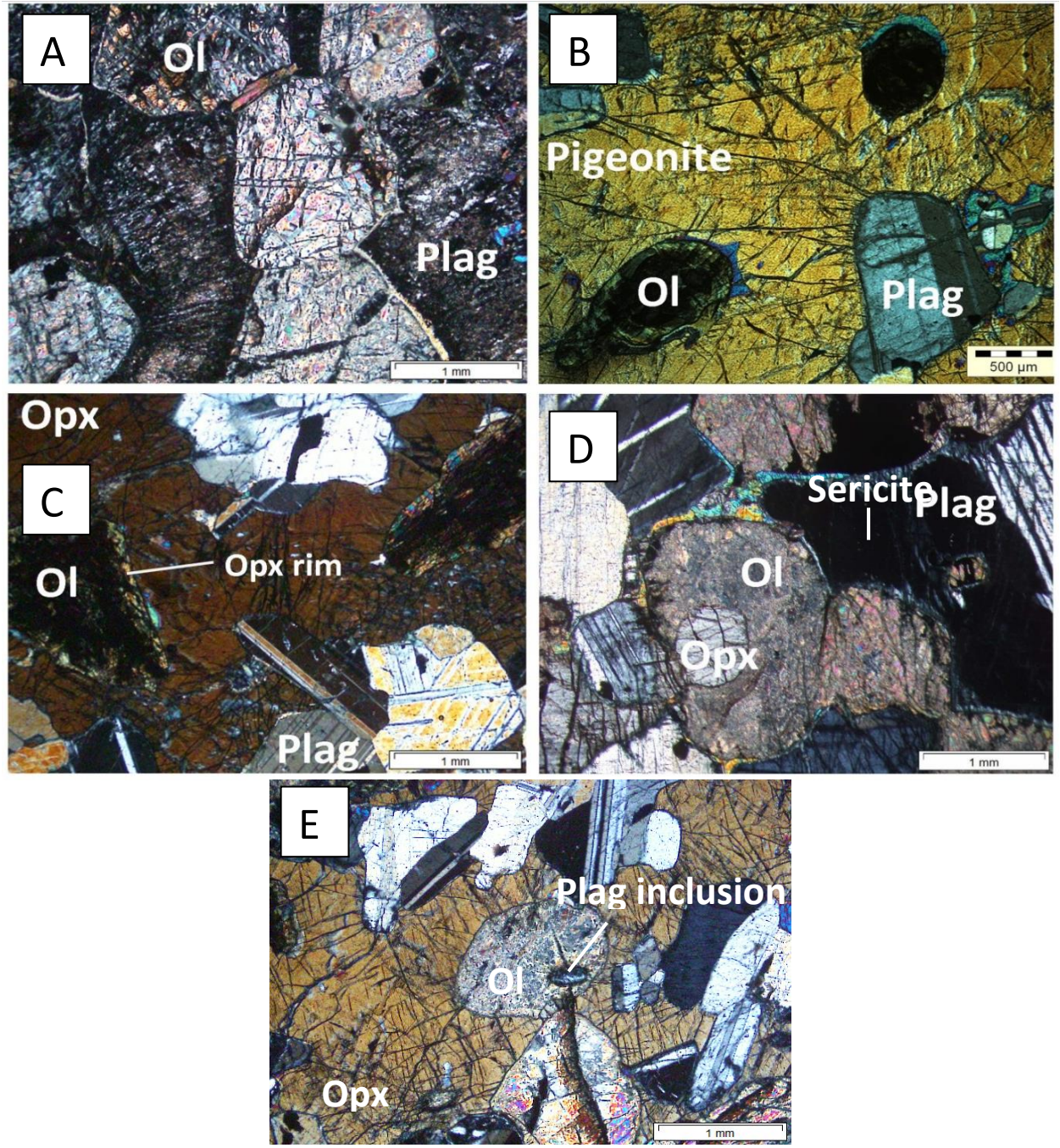

Figure 6.1: Rock textures of the lower lithologic unit on Harriet's Wish under transmitted light. A: Olivine and plagioclase in troctolite from HW024 at a depth of 306 m. B: Altered olivine and plagioclase chadacrysts in pigeonite in olivine melagabbronorite from HW024 at a depth of 314.5 m. C: Olivine with orthopyroxene rim, orthopyroxene and plagioclase laths in orthopyroxene in troctolite from HW024 at a depth of 306 m. D: Orthopyroxene in olivine and olivine in plagioclase in olivine feldspathic pyroxenite from HW024 at a depth of 348.4. E: Plagioclase inclusion in olivine pyroxenite of HW024 at a depth of 314.5 m. Abbreviations: Plag= plagioclase, Cpx= clinopyroxene, Opx= orthopyroxene, Ol= olivine.

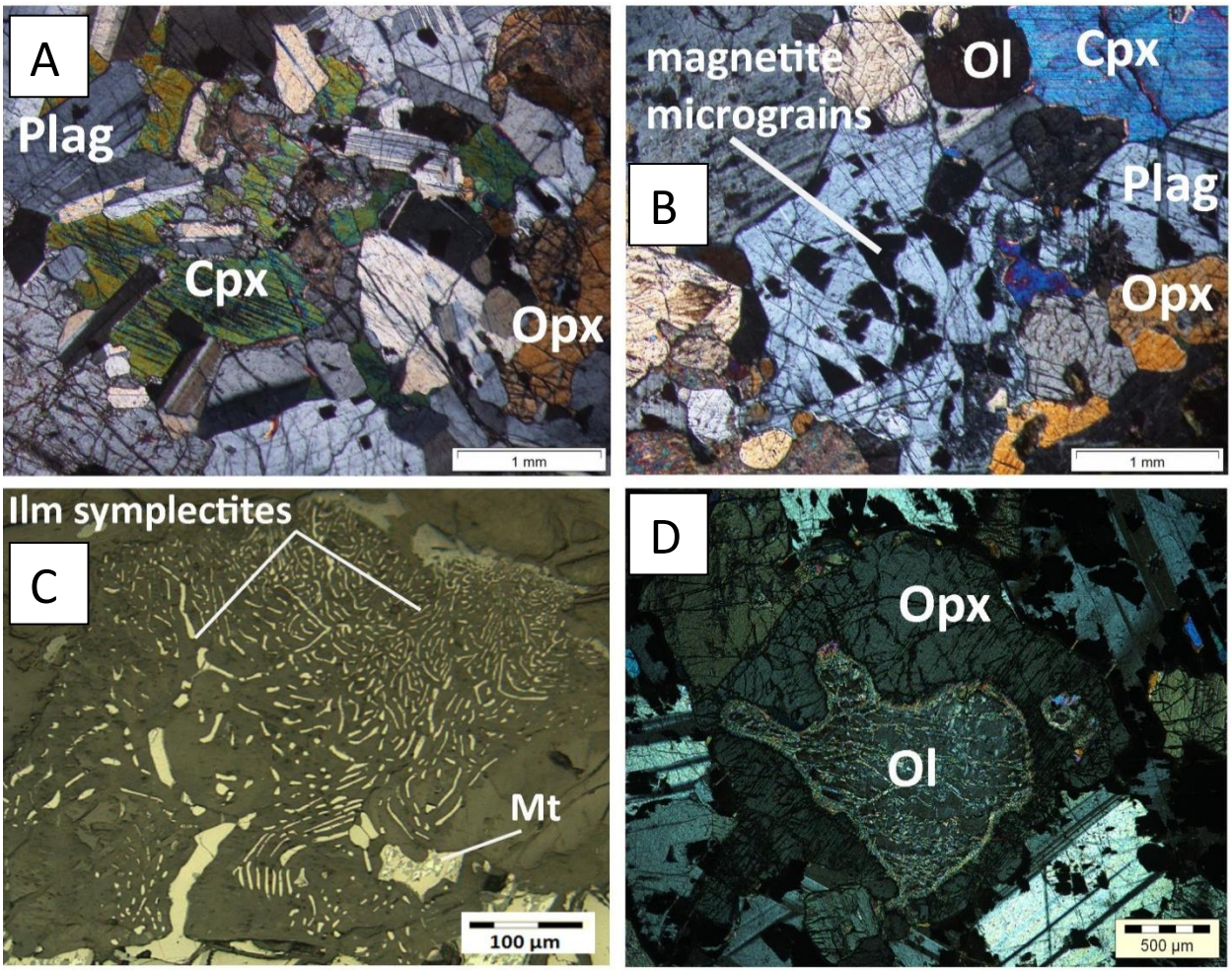

Figure 6.2: Rock textures of the lower lithologic unit on Harriet's Wish under transmitted light (A, B, D) and reflected light (C). A: Intercumulus clinopyroxene and orthopyroxene with plagioclase grains forming around them. Plagioclase grains are also included in some altered pyroxene grains in olivine-bearing gabbronorite of HW025 at a depth of 602.1 m. B: Altered plagioclase with exsolutions and inclusions of magnetite micrograins, olivine, clinopyroxene and orthopyroxene in olivine pyroxenite of HW024 at a depth of 347.9 m. C: Magnetite-ilmenite symplectites and some minor magnetite grains in troctolite of HW024 at a depth of 306.1 m. D: Olivine inside orthopyroxene in olivine gabbronorite of HW024 at a depth of 332.65 m. Abbreviations: Plag= plagioclase, Cpx= clinopyroxene, Opx= orthopyroxene, Ol= olivine, Mt= magnetite.

The pegmatoidal gabbronorite and melagabbronorite hosts significant sulphides, which occur sporadically with no particular mineral associations. The alteration intensity is moderate with plagioclase being weakly to moderately saussuritised and sericitised and pyroxenes being commonly chloritised.

6.3.2.1 *Melagabbronorite*

This rock is similar to the gabbronorite described above; however, there are some differences. The general texture is inequigranular to subophitic. The overall grain size is medium-coarse with an overall size range between 1-6 mm up to pegmatitic (<5 cm) towards the interface between the lower and upper lithologic units. Melagabbronorite comprises <80% pyroxenes, 10-65% plagioclase <10% pigeonite and <8% sulphides in thin sections. Clinopyroxene and orthopyroxene forms cumulus grains and oikocrysts as well as inclusions inside plagioclase. Inverted pigeonite is also present as oikocrysts. Sugar-textured plagioclase is found in samples close to the top of the lower lithologic unit. Interstitial sulphides occur between grains of plagioclase or pyroxenes. The overall alteration intensity is weak with some chloritisation of pyroxenes and saussuritisation and sericitisation of plagioclase seen in the thin sections.

6.3.2.2 *Olivine gabbronorite*

Olivine gabbronorite shows similar features to the gabbronorite, however, there are some differences. The overall texture is inequigranular cumulus, with olivine forming chadacrystic inclusions in poikilitic pyroxenes (Figure 6.2 d). The grain size is generally medium to coarse. Olivine gabbronorite comprises 35-65% plagioclase, 10-50% clinopyroxene, 15-40% orthopyroxene and 10-15% olivine. Interstitial sulphides are locally present in moderate to high concentrations (<8%). Accessory minerals found include biotite, secondary chlorite and interstitial magnetite. Plagioclase forms intricate intergrowths with clinopyroxene (Figure 6.2 a). Sugar-textured plagioclase is found regularly in olivine gabbronorite. The overall alteration intensity is high with clinopyroxene and orthopyroxene being locally highly chloritised whereas olivine is moderate- to highly serpentinised.

6.3.2.3 *Olivine melagabbronorite*

This rock type is also similar to gabbronorite but differs in the presence of olivine and increased proportions of pyroxenes. The overall texture is inequigranular to equigranular and the various crystals show an interlocking texture. Euhedral olivine is

found as chadacrysts in clinopyroxene, orthopyroxene and plagioclase (Figure 6.1 b). Sulphides are found interstitially accounting for <10%. The alteration intensity is moderate with plagioclase being saussuritised and sericitised. Some clinopyroxene is chloritised and olivine is low- to moderately serpentinised.

6.3.2.4 *Anorthosite*

Anorthosite is mostly composed of euhedral plagioclase grains showing an interlocking texture. Some intervals show a mottled texture, which is formed by patches or “mottles” of minor dark pyroxene in the white plagioclase matrix. The grain size is usually medium ranging from 1-6 mm, with some of plagioclase grains reaching up to 2 cm in size. Smaller grains of interstitial to poikilitic pyroxenes and interstitial specks of sulphides are locally present. The overall alteration intensity is moderate, but it varies from low- to high in some places. Highly altered anorthosite contains altered plagioclase as well as chloritised and mylonitised pyroxene grains.

6.3.2.5 *Gabbro*

The texture is inequigranular (subophitic to gabbroic) with crystals showing an interlocking texture. The overall grain size is medium ranging from 2-5 mm. Gabbro comprises 50-60% plagioclase, 15-35% clinopyroxene, 5-10% orthopyroxene and ~5% pigeonite. Accessory minerals include biotite and secondary chlorite. Euhedral orthopyroxene and pigeonite seem to have crystallised first, with postponed crystallisation of plagioclase because orthopyroxene and pigeonite are regularly enclosed by plagioclase. Exsolution lamellae of Ca-poor pyroxene are present in clinopyroxene. The alteration intensity overall is low to moderate. The plagioclase shows carlsbad, albite, and tapered polysynthetic twinning locally and is saussuritised and sericitised.

6.3.2.6 *Troctolite*

There are layers of troctolite (Figure 6.1 a) and layers of leucotroctolite in the Harriet Wish boreholes. The overall texture is equigranular. The grain size of minerals is

medium ranging between 3-5 mm with olivine and plagioclase showing equal grain sizes. Troctolite comprises 40-48% plagioclase, 40-48% olivine and 2-10% orthopyroxene whereas leucotroctolite is characterised by an elevated proportion of plagioclase up to 80%. Accessory minerals such as magnetite, sulphides and ilmenite are present and account for 0-3% locally. Plagioclase and olivine have equal euhedrality with plagioclase showing common carlsbad- and albite twinning. Orthopyroxene forms rims around certain olivine grains that resembles peritectic reaction rims (Figure 6.1 c). Magnetite-ilmenite symplectites are observed in the areas between cumulus olivine and coarse cumulus magnetite crystals (Figure 6.2 c). The alteration degree is moderate to high with plagioclase being intensely saussuritised and sericitised. Olivine shows serpentinisation and orthopyroxene is moderately altered to chlorite.

6.3.2.7 *Pyroxenite*

Pyroxenites occur in the following varieties: pyroxenite, olivine pyroxenite, olivine orthopyroxenite and feldspathic olivine pyroxenite.

The texture of pyroxenite is inequigranular. The rock is medium- to coarse-grained with the pyroxene grains ranging between 0.2-2 cm in size. Pyroxenite comprises 35-50% orthopyroxene, 15-30% clinopyroxene, 10-20% plagioclase and <10% olivine. Accessory minerals include secondary chlorite (<5%), sulphides (<10% locally) and rare grains of chromite. Euhedral clinopyroxene grains are found within sub-euhedral orthopyroxene grains and contain orthopyroxene lamellae. The plagioclase is sub- to anhedral in shape and fills interstitial space between olivine and pyroxenes. The alteration intensity is moderate with local segregations of secondary serpentine and chlorite after olivine and pyroxenes, respectively. The chromite grains are also altered and replaced by Al-rich spinel, sulphides and secondary magnetite.

6.3.2.8 *Olivine pyroxenite*

Olivine pyroxenite (Figure 6.2 b) differs from pyroxenite in that it contains a higher proportion of olivine. Olivine pyroxenite contains cumulus olivine, which forms euhedral

grains and chadacrysts inside oikocrystic orthopyroxene or inverted pigeonite. In turn, orthopyroxene can be included inside clinopyroxene grains. There are some plagioclase inclusions seen inside certain olivine grains. Sulphides make up <10% of the modal mineralogy. Phlogopite is common up to 2%. The overall alteration intensity is moderate with clinopyroxene showing chloritisation and plagioclase showing saussuritisation and sericitisation (Figure 6.1 d). Olivine is moderately serpentinised and orthopyroxene is chloritised locally.

6.3.3 **Upper lithologic unit**

For a comprehensive table describing each thin section see Appendix B. Petrographic images of concern of the rock types that are found on Harriet's Wish are shown in Figures 6.3 and 6.4 and descriptions are presented below:

6.3.3.1 *Magnetitite*

Massive and disseminated magnetitites are found only in the HW030, where they compose layers 0.4 and 1 m thick, respectively. These layers contain segregations of equigranular coarse-grained magnetite in variable proportions with pyroxenes and plagioclase. In addition, fragments of hematitised massive magnetitite are present at the bushveld-Waterberg Group contact. Disseminated magnetite is present irregularly throughout the upper lithologic unit in every rock type in the HW029 drillcore (Figures 4.11 and 4.12). Magnetite occurs mainly as specks (Figure 6.3 b and d) to blebs ranging between <0.5 mm to 2 cm in size with the biggest grains found in pegmatoidal rocks. Primary magnetite is also common in mineralised rocks.

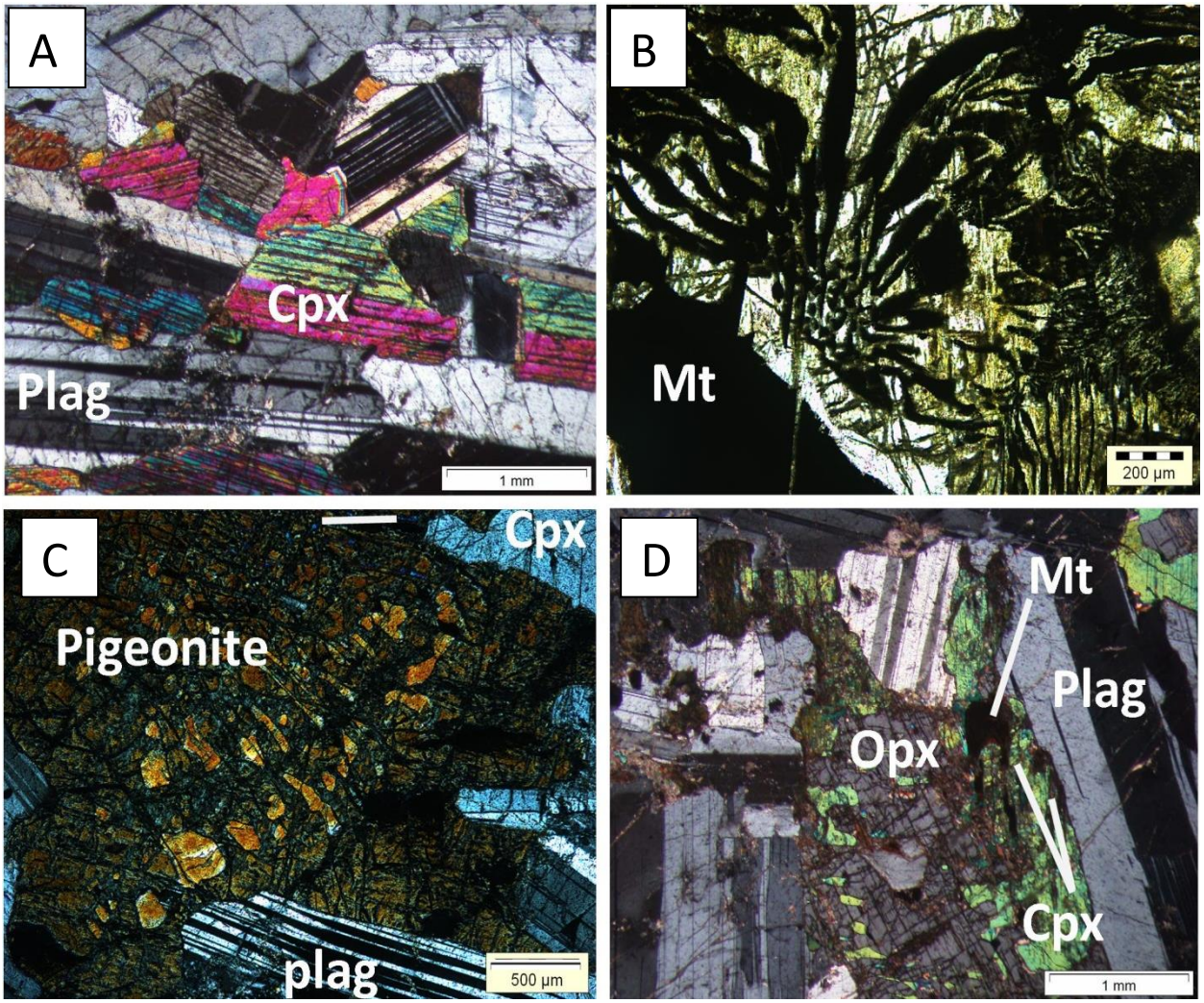

Figure 6.3: Rock textures of the upper lithologic unit on Harriet's Wish under cross-polarised transmitted light. A: Plagioclase and clinopyroxene showing the same orientation in lineated gabbro of HW029 at a depth of 378.5 m. B: Magnetite symplectites in olivine-bearing gabbronorite of HW029 at a depth of 470.2 m. C: Inverted pigeonite, clinopyroxene and plagioclase with exsolutions of clinopyroxene in pigeonite and stressed tapered twins of plagioclase in in lineated gabbro of HW029 at a depth of 378.5 m. D: An interstitial magnetite grain and exsolutions of clinopyroxene in orthopyroxene with altered plagioclase and clinopyroxene in gabbronorite of HW029 at a depth of 457.8 m. Abbreviations: Plag= plagioclase, Cpx= clinopyroxene, Opx= orthopyroxene, Ol= olivine, Mt= Magnetite.

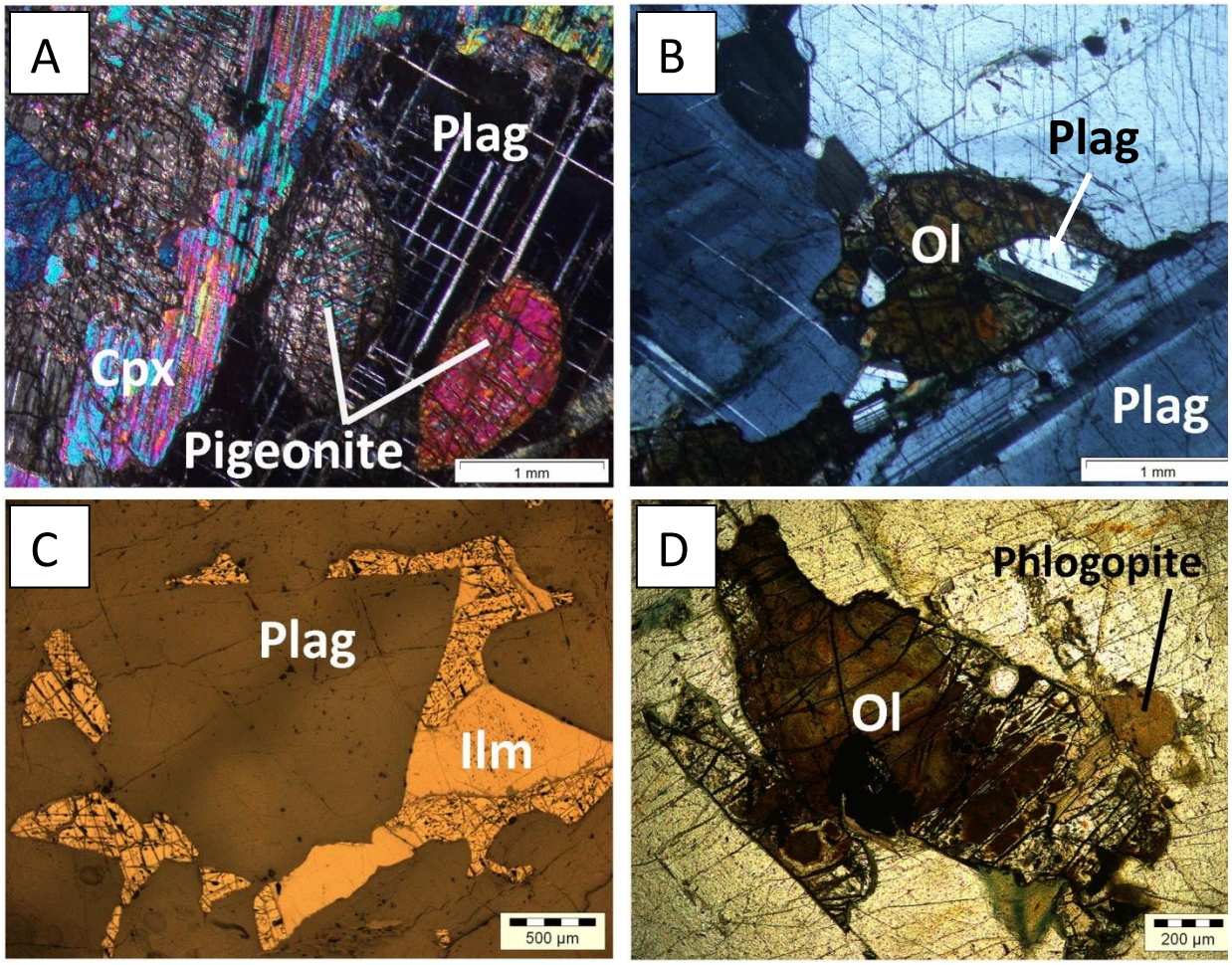

Figure 6.4: Rock textures of the upper lithologic unit on Harriet's Wish under cross-polarised transmitted light (A, B, D) and reflected light (C). A: Inverted pigeonite in plagioclase and altered clinopyroxene in melagabbronorite of HW029 at a depth of 608.1 m. B: Intercumulus altered olivine and plagioclase in olivine-bearing gabbronorite of HW029 at a depth of 470.2 m. C: Interstitial ilmenite and magnetite between plagioclase grains in mottled leucogabbro of HW029 at a depth of 389.4 m. D: Altered olivine (iddingsite) and phlogopite in orthopyroxene in olivine-bearing gabbronorite of HW029 at a depth of 470.2 m. Abbreviations: Plag= plagioclase, Cpx= clinopyroxene, Opx= orthopyroxene, Ol= olivine, Mt= Magnetite, Ilm= Ilmenite.

6.3.3.2 *Lineated gabbro*

In the upper lithologic unit, most of the gabbro occurs as lineated gabbro (Figure 6.3 a). The lineated gabbro has a predominant subophitic to ophitic texture, with some parts also having an inequigranular to equigranular gabbroic texture. The lineated ophitic texture is composed of oriented plagioclase laths with surrounding euhedral to anhedral crystals of pyroxenes. Lineated gabbro is generally medium-grained, with grain sizes

ranging between 2-6 mm. Lineated gabbro is rich in plagioclase in some sections and comprises 45-60% plagioclase, 15-30% clinopyroxene, 10-15% orthopyroxene and ~10% inverted pigeonite. In some parts, clinopyroxene, pigeonite and orthopyroxene occur as inclusions in plagioclase although orthopyroxene grains may contain plagioclase inclusions also. Inverted pigeonite contains exsolutions of high-Ca pyroxene whereas clinopyroxene contains decomposition lamella of low-Ca pyroxene. Stressed (tapered) polysynthetic twins in plagioclase locally appear in an association with pigeonite (Figure 6.3 c). Gabbro shows low alteration with saussuritisation and sericitisation developed in plagioclase and dark minerals being locally replaced by chlorite.

6.3.3.3 *Mottled leucogabbro*

Mottled leucogabbro is distinguished by a specific mottled texture with “mottles” or patches of oikocrystic to interstitial pyroxenes and magnetite in equigranular plagioclase matrix. The plagioclase content is <80%. Ilmenite and phlogopite are sometimes present along with magnetite (Figure 6.4 C). The alteration intensity ranges from moderate to high, with pyroxenes showing chloritisation.

6.3.3.4 *Anorthosite*

Anorthosite forms patches, segregations, veins and veinlets in the upper lithologic unit but does not constitute any persistent layering. The texture ranges from mottled to equigranular with mottles composed of clinopyroxene or magnetite. The grain size is from medium to coarse in the range of 0.2-1.5 cm. Interstitial specs of sulphides are found in anorthosite and may account for up to 2%. Anorthosite is also moderately to highly altered with plagioclase showing saussuritisation and sericitisation.

6.3.3.5 *Gabbronorite*

Gabbronorite is the most common rock type of the upper lithologic unit and occurs in the following varieties: gabbronorite, leucogabbronorite and olivine-bearing gabbronorite. In

the upper lithologic unit, generally, gabbronorites become more melanocratic towards the base, and more leucocratic towards the middle part of the unit.

The texture is inequigranular to equigranular with the crystals showing an interlocking texture (Figure 6.4a). Gabbronorite is medium-grained with grain sizes ranging between 1 – 6 mm. Euhedral and subhedral plagioclase laths up to 5 mm in length are present with some plagioclase grains having an anhedral, or granular shape. Orthopyroxene occurs as anhedral grains <5 mm in size. Clinopyroxene and inverted pigeonite grains vary from being anhedral to subhedral to euhedral and is generally <5 mm in size. Gabbronorite comprises 40-75% plagioclase, 20-70% pyroxenes and <15% pigeonite. Accessory minerals include magnetite (<1%), amphibole, chlorite and phlogopite. Magnetite is interstitial to plagioclase, and the small grains of magnetite are found inside pyroxenes (Figure 6.3 d). Plagioclase can also be poikilitically included and enveloped by clinopyroxene and to a lesser extent by orthopyroxene. Minor clinopyroxene is also sometimes included in plagioclase. Sulphides are present as interstitial to disseminated specks in the gabbronorite, mainly towards the base of the upper lithologic unit. The alteration intensity is weak. Plagioclase is weakly saussuritised and sericitised in some places. Some clinopyroxene is moderately replaced by phlogopite along margins and to a lesser extent by chlorite. Inverted pigeonite shows mainly lamellar exsolutions of high-Ca clinopyroxene, with some blebby exsolutions also being present (Figure 6.4 b). There are two major exsolution systems seen in inverted pigeonite.

6.3.3.6 *Olivine-bearing gabbronorite*

Olivine-bearing gabbronorite has inequigranular texture and is similar to gabbronorite with some differences outlined. The olivine grains range from 1- 2 mm in size whereas phologopite grains can be as big as 5 mm in size, with the majority of the grains ranging between 2-5 mm. Olivine gabbronorite is rich in plagioclase averaging <60% plagioclase, ~20% clinopyroxene and ~10% orthopyroxene, <5% olivine, ~3% magnetite and 1% phologopite (<9 % locally). Pyroxene grains are present inside plagioclase, and plagioclase chadacrysts may be found inside oikocrystic clinopyroxene and orthopyroxene. Olivine sometimes contains lath-like inclusions of plagioclase

(Figure 6.4b). Olivine relics are commonly trapped in oikocrystic clinopyroxene or plagioclase. Magnetite is seen to grow dendritically when close to olivine (Figure 6.3b) and magnetite symplectites are also present in olivine-bearing gabbronorite (Figure 6.3b). The rock shows moderate to high alteration with orthopyroxene and clinopyroxene being highly chloritised locally. Secondary magnetite fills cracks in all minerals. The phlogopite crystals are also highly altered to chlorite whereas olivine grains are locally altered to iddingsite and bowlingite (Figure 6.4d) and minor serpentinite. The plagioclase crystals are moderately altered to saussurite.

6.3.4 **Lower mineralised zone**

The lower mineralised zone sulphides are hosted in pyroxenite, gabbronorite and troctolite. The sulphides present in the lower mineralised zone are mainly pentlandite, chalcopyrite and minor pyrite (Figure 6.5 a) with accessory pyrrhotite. Sulphides may occur as interstitial specks, veinlets or blebs or as small inclusions in silicate minerals and chromite (Figure 6.5). Sulphides may also occur as larger clusters of sulphide minerals (Figure 6.5b). The sulphides are not associated with any specific mineral assemblage and are also not confined to specific rock types. Pyrite may form fine-grained to symplectitic intergrowths with chalcopyrite.

Cr-spinel is also present in the lower mineralised zone (Figure 6.5c). It is often associated with olivine and can be found inside sulphide grains in olivine-enriched rocks. The Cr-spinel edges are often altered, and the grains occur as relics, with unaltered cores of Cr-richer spinel.

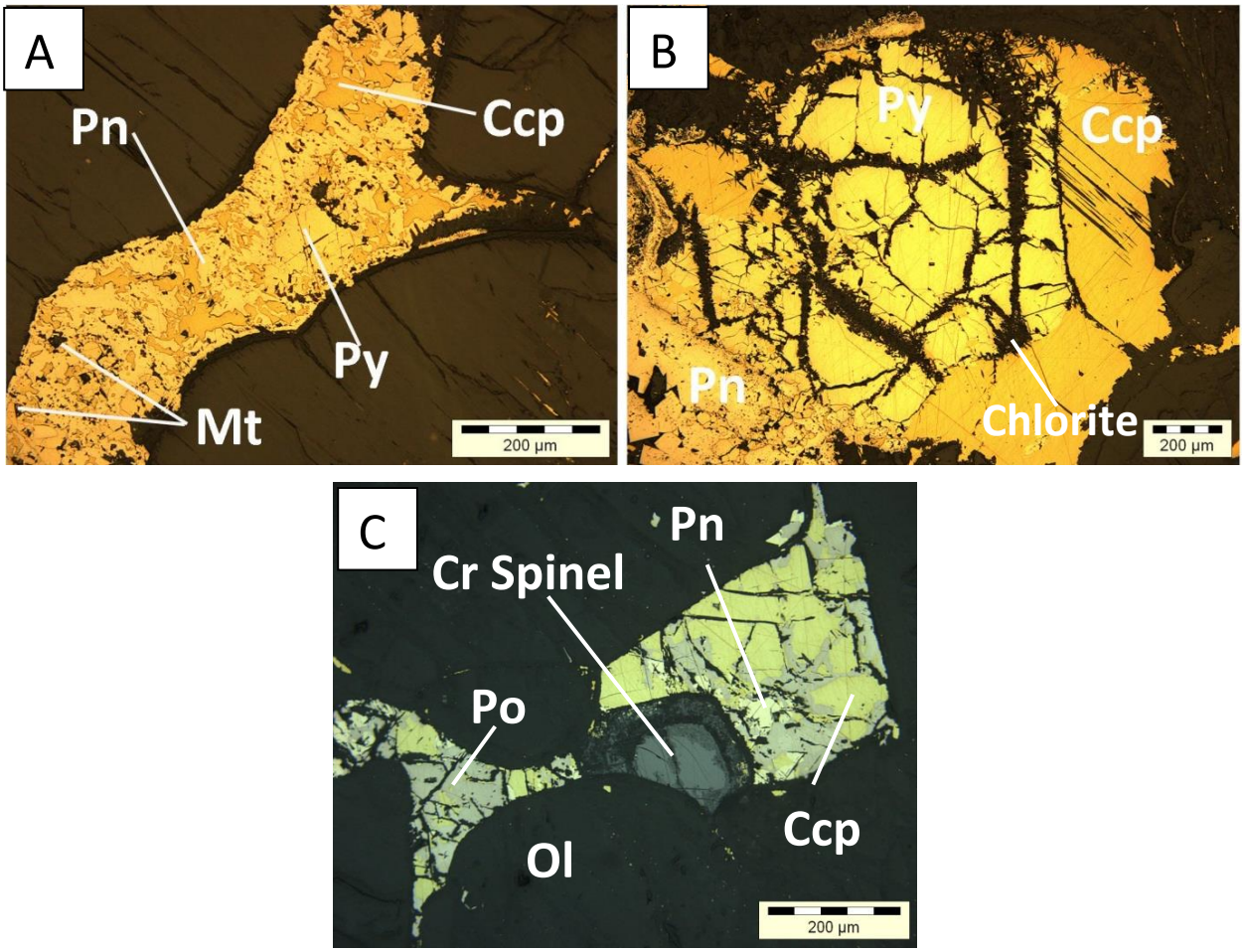

Figure 6.5: Mineral associations of base metal sulphides of the lower mineralised zone on Harriet's Wish under reflected light. A: Magnetite, pentlandite, pyrite and chalcopyrite in olivine gabbronorite of HW024 at a depth of 347.9 m. B: Pentlandite and chalcopyrite replaced by pyrite showing secondary chlorite is developed as veinlets through the sulphides and along the margins in olivine gabbronorite of HW024 at a depth of 347.9 m. C: Chromium spinel relic with chromium spinel core in sulphides in olivine gabbronorite of HW024 at a depth of 347.9 m. Abbreviations: Ccp= chalcopyrite, Ilm= ilmenite, Pn= pentlandite, Py= pyrite, Cr-spinel= chromite to Cr-spinel, Ol=olivine, Mt = magnetite.

6.3.5 **Upper mineralised zone**

The major base metal sulphides present in the upper mineralised zone are pentlandite, pyrrhotite, chalcopyrite and pyrite (Figure 6.6a and b). The style of sulphide mineralisation seen is disseminated blebs of sulphides that are truncated along boundaries of silicate minerals or as inclusions in silicate minerals. Large sulphide blebs are interstitially present and fill up cracks between all mineral grains but are mostly associated with pyroxenes (Figure 6.6 c). Pyrite euhedral crystals are often formed around primary pyrrhotite as well as occurring as a core surrounded by a rim made of quartz crystals (Figure 6.6c). Secondary pyrite is also seen replacing chalcopyrite and pentlandite with chlorite veinlets through the pyrite grains (Figure 6.6 b). The edges of sulphide blebs or cracks in sulphide grains may be replaced by secondary chlorite and amphiboles (Figure 6.6 b).

6.4 **Discussion**

Correctly classifying rocks during core logging was not always straight forward when rocks were altered, or mineral grains were too small to identify. One of the most difficult challenges in core logging was distinguishing between pyroxenes, inverted pigeonite and various dark minerals. Therefore, the petrography section aided in the confirmation of mineralogy and rock types in order to correctly correlate the Harriet's Wish stratigraphy with the Waterberg Project stratigraphy (Kinnaird *et al.,* 2017) and northern limb stratigraphy (Ashwal *et al.,* 2005). In most cases, the rock classification remained the same as in the Chapter 4, with rock names remaining the same.

6.4.1 **Lower lithologic unit**

Rock types and mineralogy of the lower lithologic unit on Harriet's Wish compare well with the TGA sequence on the Waterberg Project (Kinnaird *et al.,* 2017; Huthmann *et al.,* 2018). The most notable similarities include the presence of true troctolite (Figure 6.1 a) and anorthosite. Overall, after the petrographic inspection, the lithologies remained mainly the same as the logged lithologies in the Chapter 4. However, in the lower lithologic unit on Harriet's Wish, gabbro in HW024 at a depth of 266-270 m was proven to be more noritic than observed in the field with the higher proportions of ortho-

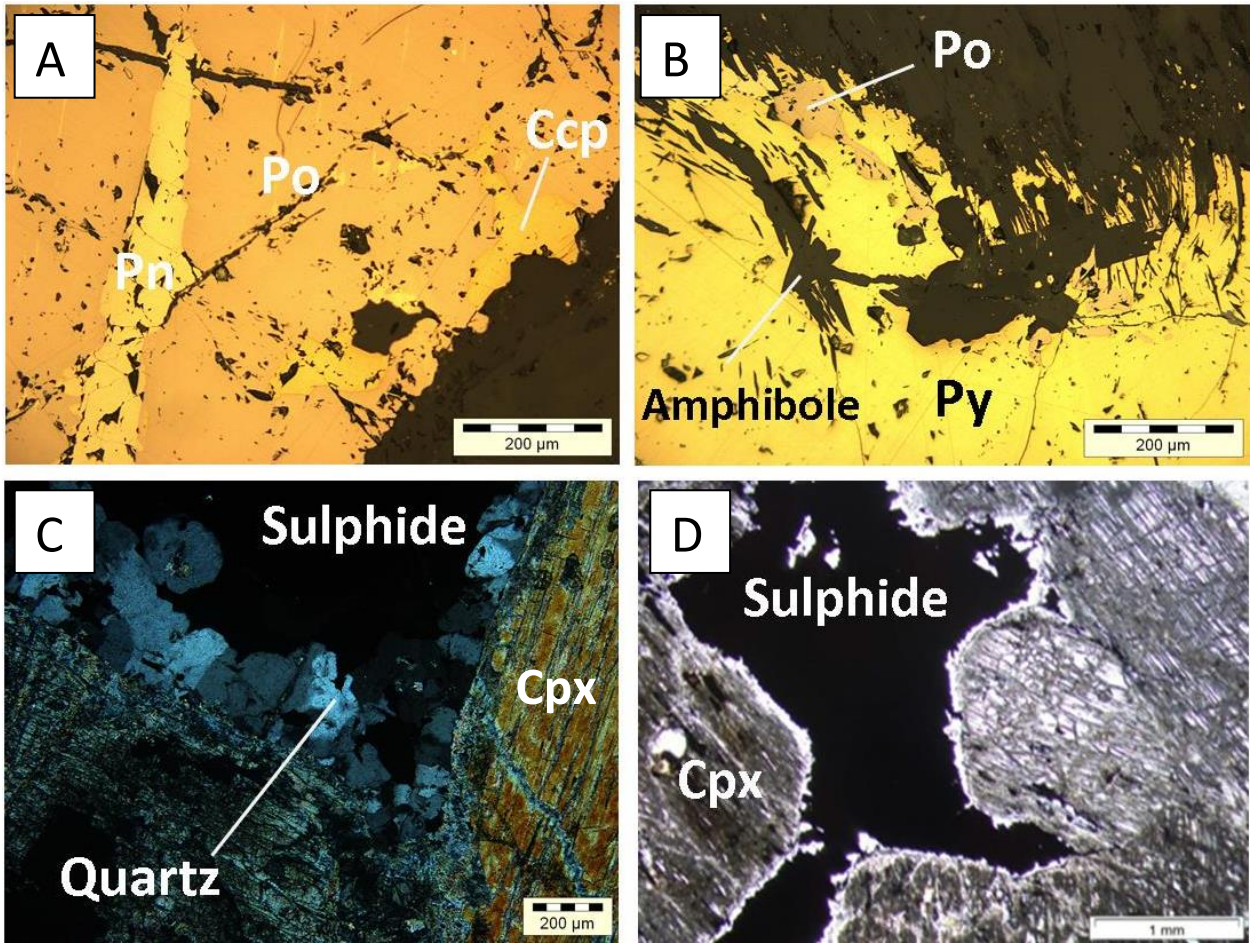

Figure 6.6: Ore minerals of the upper mineralised zone on Harriet's Wish under reflected light (A, B) and transmitted light (C, D). A: Flame textured pentlandite and chalcopyrite in pyrrhotite in pegmatoidal gabbronorite in HW029 at a depth of 614.8 m. B: Amphibole replacing pyrrhotite and pyrite in pegmatoidal gabbronorite in HW029 at a depth of 614.8 m. C: Sulphides (mostly pyrite) with quartz rim in gabbronorite in HW029 at a depth of 651.9 m. D: Interstitial sulphide between pyroxene grains in pegmatoidal gabbronorite in HW029 at a depth of 614.8 m. Abbreviations: Ccp= chalcopyrite, Ilm= ilmenite, Pn= pentlandite, Po= pyrrhotite, Py= pyrite, Plag= plagioclase.

pyroxene and pigeonite observed in thin section (Figure 6.7 a). In addition to this, norite in HW024 at a depth of 391 was proven to have more gabbroic composition than observed in the field (Figure 6.7b).

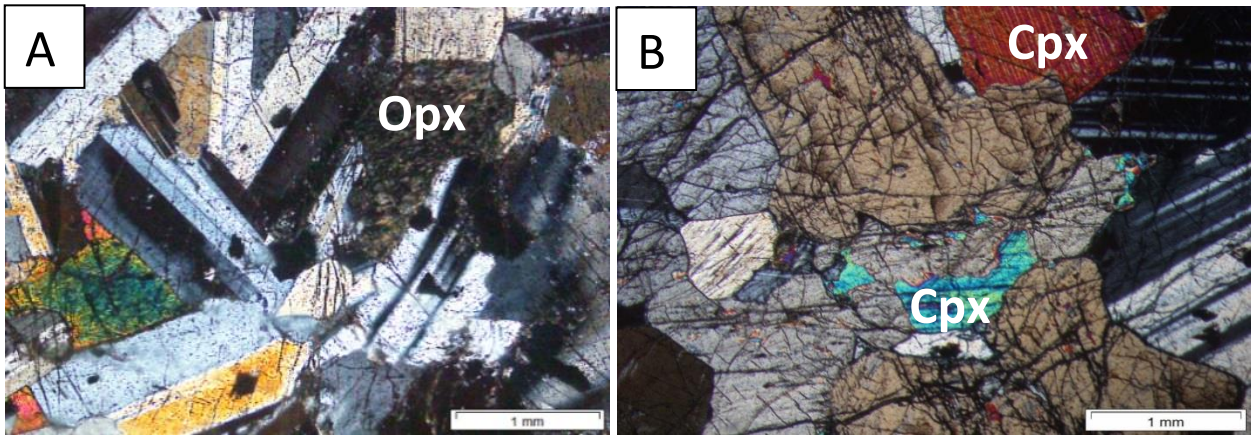

Figure 6.7: Rocks of the lower lithologic unit that differ from core logging on Harriet's Wish. A: Orthopyroxene in gabbro of HW024 at a depth of 268.2 m. B: Clinopyroxene in norite of HW024 at a depth of 391.2 m. Abbreviations: Cpx= clinopyroxene, Opx= orthopyroxene.

Nex *et al.,* (1998) divided the Main Zone on Marikana into five subzones based on the presence of certain indicator minerals, textures and field characteristics. McCreesh, (2013, 2016) and Kinnaird *et al.,* (2017) described possible correlations between the stratigraphy of the Waterberg Project TGA sequence and the subzones of the Main Zone on Marikana (Nex *et al.,* 1998). Possible correlations with the subzones C, D and E have been drawn (McCreesh, 2016). The Hexrivier Unit of subzone C is suggested to possibly correlate with the basal stratigraphy of the TGA sequence due to the occurrence of some minor olivine (<10 %), although the final conclusion was made that this possible subzone C unit is not developed on the Waterberg Project (Kinnaird *et al.,* 2017; Nex *et al.,* 1998).

Next, a possible correlation to subzone D is suggested due to a distinct lack of inverted pigeonite and the overall equigranular texture with primary orthopyroxene that is observed in the TGA sequence (Nex *et al.,* 1999; McCreesh, 2013, 2016). Then, just below the Upper Zone-TGA sequence boundary on the Waterberg Project, a correlation to subzone E is suggested (McCreesh, 2016). This section is characterised by the reappearance of inverted pigeonite oikocrysts and the presence of plagioclase and augite, although this is not always present in the northern parts of the Waterberg Project (Nex *et al.,* 1999; McCreesh, 2016). On the Aurora Project, pigeonite is present in the mineralised intervals as intercumulus and interstitial phases and abundantly present as

a cumulus phase in the upper gabbronorites (McDonald *et al.,* 2017). The presence of pigeonite in the mineralised intervals does not correlate with subzone C in the Hexrivier Unit of the Main Zone (Nex *et al.,* 1998) due the pigeonite being interstitial and not cumulus, however, the upper parts of the Aurora Project stratigraphy does contain cumulus pigeonite as well as cumulus plagioclase in some parts (McDonald *et al.,* 2017). Although the upper parts of the upper Main Zone on the Aurora Project show cumulus pigeonite and plagioclase, similar to the upper portions of the TGA sequence on the Waterberg Project, there is no associated mineralisation with this unit on the Aurora Project as is seen on the Waterberg Project (Kinnaird *et al.,* 2017; McDonald *et al.,* 2017).

The Harriet's Wish stratigraphy shows some correlations to the Waterberg Project's TGA sequence (McCreesh, 2013, 2016; Kinnaird *et al.,* 2017) and to a much lesser degree - to the Main Zone subdivisions on Marikana (Nex *et al.,* 1998). Similar to the Waterberg TGA sequence, Harriet's Wish stratigraphy does not show similarities to subzones A and B (Nex *et al.,* 1998). In drillcore HW024, however, pigeonite occurs in the lower portions of the lower lithologic unit in (Figure 6.1 b) and olivine concentrations here are <10%, which is similar to the Hexrivier unit of subzone C (Nex *et al.,* 1998). Furthermore, cumulus pigeonite is present upwards in the stratigraphy on Harriet's Wish, with cumulus pigeonite associated with the upper portions of the lower lithologic unit, however, the appearance and disappearance of inverted pigeonite is sporadic and does not correspond to the regularities seen in subzones D and E of the Main Zone (Nex *et al.,* 1998). The rhythmically layered packages, such as the Zebra Unit, the Springbok Unit and the Hexrivier Unit, which are persistent through the Marikana area, are therefore not established in the studied Harriet Wish boreholes (Nex *et al.,* 1998).

The host lithology of the ultramafic F-zone was previously correlated with the Troctolite Horizon encountered in the Bellevue drillcore (Van der Merwe, 1976; Woods, 2012; McCreesh, 2013). However, McCreesh, (2016) suggests that the modal abundance of olivine differs between these areas. Troctolite on the Waterberg Project comprises 25-65% olivine (McCreesh, 2016) and troctolite in the Bellevue drillcore comprises 21.1%

olivine on average (Ashwal *et al.,* 2005). The modal abundance of olivine in the lower lithologic unit on Harriet's Wish, more closely resembles that of the Waterberg Project comprising 40-48% olivine. Furthermore, troctolites on the Waterberg Project show clinopyroxene mainly as the small intercumulus grains with orthopyroxene forming the larger oikocrysts while in some samples the rims of orthopyroxene partially or completely surround the olivine crystals (McCreesh, 2016). On Harriet's Wish, troctolites also shows orthopyroxene forming the large oikocrysts with some samples showing the rims of orthopyroxene that surround the olivine crystals (Figure 6.1 c); therefore, suggesting a correlation between these troctolites. However, plagioclase in troctolites in the lower lithologic unit on Harriet's Wish seems to be overall coarser-grained than plagioclase in troctolite in the TGA sequence on the Waterberg Project (Figure 6.1 a).

In the UmS pyroxenite on the Waterberg Project, coarse-grained olivine with plagioclase inclusions occurs among interstitial clinopyroxene (Kinnaird *et al.,* 2017). In Harriet's Wish in the lower lithologic unit pyroxenites, small inclusions of plagioclase were also found inside euhedral olivine grains (Figure 6.1e).

In the lower lithologic unit on Harriet's Wish, it is evident that rocks have been significantly altered, with the alteration intensity overall being moderate to high (Figure 6.1b and c; Figure 6.2a). The most severely altered minerals include olivine, which is commonly replaced by serpentine or iddingsite, clinopyroxene and orthopyroxene commonly replaced by amphibole or chlorite and plagioclase, which is replaced by saussurite or sericite (Figure 6.1d). The lower lithologic unit pyroxene- and olivine-rich lithologies also show strong alteration. Highly altered olivine replaced by serpentine, iddingsite and magnetite, possibly formed during a hydrothermal stage, is common in certain samples, especially within the moderately to highly altered intervals. There is evidence, however, that the amount of liquidus olivine that was crystallised at an early magmatic stage may have been much higher, but it was replaced by pyroxene via postcumulus peritectic reactions (Figure 4.5 b).

6.4.2 **Boundary**

As described in Chapter 4 the visible boundary between the lower and upper lithologic units was taken at the first appearance of cumulus magnetite as suggested by SACS, (1980). As described in Chapter 5, Ashwal *et al.,* (2005) suggested that magnetic susceptibility readings should be used to define this boundary, since disseminated magnetite is regularly present below the visual boundary. On the Waterberg Project, the increase in magnetic susceptibility due to the presence of accessory magnetite was detected up to 100 m below the first visible cumulus magnetite (McCreesh, 2016). Petrographic studies agreed well with the magnetic susceptibility boundary and showed that accessory magnetite and symplectic intergrowths of magnetite and orthopyroxene are present in this 100 m interval with no visible magnetite recorded during the core logging (McCreesh, 2016). On Harriet's Wish, the petrographic study also reveals disseminated magnetite (Figures 6.5a; Figure 6.8a and b) and magnetite symplectic intergrowths with orthopyroxene at and above the boundary between the lower and upper lithologic units. Therefore, this suggests a likely correlation between the Upper Zone-TGA sequence boundary on the Waterberg Project and the upper lithologic unit-lower lithologic unit boundary on Harriet's Wish.

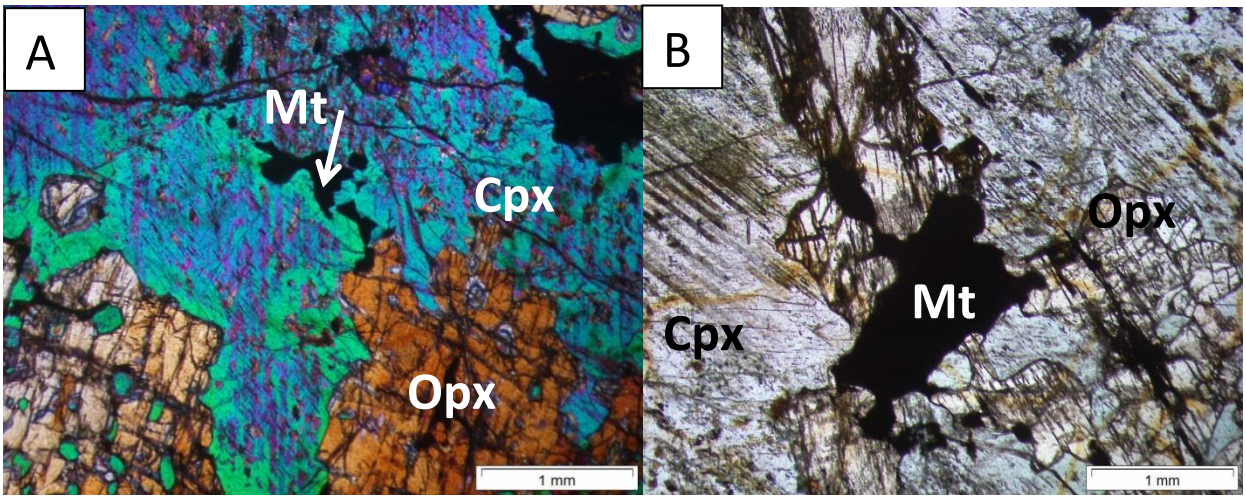

Figure 6.8: Disseminated magnetite in 20 m interval above the boundary between the lower and upper lithologic units as defined by magnetic susceptibility. A: Magnetite specks in clinopyroxene-pigeonite intergrowth of HW029 at a depth of 608.1 m. B: Magnetite specks interstitially present between clinopyroxene and orthopyroxene grains of HW029 at a depth of 608.1 m. Abbreviations: Mt= magnetite, Cpx= clinopyroxene, Opx= orthopyroxene.

6.4.3 **Upper lithologic unit**

The rock types and mineralogy of the upper lithologic unit on Harriet's Wish compare well with those of the Upper Zone on the Waterberg Project (Kinnaird *et al.,* 2017; Huthmann *et al.,* 2018). The most notable similarities include the presence of abundant gabbronorites, gabbros and anorthosite with pigeonite being sporadically present and abundant interstitial, cumulus and symplectic magnetite and throughout the entire unit. Overall, the lithologies in the upper lithologic unit on Harriet's Wish are confirmed to be the same as described in Chapter 4, however, there are some differences noted during the petrographic study. These differences and comparisons to the Waterberg Project, the Aurora Project and other northern limb localities are described below.

The occurrence of certain cumulus minerals has been used to determine subzones within the Upper Zone of the Bushveld Complex (Wager and Brown, 1968; Eales and Cawthorn, 1996; Tegner *et al.,* 2006). These include subzone UZa, classified by the first appearance of magnetite, subzone UZb, classified by the presence of ferrogabbronorite, olivine-magnetite, gabbronorite and subzone UZc classified by the presence of apatite. On the Waterberg Project, subzone UZa has been recognised due to cumulus magnetite being present (McCreesh, 2016; Kinnaird *et al.,* 2017). The use of magnetic susceptibility indicated magnetite <100 m below the visible magnetite on the Waterberg Project, which was confirmed by the petrographic studies (McCreesh, 2016). Subzone UZb has also been recognised on the Waterberg Project as the occurrence of iron-rich olivine in magnetite gabbro horizons is present in the Upper Zone, which forms complex symplectic textures with orthopyroxene and magnetite (McCreesh, 2016). This magnetite gabbro, however, is not present in all drillcores (Kinnaird *et al.,* 2017). UZc likely has been eroded from the Waterberg Project stratigraphy as there are no elevated proportions of apatite found in the lithology (McCreesh, 2016).

On Harriet's Wish, magnetite is abundantly present in the upper lithologic unit (Figure 6.3b), suggesting a correlation with UZa in the Bushveld Complex (Eales and Cawthorn, 1996; Tegner *et al.,* 2006). There is no ferrogabbronorite in the upper lithologic unit on Harriet's Wish (HW029), as seen in UZb (Eales and Cawthorn, 1996), or magnetite

gabbro as in the Upper Zone on the Waterberg Project (Kinnaird *et al.,* 2017). However, the magnetite symplectites are common in olivine-bearing gabbronorite in the Harriet's Wish upper lithologic unit (Figure 6.3 b), similar to those observed in the Waterberg Upper Zone (McCreesh, 2018). The absence of magnetite gabbro or ferrogabbronorite in the studied Harriet's Wish upper lithologic unit does not necessarily mean that those lithologies are absent in the area as they may be present in other drillcores, similar to the Waterberg project where magnetite gabbro is not present in all drillcores (McCreesh, 2016; Kinnaird *et al.,* 2017).

On the Waterberg Project widespread cumulus and oikocrystic pigeonite is present in the Upper Zone magnetite-bearing gabbro (Kinnaird *et al.,* 2017; McCreesh *et al.,* 2018). In the upper parts of the Aurora Project stratigraphy (Unit 3), pigeonite is also widespread and often occurs as irregular cores that are rimmed by primary orthopyroxene (McDonald *et al.,* 2017). Similar to the Waterberg and Aurora projects, petrographic studies on Harriet's Wish reveal the presence of widespread inverted pigeonite in the upper gabbros in the upper lithologic unit (Figure 6.4 a). However, the pigeonite in the Harriet's Wish samples is not rimmed by primary orthopyroxene, as on the Aurora Project, rather inverted pigeonite is present containing blebs of clinopyroxene (Figure 6.9) like on the Waterberg Project (Kinnaird *et al.,* 2017). Therefore, in terms of the presence of pigeonite, the upper gabbronorites on the Aurora Project (McDonald *et al.,* 2017) does not equate with the Upper Zone magnetite-bearing gabbro on the Waterberg Project and the upper gabbronorites and gabbros on Harriet's Wish.

Other similarities between the Waterberg Upper Zone (Kinnaird *et al.,* 2017) and the Harriet's Wish upper lithologic unit include 1) the irregular occurrence of the association of three co-existing pyroxenes (orthopyroxene, clinopyroxene and inverted pigeonite) in the upper lithologic unit, 2) the abundance of the orthopyroxene peritectic rims around olivine in the olivine-bearing lithologies, 3) the presence of the corroded olivine and plagioclase laths in the pyroxene oikocrysts in olivine gabbronorite and pyroxenite (Figure 6.4b), 4) the occurrence of the magnetite symplectites between cumulus olivine

and coarse cumulus magnetite, and 5) the presence of quartz in the mafic cumulates (Figure 6.6c).

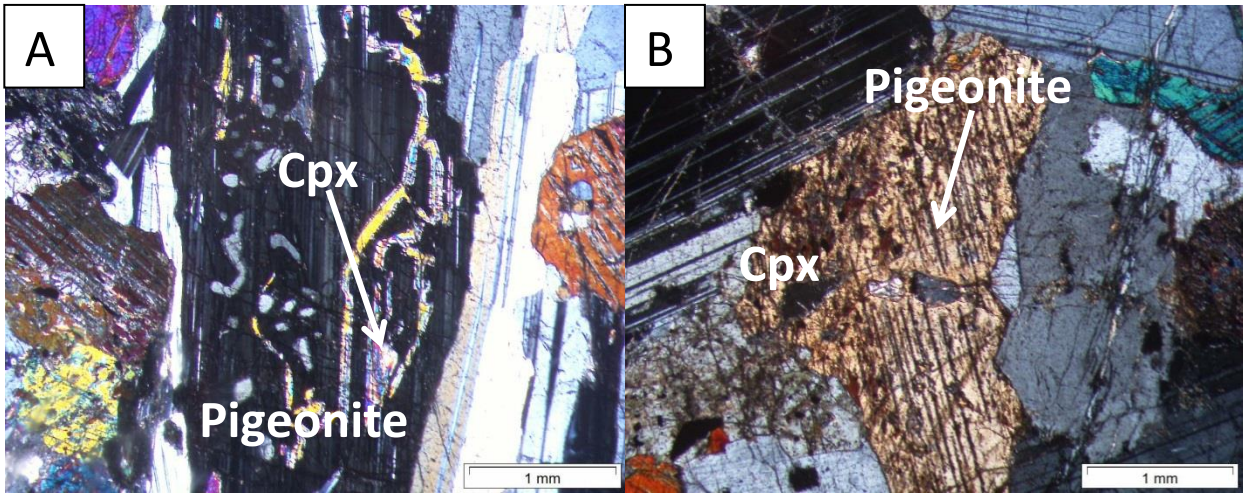

Figure 6.9: Pigeonite textures under transmitted light of the upper lithologic unit on Harriet's Wish. A: Cumulus inverted pigeonite with blebs of clinopyroxene in pigeonite in lineated gabbro of HW029 at a depth of 421.45 m. B: Cumulus orthopyroxene with an inverted pigeonite core in gabbronorite of HW029 at a depth of 516 m. Abbreviations: Opx=orthopyroxene.

The Aurora Project stratigraphy has been placed in the upper Main Zone, and not in the Upper Zone (McDonald *et al.,* 2017). However, according to the practice developed by Ashwal *et al.,* (2005), and the notion followed in this study, magnetic susceptibility should be used to define the boundary between the Upper and Main Zones. The magnetic susceptibility measurements were not done on the Aurora Project whereas the geochemical - lithologic parameters were used to define the Main Zone affiliation (McDonald *et al.,* 2017). Due to this, the correlation between Harriet's Wish, the Waterberg Project and the Aurora Project rock types is provisional. Magnetic susceptibility studies need to be done to determine the position of the boundary between the magnetite-free and magnetite-bearing lithologies.

However, so far, we can note the differences seen between the Aurora Project and Harriet's Wish magmatic sequences. These include 1) the absence of the Unit 1 correlate on Harriet's Wish contains minor pyroxenite and abundant gabbronorite (McDonald *et al.,* 2017), 2) chromite is detected in the Harriet's Wish lower lithologic

unit whereas it was not reported at all in rocks of the Aurora Project (McDonald *et al.,* 2017), 3) quartz is widespread in the Harriet's Wish upper mineralisation whereas it is not noted on the Aurora Project (McDonald *et al.,* 2017).

Similar to the Waterberg and Aurora projects (Kinnaird *et al.,* 2017; McDonald *et al.,* 2017), the lithologies in the upper lithologic unit show abundant alteration (Figure 6.3 d; Figure 6.4a and d) including serpentinisation of olivine, sericitisation and saussuritisation of plagioclase, chloritisation and epidotisation of pyroxenes.

6.4.4 **Mineralisation**

The F Zone PGE-Cu-Ni mineralisation is found at the base of the Waterberg Project stratigraphy (McCreesh, 2013; Kinnaird *et al.,* 2017; Huthmann *et al.,* 2018). The F Zone mineralisation is hosted in feldspathic pyroxenite, pyroxenite, harzburgite and true troctolite, with the olivine-rich varieties showing abundant serpentinisation. In the F Zone, secondary magnetite replaces sulphides in serpentinised harzburgite. The sulphides present in the F Zone include pyrrhotite, chalcopyrite and pentlandite with accessory chromite, chalcocite and pyrite and occur as disseminated droplets, as inclusions in silicates, in veinlets and along silicate-grain boundaries (McCreesh, 2016, 2018).

Unlike the F Zone on the Waterberg Project, the lower mineralised zone on Harriet's Wish does not occur at the base of the stratigraphy (Figure 4.16; Kinnaird *et al.,* 2017). The lower mineralised zone is hosted in generally more mafic rocks such as leucogabbronorite, leucotroctolite with minor gabbronorite, olivine-bearing leucogabbronorite and rare pyroxenites, rather than ultramafic rocks (Figure 4.4; Kinnaird *et al.,* 2017). Similar to the F Zone, sulphides in the lower mineralised zone comprise pentlandite, chalcopyrite and pyrite with accessory pyrrhotite, which occur as disseminated specks, veinlets, inclusions in silicates and along silicate grain boundaries (Figure 6.5 a and b). The lower abundance of pyrrhotite is interpreted to be a result of its replacement by later pyrite.

On the Waterberg Project in the F Zone, chromite forms rare segregations, disseminated seams and lenses, with the chromite crystals often enclosed in silicates as chadacrysts, while chromite itself may host sulphide inclusions (Kinnaird *et al.,* 2017; Huthmann *et al.,* 2018; McCreesh, 2018). In the Platreef, closer towards the surface, chromitite occurs as the disseminated seams or discontinuous lenses at a constant stratigraphic level and it becomes more copious and persistent with depth (Yudovskaya and Kinnaird, 2010, Grobler et al., 2018)). In the lower mineralised zone on Harriet's Wish the chromite does not segregate into lenses or clusters as it does in the F Zone on the Waterberg Project, or in the Platreef (Yudovskaya and Kinnaird, 2010; Kinnaird *et al.,* 2017). Instead, it occurs in some narrow intervals of ultramafic rocks as single grains or as chadacrysts enclosed by orthopyroxene or associated with olivine or sulphides (Figure 6.5c).

6.4.5 **Upper mineralised zone**

The T Zone mineralisation on the Waterberg Project consists of the T2 (lower) and the T1 (upper) mineralised zones and occurs at the interface between the TGA sequence and the Upper Zone (McCreesh, 2016; Kinnaird *et al.,* 2017; McCreesh, 2018). The T2 Zone mineralisation is predominantly hosted in gabbro and gabbronorite and occurs as disseminated and blebby pyrrhotite, pentlandite, chalcopyrite, and pyrite with minor millerite, sphalerite, and bornite (Kinnaird *et al.,* 2017; McCreesh *et al.,* 2018). The T1 zone is predominantly hosted in pyroxenite, feldspathic pyroxenite, troctolite, harzburgite and gabbronorite (McCreesh, 2016; Kinnaird *et al.,* 2017). The T1 Zone has sulphides commonly occurring as blebby to net-textured chalcopyrite and pentlandite, with minor disseminated pyrrhotite, flame-textured pentlandite in pyrrhotite, and pyrite replacing pyrrhotite, or rimming earlier sulphides (Kinnaird *et al.,* 2017; McCreesh *et al.,* 2018). On the Aurora Project, a "T-Zone-like" mineralised unit is present (McDonald *et al.,* 2017). The sulphide minerals include aggregates of pyrrhotite, pentlandite and chalcopyrite that are interstitially present between silicate minerals and along cleavage planes in clinopyroxene (McDonald *et al.,* 2017). This mineralised zone is hosted in gabbronorites and leucogabbronorites (McDonald *et al.,* 2017).

Overall the upper mineralised zone on Harriet's Wish has some common features both with the T Zone (more specifically the T2 Zone) on the Waterberg Project and the mineralisation on the Aurora Project (Kinnaird *et al.,* 2017; McDonald *et al.,* 2017). Similar to the T2 Zone, the upper mineralised zone on Harriet's Wish is hosted in gabbronorite, leucogabbronorite, melagabbronorite and anorthosite (Kinnaird *et al.,* 2017). The upper mineralised zone contains disseminated, blebby and veinlet pentlandite, pyrrhotite, and chalcopyrite that is similar to the T Zone mineralisation, but this association and the textures are typical for any other occurrence of magmatic sulphides in Bushveld rocks (Kinnaird *et al.,* 2017). However, the elevated proportion of pyrite among the sulphides and the occurrence of its euhedral crystals rimmed by quartz and chlorite both in the T Zone and on Harriet's Wish may support the correlation between these zones. At the same time, millerite, which is abundant in the T Zone, was not encountered in the lower mineralised zone on Harriet's Wish.

Similar to the T Zone on the Waterberg Project (Kinnaird *et al.,* 2017; McCreesh *et al.,* 2018), quartz is abundant in the upper mineralised zone on Harriet's Wish and is associated with the sulphide grains often forming the encrustations around sulphides (Figure 6.6 c). The quartz crustification and associated growth of chlorites and amphiboles suggests that hydrothermal fluids could have had an influence in leaching of sulphides in the lower mineralised zone and redepositing them in the Upper Zone.

The pyroxenite associated with the T Zone (or T1 Zone) has been suggested to possibly correlate with the Pyroxenite Marker in the rest of the Bushveld Complex (McCreesh, 2016). Using this Pyroxenite Marker, McCreesh, (2016) compared the T Zone with mineralisation on Moordrift (Maier and Barnes, 2010). There is no pyroxenite associated with the upper mineralised zone on Harriet's Wish (Figures 4.4 and 4.16).

6.5 **Conclusion**

There are significant similarities seen between the TGA sequence on the Waterberg Project and the lower lithologic unit on Harriet's Wish, such as the presence of major true troctolite and minor pyroxenite packages, similar rock textures and alteration types

as well as the occurrence of rare chromite grains indicative of the involvement of the Critical Zone melts at their formation (Kinnaird *et al.,* 2017). However, the primary sulphide assemblages of the lower lithologic unit on Harriet's Wish are hydrothermally reworked to a much higher extent with respect to relatively unaltered magmatic features of the TGA sequence on the Waterberg Project (Kinnaird *et al.,* 2017) when comparing the degree of alteration of host lithologies and the presence of relics of olivine and olivine norite and alteration minerals.

There are also significant petrographic overlaps between the Upper Zone on the Waterberg Project and the upper lithologic unit on Harriet's Wish, such as the three-pyroxene association, common quartz in association with pyrite+ chlorite+ amphibole, and the presence of cumulus to interstitial magnetite and its symplectites with orthopyroxene (Kinnaird *et al.,* 2017). The Unit 2 and 3 lithologies on the Aurora Project and the upper lithologic unit on Harriet's Wish can be the correlates based on the presence of magnetite and pigeonite in gabbro and gabbronorite, as well as the occurrence of similar-style PGE sulphide mineralisation (McDonald *et al.,* 2017).

The F Zone, however, cannot be directly correlated with the lower mineralised zone on Harriet's Wish. The major difference between the F Zone and the lower mineralised zone is the absence of ultramafic (harzburgitic) lithology on Harriet's Wish whereas it is a major ore-bearing rock type in the F Zone. In addition, the stratigraphic position of the lower mineralised zone is not persistent and can deviate significantly from the base of the succession. However, the scarce chromite grains and the relics of olivine replaced at peritectic reactions suggest that primary ultramafic rocks have likely been present in the Harriet's Wish sequence prior to the intrusion of gabbroic melts, which gave rise to crystallisation of the troctolite-bearing lower lithologic unit.

The Waterberg T Zone correlates well with the Harriet's Wish upper mineralised zone based on the similar textures and mineral assemblages of the host lithologies, the similarities in the sulphide mineral assemblages and the prominent presence of quartz.

In conclusion, the correlation between the Waterberg Project and the Harriet's Wish is more straightforward than with the Aurora Project.

6.6 **Recommendations**

It is recommended that PGM studies should be done on Harriet's Wish and on the Aurora Project to elaborate the correlation between the F Zone and the lower mineralised zone (see McCreesh *et al.,* 2018).

Chapter 7
Mineralisation- geochemical aspects

7.1 Introduction

The exploration results of the Waterberg Project were made known in 2012, where 4.99 million PGE ounces (2E) were identified (Lomberg, 2012). Because of this, Sylvania made the decision to enlarge the boundaries of their exploration efforts and drill additional boreholes in the northern end of the Harriet's Wish farm close to the border of the Waterberg Project area. Through this, Sylvania intersected mineralised rocks and the assay results confirmed a find of "world class PGM mineralisation" (Sylvania Resources Limited, 2012). According to Sylvania Resource Limited, (2012), when compared to the results of the intersections announced by PTM on its Waterberg Project, the mineralised intersection in the HW029 drillcore could be an equivalent to the PTM's T Zone, and the troctolitic sequence intersected in the HW024 drillcore, is possibly an equivalent of the PTM's F Zone.

According to Naldrett, (2004), the Bushveld Complex contains approximately 75 % of Pt, 52 % of Pd, Rh 82 % of Rh and 16 % of Ni that is minable on Earth. Naldrett *et al.,* (2009) describes that the stratigraphic units that contain these concentrations include the UG-2 chromitite, the Merensky Reef and the Platreef. There has been extensive work done on the tenors and geochemistry of the UG-2 and the Merensky Reef in the western and eastern Bushveld Complex, and some work done on the Platreef tenors (Kekana, 2014). PGE tenors are concentrations of metals such as Pt, Pd, Rh, Ru, Ir and Os in 100 % sulphide and are described as a representative concentration of a particular metal in the original sulphide liquid, after immiscible sulphide has segregated from its host magma (Naldrett *et al.,* 2011). The tenor calculations are therefore important to understand the overall mineralisation and processes involved in the deposition of the ore minerals better, and to evaluate if the distribution of metals and their inter-correlations are consistent with those predicted for the magmatic process.

In addition to base metal sulphides, a different set of PGE minerals can be exsolved and crystallised from sulphide liquid during cooling (McCreesh *et al.,* 2018). On Turfspruit in the northern limb of the Bushveld Complex the predominant PGM are Pt sulphides and Pt-Fe alloys similar to the assemblages typical for the Merensky Reef in the western and eastern limbs (Hutchinson *et al.,* 2015; Yudovskaya *et al.,* 2017). On the Waterberg Project, McCreesh *et al.,* (2018) found that there are two very different assemblages of PGM in the T and F zones. The overall major groups include Pt-Pd bismuthotellurides, sperrylite $PtAs_2$, Pt-Rh sulpharsenides, minerals of the system Pd-Ni-As, Pt-Fe alloys, Pt-Pd (± Ni) sulphides, minerals of the system Pt-Pd-Sn and Au-Ag alloys

7.1.1 **Aims**

The aims of the ore mineralogy study, therefore, is to test this finding by Sylvania Resources Limited, (2012), especially to determine whether the ore mineralisation (Upper and Lower mineralised zones) on Harriet's Wish does equate to the T and F zones. As mentioned in the previous chapters, if this correlation holds true, then the T and F zones on the Waterberg Project could extend 30 km along strike through to the Aurora Project farms (McDonald *et al.,* 2017). This section also aims to determine whether the mineralisation is of primary magmatic (crystallised from the magma that formed the lithologic unit) or secondary magmatic origin (crystallised through events that occurred post- deposition of lithologic unit) through the correlation of the S, Cu and Pt+ Pd+ Au values. The tenor calculations and plots will assist in discussing relationships between mineralisation and magmatic processes that have resulted in the observed stratigraphy on Harriet's Wish.

7.2 **Methods**

Pt, Pd, Au, Ni, Cu and S data presented here were provided by Sylvania Resources Limited, on the condition that the data should be used as ratios, or that data bars be removed from figures to preserve the sensitive nature of the ore grade data. The data used in this chapter is therefore from a different dataset, of the same holes, to the data

used in the geochemistry chapter of this study. Fire assay was used to obtain these results and commercial standard laboratory practices and procedures were followed.

7.2.1 **Calculation of tenors**

The holes selected for the tenor calculations were HW024, HW025 and HW029. The assay data provided by Sylvania were used for these calculations. For a full list of tenor calculations see Appendix G.

To obtain the tenor results an excel spreadsheet compiled by A. Naldrett (Naldrett *et al.,* 2011) was used. In this spreadsheet the following method was followed:

All the Cu values were calculated as chalcopyrite and all the Ni values as pentlandite (with a few exceptions outlined below). The S values of each of these were subtracted from the total S, and the remaining S was calculated as pyrrhotite (Naldrett *et al.,* 2011). The total amount of sulphides present was calculated by adding chalcopyrite, pentlandite and pyrrhotite together with the assumption that amounts of all other sulphide minerals are negligible. In the olivine-bearing lithology, Ni in the samples was assumed to be part of a silicate to avoid exaggerated values of pentlandite. Where negative pyrrhotite values were encountered the 2.65 x S method was employed to avoid distortion of the values (Naldrett *et al.,* 2000). Sulphur values of less than 0.1 wt % were considered to be too low for an accurate interpretation and were therefore not used. As it is common practice in the Bushveld Complex, where pyrrhotite values were negative, and various amounts pentlandite was subtracted based on lithology. This was done because some Ni is also incorporated into silicate minerals with up to 0.1 wt % NiO in orthopyroxene and 0.25 wt % NiO in olivine. The following procedure was followed in this regard:

- Where pyrrhotite values were negative, and the rock type was ultramafic, 0.007 wt % assuming silicate Ni was subtracted from the total Ni.
- Where pyrrhotite values were negative, and the rock type was mafic (containing significant pyroxenes), 0.005 wt % Ni was subtracted from the total.

- Where pyrrhotite values were negative, and the rocks contained a considerable amount of olivine (more than 10 %), 0.05 wt % Ni was subtracted from the total.
- This endeavour only changed a few of the pyrrhotite values to positive. The most common change was in olivine-bearing rocks.

The tenor calculation assumes the following (as described by Naldrett *et al.,* 2011):

- The S content in the sample equates to the original S content in the magma.
- All the Cu and Ni are present in sulphides, except for the silicate Ni values as described above.
- All PGEs were initially collected by immiscible sulphide liquid.

7.3 **Results**

7.3.1 **Exploration results**

Table 7.1: PGE and base metal mineralisation intervals found in Harriet's drillcores HW024 and HW025 (Sylvania Resources Limited, 2012).

Hole	From	To	Interval	2PGE+Au ppm	Pt ppm	Pd ppm	Au ppm	Ni ppm	Cu ppm	Core Recovery
HW024	346.25	349.56	3.31	8.22	2.73	5.00	0.49	3034	2214	98
HW024W1	346.24	349.58	3.34	6.60	1.83	4.25	0.51	3165	2092	92
HW029	613.54	615.40	1.86	3.24	0.82	1.11	1.30	1324	3738	97
HW029	633.70	636.62	2.92	4.59	1.00	0.52	3.06	2374	7020	100
HW029	637.77	639.71	1.94	3.72	0.87	0.51	2.33	1812	5220	92

Table 7.1 outlines the major findings of the exploration effort that was employed by Sylvania Resources Limited, (2012). The most notable intercept occurred in the HW029 drillcore at a depth of 350 m, yielding a grade of 8.22 g/t over 3.31 m (drill width) of 3E (Pt, Pd and Au). The results of the deflection yielded 6.60 g/t 3E over 3.34 m over the same interval. According to Sylvania, the HW029 drillcore also intersected a mineralised sequence of alternating pegmatoidal feldspathic pyroxenite, gabbronorite and minor troctolite. At a depth of 633.7 m, a grade of 4.59 g/t over 2.92 m was found.

Table 7.2: Ore metal ratios and ranges of assay data for the drill cores HW024, HW025 and HW029 on Harriet's Wish (data from Sylvania Resources Limited). LMZ= lower mineralised zone, UMZ= upper mineralised zone. For ratios, average values were obtained first, and then ratios were made based on the averages.

Ore ratios	UMZ Average	UMZ range	LMZ Average	LMZ range
	50 samples		166 samples	
(Pt+Pd)/Au	1.70	0.47 - 6.91	34	1.59 - 175
Ni/Cu	0.48	0.28 - 1.58	5.43	0.90 - 69.3
Pt/Pd	1.34	0.33 - 3.90	0.72	0.20 - 1.90
Cu/Pd	8147	1047 - 19024	491	17 - 1619

Overall, the lower mineralised zone has higher average (Pt+Pd)/Au and Ni/Cu ratios, and lower average Pt/Pd and Cu/Pd ratios than the upper mineralised zone.

7.3.2 **Lower mineralised zone**

The average (Pt+Pd)/Au ratio for the lower mineralised zone is 34 with a range of 1.6-175. The average Ni/Cu ratio for the lower mineralised zone is 5.43 with a range of 0.9-69. The average Pt/Pd ratio for the lower mineralised zone is 0.72 with a range of 0.2-1.9. The average Cu/Pd ratio for the lower mineralised zone is 491 with a range of 17-1619 (Table 7.2).

There is a moderate correlation between the S, Cu and Pt+ Pd+ Au contents in the HW024 drillcore and no correlation between these peaks in the HW025 drillcore when plotting these elements against depth (Figures 7.1 and 7.2). There is no apparent correlation seen between the Ni/Cu ratio and the grades within the lower mineralised zone. The Ni/Cu peaks, instead, correlate with the olivine-enriched lithologies, immediately above mineralisation in both the HW024 and HW025 drillcores. The Pt/Pd ratio is elevated over the lower mineralised zone but increases upward over the olivine-enriched lithologies immediately above the lower mineralised zone in the HW024 intersection. The Cr values generally peak over the lower mineralised zone.

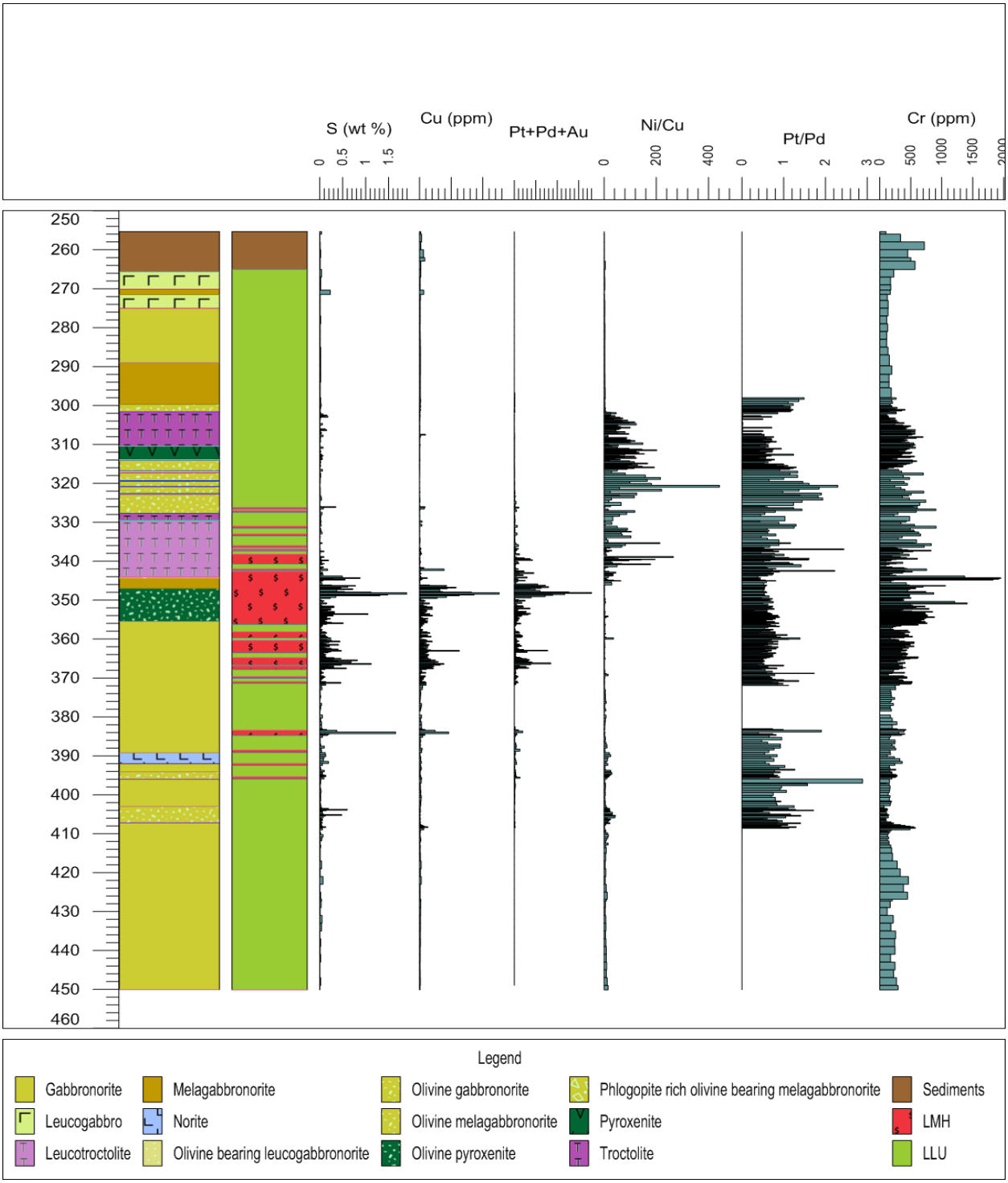

Figure 7.1: PGE grade, S, Cu and Cr contents and metal ratios plotted against depth of the various units observed in the HW024 drillcore. The column on the left shows the stratigraphy, while the column on the right shows the stratigraphic affiliation of the units. LLU= lower lithologic unit, LMH= lower mineralised zone.

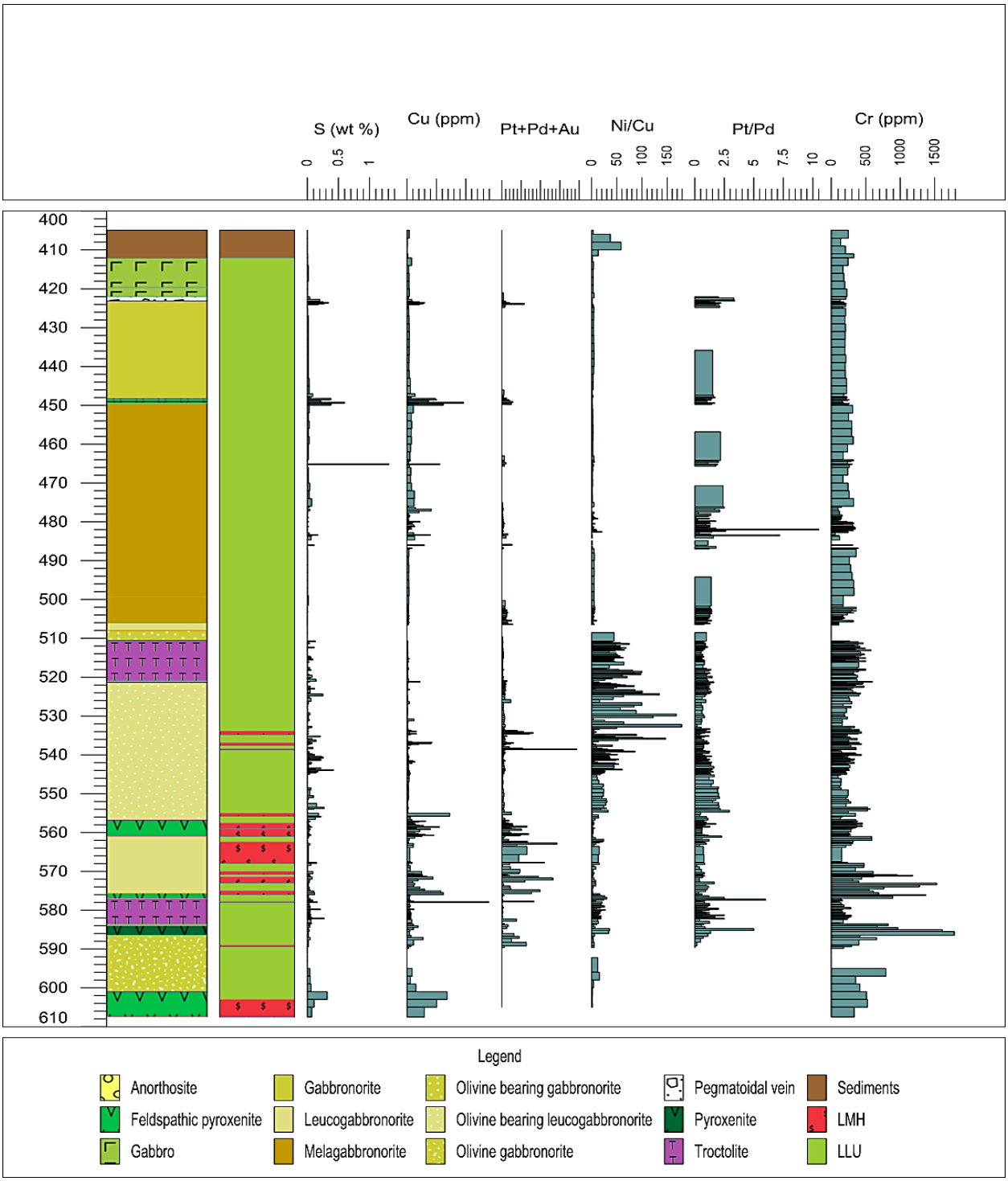

Figure 7.2: PGE grade, S, Cu and Cr contents and metal ratios plotted against depth of the various units observed in the HW025 drillcore. The column on the left shows the stratigraphy, while the column on the right shows the stratigraphic affiliation of the units. LLU= lower lithologic unit, LMH= lower mineralised zone.

7.3.3 **Upper mineralised zone**

The average (Pt+ Pd)/Au ratio for the upper mineralised zone is 1.7 with a range of 0.47-6.9. The average Ni/Cu ratio for the upper mineralised zone is 0.48 with a range of 0.28-1.6. The average Pt/Pd ratio for the upper mineralised zone is 1.34 with a range of 0.3-3.9. The average Cu/Pd ratio for the upper mineralised zone is 8147 with a range of 1064-19024.

Three major intervals of mineralisation, separated by approximately 15 to 20 m thick barren rocks, occur in the HW029 intersection (Figure 7.3). There is an excellent correlation between the peaks of S, Cu and Pt+ Pd+ Au over these mineralised intervals (Figure 7.3). The Ni/Cu ratio does not correlate with the grade; however a peak of this ratio is seen close to the upper interval of mineralisation over the olivine-bearing gabbronorites at a ~600 m depth. The Pt/Pd ratio shows an increase just above the lower interval of mineralisation at a ~630 m depth. The Cr content is somewhat elevated over the upper mineralised zone; however, it increases sharply over the contact between the lower and upper lithologic unit at a ~610 m depth, and reaches a peak value above the upper mineralised zone at a ~580 m depth. There are smaller peaks in the Ni/Cu, Pt/Pd ratios and Cr content at a ~560 m depth in the upper lithologic unit.

The Cr contents contrast sharply between the lower and upper mineralised zones and the lower and upper lithologic units (Figures 7.1, 7.2 and 7.3). In the lower mineralised zone, the Cr content reaches 2000 ppm whereas in the upper lithologic unit the Cr content does not exceed 300 ppm Cr.

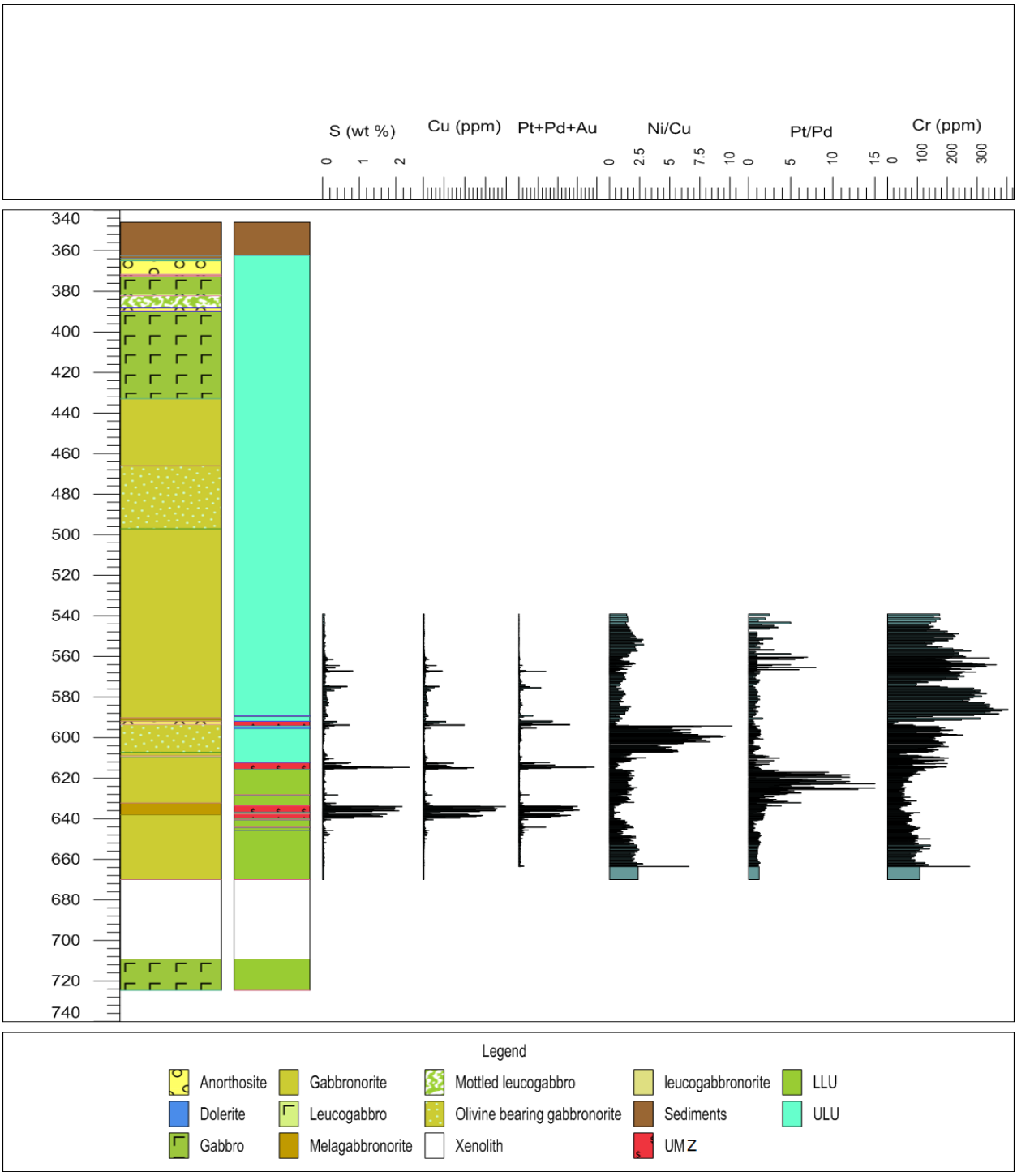

Figure 7.3: PGE grade, S, Cu and Cr contents and metal ratios plotted against depth of the various units as observed in the HW029 drillcore. The column on the left shows the stratigraphy, while the column on the right shows the stratigraphic affiliation of the units. LLU= lower lithologic unit, ULU= upper lithologic unit, UMZ= upper mineralised zone.

7.3.4 **Harriet's Wish Tenors**

Tenor variations are described using tenor values and/or metal grades (low or high), observed trends and the proportions of Pt vs Pd in each unit. A grade reference line was drawn at 100 ppm on the tenor plots. The reference line is based on an observation by Naldrett *et al.,* (2009) that the Merensky Reef Pt+ Pd tenors are generally above 100 ppm. The tenor plots for the HW024, HW025 and HW029 intersections are shown in Figures 7.4, 7.5 and 7.6. The shaded bar on the diagrams indicates a zone which corresponds to the amount of sulphide that would be contributed by 10–40 % of trapped, sulphide-saturated intercumulus silicate liquid (Naldrett *et al.,* 2009). Sulphide content that plot to the right of the shaded area is likely due to the presence of excess sulphide in the melt; and where sulphide content plots to the left of the shaded area, it is unlikely that excess immiscible sulphides were present in the melt (Naldrett *et al.,* 2009).

The lower mineralised zone occurs in drill cores HW024 and HW025 as shown in Figures 7.4 and 7.5. Overall, the lower mineralised zone PGE tenor concentration ranges from 1-6000 ppm. This mineralised zone can be divided into three broad intervals. 1) The basal mineralised section of the lower mineralised zone has a low to high tenor of 1-1000 ppm with a moderate-high sulphide contents and an upward decreasing trend. The Pt/Pd ratio has a range of 0.8-3 (Figures 7.4 and 7.5). 2) The middle interval of the lower mineralised zone has moderate-high tenors of 80-6000 ppm with a moderate-high sulphide content and an upward increasing trend. The Pt/Pd ratio has a range of 0.4-2 (Figures 7.4 and 7.5). 3) The upper interval of the lower mineralised zone has a low tenor of 1-100 ppm with a moderate-low S content and an upward decreasing trend. The Pt/Pd ratio has a range of 1-8 (Figures 7.4 and 7.5).

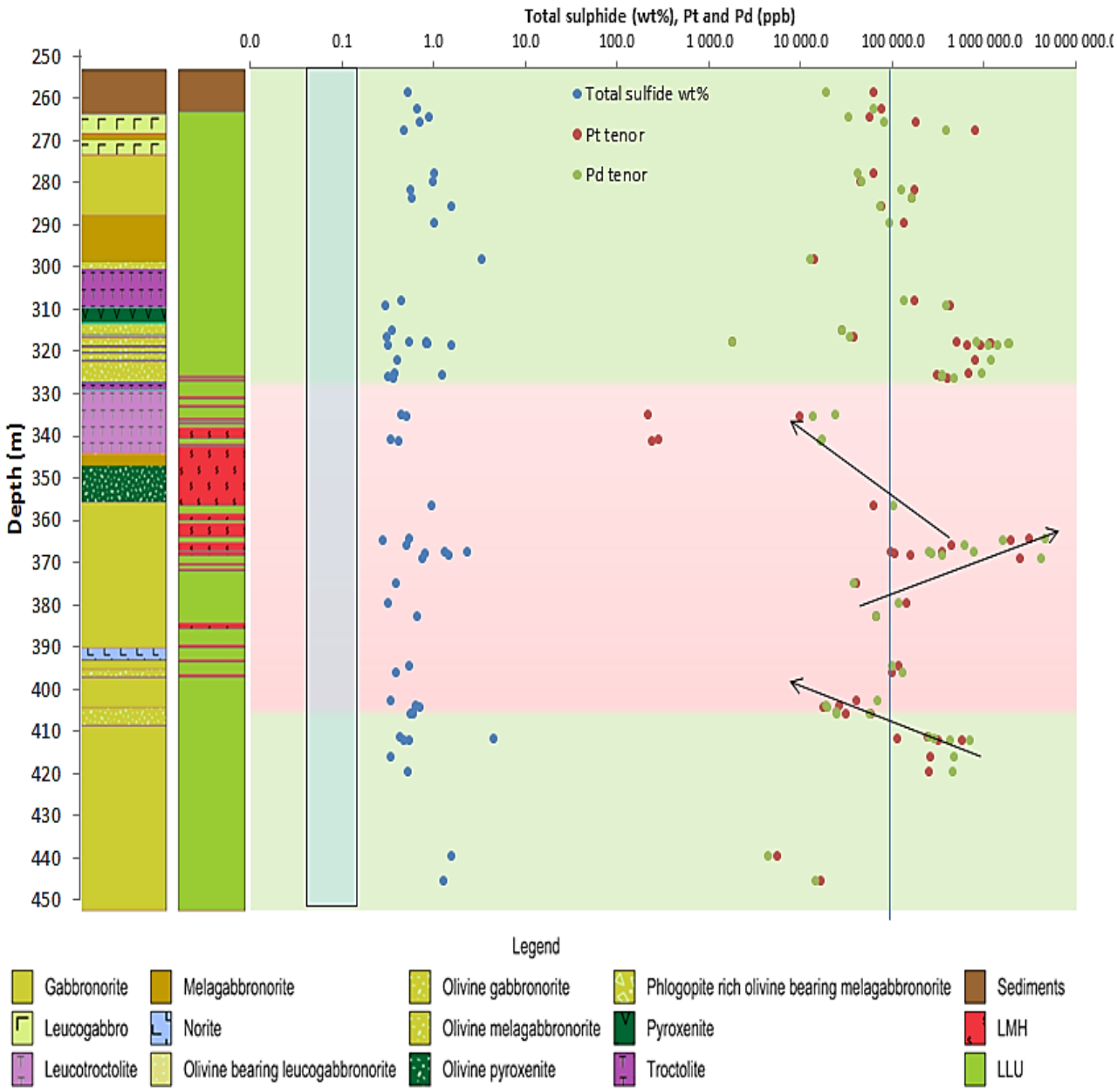

Figure 7.4: Pt and Pd tenors (ppb) and total sulphide content (wt %) plotted against depth of the HW024 drillcore. Reference line is based on an observation by Naldrett *et al.,* (2009) that the Merensky Reef Pt+ Pd tenors are generally above 100 ppm, and no tenor data is available for the Aurora and Waterberg projects. The tenors in the upper section of the Platreef in the central sector on Turfspruit plot at, or to the right of, this reference line (Yudovskaya *et al.,* 2017). The shaded bar on the diagrams indicates a zone which corresponds to the amount of sulphide that would be contributed by 10–40% of trapped, sulphide-saturated intercumulus silicate liquid (Naldrett *et al.,* 2009). LLU= lower lithologic unit, LMH= lower mineralised zone. Arrows indicate upward trends in tenors.

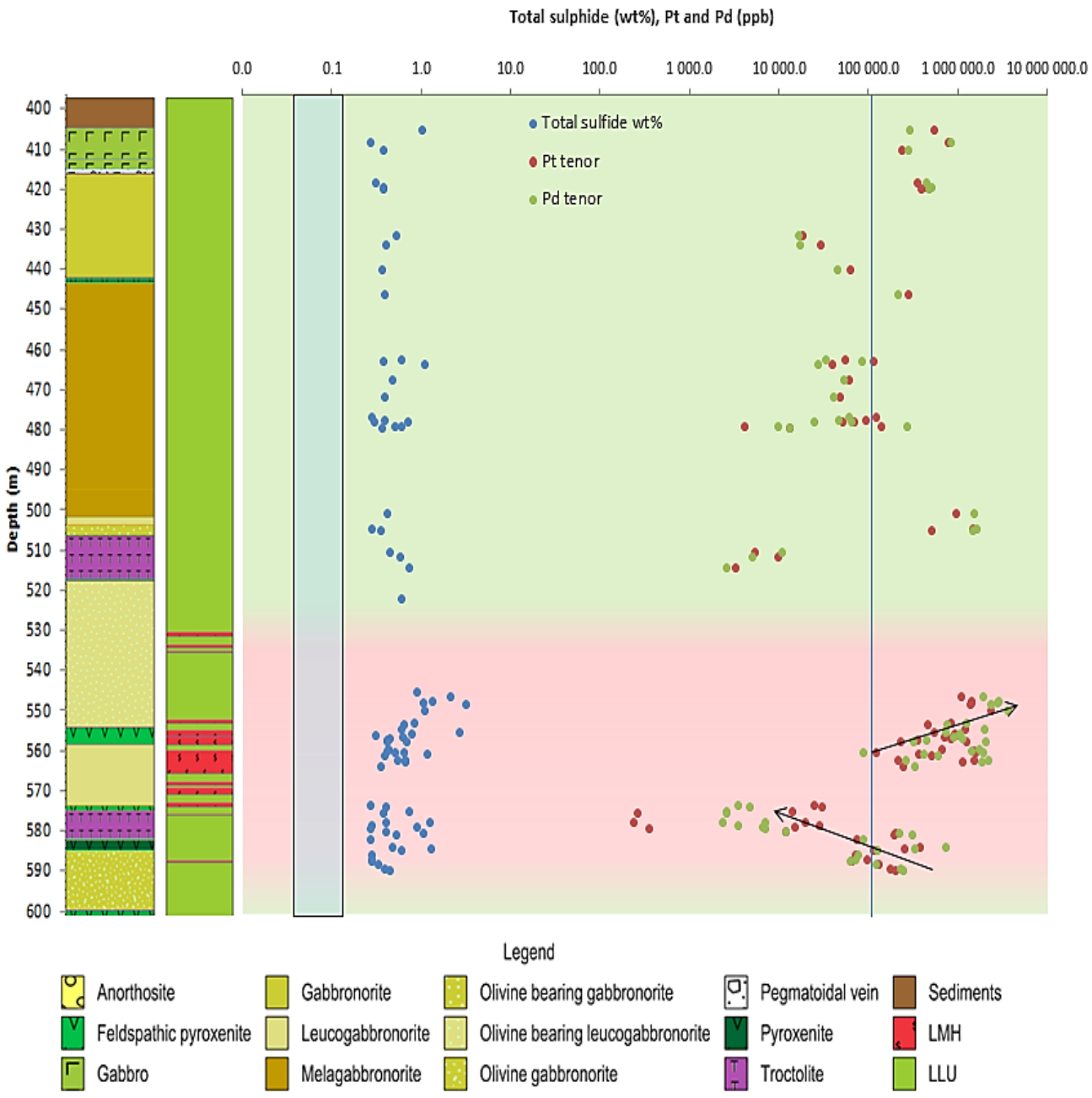

Figure 7.5: Pt and Pd tenors (ppb) and total sulphide content (wt %) plotted against depth of the HW025 drillcore. Reference line is based on an observation by Naldrett *et al.,* (2009) that Merensky Reef Pt+ Pd tenors are generally above 100 ppm, and no tenor data is available for the Aurora and Waterberg projects. The tenors in the upper section of the Platreef in the southern sector, on Turfspruit reaches up to 600 ppm and plot at or to the right of this reference line (Yudovskaya *et al.,* 2017). The shaded bar on the diagrams indicates a zone which corresponds to the amount of sulphide that would be contributed by 10–40 % of trapped, sulphide-saturated intercumulus silicate liquid (Naldrett *et al.,* 2009). LLU= lower lithologic unit, LMH= lower mineralised zone. Arrows indicate upward trends in tenors.

Overall the upper mineralised zone has PGE tenor concentrations of 1-1000 ppm. The upper mineralised zone can be divided into three intervals. 1) The basal mineralised section of the upper mineralised zone has a low to high tenor of 50-500 ppm with a moderate-high sulphide content and an upward decreasing trend. The Pt/Pd ratio has a range of 1-6 (Figure 7.1). 2) The middle interval of the upper mineralised zone has a low to high tenor of 1-1000 ppm with a moderate-high sulphide content and an upward decreasing trend. The Pt/Pd ratio has a range of 0.4-13 (Figure 7.1). 3) The upper interval of the upper mineralised zone has a moderate-high tenor of 50-1000 ppm with a moderate-high sulphide content and an upward decreasing tenor trend. The Pt/Pd ratio has a range of 0.3-6 (Figure 7.1). All intervals are distinguished by some heterogeneity in the host rock packages.

In the HW029 drillcore, some mineralisation is present above the upper mineralised zone, in the upper lithologic unit (of a provisional Upper Zone affinity; Kinnaird *et al.,* 2017) at a 560 m depth (Figure 7.6). This mineralisation has a high tenor of 100-3000 ppm and has a moderate-high sulphide content. The PGE characteristics of this interval are generally comparable with those of the upper mineralised zone at the contact, although the PGE tenor increases upwards.

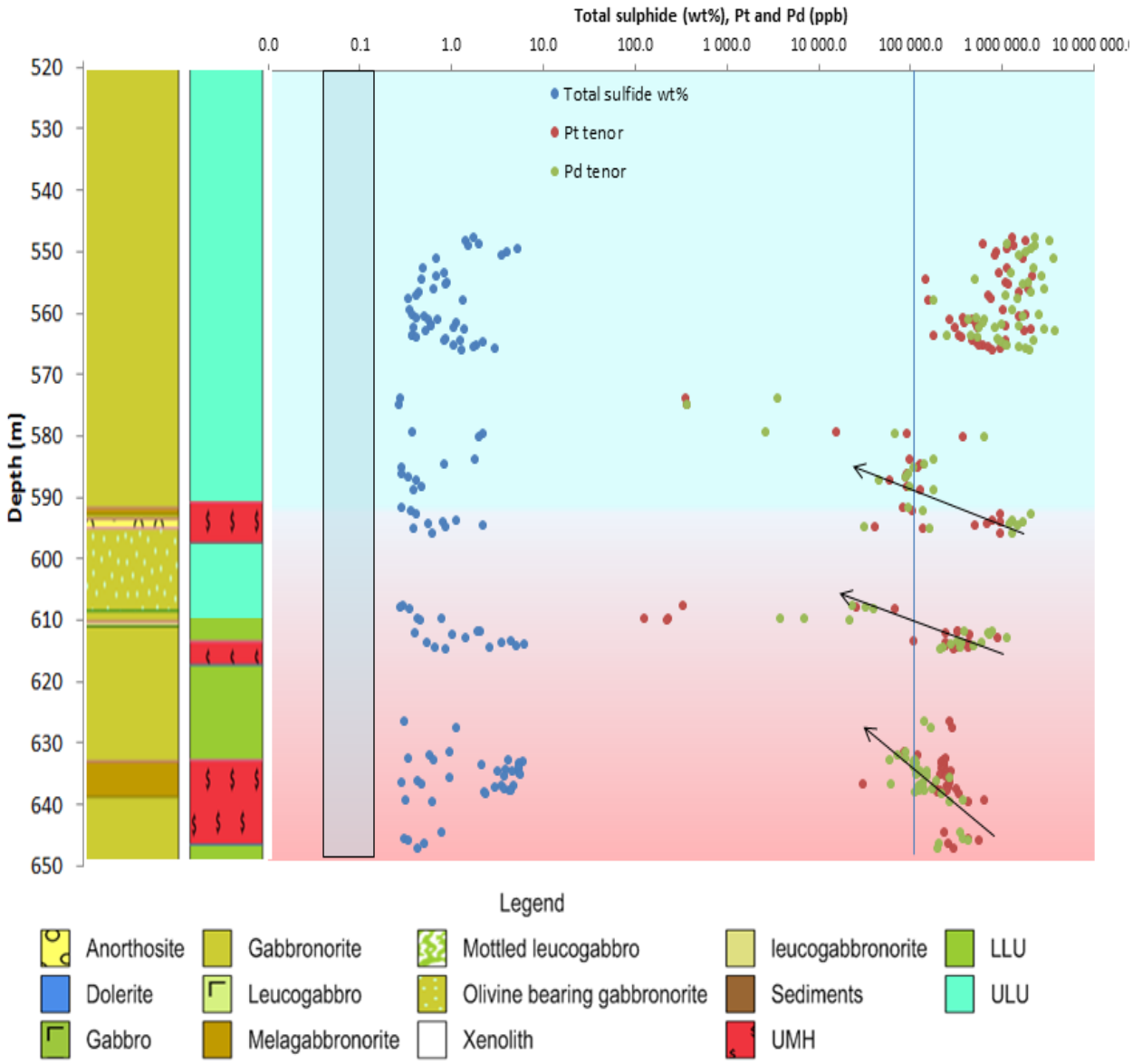

Figure 7.6: Pt, and Pd tenors and total sulphide content (wt %) plotted against depth of the HW029 drillcore. Reference line is based on an observation by Naldrett *et al.,* (2009) that Merensky Reef tenors are generally above 100 ppm, and no tenor data is available for the Aurora and Waterberg projects. The tenors in the upper section of the Platreef in the southern sector, on Turfspruit reaches up to 600 ppm and plot at or to the right of this reference line (Yudovskaya *et al.,* 2017). The shaded bar on the diagrams indicates a zone which corresponds to the amount of sulphide that would be contributed by 10–40 % of trapped, sulphide-saturated intercumulus silicate liquid (Naldrett *et al.,* 2009). LLU= lower lithologic unit, ULU= upper lithologic unit, UMH= upper mineralised zone. Arrows indicate upward trends in tenors.

7.4 **Discussion**

The F Zone mineralisation on the Waterberg Project occurs in the Ultramafic Sequence, and it is confined to the base of the igneous succession (McCreesh, 2016; Kinnaird *et al.,* 2017; Huthmann *et al.,* 2018). The F Zone mineralisation is mainly hosted in harzburgites, troctolites, and pyroxenites. Platreef reef-style mineralisation is generally restricted to pyroxenite and harzburgite (Kinnaird *et al.,* 2005; McDonald and Holwell, 2011; Yudovskaya *et al.,* 2017). Platreef contact-style mineralisation, however, is hosted by diverse rock types from mafic and ultramafic magmatic to hybrid and contact-metamorphic rocks (e.g. on Rooipoort, Townlands, Drenthe and Nonnenwerth; Viljoen and Schürmann, 1998; Kinnaird *et al.,* 2005; Maier *et al.,* 2008; Nex *et al.,* 2008; McDonald and Holwell, 2011; Kinnaird and McDonald, 2018). On Harriet's Wish, the lower mineralised zone is not confined to the base like the Ultramafic Sequence (Kinnaird *et al.,* 2017), but is found to occur irregularly throughout the lower lithologic unit (Figures 7.1 and 7.2). This mineralisation is mainly confined to leucotroctolite, olivine pyroxenite, feldspathic pyroxenite and olivine-enriched gabbronorites, similar to contact style mineralisation of the Platreef (Viljoen and Schürmann, 1998; Kinnaird *et al.,* 2005; Maier *et al.,* 2008; Nex *et al.,* 2008; McDonald and Holwell, 2011; Huthmann *et al.,* 2018).

The T Zone on the Waterberg Project occurs at the contact between the TGA (troctolite-gabbronorite-anorthosite) zone, with mineralisation occurring both below and above the boundary (Kinnaird *et al.,* 2017). The T Zone is subdivided into the T2 and T1 subzones with the T2 comprising heterogeneous gabbronorites and gabbros, and the T2 comprising troctolite, pyroxenite and feldspathic pyroxenite (Kinnaird *et al.,* 2017). On Harriet's Wish, the ore mineralisation data reveal more precisely the position of the upper mineralised zone (Figure 7.3). The upper mineralisation is confined to the boundary between the lower and upper lithologic units, with mineralisation being present in both the lower and upper lithologic units. The host rocks of this mineralisation include heterogeneous gabbronorites, gabbros and anorthosite (Figure 7.3). Overall, the position of the upper mineralised zone and the host rock compare with the T Zone on the Waterberg Project (Kinnaird *et al.,* 2017).

7.4.1 **Harriet's Wish ore grade compared to other localities in the Bushveld Complex**

Table 7.3 shows the average grades (2 PGE+ Au) for the lower and upper mineralised zones on Harriet's Wish compared to averages of the Waterberg mineralised zones (~4 g/t), the Merensky Reef in the eastern (4.09 g/t; Jones, 1999) and western (6.07 g/t; Jones, 1999) limbs, and the UG2 in the eastern (4.39 g/t) and the western (5.1 g/t; Jones, 1999) limbs. The Waterberg Project, the Aurora Project and the Harriet's Wish farm all have considerable mining potential when compared to other mined ore bodies in the rest of the Bushveld Complex (Table 7.3).

Table 7.3: Average inferred mineralisation data of various Bushveld localities. The values here may be skewed as an average of the Harriet's Wish data was taken from only 3 drillcores (HW024, HW025 and HW029), with the upper mineralised zone data only being taken from one drillcore (HW029). The Harriet's Wish values are for the mineralised zones only, and not for the entire lithologic units. The Waterberg Project data are from Lomberg, (2012); the Aurora Project data are adapted from McDonald *et al.,* (2017); the Harriet's Wish data are from the Sylvania Resources Limited, (2012) exploration report; the Merensky Reef and UG2 data are from Venmyn-Rand, (2010); the Platreef data are from Ivanhoe mines, (2018).

	Pt (ppm)	Pd (ppm)	Au (ppm)	2PGE+Au (ppm)	Pt:Pd:Au	Cu (wt%)	Ni (wt%)
Waterberg T zone (total)	0.94	1.55	0.72	3.33	29:47:24	0.18	0.1
Waterberg F zone (total)	0.91	1.74	0.35	3.01	31:57:12	0.04	0.12
Harriet's Wish UMZ	0.9	0.71	2.23	3.878	23:18:58	0.53	0.18
Harriet's Wish LMZ	2.28	4.63	0.5	7.41	31:62:07	0.22	0.31
Aurora	0.52	0.64	0.23	1.35	38:46:16	0.08	0.05
Merensky Reef (Western Bushveld)	4.42	1.885	0.2	5.00-9.00	68:29:03	0.08	0.13
Platreef	1.95	2.01	0.3	3.00-4.00	46:50:04	0.17	0.34
UG2 (average eastern and western)	3.6	3.81	0.2	3.00-7.5	47:50:03	<0.05	<0.05

What might add to the mining potential is the possible connection between the Waterberg Project T Zone, Harriet's Wish's upper mineralised zone and the mineralisation on the Aurora Project (McDonald *et al.,* 2017). So far links for the lower mineralised zones have not been fully established. On the Waterberg Project, the T Zone shows the higher average 2PGE grades than the F Zone. In comparison, the lower mineralised zone on Harriet's Wish also shows higher 2PGE grades than the upper mineralised zone (Table 7.3). The T Zone shows higher average 2PGE concentrations than the Aurora Project and the upper mineralised zone on Harriet's

Wish, with the Harriet's Wish's PGE grades plotting significantly lower than the T Zone grades (Figure 7.3; Table 7.3).

The F Zone on the Waterberg Project (Kinnaird *et al.,* 2017; Huthmann *et al.,* 2018), Aurora basal mineralisation (McDonald *et al.,* 2017), Platreef contact style mineralisation (Viljoen and Schürmann, 1998; Kinnaird *et al.,* 2005; Maier *et al.,* 2008; Nex *et al.,* 2008; McDonald and Holwell, 2011) are all Pd dominated and have Pt/Pd ratios of <1, with the F Zone Pt/Pd ratio being closer to 0.5. On Harriet's Wish, the Pt/Pd ratio of the lower mineralised zone is also <1 (0.72 on average), therefore comparing to the above-mentioned mineralised packages, including the F Zone. On the Waterberg Project, the Pt/Pd ratio in the T Zone is generally higher than the F Zone, and averages at ~0.6 (Kinnaird *et al.,* 2017). The upper mineralised zone on Harriet's Wish also has a generally higher Pt/Pd ratio than the lower mineralised zone; however, it averages at 1.3 ranging 0.3-3.9 that is notably higher than in the T Zone (Table 7.2; Kinnaird *et al.,* 2017). To avoid possible errors in calculation and considering different detection limits for Pt and Pd in the exploration analytical results, only the grade values over 0.005 ppb were used to assess the Pt/Pd ratio. In addition to this, anomalously high values of the ratio were also removed from calculation results; however, the observed range remained as described above.

When plotting Ni/Cu ratios versus (Pt+Pd)/Au of various localities in the northern limb and north of the northern limb, the lower mineralised zone on Harriet's Wish is seen to plot close to Akanani of the Platreef, as well as Rooipoort and Rooipoort LMF that are assigned to the Platreef by Maier *et al.,* (2008) or to the Main Zone by McDonald *et al.,* (2017) (Figure 7.7), and plots almost on top of the F Zone point (Figure 7.7). These areas have overall low Au and Cu concentrations compared to the Pt+Pd and Ni values, respectively, with Ni/Cu values >1. This indicates that the F Zone on the Waterberg Project (Kinnaird *et al.,* 2017) and the lower mineralised zone on Harriet's Wish are more akin to the Platreef localities than to the T Zone on the Waterberg Project and the upper mineralised zone on Harriet's Wish. The values of the upper mineralised zone on Harriet's Wish plot close to the T1 Zone values on the Waterberg Project as well as the

values from the La Pucella, Nonnenwerth and Kransplaats farms of the Aurora Project (Figure 7.7). These localities are characterised by higher Au and Cu concentrations compared to Pt+Pd and Ni values, respectively, with the Ni/Cu values <1.

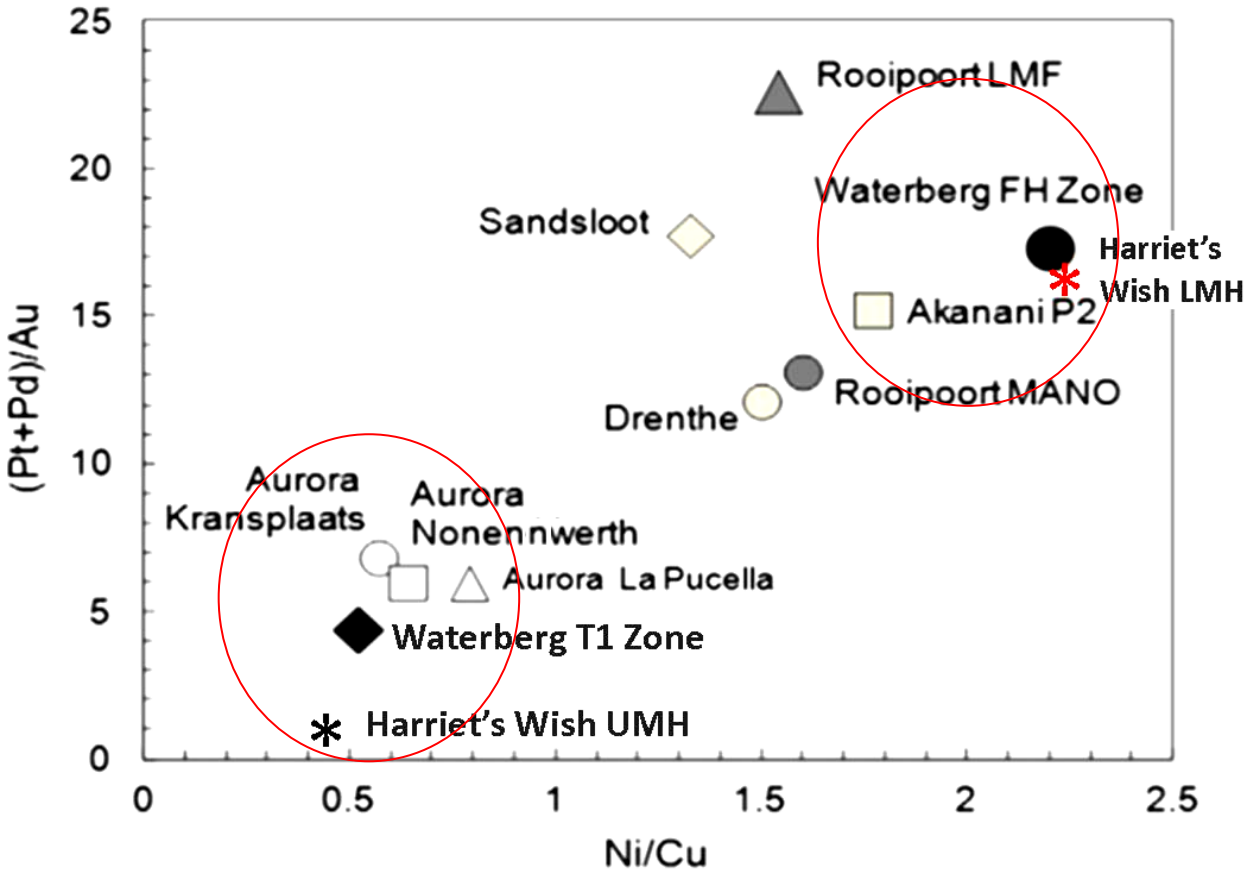

Figure 7.7: Ni/Cu values versus (Pt+Pd)/Au of the Harriet's Wish farm, the Aurora Project, the Waterberg Project and various Platreef localities (modified after McDonald and Holwell, 2011). LMH=lower mineralised zone, UMH=upper mineralised zone, red circles highlight similarities in localities.

McDonald *et al.,* (2017) use plots of Pt + Pd + Au versus Cr to compare certain northern limb localities to the Aurora Project whereas Huthmann *et al.,* (2018) reported these correlations for the F Zone on the Waterberg Project. Similarly, in this study, the Pt+ Pd+ Au versus Cr plots of Harriet's Wish and the Waterberg Project were compared and contrasted to the Aurora Project and other northern limb localities (Figure 7.8a). The lower mineralised zone values on Harriet's Wish and the F Zone on the Waterberg Project show similar scatter away from the x and y axes (Figure 7.8c and d). They also

demonstrate a more broad and consistent relationship between the PGE grade and Cr concentrations, rather than plotting close to the x and y axes as seen for the upper mineralised zone and the T Zone. This scatter could be due to the under-representation of the lower grade samples or including samples from unrelated mineralised intervals. Another interpretation is that this distribution reflects the genetic connections to the Platreef localities such as Townlands, Sandsloot-Overysel and Turfspruit as it was suggested earlier for the Waterberg F Zone by Huthmann *et al.,* (2018). The lower mineralised zone on Harriet's Wish and the F Zone on the Waterberg Project are also similar to the mineralised parts of the Lower Mafic Unit (LMF) and the Mottled Anorthosite Unit (MANO) that form the Grasvally Norite-Pyroxenite-Anorthosite (GNPA) member on the Grasvally and Rooipoort farms, as these areas also show a broad consistent relationship between the Pt + Pd + Au versus Cr plots, although the Cr concentration is higher overall (Figure 7.8e; Smith *et al.,* 2014).

The Aurora Project mineralisation, the T Zone on the Waterberg Project and the upper mineralised zone on Harriet's Wish, are seen to plot very close to the x and y axes. Any considerable grade in the upper mineralised zone on Harriet's Wish and the T Zone on the Waterberg Project, like the Aurora Project, are restricted to rocks with <300 ppm Cr. As noted by McDonald *et al.,* (2017), and as observed in this study, this contrasts distinctly with the relationship found in the Platreef, with Platreef mineralisation showing a very broad and consistent relationship between the PGE grade and Cr concentrations (Figure 7.8a). The BMS mineralisation on Moorddrift, however, does show low Cr values with corresponding high PGE values, as does the Aurora Project mineralisation, the Waterberg Project T Zone and the Harriet's Wish upper mineralised zone, however, there is an accompanying suite of Cr-richer but PGE-poor ultramafic rocks on Harriet's Wish (Figure 7.8c).

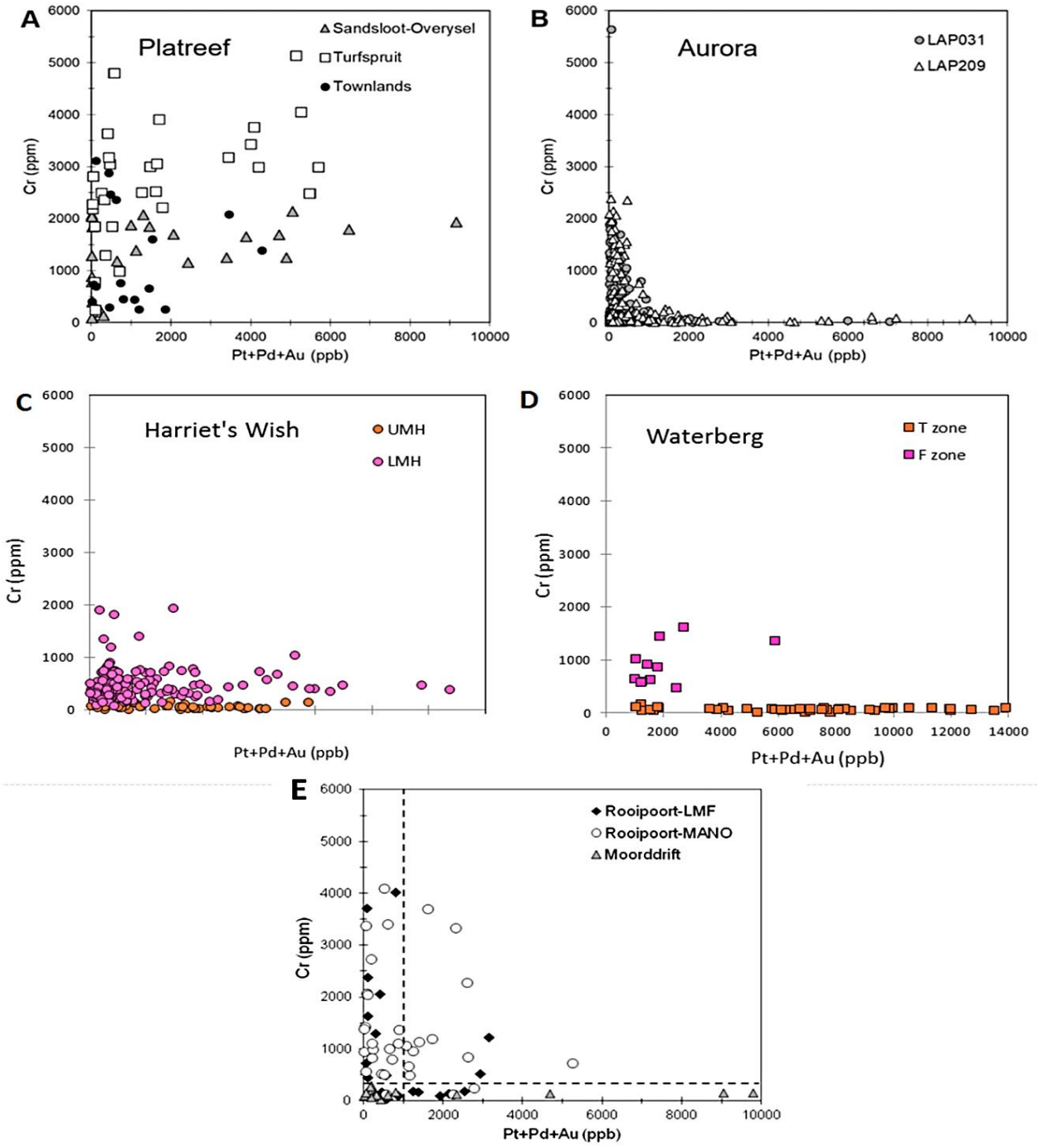

Figure 7.8: Chromium versus combined Pt+ Pd+ Au for A: different Platreef- Flatreef deposits B: Aurora boreholes LAP029 and LAP031 C: Harriet's Wish lower (LMH) and upper (UMH) mineralised zones from the HW024, HW025 and HW029 drillcores, D: Waterberg T and F zones from the WB099 drillcore, E: Rooipoort LMF and MANO, and Moorddrift. (Image A and B from McDonald *et al.,* 2017). Sandsloot- Overysel Platreef data from Holwell, (2006); Turfspruit Flatreef data from Smart, (2013); Townlands Platreef data from Manyeruke *et al.,* (2005); Aurora data from McDonald *et al.,* (2017); Lower Mafic Unit and Mottled Anorthosite Unit at Rooipoort (Maier *et al.,* 2008; Smith *et al.,* 2014) and Moorddrift (Maier and Barnes, 2010).

7.4.2 **Noble metal concentrations**

Although the localities north of the Hout River shear zone (Harriet's Wish and the T Zone on the Waterberg Project) are enriched in Au, the assay results reveal that the upper mineralised zone on Harriet's Wish is significantly enriched in Au compared to the lower mineralised zone on Harriet's Wish, the F and T Zone on the Waterberg Project (Kinnaird *et al.,* 2017), the mineralised zone on the Aurora Project and other northern limb localities (Table 7.3).

The lower mineralised zone on Harriet's Wish and the F Zone on the Waterberg Project both have higher Pd concentrations than the upper mineralised zone and the T Zone (Kinnaird *et al.,* 2017). At the same time, the lower mineralised zone as well as the T and F zones on the Waterberg Project are strongly Pd-dominated compared to the Merensky Reef and the UG2 (Figure 7.9) and better comparable with contact style mineralisation at the base of the Platreef (Viljoen and Schürmann, 1998; Kinnaird *et al.,* 2005; Maier *et al.,* 2008; Nex *et al.,* 2008; McDonald and Holwell, 2011).

The lower mineralised zone on Harriet's Wish and the F Zone on the Waterberg Project has slightly higher Pt grades than the upper mineralised zone and the T Zone on the Waterberg Project respectively (Kinnaird *et al.,* 2017). However, the Pt concentrations are generally lower than those in the other shown northern limb localities (Table 7.3).

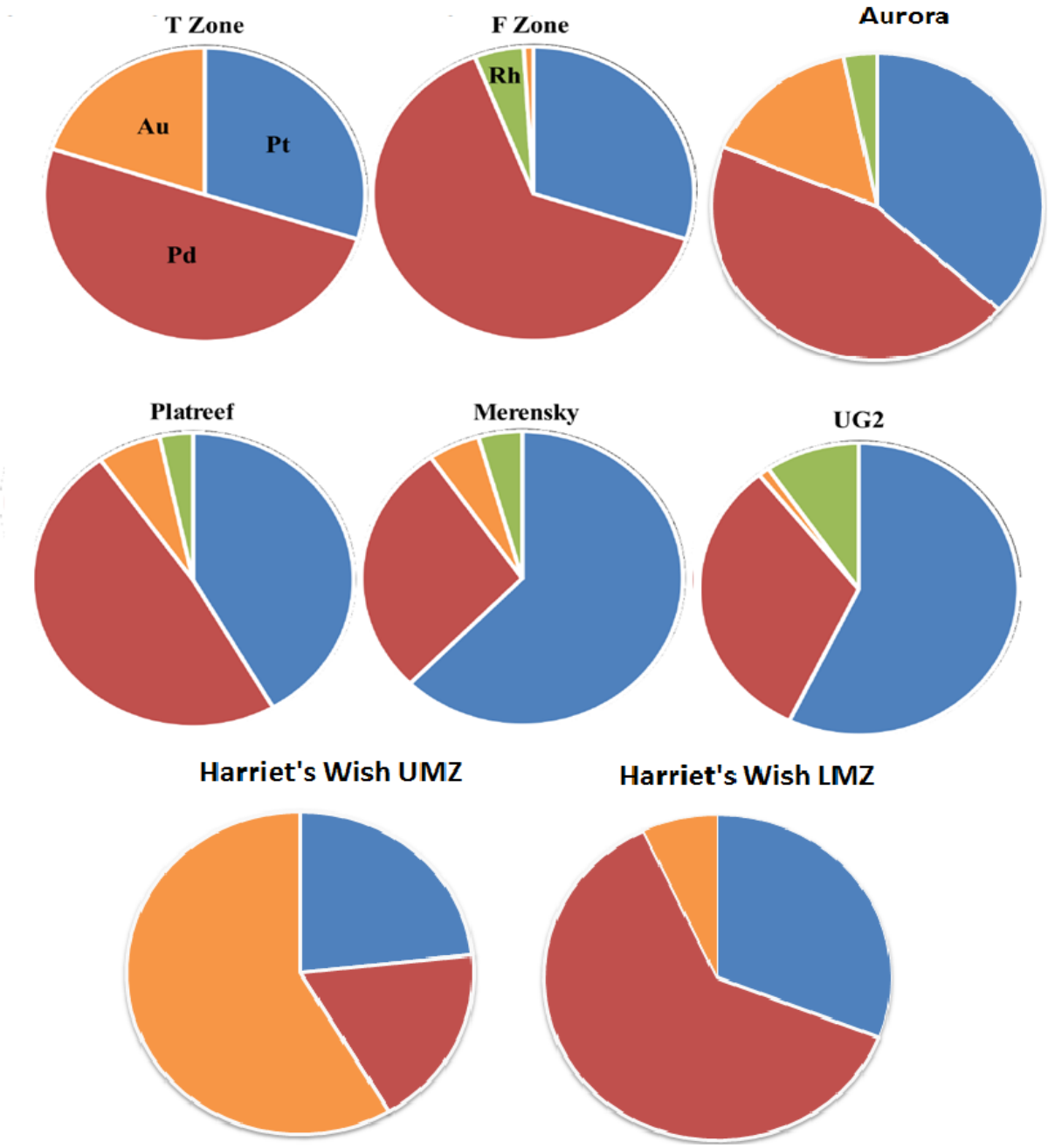

Figure 7.9: A comparison of the noble metal abundances of the Harriet's Wish lower and upper mineralised zones with the T and F mineralised zones on the Waterberg Project, the mineralisation on the Aurora Project, Platreef mineralisation, Merensky Reef mineralisation and UG2 mineralisation. This figure illustrates the dominance of Pd in the F Zone on the Waterberg Project and the lower mineralised zone on Harriet's Wish. Data for the Merensky Reef and UG2 from Barker, (2012), data for the Platreef based on Sandsloot from the Anglo Platinum annual report, (2011), data for the Waterberg Project from (Kinnaird *et al.,* 2017), data for Harriet's Wish from Sylvania Resources Limited, (2012) and data for Aurora from McDonald *et al.,* (2017). Modified after Kinnaird *et al.,* (2017).

7.4.3 **S, Cu and Pt+ Pd+ Au correlations**

The lower mineralised zone on Harriet's Wish shows a weaker correlation and decoupling between S, Cu and Pt+ Pd+ Au and therefore could be of secondary magmatic origin (Figures 7.1 and 7.2). The decoupling of sulphides and PGE could be influenced by contamination of country rock, or magma heterogeneously mixing or hybridisation. Armitage *et al.,* (2002) stated that the PGEs on Sandsloot occur mostly as compounds with metal and semi-metal ligands and not as PGE sulphides, although Yudovskaya *et al.,* (2011) showed later that Pt-Pd sulphides are present persistently throughout the sulphide reefs and chromitites on Sandsloot, Zwartfontein, Vaalkop and Tweefontein. Kinnaird *et al.,* (2005) suggested that the PGEs in the Platreef that occur in minerals other than PGE sulphides were remobilised from the base metal sulphides by hydrothermal fluid activity. Evidence for such fluids is shown by the widespread presence of tremolite, chlorite and quartz (Kinnaird *et al.,* 2005; McCreesh *et al.,* 2018). The observed decoupling between the S, Cu and PGE peaks in the lower mineralised zone (Figure 7.1) has some similarity with their distribution in certain Platreef occurrences (Figures 7.7, 7.8 and 7.9).

There is an excellent correlation between the peaks of the S, Cu and Pt+ Pd+ Au in the upper mineralised zone on Harriet's Wish (Figure 7.3). According to this observation, the sulphides are most likely primary magmatic, or that sulphide liquid was the primary metal collector. This is similar to the PGE and S relationships seen in the magmatic PGE reefs of the Platreef on Townlands and elsewhere (Manyeruke, 2005; Maier *et al.,* 2008; Yudovskaya *et al.,* 2017; Grobler *et al.,* 2018).

It could also, therefore, be useful to undertake a PGM study on Harriet's Wish to determine whether PGMs host significant grade over PGE solid solutions in pentlandite, pyrrhotite and chalcopyrite. This could serve to explain the PGE grade seen at a depth of ~560 m in the upper lithologic unit, where no sulphides were noted during the core logging and field observations (Figure 4.16). However, this should not influence the given interpretation of the tenor variations since Naldrett *et al.,* (2009) indicated based on the variations of the S/Se ratios that the occurrence of Pt and Pd intermetallide

compounds with Te, Bi, Pb, Sn, Sb and As do not have a considerable effect on sulphide tenors as these elements have been dissolved in sulphide liquid.

7.4.4 **Harriet's Wish tenors**

The tenor variations reveal that there are different subdivisions within the lower and upper mineralised zones on Harriet's Wish. The upper mineralised zone can be subdivided into three different sections based on the Pt and Pd tenor (ppm), the trends in tenors (i.e. upward tenor increase or decrease), the Pt/Pd ratios and the total sulphide content (wt %; Figures 7.4, 7.5 and 7.6).

There are normally four scenarios that cause saturation in sulphide sulphur and PGE concentration in magmatic rocks. Mineralisation can and often does occur as a result of one or more of these scenarios (de Waal, 1977; Ripley, 1990; Kinnaird *et al.,* 2005; Naldrett *et al.,* 2011; 2012; Yudovskaya *et al.,* 2017). These are outlined below:

- Sulphide saturation can be achieved due to deposition of S-free cumulates that increases S content of residual melt. The further exchange between immiscible sulphides and silicate melt results in PGE concentrating in immiscible sulphides (Mungall and Brenan, 2014). The resultant tenor depends on the rate of exchange or so-called R-factor (Campbell and Naldrett, 1979). If there is an addition of external S into the magmatic system, then mineralisation is low in S with high a PGE tenor.
- In magmatic plumbing systems (Barnes *et al.,* 2017) the highest rate of exchange is achieved in the centre of magmatic conduit where more chemically primitive and high-temperature melt flows. Trends of changes in tenor may indicate directions to the zone of the highest rate where high-tenor sulphides can be deposited (Huthmann *et al.,* 2018).
- When sulphide saturation in a magma is reached due to the incorporation of external sulphur from a xenolith, either igneous or sedimentary country rock, the sulphur content can be generally high, depending of S availability from the contaminant, but the tenors are commonly poor (Lesher, 2017). Assimilation of

S-poor country rocks also may result in sulphide saturation (Naldrett *et al.,* 2012). De Waal, (1977) proposed that devolatilisation of dolomite may increase the O fugacity of the magma, which will result in decreasing the activity of Fe^{2+} and the S solubility, which can lead to sulphide saturation.

- When sulphide saturation is reached due to mixing of different influxes of magma (Naldrett *et al.,* 2011, 2012), the sulphur concentration is generally expected to be moderate and the tenors may be high.
- Potential leaching by post-magmatic hydrothermal fluids may lead to dissolution of sulphides and PGMs followed by PGE deposition in favourable settings otherwise PGE can be scattered with no economic mineralisation formed (Holwell *et al.,* 2017).

As seen in Figure 7.4, the lower mineralised zone is interpreted to have been precipitated from three successive pulses of the same magma, based on the inter-correlations between the tenor values, tenor trends, sulphide concentrations and Pt/Pd ratios across two drillcores (HW024 and HW025). This mineralised zone is interpreted to have been formed due to magma interactions with country rocks or xenoliths (Figure 4.10) assuming the generally low PGE content of its parental magma (see Kinnaird *et al.,* 2017).

The upper mineralised zone is also interpreted to be derived from three pulses of the same magma, as the concentrations of sulphides (Figure 7.3), the tenors and the tenor variations of the three subdivisions are very similar (Figures 7.6). Due to the high and persistent tenors, and moderate total sulphide contents, it is interpreted that only magmatic sulphur was present in the open system with no external sulphur involved. The upward increasing tenor may indicate the centre of magma flowage within each influx. It is suggested that the upper mineralisation was deposited due to mixing of the several influxes of the upper unit fresh magma and resident magma or crystal mush in the chamber, with the latter possibly being a derivate of the lower unit magma. The flowage and spreading of magmas facilitate the further PGE collection and upgrading of tenors.

7.4.4.1 *Comparison to Platreef tenors*

The tenors in the upper section of the Platreef in the southern sector, on Turfspruit, plot up to 600 ppm which is identical to the Merensky Reef tenor (Kekana, 2014; Yudovskaya *et al.,* 2017). The similar values and ranges suggest that similar processes led to the formation of the reef-style mineralisation in the northern, western and eastern limbs of the Bushveld Complex. The lower and upper mineralised zones plot similar to these values; however, the upper lithologic unit plots closer to the values of Turfspruit indicating that predominantly pristine magmatic processes operated at the deposition of the upper zone.

7.5 **Conclusions**

Although the lower mineralised zone is lithologically and to some extent geochemically different from the F Zone, there are significant similarities between the lower mineralised zone and the F Zone (Kinnaird *et al.,* 2017). These similarities include: 1) the stratigraphic position in relation to the upper mineralised zone and to the footwall; 2) the range of the noble metal concentrations and 3) the metal ratios. The same similarities are observed between the lower mineralised zone on Harriet's Wish and certain Platreef localities, where mineralisation is bottom-loaded and hosted in Cr-poor contaminated magmatic sequences.

Lithologically and geochemically the upper mineralised zone is similar to the T Zone (Kinnaird *et al.,* 2017) and to some extent the Aurora Project mineralisation (McDonald *et al.,* 2017). Remarkable differences in the ore compositions are the Pd concentrations, which are significantly lower, and the Au concentrations which are significantly higher on Harriet's Wish.

7.6 **Recommendations**

PGM studies are recommended to determine the extent of mineralisation outside of sulphide blebs, and to compare with the PGM associations of the F Zone on the Waterberg Project (McCreesh *et al.,* 2018). 3D sulphide mapping could also be initiated

to show if the sulphides are connected, and how much of them was dissolved during hydrothermal alteration. Furthermore, deeper boreholes are recommended to be drilled, as it would have been clearer whether the lower mineralised zone is an extension of the F Zone, or whether it is a discrete mineralised zone related to contamination at the intrusion's margins.

Chapter 8
Whole rock geochemistry

8.1 Introduction

The stratigraphy outlined in Chapter 4, with the aid of magnetic susceptibility readings in Chapter 5 and petrographic analyses in Chapter 6 suggested that a lower and an upper lithologic unit and a lower and an upper mineralised zone exists on Harriet's Wish. Similarities between the stratigraphy on the Waterberg (Kinnaird *et al.,* 2017) and Aurora (McDonald *et al.,* 2017) projects and the northern limb of the Bushveld Complex (Eales and Cawthorn, 1996; Ashwal *et al.,* 2005) were also drawn based on the results of the previous chapters. Thus far, evidence has also pointed to a separate basin existing to the north of the Hout River shear zone (Kinnaird *et al.,* 2017). To confirm these claims, geochemical analyses are imperative. Whole rock (major and trace) geochemical analyses were carried out on three drillcores (HW024, HW025 and HW029; Figure 4.4).

8.1.1 Aims

The aims of the geochemical studies include the following:

- To establish any chemical difference between the lower and upper lithologic units, thereby confirming a subdivision.
- To compare the upper lithologic unit to the Upper Zone found on the Waterberg Project in order to evaluate the suggested connection between these, and also to compare it to the northern limb of the Bushveld Complex.
- To compare the lower lithologic unit to the troctolite-gabbronorite-anorthosite (TGA) sequence on the Waterberg Project and the Main Zone in the northern limb of the Bushveld Complex to evaluate the suggested connectivity.

- To compare the mineralised zones on Harriet's Wish to the F Zone and the T Zone found on the Waterberg project and to compare the lower mineralised zone to the Platreef contact-style mineralisation.
- To establish the geochemical affinity of the lower mineralised zone on Harriet's Wish to the Ultramafic Sequence on the Waterberg Project.

8.2 **Methodology**

Representative core samples were selected based on lithology and zones of mineralisation. Half and quarter core samples, depending on the availability of the core, were taken for the analyses. The sample lengths ranged from 10-30 cm depending on the condition of the core. At least two samples were taken for every major lithologic unit, however, more were taken in certain instances (i.e. where units were large, or in mineralised zones). A total of 117 samples were collected from three drill cores.

The major and trace element whole rock analyses were performed by XRF analysis on samples from the HW024, HW025 and HW030 drillcores. Samples were analysed at the University of the Witwatersrand using standard laboratory practice as outlined below:

8.2.1 **Crushing of samples**

The samples were crushed using a jaw crusher. The jaw crusher was cleaned between each sample with a steel brush and acetone. Once the samples were crushed, they were milled with a swing mill for 90 seconds, or until completely powdered. The milling components were cleaned with roller towel and acetone between each sample. Quartz gravel was milled between samples to remove build-up on the components of the machine.

8.2.2 **Major element analysis**

The major elements were determined using the XRF on fused disks with a Panalytical Axios max spectrometer. Major elements were analysed with the fused disk method with a Li-tetraborate flux, using the program SuperQ. Reproducibility was better than

0·7% for major elements and 5% for trace elements. The detection limits for most trace elements were: 6 ppm for Cu, Co, Ni and Zn, 3 ppm for Rb, Sr, Y and Nb and less than 12 ppm for V, Cr, Ba, Pb, Ga, La, Se, Sc, Th, As, U and Zr.

All clean Pt crucibles and porcelain LOI dishes were placed in the furnace at 1020^{o}C for half an hour to remove any organic residues. Once clean and cool approximately 1g of each sample was placed into each LOI dish. Both the LOI dish ID number and the weight of the LOI dish were recorded before and after addition on the weight chart on the laptop. Ignition then occurred at 1020^{o}C for 40 minutes. Once completed, the samples were removed from the furnace and allowed to cool in a desiccator. Approximately 1.75 g of flux (Spectroflux 105= Lithium tetraborate, Lithium carbonate and Lanthanum oxide, 47:37:16 w/w%) was weighed into each Pt crucible. Both the Pt crucibles ID number and the weight of the Pt crucible were recorded before and after addition on the weight chart on the laptop. Ignition of samples at 1020 ^{o}C for 40 minutes occurred again. Once complete, samples were removed from the furnace and allowed to cool in a desiccator. The hot plate in the furnace room was then switched on (must be on for a minimum of 1 hour prior to pouring). Once both the LOI and the Pt crucibles were cooled, the after-ignition weights of the LOI dishes were measured and recorded to determine the samples LOI.

Similarly, the weights after ignition of the Pt crucibles were measured and recorded to obtain the actual flux weights. The Pt crucible ID number and LOI dishes ID number were used to match the samples (see weighing sheet). Approximately 0.34 g of pre-ignited sample was placed into each corresponding Pt crucible. The weight of the Pt after the addition was also recorded. Samples were then ignited at 1020 ^{o}C for 50 minutes. Once completed, samples were removed from the furnace and allowed to cool in a desiccator. Once cool, if there were solid particles still present in the fused mixture, samples were reignited for an additional half an hour. The Pt crucibles were weighed and recorded and returned to the furnace at 1020^{o}C. The fusion beads were then individually poured and pressed onto the hot plate. This was done while making sure the Pt crucibles placed in the same ordering as the order in which the beads were

poured. If any beads contained bubbles or solid material, they were broken and re-poured. Once all samples were poured and the Pt crucibles were cool, the crucible ID's were mapped in order to label the beads the following day. The beads were allowed to set for 90 minutes on the hot plate. The hot plate was then switched off and allowed to anneal overnight. The Pt crucibles were then cleaned in dilute HCl for 90 minutes on the hotplate. They were then allowed to cool overnight. The remaining ignited material from the LOI dishes was then transferred to vials and stored for future use. The LOI dishes were then cleaned.

The major elements and major element ratios are reported as weight percentage (wt %) and the trace elements are analysed as parts per million (ppm). To determine the whole rock and silicate Mg#, the following formula was used: $100\frac{\mathrm{Mg}}{(\mathrm{Mg+Fe2+})}\mathrm{mol\%}$, to determine plagioclase An#, the following formula was used: $100\frac{\mathrm{Ca}}{(\mathrm{Ca+Na})}\mathrm{mol\%}$. The Cr for the Cr/MgO ratio was worked out as follows: Cr ppm= Cr_2O_3 wt % x 10000 x 0.684.

8.2.3 **Trace element analysis**

Pressed powdered pellets were made for the analysis of trace elements (10 to 100s ppm). Approximately 10 g of finely milled rock sample (<125 µm) was placed in an agate mortar and 2 ml of Elvacite or Paraloid solution was added (purely organic compound of Methyl-butyl methacrylate). The powder and binder were then mixed using a pestle until the powder is completely dry, and there is a very thin film of Elvacite around each grain. Samples were then poured in the form and pressed with a load of 10 tons. The pellets were then released. Each sample was then marked with the sample number at the bottom of the sample. Pellets were then analysed by XRF, using the program ProTrace. The lower detection limit (dl) for the trace method is 0.01 ppm for all elements analysed. Values denoted by dl were taken as 0.

The logged upper and lower lithologic units and the upper and lower mineralised zones were looked at separately and compared in terms of geochemistry to discern discrepancies.

8.3 **Results**

The major lithologic units, as defined by core logging (Chapter 4) and supported by magnetic susceptibility measurements (Chapter 5) are compared with each other in terms of geochemical parameters in this section. The mineralised zones are defined by a combination of assay data, ore mineralogy and core logging. Only parameters with some or significant geochemical variations across lithologic units are presented here. Anomalous values were left out in certain instances to maintain a holistic view of the geochemistry on Harriet's Wish. For a comprehensive list of major and trace elements see Appendices C and D.

8.3.1 **Major oxide variations through the magmatic stratigraphy**

Table 8.1: Major oxide data by lithologic units and mineralised zones on Harriet's Wish. ULU= upper lithologic unit, UMZ= upper mineralised zone, LLU= lower lithologic unit, LMZ= lower mineralised zone, FeO*=FeO total.

XRF wt % majors	ULU Ave. n=30	ULU range	UMZ Ave. n=13	UMZ range Min	LLU Ave. n=57	LLU range	LMZ Ave. n=12	LMZ range
SiO2	50.4	44.5 - 52.1	50.2	45.6 - 52.0	50.0	43.0 - 54.5	50.5	45.3 - 53.3
TiO2	0.32	0.11 - 1.91	0.22	0.14 - 0.32	0.12	0.05 - 0.25	0.13	0.05 - 0.25
Al2O3	18.1	8.8 - 25.3	15.7	8.2 - 22.1	16.5	4.0 - 24.8	12.4	3.2 - 22.0
Fe2O3	1.07	0.52 - 1.75	1.16	0.35 - 1.69	0.96	0.48 - 2.06	1.22	0.63 - 1.79
FeO	8.6	4.2 - 14.0	9.3	2.8 - 13.6	7.7	3.9 - 16.5	9.8	5.0 - 14.3
MnO	0.17	0.07 - 0.26	0.17	0.05 - 0.25	0.15	0.08 - 0.33	0.18	0.10 - 0.26
MgO	8.2	2.9 - 21.5	9.6	1.8 - 16.7	12.5	3.9 - 26.3	16.4	6.3 - 23.9
CaO	11.0	6.7 - 13.2	12.2	7.6 - 27.2	10.7	2.6 - 14.7	8.4	4.0 - 19.3
Na2O	2.1	0.9 - 3.8	1.5	0.0 - 2.4	1.4	0.1 - 2.9	0.9	0.2 - 2.0
K2O	0.19	0.08 - 0.42	0.14	0.00 - 0.26	0.16	0.02 - 0.74	0.11	0.02 - 0.20
P2O5	0.03	0.02 - 0.36	0.04	0.01 - 0.27	0.02	0.01 - 0.07	0.02	0.01 - 0.02
NiO	0.03	0.01 - 0.12	0.15	0.03 - 0.35	0.06	0.01 - 0.19	0.26	0.02 - 1.50
Cr2O3	0.04	0.01 - 0.09	0.03	0.01 - 0.07	0.07	0.02 - 0.18	0.11	0.04 - 0.19
Cr/MgO	21.2	5.7 - 41.6	12.5	5.5 - 44.3	35.8	5.1 - 89.6	39.5	15.7 - 59.9
MgO/FeO*	0.82	0.47 - 1.43	0.91	0.54 - 1.24	1.45	0.56 - 2.74	1.53	0.84 - 1.88
SiO2/Al2O3	3.0	2.0 - 5.9	3.4	2.1 - 6.2	3.5	2.0 - 13.6	5.8	2.2 - 16.4
Al2O3/(FeO*+MgO)	1.26	0.27 - 3.15	1.06	0.26 - 4.46	1.02	0.11 - 2.72	0.60	0.08 - 1.68
CaO/MgO	1.75	0.31 - 4.45	2.29	0.46 - 15.37	1.18	0.14 - 3.28	0.69	0.17 - 1.93
(Na2O+K2O)/SiO2	0.05	0.02 - 0.08	0.03	0.00 - 0.05	0.03	0.00 - 0.06	0.02	0.01 - 0.04
CaO/Al2O3	0.63	0.32 - 0.96	0.77	0.60 - 1.23	0.66	0.35 - 1.32	0.76	0.48 - 1.29

The average whole rock major oxide data per the lithologic units of the HW024, HW025 and HW029 drillcores are displayed in Table 8.1. There are slight differences in the

average content of Al_2O_3, FeO, Fe_2O_3, CaO and Na_2O between the lithologic units and the mineralised zones. Overall, the lower lithologic unit and the lower mineralised zone have the lower contents of Al_2O_3, FeO, Fe_2O_3, CaO and Na_2O than the upper lithologic unit and upper mineralised zone.

The difference in the average whole rock CaO contents of the lower lithologic (10.7 wt % CaO) and upper lithologic unit (11 wt % CaO) is minor, however, the CaO content in the upper mineralised zone (12.2 wt % CaO) is higher than in the lower and upper lithologic units and the lower mineralised zone (8.4 wt % CaO), with the latter having the lowest average CaO content (Table 8.1). The average whole rock MgO content is notably higher in the lower lithologic unit (12.5 wt % MgO) than in the upper lithologic unit (8.2 wt % MgO). The lower mineralised zone is also significantly richer in Mg (16.4 wt % MgO) than the upper mineralised zone (9.6 wt % MgO; Table 8.1). The average NiO content is higher in the lower lithologic unit (0.06 wt % NiO) than in the upper lithologic unit (0.03 wt % NiO), however, it is significantly higher in the lower mineralised zone (0.26 wt % NiO) than in the upper mineralised zone (0.15 wt %; Table 8.1). The average whole rock TiO_2 content in the lower lithologic unit (0.12 wt % TiO_2) and lower mineralised zone (0.13 wt % TiO_2) are more than twice depleted compared to those in the upper lithologic unit (0.32 wt % TiO_2) and upper mineralised zone (0.22 wt % TiO_2; Table 8.1).

The Cr/MgO ratio for the lower lithologic unit (average 35.8, range 5-90) is considerably higher than that for the upper lithologic unit (average 21.2, range 6-42) whereas the Cr/MgO ratio for the lower mineralised zone (average 39.5, range 16-60) is also higher than that for the upper mineralised zone (average 12.5, range 6-44; Table 8.1). The average SiO_2/Al_2O_3 value for the lower lithologic unit (3.5) is slightly higher than that for the upper lithologic unit (3) and, correspondingly, the value for the lower mineralised zone (5.8) is higher than the value for the upper mineralised zone (3.4; Table 8.1). The CaO/Al_2O_3 ratio for the lower lithologic unit (average 0.66, range 0.4-1.3) is slightly higher or the same as that for the upper lithologic unit (avaerage 0.63, range 0.3-1) and the CaO/Al_2O_3 ratio for the lower mineralised zone (average 0.76, range 0.5-1.3) is the

same as the value for the upper mineralised zone (average 0.77, range 0.6-1.3; Table 8.1).

When plotting certain major elements against depth, the following different trends are observed in the upper and lower lithologic units. An upward increase in the MgO content is observed from the base of the lower lithologic unit to the lower mineralised zone at a ~ 360 m depth, then un upward decrease is observed from the lower mineralsed zone to the top of the lower lithologic unit (Figure 8.1). The highest MgO contents are related to the occurrences of the olivine-enriched lithologies such as troctolite, olivine gabbronorite and olivine pyroxenite (Figure 8.1). An upward decrease in the Al_2O_3 content is observed from the base of the lower lithologic unit to the lower mineralised zone at ~360 m depth, then an upward increase is observed from the lower mineralsed zone to the top of the lower lithologic unit (Figure 8.1). The highest Al_2O_3 contents are confined to the leucocratic or olivine-barren lithologies such as leucogabbronorite, leucogabbro and gabbronorite (Figure 8.1). An upward increase in the FeO total content is observed from the base of the lower lithologic unit to the lower mineralised zone at the same ~ 360 m depth, then an upward decrease is observed from the lower mineralised zone to the top of the lower lithologic unit that is adjacent to the upper troctolite (Figure 8.1). The TiO_2 content does not show similar trends, however, but tends to increase with the increasing FeO total content, especially over gabbronortite associated with the lower mineralised zone and the upper troctolite (Figure 8.1).

In the upper lithologic unit, an upward decrease in the MgO content is observed from the base of the unit at a ~600 m depth to the top of the HW029 drillcore, with a slight increase in MgO observed over the gabbroic interval (Figure 8.2). An upward increase in the Al_2O_3 content is observed from the base of the unit at ~600 m depth to the top of the drillcore, with a slight decrease in Al_2O_3 over gabbro (Figure 8.2). An upward decrease in total FeO is observed from the base of the unit at the same ~600 m depth to the top of the drillcore, with an elevated total FeO content over the olivine-enriched and gabbroic lithologies and the upper mineralised zone (Figure 8.2). The TiO_2 content does not show a clear trend, however, coupled variations of TiO_2 and FeO total values

are noted, especially over gabbronortite hosted the upper mineralised zone and the upper gabbronorite (Figure 8.2).

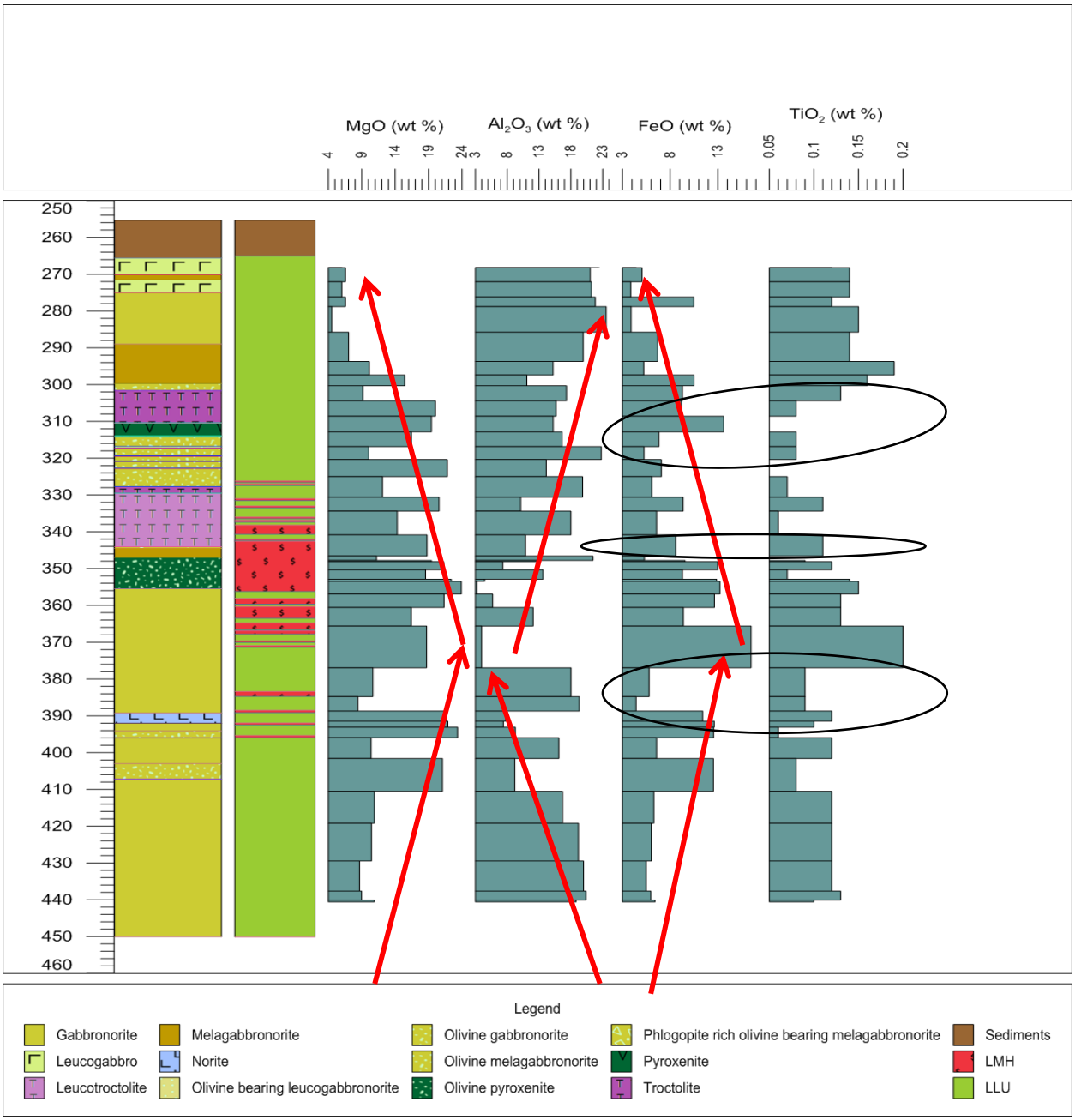

Figure 8.1: Major oxide contents plotted against depth of the lower lithologic unit and lower mineralised zone observed in the HW024 drillcore. The column on the left shows the lithology, while the column on the right shows the stratigraphic affiliation of the units. The red arrows indicate trends observed upward in the sequence and the black ellipses indicate correlations between the FeO and TiO_2 coupled peaks. LLU= lower lithologic unit, LMH= lower mineralised zone.

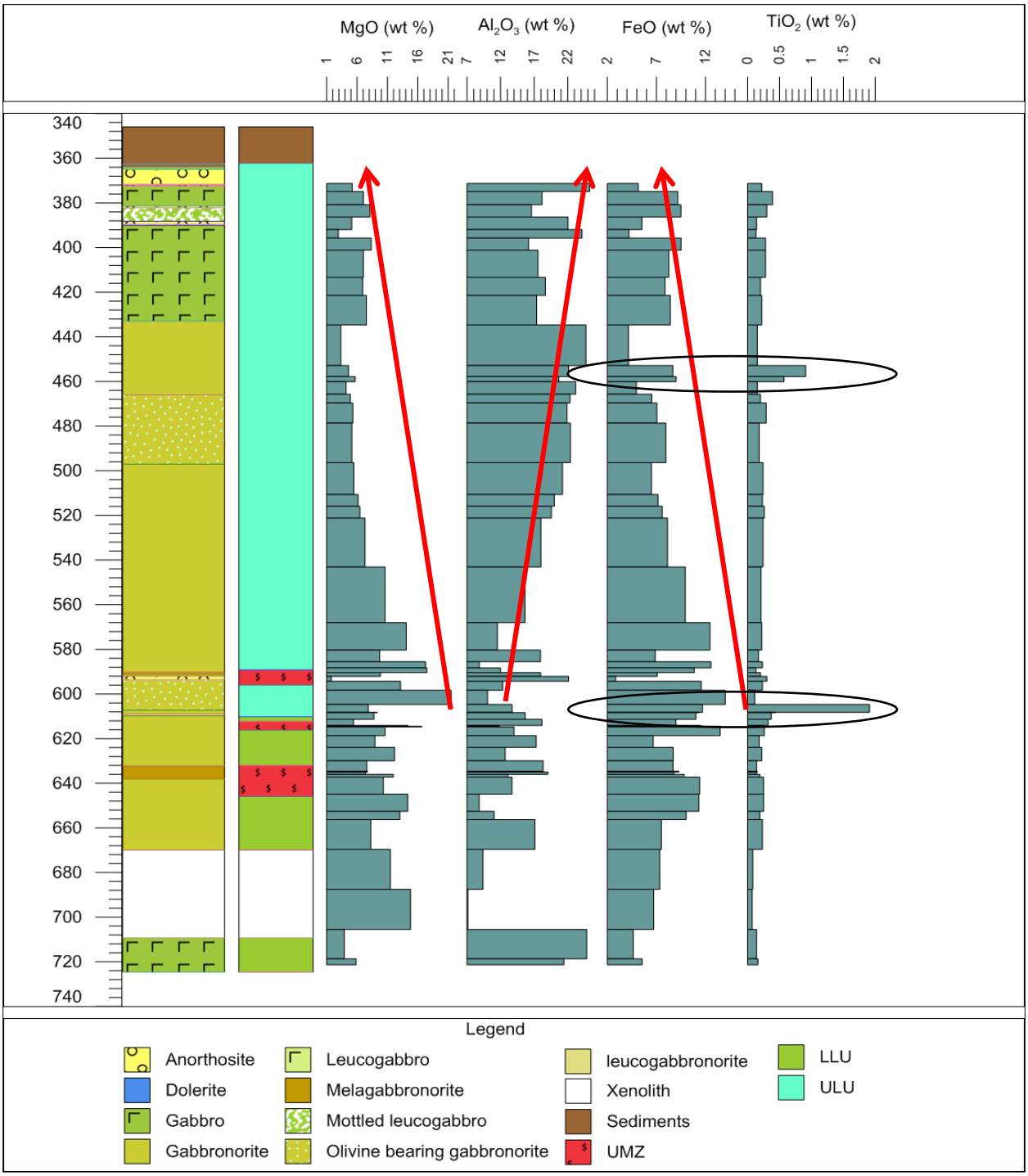

Figure 8.2: Major oxide contents plotted against depth of the lower and upper lithologic units and mineralised zones observed in the HW029 drillcore. The column on the left shows the lithology, while the column on the right shows the stratigraphic affiliation of the units. The red arrows indicate trends observed upward in the sequence and the black ellipses indicate correlations between the FeO and TiO_2 coupled peaks. LLU= lower lithologic unit, ULU= upper lithologic unit, UMZ= upper mineralised zone.

When plotting certain major oxide ratios against depth, different trends are observed in the upper and lower lithologic units. An upward decrease in the $(Na_2O+K_2O)/SiO_2$ is observed from the base of the lower lithologic unit to the lower mineralised zone at ~ 360 m depth, then an upward increase is observed from the lower mineralised zone to the top of the lower lithologic unit (Figure 8.3). Olivine-bearing rocks are characterised by lower ratios (Figure 8.3). There is no a clear trend of the Cr/MgO variations through the lower lithologic unit, however, the Cr/MgO ratio is higher in the lower mineralised zone at ~360 m depth, than within the lower lithologic unit (Figure 8.3). An upward increase in the SiO_2/Al_2O_3 ratio is observed from the base of the lower lithologic unit to the lower mineralised zone at ~ 360 m depth, then an upward decrease is observed from the lower mineralised zone to the top of the lower lithologic unit (Figure 8.3). The lower mineralised zone shows a marked increase of this ratio (Figure 8.3). An upward increase in the CaO/Al_2O_3 ratio is observed from the base of the lower lithologic unit to the lower mineralised zone at ~360 m depth, then an upward decrease is observed from the lower mineralised zone to the top of the lower lithologic unit, with a marked increase over the upper troctolite and overlying melagabbronorite (Figure 8.3).

An upward increase in the $(Na_2O+K_2O)/SiO_2$ ratio is observed in the upper lithologic unit from the base at ~600 m depth to the top of the drillcore, with a slight decrease observed over the upper gabbros (Figure 8.4). The Cr/MgO ratio shows no upward or downward trend in the upper lithologic unit, however, there is a notable decrease over olivine-bearing gabbronorite (Figure 8.4). An upward decrease in the SiO_2/Al_2O_3 ratio is observed in the upper lithologic unit from the base at ~600 m depth to the top of the drillcore, with a marked increase within the upper gabbros (Figure 8.4). The CaO/Al_2O_3 ratio shows little variation in the upper lithologic unit, with a slight increase towards the upper gabbros (Figure 8.4).

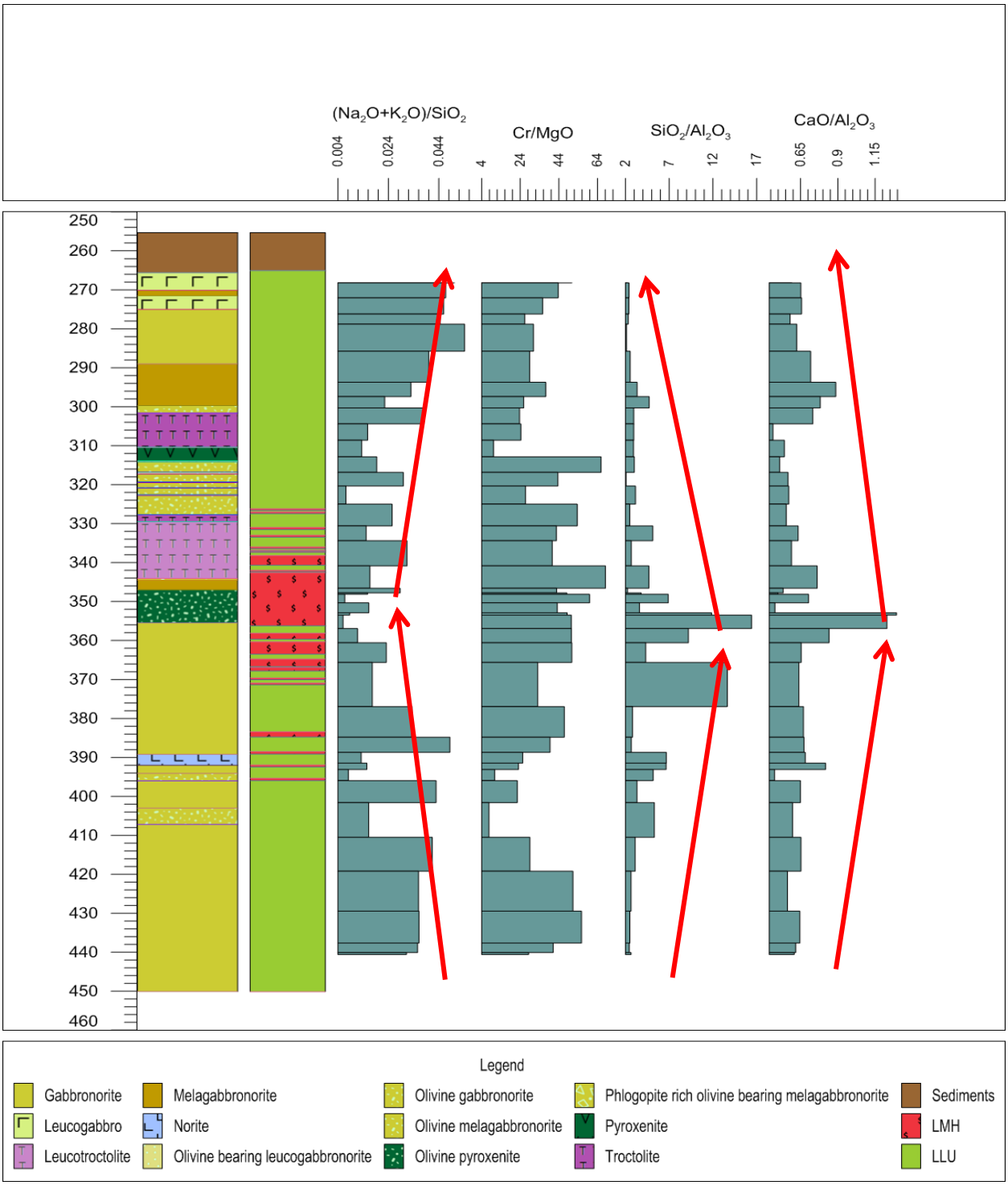

Figure 8.3: Major oxide ratios plotted against depth of the lower lithologic unit and mineralised zone observed in the HW024 drillcore. The column on the left shows the lithology, while the column on the right shows the stratigraphic affiliation of the units. The red arrows indicate trends observed upward in the sequence LLU= lower lithologic unit, LMH= lower mineralised zone.

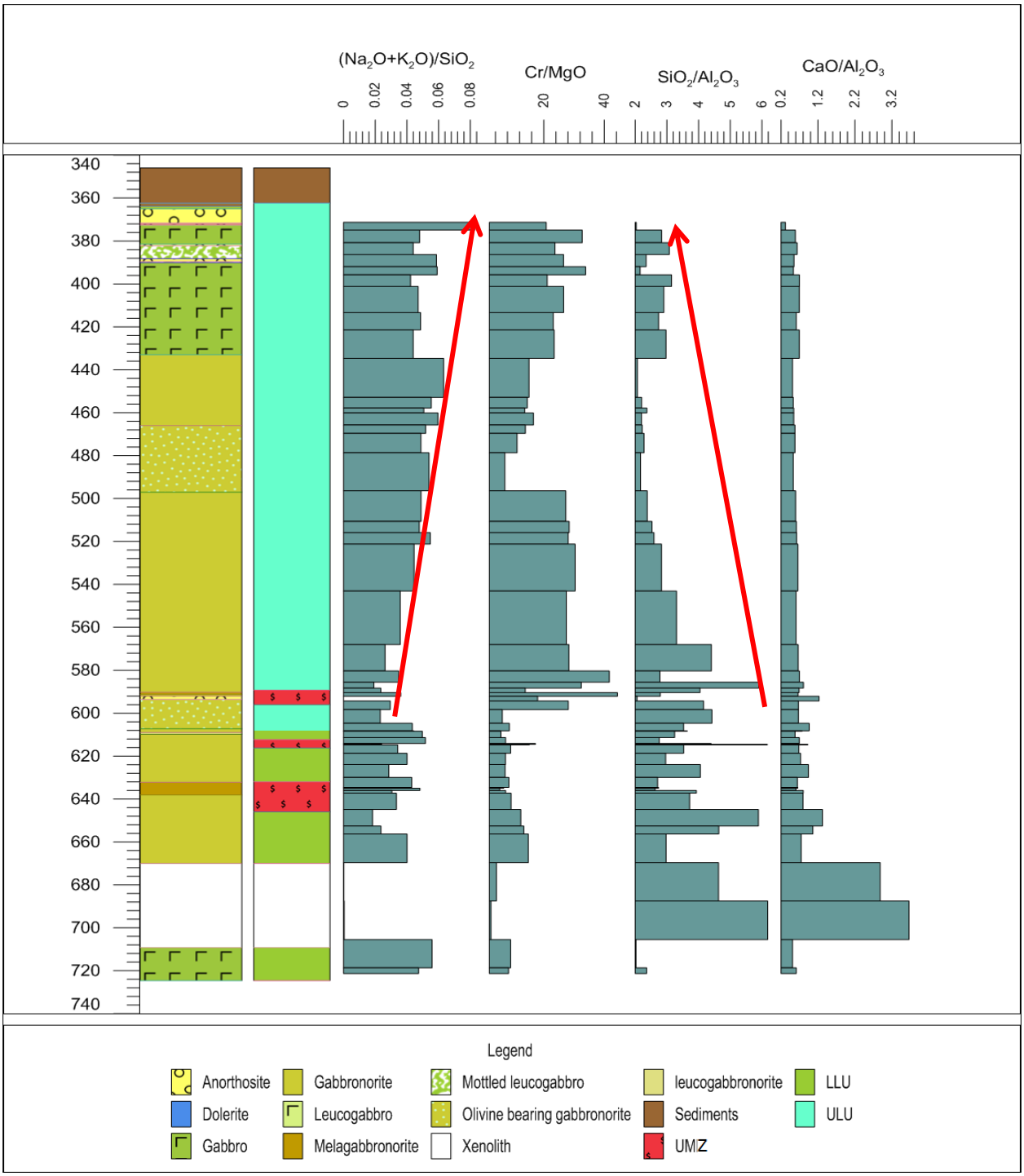

Figure 8.4: The major oxide ratios plotted against depth of the upper and lower lithologic units and upper mineralised zone observed in the HW029 drillcore. The column on the left shows the lithology, while the column to the right shows the stratigraphic affiliation of the various units. The red arrows indicate trends observed upward in the sequence. LLU= lower lithologic unit, ULU= upper lithologic unit, UMZ= upper mineralised zone.

8.3.2 **Major oxide correlations on binary diagrams**

The major oxide distributions on bivariate diagrams show that the rock compositions of the lower and upper lithologic units plot in two relatively distinct fields with distinct trends of MgO versus NiO (Figure 8.5a), TiO_2 (Figure 8.5b), CaO (Figure 8.5c) and Cr (Figure 8.5d). The compositions of the lower mineralised zone plot close to those of the lower lithologic unit and the compositions of the upper mineralised zone plot close to those of the upper lithologic unit on diagrams of MgO versus NiO, TiO_2, CaO and Cr. However, in the stratigraphy, the upper mineralised zone occurs mainly at the top of the lower lithologic unit rather than in the upper lithologic unit.

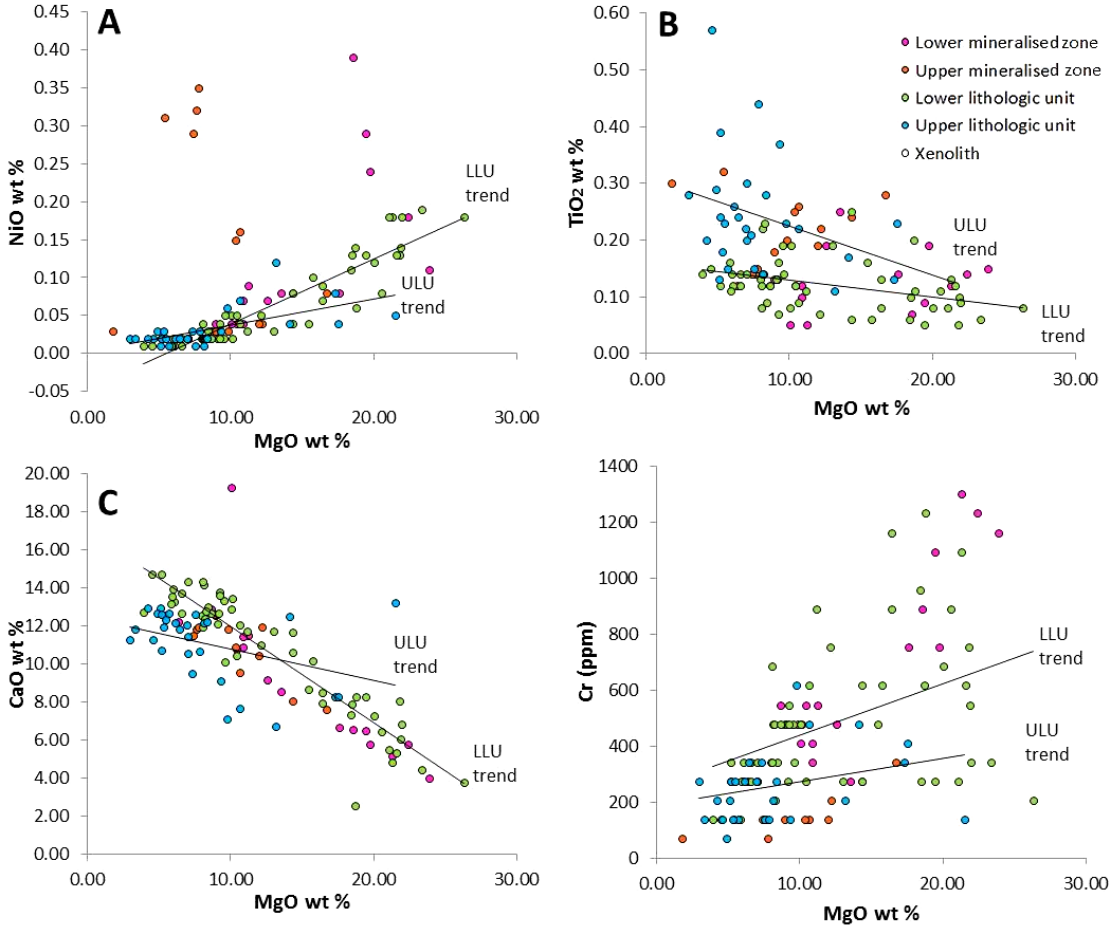

Figure 8.5: Whole rock major oxide bivariate plots of the lithologic units and the mineralised zones on Harriet's Wish. A: MgO wt% versus NiO wt%, B: MgO wt% versus TiO_2 wt%, C: MgO wt% versus CaO wt% and D: MgO wt% vs Cr (ppm). The major oxide variations show that the rock compositions of the lower and upper lithologic units in each graph fit two distinct trends. LLU= lower lithologic unit, ULU= upper lithologic unit.

The whole rock major oxide geochemistry of Harriet's Wish rocks can be easily modelled as a function of the proportions of orthopyroxene, clinopyroxene, plagioclase, and, to a lesser extent, olivine that the rocks contain (e.g., Harris and Chaumba, 2001; Manyeruke *et al.,* 2005; Maier *et al.,* 2008). Figure 8.6 indicates that the chemical compositions of rocks of the lithologic units and mineralised zones reflect the modal mineralogy of the sequence of concern as most samples fall within the range of the end-member fields. Generally, the lower lithologic unit and lower mineralised zone samples plot in both the plagioclase-clinopyroxene-orthopyroxene and the plagioclase-orthopyroxene-olivine fields, with most samples plotting in the former. The upper lithologic unit and the upper mineralised zone plot mainly in the plagioclase-clinopyroxene-orthopyroxene field.

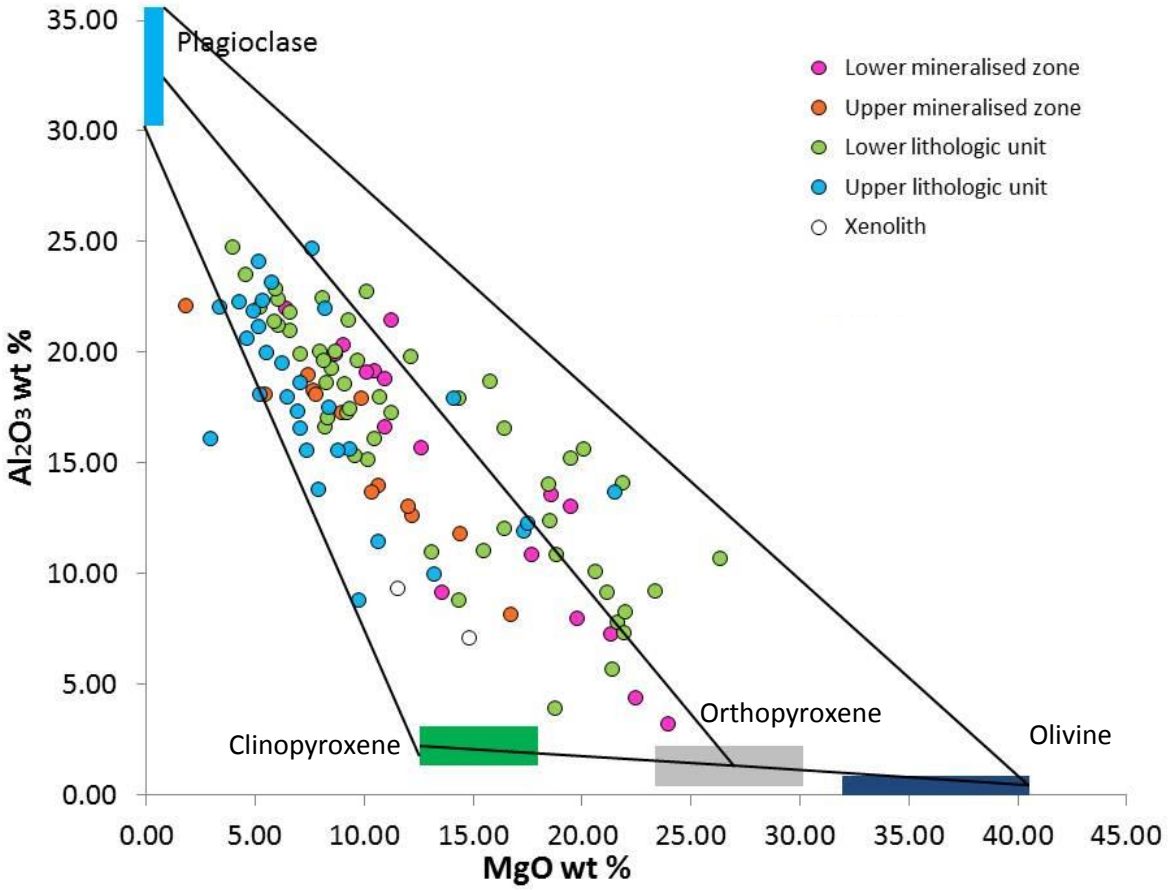

Figure 8.6: Major oxide plot showing MgO wt % versus Al_2O_3 wt % of all samples against different end member minerals. The end member mineral compositions are of the Waterberg area in the WB099 drillcore (unpublished: Yudovskaya, 2018). Different marker colours indicate the lithologic units and mineralised zones.

Figure 8.7 also indicates that the chemical compositions of rocks of the lithologic units and mineralised zones reflect the modal mineralogy of the sequence of concern as most samples fall within the range of the end member fields. Generally, the samples plot in the plagioclase-clinopyroxene-orthopyroxene field.

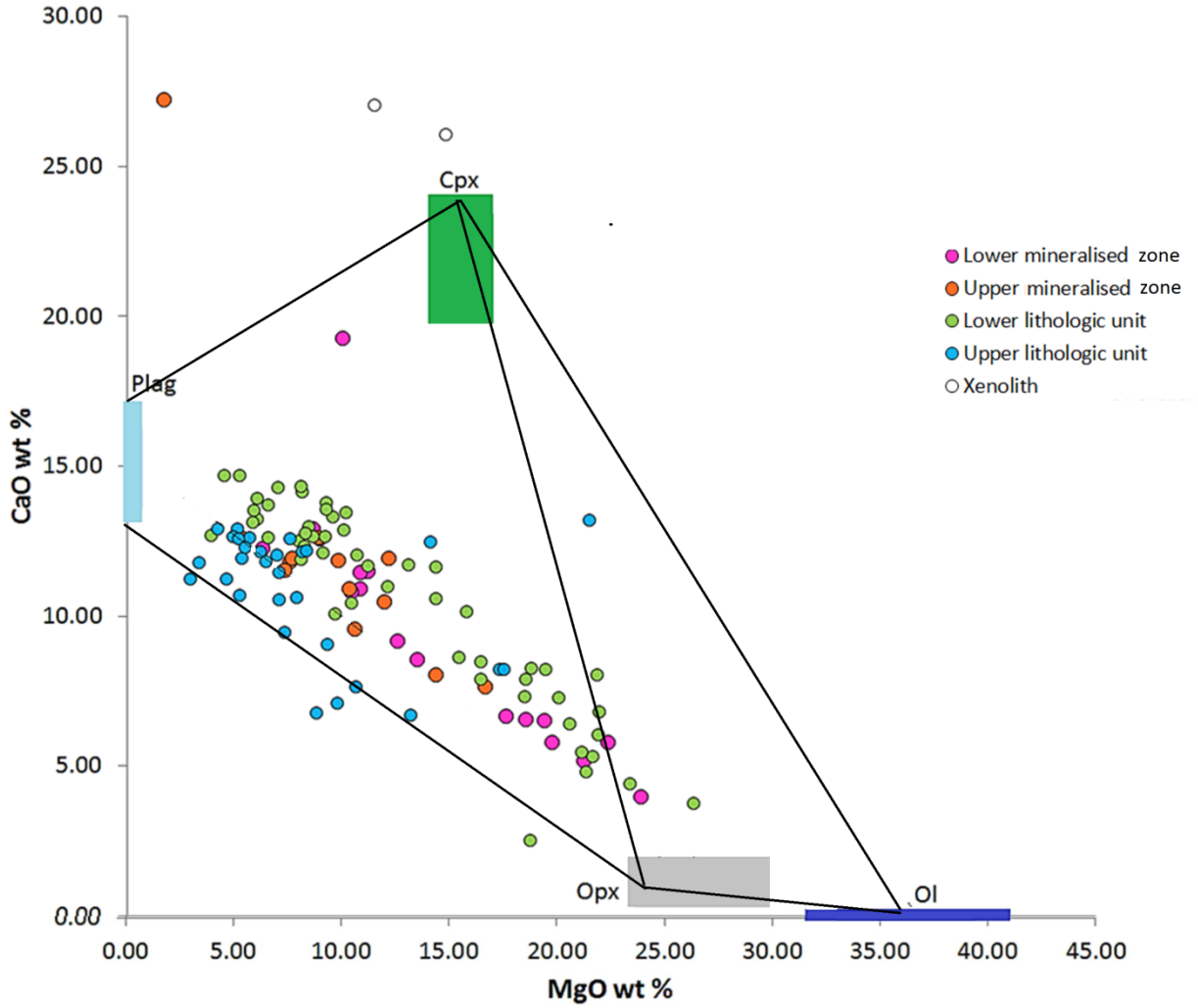

Figure 8.7: Major oxide binary plot showing MgO wt % versus CaO wt % of all samples against different end member minerals. The end member mineral compositions are of the Waterberg Project in the WB099 drillcore (unpublished: Yudovskaya, 2018). Different marker colours indicate the lithologic units and mineralised zones.

8.3.3 **CIPW normative mineralogy**

In order to identify equilibrium mineral assemblages that give rise to the observed major oxide compositions and how these assemblages change through the stratigraphy the

CIPW norms were calculated. Average values and ranges of the major minerals are shown in Table 8.2. For a full list of CIPW results (excluding PGE data) see appendix F.

Table 8.2: CIPW normative mineralogy data by lithologic and mineralised units shown. ULU= upper lithologic unit, UMZ= upper mineralised zone, LLU= lower lithologic unit, LMZ= lower mineralised zone.

	ULU Ave. 30 samples	ULU range	UMZ Ave. 13	UMZ range Min	LLU Ave. 57 samples	LLU range	LMZ Ave. 12 samples	LMZ range
Plagioclase	55.3	24.0 - 77.9	46.3	22.6 - 59.3	47.1	11.7 - 76.1	40.1	8.3 - 65.0
Clinopyroxene	11.8	0.0 - 27.8	17.2	9.1 - 40.2	11.5	0.0 - 29.4	9.5	0.0 - 35.5
Orthopyroxene	20.2	7.8 - 47.4	24.2	0.0 - 44.6	23.9	1.6 - 58.9	33.7	0.0 - 62.2
Olivine	5.0	0.0 - 42.1	3.8	0.0 - 8.1	9.0	0.0 - 37.0	6.0	0.0 - 46.9
Quartz	5.6	2.1 - 13.3	6.7	0.0 - 12.6	6.9	0.4 - 20.0	9.6	0.0 - 17.9
Other (incl. sulphides)	2.1	1.0 - 5.6	1.9	0.5 - 2.7	1.6	0.8 - 6.0	1.7	1.0 - 2.8

In general CIPW normative mineralogy (Figure 8.8) correlates closely to the observed and logged modal mineralogy (Chapter 4; Appendix A); with the exception of an increased olivine proportion in the CIPW normative contents that occur sporadically throughout the entire sequence. Both orthopyroxene and clinopyroxene are shown to occur throughout the sequence in variable proportions. The most notable difference from observed/logged modal mineralogy is the occurrence of significant amounts of orthopyroxene in the gabbro units, most notable in the HW029 drillcore (Chapter 4; Appendix A: HW029) and 8.8 c). The CIPW mineral proportions for the lithologic units are outlined below.

The CIPW calculations indicate that the lower lithologic unit has a higher orthopyroxene (average 24%, range 2-59%) and olivine (average 9%, range 0-37%) content than the upper lithologic unit (average 20%, range 8-48% and average 5%, range 0-42%, respectively; Table 8.2), which is in agreement with the elevated whole rock MgO, FeO* and NiO contents in the lower lithologic unit (Table 8.1). The lower lithologic unit also has slightly higher quartz content (average 7%, range 1-20%) than the upper lithologic unit (average 6%, range 2-13%). The CIPW calculations indicate that the lower mineralised zone has a higher orthopyroxene (average 34%, range 0-62%) and olivine (average 6%, range 0-46.7%) content than the upper mineralised zone (average 24%, range 0-45% and average 4%, range 0-8%, respectively; Table 8.2), which is also in agreement with the elevated whole rock MgO, FeO* and NiO contents in the lower

mineralised zone (Table 8.1). The lower mineralised zone also has slightly higher quartz content (average 10%, range 0-18%) than the upper mineralised zone (average 7%, range 0-13%).

The CIPW calculations indicate that the upper lithologic unit has a higher plagioclase (average 55%, range 24-80%) and clinopyroxene (average 12%, range 0-28%) content than the lower lithologic unit (average 47%, range 12-76% and average 11.5%, range 0-29%, respectively; Table 8.2), in agreement with the elevated whole rock CaO, Al_2O_3, Na_2O and K_2O contents in the upper lithologic unit (Table 8.1). The CIPW calculations indicate that the upper mineralised zone has a higher plagioclase (average 46%, range 23-59%) and clinopyroxene (average 17%, range 9-40%) content than the lower mineralised zone (average 40%, range 8-65% and average 10%, range 0-36%, respectively; Table 8.2), which is also consistent with the elevated whole rock CaO, Al_2O_3, Na_2O and K_2O contents in the upper mineralised zone (Table 8.1).

The following trends are observed in the CIPW normative mineralogy, as seen on the compositional diagrams (Figure 8.8):

In the lower lithologic unit in the HW024 drillcore, there is an upward decrease in the plagioclase proportion from the base of the lower lithologic unit (~440 m depth) to the lower mineralised zone (~355 m depth) with the plagioclase proportions ranging from ~60-6%. The plagioclase proportions also increase from ~6-75% from the mineralised zone (~355 m depth) to the top of the drillcore (270 m depth; Figure 8.8 a). The same trend is also observed in the HW025 drillcore (Figure 8.8 b).

In the HW024 drillcore there is an upward increase of the orthopyroxene proportions from the base of the lower lithologic unit (~440 m depth) to the lower mineralised zone (~355 m depth), with the proportions ranging from ~10 to 59%. The clinopyroxene proportions ranges from ~59 to 5% with an upward decrease from the mineralised zone (~355 m depth) towards the top of the drillcore (270 m depth; Fig. 8.8 a). In the HW025 drillcore, the highest orthopyroxene proportions are also associated with the lower

mineralised zone, however, there is no a clear upward or downward trend seen (Figure 8.8b). The clinopyroxene proportions in the lower lithologic unit in the HW024 (Figure 8.8a) and HW025 (Figure 8.8b) drillcores do not show clear upward trends, however, there seems to be a depletion in clinopyroxene over the lower mineralised zone in both drillcores. The olivine proportions in the lower lithologic unit shows no clear upward trend, however, in the HW024 drillcore an increase in the olivine proportion of up to 13% is seen in the upper part of the lower mineralised zone (~337 m depth; Figure 8.8b). In the HW025 drillcore the olivine proportions are <46% over the lower mineralised zone (Figure 8.8b). In both the HW024 and HW025 drillcores, the olivine proportions are elevated over the olivine-enriched lithologies with the exception of the peaks at a 270 m depth in the HW024 drillcore, and at 445 m, 480 m and 570 m depths in the HW025 drillcore (Figure 8.8a and b).

In the upper lithologic unit in the HW029 drillcore, there is an obvious upward increase in the plagioclase proportion from the top of the upper mineralised zone (~590 m depth) to the top of the magmatic sequence (377 m depth), with normative plagioclase proportions ranging from ~24 to 77%. There is an upward decrease in the orthopyroxene proportions from ~47 to 8% within the interval from ~590 m to ~450 m depth. Upwards, in the interval from ~450m to ~380 m depth, the orthopyroxene proportions increase up to 25% in the upper gabbro. Clinopyroxene proportions stay fairly constant, with a slight increase up to 27% within the upper gabbro. Olivine is present throughout the unit in varying proportions from 0 to 47%, with peaks corresponding to the occurrence of olivine-enriched lithologies (Figure 8.8c; Table 8.2).

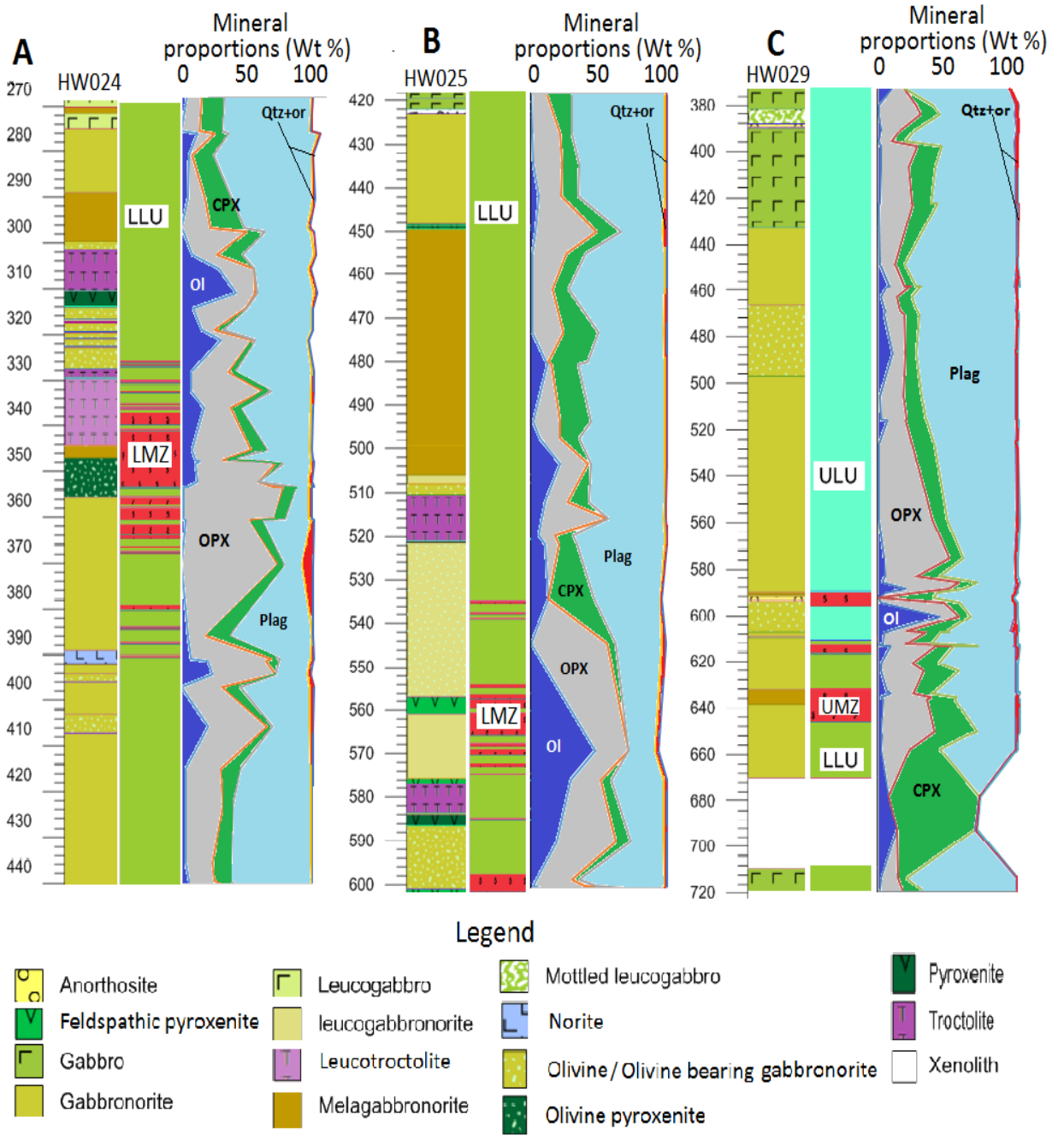

Figure 8.8: CIPW normative mineral proportions in the Harriet's Wish boreholes plotted against depth (m). A: the lower lithologic unit of the HW024 drillcore, B: the lower lithologic unit of the HW025 drillcore, C: the lower and upper lithologic units of the HW029 drillcore. In each, the column on the left represent logged lithologies, the column in the middle outlines lithologic units and mineralised zones and the graph on the right outlines the normative mineral proportions. LLU=lower lithologic unit, ULU= upper lithologic unit, LMZ=lower mineralised zone, UMZ= upper mineralised zone.

8.3.4 **Coupled variations of whole rock Mg# and normative An#**

The whole rock Mg# range for the lower lithologic unit is $Mg\#_{51-83}$, with the highest values occurring over the upper troctolite and the melagabbronorite packages (Figure 8.9). The whole rock Mg# range for the lower mineralised zone is $Mg\#_{60-77}$, with the highest values occurring over the olivine-enriched lithologies including olivine pyroxenite and troctolite (Figure 8.9). There is a general increase upward in the Mg# over the lower mineralised zone. The An# of normative plagioclase was obtained from the CIPW norm calculations. It ranges between $An\#_{50-91}$, with the highest values confined to the olivine-enriched lithologies. The normative plagioclase An# for the lower mineralised zone ranges between $An\#_{65-87}$ (Figure 8.9).

The whole rock Mg# for the upper lithologic unit ranges between $Mg\#_{46-72}$. The Mg# values generally decreases upward with the highest values occurring at the base of this unit. An increase is observed over the upper gabbronorite and gabbro (Figure 8.10). The whole rock Mg# for the upper mineralised zone is within the range of $Mg\#_{49-69}$. These values vary irregularly throughout the upper mineralised zone (Figure 8.10). The normative plagioclase An# in the upper lithologic unit and the upper mineralised zone are considerably lower than the lower lithologic unit and lower mineralised zone (Figures 8.9 and 8.10). The An# of the upper lithologic unit is $An\#_{54-76}$ with the highest values occurring at the base of the unit, showing an overall upward decrease (Figure 8.10). The An# of the upper mineralised zone is within the range of $An\#_{65-74}$.

There are a few anomalously high normative plagioclase An# values in both the lower and upper lithologic unit, however, these corresponded to either localised anorthosite veinlets, an excess of quartz or the rock corresponded to the altered and brecciated samples. These high values are therefore considered to be artefacts and were not considered.

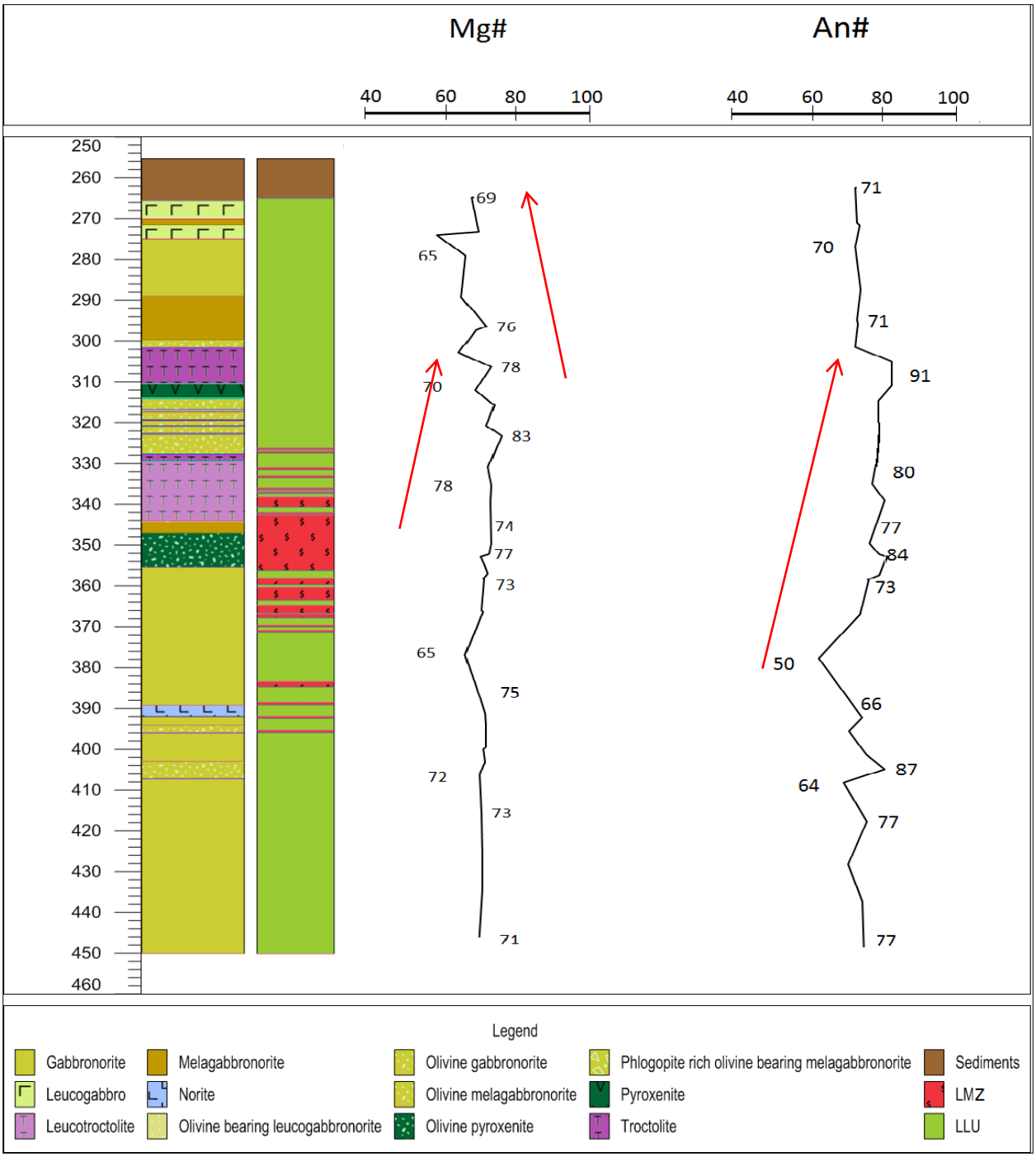

Figure 8.9: Whole rock Mg# and normative plagioclase An# for the lower lithologic unit and the lower mineralised zone of the HW024 drillcore on Harriet's Wish. The column on the left shows the lithology, while the column on the right shows the stratigraphic affiliation of the units. The red arrow indicates an upward increasing trend in Mg# and An#. Mg#= whole rock magnesium number [100*Mg/(Mg+Fe^{2+}) mol%], An#= normative plagioclase anorthite number [100*Ca/(Ca+Na) mol%], LLU= lower lithologic unit, LMZ= lower mineralised zone.

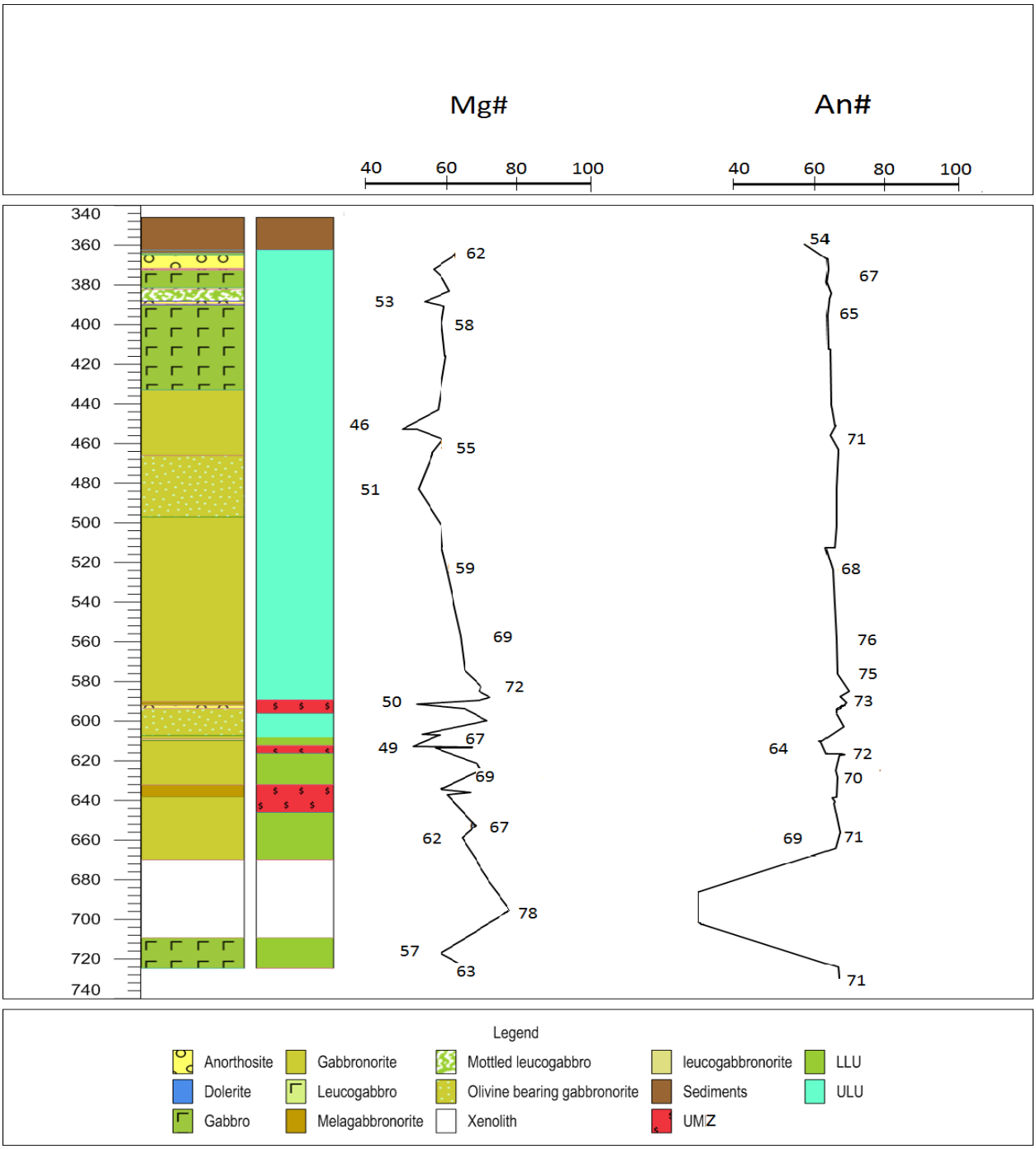

Figure 8.10: Whole rock Mg# and normative plagioclase An# for the upper lithologic unit and upper mineralised zone of the HW029 drillcore on Harriet's Wish. Mg#= magnesium number [100*Mg/(Mg+Fe^{2+}) mol%], An#= normative plagioclase anorthite number [(100*Ca/(Ca+Na) mol%], LLU= lower lithologic unit, ULU= upper lithologic unit, UMZ= upper mineralised zone.

8.3.5 **Trace element distribution**

The average whole rock trace element data for the lithologic units of the HW024, HW025 and HW029 drillcores are displayed in Table 8.3. Overall, rocks of the lower lithologic unit are characterised by lower average contents of Sc, V, Cu, Ga, Y, Zr, Nb and Pb with respect to rocks of the upper lithologic unit.

Table 8.3: Trace element data by the lithologic units and the mineralised zones. ULU= upper lithologic unit, UMZ= upper mineralised zone, LLU= lower lithologic unit, LMZ= lower mineralised zone.

XRF ppm trace	ULU Ave. n=30	ULU range	UMZ Ave. n=13	UMZ range Min	LLU Ave. n=57	LLU range	LMZ Ave. n=12	LMZ range
Sc	32.2	19.7 - 57.6	39.5	29.6 - 54.0	28.2	5.2 - 61.4	28.6	15.3 - 50.1
V	162.3	68.6 - 758.6	140.1	55.9 - 191.9	91.8	26.5 - 216.1	103.0	35.7 - 218.8
Cr	173.1	36.6 - 559.5	122.9	31.8 - 435.8	416.8	35.2 - 1277.9	686.9	189.9 - 1273.3
Co	57.6	20.6 - 146.8	83.6	15.7 - 131.7	67.1	28.2 - 154.9	98.6	38.8 - 245.3
Ni	219.3	50.4 - 944.6	1037.8	193.5 - 2597.2	467.4	77.7 - 1458.1	1794.5	116.3 - 9902.6
Cu	142.8	58.5 - 582.7	3255.5	119.3 - 10009.7	66.8	2.6 - 802.2	935.9	4.3 - 4944.8
Zn	59.9	28.0 - 126.0	59.6	5.8 - 100.5	55.3	23.8 - 187.7	73.8	33.2 - 114.3
Ga	15.4	7.8 - 20.3	12.5	6.0 - 16.2	11.8	5.6 - 18.5	9.4	5.3 - 15.0
Rb	2.7	0.0 - 14.8	1.4	0.0 - 4.4	3.5	0.0 - 29.7	2.7	0.0 - 6.5
Sr	212.7	94.9 - 427.9	161.2	47.1 - 259.6	296.7	33.4 - 1314.8	211.4	25.6 - 634.7
Y	7.5	3.2 - 26.6	6.7	2.3 - 18.5	3.5	0.0 - 13.1	3.3	1.1 - 7.2
Zr	13.3	6.4 - 34.9	11.2	4.3 - 22.1	9.8	2.6 - 25.8	7.2	2.5 - 12.6
Nb	0.4	0.0 - 4.5	1.3	0.5 - 2.4	0.6	0.0 - 2.2	0.8	0.0 - 1.8
Mo	0.5	0.0 - 1.8	0.2	0.0 - 0.7	0.4	0.0 - 1.7	0.4	0.0 - 1.5
Ba	80.8	27.7 - 166.5	53.9	0.3 - 108.1	79.7	10.0 - 476.0	60.7	15.5 - 154.3
Pb	4.2	0.0 - 10.8	6.8	2.9 - 18.8	3.9	0.0 - 12.0	5.3	3.1 - 13.7
Th	0.0	0.0 - 0.0	0.0	0.0 - 0.0	0.0	0.0 - 0.0	0.0	0.0 - 0.0
U	0.0	0.0 - 0.0	0.0	0.0 - 0.0	0.0	0.0 - 0.0	0.0	0.0 - 0.0
Cr/V	1.3	0.1 - 3.4	0.9	0.2 - 3.4	5.6	0.4 - 19.2	8.1	1.0 - 15.6
Ba/Zr	6.4	2.7 - 13.0	5.3	0.0 - 12.4	8.2	2.6 - 27.5	8.6	3.6 - 12.5
Ni/Cu	1.7	0.5 - 7.0	0.6	0.1 - 2.1	26.3	1.2 - 167.1	17.4	0.7 - 162.9

The average contents of Cr, Co, Ni, Zn, Rb, Sr and Nb are higher in rocks of the lower lithologic unit than in rocks of the upper lithologic unit. The lower mineralised zone rocks have lower contents of Sc, V, Cu, Ga, Y, Zr, Nb and Pb and higher contents of Cr, Co, Ni, Zn, Rb, Sr, Mo and Ba than the upper mineralised zone rocks.

The average Cr concentration in the lower lithologic unit is 417 ppm with a range of 35-1280 ppm, whereas the upper lithologic unit shows an average of 173 ppm with a range of 37- 560 ppm (Table 8.3). The average Cr concentration in the lower mineralised zone is 687 ppm with a range of 190-1270 ppm, whereas the upper mineralised zone shows an average of 123 ppm with a range of 32- 436 ppm (Table 8.3).

The Cr/V ratio in the lower lithologic unit is higher than that of the upper lithologic unit and, correspondingly, the Cr/V ratio of the lower mineralised zone in higher than that of the upper mineralised zone. The average Cr/V ratio in the lower lithologic unit is 5.7 with a range of 0.4-19; the upper lithologic unit shows an average ratio of 1.3 with a range of 0.09-3.4 (Table 8.3). The average Cr/V ratio in the lower mineralised zone is 8.1 with a range of 1-16, with the upper mineralised zone showing an average of 0.9 with a range of 0.2-3.4 (Table 8.3).

The Ni/Cu ratio in the lower lithologic is higher than the upper lithologic unit and the Ni/Cu ratio in the lower mineralised zone in higher than in the upper mineralised zone. The average Ni/Cu ratio in the lower lithologic unit is 26.3 with a range of 1.2-167, with the upper lithologic unit showing an average ratio of 1.7 with a range of 0.5-7 (Table 8.3). The average Ni/Cu ratio in the lower mineralised zone is 17.4 with a range of 0.7-163, whereas the upper mineralised zone shows an average ratio of 0.63 with a range of 0.1-2.1 (Table 8.3).

The Ba/Zr ratio in the lower lithologic unit is higher than that of the upper lithologic unit and the Ba/Zr ratio in the lower mineralised zone is also higher than that of the upper mineralised zone. The average Ba/Zr ratio in the lower lithologic unit is 8.2 with a range of 3-28, with the upper lithologic unit showing an average ratio of 6.4 with a range of 2.7-13 (Table 8.3). The average Ba/Zr ratio in the lower mineralised zone is 8.6 with a range of 3.6-13, with the upper mineralised zone showing an average of 5.34 with a range of 0.03-12.4 (Table 8.3).

The distribution of the trace elements and variations of their ratios in the lower and upper lithologic units and mineralised zones are shown in Figures 8.11 and 8.12 and commented below.

An upward increase in the Cr content is observed from the base of the lower lithologic unit to the lower mineralised zone, then an upward decrease is observed from the lower mineralsed zone to the top of the lower lithologic unit (Figure 8.11). The highest Cr

contents are seen over the lower mineralised zone, which includes, but is not limited to the olivine-enriched lithologies such as troctolite, olivine gabbronorite and olivine pyroxenite (Figure 8.11). An upward increase in the Cr/V value is observed from the base of the lower lithologic unit to the lower mineralised zone, followed by an increase observed just above the lower mineralsed zone from a ~330-305 m depth (Figure 8.11). The highest Cr/V values are confined to certain olivine-enriched rocks (Figure 8.11). The Ni/Cu ratio shows no clear upward trend, however, there is an increase from a 350-305 m depth associated with the olivine-enriched lithologies. The Ba/Zr value does not show a clear upward trend, however, the ratio tends to increase over the olivine-enriched rocks (Figure 8.11).

In the upper lithologic unit, an upward decrease in the Cr content is observed from the base at ~600 m to the top of the magmatic sequence, with a slight increase in Cr seen over the gabbroic layers (Figure 8.12). An upward decrease in the Cr/V value is observed from the base at ~600 m depth to the top of the sequence, with a slight increase in Cr/V within the gabbroic layers (Figure 8.12). An upward decrease in the Ni/Cu value is observed from the base at ~600 m depth to the top, with a slight increase within the olivine-enriched lithologies and the gabbroic layers (Figure 8.12). The Ba/Zr ratio shows an upward increasing trend from the base at ~600 m depth to the top of the sequence with a slight decrease within gabbro (Figure 8.12).

8.4 **Discussion**

In this chapter, the geochemical characteristics of the Harriet's Wish farm were presented with the aim of distinguishing between the lithologic units and mineralised zones and placing these into context with the known geochemical features of the Waterberg Project (Kinnaird *et al.,* 2017) and Aurora Project (McDonald *et al.,* 2017) and to a certain extent the northern limb of the Bushveld Complex.

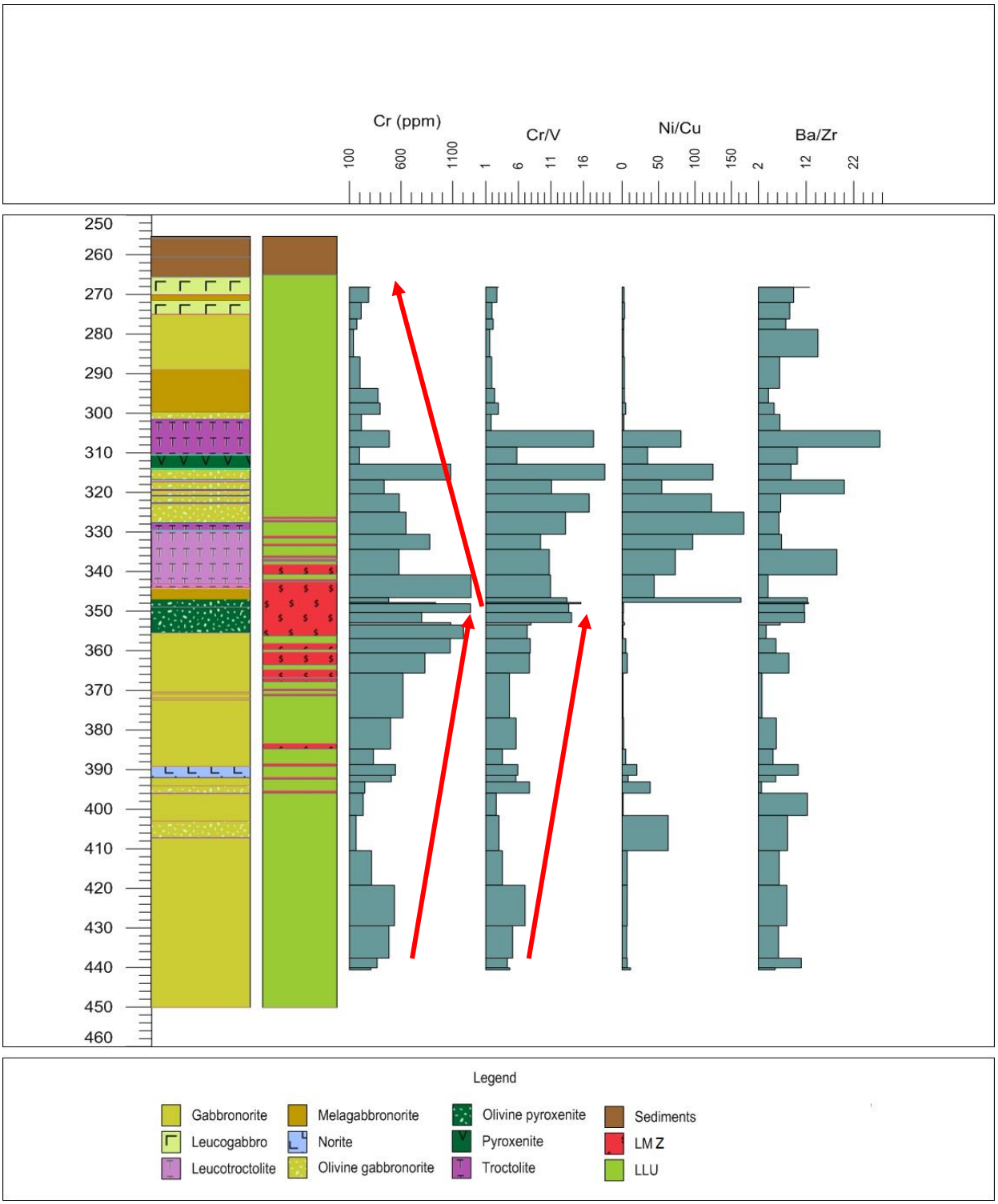

Figure 8.11: Trace element ratios and Cr content (ppm) plotted against depth (m) of the lower lithologic unit and the lower mineralised zone observed in the HW024 drillcore. The column on the left shows the lithology, while the column on the right shows the stratigraphic affiliation of the units. The red arrows indicate trends observed upward in the sequence. LLU= lower lithologic unit, LMZ= lower mineralised zone.

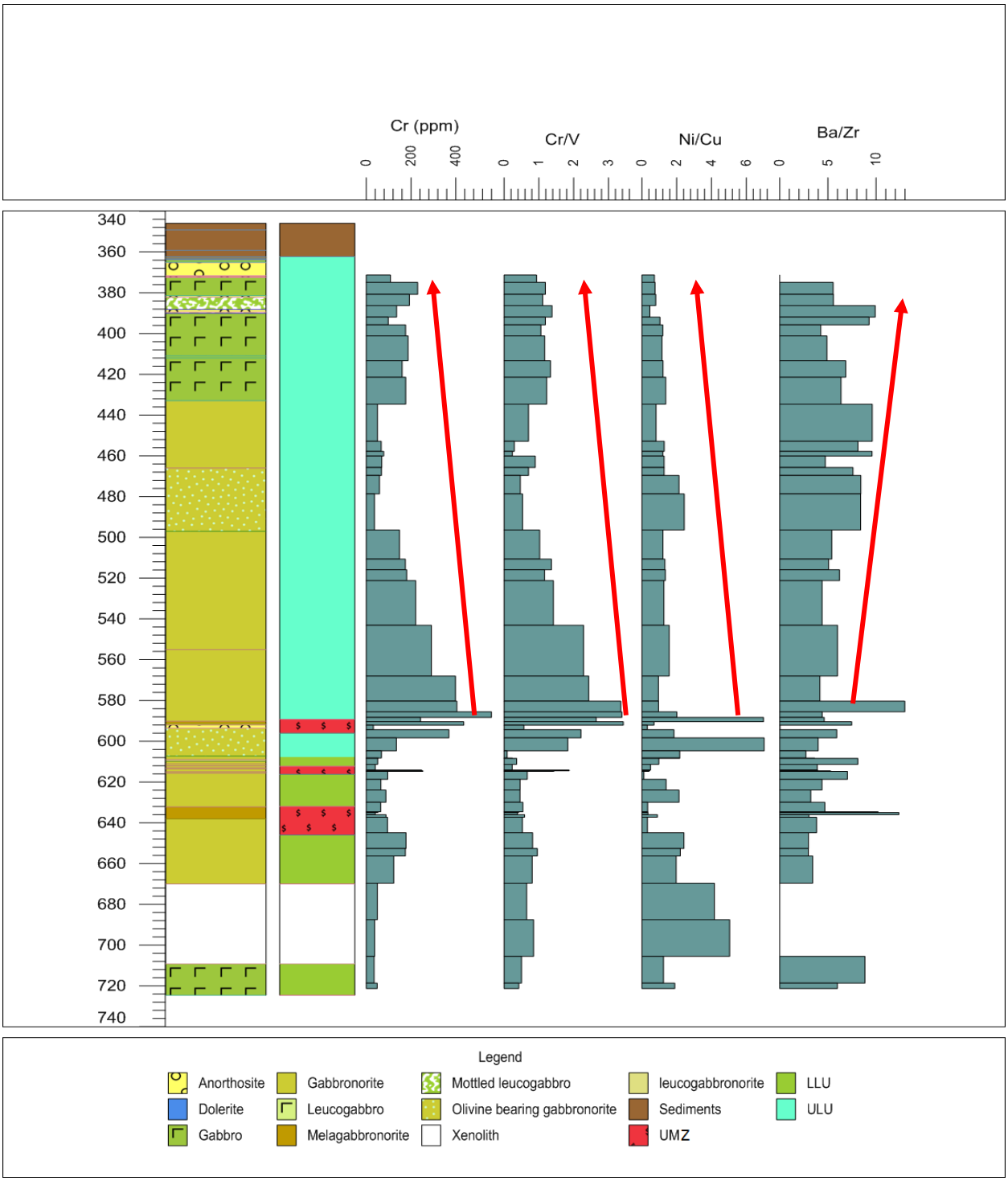

Figure 8.12: Trace element ratios and Cr content (ppm) plotted against depth (m) of the upper and the top of the lower lithologic units, as well as the upper mineralised zone observed in the HW029 drillcore. The column on the left shows the lithology, while the column on the right shows the stratigraphic affiliation of the units. The red arrows indicate trends observed upward in the sequence. LLU= lower lithologic unit, ULU= upper lithologic unit, UMZ= upper mineralised zone.

8.4.1 **Major elements**

McCreesh, (2016) and Kinnaird *et al.,* (2017) distinguish the main stratigraphic units and mineralised zones on the Waterberg Project by using certain geochemical parameters including the whole rock major oxide data such as MgO content, Cr/MgO, SiO_2/Al_2O_3 and CaO/Al_2O_3 ratios, the whole rock Mg# as well as the whole rock trace element data such as Co, Cr, V, Sr and Rb contents. These data show either a shift in concentration or a difference in averages of the various units across the boundaries. McDonald *et al.,* (2017) also used major and trace element data on the Aurora Project to aid in distinguishing the stratigraphic units. These include the changes of the Cr, Mn, Sr and Ba contents, the shifts in Ca/(Ca+Na) and Mg/(Mg+Fe) ratios of minerals etc., when plotting these against depth. Seabrook *et al.,* (2005), among other parameters, used the whole rock MgO, Cr and Al_2O_3 contents, as well as the Cr/MgO and Al_2O_3/MgO ratios to define the stratigraphy of the Merensky Reef in the Upper Critical Zone. The main stratigraphic units in the Bushveld Complex (Marginal, Lower, Critical, Main and Upper zones) can be distinguished by the whole rock and mineral chemistry and the Sr isotope compositions (Kruger, 1994; Eales and Cawthorn, 1996; Cawthorn and Walraven, 1998; Maier and Barnes, 1998; Cawthorn *et al.,* 2006; Mayer *et al.,* 2018). Geochemistry also assists in describing the magmatic history, highlighting possible contamination and determining the nature of emplacement and the style of mineralisation.

On Harriet's Wish, similar geochemical parameters were used to distinguish between major lithologic units and mineralised zones. The whole rock geochemical parameters on Harriet's Wish show a notable variation between the lower and upper lithologic units indicating that two different magmatic pulses formed this igneous sequence. Evidence for this include: 1) the contrasts in the average contents of major oxides, although the minimum and maximum values overlap (e.g. Al_2O_3, MgO, CaO, Na_2O_3 and NiO; Table 8.1). 2) The contrasts in major ratios, including the Cr/MgO and SiO_2/Al_2O_3 ratios (Figures 8.3 and 8.4 and Table 8.1). 3) The differences in the trends observed in the whole rock compositions of the lower and upper lithologic units on bivariate diagrams such as MgO vs TiO_2, MgO vs Cr, MgO vs Na_2O (Figure 8.5). 4) The whole rock Mg# and normative plagioclase An# show some contrasting behaviour between the lower

and upper lithologic units (Figures 8.9 and 8.10). 5) The contrasting CIPW normative mineralogy (Table 8.2). 6) The contrasts in trace element abundances, although some abundances may have overlapping ranges (Table 8.3). 7) The differences in the trace elements ratios (Figures 8.11 and 8.12).

As observed in Table 8.1, there are differences in the average Al_2O_3, FeO, Fe_2O_3, CaO and Na_2O contents between lithologic units, and there is no notable difference in the CaO, SiO_2 and some other minor oxides (Table 8.1) of the lower and upper lithologic units. There are, however, prominent difference in the MgO and NiO contents between the two lithologic units (Table 8.1). The observed higher average MgO and NiO contents in the lower lithologic unit over the upper lithologic unit, and the observed higher MgO and NiO concentrations in the lower mineralised zone over the upper mineralised zone (Table 8.1) support the interpretation of two separate magmas forming the sequence on Harriet's wish. These elevated values are consistent with the higher olivine and orthopyroxene normative proportions according to the CIPW normative mineralogy (Table 8.2), and to a lesser extent, the observed modal olivine proportions (Chapter 4; Appendix A).

There are also the differences in the trends of certain major oxides when plotted against depth. The most notable include the differences in the MgO and Al_2O_3 distributions across the lower lithologic unit (Figure 8.1) compared to those across the upper lithologic unit (Figure 8.2).

The SiO_2/Al_2O_3, $(Na_2O+K_2O)/SiO_2$, CaO/Al_2O_3 and Cr/MgO ratios are good indicators of defining the rock packages (Kinnaird, 2005; McDonald and Holwell, 2011; McCreesh, 2016; Kinnaird *et al.,* 2017). On Harriet's Wish, the averages and the trends of the these ratios suggest that the lower and upper ltihologic units are distinguishable form each other, and likely formed from two different magmas (Table 8.1; Figures 8.3 and 8.4).

The variations in the CaO/Al_2O_3 ratio may assist in determining whether a magma is contaminated or more pristine (Kinnaird, 2005). The CaO/Al_2O_3 ratio of plagioclase is

around 0.6, with orthopyroxene containing either CaO or Al_2O_3 in negligible amounts. When a rock has a CaO/Al_2O_3 ratio that varies from 0.6, it may be contaminated by a dolomitic rock, or it may contain notable proportions of clinopyroxene (Eales *et al.,* 1986; Kinnaird, 2005). In the lower lithologic unit, the CaO/Al_2O_3 ranges from 0.4-1.3, with an average of 0.66, and in the upper lithologic unit it ranges from 0.3-1, with an average of 0.63 (Table 8.1). These average values do not deviate significantly from 0.6, which suggests that these lithologic units most likely did not get contaminated by dolomitic rocks. The weak deviations from 0.6 in the observed ranges may be attributed to the notable proportions of clinopyroxene in the lower and upper lithologic units (Figure 8.8). In the lower mineralised zone, the CaO/Al_2O_3 ranges from 0.5-1.3, with an average of 0.76, and in the upper mineralized zone it ranges from 0.6-1.2, with an average of 0.77 (Table 8.1). The averages deviate considerably from 0.6, and the CIPW normative proportions do not indicate significant clinopyroxene over the lower and upper mineralised zones. Therefore, it is suggested that dolomitic rocks may have contaminated the magma to assist in the formation of both lower and upper mineralisation. The presence of the thick calcsilicate xenolith in the lower lithologic unit in the HW029 drillcore (Figures 4.4 and 4.10) supports this interpretation.

Seabrook *et al.,* (2005) used the Cr/MgO and Sr isotopes in orthopyroxene to determine that the Merensky Reef and Bastard unit are composed of minerals from both the Critical and Main Zone magmas. According to Seabrook *et al.,* (2005), Critical Zone rocks have Cr/MgO ratios of 80-120, whereas Main Zone rocks have Cr/MgO ratios of ~40-60. On the Waterberg Project, the Cr/MgO ratio also distinguishes the different stratigraphic units. The Ultramafic sequence has Cr/MgO values of <140, the TGA sequence has Cr/MgO values of <80, whereas the T Zone has values of <140 (mainly <50) and the Upper Zone has the values of <80 (Kinnaird *et al.,* 2017). On the Aurora Project, the Cr/MgO ratio distinguishes the units in the magmatic sequence. The sulphides are hosted predominantly in rocks that have Cr/MgO ratios <60 (more commonly <25, Manyeruke, 2007; McDonald *et al.,* 2017), which is indicative of the Main Zone (Seabrook *et al.,* 2005; McDonald and Holwell, 2011) or the Upper Zone. On Harriet's Wish, the Cr/MgO ratio for the lower lithologic unit (<90) are higher than that on

the Main Zone in the northern limb (Seabrook *et al.,* 2005; McDonald and Holwell *et al.,* 2011) but falls in the range of the values for the TGA sequence on the Waterberg Project (Kinnaird *et al.,* 2017). The upper lithologic unit Cr/MgO values (<42) fall in the range of the Main Zone (Seabrook *et al.,* 2005) and the Upper Zone on the Waterberg Project (Kinniard *et al.,* 2017). On Harriet's Wish, the lower mineralised zone Cr/MgO values (60) are lower than those of the Critical Zone and the Ultramafic Sequence on the Waterberg Project, although it falls into the range of the TGA values (Seabrook *et al.,* 2005; Kinnaird *et al.,* 2017). The upper mineralised zone on Harriet's Wish Cr/MgO values (<44) fall into the range of the Waterberg Upper Zone (Kinnaird *et al.,* 2017).

The whole rock Mg# is one of the major differentiation indexes that is useful in determining how primitive or evolved a magma is (Eales and Cawthorn, 1996). The compositions of mantle olivine commonly range from Fo_{88}-Fo_{98}, and this may crystallise from a primary melt with an <Mg# 70 (Gill, 2010). The higher Mg# determines the more chemically primitive compositions of the parental melts. The whole rock Mg# on the Waterberg Project shows different values for the stratigraphic subdivisions, therefore supporting these subdivisions, with the upward decrease from the base of the sequence to the top (Kinnaird *et al.,* 2017). The Ultramafic Sequence has generally the range of $Mg\#_{43\text{-}70}$, the TGA sequence, a range of $Mg\#_{43\text{-}68}$, the T Zone is more evolved with a range of $Mg\#_{40\text{-}57}$ and the Upper Zone which has the highest range of $Mg\#_{25\text{-}60}$ (McCreesh, 2016; Kinnaird *et al.,* 2017).

The whole rock Mg# values on Harriet's Wish also support the subdivision of the sequence into two lithologic units (Table 8.2). The whole rock Mg# values indicate that the lower lithologic unit ($Mg\#_{50\text{-}83}$) is Mg-richer than the upper lithologic unit ($Mg\#_{45\text{-}72}$) whereas the mineralised zones, overall, are Mg-richer than the adjacent rocks. The lower mineralised zone ($Mg\#_{60\text{-}77}$) is also Mg-richer than the upper mineralised zone ($Mg\#_{49\text{-}69}$; Figures 8.9 and 8.10) that is in agreement with the observed olivine proportions and the variations of Mg# of silicates (olivine and orthopyroxene; Figure 8.8; Table 8.3). There is also an overall upward decrease in the whole rock Mg# from the base of the sequence to the top, with the sequence being more chemically primitive at

the base and more evolved at the top, similar to the Waterberg Project (Figures 8.9 and 8.10; McCreesh, 2016; Kinnaird *et al.,* 2017). It is worth noting that some rocks from the lower lithologic unit on Harriet's Wish have very high Mg# values of <83, which is higher than the values observed in the Waterberg Ultramafic Sequence (McCreesh, 2016; Kinnaird *et al.,* 2017). However, the stratigraphic positions of the rocks with the elevated Mg# values, in the lower mineralised zone, do not correlate with the basal position of the most primitive ultramafic rocks on the Waterberg Project (Kinnaird *et al.,* 2017). As noted in Chapter 4, the rock types of the lower unit do not correspond to the Ultramafic Sequence on the Waterberg Project, since the persistent layers of harzburgite and disseminated chromite are absent, and pyroxenite is less common on Harriet's Wish (Figure 4.4; Figure 4.19; Kinnaird *et al.,* 2017). Rather, these high Mg# values are comparable with the Mg# of the olivine-bearing layers of the Critical Zone and the Platreef and are not consistent with the Main Zone parentage (Yudovskaya *et al.,* 2017).

The normative plagioclase An# also support the subdivision of the stratigraphy into two lithologic units as there is a notable difference seen in these proposed units (Figures 8.9 and 8.10).

8.4.2 **CIPW normative mineralogy**

In the logged core, olivine is not present throughout the entire sequence, but rather is enriched at certain intervals. In the CIPW normative mineralogy, however, olivine is present throughout almost the entire system, in both the lower and upper lithologic units (Figure 8.8). The idea that best fits this observation is that the primary olivine-bearing cumulates were transformed through peritectic reactions and the interaction with silica-richer melts so that olivine that was once present was replaced by orthopyroxene (Chapter 6). This is consistent with the higher proportions of orthopyroxene in the mineralised zones.

However, at least some of the disagreement between the CIPW normative olivine proportions (Figure 8.8) and the observed modal olivine in the core logs (Chapter 4;

Appendix A; HW029) could be attributed to the FeO/Fe_2O_3 ratio that was used for recalculation of the XRF analytical results. To confirm this, different ratios were tried and the results of the CIPW normative mineralogy were compared with the thin section petrographic analyses. A thin section was chosen with no olivine observed under the microscope, and the ratio was changed so that the calculation would not show normative olivine in this sample. The change, however, was insignificant, and olivine is still present in most of the CIPW normative results. The preferred FeO/Fe_2O_3 ratio of 1:9 was estimated as the best fit between the normative mineralogy proportions and those from the thin sections (Chapter 6). The preferred FeO/Fe_2O_3 ratio for magnetite-poor Waterberg rocks and magnetite-free Platreef ultramafic-mafic rocks is reported as 1:10 (Yudovskaya *et al.,* 2017). Therefore, the interpretation that is favoured in this study, is that olivine used to be present as an early liquidus phase in the magmas; but the liquidus olivine was replaced by orthopyroxene due to peritectic reactions, although it cannot be excluded that the olivine-enriched cumulates may have been eroded, reworked and consumed by later dynamic magmatic influxes (Figures 4.5 b and 4.6 a).

8.4.3 **Mineral chemistry**

Although there were no mineral chemistry data acquired in this study, unpublished microprobe data from M. Yudovskaya on the Waterberg samples were used to plot the end member compositions.

In Figure 8.13, almost all the samples plot within the fields restricted by the proportions of the major minerals, although upper lithologic unit and upper mineralised zone points plot slightly closer to the plagioclase-clinopyroxene line (Figure 8.13) indicating the presence of Mg-poor Fe-richer clinopyroxene compared to that on the Waterberg Project. There is a significant overlap between the Aurora Project samples, the Waterberg Project samples and the Harriet's Wish samples. The Aurora rocks appear to be Mg- poorer and Al-richer than the Waterberg rocks overall. Harriet's Wish rocks have intermediate compositions between Waterberg and Aurora in terms of the Al and Mg contents. This north to south general decrease in the Mg content and increases in the Al

content can be interpreted as an indication of a north to south evolution from more primitive to more evolved magmas more distal from a source.

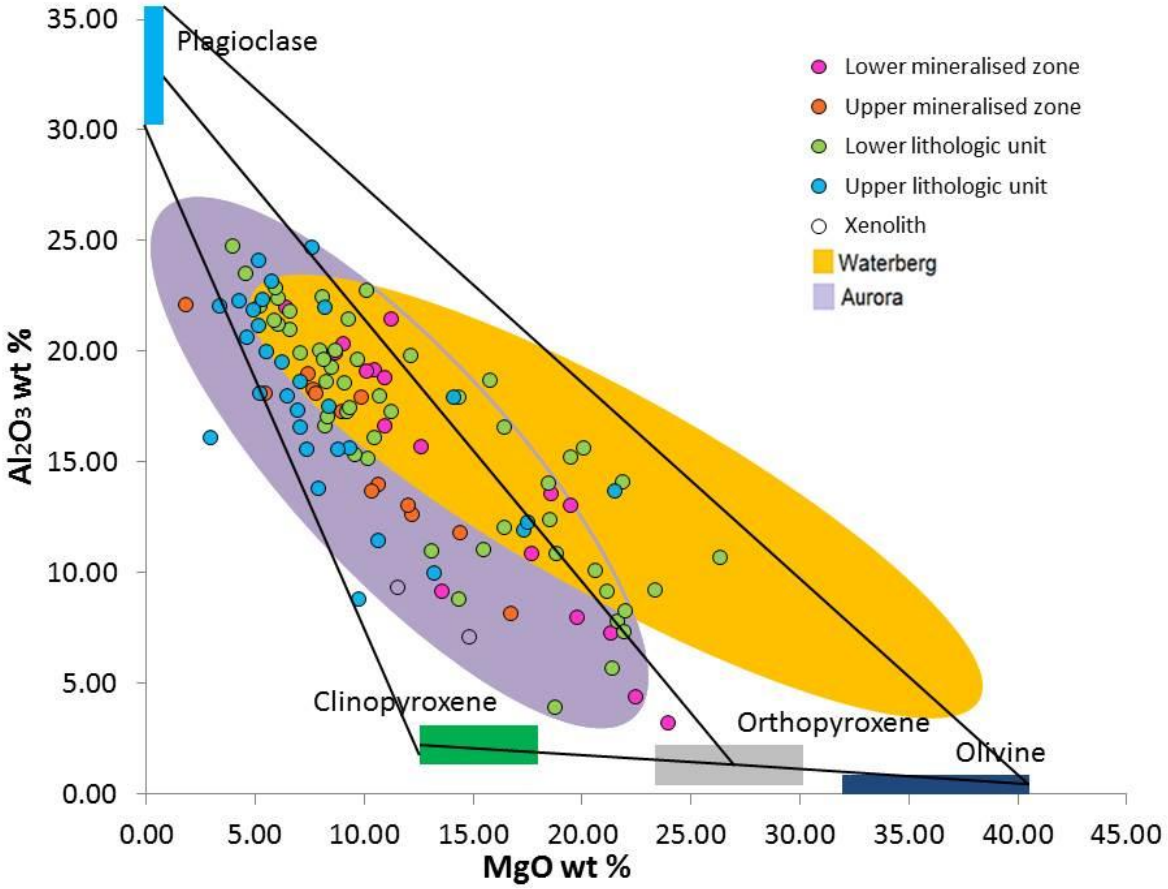

Figure 8.13: Major oxide plot showing MgO wt % versus Al_2O_3 wt % for all samples against different end member minerals. The end member mineral compositions are from the WB099 drillcore of the Waterberg area (unpublished data from M. Yudovskaya). The Waterberg data are from Kinnaird *et al.,* (2017), the Aurora data are from McDonald *et al.,* (2017).

The CaO and MgO binary plot showing the same mineral proportions also highlights the similarity between Harriet's Wish, and the Aurora and Waterberg projects, however, the upper lithologic unit on Harriet's Wish is Ca and Mg-poorer than Waterberg rocks, although is not as Ca- and Mg- poor as Aurora rocks, thus, confirming the regional trend of decreasing CaO and MgO southward (Figure 8.14).

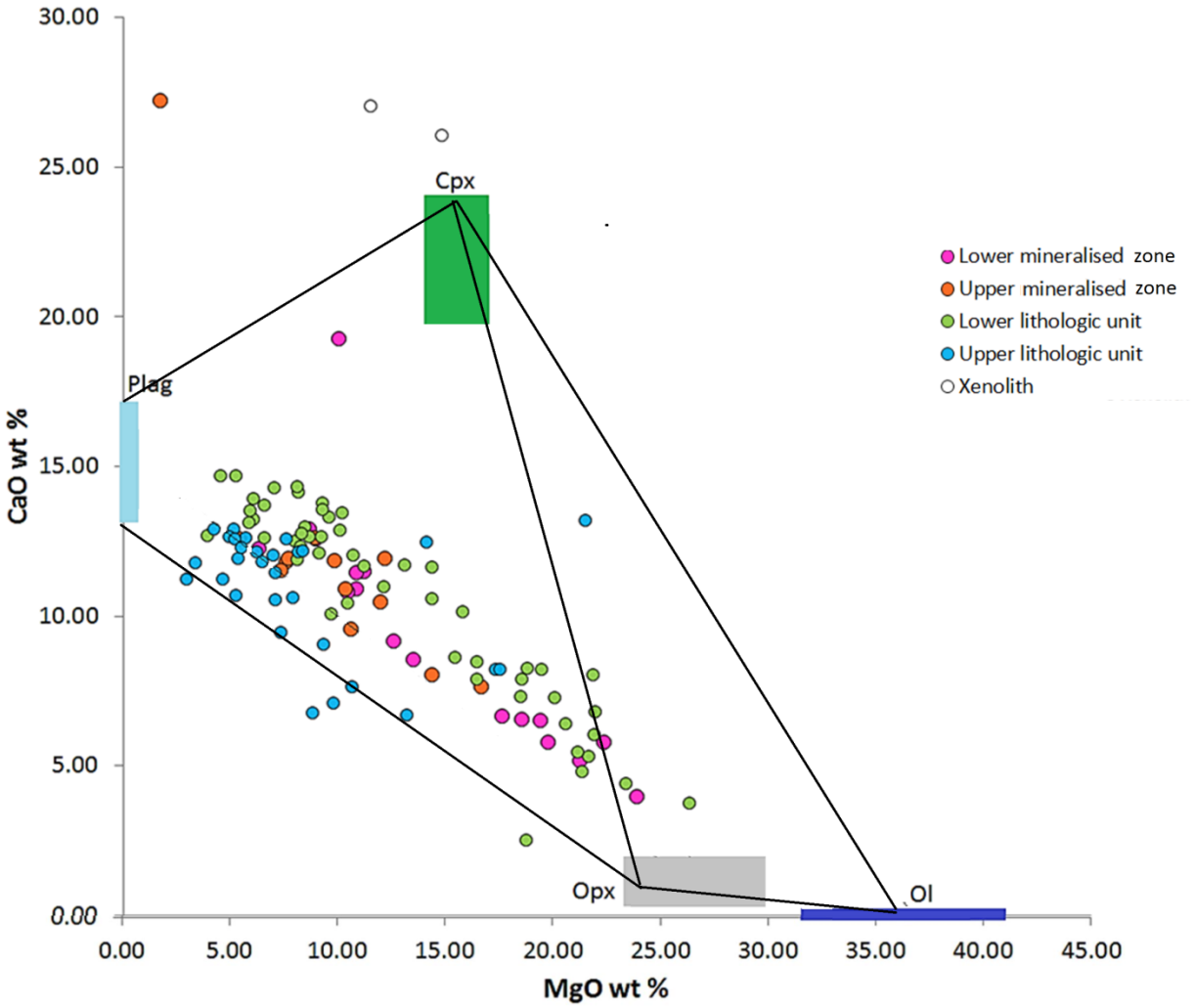

Figure 8.14: Major oxide plot showing MgO wt % versus CaO wt % of all samples against the different end member minerals. The end member mineral proportions are from the WB099 drillcore of the Waterberg area (unpublished data from M. Yudovskaya). Waterberg data are from Kinnaird *et al.,* (2017), Aurora data are from McDonald *et al.,* (2017).

8.4.4 **Trace elements**

There is a slight contrast in the trace element trends and abundances between the lower and upper lithologic units except for the Cr content, which shows a significant contrast (Table 8.3). The different Cr content is coupled with the contrasting Cr/V ratio of the lower and upper lithologic units (Figure 8.11 and 8.12; Table 8.3). This aids in the interpretation that two separate magmas formed the units on Harriet's Wish.

There is some overlap seen between the Ni and Cu values of the lower lithologic unit on Harriet's Wish, the Main Zone on the Aurora Project and the TGA sequence on the Waterberg Project (Figure 8.15). The lowest Cu occurs in the Harriet's Wish samples, with increased Cu values but the lowest Ni contents seen in the Aurora Project samples and the highest Cu and Ni values in the Waterberg Project samples (Figure 8.15). Furthermore, geographically this trend suggests depletion in Cu and Ni from north to south within the proposed basin north of the northern limb. The changes of lithologies through these areas are in agreement with this depletion trend. The olivine proportions and Mg# values are the highest on the Waterberg Project (Kinnaird *et al.,* 2017) whereas the Harriet's Wish (Figure 8.8; Figure 4.4) and the Aurora sequences at La Pucella, Nonnenwerth and Kransplaats are hosted by much more leucocratic rocks such as gabbronorite and gabbro rather than olivine-enriched rocks such as troctolite and olivine pyroxenite (Harmer *et al.,* 2004; Maier *et al.*, 2008; McDonald and Harmer, 2010). This trend also agrees well with the previously noted Ca- and Mg-depletion trend southward (Figure 8.14), and the north to south mafic to more felsic gradation of rocks in the upper and lower lithologic units (Figure 8.13). Overall, there is a slightly higher Ni/Cu ratio (a shallower slope of the trend) on Harriet's Wish compared to that on the Aurora Project and the F Zone on the Waterberg Project (Figure 8.15).

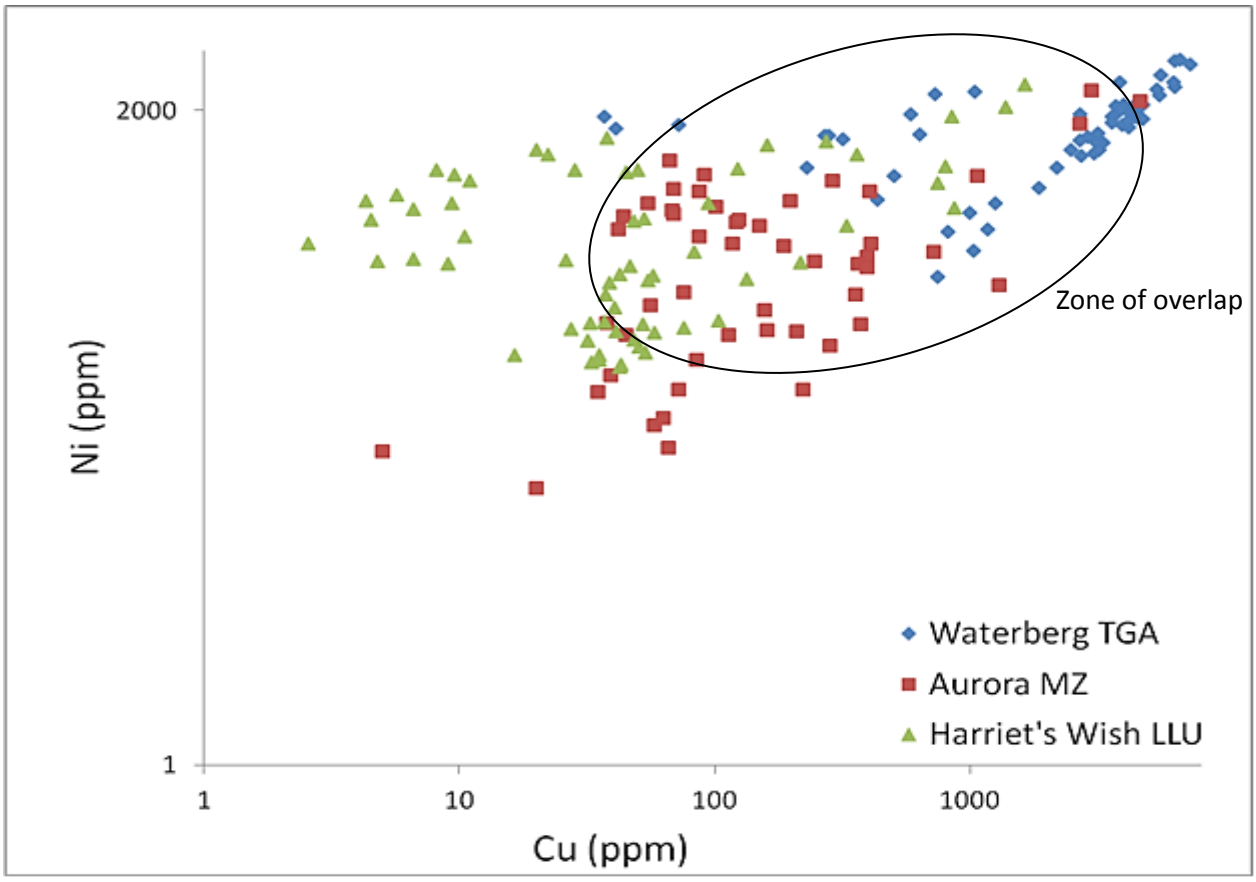

Figure 8.15: Ni (ppm) and Cu (ppm) log scaled values of the lower lithologic unit in the HW024 and HW025 drillcores at the Harriet's Wish, the TGA sequence in the drillcore WB099 from the Waterberg Project (McCreesh *et al.,* 2018), and the Main Zone of the Aurora LAP29 drillcore (McDonald *et al.,* 2017). The Waterberg Project samples, the Aurora Project samples and the Harriet's wish samples include mineralised rocks.

8.4.5 **A possible formation mechanism of the Harriet's Wish magmatic sequence**

The lower lithologic unit and the lower mineralised zone expectedly show some similarities to each other, but also some differences, when comparing certain whole rock geochemical parameters. This includes the very similar averages of such major oxides as TiO_2, MgO, CaO, and P_2O_5, but the distinguishably different Al_2O_3 and NiO contents (Table 8.1). The similarities in the Na_2O+K_2O/SiO_2 values are notable, but the differences in the CaO/Al_2O_3 ratio are also prominent (Table 8.1). Both the lower lithologic unit and the lower mineralised zone have elevated whole rock Mg# values, within the range of the ultramafic rock compositions, however, the lower lithologic unit is characterised by a wider range ($Mg\#_{51-83}$) than the lower mineralised zone ($Mg\#_{60-77}$;

Figures 8.9 and 8.10). Although the similarities in geochemical parameters are obvious, the considerable contrast makes it difficult to suggest that the same pulse of magma deposited the lower lithologic unit and the lower mineralised zone. Furthermore, within the lower lithologic unit, rocks above the lower mineralised zone show the differentiation trends in both the HW024 and HW025 drillcores (Figure 8.8 a and b). At the same time, rocks below the lower mineralised zone in both drillcores show a reverse trend with the more mafic (primitive) rocks higher in the sequence. This trend is also confirmed by the variation of the whole rock Mg# (Figure 8.9). These variations may have resulted from the different pulses of the same magma entering the system, starting with a more felsic, probably more contaminated or cooler portion of the melt that lost its energy along the cold pathways. As the entire plumbing system became heated with time more primitive melts entered the resident chamber. The final larger primitive influx (above the lower mineralisation), therefore, could have formed the upper part of the lower lithologic unit, which fractionated after the deposition in a conventional manner (more felsic at the top). The incorporation of S during consumption and digestion of the dolomitic xenoliths (as followed from the variations of the CaO/Al_2O_3 ratio; Table 8.1), and the interaction between crustally-contaminated resident melts and later, primitive melts carrying more dissolved magmatic S induce the formation of Cu-Ni-PGE mineralisation in the lower lithologic unit.

Another idea that could explain the formation of the basal mineralisation is that ultramafic, sulphide rich gabbroic melt could have entered the system in a period between the deposition of the sections below and above the mineralisation. This observation is consistent with the observed normative mineralogy of the HW025 drillcore (Figures 4.4, 8.8 b), and also consistent with the variations in major and trace element concentrations of the lower mineralised zone (Tables 8.1 and 8.3), and variations in major and trace element trends above and below the lower mineralised zone (Figures 8.1, 8.3 and 8.11). The mineralised zone appearing just below the olivine rich interval in the HW024 drillcore (Figure 8.8 a) could be explained by leaching of sulphides into the rocks below.

The major oxide compositions of the upper mineralised zone indicate its affinity for the upper lithologic unit (Table 8.1; Figure 8.5), albeit the upper mineralised zone occurs at the top of the lower lithologic unit. The unit and the zone have similar average abundances of such major oxides as TiO_2, FeO, MnO, MgO, CaO, and Cr_2O_3, as well as identical Cr/MgO (both <45) and Mg/FeO (both <1; Table 8.1). They also reveal similar trends on the bivariate diagrams and their rock compositions fall in the same fields (Figure 8.5). The whole rock Mg# values of these units also fall into the same range of $Mg\#_{46\text{-}72}$. This supposes that the Upper Zone magma influxes and the underlying cumulate mush have likely interacted with each other through mingling and mixing that have triggered sulphide immiscibility, therefore forming the upper mineralised zone. Overall, the normative mineral proportions show that the upper lithologic unit was fractionated upward (Figure 8.8 c) with more mafic rocks with the higher Mg# at the base and more felsic rocks with the lower Mg# at the top (Figure 4.4 and Figure 8.10). The occurrence of the olivine-rich layer in the upper lithologic unit could be attributed to a more mafic or primitive pulse of the same magma with olivine on the liquidus (Figure 8.8 c) that entered the system.

Although there are similarities between the upper lithologic unit and the upper mineralised zone, the upper mineralised zone is unique. The distinctions of this unit include the high compositional variability of the mineral proportions, the local enrichment in normative olivine, and generally a smaller proportion of plagioclase (Figure 8.8c; Figure 8.10). Furthermore, the highly variable host lithology is a distinguishing feature of the upper mineralised zone, like the heterogeneity of the package hosting the T Zone on the Waterberg Project (Kinnaird *et al.,* 2017). This could also serve as evidence for multiple influxes with accompanied mixing and mingling of magmas. In addition, as previously noted, calcsilicate xenoliths are common in the lower lithologic unit throughout Aurora (McDonald *et al.,* 2017) although rare on the Waterberg Project (Kinnaird *et al.,* 2017). On Harriet's Wish, there may have been some influence of calcsilicate xenoliths on the formation of the mineralised zones as noted by the deviation of the CaO/Al_2O_3 ratio from 0.6 in the upper mineralised zone (Table 8.1).

8.5 **Conclusions**

With some overlap, whole rock geochemistry shows a distinction between the lower and upper lithologic units and the lower and upper mineralised zones. This finding is supported by major oxide and trace element abundances and trends, as well as CIPW normative mineralogy that are different across the boundary at the 610 m depth of HW029 as defined by magnetic susceptibility measurements (Figure 5.4).

There is significant overlap between the whole rock major and trace element geochemistry of the Harriet's Wish, Aurora and Waterberg magmatic sequences. Harriet's Wish rocks show a higher geochemical affinity for rocks of the Waterberg Project rocks than for Aurora Project rocks.

There seems to be a north to south provisional gradation from generally more mafic to less mafic sequences from the Waterberg through Harriet's Wish and towards Aurora areas.

8.6 **Recommendations**

It is advisable to differentiate between the upper and lower lithologic unit based on multiple analyses, and not just magnetic susceptibility. Isotopic studies, particularly of Sr, are recommended to see if a shift occurs at their boundary in order to conclusively differentiate the upper and lower lithologic units. It would be especially important to look at the Aurora Project succession, because of the geochemical similarities found between this succession and the Waterberg Project succession by McDonald *et al.,* (2017). Mineral chemistry studies are also recommended to see if there are any cryptic variations within the units, to confirm the boundary between the lower and upper lithologic units and to assist in the interpretation of the CIPW results.

Chapter 9
Discussion

9.1 Introduction

To assist in the understanding of the geology and the mineralisation processes involved in the formation of the Harriet's Wish succession, the following techniques were employed on the HW024, HW025 and HW029 drillcores. 1) An in depth study of the stratigraphy, 2) A magnetic susceptibility study to determine a boundary, 3) A petrographic study, 4) a study of the geochemical aspects of the mineralisation and 5) A whole rock geochemical study.

9.1.1 Aims

This chapter aims to discuss and to evaluate:

- Probable correlations between the lithological units and the mineralised zones on the adjacent areas of Harriet's Wish, namely the Waterberg Project to the north and the Aurora Project the south.
- A continuity or discontinuity of the magmatic stratigraphy across the Hout River shear zone in the northern sector of the northern limb of the Bushveld Complex.
- Processes involved in the formation of the magmatic sequence and its mineralisation north of the Hout River shear zone.

An in-depth discussion on each technique is found at the end of each chapter. The purpose of this chapter is to highlight main points and ideas of each section and to draw overall conclusions.

9.2 **Discussion of results**

9.2.1 **Stratigraphy**

The magmatic sequence on Harriet's Wish can be divided into two broad stratigraphic subdivisions, referred to as the lower and upper lithologic units. Although some of the major and trace element data for the lower and upper lithologic units overlap (Tables 8.1, 8.2 and 8.3), the notable differences in the major and trace element abundances, the trends of their variations on binary diagrams and in vertical sections indicate that two separate magmas, or major two pulses of magma, formed these two parts of the magmatic stratigraphy on Harriet's Wish (Chapter 8; Table 8.1; Figures 8.1, 8.2, 8.3, 8.5 and 8.6).

The lower lithologic unit consists of the following rock types as logged in the field (Chapter 4) and confirmed by petrographic studies (Chapter 6): 1) gabbronorites (including melagabbronorite, olivine-bearing and olivine melagabbronorite), 2) a true troctolite package comprising distinct layers of leucotroctolite and troctolite with minor segregations of olivine norite with the variable proportions of cumulus olivine and plagioclase and minor pyroxenes, gabbro (including leucogabbro and anorthosite), norite (including melanorite), 3) pyroxenites (including feldspathic and olivine pyroxenite, orthopyroxenite and olivine-bearing orthopyroxenite), and 4) a calcsilicate xenolith. This rock assemblage is similar to the troctolite-anorthosite-gabbronorite (TGA) sequence in the occurrence of true troctolite and anorthosite amongst other common lithologies. The lower lithologic unit on Harriet's Wish does not contain harzburgite, which is the major rock type of the Ultramafic Sequence on the Waterberg Project (McCreesh, 2016; Kinnaird *et al.,* 2017); therefore, these units do not correlate. In addition, the more mafic lithologies are also not confined to the base of lower lithologic unit, on Harriet's Wish, as seen on the Waterberg Project (Kinnaird *et al.,* 2017).

Magnetic susceptibility values over the lower lithologic unit are generally ~0, with some local peaks over barren norite, mineralised gabbronorite (in the HW025 drillcore; Figure 5.3) and barren troctolite (in the HW024 drillcore; Figure 5.2). These sporadic peaks are not restricted exclusively to the mineralised and serpentinised parts of the unit. This is

dissimilar to the distribution of the magnetic susceptibility values within the Ultramafic Sequence that shows the persistent elevated magnetic susceptibility values at the base (McCreesh, 2016; Kinnaird *et al.*, 2017). Instead, the magnetic susceptibility readings on the Harriet's Wish lower lithologic unit favour a correlation with the TGA sequence (Kinnaird *et al.,* 2017). The core logging (Chapter 4) suggests that the lower lithologic unit is not a correlate of the Main Zone of the northern limb (Nex *et al.,* 1998; Ashwal *et al.,* 2005) since it contains true troctolite and economic sulphide mineralisation.

Petrography confirms the logged lithologies and suggests that the lower lithologic unit is distinct from the upper lithologic unit in that it contains much more olivine and bears rare chromite phenocrysts and their relics (Chapter 6). Furthermore, the true troctolite package of the olivine-plagioclase cumulates is confirmed by the petrographic study (Figure 6.1 a). The common although minor olivine relics inside predominant oikocrystic pyroxenes in the lower lithologic unit suggests that the proportion of liquidus olivine has been higher and the earlier ultramafic cumulates may have been partly reworked or "digested" by later gabbroic melts. The true troctolite texture and composition are suggestive of their correlation with the true troctolite in the TGA sequence on the Waterberg Project (Kinnaird *et al.,* 2017). Rare chromite grains are also found at the base of the TGA (McCreesh *et al.,* 2018). It is known that chromite is an indicative mineral of the Critical Zone, so its presence favours a derivation of the lower package from a Critical Zone-type magma rather than from a Main Zone-type magma (Eales and Cawthorn, 1996).

The field observations and core logging varied slightly from the magnetic susceptibility readings (Figures 4.16 and 5.4) in recognising the boundary between the two lithologic units in the HW029 drillcore. This inconsistency was due to the presence of secondary magnetite and base metal sulphides that occur at the interface between these two lithologic units (Figure 6.3b and d). The boundary between the lower and upper lithologic units was drawn at the 590-592 m, in the HW029 drillcore, using the magnetic pen and visual observations (Figure 4.16; SACS, 1980), whereas it was established at the 610 m depth based on the magnetic susceptibility measurements (Figure 5.3;

Ashwal *et al.,* 2005). The position of the upper mineralised zone, which straddles the boundary between the units, is identical to the position of the T zone, which straddles the wide interfingering contact between the TGA and the overlying-Upper Zone on the Waterberg Project (Kinnaird *et al.,* 2017).

The upper lithologic unit consists of the following rock types as logged in the field (Chapter 4) and confirmed by petrographic studies (Chapter 6): 1) gabbro (including mottled leucogabbro, lineated, non-lineated and magnetite-bearing varieties), 2) anorthosite (including mottled anorthosite), 3) gabbronorites (including olivine-bearing, mottled, leuco- and melagabbronorite and magnetite-bearing), and 4) massive and disseminated magnetitites. It was found that the upper lithologic unit is similar to the Upper Zone in the northern limb of the Bushveld Complex in terms of lithology and stratigraphic position; however, the observed thickness of the unit in the studied drillcores is significantly thinner due to Proterozoic and modern erosional processes (Huthmann *et al.,* 2016; Kinnaird *et al.,* 2017; Huthmann *et al.,* 2018). The magnetic susceptibility (Figure 5.4) and petrography (Figure 6.3 b and d) suggest disseminated magnetite present throughout the upper lithologic unit, although no magnetitite layers occur in the HW029 drillcore, which is located north of the Hout River shear zone (Ashwal *et al.,* 2005). However, massive and disseminated magnetitite layers are logged in the HW030 drillcore, which is located within the Hout River shear zone, as well as persistent layers that are present through the Harriet's Wish property forming reliable markers on the aeromagnetic maps (Figure 4.18). It is still questionable whether these layers were removed due to pre-Waterberg Proterozoic tectonism and erosion of the exposed Bushveld top (Huthmann *et al.,* 2016) or whether these layers are absent in the Upper Zone stratigraphy north of the Hout River shear zone (Chapters 2 and 3). The presence of the coarse hematitised magnetite clasts in Waterberg basal conglomerate (Figure 4.15 b) in the studied drillcores suggest that the clasts may be derived from eroded massive magnetitites although this hypothesis needs additional confirmation. The composition of the upper lithologic unit has much in common with the composition of the Upper Zone on the Waterberg Project with the occurrence of the disseminated interstitial, symplectic and cumulus magnetite (±ilmenite) grains and intergrowths being the major indicative feature (Figure 6.3 b and d; Kinnaird *et al.,* 2017;

McCreesh *et al.,* 2018). The log data support the earlier vision that the magnetitite layers are present only south of the Hout River shear zone (Ashwal *et al.,* 2005; Huthmann *et al.,* 2016; Kinnaird *et al.,* 2017; Chapters 3, 4 and 6).

9.2.2 **Mineralisation**

The lower mineralised zone occurs below the upper mineralised zone, within the lower lithologic unit and is not confined to the base of the sequence (Figures 4.16 and 7.3). This unit is hosted in a lithologically variable package of gabbronorites, pyroxenites and troctolites (Figure 4.4; Figure 7.3).

The lower mineralised zone shows the following differences to the F Zone on the Waterberg Project (Kinnaird *et al.,* 2017): 1) differences in the host lithology since harzburgitic rocks are absent (Chapter 4; Figure 4.4), 2) disagreement in the stratigraphic position (Figure 4.19), 3) a lack of elevated magnetic susceptibility readings over the lower mineralised zone (Figures 5.2 and 5.3) in petrographic differences, as chromite occurs as single grains and relics rather than in disseminated lenses or clusters (Figure 6.5 c).

There are, however, some geochemical similarities between the F Zone and the lower mineralised zone on Harriet's Wish. The most striking is the overlap on the plot of Ni/Cu versus (Pt+Pd)/Au (Figure 9.1) where their average compositions plot very close to each other. There are also notable similarities between the lower mineralised zone, the F Zone and certain Platreef localities. These similarities include coinciding Ni/Cu values >1 (Figure 9.1), similar noble metal abundances (Figure 7.9) and comparable miscorrelations between S, Cu and Pt+ Pd+ Au peaks (Chapter 7; Figure 7.2).

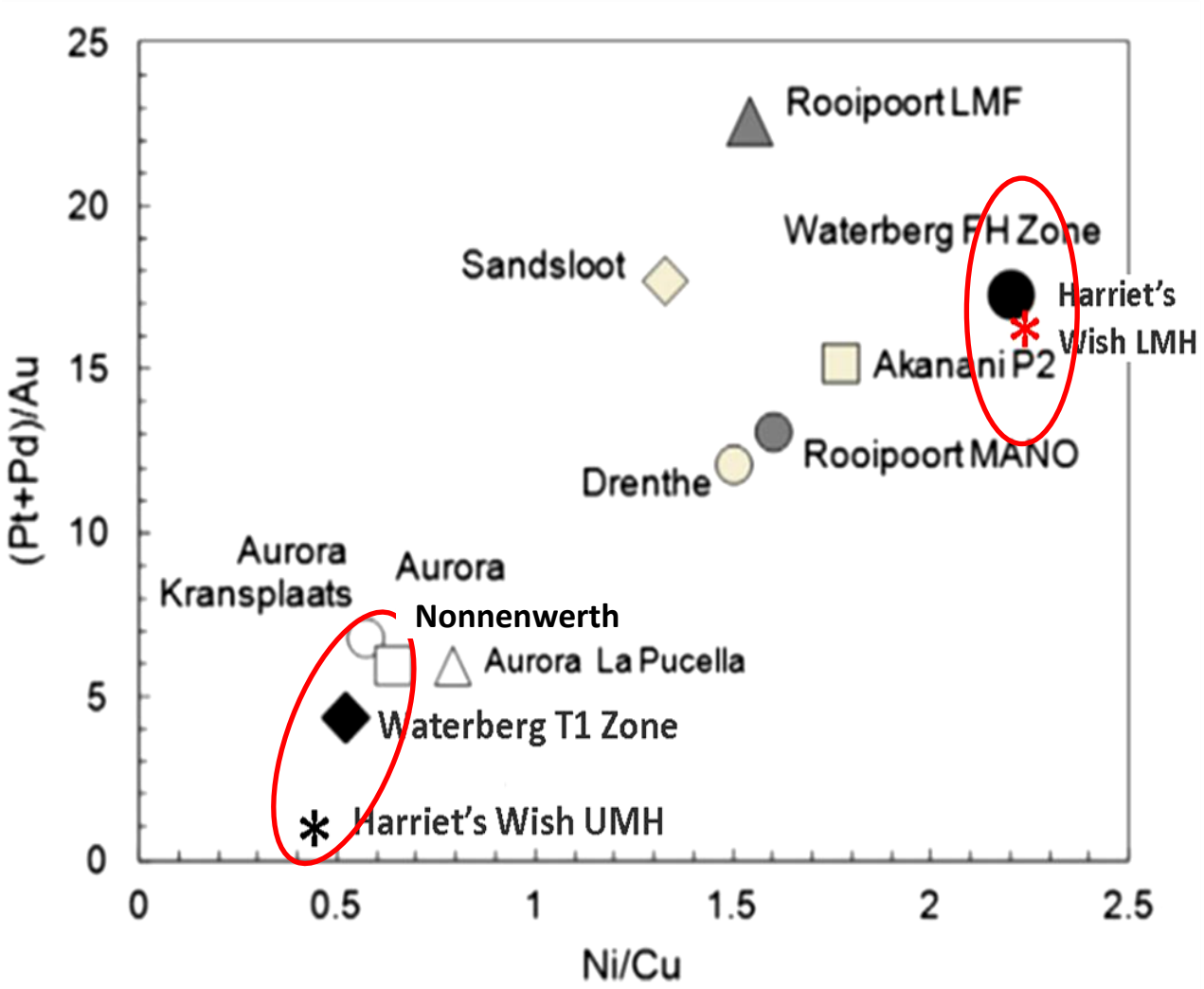

Figure 9.1: Average Ni/Cu values versus (Pt+Pd)/Au of Harriet's Wish, Aurora, Waterberg and various Platreef localities (modified after McDonald and Holwell, 2011). The red circle on the right shows similarities between the Harriet's Wish lower mineralised zone and the Waterberg F Zone as well as some Platreef localities. The red circle on the left shows similarities between the upper mineralised zone on Harriet's Wish and the T Zone on Waterberg. (LMH=lower mineralised zone, UMH=upper mineralised zone).

The lower mineralised zone on Harriet's Wish also shows notable similarities to the contact style mineralisation at the base of the Platreef on the plot of Cr versus combined Pt+ Pd+ Au (Figure 9.2). The observed scatter of the elevated Cr values with the increasing PGE content is observed in the F Zone on the Waterberg Project, as well as in the Platreef at Townlands and Sandsloot, but this feature is absent in the Aurora Project pattern (Figure 9.2).

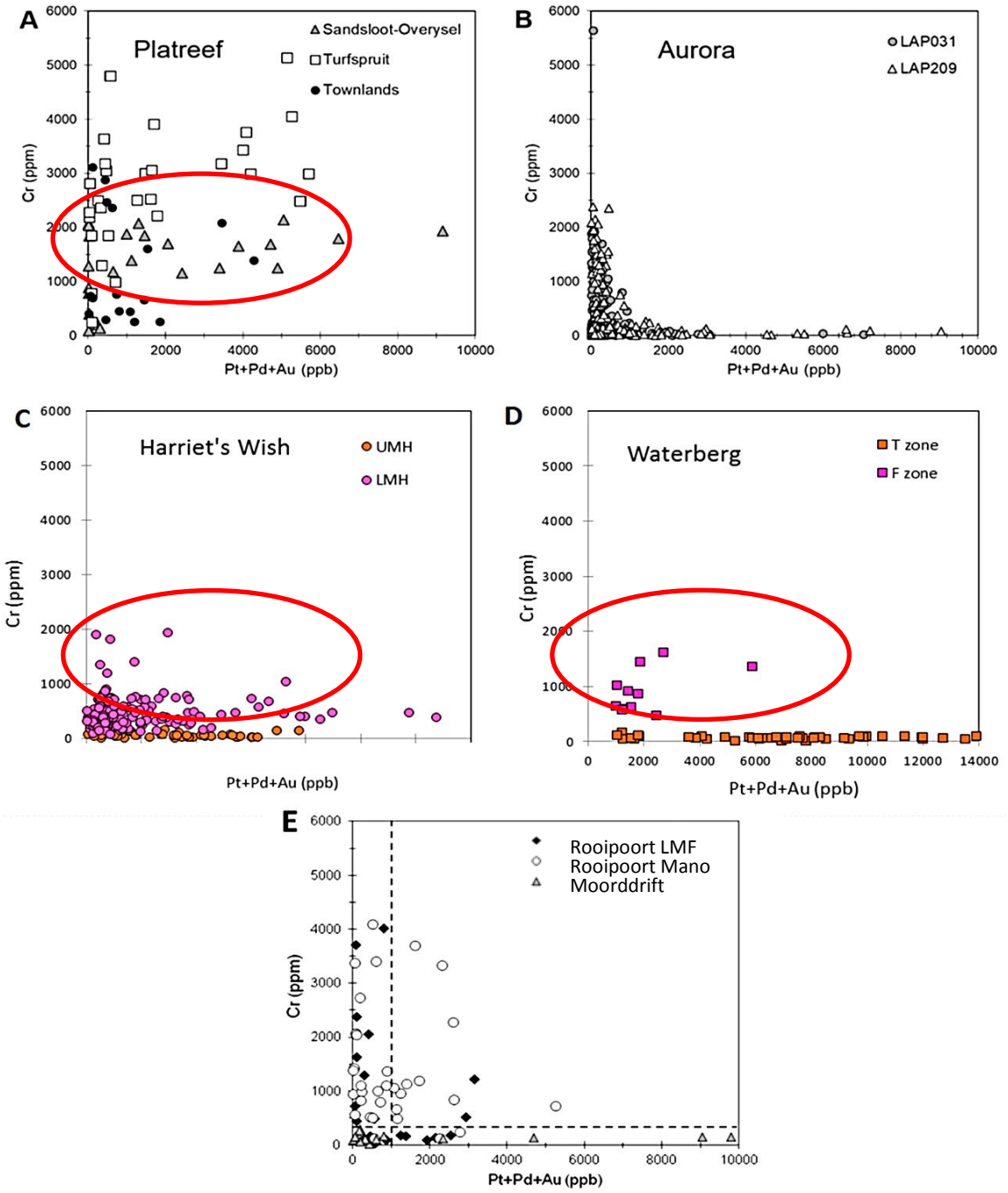

Figure 9.2: Chromium versus combined Pt+ Pd+ Au for samples of A) different Platreef-Flatreef deposits B) the LAP029 and LAP031 drillcores of Aurora C) the upper (UMH) and lower mineralised zones (LMH) from the HW024, HW025 and HW029 drillcores on Harriet's Wish, D) the T and F zones in the WB099 drillcore on the Waterberg Project and E) Rooipoort LMF and MANO, and Moorddrift drillcores. (Image A and B from McDonald *et al.,* 2017). Sandsloot-Overysel Platreef data from Holwell, (2006), Turfspruit Flatreef data from Smart, (2013), Townlands Platreef data from Manyeruke *et al.,* (2005), Aurora data from McDonald *et al.,* (2017). The red ellipses highlight the scatter of points away from x- and y axes.

The CIPW normative mineralogy (Figure 8.8) and the observed modal mineralogy (Chapters 4 and 6; Appendix A) correlate well with each other, with the exception of the proportions of olivine and pyroxenes in some intervals. The CIPW normative mineralogy indicates the presence of olivine throughout almost the entire sequence on Harriet's Wish, as well as an enrichment of olivine at the intervals where olivine is observed in the field and in the petrographic study (Figure 4.4; Chapter 6). Figures 4.5 b and 4.6 provide the textural evidence on mingling between olivine norite and olivine-bearing melagabbronorite and troctolites. The widespread evidence of mingling in the heterogeneous packages may possibly indicate digestion and reworking of earlier resident cumulates by new influxes of magma. The evidence on widespread postcumulus growth such as peritectic rims transitional into oikocrysts indicates that an initial amount of liquidus olivine might have been higher in these rocks. Therefore, it is suggested that the earlier ultramafic cumulates once present in the resident chamber were later eroded, dissolved and replaced by later dynamic influxes parental to the sequence similar to the TGA sequence (Kinnaird *et al.,* 2017).

The Mg# values of the lower mineralised zone correspond well to those of the F Zone on the Waterberg Project (Chapter 6: CIPW discussion) even though they do not average as high. It is therefore suggested that the lower mineralised zone was formed from the same magma as the F Zone, but that it had more interaction with xenoliths (Figure 4.10) and magma mixing to mingling occurred with the resulting sequence, thus becoming more gabbroic and dissimilar to the Ultramafic Sequence (Figure 4.19 b).

The upper mineralised zone on Harriet's Wish is correlative with the T Zone on the basis of their similar stratigraphic position straddling the contact between the lower and upper lithologic units (Figure 4.16 and 7.3), similar heterogeneous host rock package (including gabbro, gabbronorite, pegmatoidal gabbronorite, minor anorthosite and magnetite-bearing varieties), indicative minerals (pigeonite, magnetite and ilmenite) and major sulphides (such as chalcopyrite, pentlandite and pyrrhotite; Figure 6.6). Furthermore, the major and trace element geochemistry (Table 8.1 and 8.2) indicate that the upper mineralised zone shows more significant affinity to the upper lithologic

unit, than the lower lithologic unit which supports the idea of Upper Zone magma involvement in the formation of the upper mineralised zone.

Finally, a comparison is shown between the stratigraphic units and the mineralised zones of Harriet's Wish and the Waterberg Project, the Aurora Project and the generalised northern limb stratigraphy (Figure 9.3).

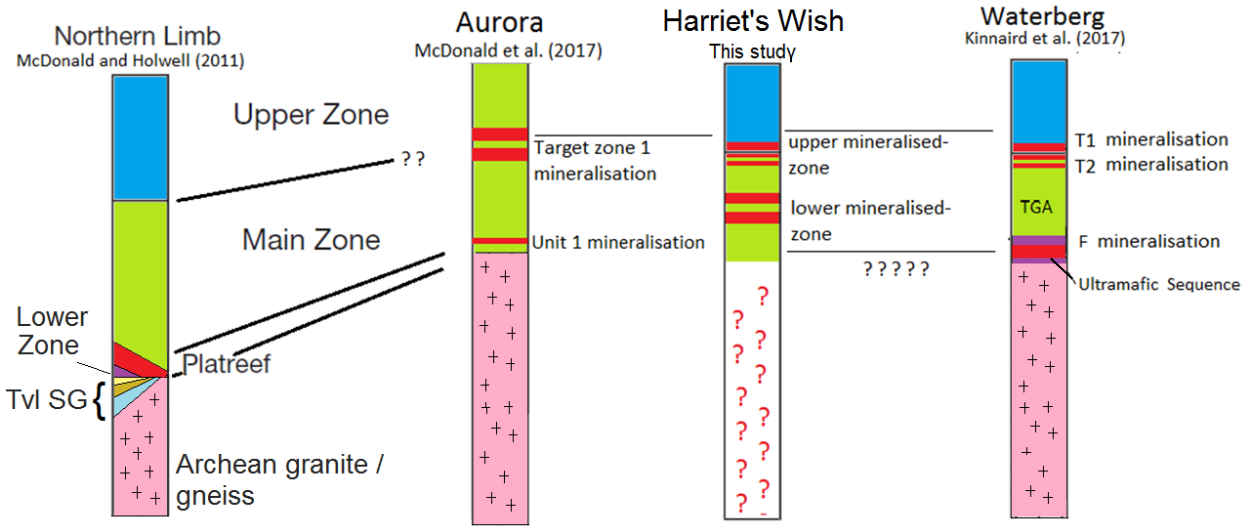

Figure 9.3: Schematic comparison of the positions of stratigraphic units of the northern limb (left), the Aurora succession (middle left), Harriet's Wish (middle right) and the Waterberg succession (right; Figure modified after McDonald and Holwell, 2011). TGA=Troctolite-gabbronorite-anorthosite sequence.

9.2.3 **A model for the formation of the mineralised zones**

The model for the formation of the upper and lower mineralised zones is based mainly on the tenor calculations. However, as discussed in Chapter 7, many of the exploration S analytical values were too low to be used in the tenor calculations. The results could therefore be somewhat skewed; however, the analytical database that was used is large and, therefore, statistically reliable as well as representing the only data source available for the studied area so far.

The lower mineralised zone is interpreted to have been formed from at least three major pulses of the same magma, confirmed by the correspondence between tenor values,

tenor trends, sulphide contents and Pt/Pd ratios across two drillcore intersections (Chapter 7; Figures 7.5 and 7.6). The magma influxes interacted with each other and their following differentiation due to the crystallisation of the PGE-free cumulates making the residual magma more evolved and richer in PGE and S from the base to the top. The incorporation of country rock xenoliths might have diluted the metal contents but facilitated sulphide immiscibility. The presence of the thick calcsilicate xenolith in the HW029 drillcore (Figure 4.10) supports this interpretation. It is likely that the early batch of magma incorporated higher amounts of the xenolithic material than two later batches, as it is elevated in S content but has a low PGE tenor (Table 8.1). The involvement of crustal components, which likely provide a flux of volatiles, facilitated an enhanced hydrothermal remobilisation of the ore components at the post-magmatic stage that resulted in the observed miscorrelation between the peaks of S, Cu and Pt+ Pd+ Au (Figure 9.4). There may also be alternative explanations for the miscorrelation of peaks, such as Rayleigh fractionation, as seen in the Great Dyke Main Sulphide Zone (Naldrett and Wilson, 1990).

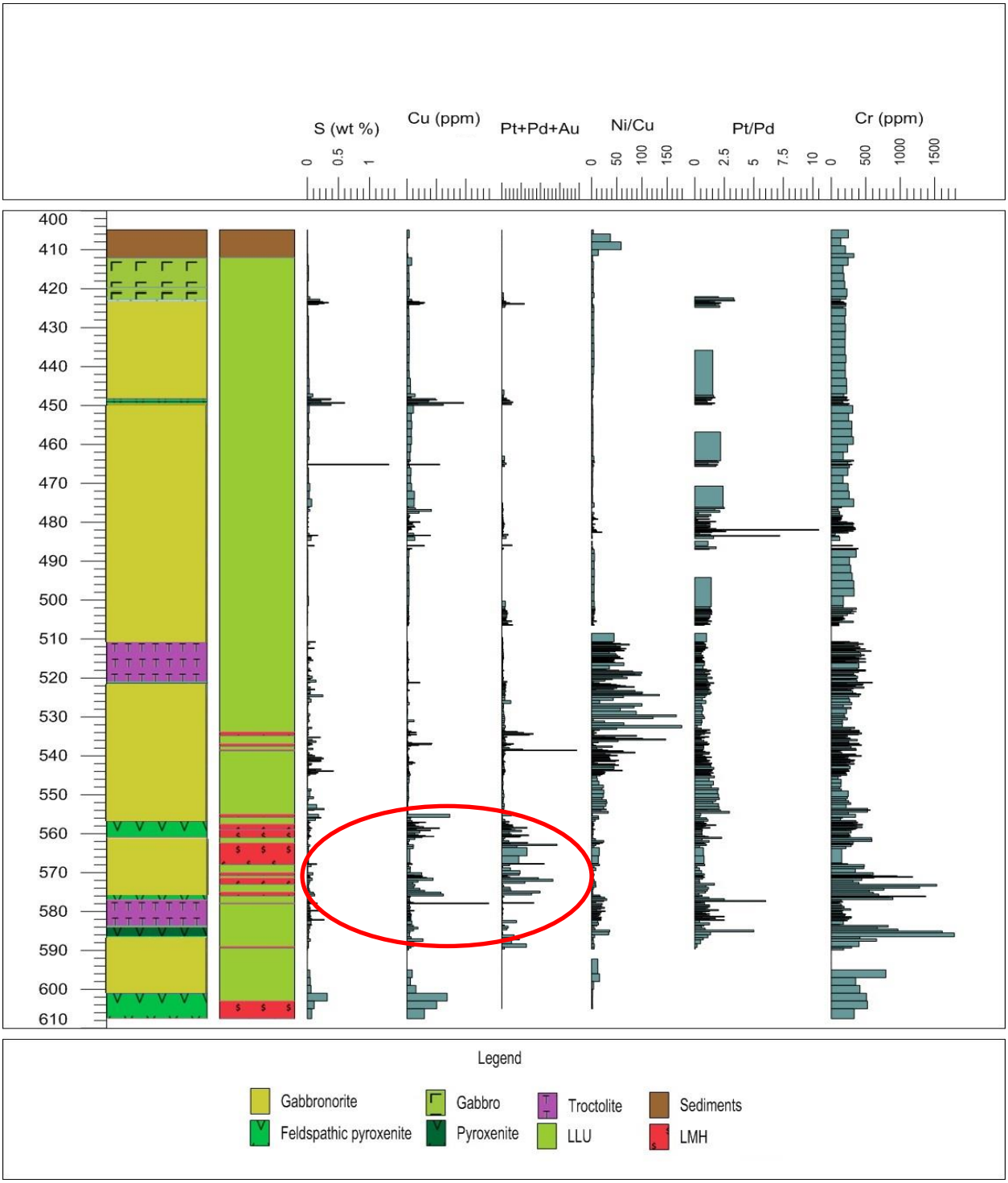

Figure 9.4: Ore metals, Cr and S content as well as the metal ratios plotted against depth of the units in the HW025 drillcore. The column on the left shows the stratigraphy, while the column on the right shows the stratigraphic affiliation of the units. The elipse higlights the miscorrelation between the peaks of the elements. LLU= lower lithologic unit, LMH= lower mineralised zone. Confidential data was provided by Sylvania Resources Limited, (2012), and to protect the sensitive nature of the data, the PGE grade values are not shown on the plots.

The upper mineralised zone probably formed from at least three major pulses of the same magma, since the sulphide contents (Figure 7.1), the PGE tenors and the trends in the tenors in the three intersections are very similar (Figure 7.4). The high and persistent tenor, and the moderate total sulphide amounts, is used in the interpretation that the magmas parental to the lower lithologic unit contained some magmatic S and a partial saturation in sulphide S was reached locally due to the cumulate deposition at the cooler margins of the magma flowed. The further exchange with a higher volume of flowing magma resulted in the observed increase in the PGE tenor upwards. The separate finger-like influxes of this magma deposited mineralisation in this manner with widespread mingling and mixing between derivates in the resident chamber. The first and second influxes have similar tenors and sulphide amounts, being in relative equilibrium with each other. The PGE-rich upper mineralisation was then deposited as a result of mixing between the latest influx and the resident residual melts and crystal mushes. This mixing induced sulphide immiscibility and facilitated further PGE concentration and tenor upgrading, therefore, forming the upper mineralised zone. The pristine magmatic origin of upper mineralisation is supported by the excellent correlation between the S, Cu and Pt+ Pd+ Au (Figure 9.5). The suggested model agrees with a PGE-fertile nature of the Upper Zone-type magmas proposed by Kinnaird *et al.,* (2017) and McCreesh *et al.,* (2018).

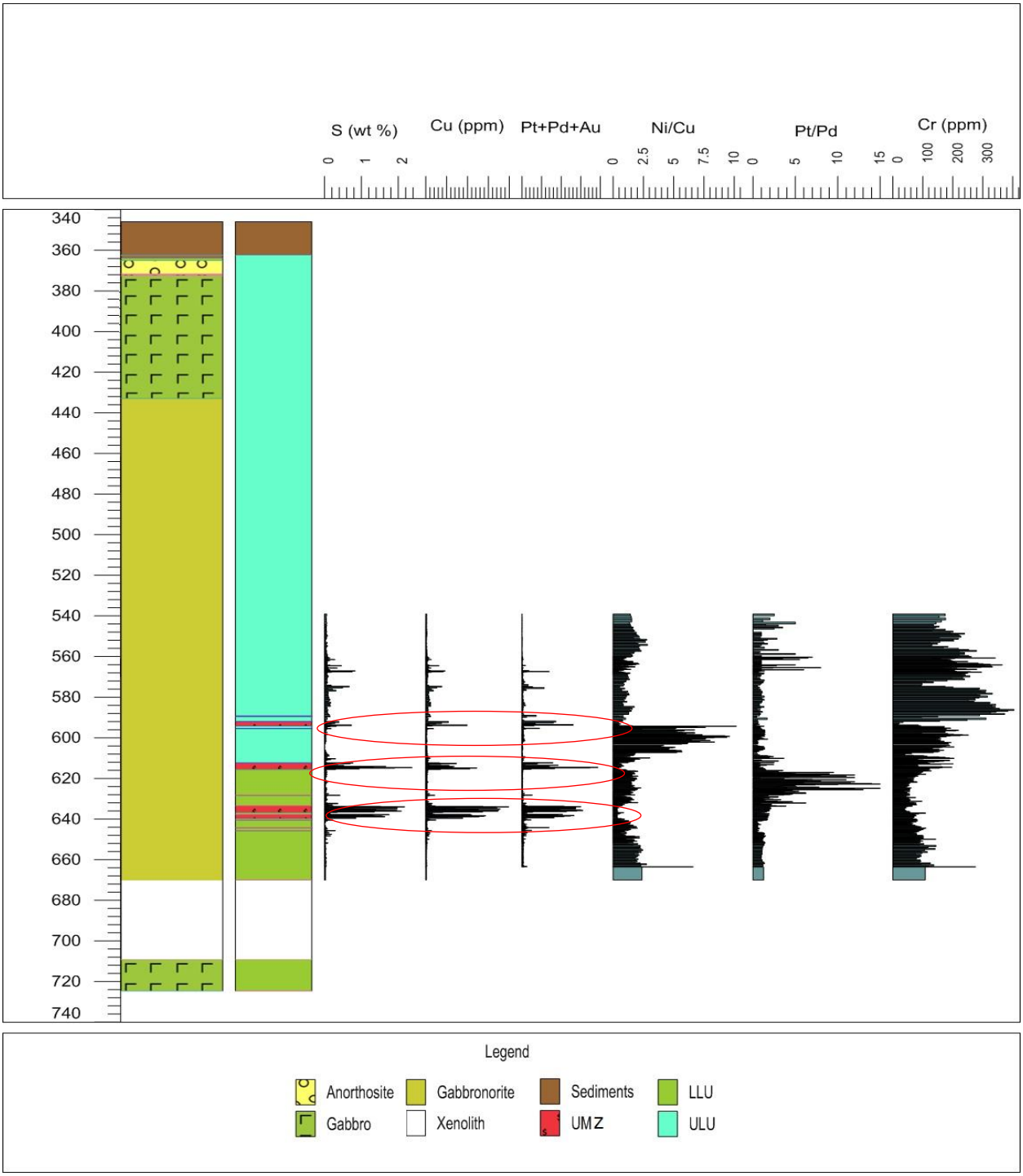

Figure 9.5: Ore metals, Cr and S content as well as the metal ratios plotted against depth of the various units in the HW029 drillcore. The column on the left shows the major stratigraphy, while the column on the right shows the stratigraphic affiliation of the units. The red elipses indicate correlated peaks of elements. LLU= lower lithologic unit, ULU= upper lithologic unit, UMZ= upper mineralised zone. Confidential data was provided by Sylvania Resources Limited, (2012), and to protect the sensitive nature of the data, the PGE grade values are not shown on the plots.

9.3 **Conclusions**

- The magmatic sequence on Harriet's Wish consists of two lithologic units.
- The lower lithologic unit is closely analogous to the basal part of the TGA sequence on the Waterberg Project area, where gabbroic melts parental to basal troctolite interacted with and eroded ultramafic rocks inheriting some scarce chromite grains (Huthmann *et al.,* 2018; McCreesh *et al.,* 2018).
- The upper lithologic unit is analogous to the base of the Upper Zone on the Waterberg Project.
- There is no stratigraphic and petrographic equivalent of the Waterberg Project Ultramafic Sequence on Harriet's Wish, but there is evidence that some earlier ultramafic cumulates might have been present in the resident chamber that were digested by later gabbroic melts.
- The lower mineralised zone shows some similarities to the F Zone in terms of ore mineralisation style, such as being hosted in similar sulphide assemblages and correspondence in noble metal concentrations such as Pd and Pt concentrations, although the host rock petrographic and chemical compositions are different. This could be due to magmatic facies variations along the strike of the sequence.
- There are some similarities between basal contact-style Platreef mineralisation, the lower mineralised zone on Harriet's Wish and the F Zone on the Waterberg Project. These similarities are, however, not strong enough to draw definitive correlations of the mineralised zone between these areas.
- The upper mineralised zone on Harriet's Wish is geochemically analogous to the T Zone on the Waterberg Project, and the mineralisation on the Aurora Project. However, it is characterised by notably higher Au proportion of 2.23 g/t (compared with 0.72 g/t on the Waterberg Project and 0.23 g/t on the Aurora Project) and has a quartz-chlorite-amphibole-pyrite assemblage similar to the Waterberg Project, but absent on Aurora (McDonald *et al.,* 2017). It is, therefore, suggested that the T Zone does indeed continue down strike from the proximal Waterberg facies to Harriet Wish and finally to the distal Aurora facies as suggested by Kinnaird *et al.,* (2017) and McDonald *et al.,* (2017).

- The upper mineralised zone on Harriet's Wish, the mineralisation on the Aurora Project and the T Zone mineralisation on the Waterberg Project differ from the Platreef-style ore mineralisation in terms of stratigraphic position. The stratigraphic position of the Platreef correlates to the Critical Zone, at the base of the Main Zone (Maier *et al.,* 2008; Yudovskaya *et al.,* 2017), whereas the stratigraphic level of the mineralisation of concern corresponds to the boundary between the Main and Upper Zones.
- The lithology, geochemistry, ore mineralisation and petrography suggest definitive differences across the Hout River shear zone. The idea that a separate magmatic basin or sub-chamber exists north of the Hout River shear zone (Huthmann *et al.,* 2016, 2018; Kinnaird *et al.,* 2017) is, therefore, supported by this study.
- It is suggested that the S- and PGE-poor Main Zone-type magmas in the resident chamber were mixed with the later pulses of the PGE- and S-rich fertile Upper Zone magma entering the chamber to form the upper mineralised zone correlative to the T Zone. The Upper Zone geochemical similarities to the T Zone equivalent on Harriet's Wish support its involvement in the formation of this mineralisation. Different processes related to proximity to the footwall may have triggered the deposition of the lower mineralised zone. These processes include magma mixing and mingling, assimilation of xenoliths and hydrothermal fluid circulation initiated by interaction with sediment-derived volatiles.

9.4 **Recommendations**

It is recommended that deeper boreholes be drilled to elucidate on the matter of the possible alteration of the Ultramafic Sequence and because a possible F Zone equivalent may be present deeper in the sequence. PGM studies should be done in order to fully compare the lower mineralised zone on Harriet's Wish with the F Zone on the Waterberg Project. Further studies are needed to determine a definitive correlation with or distinctiveness from the Platreef.

References

Appiah-Nimoh, F., 2004. A geological study of the Platreef at Potgietersrus platinum mine with emphasis on the magmatic processes, contamination and metasomatism (Doctoral dissertation, University of Johannesburg).

Armitage, P.E.B., 2011. Development of the Platreef in the northern limb of the Bushveld Complex at Sandsloot, Mokopane District, South Africa. Doctoral dissertation, University of Greenwich.

Armitage, P.E.B., McDonald, I., Edwards, S.J. and Manby, G.M., 2002. Platinum- group element mineralisation in the Platreef and calcsilicate footwall at Sandsloot, Potgietersrus district, South Africa: *Transactions of the Institution of Mining and Metallurgy*. 111, 36–45.

Armstrong, R.A., Compston, W., Retief, E.A., Williams, I.S. and Welke, H.J., 1991. Zircon ion microprobe studies bearing on the age and evolution of the Witwatersrand triad. Precambrian Research, 53, 243-266.

Ashwal, L.D., Webb S.J. and Knoper, M.W., 2005. Magmatic stratigraphy in the Bushveld Northern Lobe: continuous geophysical and mineralogical data from the 2950 m Bellevue drill core. *South African Journal of Geology*. 108, 199–232.

Bailie, R.H. and Robb, L.J., 2004. Polymetallic mineralization in the granites of the Bushveld Complex - examples from the central southeastern lobe. *South African Journal of Geology.* 107(4), 633-652.

Barker, O.B., 2012. Barker's platinum map of southern Africa [4th ed.]: Johannesburg*. Books on the Wall Publishing CC*.

Barnes, S.J., Holwell, D.A., and Le Vaillant, M., 2017. Magmatic sulfide ore deposits. *Elements*, *13*(2), 89-95.

Barnes, S-J. and Maier, W.D., 2002. Platinum-group element distributions in the Rustenburg layered suite of the Bushveld Complex, South Africa. In: Cabri LJ (ed) The geology, geochemistry, mineralogy and mineral beneficiation of platinum-group elements. *Can I Min Metal Petrol, Special Issu.*54, 431–458.

Barnes, S-J., Maier, W. D. and Ashwal, L. D., 2004. Platinum-group element distribution in the main zone and upper zone of the Bushveld Complex, South Africa. *Chemical Geology*. *208*(1-4), 293-317.

Barnes, S-J., Cruden, A.R., Arndt, N., and Saumur, B.M., 2016. The mineral system approach applied to magmatic Ni_Cu_PGE sulphide deposits. *Ore Geology Reviews.* 76(C), 296-316.

Barton, J.M., Cawthorn, R. C. and White, J., 1986. The role of contamination in the evolution of the Platreef of the Bushveld Complex. *Economic Geology*, 81, 1096-1104.

Bekker, A., Kaufman, A. J., Karhu, J. A., Beukes, N. J., Swart, Q. D., Coetzee, L. L. and Eriksson, K. A., 2001. Chemostratigraphy of the Paleoproterozoic Duitschland Formation, South Africa: implications for coupled climate change and carbon cycling. *American Journal of Science*, *301*(3), 261-285.

Biesheuvel, K., 1970. An interpretation of a gravimetric survey in the area west of Pilanesberg in the western Transvaal. Geological Society of South Africa, *Special Publication*. 1, 266–282.

Boorman, S., Boudreau, A. and Kruger, F. J., 2004. The Lower Zone–Critical Zone transition of the Bushveld Complex: a quantitative textural study. *Journal of Petrology*. *45*(6), 1209-1235.

Buchanan, D. and Rouse, J.E., 1984. Role of contamination in the precipitation of sulphides in the Platreef of the Bushveld Complex. In: Buchanan DL, Jones MJ (eds) Sulphide deposits in mafic and ultramafic rocks. Institution of Mining and Metallurgy, Stephen Austin, Hereford 141–146.

Buchanan, D.L, Nolan, J., Sudaby, P., Rouse, J.E., Viljoen, M.J. and Davenport, J.W.J., 1981. The genesis of sulphide mineralization in a portion of the Potgietersrus Limb of the Bushveld Complex. *Economic Geology.* 76,568–579.

Buchanan, D.L., 1988. Platinum group elements exploration (Amsterdam Elsevier). *Development in Economic Geology.* 26, 184.

Buchanan, P.C., Koeberl, C. and Reimold, W.U., 1999. Petrogenesis of the Dullstroom Formation, Bushveld Magmatic Province, South Africa. *Contrib. Mineral. Petrol*. 137, 133-146.

Buchanan, P.C., Reimold, W.U., Koeberl, C. and Kruger, F.J., 2002. Geochemistry of intermediate to siliceous volcanic rocks from the Dullstroom Formation and the Rooiberg Group, South Africa. *Contrib. Mineral. Petrol*. 144, 131-143.

Buchanan, P.C., Reimold, W.U., Koeberl, C. and Kruger, F.J., 2004. Rb–Sr and Sm–Nd isotopic compositions of the Rooiberg Group, South Africa: early Bushveld-related volcanism. *Lithos*, *75*(3-4), 373-388.

Buick, I.S., Maas, R. and Gibson, R., 2001. Precise U–Pb titanite age constraints on the emplacement of the Bushveld Complex, South Africa. *Journal of the Geological Society*. *158*(1), 3-6.

Bullen, W.D., Wilson, M.G.C. and Vorster, C.J., 1995. The Metallogeny of the Pietersburg and Tzaneen Area. *Geological Survey of South Africa*, 85.

Button, A., 1973. The stratigraphic history of the Malmani Dolomite in the eastern and north-eastern Transvaal*. Transactions of the Geological Society of South Africa*. 76, 229-247.

Bye, A. R. and Bell, F. G., 2001. Stability assessment and slope design at Sandsloot open pit, South Africa. *International Journal of Rock Mechanics and Mining Sciences*. *38*(3), 449-466.

Bye, A., 2005. Sandsloot open-pit applies 3-D geotechnical modelling. *Engineering and Mining Journal*. *206*(6), 44-46.

Callaghan, C.C., 1993. The geology of the Waterberg Group in the southern portion of the Waterberg basin. Masters dissertation, University of Pretoria.

Callaghan, C.C., Eriksson, P.G. and Snyman, C.P., 1991. The sedimentology of the Waterberg Group in the Transvaal, South Africa: an overview. *Journal of African Earth Sciences (and the Middle East). 13*(1), 121-139.

Cameron, E.N., 1978. The Lower Zone of the Eastern Bushveld Complex in the Olifants River Trough. *Journal of Petrology,* 19, 437-462.

Cameron, E.N., 1980. Evolution of the lower critical zone, central sector, eastern Bushveld Complex and its chromite deposits. *Economic Geology. 75*(6), 845-871.

Cameron, E.N., 1982. The Upper Critical Zone of the Eastern Bushveld Complex—Precursor of the Merensky Reef. *Economic Geology,* 77, 1307–1327.

Campbell, I.H. and Naldrett, A.J., 1979. The influence of silicate: sulfide ratios on the geochemistry of magmatic sulfides. *Economic Geology.* 74(6), 1503-1506.

Catuneanu, O. and Eriksson, P.G., 1999. The sequence stratigraphic concept and the Precambrian rock record: an example from the 2.7-2.1 Transvaal Supergroup, Kaapvaal craton. *Precambrian Research*. 97, 215-251.

Cawthorn, R.G., 1999. The Platinum and Palladium Resources of the Bushveld Complex. Platinum in South Africa. *South African Journal of Science* (95), Issue 11/12, pg: 481-489.

Cawthorn, R.G., 2010. The platinum group element deposits of the Bushveld Complex in South Africa. *Platinum Metals Review. 54*(4), 205-215.

Cawthorn, R.G., McCarthy, T.S., 1980. Variations in Cr content of magnetite from the upper zone of the Bushveld Complex—evidence for heterogeneity and convection currents in magma chambers. *Earth Planet Sci Lett.* 46, 335–343.

Cawthorn, G.G. and Molyneux, T., 1986. Vanadiferous magnetite deposits of the Bushveld Complex. In: Anhaeusser, C. R. and Maske, S., (Eds) Mineral deposits of Southern Africa. *Geol. Soc. S. Afr. Johannesburg.*1251-1266.

Cawthorn, R.G. and Walraven, F., 1998. Emplacement and crystallization time for the Bushveld Complex. *Journal of Petrology*. 39, 1669-1687.

Cawthorn, R.G. and Webb, S.J., 2001. Connectivity between the western and eastern limbs of the Bushveld Complex. *Tectonophysics*. *330*(3-4), 195-209.

Cawthorn, R. G. and Spies, L., 2003. Plagioclase content of cyclic units in the Bushveld Complex, South Africa. *Contributions to Mineralogy and Petrology*. *145*(1), 47-60.

Cawthorn, R.G., Davies, G., Clubley-Armstrong, A. and McCarthy T.S., 1981. Sills associated with the Bushveld Complex, South Africa: an estimate of the parental magma composition. *Lithos*. *14*(1), 1-16.

Cawthorn, R.G., Barton, J.M. and Viljoen, M.J., 1985. Interaction of floor rocks within the Platreef at Overysel, Potgietersrus, Northern Transvaal. *Economic Geology*. 80, 988-1006.

Cawthorn, R.G., Meyer, P.S. and Kruger, F.J., 1991. Major addition of magma at the Pyroxenite Marker in the western Bushveld Complex, South Africa. *Journal of Petrology*. *32*(4), 739-763.

Cawthorn, R.G., Lee, C.A., Schouwstra, R. P. and Mellowship, P., 2002. Relationship between PGE and PGM in the Bushveld Complex. *The Canadian Mineralogist*, *40*(2), 311-328.

Cawthorn, R.G., Eales, H.V., Walvaren, F., Uken, R. and Watkeys, M.K., 2006. The Bushveld Complex. In: Johnson, M.R., Anhaeusser, C.R. and Thomas, R.J., (Eds.) (2006). The Geology of South Africa Geological Society of South Africa, Johannesburg/Council for Geoscience, Pretoria. 261 - 281.

Cheney, E.S. and Twist, D., 1991. The conformable emplacement of the Bushveld mafic rocks along a regional unconformity in the Transvaal succession of South Africa. *Precambrian Research*. *52*(1-2), 115-132.

Clark, D.A. and Emerson, D.W., 1991. Notes on rock magnetization characteristics in applied geophysical studies. *Exploration Geophysics*. 22, 547-555.

Clark, D.A., 1997. Magnetic petrophysics and magnetic petrology: aids to geological interpretation of magnetic surveys. *Journal of Australian Geology and Geophysics.* 17 (2), 83-103.

Clarke, B., Uken, R. and Reinhardt, J., 2009. Structural and compositional constraints on the emplacement of the Bushveld Complex, South Africa. *Lithos*. *111*(1-2), 21-36.

Cornell, D.H., Armstrong, R.A. and Walraven, F., 1998. Geochronology of the Proterozoic Hartley Basalt formation, South Africa: constraints on the Kheis tectogenesis and the Kaapvaal Craton's earliest Wilson cycle. *Journal of African Earth Sciences. 26*(1), 5-27.

Cousins, C.A., 1959. The structure of the mafic portion of the Bushveld Igneous Complex. Transactions of the Geological Society of South Africa. 62, 79–189.

De Klerk, L., 2005. Bushveld stratigraphy on Rooipoort, Potgietersrus limb. In Workshop on Platinum exploration and exploitation in Africa., October 2005.

De Villiers, J.S., 1970. The structure and petrology of the mafic rocks of the Bushveld Complex south of Potgietersrus: *Geol. Soc. South Africa Spec. Pub*. 1: 23-35.

De Villiers, J. and Burger, A.J., 1967. Note on the minimum age of certain granites from the Richtersveld area. *Ann. Geol. Surv. S. Afr. 6*, 83-84.

De Waal, S.A., 1977. Carbon dioxide and water from metamorphic reactions as agents for sulphide and spinel precipitation in mafic magmas. *South African Journal of Geology*. *80*(3), 193-196.

De Wit, M.J., de Ronde, C.E., Tredoux, M., Roering, C., Hart, R.J., Armstrong, R.A. and Hart, R.A., 1992. Formation of an Archaean continent. *Nature*, *357*(6379), 553.

Dorland, H.C., Beukes, N.J., Gutzmer, J., Evans, D.A.D. and Armstrong, R.A., 2006. Precise SHRIMP U-Pb zircon age constraints on the lower Waterberg and Soutpansberg Group, SouthAfrica. *South African Journal of Geology*. 109, 139-156.

Du Toit , A.L., 1954. The Geology of South Africa. Oliver and Boyd, Edinburgh, U.K. 539.

Dunnett, T., Grobler, D.F., Simmonotti, N. M. E. M. and Mapeka, J. M., 2012. Lithological variations within Upper Critical Zone stratigraphy, Turfspruit 241KR, northern limb, Bushveld Complex. In *Platreef Workshop, 5th, Mokopane, South Africa, 9th–11th November 2012, Abstracts*.

Eales, H.V., 2002. Caveats in defining the magmas parental to the mafic rocks of the Bushveld Complex and the manner of their emplacement: review and commentary, *Mineralogical Magazine*. 66, 815-822.

Eales, H.V. and Cawthorn, R.G., 1996. The bushveld complex. *Developments in Petrology*. *15,* 181-229.

Eales, H.V. and Costin, G., 2012. Crustally contaminated komatiite: primary source of the chromitites and Marginal, Lower and Critical Zone magmas in a staging chamber beneath the Bushveld Complex. *Economic Geology*. *107*(4), 645-665.

Eales, H.V., Marsh, J.S., Mitchell, A.A., De Klerk, W.J., Kruger, F.J. and Field, M., 1986. Some geochemical constraints upon models for the crystallisation of the Upper Critical Zone – Main Zone interval, northwestern Bushveld Complex. *Mineralogical Magazine* 50, 567-582.

Eales, H.V., De Klerk, W.J., Butcher, A.R. and Kruger, F.J., 1990. The cyclic unit beneath the UG1 chromitite (UG1FW unit) at RPM union section platinum mine—Rosetta stone of the Bushveld upper critical zone. *Mineralogical Magazine*. *54*(374), 23-43.

Eales, H.V., Teigler, B. and Maier, W.D., 1993. Cryptic variations of minor elements Al, Cr, Ti and Mn in Lower and Critical Zone orthopyroxenes of the Western Bushveld Complex. *Mineralogical Magazine*. 57, 257-264.

Eglinton, R.M. and Armstrong, R.A. 2004. The Kaapvaal Craton and adjacent orogens, southern Africa: a geochronological database and overview of the geological development of the crato. *South African Journal of Geology*. 107, 13-32.

Engela, A., 2014. An evaluation of the contact between the Bushveld Complex and the Waterberg sedimentary sequence in the Waterberg Project. Honour's thesis. The University of the Witwatersrand.

Eriksson, P.G., Altermann, W., Catuneanu, O., Van der Merwe, R. and Bumby, A.J., 2001. Major influences on the evolution of the 2.67 – 2.1 Ga Transvaal basin, Kaapvaal craton. *Sedimentary Geology* 141-142 205-231.

Finn, C.A., Bedrosian, P.A., Cole, J.C., Khoza T.D. and Webb S.J., 2015. Mapping the 3D extent of the Northern Lobe of the Bushveld layered mafic intrusion from geophysical data. P*recambrian Research.* 268, 279-294.

Fossen, H. and Cavalcante, G.C.G., 2017. Shear zones–A review. *Earth-Science Reviews. 171*, 434-455.

Friese, A.E.W., 2004. Geology and tectono-magmatic evolution of the PPL concession area, Villa Nora-Potgietersrus Limb, Bushveld Complex. *Geological visitor guide*. *57*.

Gain, S.B. and Mostert, A.B., 1982. The geological setting of the platinoid and base metal sulfide mineralization in the Platreef of the Bushveld Complex in Drenthe, north of Potgietersrus. *Economic Geology. 77*(6), 1395-1404.

Gap geophysics, 2008. Date accessed 19 February 2019. Found online at http://www.gapgeo.com/.

Gauert, C., 2001. Sulphide and oxide mineralisation in the Uitkomst Complex, South Africa: origin in a magma conduit. *Journal of African Earth Sciences.* 32(2), 149-161.

Gill, R., 2010. Igneous Rocks and Processes a practical guide. *Blackwell Publishing*. 1-415.

Good, N. and de Wit M.J., 1997. The Thabazimbi-Murchison Lineament of the Kaapvaal Craton, South Africa: 2700 Ma of episodic deformation. *J Geol Soc Lond.* 154, 93–97.

Griffin, W.L., Graham, S., O'Reilly, S.Y. and Pearson, N.J., 2004. Lithosphere evolution beneath the Kaapvaal Craton: Re–Os systematics of sulfides in mantle-derived peridotites. *Chemical Geology*. *208*(1-4), 89-118.

Grobler, D.F, Brits, J.A.N., Maier, WD, Crossingham, A., 2018 Litho-chemostratigraphy of the Flatreef PGE deposit, northern Bushveld Complex. *Mineral Deposita*.

Grobler, D. F., Nielsen, S. A. and Broughton, D. W., 2012. Upper Critical Zone (Merenksy Reef) correlates within the Platreef on Turfspruit 241KR, northern limb, Bushveld Complex. In *Platreef Workshop, 5th, Mokopane, South Africa, 9th–11th November 2012, Abstracts*.

Grobler, N.J. and Whitfield, G.G., 1970. The olivineapatite magnetitites and related rocks in the Villa Nora occurrence of the Bushveld Igneous Complex. Pp. 208–231 in: Symposium on the Bushveld Complex and other Layered Intrusions (D.J.L. Visser and G. Von Gruenewaldt, editors). *Geological Society of South Africa, Special Publication.* 1.

Hall, A.L., 1932. The Bushveld Igneous Complex of the central Transvaal: *South Africa Geol. Survey Mem.* 28, 560.

Hall, A.L. and Humphrey, W.A., 1908. On the occurrence of chromite along the southern and eastern margins of the Bushveld plutonic complex. *Trans. Geol. Soc. S. Afr*. 11: 69-77.

Harmer, R.E and Von Gruenewaldt, G., 1991. A review of magmatism associated with the Transvaal Basin-implications for its tectonic settings. *South African Journal of Geology*. 94, 104-122.

Harmer, R.E. and Armstrong, R.A., 2000. Duration of Bushveld Complex (sensu lato) magmatism: constraints from new SHRIMP zircon chronology. In *workshop on the Bushveld Complex,* 18-21.

Harmer, R.E. and Armstrong, R.A., 2000. New precise dates on the acid phase of the Bushveld and their implications. Circular of Workshop on the Bushveld Complex, University of the Witwatersrand, Johannesburg, South Africa (Vol. 11, p. 12).

Harmer R.E., Pillay N. and Davis P.G., 2004. The Aurora project - Main Zone hosted PGE-base floor interaction, magmatic unconformities and the formation of giant chromitite, PGE and Ti-V magnetitite deposits. *Mineralium Deposita.* 40 (5), 451-472.

Harris, C. and Chaumba, J.B., 2001. Crustal contamination and fluid–rock interaction during the formation of the Platreef, northern limb of the Bushveld Complex, South Africa. *Journal of Petrology*. *42*(7), 1321-1347.

Hatch, F.H. and Corstorphine, G.S., 1905. The Geology of South Africa. 2nd edition, *MacMillan and Co., London.* 394.

Hatton, C.J. and Schweitzer, J.K., 1995. Evidence for syn-chronous extrusive and intrusive Bushveld magmatism. *Journal of African Earth Science*. 21, 579-594.

Holwell, D.A. and Armitage, P.E.B., 2005. Geochemistry and mineralogy of the Platreef and “Critical Zone” of the northern lobe of the Bushveld Complex, South Africa: Implications for Bushveld stratigraphy and the development of PGE mineralisation. *Mineralium Deposita*. 40, 526-549.

Holwell, D.A. and McDonald, I., 2006. Petrology, geochemistry and the mechanisms determining the distribution of platinum-group element and base metal sulphide mineralisation in the Platreef at Overysel, northern Bushveld Complex, South Africa. *Mineral. Deposita.* 41, 575–598.

Holwell, D.A. and Jordaan, A., 2006. Three-dimensional mapping of the Platreef at the Zwartfontein South mine: implications for the timing of magmatic events in the northern limb of the Bushveld Complex, South Africa", *Applied Earth Science: Transactions of the Institutions of Mining and Metallurgy*: Section B, 115, 2, 41-48.

Holwell, D.A., McDonald, I. and Armitage, P.E.B., 2006. Platinum-group mineral assemblages in the Platreef at the Sandsloot Mine, northern Bushveld Complex, South Africa. *Mineralogical Magazine*. 70, 83-101.

Holwell, D.A., Adeyemi, Z., Ward, L. A., Smith, D. J., Graham, S. D., McDonald, I. and Smith, J. W., 2017. Low temperature alteration of magmatic Ni-Cu-PGE sulfides as a source for hydrothermal Ni and PGE ores: A quantitative approach using automated mineralogy. *Ore Geology Reviews*. *91*, 718-740.

Holwell, D.A., Boyce, A., McDonald, I., 2007. Sulphur isotope variations within the Platreef Ni-Cu-PGE deposit: Genetic implications for the origin of sulphide mineralization. *Economic Geology*. 102(6), 1091-1110.

Holwell, D.A., McDonald, I. and Butler, I.B., 2011. Precious metal enrichment in the Platreef, Bushveld Complex, South Africa: evidence from homogenized magmatic sulphide melt inclusions*. Contributions Mineral. Petrol.* 161: 1011-1026.

Hulbert, L.J., 1983. A petrographical investigation of the Rustenburg Layered Suite and associated mineralization south of Potgietersrus. Unpublished DSc dissertation, University of Pretoria. 1-511.

Hulbert, L.J. and Von Gruenewaldt, G., 1982. Nickel, copper and platinum mineralization in the lower zone of the Bushveld Complex, south of Potgietersrus. *Economic Geology*. *77*(6), 1296-1306.

Hulbert, L.J. and Von Gruenewaldt, G., 1985. Textural and Compositional Features of Chromite in the Lower and Critical Zone of the Bushveld Complex South of Potgietersrus. *Economic Geology*. 80, 872-895.

Hunt, E.J., Latypov, R. and Horváth, P., 2018. The Merensky Cyclic Unit, Bushveld Complex, South Africa: Reality or Myth?. *Minerals*. *8*(4), 144.

Hutchinson, D. and Kinnaird, J.A., 2005. Complex multistage genesis for the Ni–Cu–PGE mineralisation in the southern region of the Platreef, Bushveld Complex, South Africa", *Applied Earth Science: Transactions of the Institutions of Mining and Metallurgy*. Section B, 114, 4, 208-224.

Hutchinson, D. and McDonald, I., 2008. Laser ablation ICP-MS study of platinum-group elements in sulphides from the Platreef at Turfspruit, northern limb of the Bushveld Complex, South Africa. *Mineralium Deposita.* 43,695-711.

Huthmann, F.M., Yudovskaya, M.A., Frei D. and Kinnaird, J.A., 2016. Geochronological evidence for an extension of the Northern Lobe of the Bushveld Complex, Limpopo Province, South Africa. *Precambrian Research*. 280, 61-75.

Huthmann, F. M., Yudovskaya, M. A., Kinnaird, J. A., McCreesh, M. and McDonald, I., 2018. Geochemistry and PGE of the lower mineralized Zone of the Waterberg Project, South Africa. *Ore Geology Reviews*. *92*, 161-185.

IUPAC, 1997. Compendium of Chemical Terminology— The Gold Book (2nd ed.). International Union of Pure and Applied Chemistry.

Ivanhoe mines, 2018. Found online at: https://www.ivanhoemines.com/projects/platreef-project/(2018). Date accessed: August 2018

Jansen, H., 1976. The Waterberg and Soutpansberg Groups in the Blouberg Area, Northern Transvaal: Transactions of the Geological Society of South Africa. 79, 281–91.

Jansen, H., 1982. The geology of the Waterberg basins in the Transvaal, Republic of South Africa (Vol. 71). Republic of South Africa, Department of Mineral and Energy Affairs.

Jones, R.T., 1999. Platinum Smelting in South Africa. Specialist report for Mintek. Found online at: http://www.mintek.co.za/Pyromet/Platinum/Platinum.htm. Date accessed: 13 November 2018.

Kawohl, A. and Frimmel, H.E., 2016. Isoferroplatinum-pyrrhotite-troilite intergrowth as evidence of desulfurization in the Merensky Reef at Rustenburg (western Bushveld Complex, South Africa). *Mineralogical Magazine*. *80*(6), 1041-1053.

Kekana, S.M., 2014. An investigation of mineralisation controls in the upper section of the Platreef in the southern sector, on Turfspruit, Northern Limb, Bushveld Complex, South Africa (Masters dissertation). University of the Witwatersrand.

Kendall, T., 2006. Platinum 2006. Johnson Matthey, Royston, UK, 52.

Kinnaird, J. A., 2005. The Bushveld large igneous province. *Review Paper, The University of the Witwatersrand Johannesburg, South Africa, 39pp*.

Kinnaird, J.A. and McDonald, I., 2005. An introduction to mineralisation in the northern limb of the Bushveld Complex. *Applied Earth science (Trans. Inst. Min. Metall. B)*. 114, 194-198.

Kinnaird, J.A. and Nex, P.A.M., 2015. Platinum-group elements (PGE) Mineralisation and Resources of the Bushveld Complex, South Africa. Edited by Napoleon Q. Hammond and Christopher Hatton, Council for Geoscience, publ. 2015, 193-342.

Kinnaird, J.A., and McDonald, I., 2018. The Northern Limb of the Bushveld Complex: A New Economic Frontier. SEG Spec. Publ. Metals. Miner. Soc. 21, 157-177.

Kinnaird, J.A., Kruger, F.J., Nex, P.A.M. and Cawthorn, R. G., 2002. Chromitite Formation- a key to understanding processes of platinum enrichment. *The Institution of Mining and Metallurgy*. 23-35.

Kinnaird, J.A., White, J.A. and Schurmann, L. W., 2004. The importance of multiphase emplacement in the Platreef, a critical link with the eastern and western limbs of the Bushveld Complex.

Kinnaird, J.A., Hutchinson D., Schurmann L., Nex P.A.M. and de Lange R., 2005. Petrology and mineralisation of the southern Platreef: northern limb of the Bushveld Complex, South Africa. *Mineralium Deposita.* 40, 576–597.

Kinnaird, J.A., Yudovskaya, M.A. and Botha, M.J., 2014. The waterberg extension to the bushveld complex. In: *12th International Platinum Symposium.* Yekaterinburg, Russia.

Kinnaird, J.A., Yudovskaya, M., McCreesh, M., Huthmann, F. and Botha, T.J., 2017. The Waterberg platinum group element deposit: atypical mineralization in mafic-ultramafic rocks of the Bushveld Complex, South Africa. *Economic Geology*. 112(6), 1367-1394.

Kinnaird, K.A. and McDonald, I., 2014. The update on the Waterberg site (PTM) (Internal report). Unpublished, The University of the Witwatersrand Johannesburg, South Africa.

Klemd, R., Herderich, T., and Junge, M., 2016. Platinum-group element concentrations in base-metal sulphides from the Platreef, Mogalakwena Platinum Mine, Bushveld Complex, South Africa. *South African Journal of Geology*. 119(4), 623-638.

Klemd, R., Junge M., Oberthür T., Herderich T., Schouwstra R., and Roberts J., 2016. Platinum-group element concentrations in base-metal sulphides from the Platreef, Mogalakwena Platinum Mine, Bushveld Complex, South Africa. *South African Journal of Geology.* 119(4), 623-638.

Knoper, M.W. and Von Gruenewaldt, G., 1996. The Bellevue (BV-1) borehole core log: 2.9 km of Bushveld Complex stratigraphy (northern lobe), Potgietersrus, South Africa.

Kruger, F.J., 1990. The stratigraphy of the Bushveld Complex: a reappraisal and the relocation of the Main Zone boundaries. *South African journal of geology*. *93*(2), 376-381.

Kruger, F.J., 1992. The origin of the Merensky cyclic unit: Sr-isotopic and mineralogical evidence for an alternative orthomagmatic model. *Australian Journal of Earth Sciences*. *39*(3), 255-261.

Kruger, F.J., 2004. Filling the Bushveld Complex magma chamber: Lateral expansion, roof and floor interaction, magmatic unconformities and the formation of giant chromitite, PGE and Ti-V-magnetite deposits. EGRI circular 34, University of the Witwatersrand.

Kruger, F.J., 2005. Filling the Bushveld Complex magma chamber: lateral expansion, roof and metal mineralisation at the northern outcrop limit of the Bushveld northern limb, north of Mokopane. *1st Platreef Workshop Field Guide*, Mokopane 16–19 July 2004 Geoscience Africa. University of the Witwatersrand.

Kruger, F.J. and Marsh, J.S., 1985. The mineralogy, petrology and origin of the Merensky cyclic unit in the western Bushveld Complex. *Economic Geology*. *80*(4), 958-974.

Kruger, F.J. and Smart, R., 1987. Diffusion of trace elements during bottom crystallization of double-diffusive convection systems: the magnetitite layers of the Bushveld Complex. *Journal of Volcanology and Geothermal Research*. 34(1-2), 133-142.

Kruger, F.J., Cawthorn, R.G., Walsh, K.L., 1987. Strontium isotopic evidence against magma addition in the upper zone of the Bushveld Complex. *Earth Planet Sci Lett.* 84:51–58.

Le Bas, M.J. and Streckeisen, A.L., 1991. The IUGS systematics of igneous rocks. *Journal of the Geological Society*. *148*(5), 825-833.

Lee, C.A., 1996. A review of mineralisation in the Bushveld Complex and some other layered mafic intrusions. In: R.G. Cawthorn (Editor), Layered Intrusions. *Elsevier, Amsterdam.* 103-145.

Lenthall, D. H., 1973. A proposed nomenclature system for the granophyre's associated with the Bushveld Complex. *Trans. Geol. S. Afr*. 76, 75-76.

Lesher, C.M., 2017. Roles of xenomelts, xenoliths, xenocrysts, xenovolatiles, residues, and skarns in the genesis, transport, and localization of magmatic Fe-Ni-Cu-PGE sulfides and chromite. *Ore Geology Reviews*. 90, 465-484.

Lomberg, K., 2012. Updated exploration results and mineral resource estimate for the Waterberg platinum project, South Africa., (Latitude 23° 21′ 53″S, Longitude 28° 48′ 23″E). NI-43-101 Report Prepared for Platinum Group Metals Ltd by Coffey Mining, 1st September 2012: 89.

Lomberg, K., 2013. Revised and Updated mineral resource estimate for the Waterberg platinum project, South Africa., (Latitude 23° 21′ 53″S, Longitude 28° 48′ 23″E). NI-43-101 Report Prepared for Platinum Group Metals Ltd by Coffey Mining, 1st February 2013: 98.

Lomberg, K. and Goldschmidt, A., 2014. Platinum Group Metals Ltd. Technical Report for the Update on Exploration Drilling at the Waterberg Joint Venture and Waterberg Extension Project, South Africa (Latitude 23° 14' 11'' S, Longitude 28° 54' 42'' E) Platinum Group Metals (RSA)(Pty)Ltd (Internal report).

Lotter, N.O., Oliveira, J. and Nicholson, D.R., 2011. Ivanhoe Platreef - Phase I Geomet Unit Characterisation. *Internal report.* 1-71.

Maier, W.D. and Eales, H.V., 1997. Correlation within the UG2-Merensky Reef interval of the Western Bushveld Complex, based on geochemical, mineralogical and petrological data. Geological Survey of South Africa, Council for Geoscience. 120.

Maier, W.D. and Barnes, S.J., 2010. The petrogenesis of platinum-group element reefs in the upper Main Zone of the Northern lobe of the Bushveld Complex on the farm Moorddrift, South Africa. *Econ. Geol.* 105, 841–854.

Maier, W.D., Barnes, S.J. and De Waal, S.A., 1998. Exploration for magmatic Ni-Cu-PGE sulphide deposits: A review of recent advances in the use of geochemical tools and their application to some South African ores. *South African Journal of Geology*, *101*(3), 237-253.

Maier, W.D., de Klerk, L., Blaine, J., Manyeruke, T., Barnes, S-J., Stevens, M.V.A. and Mavrogenes, J.A., 2007. Petrogenesis of contact-style PGE mineralization in the northern

lobe of the Bushveld Complex: comparison of data from the farms Rooipoort, Townlands, Drenthe and Nonnenwerth. *Mineralium Deposita*. 43(3), 255-280.

Maier, W.D., De Klerk, L., Blaine, J., Manyeruke, T., Barnes, S.J., Stevens, M.V.A. and Mavrogenes, J.A., 2008. Petrogenesis of contact-style PGE mineralization in the northern lobe of the Bushveld Complex: comparison of data from the farms Rooipoort, Townlands, Drenthe and Nonnenwerth. *Mineralium Deposita*. *43*(3), 255-280.

Mangwegape, M., Roelofse, F., Mock, T. and Carlson, R.W., 2016. The Sr-isotopic stratigraphy of the Northern Limb of the Bushveld Complex, South Africa. *Journal of African Earth Sciences*. *113,* 95-100.

Manyeruke, T.D., 2003. The petrography and geochemistry of the Platreef on the farm Townlands, near Potgietersrus, northern Bushveld Complex (Doctoral dissertation), University of Pretoria.

Manyeruke T.D., 2007. Geochemical Variation of the Platreef in the Northern Limb of the Bushveld Complex: Implications for the Origin of the PGE Mineralisation (Doctoral thesis), University of Pretoria. 206.

Manyeruke, T.D., Maier, W.D. and Barnes, S.J., 2005. Major and trace element geochemistry of the Platreef on the farm Townlands, northern Bushveld Complex. *South African Journal of Geology*. *108*(3), 381-396.

Martini, J.E.J., 1979. A copper-bearing bed in the Pretoria Group in the northeastern Transvaal. In: Anderson, A.L. and Van Biljoen W.J., (Eds.) Some sedimentary basins and associated ore deposits of South Africa. Geological Society of South Africa. Special Publication. 6 65-72.

Mayer, C., 2018. Strontium isotope stratigraphy of the platreef at Turfspruit, Northern Limb, Bushveld Igneous Complex (Doctoral dissertation, Laurentian University of Sudbury).

McCreesh, M.J.G., 2013. A study of the Main Zone-Upper Zone boundary beneath a thick succession of Waterberg sediments in the far north of the Northern limb of the Bushveld Complex: B.Sc. thesis, University of the Witwatersrand 148.

McCreesh, M. J., Yudovskaya, M. A., Kinnaird, J. A. and Reinke, C., 2018. Platinum-group minerals of the F and T zones, Waterberg Project, far northern Bushveld Complex: implication for the formation of the PGE mineralization. *Mineralogical Magazine*, 82(3), 539-575.

McDonald, I. and Holwell, D.A., 2007. Did Lower Zone magma conduits store PGE-rich sulfides that were later supplied to the Platreef? *South African Journal of Geology*, 110, 611−616.

McDonald, I. and Holwell, D.A., 2011. Geology of the northern Bushveld Complex and the setting and genesis of the Platreef Ni-Cu-PGE deposit. *Reviews in Economic Geology.* (17), 297-327.

McDonald, I., Holwell, D.A. and Armitage, P.E.B., 2005. Geochemistry and mineralogy of the Platreef and “Critical Zone” of the northern lobe of the Bushveld Complex, South Africa: Implications for Bushveld Stratigraphy and the development of PGE mineralization. *Mineralium Deposita*. 40, 526-549.

McDonald, I., Holwell, D.A. and Wesley, B., 2009. Assessing the potential involvement of an early magma staging chamber in generation of the Platreef Ni-Cu-PGE deposit in the northern limb of the Bushveld Complex: A pilot study of the Lower Zone complex at Zwartfontein. *Transactions of the Institution of Mining and Metallurgy*. 118, 5−20.

McDonald, I. and Harmer, R.E., 2010. The nature of PGE mineralisation in the Aurora Project area, northern Bushveld Complex, South Africa. Abstract, 11th International Platinum Symposium, 21st–24th June 2010, Sudbury, Ontario. In: Jugo, P.J., Lesher, C.M., Mungall, J.E., (Eds.), *Ontario Geological Survey*. Miscellaneous Release Data-269.

McDonald, I., Harmer, R.E., Holwell, Hughes, H.S.R. and Boyce, A.J., 2017. Cu-Ni-PGE Mineralisation at the Aurora Project and potential for a new PGE province in the Northern Bushveld Main Zone. *Ore Geology Reviews*. 80, 1135–1159.

McNaughton, N.J., Pollard, P.J., Groves, D. I. and Toylor, R.G., 1993. A long-lived hydrothermal system in Bushveld Granites at the Zaaiplaats Tin Mine: Lead Isotope Evidence. *Economic Geology*. 88, 27-43.

Meyer, R. and De Beer, J.H., 1987. Structure of the Bushveld Complex from resistivity measurements. *Nature*. 325, 610–612.

Mitchell, A.A., 1986. The petrology, mineralogy and geochemistry of the Main Zone of the Bushveld Complex at Rustenburg Paltinum Mines, Union Section. Unpubl. PhD thesis, Rhodes University, South Africa 122.

Mitchell A.A., 1990. The stratigraphy, petrography and mineralogy of the Main Zone of the northwestern Bushveld Complex. *South African Journal of Geology*. 93, 818–831.

Mitchell, A.A. and Manthree, R., 2002. The Giant Mottled Anorthosite: a transitional sequence at the top of the Upper Critical Zone of the Bushveld Complex. *South African Journal of Geology*, *105*(1), 15-24.

Molyneux T.G., 1974. A Geological investigation of the Bushveld Complex in Sekhukhuneland and part of the Steelport Valley. *The Geological Society of South Africa*. 77, 329–338.

Molyneux, T.G and Klinkert, P. S., 1978. A structural interpretation of part of the eastern mafic lobe of the Bushveld Complex and its surroundings. *Transaction of the Geological Society of South Africa*. 81, 359-368.

Mungall, J. and Brenan, J., 2014. Partitioning of platinum-group elements and Au between sulfide liquid and basalt and the origins of mantle-crust fractionation of the chalcophile elements. *Geochimica et Cosmochimica Acta*. 125, 265-289.

Mungall, J.E. and Naldrett, A.J., 2008. Ore deposits of the platinum-group elements. *Elements.* 4(4), 253-258.

Naldrett A.J., Wilson A., Kinnaird J.A., Yudovskaya M. and Chunnett G., 2012. The origin of chromitites and related PGE mineralisation in the Bushveld Complex: new mineralogical and petrological constraints. *Miner. Deposita.* 47, 209–232.

Naldrett, A.J., 2004. Magmatic sulfide deposits. Geology, geochemistry and exploration. 727.

Naldrett, A.J., 2011. Fundamentals of magmatic sulfide deposits. *Reviews in Economic Geology*. 17(1), 50.

Naldrett, A.J., and Wilson, A.H., 1990. Horizontal and vertical variations in noble-metal distribution in the Great Dyke of Zimbabwe: A model for the origin of the PGE mineralization by fractional segregation of sulfide. *Chemical Geology*. 88(3-4), 279-300.

Naldrett, A.J., Gasparrini, E.C., Barnes, S.J., Von Gruenewaldt, G. and Sharpe, M.R., 1986. The Upper Critical Zone of the Bushveld Complex and the origin of Merensky-type ores. *Economic Geology*. *81*(5), 1105-1117.

Naldrett, A.J., Wilson, A., Kinnaird, J.A. and Chunnett, G., 2009. PGE Tenor and Metal Ratios within and below the Merensky Reef, Bushveld Complex: Implications for its Genesis. *Journal of Petrology*. 50, 625-659.

Naldrett, A.J., Wilson, A., Kinnaird, J., Yudovskaya, M. and Chunnett, G., 2012. The origin of chromitites and related PGE mineralization in the Bushveld Complex: new mineralogical and petrological constraints. *Mineralium Deposita*. 47(3), 209-232.

Nex, P.A.M., 2005. The structural setting of mineralisation on Tweefontein Hill, northern limb of the Bushveld Complex, South Africa. *Applied Earth Science*, *114*(4), 243-251.

Nex, P.A.M., Kinnaird, J.A., Ingle, L.J., Van der Vyver, B.A. and Cawthorn, R.G., 1998. A new stratigraphy for the Main Zone of the Bushveld Complex, in the Rustenburg area. *South African Journal of Geology*. 101(3), 215-223.

Nex, P.A.M., Cawthorn, R.G. and Kinnaird, J.A., 2002. Geochemical effects of magma addition: compositional reversals and decoupling of trends in the Main Zone of the western Bushveld Complex. *Mineralogical Magazine.* 66, 833-856.

Nex, P.A.M., Nichol, S. and Ixer, R.A., 2008. Geological evidence for hydrothermal and supergene PGE mineralization in the footwall to the Platreef from Tweefontein Hill, South Africa [abs.]: Platreef Workshop, 3rd, Mokopane, South Africa, 11th−13th July, 2008, Abstracts.

Oosterhuis, W.R., 1998. Andalusite, sillimanite and Kyanite, pg: 53-58. In: Wilson, M. G. C. and Anhaeusser, C. R., (Eds) the mineral recourses of South Africa, handbook. *Council for Geoscience*. 740.

Pronost, J., Harris, C. and Pin, C., 2008. Relationship between footwall composition, crustal contamination and fluid-rock interaction in the Platreef, Bushveld complex, South Africa. *Miner. Deposita*. 43, 825-848.

Reid, D.L. and Basson, I.J., 2002. Iron-rich ultramafic pegmatite replacement bodies within the upper critical zone, Rustenburg layered suite, Northam platinum mine, South Africa. *Mineralogical Magazine*. 66(6), 895–914.

Reynolds, I.M., 1985. Contrasted mineralogy and textural relationships in the uppermost titaniferous magnetite layers of the Bushveld Complex in the Bierkraal area north of Rustenburg. *Economic Geology*. *80*(4), 1027-1048.

Ripley, E.M., Alawi J.A., 1988 Petrogenesis of pelitic xenoliths at the Babbitt Cu- Ni deposit, Duluth Complex, Minnesota, USA. *Lithos* 21,143–159.

Ripley, E.M., Park, Y. R., Li, C. and Naldrett, A.J., 1999. Sulfur and oxygen isotopic evidence of country rock contamination in the Voisey's Bay Ni–Cu–Co deposit, Labrador, Canada. *Lithos. 47*(1-2), 53-68.

Roelofse, F. and Ashwal, L.D., 2012. The lower main zone in the northern limb of the bushveld complex e a >1.3 km Thick sequence of Intruded and variably contaminated crystal mushes. *J. Petrol.* 53, 1449-1476.

Sagnotti, L., 2007. Sagnotti Istituto Nazionale di Geofisica e Vulcanologia. *Via di Vigna Murata*. 605 – 00143.

Schmitz, M.and Bowring S.A., 2003. Ultrahigh-temperature metamorphism in the lower crust during Neoarchean Ventersdorp rifting and magmatism, Kaapvaal Craton, southern Africa. Geological Society of America Bulletin. 115(5), 533-548.

Schweitzer, J.K., Hatton, C.J. and de Waal, S.A., 1995. Regional lithochemical stratigraphy of the Rooiberg Group, upper Transvaal Supergroup: a proposed new subdivision. *South African Journal Geology.* 98,245-255.

Scoates. J.S. and Friedmann, R.M., 2008. Precise Age of the Platiniferous Merensky Reef, Bushveld Complex, South Africa, by the U-Pb Zircon Chemical Abrasion ID-TIMS Technique. *Economic Geology*. 103, 465-471

Scoon, R.N. and Mitchell, A.A., 2012. The Upper Zone of the Bushveld Complex at Roossenekal, South Africa: geochemical stratigraphy and evidence of multiple episodes of magma replenishment. *South African Journal of Geology*. *115*(4), 515-534.

Scoon, R.N. and Mitchell, A.A., 2014. Discussion of “The Bushveld Complex, South Africa: formation of platinum–palladium, chrome-and vanadium-rich layers via hydrodynamic sorting of a mobilized cumulate slurry in a large, relatively slowly cooling, subsiding magma chamber” by Maier *et al*., (2013) Miner Deposita 48: 1–56. *Mineralium Deposita. 49*(3), 399-404.

Scoon, R.N. and Costin, G., 2018. Chemistry, Morphology and Origin of Magmatic-Reaction Chromite Stringers Associated with Anorthosite in the Upper Critical Zone at Winnaarshoek, eastern limb of the Bushveld Complex. *Journal of Petrology. 59*(8), 1551-1578.

Seabrook, C.L., Cawthorn, R.G. and Kruger, F.J., 2005. The Merensky Reef, Bushveld Complex: Mixing of minerals not mixing of magmas. *Economic Geology*. 100, 1191-1205.

Sharpe, M.R., Bahat, D. and Von Gruenewaldt, G. 1981. The concentric elliptical feeder sites to the Bushveld Complex and possible economic implications. Transactions of the Geological Society of South Africa. 84, 239–244.

Silver, P.G., Fouch, M. J., Gao, S.S., Schmitz, M. and Kaapvaal Seismic Group., 2004. Seismic anisotropy, mantle fabric and the magmatic evolution of Precambrian southern Africa. *South African Journal of Geology*. *107*(1-2), 45-58.

Smart, G.D., 2013. PGE in the Platreef: A Petrological and Geochemical Study of the Turfspruit Cyclic Unit on the Farm Turfspruit., (Unpublished MESci dissertation), Cardiff University, 163.

Smith, J.W., Holwell, D.A., McDonald, I., 2014. Precious and base metal geochemistry and mineralogy of the Grasvally norite–pyroxenite–anorthosite (GNPA) member, northern Bushveld Complex, South Africa: implications for a multistage emplacement. *Mineral Deposita*, 49, 667–692.

South African Committee on Stratigraphy (SACS), 1980. Stratigraphy of South Africa. Part 1 (Comp. L.E. Kent). Lithostratigraphy of the Republic of South Africa, South West Africa/Namibia and the Republics of Botswana, Transkei and Venda. Handb. Geol. Surv. S .Afr. 8, 690.

Stanistreet, I.G. and McCarthy, T.S., 1991. Changing tectono-sedimentary scenarios relevant to the development of the Late Archaean Witwatersrand Basin. *Journal of African Earth Sciences (and the Middle East)*. *13*(1), 65-81.

Sylvania Platinum Resources, 2016. Northern Limb Exploration Drilling Update. Found online at: www.sylvaniaplatinum.com. Date accessed: 01 April 2017.

Tankard A.J., Jackson M.P.A., Eriksson K.A., Hobday D.K., Hunter D.R., Minter W.E.L., 1982. Crustal Evolution of Southern Africa. Springer-Verlag, New York, 523.

Tanner D., Mavrogenes J.A., Arculus R.J. and Jenner F.E., 2014. Trace element stratigraphy of the Bellevue core, Northern Bushveld: multiple magma injections obscured by diffusive processes. *Journal of Petrology.* 55, 859–882.

Tegner, C., Cawthorn, R.G. and Kruger, F.J., 2006. Cyclicity in the Main and Upper zones of the Bushveld Complex, South Africa: crystallization from a zoned magma sheet. *Journal of Petrology*. *47*(11), 2257-2279.

Teigler, B. and Eales, H.V., 1996. The Lower and Critical zones of the western limb of the Bushveld Complex as intersected by the Nooitgedacht boreholes (No. 111-112). Geological Survey of South Africa, Council for Geoscience.

Truter, F.C., 1947. A remarkable transcurrent fauly near Potgietersrust, Transvaal. *South African Journal of Geology*. *50* (Transactions 1947), 1-15.

Twist, D. and French, B.M., 1983 Voluminous acid volcanism in the Bushveld Complex: A review of the Rooiberg Felsite. *Bulletin Volcanology.* 46, 225-242.

Van der Merwe M.J., 1976. The layered sequence of the Potgietersrus limb of the Bushveld Complex. *Economic Geology.* 71, 1337–1351.

Van der Merwe M.J., 1978. The geology of the basic and ultramafic rocks of the Potgietersrus limb of the Bushveld Complex., (Doctoral Thesis), University of the Witwatersrand.

Van der Merwe, M.J., 2008. The geology and structure of the Rustenburg Layered Suite in the Potgietersrus/Mokopane area of the Bushveld Complex, South Africa. *Mineralium Deposita*. *43*(4), 405-419.

Van der Merwe, F., Viljoen, F. and Knoper, M., 2012. The mineralogy and mineral associations of platinum group elements and gold in the Platreef at Zwartfontein, Akanani Project, Northern Bushveld Complex, South Africa. *Miner Petrol*. 106, 25-38.

Van Rooyen, D.P., 1954. Die geologie Van ‘n gedeelte van gebied 7 (Potgietersrus). Report. Geological Survey of South Africa, Pretoria.

Van Tongeren, J.A., Mathez, E.A., 2013. Incoming magma composition and style of recharge below the pyroxenite marker, eastern Bushveld Complex, South Africa. J Petrol. 54:1585–1605

Venmyn-Rand, 2010. Independent Technical Experts Report on the Mineral Assets of Sylvania Resources Limited – In the Form of a Competent Persons Report by Venmyn-Rand (Pty) Limited 151.

Viljoen, M. J., Theron, J., Underwood, B., Walters, B. M., Weaver, J., Peyerl, W. and Maske, S., 1986. The Amandelbult section of Rustenburg Platinum Mines Limited, with reference to the Merensky reef. *Mineral deposits of southern Africa*. *2*, 1041-1060.

Viljoen, M.J. and Schürmann, L.W., 1998. Platinum group metals. In: Wilson, M.G.C. and Anhaeusser, C.R., (eds) The Mineral Resources of Southern Africa. Council for Geosciences. 532-568.

Von Gruenewaldt G., 1979. A review of some recent concepts of the Bushveld Complex, with particular reference to sulfide mineralization. *Canada Mineral*. 17:233–256.

Von Gruenewaldt, G., 1970. On the phase change orthopyroxene-pigeonite and resulting textures in the main and upper zones of the Bushveld Complex in the eastern Transvaal. In Visser DJL, Von Gruenewaldt G (eds) Symposium on the bushveld igneous complex

and other layered intrusions. Geological Society of South Africa Special Publications. 1:67–73

Von Gruenewaldt, G., 1973. The Main and Upper zones of the Bushveld Complex in the Roossenekal area, eastern Transvaal. *Transactions of the Geological Society of South Africa*. 76, 207-227.

Von Gruenewaldt, M., Sharpe, M.R. and Hatton, C.J., 1985. The Bushveld Complex: Introduction and Review. *Economic Geology*. 80, 803-812.

Von Gruenewaldt, G. Hulbert, L. J. and Naldrett, A.J., 1989. Contrasting platinum-group element concentrations in cumulates of the Bushveld Complex. *Miner Deposita*. 24, 219-229.

Wager, L.R. and Brown, G.M., 1968. Layered igneous rocks. Oliver and Boyd, Edinburgh. 588.

Wagner, P.A., 1929. Platinum deposits and mines of South Africa: Edinburgh. *Oliver and Boyd*. 329.

Walraven, F. and Hattingh, E., 1993. Geochronology of the Nebo Granites, Bushveld Complex. *South African Journal of Geology*. 96, 31-41.

Walraven, F. and Martini, J., 1995. Zircon Pb-evaporation age determination of the Oaktree Formation, Chuniespoort Group, Transvaal Sequence: implications for Transvaal-Griqualand West basin correlations. *South African J. Geol.* 98, 58-67.

Walraven, F., 1987. Textural, geochemical and genetic aspects of the granophyric rocks of the Bushveld Complex. Memoir 72, Geological Survey South Africa.145.

Walraven, F., 1988. Notes of the age and genetic relationships of the Makhutso Granite, Bushveld Complex, South Africa. *Chemical Geology (Isotope Geoscience Section)*. 72, 17-28.

Walraven, F., Armstrong, R.A. and Kruger, F.J., 1990. A chronostratigraphic framework for the north-central Kaapvaal craton, the Bushveld Complex and the Vredefort structure. *Tectonophysics*. *171*(1-4), 23-48.

Webb, S.J., Cawthorn, R.G., Nguuri, T. and James, D., 2004. Gravity modeling of Bushveld Complex connectivity supported by Southern African seismic experiment results. *South African Journal of Geology*. *107*(1-2), 207-218.

White, J.A., 1994. The Potgietersrus prospect–geology and exploration history XVth CMMI congress. Johannesburg SAIMM. 3, 173–181.

Willemse, J., 1969. The vanadiferous magnetic iron ore of the Bushveld Igneous Complex. *Econ Geol Monogr*. 4, 137–208.

Wilson, A.H., 2012. A chill sequence to the Bushveld Complex: insight into the first stage of emplacement and implications for the parental magmas. *Journal of Petrology. 53*(6), 1123-1168.

Wilson, M.G.C. and Anhaeusser, C.R., 1998. The mineral resources of South Africa. Council for Geoscience, Handbook. 16, 740.

Woods, T., 2012. Nature and Origin of Mineralization within the Main Zone beyond the North End of the Northern Limb of the Bushveld Complex. Unpublished, Honours Research Project, University of the Witwatersrand Johannesburg, South Africa. 1-82.

Yudovskaya, M.A. and Kinnaird, J.A., 2010. Chromite in the Platreef (Bushveld Complex, South Africa): occurrence and evolution of its chemical composition. *Mineralium Deposita*. 45, 4, 369-391.

Yudovskaya, M.A., Kinnaird, J.A., Udachina, L.V., Distler, V.V. and Kuz'min, D.V., 2014. Role of magmatic and fluid concentrating in formation of platinum mineralization in the Lower Zone and Platreef as follows from composition of phlogopite, cumulus silicates and sulfide melt, the northern limb of Bushveld Complex. *Geology of Ore Deposits*. 56(6), 451-478.

Yudovskaya, M., Kinnaird, J.A., McCreesh, M.J.G. and Frei, D., 2015. The lithology at the contact between the Bushveld Mafic-Ultramafic sequence and overlying Waterberg sediments on the Waterberg: Extended Abstract Volume 6th Platreef Workshop, Mokopane 8th -10th May. 59-61.

Yudovskaya, M.A., Kinnaird, J.A., Grobler, D.F., Costin, G., Abramova, V.D., Dunnett, T. and Barnes, S.J., 2017. Zonation of Merensky-style platinum-group element mineralization in Turfspruit thick reef facies (northern limb of the Bushveld Complex). *Economic Geology*. *112*(6), 1333-1365.

Zeh, A., Ovtcharova, M., Wilson, A.H. and Schaltegger, U., 2015. The Bushveld Complex was emplaced and cooled in less than one million years–results of zirconology and geotectonic implications. *Earth and Planetary Science Letters*. 418, 103-114.

Appendices

11.1 Appendix A: in-field descriptions of core logs

The descriptions of the drillcores are directly from a field notebook, and discussions, deliberations and successive field visits resulted in some changes to interpretation. The drillcore descriptions are outlined below.

11.1.1 **Drillcore HW024**

Depth		Contacts		Rock type	Proportion of minerals	Grain size (overall)	Description of layer
From	To	Top	Bottom				
255.34	255.95		Brecciated but obvious contact	Conglomerate			Reddish, pinkish matrix. Matrix of sandstone. Feldspar altered into clay. First 10 cm is matrix supported and then becomes clast supported. No hematite clasts found. Clast sizes: 1 cm- 10 cm, with quartz clasts being largest
255.95	260.6	Brecciated but obvious contact	Transitional contact. A lot less hematite suddenly, but still present	Brecciated clay	70 % hematite	Fine	Cannot tell if this section is altered bushveld rocks or waterberg sediments. This section is also hematitised.
260.6	265.6	Transitional contact. A lot less hematite suddenly, but still present	Transitional contact	Hematitised, altered bushveld rocks			
265.6	270.1	Transitional contact	Sharp contact	Leucogabbro	15- 20 % clinopyroxene, 80-85 % plagioclase	Medium	Light coloured igneous rock.
270.1	271.5	Sharp contact	Sharp contact	Melagabbronorite		Fine	
271.5	289	Sharp contact	Transitional contact	Leucogabbro-gabbro, transitions into gabbronorite		Medium	Start seeing oikocrysts pigeonite in this section, do not confuse with shimmering clinopyroxene.
289	299.7	Transitional (no more pigeonite seen)	Sudden appearance of Olivine, rock type still similar	Melagabbronorite		Medium	No visible pigeonite seen orthopyroxene appears
299.7	301.6	Sudden appearance of Olivine, rock type still similar	Unclear contact (missing core)	Olivine gabbronorite	> 10 % olivine,	Medium	No clear change in rock type, but sudden appearance of visible olivine crystals. Olivine is black (serpentinised).
301.6	310.4	Unclear contact (missing core)	Sharp contact	Troctolite	47.5 % plagioclase, 47.5 % olivine, 5% orthopyroxene	Medium	Strong alteration below contact. Transitions into true troctolite after alteration.
310.4	310.5	Sharp contact	Sharp contact	Leucotroctolite	55 % plagioclase, 40 % olivine, 5 % orthopyroxene	Medium	Larger proportion of plagioclase than olivine.
310.5	310.6	Sharp contact	Sharp contact	Orthopyroxenite		Medium	Has 2 mm olivine crystals in this interval.
310.6	313.9	Sharp contact	Sharp/ irregular contact	Orthopyroxenite			
313.9	314	Sharp/ irregular contact	Irregular contact	Leucotroctolite	55 % plagioclase, 40 % olivine, 5 % orthopyroxene	Medium	
314	314.2	Sharp contact	Sharp contact	Orthopyroxenite			
314.2	316.8	Sharp contact	Sharp contact	Olivine melagabbronorite			Package of Olivine melagabbronorite, with vein like olivine bearing leucogabbronorite
316.8	317.3	Sharp contact	Sharp contact	Vein like Olivine bearing leucogabbronorite			
317.3	319.3	Sharp contact	Sharp contact	Olivine melagabbronorite			
319.3	319.5	Sharp contact	Sharp contact	Vein like Olivine bearing leucogabbronorite			
319.5	320.8	Sharp contact	Sharp contact	Olivine melagabbronorite			
320.8	320.9	Sharp contact	Sharp contact	Vein like Olivine bearing leucogabbronorite			
320.9	322.6	Sharp contact	Sharp contact	Olivine melagabbronorite			
322.6	322.8	Sharp contact	Sharp contact	Vein like Olivine bearing leucogabbronorite			
322.8	327.7	Sharp contact	Sharp contact	Olivine melagabbronorite			

Depth		Contacts		Rock type	Proportion of minerals	Grain size (overall)	Description of layer
From	To	Top	Bottom				
327.7	329.5	Sharp contact	Sharp contact	Troctolite	60 % plagioclase, 35% olivine, 5 % orthopyroxene		
329.5	343.1	Transitional contact	sudden appearance of sulphides	More leucocratic troctolite			More leucocratic troctolite
343.1	344.1	Sudden disappearance of sulphides.	Transitional contact	More leucocratic troctolite	0.1 % sulphides seen		Mineralised with 0.1 % sulphides
344.1	344.5	Transitional contact	Transitional contact	Phlogopite rich olivine bearing melagabbronorite			
344.5	347	Transitional contact	Sharp contact	Melagabbronorite			
347	349	Sharp contact	Sharp contact	Olivine pyroxenite	2 % sulphides, 3-5 % plagioclase, 10-15 % olivine		Altered layer, cannot see clearly. Olivine crystals are also altered.
349	355.5	Sharp contact	Transitional contact	Olivine pyroxenite with olivine melagabbronorite.	2 % sulphides (locally higher), < 10 % olivine, 1 % phlogopite (< 5% locally)		Heterogeneous mix of olivine pyroxenite with olivine melagabbronorite.
355.5	370.4	Transitional contact	Sharp contact	Heterogeneous gabbronorite		Medium	Olivine free?
370.4	370.9	Sharp contact	Sharp contact	Norite or gabbronorite		Fine	Cannot tell exact rock type as layer is too fine grained.
370.9	371.9	Sharp contact	Sharp contact	Heterogeneous gabbronorite		Medium	Heterogeneous
371.9	372.4	Sharp contact	Sharp contact	Norite or gabbronorite		Fine	
372.4	389.2	Sharp contact	Transitional contact	Heterogeneous gabbronorite		Medium	No olivine seen
389.2	392	Transitional contact	Transitional contact	Norite	20- 30 % Olivine, 30- 40 % orthopyroxene, 30- 40 % plagioclase	Medium	Transitions into norite
392	394.1	Transitional contact	Transitional contact	Gabbronorite		Medium	No olivine?
394.1	396	Transitional contact	Transitional contact	Olivine gabbronorite		Medium	
396	403	Transitional contact	Transitional contact	Gabbronorite		Medium	
403	407.2	Transitional contact	Transitional contact	Olivine gabbronorite		Medium	Olivine appears
407.2	450.1	Transitional contact		Gabbronorite	0.1 % sulphides, 0.5 % phlogopite	Medium	Olivine disappears (check polished section to confirm), transitions into "normal" gabbronorite, with some intervals being more leucocratic (50- 60% plagioclase), and some intervals being more melanocratic.

11.1.2 **Drillcore HW025**

Depth		Contacts		Rock type	Proportion of minerals	Grain size (overall)	Description of layer
From	To	Top	Bottom				
404.9	412.1		Sharp	Hematitised clay		Very fine	
412.1	419.6	Sharp	Sharp	Gabbro		Medium	Altered bushveld gabbro, gest less altered as you go down hole, clinopyroxene is also replaced by chlorite.
419.6	419.7	Sharp	Sharp	Anorthosite	60 % plagioclase, 40 % clinopyroxene	Medium	
419.7	422	Sharp	Sharp	Gabbro		Medium	Altered bushveld gabbro
422	423.1	Sharp	Sharp	Pegmatoidal vein		Coarse	Plagioclase, pyroxene, magnetite pegmatoidal vein. Highly altered.
423.1	427	Sharp	Transitional	Gabbronorite	60 % plagioclase, 40 % clinopyroxene and orthopyroxene, 0.05 % sulphides	Medium	Transitions into gabbronorite. Small specs of sulphides found.
427	448.2	Transitional	Sharp	Gabbronorite		Medium	
448.2	448.6	Transitional	Sharp	Pyroxenite	70 % orthopyroxene, 20% clinopyroxene, 2- 5 % sulphide (mainly pyrite, with chalcopyrite and possibly bornite), speckles of magnetite, < 10 % interstitial plagioclase	Medium	Pyroxenite, but some veins of gabbronorite, with not mineralization, so mineralization is controlled by lithology.
448.6	448.7	Sharp	Sharp	Melagabbronorite		Medium	Veinlike melagabbronorite, with no sulphides.
448.7	449.4	Sharp	Sharp	Pyroxenite	70 % orthopyroxene, 20% clinopyroxene, 2- 5 % sulphide (mainly pyrite, with chalcopyrite and possibly bornite), speckles of magnetite, < 10 % interstitial plagioclase	Medium	Pyroxenite, but some veins of gabbronorite, with not mineralization, so mineralization is controlled by lithology.
449.4	449.7	Sharp	Transitional but sharp	Melagabbronorite	1 % sulphides	Medium	Mineralization found over interval of around 1 %, but up to 5 % locally.
449.7	506	Transitional but sharp	Broken contact	Melagabbronorite		Medium	Same rock, but sudden stop in presence of mineralisation.
506	508	Broken contact	Broken contact	Leucogabbronorite	70- 80 % plagioclase	Medium	Bottom contact is broken, but obvious contact.
508	510.5	Broken contact	Broken contact	Olivine bearing lithology			interval is brecciated, and cannot see what rock type is.

Depth		Contacts		Rock type	Proportion of minerals	Grain size (overall)	Description of layer
From	To	Top	Bottom				
510.5	521	Broken contact	Sharp, but brecciated	Troctolite (with minor segregations of olivine norite)		Medium	0 % orthopyroxene in troctolite, but up to 50 % in some patches described locally. Some oikocrysts or segregations of olivine norite distributed irregularly throughout interval.
521	521.3	Sharp, but brecciated	Sharp	Olivine bearing orthopyroxenite		Medium	
521.3	524.3	Sharp	Brecciated	Olivine bearing leucogabbronorite	< 10 % olivine, 7- % plagioclase, 20 % pyroxenes	Medium	
524.3	556.8	Brecciated	Brecciated/ unclear	Olivine bearing leucogabbronorite	< 10 % olivine, 7- % plagioclase, 20 % pyroxenes	Medium	Almost same as above, but will call this olivine norite. Olivine seen in Orthopyroxene (not pigeonite, but orthopyroxene), Pigeonite has lamellae (post cumulus). See oikocrysts with olivine inside. Package of intercalated/ interveinded olivine norite predominately, then we have olivine gabbronorite, and small proportion of troctolite. Small feldspathic harzburgite, poikilitic, small pieces < 5 cm. All is highly altered and brecciated. Darker lithology has some pyrite sulphide, but remnants only, looks altered. 0.1- 1 %. (mostly pyrite). Sulphides look reduced due to alteration. Maybe because it is close to the HRSZ (just check location me:).
556.8	561	Brecciated/ unclear	Sharp but irregular	Feldspathic pyroxenite-melanorite	70- 80 % orthopyroxene, up to 3 % phlogopite, < 0.5 % sulphides (mostly pyrite)	Medium	Interstitial clinopyroxene and plagioclase. Plagioclase is interstitial then becomes cumulous (then name changes to melanorite).
561	575.7	Sharp but irregular	Sharp	Leucogabbronorite		Medium	Vein like contact. Interval is altered, Maybe more clinopyroxene in interval, but due to alteration, cannot see clearly.
575.7	577	Sharp	Sharp	Feldspathic pyroxenite-melanorite		Medium	Altered, with unclear transition into troctolite.
577	583.7	Sharp	Sharp but brecciated	Heterogeneous troctolite		Medium	10- 20 cm intervals of leucotroctolite.
583.7	584	Sharp but brecciated	Sharp	Gabbronorite		Medium	Typical lower zone lineation seen (orthopyroxene lineated, not plagioclase like upper zone).
584	586.5	Sharp	Brecciated	Lineated pyroxenite	0.1 % sulphides		Orthopyroxene crystals up to 1 cm.
586.5	601	Brecciated	Sharp	Olivine gabbronorite	30 % olivine	Medium (with some intervals of fine)	With intervals of leuco- and melagabbronorite (predominantly olivine gabbronorite). So medium grained with some intervals where grain size in fine.
601	607.5	Sharp		Feldspathic pyroxenite			Clear change into feldspathic pyroxenite. Interstitial plagioclase quite high, up to 15 %. Sulphides from 0.1- 2 % (pyrite and chalcopyrite). Transitions downward into melanorite or melagabbronorite (no clear boundary).

11.1.3 **Drillcore HW029**

Depth		Contacts		Rock type	Proportion of minerals	Grain size (overall)	Description of layer
From	To	Top	Bottom				
	349.2	?	Sharp	Quartz conglomerate			Poorly sorted conglomerate with clasts up to 6 cm. Medium grained matrix, matrix is red-green. Clasts are well rounded- angular. 100% of clasts are composed of quartz.
349.2	359.2	Sharp	Sharp	Bedded sediments			Bedded sediment grading from conglomerate to delta-like deposits.
359.2	362.3			Quartz conglomerate			Poorly sorted conglomerate with clasts up to 6 cm. Medium grained matrix, matrix is red-green. Clasts are well rounded- angular. 100% of clasts are composed of quartz.
362.3	362.85	Sharp	Sharp	Dolerite sill		Very fine	Very fine grained recrystallised glass. No longer glassy.
362.85	363			Quartz conglomerate			Poorly sorted conglomerate with clasts up to 6 cm. Medium grained matrix, matrix is red-green. Clasts are well rounded- angular. 100% of clasts are composed of quartz. Contains 2 cm thick layer of greenish clay
363	363.4	Sharp	Sharp	Conglomerate			Clayish matrix, pebbles up to 5 cm. Conglomerate with hematite clasts, some clasts are magnetic. Pebbles are rounded and not angular.
363.4	363.9	Sharp	Sharp	Clay			Red clay, semi lithified
363.9	365	Sharp	Transitional	Altered gabbro		Medium	Strongly- less altered bushveld gabbro (whitish-greenish in colour)
365	365.2	Transitional	Sharp	Anorthosite			Veins along sharp contact.
365.2	371.7	Sharp	Sharp	Anorthosite	90% plagioclase, 10% clinopyroxene		
371.7	372	Sharp	Sharp	Leucogabbro	80- 85 % plagioclase, 15- 20 % clinopyroxene		Looks dark, due to it being altered.
372	372.5	Sharp	Sharp	Anorthosite	90% plagioclase, 10% clinopyroxene		
372.5	381.5	Sharp	Sharp	Lineated gabbro	60 % plagioclase, 40 % clinopyroxene	Medium	Altered plagioclase dominates over clinopyroxene.
381.5	390	Sharp	Transitional	Mottled leucogabbro-Anorthosite	80- 90 % plagioclase, 10- 20% dark minerals	Medium	Mottles up to 3 cm made of magnetite, mostly cpx, and possibly some olivine and rare pigeonite oikocrysts. This interval shows alteration. Contact is transitional, but obvious.
390	411	Transitional	Sharp	Lineated gabbro	60 % plagioclase, 40 % clinopyroxene, 1 % magnetite	Medium	Typical upper zone gabbro. Cannot see pigeonite anymore. Possibly some orthopyroxene present.
411	412	Sharp	Transitional	Gabbro		Coarse	Altered plagioclase dominates over clinopyroxene.
412	433	Transitional	Transitional	Lineated gabbro		Medium	Upper zone gabbro
433	466	Transitional	Transitional	Gabbronorite	60- 70 % plagioclase, 30- 40 % dark minerals, 1-2 % magnetite	Medium	Massive magnetite bearing gabbronorite. Interstitial, mottled magnetite seen. Orthopyroxene definitely seen, grows with clinopyroxene, no pigeonite seen? Rare relics of olivine seen (sometimes olivine is surrounded by rim of orthopyroxene).
466	497	Transitional	Transitional	Olivine bearing gabbronorite		Medium	Up to 7 % gradual transition more olivine downward, up to 7 mm in size, irregular spots of olivine. Boundary is mostly controlled by plagioclase, some surrounded by orthopyroxene, probably not the first mineral formed. Plagioclase is still dominant. Magnetite 0.5- 3 %.
497	555	Transitional	Transitional	Gabbronorite		Medium	Olivine free rocks, sudden stop of olivine. 0.5-10 % magnetite (segregated small bits). Orthopyroxene and clinopyroxene are present and show lineated texture. Plagioclase also more oriented than previous layer.

Depth		Contacts		Rock type	Proportion of minerals	Grain size (overall)	Description of layer
From	To	Top	Bottom				
555	590.2	Transitional	Sharp	Gabbronorite		Medium	Still magnetic. The plagioclase appears sugar like and is fine grained. The plagioclase is interstitial, but still euhedral. POSSIBLE BOUNDARY BETWEEN MAIN ZONE AND UPPER ZONE.
590.2	591.3	Sharp	Sharp	Melagabbronorite	20 % plagioclase, < 0.2 % sulphides (pyrite)	Fine	Pinhead sized sulphides in interval.
591.3	592	Sharp	Sharp	Gabbronorite		Medium	Sugar like plagioclase present. POSSIBLE BOUNDARY BETWEEN MAIN ZONE AND UPPER ZONE?
592	593.6	Sharp	Sharp	Anorthosite	95 % plagioclase, 5 % clinopyroxene, 0.1 % sulphides (chalcopyrite)	Coarse	Pegmatoidal anorthosite, with some sulphides and interstitial clinopyroxene.
593.6	607.3	Sharp	Sharp	Olivine bearing gabbronorite			Medium grained olivine, serpentinised slightly, but locally magnetic. 2- 20 % olivine that dissipates downward, close to interval boundary, only relics are present.
607.3	609	Sharp	Sharp	Gabbronorite (pegmatoidal vein)	up to 30 %plagioclase, 65- 80 % pyroxenes, 2 % magnetite, 1 % phlogopite	Coarse	Plagioclase up to 30 %, not dominant. Pyroxenes dominate. 2 % magnetite found locally. Course grained segregations, possibly apatite (3 mm crystals). White looks like plagioclase, could be saussurised in to sugar like texture? Also phlogopite found.
609	609.8	Sharp	Sharp	leucogabbronorite		Medium	
609.8	611.2	Sharp	Sharp	Gabbronorite (pegmatoidal vein)	30 % plagioclase, 60 % pyroxenes, 5 % magnetite, 1 % phlogopite, 0.2 % sulphides, 5 grains of serpentinised olivine.	Coarse	Orthopyroxene could be confused with pigeonite, just confirm with polished section.
611.2	612.15	Sharp	Sharp	Gabbronorite		Medium	Sugar like plagioclase present.
612.15	613.11	Sharp	Sharp	Gabbronorite (pegmatoidal vein)	30 % plagioclase, 60 % pyroxenes, 5 % magnetite, 1 % phlogopite, 2 % sulphides, 5 grains of serpentinised olivine.	coarse	Same as previous, but sulphides are more prominent. 8 % sulphides at interval 612.5-612.6.
613.11	613.5	Sharp	Sharp	Gabbronorite		Medium	Normal gabbronorite
613.5	615	Sharp	Sharp	Gabbronorite (pegmatoidal vein)	30 % plagioclase, 60 % pyroxenes, can't see magnetite, 1 % phlogopite, 10 % sulphides, 3 %olivine.	Coarse	Pegmatoids same as above, but 10 % sulphides, 3 % olivine, less magnetite (not seen, but still magnetic), Inter veining with gabbronorite (same as above), It is not clear if is a vertical or sub-vertical contact, or if it's true intercalation. So could be same vein as above? Or it could be higher.
615	615.6	Sharp	Transitional	Gabbronorite	50 % plagioclase, 45 % pyroxenes, 5 % sulphides	Medium	Sugar like plagioclase seen, sulphides small disseminated and interstitial.
615.6	632.2	Transitional	Transitional	Gabbronorite		Medium	Same as above, but no sulphides seen.
632.2	638.1	Transitional	Transitional but sharp	Melagabbronorite		Medium-fine	Sulphide rich (chalcopyrite and pyrrhotite seen), Less plag (20 %), just a bit finer than medium grained. CHECK PAPER FOR EXACT GRADES.
638.1	670	Transitional but sharp	Sharp	Gabbronorite		Medium	
670	709.2	Sharp	Sharp	Xenolith			Xenolith (from quartzite to calc silicate), so quartz rich hornfels and calc silicate.
709.2	724.6	Sharp		Gabbro		Medium	Normal gabbro

11.2 Appendix B: petrography table

Sample name	From (m)	to (m)	Grain size	Texture	Alteration Type	Alteration Intensity	Comments	Modal mineralogy	Abun-dance	Rock name
HW024/ 268.2	268.2	268.5	Medium	Inequigranular (subophitic). Euhedral early cpx, opx and pigeonite, late interstitial plagioclase	Plagioclase saussuritised and sericitised	Moderate	Carlsbad and albite twinning in plagioclase. Some twins are stressed (Polysynthetic deformation twins). Ca rich exsolution lamellae in cpx. Sugar like plag sporadically present.	Orthopyroxene Clinopyroxene Plagioclase Magnetite Inverted pigeonite phlogopite Chlorite	6 20 67 2 5 < 1 < 1	Leucogabbro
HW024/2 81	281.1	281.3	Medium	Inequigranular (subophitic). Euhedral plagioclase laths with cpx growing around them and later opx. Some minor cpx also enclosed in	Plagioclase saussuritised and sericitised	Moderate-High	Carlsbad and albite twinning in plagioclase. Some twins are stressed (Polysynthetic deformation twins). Ca rich exsolution lamellae in cpx. Granular plag sporadically present.	Clinopyroxene Pigeonite Plagioclase phlogopite Magnetite Sulphides Chlorite Orthopyroxene	20 10 65 < 1 < 1 < 1 1 <8	Leucogabbro-gabbro, transitions into gabbronorite
HW024/ 297.8	297.8	298	Medium	Inequigranular (subophitic). Plag formed around cpx and opx. Euhedral olivine found in cpx and opx and plag.	Plagioclase saussuritised and sericitised. Some cpx chloritised. Olivine serpentinised.	High	Carlsbad and albite twinning in plagioclase. Some twins are stressed (Polysynthetic deformation twins). Granular plag sporadically present.	Orthopyroxene Clinopyroxene Plagioclase Olivine Inverted pigeonite phlogopite Chlorite	30 25 35 3 5 < 1 2	Melagabbronorite
HW024/ 306	306	306.2	Medium	Cumulus	Plagioclase intensely saussuritised and sericitised. Some cpx chloritised. Olivine serpentinised. highly Serpentinised	High	Minor magnetite and sulphide grains sporadically throughout plag and ol. Carlsbad and albite twinning in plagioclase. Ilmenite symplectites seen. Also orthopyroxene rims seen around certain olivines.	Orthopyroxene Plagioclase Olivine Magnetite Sulphides Ilmenite	5 47 47 1 < 1 1	Troctolite
HW024/ 314.5	314.5	314.7	Medium to coarse	Plagioclase and olivine found in opx and cpx.	Olivine moderately serpentinised, plag weakly altered, opx moderately altered.	Low	Carlsbad and albite twinning in plagioclase.	Orthopyroxene Clinopyroxene Plagioclase Olivine Pigeonite phologopite Magnetite Sulphides Chlorite	35 10 30 18 5 < 1 < 1 < 1 < 1	Olivine melagabbronorite
HW024/ 319.2	319.2	319.5	Medium	Inequigranular (subophitic). Plag is eu- to anhedral in shape. Cpx and opx form around plag.	Cpx and opx moderately altered, plag, weakly to moderately altered. Olivine serpentinised	Weak-Moderate	Granulated plag grains abundantly found throughout. Carlsbad and albite twinning in plagioclase.	Orthopyroxene Clinopyroxene Plagioclase Olivine phlogopite Chlorite	23 5 70 2 < 1 < 1	Olivine bearing Leucogabbronorite
HW024/ 332.65	332.7	332.9	Medium to coarse	Cumulus. Olivine is euhedral, plag sub to anhedral	Olivine moderately serpentinised, plag weakly altered, opx moderately altered.	Moderate	Some granulated plag found within interstitial plag. Carlsbad and albite twinning in plagioclase.	Orthopyroxene Clinopyroxene Plagioclase Olivine	7 3 50 40	Olivine gabbronorite to olivine feldspathic pyroxenite

Sample	From	to (m)	Grain size	Texture	Alteration Type	Alteration	Comments	Modal mineralogy	Abun-	Rock name
HW024/ 347.9	347.9	348.1	Medium to coarse	Inequigranular (subophitic). Plag is sub- to anhedral in shape and forms around olivine and pyroxenes. Cpx found in opx.	Olivine moderately-highly serpentinised. Opx chloritised/ moderately altered overall. Plag moderately altered.	Moderate	Granulated plag grains found in interstitial plag. Carlsbad and albite twinning in plagioclase. Sulphides found within and interstitial to opx and olivine.	Orthopyroxene Clinopyroxene Plagioclase Olivine Sulphides Chlorite Spinel	40 12 15 25 3 5 <1	Olivine gabbronorite to olivine feldspathic pyroxenite
HW024/ 348.4	348.4	348.5	Medium to coarse	Inequigranular (subophitic). Plag is sub- to anhedral in shape and forms around olivine and pyroxenes. Cpx found in opx.	Olivine moderately-highly serpentinised. Opx chloritised/ moderately altered overall. Plag moderately altered.	Moderate	Granulated plag grains found in interstitial plag. Carlsbad and albite twinning in plagioclase. Sulphides found within and interstitial to opx and olivine.	Orthopyroxene Clinopyroxene Plagioclase Olivine Sulphides Chlorite	50 12 10 15 8 5	Olivine gabbronorite to olivine feldspathic pyroxenite
HW024/ 353.45	353.5	353.6	Medium to coarse	Olivine is cumulus. Opx present in cpx, plag is interstitial.	Olivine moderately serpentinised. Opx chloritised/ moderately-highly altered overall. Plag moderately altered.	Moderate	Sulphides found within plagioclase. Phlogopite found adjacent to opx. Cpx shows exsolution.	Orthopyroxene Clinopyroxene Plagioclase Olivine Sulphides Chlorite	40 20 10 15 10 5	Olivine pyroxenite with olivine melagabbronorite.
HW024/ 360.75	360.8	361	Medium	Olivine is cumulus. Opx in cpx, plag interstitial.	Olivine moderately-highly serpentinised. Opx chloritised/ moderately-highly altered overall. Plag moderately	Moderate	Sulphides found within plagioclase. Granulated plag found within interstitial plag.	Orthopyroxene Clinopyroxene Plagioclase Olivine Inverted pigeonite phlogopite Sulphides Chlorite	20 20 40 10 5 < 1 < 1 5	Heterogeneous gabbronorite
HW024/ 391.2	391.2	391.4	Medium	Inequigranular (subophitic). Plag is sub- to anhedral in shape and forms around olivine and pyroxenes. Cpx found in opx. Opx sub- euhedral.	Olivine is serpentinised, opx is chloritised, cpx shows some exsolution.	Moderate	Granulated plag found within interstitial plag.	Orthopyroxene Clinopyroxene Plagioclase Olivine Inverted pigeonite phlogopite Chlorite	45 20 15 10 5 < 1 5	olivine orthopyroxenite or olivine melanorite
HW024/ 439.6	439.6	439.8	Medium	Inequigranular (subophitic). Plag is sub- euhedral in shape and is found within cpx and opx.	Serpentinised	Moderate	Olivine relics seen? Granulated plag seen throughout slide.	Orthopyroxene Clinopyroxene Plagioclase Inverted pigeonite Magnetite	25 15 45 5 5	Gabbronorite
HW025/ 602.1	602.1	602.5	Medium	Inequigranular. Olivine is cumulus, opx and cpx also found in plag. Some plag also found in cpx.	Cpx and opx locally highly altered (chloritised). Olivine is serpentinised.	Moderate to High locally	Sulphides present interstitially mainly between dark minerals. Granulated plag found throughout.	Orthopyroxene Clinopyroxene Plagioclase Olivine phlogopite Sulphides Chlorite	12 27 30 23 1 2 5	Olivine gabbronorite

Sample	From	to (m)	Grain size	Texture	Alteration Type	Alteration	Comments	Modal mineralogy	Abun-	Rock name
HW029/ 378.5	378.5	378.6	Medium	Inequigranular	Opx is chloritized, some cpx altered to pigeonite	Moderate-intermedia te	Inverted pigeonite present. Pyroxenes occur in a linear pattern.	Clinopyroxene Orthopyroxene Plagioclase Inverted pigeonite Magnetite	20 15 55 10 < 1	Lineated gabbro
HW029/ 389.4	389.4	389.7	Medium	Inequigranular. Magnetite grows interstitially to plag and cpx. Plag is lathlike and euhedral to subhedral. Magnetite and cpx are anhedral and	Plagioclase sericitised, cpx chloritised.	Low alteration intensity.	Some sulphide grains seen in plagioclase.	Clinopyroxene Plagioclase phlogopite Magnetite Chlorite	5 80 < 1 15 < 1	Mottled leucogabbro-Anorthosite
HW029/ 421.45	421.5	421.6	Medium	Equigranular. Plag found in pigeonite, some parts plag is in cpx and opx, some parts cpx and opx is in plag.	Saussuritised plagioclase,	Weak	Blebby exsolution in pigeonite seen	Orthopyroxene Clinopyroxene Plagioclase Inverted pigeonite phlogopite Chlorite	13 17 60 10 < 1 < 1	Lineated gabbro
HW029/ 457.8	457.8	458.2	Medium	Inequigranular. Plag found in cpx, opx and pigeonite. Plag is eu to subhedral, cpx, opx and pigeonite is anhedral to subhedral.	Plagioclase weakly saussuritised and sericitised. Some cpx altered moderately to phlogopite.	weak	Interstitial Magnetite. Pigeonite oikocryst present. Mainly laminar exsolution in pigeonite, with some blebby exsolution. Magnetite interstitial to plag, and some small grains of magnetite found in dark minerals. Granular plag found throughout plag. Pigeonite	Orthopyroxene Clinopyroxene Plagioclase Inverted pigeonite phlogopite Magnetite	5 10 60 15 < 1 10	Gabbronorite
HW029/ 470.2	470.2	470.5	Medium	Inequigranular. Dark minerals grow in plag, and plag grows in dark minerals. Magnetite fills cracks in all minerals.	Some opx is chloritised, magnetite grows dendritically between phlogopite. Cpx highly altered and olivine highly altered,	Moderate overall	Magnetite dendrites seen. Also large phlogopite crystals seen. Olivine relics present which seem to be filled with cpx or plag.	Clinopyroxene Orthopyroxene Plagioclase Olivine Magnetite Phlogopite	18 5 65 < 1 3 9	Olivine bearing gabbronorite
HW029/ 516	516		Medium	Inequigranular. Cpx found in plag, plag found in opx.	low to moderate alteration of opx, plag and cpx locally. Some chloritisation of cpx and opx, some sericitisation and saussuritisation	Low to Moderate	Decrease in Magnetite content. Small specs seen within cpx and opx mainly. White granular plagioclase seen. Cpx grown in olivine relic.	Orthopyroxene Clinopyroxene Plagioclase phlogopite Magnetite Sulphides Chlorite	9 15 75 < 1 1 < 1 < 1	Leucogabbronorite
HW029/ 559.7	559.7	559.9	Medium	Equigranular. Opx, Cpx and plag are similar size. Cpx and opx grains are eu to subhedral, plag is subhedral to anhedral.	Saussuritisation of plag.	Weak	Minor magnetite grown interstitially to plag and dark minerals. Some granulated plag seen throughout.	Orthopyroxene Clinopyroxene Plagioclase Inverted pigeonite Magnetite Phlogopite	12 15 65 8 < 1 < 1	Gabbronorite

Sample	From	to (m)	Grain size	Texture	Alteration Type	Alteration	Comments	Modal mineralogy	Abun-	Rock name
HW029/ 586.8	586.8	587.1	Medium	Equigranular. Opx, Cpx and plag are similar size. Cpx and opx grains are anhedral to subhedral, plag is subhedral to euhedral. Plag in cpx (mostly), with	Saussuritisation of plag. Minor chloritisation of cpx.	Weak	Poikilitic pigeonite seen.	Orthopyroxene Clinopyroxene Plagioclase Inverted pigeonite	10 40 40 10	Gabbronorite
HW029/ 593.2	593.2	593.5	moderate	Recrystallized mottled plagioclase	Chloritised	Moderate	Mylonitic in places	Clinopyroxene Plagioclase Sulphides Chlorite	3 90 2 5	Anorthosite
HW029/ 608.1	608.1		Coarse	Pegmatitic	Some chloritisation, of pyroxenes. Weak saussuritisation and sericitisation.	Weak	Pigeonite present (oikocrytstic). Sulphides interstitially present and fill up cracks between either mineral grains.	Orthopyroxene Clinopyroxene Plagioclase Inverted pigeonite Phlogopite Magnetite Sulphides Chlorite	20 48 20 10 < 1 1 1 < 1	melagabbronorite (pegmatoidal vein)
HW029/ 614.25	614.3	614.4	Coarse	Pegmatitic	Some chloritisation, of pyroxenes. Weak saussuritisation and sericitisation. Minor serpentine seen	Weak	Pigeonite present (oikocrytstic). Sulphides interstitially present and fill up cracks between all mineral grains.	Orthopyroxene Clinopyroxene Plagioclase Chlorite Inverted pigeonite phlogopite Hornblende Sulphides Phlogopite	10 12 58 5 5 1 2 5 2	Gabbronorite (pegmatoidal vein)
HW029/ 614.8	614.8		Coarse	Pegmatitic. Plag seen in cpx, cpx seen in opx.	Some chloritisation, of pyroxenes. Weak saussuritisation and sericitisation. Minor serpentine seen.	Weak	Pigeonite present (oikocrytstic). Large sulphides interstitially present and fill up cracks between all mineral grains, mostly pyroxenes.	Orthopyroxene Clinopyroxene Plagioclase Inverted pigeonite phlogopite Sulphides Chlorite	23 40 15 8 1 10 3	Gabbronorite (pegmatoidal vein)
HW029/ 634.7	634.7	634.9	Medium	Equigranular. Plag in opx, not in cpx. Plag lathlike and sub to euhedral. Cpx subhedral, opx anhedral.	Some chloritisation, of pyroxenes. Weak saussuritisation and sericitisation. Minor serpentine seen.	weak	Disseminated sulphides interstitially to all minerals. Granular plagioclase present throughout. Possible olivine relics. Minor phlogopite in opx.	Orthopyroxene Clinopyroxene Plagioclase Inverted pigeonite phlogopite Sulphides Chlorite	17 12 60 5 < 1 6 < 1	gabbronorite / melagabbronorite
HW029/ 635.2	635.2	635.5	Medium	Equigranular. Plag in cpx, cpx in opx. . Plag lathlike and sub to euhedral. Cpx subhedral, opx anhedral.	Some chloritisation, of pyroxenes. Weak saussuritisation and sericitisation.	weak to Moderate	Disseminated sulphides interstitially to all minerals. Granular plagioclase present throughout. Possible olivine relics. Minor phlogopite in opx.	Orthopyroxene Clinopyroxene Plagioclase phlogopite Sulphides Chlorite	25 15 50 1 4 5	Melagabbronorite

Sample	From	to (m)	Grain size	Texture	Alteration Type	Alteration	Comments	Modal mineralogy	Abun-	Rock name
HW029/ 637.8	637.8	638	pegmatoidal	Pegmatitic. Plag seen in cpx and opx, cpx seen in opx.	Some chloritisation, of pyroxenes. Weak to moderate saussuritisation and sericitisation. Minor serpentine seen.	Moderate	Pigeonite present (oikocrytstic). Large sulphides interstitially present and fill up cracks between all mineral grains, mostly pyroxenes. Sulphides seem to digest surrounding plag locally. Opx shows high laminar exsolution.	Orthopyroxene Clinopyroxene Plagioclase Inverted pigeonite phlogopite Chlorite	15 40 30 10 1 4	Melagabbronorite (pegmatic)
HW029/ 651.9	651.9	652.2	Medium	Inequigranular. Opx and pigeonite in cpx. Cpx, opx and pigeonite are seen in plag. Most grains are and hedral to subhedral with some opx and pigeonite grains	saussuritisation of plag. Minor chloritisation of cpx and opx.	Weak	Poikilitic pigeonite seen.	Orthopyroxene Clinopyroxene Plagioclase Inverted pigeonite phlogopite Chlorite	10 20 60 10 < 1 < 1	Gabbronorite
HW030/ 440.4	440.4	440.5	Medium	Inequigranular or blebby	Chloritisation of cpx. Plag low alteration.	Low to Moderate	Sulphides ingested cpx host. Minor phlogopite seen. Blebs of magnetite seen interstitially to plag and cpx.	Magnetite Clinopyroxene Sulphides Plagioclase Phlogopite	20 15 3 62 1	Magnetite gabbro?
HW030/ 445.7	445.7		massive	Massive			Thin veins of plag and cpx cross cutting magnetite. Seems to form part of a magnetitite layer.	Magnetite Clinopyroxene Plagioclase	98 1 1	Magnetitite

Thin sections (XPL), picture of samples and Picture of slides as part of petrography table.

Sample name	Thin section cross polars	Picture of sample	Picture of slide
HW024/ 268.2	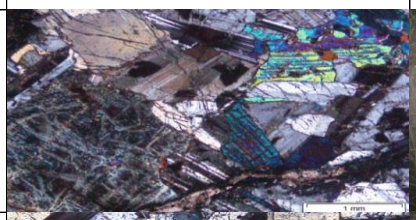	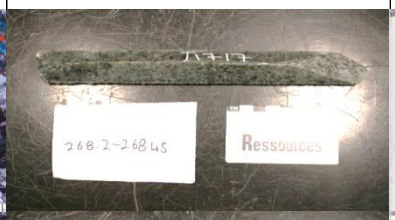	
HW024/ 281			
HW024/ 297.8	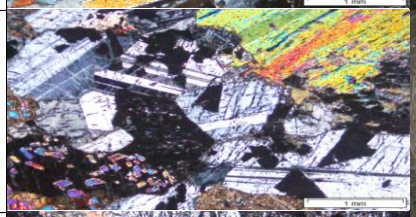		
HW024/ 306	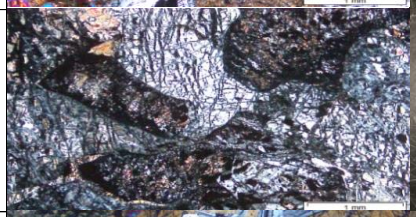		
HW024/ 314.5	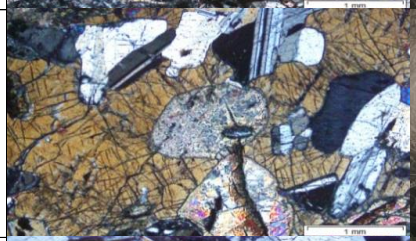	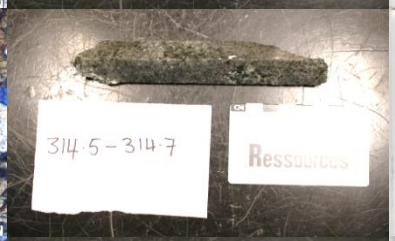	
HW024/ 319.2	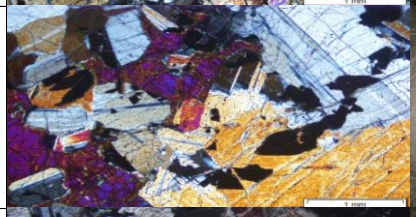	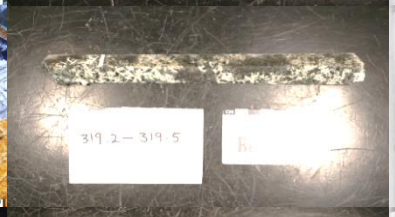	
HW024/ 332.65	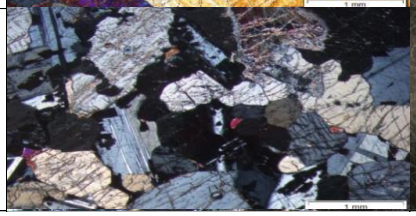		

Sample name	Thin section cross polars	Picture of sample	Picture of slide
HW024/ 347.9	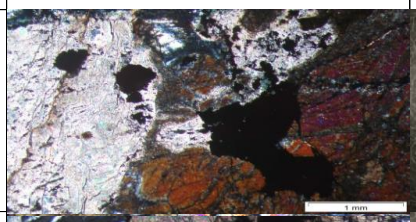	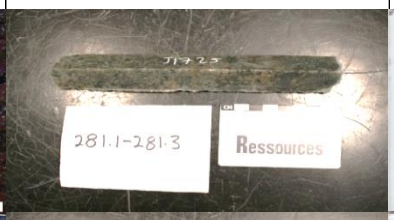	
HW024/ 348.4	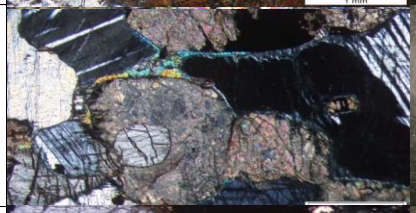		
HW024/ 353.45			
HW024/ 360.75			
HW024/ 391.2	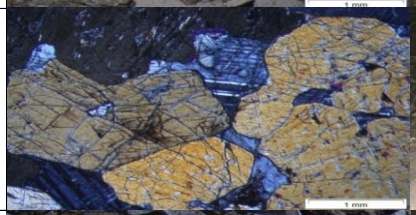		
HW024/ 439.6			
HW025/ 602.1	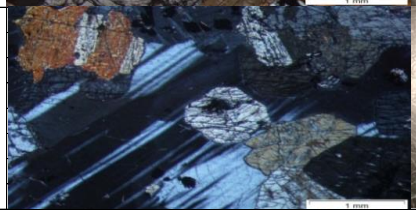	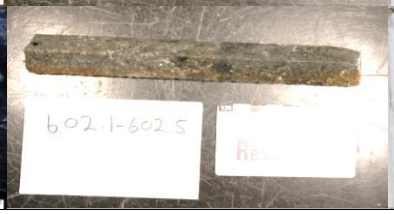	

Sample name	Thin section cross polars	Picture of sample	Picture of slide
HW029/ 586.8	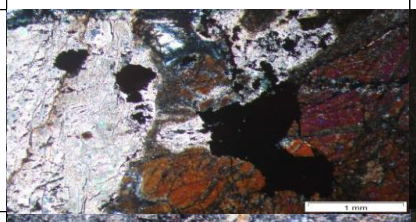		
HW029/ 593.2	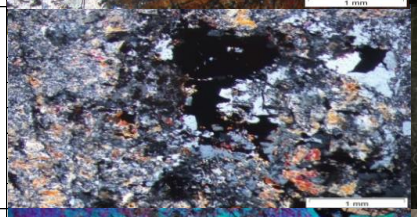	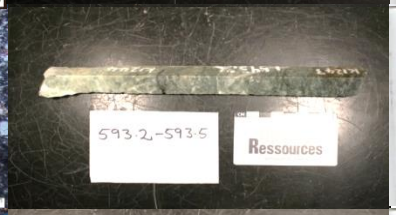	
HW029/ 608.1	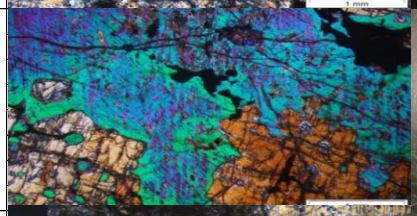		
HW029/ 614.25	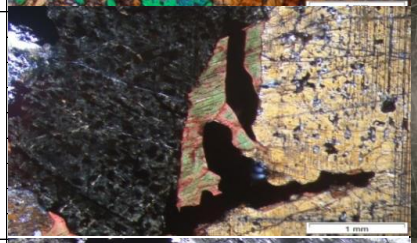		
HW029/ 614.8			
HW029/ 634.7	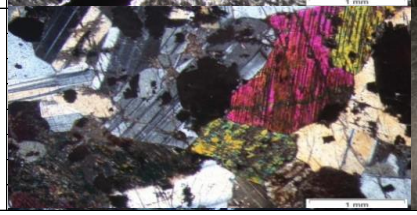		

Sample name	Thin section cross polars	Picture of sample	Picture of slide
HW029/ 635.2	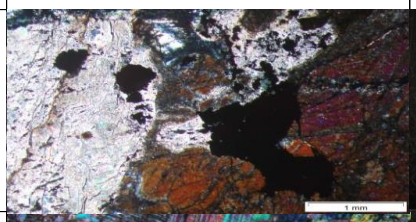		
HW029/ 637.8	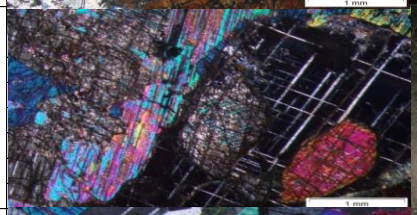		
HW029/ 651.9	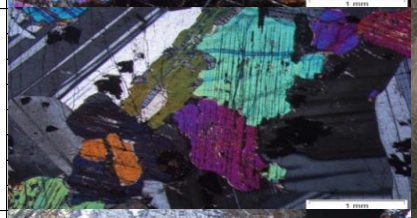		
HW030/ 440.4	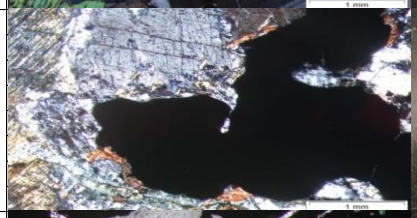		
HW030/ 445.7	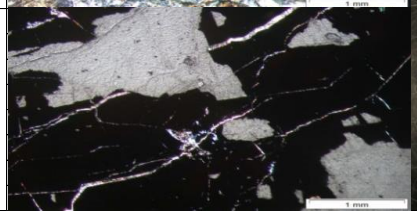		

11.3 Appendix C: major elements XRF

Sample #	SiO_2	TiO_2	$Al2O_3$	Fe_2O_3	FeO	MnO	MgO	CaO	Na_2O	K_2O	P_2O5	NiO	$Cr2O_3$	Total
HW29/371.3	51.43	0.22	25.27	0.64	5.15	0.15	5.19	8.14	3.84	0.42	0.02	0.01	0.02	100.50
HW29/378.5	51.47	0.39	18.17	1.15	9.18	0.17	7.03	10.71	2.32	0.15	0.02	0.02	0.04	100.83
HW29/383.15	51.14	0.30	16.61	1.19	9.50	0.21	8.13	10.57	2.10	0.15	0.02	0.02	0.04	99.99
HW29/389.4	51.68	0.14	22.03	0.69	5.52	0.10	5.12	12.16	2.87	0.16	0.02	0.01	0.03	100.54
HW29/394.5	51.95	0.13	24.12	0.53	4.21	0.08	2.91	12.94	2.89	0.18	0.02	0.01	0.03	100.00
HW29/397.02	50.84	0.28	16.15	1.19	9.51	0.20	8.33	11.26	2.01	0.14	0.02	0.02	0.04	99.99
HW29/405.3	50.97	0.28	17.56	1.03	8.26	0.17	7.04	12.20	2.24	0.16	0.02	0.02	0.04	100.01
HW29/421.4	51.18	0.20	18.67	0.98	7.87	0.16	6.93	11.46	2.34	0.15	0.02	0.02	0.04	100.01
HW29/421.45	51.64	0.22	17.36	1.05	8.41	0.17	7.53	12.04	2.13	0.14	0.02	0.02	0.04	100.78
HW29/447.9	51.14	0.15	24.71	0.52	4.15	0.07	3.34	12.62	2.96	0.27	0.02	0.01	0.02	100.00
HW29/457.8	48.73	0.91	22.11	1.08	8.67	0.15	4.60	11.81	2.48	0.22	0.02	0.02	0.02	100.82
HW29/457.8	48.97	0.57	20.67	1.13	9.01	0.16	5.69	11.25	2.28	0.20	0.02	0.02	0.02	100.00
HW29/462.38	51.02	0.15	23.19	0.62	4.96	0.10	4.19	12.65	2.82	0.22	0.04	0.01	0.02	100.00
HW29/469.1	49.58	0.20	22.33	0.81	6.52	0.11	4.89	12.93	2.34	0.23	0.02	0.02	0.03	100.01
HW29/470.2	49.94	0.29	21.89	0.88	7.04	0.14	5.31	12.66	2.27	0.17	0.02	0.03	0.01	100.66
HW29/487.2	48.57	0.18	22.40	0.99	7.96	0.11	5.14	11.96	2.42	0.20	0.02	0.03	0.02	100.00
HW29/505.57	50.50	0.24	21.22	0.81	6.49	0.12	5.46	12.61	2.30	0.17	0.02	0.02	0.04	100.01
HW29/515.8	50.61	0.23	20.01	0.90	7.16	0.13	6.16	12.31	2.23	0.19	0.02	0.02	0.04	100.01
HW29/516	50.75	0.26	19.56	0.95	7.59	0.15	6.45	12.16	2.58	0.20	0.03	0.02	0.04	100.73
HW29/526.45	50.98	0.24	18.01	1.02	8.13	0.15	7.29	11.84	2.07	0.20	0.02	0.02	0.05	100.02
HW29/559.7	51.64	0.21	15.63	1.24	9.94	0.19	10.61	9.49	1.71	0.14	0.02	0.03	0.05	100.91
HW29/576.3	50.75	0.22	11.52	1.56	12.46	0.24	14.09	7.65	1.23	0.10	0.02	0.07	0.07	99.99
HW29/584.4	49.93	0.17	17.94	0.86	6.88	0.13	9.72	12.49	1.48	0.26	0.02	0.04	0.07	100.01
HW29/586.8	52.13	0.23	8.83	1.57	12.56	0.25	17.27	7.12	0.90	0.10	0.02	0.06	0.09	101.12
HW29/589.8	48.46	0.13	11.98	1.36	10.85	0.18	17.49	8.26	1.05	0.09	0.02	0.08	0.05	100.00
HW29/591.1	50.14	0.20	17.95	0.89	7.08	0.14	9.83	11.85	1.66	0.15	0.02	0.03	0.07	100.02
HW29/593.2	45.58	0.30	22.12	0.35	2.84	0.05	1.77	27.20	0.00	0.00	0.02	0.03	0.01	100.29
HW29/595.35	51.19	0.23	12.31	1.45	11.56	0.22	13.15	8.26	1.34	0.17	0.03	0.04	0.06	100.00
HW29/601.35	44.45	0.11	10.05	1.75	14.01	0.21	21.48	6.73	0.95	0.08	0.02	0.12	0.03	99.99
HW29/608.1	48.39	1.91	13.72	1.46	11.70	0.26	7.85	13.21	1.90	0.20	0.36	0.05	0.02	101.05
HW29/608.25	50.46	0.44	13.85	1.42	11.33	0.24	9.31	10.65	2.00	0.24	0.03	0.03	0.02	100.01
HW29/608.59	50.85	0.37	15.67	1.38	11.02	0.23	8.77	9.08	2.20	0.33	0.04	0.03	0.02	100.00
HW29/614.05	50.11	0.32	18.15	1.12	8.99	0.13	5.41	12.58	2.35	0.24	0.27	0.31	0.02	99.98
HW29/614.25	51.99	0.24	11.82	1.44	11.53	0.24	14.37	8.02	1.15	0.10	0.02	0.08	0.04	101.04
HW29/614.7	50.71	0.28	8.22	1.69	13.55	0.25	16.67	7.61	0.75	0.12	0.02	0.08	0.05	100.00
HW29/614.8	49.41	0.26	14.00	1.69	13.49	0.20	10.61	9.56	1.43	0.26	0.09	0.16	0.02	101.17
HW29/622.49	51.21	0.18	17.29	0.83	6.67	0.14	8.94	12.62	1.91	0.14	0.02	0.03	0.02	100.02
HW29/625.4	51.45	0.22	12.68	1.09	8.72	0.20	12.17	11.93	1.36	0.11	0.02	0.04	0.03	100.02
HW29/634.5	49.68	0.14	18.34	1.09	8.69	0.15	7.61	11.81	1.98	0.16	0.02	0.32	0.02	100.01
HW29/634.7	49.76	0.15	18.17	1.16	9.29	0.14	7.73	11.93	1.98	0.15	0.01	0.35	0.01	100.85
HW29/635.2	50.02	0.14	19.04	1.10	8.77	0.14	7.37	11.50	2.26	0.15	0.01	0.29	0.02	100.82
HW29/636.78	51.39	0.19	13.07	1.23	9.82	0.21	11.97	10.46	1.46	0.11	0.02	0.04	0.02	99.99
HW29/637.8	50.95	0.25	13.70	1.42	11.40	0.20	10.33	10.89	1.57	0.13	0.02	0.15	0.02	101.03
HW29/651.9	51.93	0.25	8.82	1.41	11.31	0.25	14.33	11.65	0.89	0.06	0.02	0.04	0.04	101.01
HW29/653.3	51.22	0.19	11.04	1.25	10.03	0.22	13.04	11.72	1.13	0.08	0.01	0.03	0.04	100.00
HW29/659.25	50.90	0.23	17.11	0.94	7.51	0.15	8.26	12.77	1.89	0.15	0.02	0.02	0.03	100.00
HW29/680	43.44	0.08	9.38	0.92	7.34	0.22	11.48	27.05	0.00	0.01	0.01	0.01	0.03	99.99
HW29/695	44.08	0.07	7.13	0.84	6.72	0.20	14.80	26.10	0.01	0.01	0.01	0.01	0.01	100.01
HW29/716	50.28	0.14	24.82	0.58	4.64	0.08	3.89	12.72	2.58	0.23	0.02	0.01	0.02	100.02
HW29/721.3	50.65	0.16	21.43	0.69	5.54	0.11	5.84	13.14	2.22	0.18	0.02	0.01	0.02	100.01
HW30/440.4	27.63	6.46	15.59	4.40	35.20	0.35	2.87	6.80	1.45	0.13	0.01	0.10	1.24	102.24
HW25/417.5	50.43	0.12	22.09	0.58	4.60	0.11	5.19	14.72	1.95	0.11	0.02	0.02	0.05	100.00
HW25/426.3	50.16	0.12	22.01	0.75	5.98	0.11	6.34	12.24	2.03	0.17	0.02	0.02	0.04	99.99
HW25/433.53	50.44	0.13	20.10	0.74	5.92	0.13	7.94	12.53	1.85	0.14	0.02	0.02	0.05	100.01
HW25/440.9	50.65	0.12	19.68	0.76	6.08	0.12	8.07	11.92	2.27	0.22	0.02	0.02	0.05	99.99
HW25/449.2	50.70	0.25	9.22	1.79	14.34	0.26	13.52	8.53	1.17	0.08	0.01	0.08	0.04	99.99
HW25/454.3	50.71	0.13	18.62	0.81	6.47	0.14	9.06	12.12	1.72	0.11	0.02	0.02	0.07	100.00
HW25/462.7	50.23	0.11	22.90	0.55	4.37	0.10	5.89	13.56	2.09	0.13	0.01	0.01	0.04	99.99
HW25/472.8	50.93	0.19	15.38	0.96	7.68	0.14	9.54	13.34	1.42	0.29	0.02	0.02	0.07	99.98

Sample #	SiO_2	TiO_2	$Al2O_3$	Fe_2O_3	FeO	MnO	MgO	CaO	Na_2O	K_2O	P_2O5	NiO	$Cr2O_3$	Total
HW25/479.71	50.54	0.22	16.68	0.81	6.47	0.16	8.13	14.17	2.42	0.28	0.02	0.02	0.07	100.01
HW25/480.3	51.31	0.14	18.66	0.64	5.09	0.14	8.23	12.36	2.92	0.40	0.02	0.02	0.07	99.99
HW25/493.53	50.76	0.16	17.49	0.73	5.85	0.13	9.26	13.79	1.57	0.15	0.02	0.02	0.08	100.02
HW25/497.6	49.96	0.12	20.07	0.68	5.44	0.12	8.64	12.68	1.85	0.33	0.02	0.02	0.07	100.00
HW25/503.49	46.29	0.06	18.76	0.87	6.95	0.13	15.76	10.15	0.74	0.11	0.02	0.10	0.09	100.02
HW25/512.5	50.16	0.11	17.34	0.78	6.25	0.13	11.17	11.71	1.90	0.24	0.02	0.03	0.13	99.99
HW25/516.2	50.06	0.06	14.11	0.99	7.88	0.15	18.43	7.34	0.68	0.05	0.01	0.11	0.14	100.00
HW25/520.14	48.87	0.08	22.47	0.48	3.85	0.08	8.06	14.33	1.52	0.10	0.01	0.04	0.10	100.00
HW25/522.3	48.22	0.07	21.51	0.61	4.90	0.10	9.21	13.60	1.45	0.19	0.01	0.04	0.07	100.00
HW25/535.1	45.31	0.05	19.12	0.63	5.01	0.11	10.05	19.26	0.31	0.02	0.01	0.04	0.06	100.00
HW25/545.5	53.30	0.14	10.88	1.11	8.86	0.16	17.62	6.64	1.01	0.08	0.02	0.08	0.11	100.01
HW25/570.5	42.95	0.08	10.74	1.73	13.83	0.23	26.29	3.76	0.11	0.04	0.02	0.18	0.03	100.01
HW25/577.28	46.61	0.10	12.41	1.44	11.54	0.17	18.50	7.90	0.99	0.16	0.02	0.13	0.04	100.01
HW25/591.56	48.84	0.09	8.30	1.45	11.63	0.19	21.93	6.84	0.33	0.16	0.02	0.18	0.05	100.01
HW25/600.5	51.14	0.14	19.70	0.74	5.88	0.11	9.63	10.10	2.14	0.28	0.02	0.05	0.05	100.00
HW25/602.1	52.15	0.19	15.75	0.96	7.67	0.15	12.59	9.15	1.80	0.15	0.02	0.07	0.07	100.71
HW25/602.6	51.16	0.19	8.05	1.51	12.11	0.21	19.75	5.76	0.71	0.17	0.02	0.24	0.11	100.00
HW24/268.2	50.43	0.12	22.44	0.55	4.43	0.11	6.02	13.27	2.33	0.20	0.02	0.01	0.05	100.00
HW24/268.2	50.76	0.14	21.05	0.63	5.05	0.13	6.55	13.72	2.23	0.14	0.02	0.02	0.05	100.50
HW24/275.9	50.72	0.14	21.25	0.48	3.87	0.11	6.01	13.96	2.17	0.16	0.02	0.02	0.04	98.97
HW24/276.5	50.74	0.12	21.83	1.31	10.48	0.11	6.55	12.65	2.10	0.16	0.02	0.01	0.04	106.11
HW24/281.1	50.19	0.15	23.55	0.49	3.91	0.10	4.49	14.71	2.48	0.24	0.02	0.01	0.02	100.36
HW24/290.45	50.73	0.14	19.94	0.84	6.69	0.11	7.02	14.31	1.89	0.14	0.02	0.02	0.05	101.90
HW24/297	50.68	0.19	15.20	0.66	5.24	0.16	10.13	13.47	1.56	0.11	0.02	0.02	0.07	97.51
HW24/297.8	52.29	0.16	11.08	1.31	10.50	0.22	15.41	8.66	1.10	0.08	0.02	0.04	0.07	100.94
HW24/302.85	51.14	0.13	17.31	1.16	9.29	0.14	9.16	12.68	1.83	0.11	0.02	0.02	0.04	103.04
HW24/306	46.29	0.08	15.68	1.15	9.19	0.17	20.03	7.29	0.41	0.32	0.02	0.12	0.10	100.84
HW24/311.2	44.56	0.05	15.23	1.70	13.62	0.17	19.43	8.25	0.44	0.16	0.02	0.13	0.04	103.83
HW24/314.5	49.99	0.08	16.63	0.85	6.83	0.14	16.42	8.49	0.93	0.04	0.01	0.07	0.17	100.65
HW24/319.2	47.15	0.08	22.77	0.66	5.26	0.11	10.04	12.89	1.26	0.15	0.02	0.05	0.07	100.52
HW24/321.52	44.48	0.05	14.14	0.88	7.07	0.16	21.81	8.07	0.15	0.17	0.02	0.13	0.11	97.26
HW24/328.5	49.42	0.07	19.84	0.76	6.07	0.11	12.10	11.00	1.21	0.05	0.01	0.05	0.11	100.81
HW24/332.65	51.89	0.11	10.13	1.17	9.36	0.20	20.56	6.42	0.69	0.10	0.01	0.08	0.13	100.86
HW24/336.15	47.82	0.06	17.99	0.82	6.58	0.14	14.31	10.60	0.76	0.74	0.01	0.08	0.09	100.00
HW24/345.55	50.99	0.11	10.89	1.07	8.58	0.19	18.76	8.29	0.80	0.05	0.01	0.06	0.18	99.99
HW24/347.65	48.15	0.05	21.48	0.66	5.30	0.10	11.21	11.47	1.18	0.20	0.01	0.09	0.08	99.99
HW24/347.9	49.62	0.09	13.06	1.19	9.55	0.18	19.43	6.51	0.69	0.09	0.02	0.29	0.16	100.89
HW24/348.4	50.46	0.12	7.32	1.62	12.99	0.17	21.26	5.15	0.29	0.05	0.01	1.50	0.19	101.14
HW24/352.3	49.29	0.07	13.64	1.16	9.29	0.16	18.55	6.52	0.71	0.09	0.01	0.39	0.13	100.00
HW24/353.45	52.82	0.14	4.46	1.61	12.86	0.26	22.39	5.77	0.34	0.12	0.02	0.18	0.18	101.14
HW24/353.5	53.01	0.15	3.23	1.65	13.21	0.25	23.89	3.97	0.24	0.08	0.01	0.11	0.17	99.99
HW24/360.4	52.58	0.13	5.72	1.58	12.64	0.22	21.32	4.81	0.53	0.09	0.01	0.18	0.16	99.98
HW24/360.75	52.14	0.13	12.09	1.17	9.39	0.19	16.40	7.91	1.13	0.08	0.01	0.09	0.13	100.87
HW24/370.5	54.45	0.20	3.99	2.06	16.47	0.33	18.70	2.55	0.77	0.19	0.07	0.14	0.09	100.02
HW24/383.4	50.70	0.09	18.02	0.72	5.80	0.12	10.65	12.07	1.63	0.06	0.01	0.04	0.09	100.01
HW24/386.2	51.45	0.09	19.33	0.55	4.43	0.10	8.43	13.01	2.36	0.13	0.01	0.03	0.05	99.99
HW24/391.2	52.17	0.12	7.82	1.43	11.42	0.22	21.59	5.33	0.64	0.05	0.01	0.13	0.09	101.04
HW24/391.7	49.18	0.10	7.40	1.58	12.62	0.21	21.88	6.05	0.55	0.21	0.01	0.14	0.08	100.00
HW24/394.5	47.89	0.06	9.28	1.57	12.56	0.20	23.34	4.42	0.37	0.02	0.02	0.19	0.05	100.00
HW24/397.4	53.60	0.12	16.12	0.82	6.57	0.12	10.40	10.46	2.16	0.14	0.02	0.05	0.04	100.63
HW24/405.8	48.80	0.08	9.20	1.57	12.54	0.21	21.09	5.49	0.74	0.05	0.02	0.18	0.04	100.01
HW24/415.2	51.92	0.12	16.70	0.79	6.29	0.14	10.88	10.90	2.04	0.11	0.02	0.04	0.05	100.00
HW24/423.2	50.60	0.12	19.18	0.75	6.03	0.13	10.45	10.79	1.73	0.09	0.02	0.04	0.08	100.02
HW24/435.72	50.08	0.12	19.99	0.69	5.49	0.12	8.66	12.90	1.70	0.11	0.02	0.03	0.08	100.00
HW24/439.6	49.76	0.13	20.36	0.75	5.98	0.12	8.97	12.58	1.63	0.14	0.02	0.04	0.07	100.55
HW24/440.6	49.74	0.10	18.82	0.80	6.42	0.12	10.88	11.43	1.44	0.11	0.02	0.07	0.06	100.02

11.4 Appendix D: trace element XRF

Sample #	Sc	V	Cr	Co	Ni	Cu	Zn	Ga	Rb	Sr	Y	Zr	Nb	Mo	Ba	Pb	Th	U
HW29/371.3	27.93	115.85	108.02	20.56	50.35	69.8	32.39	18.27	8.6	427.93	3.15	11.49	0	1.36		5.32	0	0
HW29/378.5	34.34	193.50	229.78	56.84	169.67	224.26	69.26	16.60	0.20	198.23	6.74	9.40	0.38	0.45	52.14	2.78	0.00	0.00
HW29/383.15	33.17	173.56	192.67	62.68	178.30	224.15	61.75	14.58		210.49	9.74	13.18	1.99	0.19	73.44	2.99	0.00	0.00
HW29/389.4	29.87	98.56	135.86	29.74	100.88	221.25	38.79	15.99	0.66	237.86	5.30	6.42	0.00	0.30	63.62	3.32	0.00	0.00
HW29/394.5	25.83	83.03	98.42	27.91	62.86	60.49	28.02	17.42	0.67	293.36	4.67	12.00	0.00	0.56	111.27	5.73	0.00	0.00
HW29/397.02	36.49	166.33	176.07	53.15	142.02	118.12	60.17	16.25	0.00	216.29	8.43	16.44	0.00	0.04	70.06	5.18	0.00	0.00
HW29/405.3	36.65	160.23	187.12	46.32	111.96	97.26	53.96	16.99	0.24	232.23	9.67	15.87	0.00	0.25	77.90	2.83	0.00	0.00
HW29/421.4	32.44	120.27	160.46	45.40	114.54	94.40	49.75	15.94	0.64	235.71	5.04	10.49	0.00	0.36	71.88	2.34	0.00	0.00
HW29/421.45	37.75	144.11	176.30	50.69	127.89	93.17	56.99	14.85	0.41	237.79	5.96	8.95	0.00	0.40	56.91	3.12	0.00	0.00
HW29/447.9	21.01	72.04	50.44	28.00	59.52	72.80	30.05	18.48	2.54	283.98	4.91	11.64	0.00	0.00	111.82	3.27	0.00	0.00
HW29/457.8	21.89	226.42	66.88	51.29	123.73	96.37	55.09	17.66	1.84	246.97	6.28	11.82	0.00	0.41	95.96	3.18	0.00	0.00
HW29/457.8	25.39	326.44	77.94	41.19	127.99	106.63	54.20	17.84	2.42	252.05	4.55	10.89	0.55	1.39	104.37	5.55	0.00	0.00
HW29/462.38	19.73	77.51	69.45	33.82	74.87	58.53	30.19	20.26	2.63	258.33	7.38	18.73	0.00	0.00	88.64	4.98	0.00	0.00
HW29/469.1	25.84	96.78	68.04	37.76	106.62	83.37	39.97	18.13	4.12	230.88	7.17	13.40	0.00	0.02	101.83	3.41	0.00	0.00
HW29/470.2	30.55	127.00	59.26	52.13	178.12	83.48	44.53	17.19	1.01	223.04	4.84	8.95	0.00	0.69	75.28	2.37	0.00	0.00
HW29/487.2	22.10	68.62	36.57	54.08	192.07	78.87	45.60	17.89	1.94	248.07	6.31	12.49	0.00	0.91	104.85	0.00	0.00	0.00
HW29/505.57	31.45	145.40	148.78	40.18	102.39	84.53	38.92	16.53	1.50	228.14	7.85	14.59	0.00	0.31	78.86	4.07	0.00	0.00
HW29/515.8	33.37	128.27	174.81	40.97	111.89	84.66	48.04	16.32	1.83	211.48	6.36	14.47	0.00	0.00	73.40	0.79	0.00	0.00
HW29/516	29.88	155.33	180.89	45.43	130.18	96.64	52.63	15.58	1.48	202.28	6.16	11.13	0.00	0.00	69.04	1.81	0.00	0.00
HW29/526.45	34.51	156.09	221.23	46.80	125.44	99.30	52.09	14.83	4.34	194.78	7.06	17.27	0.00	0.00	75.91	4.07	0.00	0.00
HW29/559.7	37.83	127.46	291.03	59.88	234.18	149.29	70.43	14.15	1.43	159.94	5.99	9.41	0.00	0.79	56.47	4.14	0.00	0.00
HW29/576.3	37.48	163.84	398.55	86.91	553.45	582.74	92.04	10.31	1.01	144.96	6.37	11.87	0.00	0.45	49.51	6.03	0.00	0.00
HW29/584.4	32.73	120.64	404.79	62.58	294.27	307.52	55.53	13.04	6.95	254.53	6.06	12.82	0.00	0.51	166.46	5.31	0.00	0.00
HW29/586.8	40.04	165.34	559.52	93.85	427.75	213.09	93.72	9.49	1.62	101.57	6.12	10.76	1.99	0.60	47.42	2.66	0.00	0.00
HW29/589.8	30.60	91.58	242.54	123.01	654.41	93.62	71.61	7.80	2.25	121.94	3.31	6.78	0.00	0.71	31.30	4.64	0.00	0.00
HW29/591.1	30.63	127.22	435.79	56.93	244.21	351.90	57.06	13.60	1.87	259.62	6.18	12.67	0.46	0.31	94.68	4.95	0.00	0.00
HW29/593.2	29.64	55.85	31.77	15.73	239.60	768.70	5.82	14.68	0.50	47.07	2.27	9.72	1.40	0.63	0.31	3.09	0.00	0.00
HW29/595.35	37.06	167.09	369.29	76.95	299.94	163.18	83.08	12.17	3.13	133.37	8.01	12.56	0.78	0.00	74.39	4.93	0.00	0.00
HW29/601.35	22.69	73.64	134.84	146.78	944.59	134.47	78.15	8.64	0.02	94.86	3.19	6.94	0.00	0.00	27.71	3.38	0.00	0.00
HW29/608.1	57.62	758.56	67.72	83.02	328.42	150.81	125.99	17.81	3.42	147.36	26.59	34.87	4.54	0.00	94.86	9.45	0.00	0.00
HW29/608.25	44.73	223.63	53.12	65.63	211.85	97.48	91.18	13.45	6.57	165.35	18.79	26.23	0.77	1.81	94.94	8.47	0.00	0.00
HW29/608.59	33.79	141.55	51.12	63.52	237.57	243.70	91.87	16.09	14.84	188.60	13.16	17.73	0.16	1.82	143.81	10.80	0.00	0.00
HW29/614.05	38.87	172.25	39.97	131.71	2068.14	4195.35	87.58	16.21	4.35	200.61	18.46	22.08	1.73	0.00	86.19	8.87	0.00	0.00
HW29/614.25	34.68	132.33	247.82	93.39	585.19	1303.47	79.96	10.68	0.44	109.22	5.97	9.43	2.41	0.02	37.11	3.28	0.00	0.00
HW29/614.7	48.62	177.20	253.43	93.57	598.66	1463.87	88.36	6.00	2.24	81.45	6.52	8.85	1.16	0.14	46.70	7.09	0.00	0.00
HW29/614.8	41.44	144.19	96.12	98.49	1131.59	10009.67	100.47	13.30	0.96	151.63	9.81	15.38	1.76	0.00	108.08	18.82	0.00	0.00
HW29/622.49	40.33	142.62	65.61	47.05	193.52	139.06	36.66	14.58	2.64	200.76	5.34	13.11	1.17	0.00	57.48	4.10	0.00	0.00
HW29/625.4	53.95	191.85	87.60	63.37	254.52	119.26	52.61	10.11	2.20	161.14	6.97	13.28	0.76	0.44	42.72	3.52	0.00	0.00
HW29/634.5	34.35	118.48	64.41	99.45	2059.40	6198.71	39.46	13.91	2.39	197.93	4.02	8.96	1.14	0.00	42.03	5.95	0.00	0.00
HW29/634.7	38.67	123.85	52.13	121.27	2597.23	7766.46	53.13	12.31	0.00	189.58	3.53	5.62	1.35	0.18	57.40	9.40	0.00	0.00
HW29/635.2	33.16	104.98	40.19	106.66	2176.70	6326.73	42.86	15.93	0.00	201.96	3.72	4.34	1.19	0.00	53.69	8.69	0.00	0.00
HW29/636.78	44.82	149.86	88.24	69.57	265.14	297.87	62.26	10.04	0.78	146.96	5.11	10.07	1.09	0.00	30.51	2.92	0.00	0.00
HW29/637.8	44.60	179.99	94.87	89.69	1077.99	3380.02	69.12	10.82	0.35	147.33	8.81	11.47	1.45	0.74	43.92	7.90	0.00	0.00
HW29/651.9	61.40	216.14	177.62	82.43	305.30	126.52	71.95	7.95	0.00	91.93	7.73	10.25	1.47	0.89	30.54	2.27	0.00	0.00
HW29/653.3	48.48	182.93	174.66	77.08	254.91	115.45	62.56	12.68	0.11	126.95	6.39	9.36	1.98	0.04	27.78	1.35	0.00	0.00
HW29/659.25	37.88	152.52	123.04	48.86	156.22	79.22	48.40	14.42	0.92	208.43	6.94	15.07	1.35	0.67	51.54	4.49	0.00	0.00
HW29/680	29.60	76.91	49.84	15.01	47.80	11.47	25.99	4.61	0.00	152.31	2.40	4.41	1.70	0.32	0.00	5.15	0.00	0.00
HW29/695	21.63	44.19	37.54	11.13	43.12	8.55	23.03	3.51	0.88	376.64	2.10	9.59	0.80	1.38	0.00	3.35	0.00	0.00
HW29/716	21.20	70.33	35.20	32.06	77.74	62.72	36.87	18.50	4.15	297.43	2.75	9.96	0.25	0.11	88.06	2.96	0.00	0.00
HW29/721.3	29.63	115.57	48.84	33.33	94.22	49.86	34.01	16.84	2.51	251.66	4.62	11.94	1.26	0.63	71.54	2.59	0.00	0.00
HW30/440.4	34.25	3884.96	8208.37	138.43	838.12	2005.63	203.57	35.04	0.00	203.54	2.36	19.65	3.41	0.80	57.83	10.14	0.00	0.00
HW25/417.5	31.53	98.38	275.56	31.77	116.63	35.51	32.31	15.81	1.57	243.56	3.92	9.42	1.61	0.55	62.15	4.03	0.00	0.00
HW25/426.3	25.24	75.07	189.85	45.54	116.27	16.54	44.97	14.80	1.75	282.24	2.15	10.31	0.87	0.00	89.00	3.10	0.00	0.00
HW25/433.53	27.09	99.41	273.24	39.57	136.97	31.82	44.43	13.87	1.32	498.76	4.44	16.25	0.52	0.00	90.88	3.05	0.00	0.00
HW25/440.9	27.20	93.21	291.98	39.85	137.31	31.78	44.21	14.37	3.44	291.38	4.26	10.71	0.57	0.65	123.62	1.98	0.00	0.00
HW25/449.2	50.12	218.80	212.62	97.04	641.16	870.76	105.76	11.79	0.53	134.21	7.15	8.70	0.95	0.00	37.98	3.93	0.00	0.00
HW25/454.3	28.08	104.05	343.38	48.90	159.56	75.92	41.10	14.52	0.00	223.25	5.54	9.67	0.00	0.00	56.58	4.30	0.00	0.00
HW25/462.7	30.94	66.58	217.53	32.00	102.31	42.41	28.51	17.31	0.57	282.13	3.62	9.97	0.00	0.00	61.24	2.84	0.00	0.00
HW25/472.8	48.69	153.58	379.33	50.43	173.63	103.62	92.86	13.13	6.24	185.49	6.25	10.31	0.00	1.67	118.71	6.61	0.00	0.00

Sample #	Sc	V	Cr	Co	Ni	Cu	Zn	Ga	Rb	Sr	Y	Zr	Nb	Mo	Ba	Pb	Th	U
HW25/479.71	46.66	164.87	422.28	54.68	154.44	41.05	57.97	12.00	5.50	249.66	7.44	19.32	0.00	0.02	125.40	7.86	0.00	0.00
HW25/480.3	32.71	111.53	408.93	34.71	168.74	32.62	33.17	11.25	12.46	751.20	4.16	21.36	0.00	0.00	228.08	0.00	0.00	0.00
HW25/493.53	39.95	129.58	492.05	44.77	172.56	37.11	36.17	12.61	3.49	304.53	4.87	14.95	1.72	0.67	90.34	4.66	0.00	0.00
HW25/497.6	27.41	99.74	428.33	44.08	158.93	27.52	34.75	13.24	7.60	460.25	3.82	14.76	1.11	1.19	192.72	2.92	0.00	0.00
HW25/503.49	11.13	29.39	449.10	87.84	753.64	5.66	42.16	11.20	2.01	419.57	0.42	9.98	0.61	0.00	52.65	1.43	0.00	0.00
HW25/512.5	32.09	105.44	1001.11	51.11	295.39	57.71	53.68	10.72	5.35	885.12	3.57	20.15	0.73	0.27	191.39	5.21	0.00	0.00
HW25/516.2	17.12	48.05	736.78	107.16	944.40	9.55	53.82	8.93	0.46	160.81	1.50	4.97	0.92	0.00	23.33	4.40	0.00	0.00
HW25/520.14	24.04	69.72	631.75	33.51	346.22	4.78	23.77	13.13	0.53	313.43	0.61	7.79	0.00	0.12	80.61	2.78	0.00	0.00
HW25/522.3	26.73	67.79	511.98	47.30	338.81	8.99	33.07	11.23	4.00	1060.53	0.03	20.03	0.00	0.00	145.63	1.13	0.00	0.00
HW25/535.1	24.19	52.82	302.75	38.81	353.12	26.03	33.24	10.15	0.00	108.42		2.64	0.00	0.00	29.62	3.62	0.00	0.00
HW25/545.5	26.26	97.11	671.27	77.57	569.83	52.82	65.73	8.51	0.43	187.87	1.10	8.89	0.00	0.28	48.77	6.02	0.00	0.00
HW25/570.5	5.18	26.45	134.07	96.61	1207.23	22.22	87.57	7.51	0.00	33.36	0.02	3.69	0.00	0.02	17.67	4.55	0.00	0.00
HW25/577.28	15.58	55.48	139.69	126.01	973.22	45.00	75.00	8.27	4.47	191.07	2.99	7.53	1.65	0.00	63.07	4.41	0.00	0.00
HW25/591.56	17.14	51.65	217.90	154.91	1336.15	160.96	108.87	7.30	3.01	112.08	4.46	4.38	1.34	0.00	46.38	10.90	0.00	0.00
HW25/600.5	23.62	80.32	294.83	53.91	385.71	82.75	42.17	14.52	6.44	442.08	3.85	15.80	1.14	0.54	161.69	3.41	0.00	0.00
HW25/602.1	28.38	115.58	432.64	57.21	526.12	327.67	60.86	15.03	0.98	231.62	4.29	9.48	0.00	0.10	85.38	4.18	0.00	0.00
HW25/602.6	34.99	131.78	660.12	122.11	1868.48	850.51	100.21	8.38	4.56	217.94	4.74	11.75	1.61	0.05	73.03	7.27	0.00	0.00
HW24/268.2	36.24	102.89	305.67	36.23	128.05	50.54	31.63	14.93	2.57	286.75	3.11	11.80	0.59	0.00	150.34	10.99	0.00	0.00
HW24/268.2	28.37	105.72	285.83	37.89	139.64	48.31	31.24	14.13	3.30	253.08	5.16	7.97	0.00	0.24	74.75	11.99	0.00	0.00
HW24/275.9	32.08	110.36	214.01	34.98	106.77	32.95	33.05	15.85	0.87	259.75	3.53	10.18	1.21	0.34	87.34	0.57	0.00	0.00
HW24/276.5	27.70	80.43	172.73	33.39	104.54	42.87	33.10	17.17	0.66	255.70	2.37	10.75	0.72	0.00	83.23	2.82	0.00	0.00
HW24/281.1	32.09	86.09	138.52	31.21	119.42	53.50	27.98	15.87	5.66	272.50	4.33	7.50	0.00	0.00	108.62	3.35	0.00	0.00
HW24/290.45	33.08	106.20	202.58	28.86	110.27	35.21	31.98	15.03	1.33	219.50	3.51	11.34	1.75	0.78	73.08	4.10	0.00	0.00
HW24/297	40.34	159.36	377.13	49.99	166.87	52.36	48.61	14.10	0.05	177.78	6.03	13.63	1.86	0.00	56.03	2.92	0.00	0.00
HW24/297.8	41.87	135.45	397.16	87.93	278.18	55.00	80.62	8.34	1.42	139.51	5.43	8.43	1.31	1.24	44.59	1.73	0.00	0.00
HW24/302.85	33.60	119.29	216.52	40.00	150.82	58.22	41.19	14.06	1.00	209.66	4.54	9.09	0.24	0.63	59.28	2.40	0.00	0.00
HW24/306	11.63	27.75	486.47	103.45	883.92	10.94	56.74	8.95	8.23	138.45	1.90	3.20	0.53	0.02	88.03	3.22	0.00	0.00
HW24/311.2	11.06	34.32	197.54	111.31	1000.04	28.50	64.49	7.37	3.11	196.04	0.75	6.15	0.66	1.56	62.58	4.97	0.00	0.00
HW24/314.5	18.93	56.17	1080.88	66.70	560.82	4.50	46.33	8.90	1.07	134.68	2.29	3.02	0.48	0.90	26.68	1.14	0.00	0.00
HW24/319.2	17.53	39.34	436.46	43.34	358.54	6.60	34.96	13.54	3.02	946.45	2.02	5.78	0.00	0.83	115.58	3.47	0.00	0.00
HW24/321.52	11.14	34.61	583.15	114.82	996.71	8.13	56.21	6.97	5.33	71.43	1.41	4.60	1.96	1.39	30.68	3.54	0.00	0.00
HW24/328.5	18.61	48.96	647.91	52.08	427.86	2.56	32.96	11.72	1.19	167.83	1.17	4.92	0.81	0.08	31.04	1.74	0.00	0.00
HW24/332.65	24.77	93.32	878.45	84.53	635.93	6.57	68.16	7.05	3.85	236.35	2.54	5.76	0.13	0.99	39.35	2.24	0.00	0.00
HW24/336.15	21.06	53.98	580.25	75.50	681.70	9.33	58.18	10.31	29.72	1314.84	1.14	25.77	0.00	0.59	476.02	2.21	0.00	0.00
HW24/345.55	33.75	116.97	1277.89	79.24	463.30	10.51	60.61	8.95	1.32	299.71	3.59	9.51	0.21	0.00	38.46	1.75	0.00	0.00
HW24/347.65	15.32	35.72	479.76	80.91	702.06	4.31	42.35	11.33	6.48	634.67	1.05	12.57	1.19	0.00	154.33	3.75	0.00	0.00
HW24/347.9	20.21	59.94	934.40	100.84	2073.03	1382.50	64.82	7.75	3.02	309.56	2.24	3.59	0.31	1.05	44.90	3.57	0.00	0.00
HW24/348.4	27.60	92.87	1273.27	245.25	9902.60	4944.80	81.56	6.17	0.00	110.90	2.91	3.63	0.71	1.16	42.28	13.73	0.00	0.00
HW24/352.3	17.75	56.54	800.37	111.64	2719.38	1646.30	67.85	8.16	2.46	263.00	2.29	7.75	1.66	0.48	90.61	3.95	0.00	0.00
HW24/353.45	35.30	136.30	1081.40	106.67	1200.52	361.86	103.63	5.85	6.24	31.05	4.51	2.50	0.00	1.46	16.43	7.23	0.00	0.00
HW24/353.5	37.93	163.90	1204.72	99.77	861.29	747.19	114.32	5.30	5.50	25.63	3.50	4.27	1.84	0.00	15.51	3.05	0.00	0.00
HW24/360.4	36.40	137.71	1076.79	117.28	1398.14	271.86	102.26	5.62	3.79	59.00	4.35	4.89	2.19	0.00	27.85	7.38	0.00	0.00
HW24/360.75	34.13	107.90	831.58	81.17	678.36	94.38	66.45	10.75	0.27	192.50	3.45	3.81	0.00	0.00	31.95	6.81	0.00	0.00
HW24/370.5	33.71	133.24	618.37	117.71	1046.61	802.17	187.68	8.62	23.41	54.02	13.13	12.24	2.14	0.54	33.58	6.93	0.00	0.00
HW24/383.4	30.47	88.34	498.36	52.48	282.84	133.48	32.77	12.65	0.00	196.29	2.70	5.64	0.00	0.21	32.38	3.44	0.00	0.00
HW24/386.2	31.45	93.67	332.56	28.24	202.84	40.35	27.93	13.97	1.68	441.28	3.03	12.63	0.00	0.00	64.09	5.02	0.00	0.00
HW24/391.2	31.17	92.53	546.03	123.33	1007.13	49.86	83.87	6.00	0.00	92.83	1.83	2.57	0.00	0.00	26.62	2.48	0.00	0.00
HW24/391.7	29.18	90.13	504.97	117.36	1017.95	123.40	111.01	6.62	7.62	294.92	2.47	8.24	0.00	0.37	46.45	8.12	0.00	0.00
HW24/394.5	11.04	32.47	249.98	132.83	1458.05	37.73	69.96	7.52	0.00	48.78	1.73	3.79	0.00	1.02	9.98	3.71	0.00	0.00
HW24/397.4	29.24	89.70	233.64	61.38	340.45	216.36	61.72	12.39	0.67	306.58	2.21	5.18	0.00	0.44	63.56	4.02	0.00	0.00
HW24/405.8	17.70	54.70	164.89	143.76	1259.55	19.93	77.67	6.93	1.63	105.68	1.41	4.89	0.00	0.00	39.75	3.84	0.00	0.00
HW24/415.2	30.25	89.08	315.28	57.83	326.18	46.54	99.49	13.35	1.94	303.91	3.43	10.27	0.00	0.11	65.27	4.07	0.00	0.00
HW24/423.2	26.10	76.26	535.77	48.88	270.90	38.68	39.72	12.66	1.67	282.48	2.19	8.84	0.33	0.00	70.35	0.00	0.00	0.00
HW24/435.72	28.85	94.50	482.63	45.04	235.46	37.21	38.70	12.88	2.39	283.35	3.26	9.28	0.00	0.00	57.80	4.13	0.00	0.00
HW24/439.6	26.98	85.45	368.22	49.02	297.69	42.36	40.92	13.89	1.84	317.78	3.05	6.57	0.00	0.00	72.28	2.80	0.00	0.00
HW24/440.6	23.93	65.68	307.82	86.72	557.44	48.10	54.11	13.02	1.29	265.27	1.89	10.03	0.43	0.00	55.10	3.79	0.00	0.00

11.5 **Appendix E: Magnetic susceptibility data**

11.5.1 **Drillcore HW024**

Hole ID	Depth	Reading 1	Reading 2	Reading 3	Average	Hole ID	Depth	Reading 1	Reading 2	Reading 3	Average
HW024	255	0.092	0.09	0.119	0.1	HW024	300	0.28	0.258	0.273	0.3
HW024	256	2.88	3.11	3.05	3.0	HW024	301	0.211	0.213	0.218	0.2
HW024	257	0.075	0.08	0.076	0.1	HW024	302	0.23	0.32	0.23	0.3
HW024	258	0.091	0.103	0.11	0.1	HW024	303	0.382	0.404	0.432	0.4
HW024	259	0.091	0.093	0.084	0.1	HW024	304	0.418	0.403	0.436	0.4
HW024	260	0.061	0.06	0.058	0.1	HW024	305	0.726	0.773	0.768	0.8
HW024	261	0.305	0.304	0.324	0.3	HW024	306	0.714	0.729	0.718	0.7
HW024	262	0.499	0.443	0.495	0.5	HW024	307	0.481	0.477	0.485	0.5
HW024	263	13.4	15.2	15.2	14.6	HW024	308	0.223	0.214	0.263	0.2
HW024	264	0.79	0.78	0.083	0.6	HW024	309	0.293	0.286	0.294	0.3
HW024	265	0.13	0.13	0.123	0.1	HW024	310	0.144	0.139	0.138	0.1
HW024	266	0.236	0.235	0.249	0.2	HW024	311	0.272	0.277	0.286	0.3
HW024	267	0.232	0.223	0.218	0.2	HW024	312	0.282	0.276	0.289	0.3
HW024	268	0.044	0.043	0.045	0.0	HW024	313	0.257	0.234	0.259	0.3
HW024	269	0.223	0.234	0.229	0.2	HW024	314	0.199	0.184	0.201	0.2
HW024	270	0.196	0.193	0.198	0.2	HW024	315	0.175	0.184	0.177	0.2
HW024	271	22.8	22.6	21.9	22.4	HW024	316	0.138	0.138	0.147	0.1
HW024	272	0.135	0.141	0.137	0.1	HW024	317	0.093	0.094	0.111	0.1
HW024	273	0.296	0.262	0.236	0.3	HW024	318	0.13	0.107	0.111	0.1
HW024	274	0.149	0.183	0.187	0.2	HW024	319	0.125	0.14	0.136	0.1
HW024	275	0.257	0.268	0.271	0.3	HW024	320	0.214	0.22	0.201	0.2
HW024	276	0.544	0.545	0.576	0.6	HW024	321	0.143	0.166	0.15	0.2
HW024	277	0.531	0.539	0.56	0.5	HW024	322	0.128	0.112	0.117	0.1
HW024	278	0.385	0.356	0.349	0.4	HW024	323	0.215	0.207	0.243	0.2
HW024	279	0.262	0.267	0.27	0.3	HW024	324	0.242	0.243	0.25	0.2
HW024	280	0.321	0.384	0.345	0.4	HW024	325	0.32	0.294	0.321	0.3
HW024	281	0.105	0.111	0.127	0.1	HW024	326	0.66	0.716	0.694	0.7
HW024	282	0.201	0.205	0.206	0.2	HW024	327	0.229	0.235	0.245	0.2
HW024	283	0.141	0.143	0.146	0.1	HW024	328	0.421	0.456	0.367	0.4
HW024	284	0.115	0.115	0.122	0.1	HW024	329	0.143	0.152	0.17	0.2
HW024	285	0.091	0.107	0.106	0.1	HW024	330	0.367	0.362	0.329	0.4
HW024	286	0.122	0.13	0.124	0.1	HW024	331	0.447	0.539	0.618	0.5
HW024	287	0.332	0.331	0.337	0.3	HW024	332	0.361	0.344	0.307	0.3
HW024	288	0.156	0.156	0.161	0.2	HW024	333	0.279	0.262	0.309	0.3
HW024	289	0.443	0.449	0.453	0.4	HW024	334	0.16	0.164	0.172	0.2
HW024	290	0.492	0.414	0.51	0.5	HW024	335	0.21	0.221	0.184	0.2
HW024	291	0.425	0.46	0.47	0.5	HW024	336	0.3	0.285	0.295	0.3
HW024	292	0.191	0.186	0.196	0.2	HW024	337	0.203	0.207	0.216	0.2
HW024	293	0.131	0.14	0.137	0.1	HW024	338	0.429	0.465	0.454	0.4
HW024	294	0.145	0.157	0.163	0.2	HW024	339	0.439	0.45	0.456	0.4
HW024	295	0.188	0.19	0.176	0.2	HW024	340	0.316	0.282	0.327	0.3
HW024	296	0.203	0.201	0.216	0.2	HW024	341	0.192	0.177	0.187	0.2
HW024	297	0.197	0.189	0.209	0.2	HW024	342	0.231	0.242	0.236	0.2
HW024	298	0.326	0.327	0.308	0.3	HW024	343	0.187	0.188	0.198	0.2
HW024	299	0.514	0.524	0.496	0.5	HW024	344	1.75	1.64	1.65	1.7

11.5.2 **Drillcore HW025**

Hole ID	Depth	Reading 1	Reading 2	Readin 3	Average	Hole ID	Depth	Reading 1	Reading 2	Readin 3	Average
HW025	409	0.103	0.103	0.146	0.1	HW025	453	0.29	0.299	0.287	0.3
HW025	410	0.073	0.065	0.075	0.1	HW025	454	0.19	0.188	0.198	0.2
HW025	411	0.074	0.072	0.078	0.1	HW025	455	0.165	0.15	0.137	0.2
HW025	412	0.042	0.043	0.023	0.0	HW025	456	0.38	0.389	0.399	0.4
HW025	413	0.182	0.183	0.182	0.2	HW025	457	0.227	0.231	0.23	0.2
HW025	414	0.264	0.28	0.273	0.3	HW025	458	0.165	0.141	0.159	0.2
HW025	415	0.134	0.169	0.171	0.2	HW025	459	0.178	0.242	0.259	0.2
HW025	416	0.376	0.359	0.407	0.4	HW025	460	0.172	0.209	0.208	0.2
HW025	417	0.737	0.805	0.802	0.8	HW025	461	0.144	0.132	0.119	0.1
HW025	418	0.269	0.283	0.288	0.3	HW025	462	0.093	0.087	0.103	0.1
HW025	419	0.358	0.368	0.382	0.4	HW025	463	0.118	0.121	0.133	0.1
HW025	420	0.211	0.208	0.221	0.2	HW025	464	0.508	0.466	0.456	0.5
HW025	421	0.559	0.552	0.52	0.5	HW025	465	7.66	7.86	8.26	7.9
HW025	422	0.889	0.962	1.2	1.0	HW025	466	0.165	0.168	0.212	0.2
HW025	423	84	81.9	80.7	82.2	HW025	467	0.161	0.212	0.202	0.2
HW025	424	1.64	1.79	1.97	1.8	HW025	468	0.087	0.083	0.086	0.1
HW025	425	0.371	0.306	0.372	0.3	HW025	469	0.064	0.049	0.076	0.1
HW025	426	0.303	0.325	0.325	0.3	HW025	470	0.168	0.162	0.154	0.2
HW025	427	0.351	0.263	0.261	0.3	HW025	471	0.745	0.796	0.843	0.8
HW025	428	0.276	0.345	0.348	0.3	HW025	472	2.01	1.97	1.91	2.0
HW025	429	0.308	0.283	0.438	0.3	HW025	473	2.52	2.3	2.45	2.4
HW025	430	0.217	0.207	0.227	0.2	HW025	474	0.228	0.312	0.31	0.3
HW025	431	0.383	0.299	0.386	0.4	HW025	475	0.902	0.882	0.872	0.9
HW025	432	0.299	0.271	0.31	0.3	HW025	476	0.071	0.073	0.071	0.1
HW025	433	0.382	0.396	0.423	0.4	HW025	477	0.106	0.122	0.11	0.1
HW025	434	0.454	0.484	0.486	0.5	HW025	478	0.271	0.245	0.23	0.2
HW025	435	0.334	0.367	0.375	0.4	HW025	479	0.269	0.253	0.275	0.3
HW025	436	0.331	0.352	0.338	0.3	HW025	480	0.691	0.695	0.626	0.7
HW025	437	0.167	0.157	0.152	0.2	HW025	481	3.06	3.17	3.02	3.1
HW025	438	0.783	0.807	0.855	0.8	HW025	482	2.48	2.41	2.14	2.3
HW025	439	0.223	0.23	0.232	0.2	HW025	483	0.144	0.118	0.117	0.1
HW025	440	0.264	0.324	0.352	0.3	HW025	484	6.08	6.34	6.2	6.2
HW025	441	0.275	0.34	0.349	0.3	HW025	485	0.258	0.272	0.276	0.3
HW025	442	0.119	0.174	0.183	0.2	HW025	486	0.22	0.22	0.217	0.2
HW025	443	0.115	0.147	0.157	0.1	HW025	487	0.094	0.087	0.093	0.1
HW025	444	0.098	0.101	0.125	0.1	HW025	488	0.097	0.108	0.107	0.1
HW025	445	0.271	0.359	0.364	0.3	HW025	489	0.088	0.077	0.063	0.1
HW025	446	0.109	0.114	0.107	0.1	HW025	490	0.043	0.062	0.069	0.1
HW025	447	0.238	0.254	0.259	0.3	HW025	491	0.105	0.107	0.114	0.1
HW025	448	0.171	0.16	0.187	0.2	HW025	492	0.099	0.091	0.106	0.1
HW025	449	29.7	28.6	28.8	29.0	HW025	493	0.074	0.075	0.082	0.1
HW025	450	0.208	0.198	0.175	0.2	HW025	494	0.113	0.112	0.116	0.1
HW025	451	0.223	0.221	0.216	0.2	HW025	495	0.08	0.09	0.084	0.1
HW025	452	0.244	0.26	0.254	0.3	HW025	496	0.126	0.123	0.127	0.1

Hole ID	Depth	Reading 1	Reading 2	Readin 3	Average	Hole ID	Depth	Reading 1	Reading 2	Readin 3	Average
HW025	497	0.241	0.246	0.253	0.2	HW025	553				0.0
HW025	498	0.142	0.144	0.148	0.1	HW025	554				0.0
HW025	499	0.096	0.097	0.093	0.1	HW025	555				0.0
HW025	500	0.076	0.071	0.075	0.1	HW025	556				0.0
HW025	501	0.077	0.068	0.07	0.1	HW025	557	0.268	0.272	0.258	0.3
HW025	502	0.268	0.233	0.265	0.3	HW025	558	0.465	0.481	0.504	0.5
HW025	503	0.201	0.19	0.2	0.2	HW025	559	0.305	0.279	0.268	0.3
HW025	504	0.124	0.126	0.126	0.1	HW025	560	0.168	0.159	0.182	0.2
HW025	505	0.097	0.137	0.134	0.1	HW025	561	0.404	0.394	0.39	0.4
HW025	506	0.092	0.098	0.08	0.1	HW025	562	0.258	0.259	0.228	0.2
HW025	507	0.06	0.054	0.041	0.1	HW025	563	0.493	0.466	0.446	0.5
HW025	508	0.194	0.222	0.22	0.2	HW025	564				0.0
HW025	509				0.0	HW025	565				0.0
HW025	510				0.0	HW025	566				0.0
HW025	511	0.283	0.301	0.306	0.3	HW025	567				0.0
HW025	512	0.205	0.171	0.208	0.2	HW025	568				0.0
HW025	513	0.163	0.199	0.197	0.2	HW025	569				0.0
HW025	514	0.284	0.329	0.323	0.3	HW025	570	0.156	0.153	0.139	0.1
HW025	515	0.311	0.31	0.317	0.3	HW025	571	0.508	0.523	0.516	0.5
HW025	516	0.368	0.36	0.364	0.4	HW025	572	0.164	0.153	0.138	0.2
HW025	517	0.192	0.178	0.194	0.2	HW025	573	0.308	0.325	0.247	0.3
HW025	518	0.177	0.165	0.17	0.2	HW025	574	0.161	0.171	0.16	0.2
HW025	519	0.335	0.317	0.288	0.3	HW025	575	0.343	0.356	0.347	0.3
HW025	520	0.24	0.251	0.25	0.2	HW025	576	0.382	0.303	0.361	0.3
HW025	521	0.825	0.8	0.78	0.8	HW025	577	0.152	0.138	0.133	0.1
HW025	522	0.086	0.083	0.082	0.1	HW025	578	0.107	0.084	0.047	0.1
HW025	523	0.157	0.156	0.158	0.2	HW025	579	0.325	0.365	0.365	0.4
HW025	524	0.169	0.159	0.13	0.2	HW025	580	24.6	23.6	20.7	23.0
HW025	525	0.155	0.15	0.155	0.2	HW025	581				0.0
HW025	526	8.27	7.33	7.73	7.8	HW025	582	42.9	43.1	46.4	44.1
HW025	527	0.089	0.061	0.07	0.1	HW025	583				0.0
HW025	528	0.137	0.142	0.136	0.1	HW025	584	0.292	0.299	0.227	0.3
HW025	529	0.077	0.066	0.093	0.1	HW025	585	0.33	0.463	0.468	0.4
HW025	530	0.104	0.113	0.126	0.1	HW025	586				0.0
HW025	531	0.104	0.113	0.126	0.1	HW025	587	0.239	0.218	0.27	0.2
HW025	532				0.0	HW025	588				0.0
HW025	533				0.0	HW025	589	0.277	0.266	0.296	0.3
HW025	534	0.298	0.315	0.317	0.3	HW025	590	0.052	0.047	0.052	0.1
HW025	535	0.159	0.161	0.079	0.1	HW025	591	1.93	1.87	1.82	1.9
HW025	536	0.326	0.31	0.318	0.3	HW025	592	21	20.9	21.9	21.3
HW025	537	0.627	0.623	0.639	0.6	HW025	593				0.0
HW025	538	0.506	0.46	0.456	0.5	HW025	594	0.406	0.391	0.356	0.4
HW025	539	0.276	0.311	0.318	0.3	HW025	595	0.217	0.212	0.21	0.2
HW025	540	0.285	0.257	0.268	0.3	HW025	596	0.354	0.32	0.37	0.3
HW025	541	0.24	0.23	0.23	0.2	HW025	597	2.53	1.81	2.39	2.2
HW025	542	0.416	0.343	0.371	0.4	HW025	598	1.96	1.69	2.02	1.9
HW025	543				0.0	HW025	599	0.449	0.426	0.296	0.4
HW025	544	0.31	0.33	0.318	0.3	HW025	600	0.263	0.284	0.215	0.3
HW025	545	0.164	0.153	0.159	0.2	HW025	601	0.252	0.239	0.237	0.2
HW025	546	0.126	0.123	0.114	0.1	HW025	602		0.231	0.211	0.1
HW025	547	0.101	0.092	0.089	0.1	HW025	603	0.206	0.2	0.213	0.2
HW025	548	0.114	0.116	0.105	0.1	HW025	604	0.188	0.18	0.208	0.2
HW025	549	0.08	0.07	0.07	0.1	HW025	605	0.213	0.215	0.22	0.2
HW025	550				0.0	HW025	606	0.119	0.123	0.14	0.1
HW025	551	0.126	0.128	0.124	0.1	HW025	607	0.197	0.194	0.182	0.2
HW025	552	0.145	0.134	0.151	0.1						

11.5.3 **Drillcore HW029**

Hole ID	Depth	Reading 1	Reading 2	Reading 3	Average	Average/100	Hole ID	Depth	Reading 1	Reading 2	Reading 3	Average	Average/100
HW029	361	47	24	44	38.3	0.44	HW029	543	304	354	348	335.3	3.48
HW029	362	62	31	27	40.0	0.27	HW029	544	436	448	468	450.7	4.68
HW029	363	22	21	33	25.3	0.33	HW029	545	355	325	378	352.7	3.78
HW029	364	19	22	18	19.7	0.18	HW029	546	185	200	144	176.3	1.44
HW029	365	12	10	10	10.7	0.10	HW029	547	1954	2137	1872	1987.7	18.72
HW029	366	6	3	4	4.3	0.04	HW029	548	302	337	292	310.3	2.92
HW029	367	923	1029	648	866.7	6.48	HW029	549	804	815	838	819.0	8.38
HW029	368	310	427	319	352.0	3.19	HW029	550	412	441	447	433.3	4.47
HW029	369	702	915	844	820.3	8.44	HW029	551	173	184	203	186.7	2.03
HW029	370	880	1095	1036	1003.7	10.36	HW029	552	1	0	0	0.3	0.00
HW029	371	0	0	0	0.0	0.00	HW029	553	238	267	132	212.3	1.32
HW029	372	4	10	4	6.0	0.04	HW029	554	1262	1285	1168	1238.3	11.68
HW029	373	555	314	333	400.7	3.33	HW029	555	1057	1116	1133	1102.0	11.33
HW029	374	454	424	421	433.0	4.21	HW029	556	12	7	4	7.7	0.04
HW029	375	1023	1075	1271	1123.0	12.71	HW029	557	10	24	41	25.0	0.41
HW029	376	575	505	858	646.0	8.58	HW029	558	54	100	71	75.0	0.71
HW029	377	673	544	555	590.7	5.55	HW029	559	19	31	25	25.0	0.25
HW029	378	488	918	1005	803.7	10.05	HW029	560	19	115	124	86.0	1.24
HW029	379	162	120	112	131.3	1.12	HW029	561	101	138	165	134.7	1.65
HW029	380	885	524	457	622.0	4.57	HW029	562	1224	1238	1127	1196.3	11.27
HW029	381	438	505	462	468.3	4.62	HW029	563	375	489	492	452.0	4.92
HW029	382	7	4	6	5.7	0.06	HW029	564	158	144	147	149.7	1.47
HW029	383	73	127	94	98.0	0.94	HW029	565	47	57	30	44.7	0.30
HW029	384	66	100	184	116.7	1.84	HW029	566	340	377	438	385.0	4.38
HW029	385	4980	3970	1536	3495.3	15.36	HW029	567	101	106	80	95.7	0.80
HW029	386	1461	1706	1553	1573.3	15.53	HW029	568	333	441	397	390.3	3.97
HW029	387	124	111	111	115.3	1.11	HW029	569	3	0	0	1.0	0.00
HW029	388	416	293	444	384.3	4.44	HW029	570	359	362	389	370.0	3.89
HW029	389	212	188	184	194.7	1.84	HW029	571	48	89	74	70.3	0.74
HW029	390	362	410	375	382.3	3.75	HW029	572	19	16	10	15.0	0.10
HW029	391	313	512	394	406.3	3.94	HW029	573	400	372	229	333.7	2.29
HW029	392	774	657	800	743.7	8.00	HW029	574	187	293	202	227.3	2.02
HW029	393	661	648	564	624.3	5.64	HW029	575	736	759	1145	880.0	11.45
HW029	394	848	725	748	773.7	7.48	HW029	576	3	1	0	1.3	0.00
HW029	395	582	593	559	578.0	5.59	HW029	577	0	0	0	0.0	0.00
HW029	396	454	416	381	417.0	3.81	HW029	578	0	16	33	16.3	0.33
HW029	397	351	378	471	400.0	4.71	HW029	579	6	7	3	5.3	0.03
HW029	398	532	517	538	529.0	5.38	HW029	580	91	50	24	55.0	0.24
HW029	399	462	657	616	578.3	6.16	HW029	581	1	0	0	0.3	0.00
HW029	400	594	541	775	636.7	7.75	HW029	582	269	325	354	316.0	3.54
HW029	401	670	810	462	647.3	4.62	HW029	583	129	80	44	84.3	0.44
HW029	402	401	564	419	461.3	4.19	HW029	584	152	150	168	156.7	1.68
HW029	403	658	579	430	555.7	4.30	HW029	585	0	0	0	0.0	0.00
HW029	404	631	721	654	668.7	6.54	HW029	586	0	0	0	0.0	0.00

Hole ID	Depth	Reading 1	Reading 2	Reading 3	Average	Average/100	Hole ID	Depth	Reading 1	Reading 2	Reading 3	Average	Average/100
HW029	405	800	473	590	621.0	5.90	HW029	587	0	0	0	0.0	0.00
HW029	406	463	546	560	523.0	5.60	HW029	588	0	0	0	0.0	0.00
HW029	407	384	441	645	490.0	6.45	HW029	589	0	0	0	0.0	0.00
HW029	408	847	854	789	830.0	7.89	HW029	590	0	0	0	0.0	0.00
HW029	409	597	287	819	567.7	8.19	HW029	591	0	0	0	0.0	0.00
HW029	410	578	533	547	552.7	5.47	HW029	592	0	0	0	0.0	0.00
HW029	411	667	634	740	680.3	7.40	HW029	593	0	0	0	0.0	0.00
HW029	412	716	1239	1226	1060.3	12.26	HW029	594	0	0	0	0.0	0.00
HW029	413	324	436	351	370.3	3.51	HW029	595	0	0	0	0.0	0.00
HW029	414	789	844	934	855.7	9.34	HW029	596	990	993	1042	1008.3	10.42
HW029	415	809	789	710	769.3	7.10	HW029	597	0	0	0	0.0	0.00
HW029	416	562	538	546	548.7	5.46	HW029	598	0	0	0	0.0	0.00
HW029	417	801	961	724	828.7	7.24	HW029	599	0	0	0	0.0	0.00
HW029	418	746	917	997	886.7	9.97	HW029	600	1151	1404	1306	1287.0	13.06
HW029	419	643	521	412	525.3	4.12	HW029	601	1197	1227	1159	1194.3	11.59
HW029	420	164	101	126	130.3	1.26	HW029	602	1594	1787	1484	1621.7	14.84
HW029	421	199	226	211	212.0	2.11	HW029	603	216	273	302	263.7	3.02
HW029	422	620	445	468	511.0	4.68	HW029	604	1066	1037	1087	1063.3	10.87
HW029	423	383	305	389	359.0	3.89	HW029	605	932	943	909	928.0	9.09
HW029	424	395	363	453	403.7	4.53	HW029	606	459	508	514	493.7	5.14
HW029	425	544	380	509	477.7	5.09	HW029	607	1723	1772	1793	1762.7	17.93
HW029	426	409	448	442	433.0	4.42	HW029	608	514	546	622	560.7	6.22
HW029	427	331	401	357	363.0	3.57	HW029	609	7	4	1	4.0	0.01
HW029	428	100	89	60	83.0	0.60	HW029	610	0	0	0	0.0	0.00
HW029	429	500	222	273	331.7	2.73	HW029	611	0	0	0	0.0	0.00
HW029	430	422	372	418	404.0	4.18	HW029	612	0	0	0	0.0	0.00
HW029	431	400	286	298	328.0	2.98	HW029	613	0	0	0	0.0	0.00
HW029	432	456	690	597	581.0	5.97	HW029	614	0	0	0	0.0	0.00
HW029	433	1930	1992	1998	1973.3	19.98	HW029	615	0	0	0	0.0	0.00
HW029	434	260	419	541	406.7	5.41	HW029	616	0	0	0	0.0	0.00
HW029	435	362	444	451	419.0	4.51	HW029	617	0	0	0	0.0	0.00
HW029	436	871	777	877	841.7	8.77	HW029	618	0	0	0	0.0	0.00
HW029	437	1049	1168	1010	1075.7	10.10	HW029	619	0	0	0	0.0	0.00
HW029	438	899	759	778	812.0	7.78	HW029	620	0	0	0	0.0	0.00
HW029	439	328	365	270	321.0	2.70	HW029	621	0	0	0	0.0	0.00
HW029	440	555	467	270	430.7	2.70	HW029	622	0	0	0	0.0	0.00
HW029	441	330	368	324	340.7	3.24	HW029	623	0	0	0	0.0	0.00
HW029	442	143	135	184	154.0	1.84	HW029	624	0	0	0	0.0	0.00
HW029	443	395	359	375	376.3	3.75	HW029	625	0	0	0	0.0	0.00
HW029	444	146	158	165	156.3	1.65	HW029	626	0	0	0	0.0	0.00
HW029	445	7	10	6	7.7	0.06	HW029	627	0	0	0	0.0	0.00
HW029	446	12	24	28	21.3	0.28	HW029	628	0	0	0	0.0	0.00
HW029	447	3	0	3	2.0	0.03	HW029	629	0	0	0	0.0	0.00
HW029	448	83	86	94	87.7	0.94	HW029	630	0	0	0	0.0	0.00

Hole ID	Depth	Reading 1	Reading 2	Reading 3	Average	Average/100	Hole ID	Depth	Reading 1	Reading 2	Reading 3	Average	Average/100
HW029	449	225	231	188	214.7	1.88	HW029	631	0	0	0	0.0	0.00
HW029	450	404	395	301	366.7	3.01	HW029	632	0	0	0	0.0	0.00
HW029	451	1802	1909	1740	1817.0	17.40	HW029	633	0	0	0	0.0	0.00
HW029	452	6555	6886	6570	6670.3	65.70	HW029	634	0	0	0	0.0	0.00
HW029	453	95	101	98	98.0	0.98	HW029	635	0	0	0	0.0	0.00
HW029	454	1004	927	1042	991.0	10.42	HW029	636	0	0	0	0.0	0.00
HW029	455	1632	1623	1834	1696.3	18.34	HW029	637	0	0	0	0.0	0.00
HW029	456	713	791	861	788.3	8.61	HW029	638	0	0	0	0.0	0.00
HW029	457	923	932	927	927.3	9.27	HW029	639	0	0	0	0.0	0.00
HW029	458	946	938	935	939.7	9.35	HW029	640	0	0	0	0.0	0.00
HW029	459	42	74	86	67.3	0.86	HW029	641	0	0	0	0.0	0.00
HW029	460	307	298	334	313.0	3.34	HW029	642	0	0	0	0.0	0.00
HW029	461	1102	1140	1183	1141.7	11.83	HW029	643	0	0	0	0.0	0.00
HW029	462	775	824	931	843.3	9.31	HW029	644	0	0	0	0.0	0.00
HW029	463	170	155	141	155.3	1.41	HW029	645	0	0	0	0.0	0.00
HW029	464	654	725	707	695.3	7.07	HW029	646	0	0	0	0.0	0.00
HW029	465	199	129	136	154.7	1.36	HW029	647	0	0	0	0.0	0.00
HW029	466	2000	1997	1919	1972.0	19.19	HW029	648	0	0	0	0.0	0.00
HW029	467	949	982	990	973.7	9.90	HW029	649	0	0	0	0.0	0.00
HW029	468	176	199	410	261.7	4.10	HW029	650	0	0	0	0.0	0.00
HW029	469	0	0	47	15.7	0.47	HW029	651	0	0	0	0.0	0.00
HW029	470	7	4	4	5.0	0.04	HW029	652	0	0	0	0.0	0.00
HW029	471	827	695	599	707.0	5.99	HW029	653	0	0	0	0.0	0.00
HW029	472	584	654	483	573.7	4.83	HW029	654	0	0	0	0.0	0.00
HW029	473	0	0	21	7.0	0.21	HW029	655	0	0	0	0.0	0.00
HW029	474	0	0	0	0.0	0.00	HW029	656	0	0	0	0.0	0.00
HW029	475	1026	830	1209	1021.7	12.09	HW029	657	0	0	0	0.0	0.00
HW029	476	2522	2602	2304	2476.0	23.04	HW029	658	0	0	0	0.0	0.00
HW029	477	2937	3244	3100	3093.7	31.00	HW029	659	0	0	0	0.0	0.00
HW029	478	969	978	903	950.0	9.03	HW029	660	0	0	0	0.0	0.00
HW029	479	9	6	30	15.0	0.30	HW029	661	0	0	0	0.0	0.00
HW029	480	841	883	858	860.7	8.58	HW029	662	0	0	0	0.0	0.00
HW029	481	1303	1296	1139	1246.0	11.39	HW029	663	48	16	12	25.3	0.12
HW029	482	54	50	56	53.3	0.56	HW029	664	0	0	0	0.0	0.00
HW029	483	3778	3791	3652	3740.3	36.52	HW029	665	0	0	0	0.0	0.00
HW029	484	33	39	94	55.3	0.94	HW029	666	0	0	0	0.0	0.00
HW029	485	2438	2158	1957	2184.3	19.57	HW029	667	0	0	0	0.0	0.00
HW029	486	152	179	234	188.3	2.34	HW029	668	0	0	0	0.0	0.00
HW029	487	999	984	1334	1105.7	13.34	HW029	669	0	0	0	0.0	0.00
HW029	488	1104	1169	1118	1130.3	11.18	HW029	670	0	0	0	0.0	0.00
HW029	489	1726	1630	1398	1584.7	13.98	HW029	671	0	0	0	0.0	0.00
HW029	490	380	397	433	403.3	4.33	HW029	672	0	0	0	0.0	0.00
HW029	491	599	771	880	750.0	8.80	HW029	673	0	0	0	0.0	0.00
HW029	492	1338	1398	1489	1408.3	14.89	HW029	674	0	0	0	0.0	0.00

Hole ID	Depth	Reading 1	Reading 2	Reading 3	Average	Average/100	Hole ID	Depth	Reading 1	Reading 2	Reading 3	Average	Average/100
HW029	493	927	994	1007	976.0	10.07	HW029	675	0	0	0	0.0	0.00
HW029	494	3059	3454	3818	3443.7	38.18	HW029	676	0	0	0	0.0	0.00
HW029	495	1322	1422	1428	1390.7	14.28	HW029	677	0	0	0	0.0	0.00
HW029	496	450	503	591	514.7	5.91	HW029	678	0	0	0	0.0	0.00
HW029	497	1248	1280	1288	1272.0	12.88	HW029	679	0	0	0	0.0	0.00
HW029	498	80	83	91	84.7	0.91	HW029	680	0	0	0	0.0	0.00
HW029	499	181	136	208	175.0	2.08	HW029	681	0	0	0	0.0	0.00
HW029	500	3	1	0	1.3	0.00	HW029	682	0	0	0	0.0	0.00
HW029	501	255	336	325	305.3	3.25	HW029	683	0	0	0	0.0	0.00
HW029	502	292	275	365	310.7	3.65	HW029	684	0	0	0	0.0	0.00
HW029	503	517	407	339	421.0	3.39	HW029	685	0	0	0	0.0	0.00
HW029	504	30	101	79	70.0	0.79	HW029	686	0	0	0	0.0	0.00
HW029	505	544	605	524	557.7	5.24	HW029	687	0	0	0	0.0	0.00
HW029	506	398	415	476	429.7	4.76	HW029	688	0	0	0	0.0	0.00
HW029	507	336	416	474	408.7	4.74	HW029	689	0	0	0	0.0	0.00
HW029	508	301	398	346	348.3	3.46	HW029	690	0	0	0	0.0	0.00
HW029	509	500	543	482	508.3	4.82	HW029	691	0	0	0	0.0	0.00
HW029	510	610	713	628	650.3	6.28	HW029	692	0	0	0	0.0	0.00
HW029	511	1140	835	862	945.7	8.62	HW029	693	0	0	0	0.0	0.00
HW029	512	500	565	550	538.3	5.50	HW029	694	0	0	0	0.0	0.00
HW029	513	523	471	479	491.0	4.79	HW029	695	0	0	0	0.0	0.00
HW029	514	450	468	546	488.0	5.46	HW029	696	0	0	0	0.0	0.00
HW029	515	387	403	524	438.0	5.24	HW029	697	0	0	0	0.0	0.00
HW029	516	444	454	392	430.0	3.92	HW029	698	0	0	0	0.0	0.00
HW029	517	374	413	447	411.3	4.47	HW029	699	0	0	0	0.0	0.00
HW029	518	477	527	540	514.7	5.40	HW029	700	0	0	0	0.0	0.00
HW029	519	546	449	546	513.7	5.46	HW029	701	0	0	0	0.0	0.00
HW029	520	459	520	495	491.3	4.95	HW029	702	0	0	0	0.0	0.00
HW029	521	459	474	378	437.0	3.78	HW029	703	0	0	0	0.0	0.00
HW029	522	561	568	549	559.3	5.49	HW029	704	0	0	0	0.0	0.00
HW029	523	514	602	620	578.7	6.20	HW029	705	0	0	0	0.0	0.00
HW029	524	1049	950	908	969.0	9.08	HW029	706	0	0	0	0.0	0.00
HW029	525	1624	1457	1478	1519.7	14.78	HW029	707	0	0	0	0.0	0.00
HW029	526	754	733	722	736.3	7.22	HW029	708	0	0	0	0.0	0.00
HW029	527	1115	1169	807	1030.3	8.07	HW029	709	0	0	0	0.0	0.00
HW029	528	527	578	731	612.0	7.31	HW029	710	0	0	0	0.0	0.00
HW029	529	673	711	625	669.7	6.25	HW029	711	0	0	0	0.0	0.00
HW029	530	564	588	584	578.7	5.84	HW029	712	0	0	0	0.0	0.00
HW029	531	608	620	556	594.7	5.56	HW029	713	0	0	0	0.0	0.00
HW029	532	404	435	362	400.3	3.62	HW029	714	0	0	0	0.0	0.00
HW029	533	724	745	781	750.0	7.81	HW029	715	0	0	0	0.0	0.00
HW029	534	661	683	756	700.0	7.56	HW029	716	0	0	0	0.0	0.00
HW029	535	701	693	704	699.3	7.04	HW029	717	0	0	0	0.0	0.00
HW029	536	533	579	648	586.7	6.48	HW029	718	0	0	0	0.0	0.00
HW029	537	359	383	394	378.7	3.94	HW029	719	0	0	0	0.0	0.00
HW029	538	485	463	468	472.0	4.68	HW029	720	0	0	0	0.0	0.00
HW029	539	497	508	814	606.3	8.14	HW029	721	0	0	0	0.0	0.00
HW029	540	286	298	296	293.3	2.96	HW029	722	0	0	0	0.0	0.00
HW029	541	567	581	613	587.0	6.13	HW029	723	0	0	0	0	0.00
HW029	542	880	870	860	870.0	8.60	HW029	724	0	0	0	0	0.00

11.6 **Appendix F: CIPW normative results (wt %)**

Abbreviations of concern: ap-apatite, cm-chromite, ilm- ilmenite, mt- magnetite, q- quartz, c-calcite, or- orthoclase, ab- albite, an- anorthite, wo- wollastonite, en- enstatite, fs- ferrosilite, fo-forsterite, fa-fayalite, gh- goethite, di- diopside, hd- hedenbergite.

Sample #	ap	cm	ilm	mt	pf	q	c	als	or	ab	an	lc
HW29/362.1	0.24	0.03	1.81	0.91	0	79.64	0	4.81	5.16	0.34	0.75	0
HW29/363.55	0.12	0.28	33.83	9.20	0	0	3.91	0	0	0	0	2.27
HW29/371.3	0.05	0.03	0.41	0.84	0	0	0	5.96	2.49	32.48	40.24	0
HW29/378.5	0.05	0.06	0.75	1.50	0	0	0	0	0.88	19.63	38.72	0
HW29/383.15	0.05	0.06	0.57	1.55	0	0	0	0	0.89	17.78	35.45	0
HW29/389.4	0.05	0.04	0.27	0.90	0	0	0	0	0.96	24.31	46.74	0
HW29/394.5	0.05	0.05	0.25	0.69	0	1.66	0	0	1.09	24.42	52.31	0
HW29/397.02	0.05	0.06	0.53	1.55	0	0	0	0	0.83	16.99	34.64	0
HW29/405.3	0.05	0.06	0.54	1.35	0	0	0	0	0.95	18.98	37.36	0
HW29/421.4	0.05	0.06	0.38	1.28	0	0	0	0	0.89	19.76	40.03	0
HW29/421.45	0.05	0.06	0.42	1.37	0	0	0	0	0.83	18.01	37.41	0
HW29/447.9	0.05	0.03	0.29	0.68	0	0	0	0	1.62	25.02	53.35	0
HW29/457.8	0.05	0.03	1.73	1.41	0	0	0	0	1.30	20.97	48.55	0
HW29/457.8	0.05	0.03	1.09	1.47	0	0	0	0	1.19	19.33	45.56	0
HW29/462.38	0.10	0.03	0.29	0.81	0	0	0	0	1.31	23.83	49.97	0
HW29/469.1	0.05	0.04	0.38	1.06	0	0	0	0	1.37	19.76	49.75	0
HW29/470.2	0.05	0.01	0.55	1.15	0	0	0	0	1.01	19.24	49.02	0
HW29/487.2	0.05	0.03	0.34	1.30	0	0	0	0	1.19	20.47	49.66	0
HW29/505.57	0.05	0.06	0.46	1.06	0	0	0	0	1.01	19.47	47.07	0
HW29/515.8	0.05	0.06	0.44	1.17	0	0	0	0	1.13	18.86	44.03	0
HW29/516	0.07	0.06	0.49	1.24	0	0	0	0	1.18	21.79	41.21	0
HW29/526.45	0.05	0.07	0.46	1.33	0	0	0	0	1.20	17.49	39.27	0
HW29/559.7	0.05	0.07	0.40	1.62	0	0	0	0	0.83	14.43	34.58	0
HW29/576.3	0.05	0.10	0.42	2.03	0	0	0	0	0.59	10.41	25.62	0
HW29/584.4	0.05	0.10	0.33	1.12	0	0	0	0	1.56	12.49	41.55	0
HW29/586.8	0.05	0.13	0.43	2.05	0	0	0	0	0.59	7.58	19.78	0
HW29/589.8	0.05	0.07	0.25	1.77	0	0	0	0	0.54	8.92	27.68	0
HW29/591.1	0.05	0.10	0.39	1.16	0	0	0	0	0.90	14.09	41.05	0
HW29/593.2	0.05	0.02	0	0.46	0.51	0	0	0	0	0	57.31	0
HW29/595.35	0.07	0.09	0.44	1.89	0	0	0	0	1.00	11.30	27.10	0
HW29/601.35	0.05	0.04	0.21	2.29	0	0	0	0	0.48	8.02	22.92	0
HW29/608.1	0.86	0.03	3.63	1.91	0	0	0	0	1.20	16.09	28.30	0
HW29/608.25	0.07	0.03	0.83	1.85	0	0	0	0	1.42	16.89	28.12	0
HW29/608.59	0.09	0.03	0.70	1.80	0	0	0	0	1.95	18.65	31.90	0
HW29/614.05	0.63	0.03	0.60	1.47	0	0	0	0	1.39	19.87	38.27	0
HW29/614.25	0.05	0.06	0.45	1.88	0	0	0	0	0.61	9.71	26.79	0
HW29/614.7	0.05	0.07	0.53	2.21	0	0	0	0	0.71	6.37	18.69	0
HW29/614.8	0.22	0.03	0.49	2.20	0	0	0	0	1.54	12.07	31.04	0
HW29/622.49	0.05	0.03	0.35	1.09	0	0	0	0	0.84	16.16	38.19	0
HW29/625.4	0.05	0.04	0.42	1.42	0	0	0	0	0.65	11.49	28.18	0
HW29/634.5	0.05	0.03	0.27	1.42	0	0	0	0	0.96	16.79	40.66	0
HW29/634.7	0.02	0.02	0.29	1.52	0	0	0	0	0.90	16.73	40.25	0
HW29/635.2	0.02	0.03	0.27	1.43	0	0	0	0	0.90	19.10	41.38	0
HW29/636.78	0.05	0.03	0.36	1.60	0	0	0	0	0.65	12.33	28.80	0
HW29/637.8	0.05	0.03	0.48	1.86	0	0	0	0	0.78	13.27	29.94	0
HW29/651.9	0.05	0.06	0.48	1.85	0	0	0	0	0.36	7.56	19.88	0
HW29/653.3	0.02	0.06	0.36	1.64	0	0	0	0	0.48	9.54	24.83	0
HW29/659.25	0.05	0.04	0.44	1.23	0	0	0	0	0.89	16.02	37.75	0
HW29/680	0.03	0.04	0	1.20	0.14	0	0	0	0	0	0	0.06
HW29/695	0.03	0.02	0.13	1.10	0	0	0	0	0	0	0	0.06
HW29/716	0.05	0.03	0.27	0.76	0	0	0	0	1.33	21.85	55.48	0
HW29/721.3	0.05	0.03	0.31	0.90	0	0	0	0	1.08	18.75	47.98	0
HW30/440.4	0.02	1.83	12.27	5.74	0	0	2.90	0	0	0	21.79	0.62

Sample #	ne	di	hd	wo	en	fs	fo	fa	gh	ak	Feak	per
HW29/362.1	0	0	0	0	0	0	0.48	6.41	0	0	0	0
HW29/363.55	0.43	0	0	0	0	0	-7.71	54.23	0.60	0	0	5.03
HW29/371.3	0	0	0	0	4.36	3.04	6.00	4.61	0	0	0	0
HW29/378.5	0	6.56	5.18	0	14.31	12.97	0.11	0.11	0	0	0	0
HW29/383.15	0	8.06	5.78	0	15.91	13.08	0.43	0.39	0	0	0	0
HW29/389.4	0	6.63	4.40	0	8.04	6.11	1.14	0.96	0	0	0	0
HW29/394.5	0	5.16	4.57	0	4.85	4.92	0	0	0	0	0	0
HW29/397.02	0	10.19	7.14	0	14.17	11.39	1.30	1.15	0	0	0	0
HW29/405.3	0	11.03	7.91	0	10.66	8.77	1.24	1.12	0	0	0	0
HW29/421.4	0	8.05	5.64	0	12.52	10.05	0.69	0.61	0	0	0	0
HW29/421.45	0	10.78	7.41	0	13.42	10.59	0.22	0.19	0	0	0	0
HW29/447.9	0	4.27	3.23	0	5.61	4.85	0.52	0.49	0	0	0	0
HW29/457.8	0	3.98	4.27	0	4.62	5.68	3.49	4.73	0	0	0	0
HW29/457.8	0	4.33	4.07	0	7.83	8.44	3.03	3.60	0	0	0	0
HW29/462.38	0	5.97	4.33	0	6.26	5.21	0.99	0.91	0	0	0	0
HW29/469.1	0	6.49	5.28	0	5.42	5.05	2.64	2.71	0	0	0	0
HW29/470.2	0	6.23	5.03	0	7.32	6.77	2.12	2.16	0	0	0	0
HW29/487.2	0	4.04	3.85	0	4.03	4.40	4.83	5.81	0	0	0	0
HW29/505.57	0	7.32	5.29	0	9.29	7.70	0.64	0.58	0	0	0	0
HW29/515.8	0	8.13	5.77	0	10.30	8.39	0.89	0.80	0	0	0	0
HW29/516	0	9.04	6.49	0	6.74	5.56	3.59	3.26	0	0	0	0
HW29/526.45	0	9.42	6.43	0	13.20	10.33	0.40	0.35	0	0	0	0
HW29/559.7	0	6.40	3.71	0	22.98	15.25	0.34	0.25	0	0	0	0
HW29/576.3	0	6.41	3.53	0	28.61	18.04	2.46	1.71	0	0	0	0
HW29/584.4	0	11.44	4.99	0	14.11	7.05	3.36	1.85	0	0	0	0
HW29/586.8	0	8.59	3.88	0	36.18	18.74	1.98	1.13	0	0	0	0
HW29/589.8	0	7.64	2.96	0	20.84	9.26	13.42	6.57	0	0	0	0
HW29/591.1	0	9.87	4.37	0	15.22	7.72	3.27	1.83	0	0	0	0
HW29/593.2	0	9.52	9.69	19.73	0	0	0	0	3.00	0	0	0
HW29/595.35	0	7.23	3.93	0	27.62	17.25	1.23	0.85	0	0	0	0
HW29/601.35	0	5.92	2.42	0	9.05	4.25	29.22	15.11	0	0	0	0
HW29/608.1	0	15.94	12.82	0	6.06	5.59	4.28	4.35	0	0	0	0
HW29/608.25	0	11.58	8.60	0	13.03	11.10	3.34	3.14	0	0	0	0
HW29/608.59	0	5.99	4.61	0	15.80	13.97	2.28	2.22	0	0	0	0
HW29/614.05	0	9.11	9.50	0	7.15	8.56	1.46	1.92	0	0	0	0
HW29/614.25	0	6.95	3.47	0	32.18	18.44	0.26	0.16	0	0	0	0
HW29/614.7	0	10.22	5.15	0	32.05	18.53	3.30	2.10	0	0	0	0
HW29/614.8	0	7.25	5.74	0	16.31	14.82	4.72	4.72	0	0	0	0
HW29/622.49	0	13.47	6.21	0	13.99	7.40	1.42	0.83	0	0	0	0
HW29/625.4	0	17.30	7.69	0	20.22	10.31	1.44	0.81	0	0	0	0
HW29/634.5	0	8.44	6.17	0	10.03	8.41	3.52	3.25	0	0	0	0
HW29/634.7	0	8.78	6.76	0	9.11	8.05	4.26	4.14	0	0	0	0
HW29/635.2	0	7.30	5.55	0	8.57	7.47	4.49	4.31	0	0	0	0
HW29/636.78	0	12.35	6.31	0	22.53	13.20	1.08	0.70	0	0	0	0
HW29/637.8	0	11.63	8.01	0	17.40	13.74	2.05	1.78	0	0	0	0
HW29/651.9	0	20.60	10.09	0	24.48	13.75	1.15	0.71	0	0	0	0
HW29/653.3	0	18.24	8.72	0	21.48	11.79	1.76	1.06	0	0	0	0
HW29/659.25	0	13.33	7.44	0	12.62	8.07	1.24	0.87	0	0	0	0
HW29/680	0	45.74	18.63	0	0	0	4.89	2.52	25.19	1.09	0.43	0
HW29/695	0.06	43.74	12.55	0	0	0	9.54	3.46	19.08	7.99	2.23	0
HW29/716	0	3.56	2.59	0	6.71	5.60	0.93	0.86	0	0	0	0
HW29/721.3	0	8.80	5.12	0	9.45	6.31	0.71	0.52	0	0	0	0
HW30/440.4	6.63	0	0	0	0.00	0.00	5.02	39.52	5.85	0	0	0

Sample #	ap	cm	ilm	mt	q	als	or	ab	an	lc	ne	di	hd	en	fs	fo	fa	gh
HW25/417.5	0.05	0.08	0.24	0.75	0.45	0	0.67	16.50	51.19	0	0	11.41	6.25	7.62	4.79	0	0	0
HW25/426.3	0.05	0.06	0.23	0.97	0	0	1.02	17.18	50.42	0	0	5.24	3.06	12.21	8.16	0.79	0.58	0
HW25/433.53	0.05	0.08	0.25	0.97	0	0	0.84	15.62	46.15	0	0	8.79	4.06	13.84	7.33	1.29	0.75	0
HW25/440.9	0.05	0.08	0.24	0.99	0	0	1.28	19.25	42.84	0	0	8.94	4.17	10.46	5.60	3.84	2.26	0
HW25/449.2	0.02	0.06	0.48	2.34	0	0	0.48	9.89	19.68	0	0	11.14	7.35	25.31	19.15	2.23	1.86	0
HW25/454.3	0.05	0.10	0.25	1.06	0	0	0.65	14.52	42.79	0	0	9.65	4.27	16.69	8.46	0.97	0.54	0
HW25/462.7	0.02	0.06	0.21	0.71	0	0	0.77	17.71	52.70	0	0	8.06	3.68	9.49	4.98	1.01	0.58	0
HW25/472.8	0.05	0.11	0.36	1.25	0	0	1.73	12.05	34.71	0	0	17.03	8.41	14.55	8.24	0.91	0.57	0
HW25/479.71	0.05	0.11	0.42	1.05	0	0	1.63	20.51	33.83	0	0	19.85	9.66	0.89	0.50	7.12	4.38	0
HW25/480.3	0.05	0.11	0.26	0.83	0	0	2.34	24.74	36.62	0	0	14.34	5.47	2.13	0.93	8.21	3.96	0
HW25/493.53	0.05	0.12	0.31	0.95	0	0	0.89	13.32	40.22	0	0	16.30	6.33	13.34	5.94	1.51	0.74	0
HW25/497.6	0.05	0.11	0.23	0.89	0	0	1.93	15.67	45.50	0	0	10.02	3.90	10.22	4.56	4.65	2.29	0
HW25/503.49	0.05	0.13	0.12	1.13	0	0	0.63	6.30	47.52	0	0	1.68	0.47	15.03	4.78	16.42	5.76	0
HW25/512.5	0.05	0.20	0.22	1.02	0	0	1.41	16.06	38.08	0	0	11.89	4.11	11.52	4.57	7.56	3.30	0
HW25/516.2	0.02	0.20	0.12	1.29	0	0	0.31	5.73	35.30	0	0	0.64	0.17	36.27	11.19	6.54	2.22	0
HW25/520.14	0.02	0.15	0.16	0.63	0	0	0.61	12.83	54.21	0	0	10.40	3.07	8.64	2.93	4.62	1.72	0
HW25/522.3	0.02	0.11	0.14	0.80	0	0	1.10	12.30	51.60	0	0	9.54	3.16	7.28	2.77	7.87	3.30	0
HW25/535.1	0.03	0.10	0.10	0.82	0	0	0	0	48.35	0.10	1.43	25.93	8.11	0.00	0	9.11	3.60	2.31
HW25/545.5	0.05	0.17	0.26	1.45	1.23	0	0.49	8.53	24.90	0	0	4.84	1.51	41.63	14.94	0	0	0
HW25/570.5	0.05	0.05	0.15	2.26	0	5.93	0.26	0.94	18.50	0	0	0	0	17.30	6.60	33.76	14.20	0
HW25/577.28	0.05	0.06	0.19	1.88	0	0	0.96	8.35	28.95	0	0	5.86	2.30	14.92	6.70	19.92	9.86	0
HW25/591.56	0.05	0.08	0.16	1.90	0	0	0.95	2.80	20.69	0	0	7.88	2.64	31.07	11.95	13.93	5.90	0
HW25/600.5	0.05	0.08	0.27	0.96	0	0	1.64	18.14	43.33	0	0	3.89	1.47	18.14	7.86	2.82	1.35	0
HW25/602.1	0.05	0.10	0.36	1.25	0	0	0.89	15.22	34.46	0	0	6.31	2.38	25.86	11.18	1.78	0.85	0
HW25/602.6	0.05	0.16	0.36	1.98	0	0	1.02	5.99	18.28	0	0	5.90	2.28	38.86	17.20	5.32	2.59	0
HW24/268.2	0.05	0.08	0.23	0.72	0	0	1.20	19.75	50.16	0	0	8.66	3.92	7.50	3.90	2.44	1.40	0
HW24/268.2	0.05	0.08	0.27	0.82	0	0	0.85	18.90	46.98	0	0	11.51	5.48	7.69	4.20	2.30	1.38	0
HW24/275.9	0.05	0.06	0.27	0.63	0.20	0	0.97	18.34	47.77	0	0	12.35	4.90	9.24	4.20	0	0	0
HW24/276.5	0.05	0.06	0.23	1.71	0	0	0.94	17.74	49.67	0	0	5.41	5.34	5.77	6.54	5.63	7.02	0
HW24/281.1	0.05	0.03	0.28	0.64	0	0	1.41	20.98	52.43	0	0	10.83	5.78	1.62	0.99	3.18	2.15	0
HW24/290.45	0.05	0.07	0.27	1.09	0	0	0.83	15.98	45.53	0	0	13.03	7.64	7.62	5.13	2.68	1.99	0
HW24/297	0.05	0.11	0.37	0.85	0.15	0	0.67	13.16	34.16	0	0	19.81	6.30	16.04	5.85	0	0	0
HW24/297.8	0.05	0.10	0.30	1.71	0	0	0.47	9.31	25.05	0	0	10.11	4.29	32.38	15.76	0.91	0.49	0
HW24/302.85	0.05	0.06	0.25	1.52	0	0	0.65	15.48	38.70	0	0	12.09	7.60	10.83	7.81	4.46	3.54	0
HW24/306	0.05	0.14	0.14	1.50	0	2.31	1.92	3.48	36.01	0	0	0	0	20.20	6.69	20.79	7.59	0
HW24/311.2	0.05	0.06	0.10	2.22	0	0	0.97	3.69	39.12	0	0	0.94	0.41	9.49	4.79	26.96	15.01	0
HW24/314.5	0.02	0.26	0.15	1.11	0	0	0.24	7.85	41.08	0	0	0.60	0.16	31.07	9.23	6.69	2.19	0
HW24/319.2	0.05	0.11	0.16	0.86	0	0	0.91	10.69	56.01	0	0	4.71	1.54	7.52	2.82	10.72	4.43	0
HW24/321.52	0.05	0.16	0.10	1.15	0	0	1.03	1.29	37.38	0	0	1.64	0.34	19.29	4.56	24.01	6.25	0
HW24/328.5	0.02	0.17	0.14	0.99	0	0	0.30	10.22	48.57	0	0	3.61	1.13	20.59	7.37	5.52	2.18	0
HW24/332.65	0.02	0.20	0.21	1.53	0	0	0.60	5.87	24.22	0	0	4.69	1.34	41.36	13.51	5.36	1.93	0
HW24/336.15	0.02	0.14	0.12	1.07	0	0	4.36	6.42	43.51	0	0	5.58	1.61	14.79	4.91	12.78	4.68	0
HW24/345.55	0.02	0.27	0.21	1.40	0	0	0.30	6.78	25.97	0	0	9.39	2.67	33.73	11.02	6.05	2.18	0
HW24/347.65	0.02	0.12	0.10	0.87	0	0	1.16	9.99	52.73	0	0	2.54	0.76	15.66	5.36	7.75	2.92	0
HW24/347.9	0.05	0.23	0.18	1.56	0	0.06	0.55	5.86	32.16	0	0	0	0	33.84	12.17	10.19	4.04	0
HW24/348.4	0.03	0.28	0.22	2.12	0	0	0.32	2.46	18.51	0	0	3.96	1.66	40.77	19.65	7.24	3.84	0
HW24/352.3	0.02	0.18	0.14	1.52	0	0.86	0.55	5.99	32.28	0	0	0	0	33.46	12.40	8.92	3.64	0
HW24/353.45	0.05	0.26	0.27	2.10	0	0	0.73	2.88	10.28	0	0	10.77	3.89	46.02	19.05	3.32	1.51	0
HW24/353.5	0.02	0.25	0.29	2.16	0	0	0.48	2.05	7.50	0	0	7.25	2.50	53.87	21.34	1.58	0.69	0
HW24/360.4	0.02	0.24	0.25	2.06	0	0	0.54	4.46	12.96	0	0	6.37	2.37	47.99	20.49	1.50	0.71	0
HW24/360.75	0.02	0.19	0.25	1.53	0	0	0.48	9.58	27.67	0	0	6.81	2.43	34.55	14.17	2.19	0.99	0
HW24/370.5	0.16	0.13	0.38	2.69	3.82	0	1.12	6.55	6.86	0	0	2.81	1.55	45.26	28.68	0	0	0
HW24/383.4	0.02	0.14	0.17	0.95	0	0	0.36	13.79	41.68	0	0	10.90	3.69	17.65	6.85	2.66	1.14	0
HW24/386.2	0.02	0.08	0.17	0.72	0	0	0.79	19.98	41.75	0	0	13.76	4.50	9.75	3.66	3.41	1.41	0
HW24/391.2	0.02	0.13	0.23	1.86	0	0	0.30	5.41	18.32	0	0	4.86	1.62	43.98	16.79	5.26	2.21	0
HW24/391.7	0.02	0.12	0.20	2.06	0	0	1.22	4.62	17.13	0	0	7.57	2.74	31.01	12.89	13.99	6.41	0
HW24/394.5	0.05	0.08	0.12	2.05	0	1.04	0.13	3.17	21.79	0	0	0	0	34.20	13.37	16.76	7.22	0
HW24/397.4	0.05	0.06	0.23	1.07	1.22	0	0.84	18.24	33.90	0	0	10.36	4.07	21.10	9.50	0	0	0
HW24/405.8	0.05	0.06	0.16	2.05	0	0	0.31	6.24	21.63	0	0	3.20	1.20	31.05	13.40	13.99	6.65	0
HW24/415.2	0.05	0.07	0.23	1.03	0	0	0.66	17.28	36.06	0	0	10.60	3.81	19.33	7.97	2.00	0.91	0
HW24/423.2	0.05	0.12	0.23	0.98	0	0	0.54	14.62	44.31	0	0	5.40	1.93	20.15	8.27	2.36	1.07	0
HW24/435.72	0.05	0.12	0.23	0.90	0	0	0.67	14.37	46.60	0	0	0.00	3.92	13.46	6.05	2.43	1.20	0
HW24/439.6	0.05	0.10	0.25	0.98	0	0	0.83	13.82	47.82	0	0	8.27	3.41	13.05	6.17	3.82	1.99	0
HW24/440.6	0.05	0.09	0.20	1.05	0	0	0.67	12.18	44.55	0	0	7.08	2.61	17.96	7.59	4.09	1.91	0

11.7 **Appendix G: tenor results**

The tenors were calculated by an unpublished spreadsheet created by A.J. Naldrett.

Sample #	depth_from	wt% Chalcopy	wt% pentlandite	wt% pyrrhotite	if j neg opt+cmd+t	Total sulfide	Factor	100% S	100% Ni	100% Cu	100% Rh	100% Pd	100% Au	100% Pt
HW029	547.5	0.48	0.72	0.52	0.72	1.73	57.92	35.33	14.89	9.62	0.00	231.11	24.10	128.01
HW029	548	0.67	0.66	0.11	0.66	1.44	69.35	31.21	16.44	16.02	0.00	332.21	39.60	180.32
HW029	548.5	0.29	0.66	1.02	0.66	1.98	50.52	36.38	11.92	5.10	0.00	114.18	9.09	61.89
HW029	549	0.43	0.67	0.44	0.67	1.53	65.25	35.24	15.47	9.59	0.00	232.31	23.43	134.42
HW029	549.5	1.46	1.69	2.12	1.69	5.26	19.01	35.93	11.39	9.56	0.00	210.06	19.20	112.92
HW029	550	1.00	1.22	1.87	1.22	4.09	24.46	36.20	10.59	8.44	0.00	183.93	16.90	86.83
HW029	550.5	0.73	0.87	1.97	0.87	3.57	28.01	36.69	8.68	7.03	0.00	151.52	15.07	84.02
HW029	551	0.32	0.40	-0.02	0.39	0.69	144.44	33.22	20.51	16.03	0.00	361.10	35.97	168.27
HW029	552.47	0.18	0.48	-0.17	0.47	0.48	206.33	30.95	35.28	12.83	0.00	223.86	22.08	113.07
HW029	553.5	0.13	0.21	0.50	0.21	0.84	118.94	36.87	8.71	5.49	0.00	125.48	13.80	92.77
HW029	554	0.24	0.34	0.12	0.34	0.69	144.52	34.68	17.20	11.76	0.00	275.30	38.73	211.72
HW029	554.5	0.14	0.14	0.20	0.14	0.47	212.23	36.08	10.23	9.93	0.00	51.57	12.31	14.86
HW029	555	0.12	0.35	0.42	0.35	0.89	112.76	36.08	13.87	4.81	0.00	192.25	12.74	108.25
HW029	555.33	0.09	0.30	0.48	0.30	0.88	114.05	36.50	12.26	3.62	0.00	172.22	8.90	117.48
HW029	556	0.11	0.31	0.23	0.31	0.65	154.17	35.46	16.73	5.98	0.00	293.70	10.79	194.26
HW029	556.5	0.02	0.24	0.19	0.24	0.45	222.51	35.60	19.25	1.27	0.00	206.72	2.89	150.86
HW029	557	0.06	0.18	0.18	0.18	0.42	238.88	35.83	15.43	4.71	0.00	107.97	18.87	71.66
HW029	557.5	0.15	0.22	-0.03	0.22	0.34	294.73	32.42	23.70	14.85	0.00	147.36	25.64	75.45
HW029	558	0.07	0.18	1.09	0.18	1.34	74.44	37.96	4.82	1.86	0.00	17.79	2.61	15.71
HW029	559.5	0.14	0.20	0.02	0.20	0.35	283.44	34.01	19.98	13.44	0.00	128.68	29.48	102.89
HW029	560.4	0.14	0.28	-0.05	0.27	0.37	268.05	32.17	26.80	13.21	0.00	254.91	19.84	182.54
HW029	560.6	0.04	0.28	0.19	0.28	0.51	196.33	35.34	19.83	2.63	0.00	166.88	4.52	154.91
HW029	560.8	0.11	0.16	0.15	0.16	0.42	237.65	35.65	13.17	9.41	0.00	52.52	9.98	37.07
HW029	561	0.14	0.19	0.38	0.19	0.71	140.74	36.59	9.36	6.88	0.00	42.50	5.49	26.74
HW029	561.2	0.08	0.22	0.25	0.22	0.56	179.93	35.99	14.11	5.27	0.00	64.60	5.04	47.68
HW029	561.6	0.18	0.45	0.52	0.45	1.14	87.85	36.02	13.88	5.33	0.00	62.64	7.99	38.92
HW029	561.8	0.15	0.26	0.18	0.26	0.60	168.06	35.29	15.66	8.86	0.00	98.82	19.83	52.10
HW029	562	0.15	0.34	0.12	0.34	0.61	164.94	34.64	19.63	8.74	0.00	152.74	12.70	108.04
HW029	562.32	0.15	0.22	0.02	0.22	0.38	261.85	34.04	20.01	13.17	0.00	85.36	20.69	55.25
HW029	562.51	0.13	0.19	0.74	0.19	1.07	93.52	37.41	6.42	4.25	0.00	56.48	7.86	30.77
HW029	562.7	0.73	0.51	0.12	0.51	1.36	73.45	34.52	13.33	18.51	0.00	293.81	71.54	205.67
HW029	563	0.14	0.30	0.08	0.30	0.52	191.35	34.44	20.47	9.18	0.00	379.82	19.33	175.65
HW029	563.6	0.17	0.20	0.02	0.20	0.38	262.01	34.06	18.63	14.93	0.00	46.11	16.51	34.32
HW029	563.8	0.16	0.15	0.07	0.10	0.37	267.86	26.79	19.31	14.33	0.00	25.45	12.05	18.21
HW029	564	0.13	0.24	0.04	0.24	0.41	243.85	34.14	21.12	10.80	0.00	54.38	16.34	36.33
HW029	564.2	0.16	0.35	0.36	0.35	0.87	115.60	35.84	14.28	6.29	0.00	91.09	9.25	53.87
HW029	564.4	0.08	0.35	0.81	0.35	1.24	80.53	37.04	10.03	2.21	0.00	92.61	2.50	47.43
HW029	564.6	0.20	0.29	0.35	0.29	0.83	119.81	35.94	12.16	8.35	0.00	224.65	12.94	108.43
HW029	564.86	0.29	0.31	1.58	0.31	2.18	45.84	37.59	5.09	4.58	0.00	100.85	6.10	52.49
HW029	565.23	0.19	0.19	0.67	0.19	1.05	95.27	37.16	6.46	6.26	0.00	114.81	7.15	62.02
HW029	565.42	0.34	0.32	1.19	0.32	1.85	53.92	37.21	6.12	6.34	0.00	110.00	8.20	55.54
HW029	565.6	0.28	0.35	1.15	0.35	1.77	56.35	37.19	6.90	5.36	0.00	151.58	9.41	71.00
HW029	565.8	0.45	0.54	2.01	0.54	3.00	33.30	37.30	6.43	5.13	0.00	180.17	6.93	95.91
HW029	566	0.38	0.33	0.59	0.33	1.30	77.16	36.27	9.03	10.07	0.00	202.93	11.65	78.70
HW029	574	0.08	0.09	0.11	0.09	0.28	359.41	35.94	10.85	10.21	0.00	0.36	14.74	0.04
HW029	575	0.07	0.05	0.15	0.05	0.27	367.88	36.79	6.73	8.94	0.00	0.04	10.30	0.04
HW029	579.5	0.10	0.07	0.21	0.07	0.38	263.10	36.83	6.60	8.74	0.00	0.26	11.05	1.58
HW029	580	0.67	0.25	1.32	0.25	2.24	44.68	37.09	3.97	10.32	0.00	6.93	15.01	9.34
HW029	580.44	0.61	0.28	1.14	0.28	2.03	49.23	36.92	4.92	10.34	0.00	63.76	35.30	37.61
HW029	584	0.56	0.30	0.96	0.30	1.82	54.83	36.74	5.92	10.50	0.00	18.20	4.55	9.92
HW029	585	0.26	0.18	0.40	0.18	0.85	117.49	36.42	7.65	10.69	0.00	14.33	23.03	12.81
HW029	585.5	0.11	0.11	0.06	0.11	0.29	350.59	35.06	14.06	13.04	0.00	10.87	15.78	11.92
HW029	586.5	0.10	0.11	0.08	0.11	0.28	353.39	35.34	13.18	11.94	0.00	9.54	14.49	9.19
HW029	587	0.12	0.11	0.11	0.11	0.34	296.58	35.59	11.71	11.92	0.00	8.90	14.24	8.90
HW029	587.5	0.14	0.11	0.16	0.11	0.42	239.93	35.99	9.65	11.49	0.00	4.56	15.36	6.00
HW029	588.5	0.17	0.13	0.18	0.13	0.47	211.22	35.91	9.48	12.40	0.00	9.72	17.32	9.29
HW029	589.21	0.15	0.13	0.12	0.13	0.39	253.36	35.47	11.38	13.38	0.00	18.24	22.04	12.92
HW029	591.96	0.10	0.12	0.07	0.12	0.28	350.96	35.10	14.88	11.58	0.00	9.48	16.85	8.42
HW029	592.5	0.14	0.11	0.11	0.11	0.37	273.24	35.52	11.01	13.47	0.00	13.94	22.68	10.66
HW029	593	0.16	0.08	0.17	0.08	0.41	241.63	36.24	6.57	13.68	0.00	210.70	44.22	94.72
HW029	594.2	0.78	0.33	0.02	0.33	1.13	88.19	34.39	10.32	23.81	0.00	130.52	93.92	79.81
HW029	594.4	0.55	0.24	0.02	0.24	0.81	122.91	34.41	10.61	23.23	0.00	169.61	127.21	95.74

Sample #	depth_from	wt% Chalcopy	wt% pentlandite	wt% pyrrhotite	if j neg opt+cmd+t	Total sulfide	Factor	100% S	100% Ni	100% Cu	100% Rh	100% Pd	100% Au	100% Pt
HW029	595.2	0.02	0.24	0.59	0.24	0.86	116.21	37.19	10.05	0.99	0.00	3.14	1.28	4.07
HW029	595.4	0.03	0.20	0.16	0.20	0.39	254.52	35.63	17.92	2.88	0.00	16.54	4.07	13.74
HW029	596.4	0.27	0.32	0.03	0.27	0.62	162.49	29.25	21.12	14.97	0.00	131.78	64.51	96.20
HW029	608.2	0.04	0.07	0.18	0.07	0.30	336.10	36.97	8.44	5.04	0.00	2.35	6.39	0.03
HW029	608.4	0.06	0.08	0.14	0.08	0.27	364.41	36.44	9.95	7.32	0.00	3.28	9.11	2.55
HW029	608.79	0.07	0.08	0.20	0.08	0.35	282.61	36.74	8.51	6.87	0.00	3.96	8.76	6.78
HW029	610.2	0.03	0.07	0.68	0.07	0.78	127.70	38.31	3.03	1.48	0.00	0.38	0.77	0.01
HW029	610.4	0.04	0.09	0.30	0.09	0.43	233.25	37.32	7.53	3.41	0.00	0.70	2.57	0.02
HW029	610.59	0.05	0.08	0.32	0.08	0.45	220.59	37.50	5.93	4.15	0.00	2.21	5.51	0.02
HW029	612.32	0.48	0.24	1.34	0.24	2.06	48.47	37.32	4.16	8.09	0.00	77.31	42.70	33.01
HW029	612.5	1.06	0.29	0.60	0.29	1.95	51.21	35.85	5.27	18.79	0.00	38.72	12.24	32.83
HW029	612.75	0.20	0.13	0.07	0.13	0.40	249.63	34.95	11.71	17.25	0.00	71.64	20.47	24.71
HW029	612.91	0.52	0.21	0.28	0.21	1.01	98.95	35.62	7.25	17.91	0.00	72.33	35.82	44.03
HW029	613.54	0.81	0.23	0.42	0.23	1.45	68.76	35.75	5.60	19.11	0.00	113.79	48.89	91.10
HW029	614	0.99	0.51	2.95	0.51	4.44	22.53	37.39	4.05	7.66	0.00	32.55	17.39	10.75
HW029	614.2	0.92	0.43	2.19	0.43	3.55	28.17	37.19	4.34	8.99	0.00	36.48	18.48	24.34
HW029	614.4	0.23	0.15	0.15	0.15	0.54	186.87	35.51	9.98	15.04	0.00	60.17	36.63	42.42
HW029	614.6	0.00	0.45	5.70	0.45	6.15	16.27	38.57	2.57	0.00	0.00	27.74	64.60	33.68
HW029	614.8	1.77	0.81	2.60	0.81	5.19	19.28	36.64	5.57	11.78	0.00	49.37	59.98	24.20
HW029	615.02	0.47	0.19	0.00	0.19	0.67	149.30	34.34	10.32	24.26	0.00	34.64	65.69	42.40
HW029	615.2	1.53	0.53	0.59	0.53	2.65	37.67	35.41	7.12	19.85	0.00	22.83	70.25	32.32
HW029	615.4	0.51	0.23	0.12	0.23	0.86	116.37	34.91	9.67	20.42	0.00	21.06	56.67	30.14
HW029	627.4	0.13	0.09	0.08	0.09	0.31	321.99	35.42	10.75	14.68	0.00	14.17	40.57	27.05
HW029	628.2	0.31	0.17	0.66	0.17	1.14	88.05	36.98	5.26	9.42	0.00	17.08	45.87	28.44
HW029	632.2	0.22	0.18	0.58	0.18	0.97	102.75	36.99	6.39	7.75	0.00	9.04	25.58	8.63
HW029	632.89	0.20	0.13	0.25	0.13	0.58	172.54	36.23	7.85	11.97	0.00	7.42	38.13	11.91
HW029	633.3	0.15	0.10	0.09	0.10	0.34	295.12	35.41	10.68	14.82	0.00	8.85	53.42	24.20
HW029	633.5	0.33	0.13	0.19	0.13	0.64	155.11	35.68	7.20	17.53	0.00	6.05	49.17	23.58
HW029	633.7	1.99	0.57	1.64	0.57	4.20	23.83	36.22	4.84	16.34	0.00	11.17	67.67	23.28
HW029	633.9	2.88	0.84	2.28	0.84	6.00	16.67	36.17	4.98	16.55	0.00	10.78	67.33	21.92
HW029	634.1	2.45	0.75	2.25	0.75	5.45	18.34	36.31	4.91	15.49	0.00	11.64	67.11	21.91
HW029	634.5	1.02	0.34	0.80	0.34	2.16	46.28	36.10	5.55	16.29	0.00	11.11	69.89	23.60
HW029	634.7	2.48	0.85	2.12	0.85	5.45	18.36	36.17	5.55	15.70	0.00	10.93	67.02	22.77
HW029	635	2.58	0.80	2.02	0.80	5.40	18.53	36.13	5.26	16.51	0.00	11.12	67.99	21.95
HW029	635.2	1.83	0.61	1.42	0.61	3.85	25.96	36.09	5.58	16.36	0.00	11.53	66.47	22.46
HW029	635.4	1.50	0.49	1.20	0.49	3.18	31.42	36.13	5.43	16.24	0.00	12.97	78.54	24.91
HW029	635.6	2.54	0.88	1.24	0.88	4.66	21.45	35.60	6.73	18.77	0.00	15.31	85.58	28.31
HW029	635.75	2.39	0.79	2.22	0.79	5.40	18.51	36.29	5.20	15.24	0.00	12.48	78.13	24.25
HW029	636	2.50	0.85	2.38	0.85	5.73	17.45	36.30	5.25	15.08	0.00	11.81	64.39	21.46
HW029	636.2	1.97	0.71	1.10	0.71	3.78	26.46	35.72	6.64	17.96	0.00	15.42	80.16	24.55
HW029	636.62	0.59	0.22	0.16	0.22	0.97	103.36	35.14	7.97	20.88	0.00	26.77	59.84	26.56
HW029	637	0.23	0.14	0.06	0.14	0.43	232.59	34.89	11.16	18.51	0.00	19.54	73.73	27.21
HW029	637.29	0.19	0.09	0.01	0.09	0.29	344.32	34.43	11.33	22.07	0.00	13.77	45.79	26.51
HW029	637.56	0.30	0.10	0.09	0.10	0.48	207.33	35.25	7.01	21.36	0.00	6.22	66.14	3.11
HW029	637.77	1.55	0.54	2.64	0.54	4.74	21.12	36.95	4.08	11.28	0.00	12.59	55.96	18.88
HW029	637.95	1.59	0.52	1.48	0.52	3.58	27.92	36.29	5.11	15.33	0.00	13.51	63.65	24.82
HW029	638.14	1.30	0.44	1.21	0.44	2.95	33.91	36.28	5.29	15.16	0.00	13.97	67.14	25.84
HW029	638.33	2.08	0.71	1.03	0.71	3.82	26.19	35.62	6.63	18.75	0.00	17.60	89.32	32.09
HW029	638.53	2.02	0.68	1.62	0.68	4.32	23.15	36.11	5.62	16.13	0.00	14.42	74.76	25.00
HW029	638.72	1.85	0.59	2.03	0.59	4.47	22.38	36.49	4.70	14.28	0.00	12.40	61.56	21.60
HW029	639	0.77	0.26	1.24	0.26	2.28	43.93	36.90	4.13	11.64	0.00	11.25	46.79	19.77
HW029	639.23	1.28	0.44	0.66	0.44	2.38	41.95	35.66	6.59	18.54	0.00	22.07	80.75	34.40
HW029	640.2	0.16	0.10	0.06	0.10	0.31	318.32	35.02	10.85	17.89	0.00	37.88	62.07	64.30
HW029	640.4	0.35	0.15	0.13	0.15	0.62	160.17	35.24	8.59	19.22	0.00	26.91	76.72	43.73
HW029	645.6	0.20	0.12	0.46	0.12	0.78	127.63	37.01	5.59	8.67	0.00	35.10	65.60	23.48
HW029	646.6	0.12	0.07	0.11	0.07	0.31	326.84	35.95	8.37	13.60	0.00	38.24	45.76	43.14
HW029	646.8	0.15	0.08	0.10	0.08	0.34	297.33	35.68	8.65	15.46	0.00	43.11	60.36	56.19
HW029	647.4	0.12	0.09	0.30	0.09	0.51	194.62	36.98	6.05	8.31	0.00	20.63	34.64	26.47
HW029	648.2	0.11	0.09	0.24	0.09	0.44	229.41	36.71	7.41	8.67	0.00	20.19	48.41	30.05

100% Ir	100% Os	100% Ru	100% S	100% Ni	100% Cu	100% Rh	100% Pd	100% Au	100% Pt	100% Ir	100% Os	100% Ru	Total
0.00	0.00	0.00	353323.7	148859.3	96150.4	0.0	2311084.7	240955.2	1280074.5	0.0	0.0	0.0	4430447.8
0.00	0.00	0.00	312096.2	164370.7	160209.4	0.0	3322090.6	396015.4	1803222.4	0.0	0.0	0.0	6158004.6
0.00	0.00	0.00	363753.4	119230.3	51026.5	0.0	1141781.5	90938.4	618886.0	0.0	0.0	0.0	2385616.1
0.00	0.00	0.00	352374.2	154653.1	95924.1	0.0	2323059.5	234263.6	1344242.3	0.0	0.0	0.0	4504516.8
0.00	0.00	0.00	359286.7	113869.2	95619.7	0.0	2100591.5	191999.8	1129186.7	0.0	0.0	0.0	3990553.5
0.00	0.00	0.00	361983.0	105904.5	84381.2	0.0	1839264.8	169006.9	868270.0	0.0	0.0	0.0	3428810.3
0.00	0.00	0.00	366896.0	86822.7	70298.4	0.0	1515196.7	150679.4	840220.0	0.0	0.0	0.0	3030113.2
0.00	0.00	0.00	332212.1	205104.8	160328.4	0.0	3611000.6	359655.7	1682726.3	0.0	0.0	0.0	6351027.9
0.00	0.00	0.00	309490.7	352819.4	128335.5	0.0	2238649.6	220770.1	1130672.8	0.0	0.0	0.0	4380738.2
0.00	0.00	0.00	368704.4	87061.8	54948.8	0.0	1254784.2	137966.8	927707.8	0.0	0.0	0.0	2831173.8
0.00	0.00	0.00	346839.1	171974.4	117636.3	0.0	2753035.2	387303.6	2117163.5	0.0	0.0	0.0	5893952.0
0.00	0.00	0.00	360791.9	102295.1	99323.9	0.0	515720.1	123093.7	148561.4	0.0	0.0	0.0	1349786.0
0.00	0.00	0.00	360819.5	138690.0	48146.8	0.0	1922491.3	127414.4	1082458.5	0.0	0.0	0.0	3680020.5
0.00	0.00	0.00	364974.8	122608.7	36155.3	0.0	1722225.0	88962.6	1174762.8	0.0	0.0	0.0	3509689.4
0.00	0.00	0.00	354594.4	167276.1	59818.5	0.0	2936967.0	107920.0	1942560.8	0.0	0.0	0.0	5569136.9
0.00	0.00	0.00	356022.9	192474.9	12683.3	0.0	2067157.7	28926.9	1508646.8	0.0	0.0	0.0	4165912.4
0.00	0.00	0.00	358316.3	154314.9	47058.9	0.0	1079726.4	188713.2	716632.6	0.0	0.0	0.0	2544762.3
0.00	0.00	0.00	324202.6	236962.6	148543.7	0.0	1473648.1	256414.8	754507.8	0.0	0.0	0.0	3194279.6
0.00	0.00	0.00	379639.0	48162.0	18609.8	0.0	177909.3	26053.7	157066.3	0.0	0.0	0.0	807440.1
0.00	0.00	0.00	340130.3	199826.6	134351.5	0.0	1286826.4	294779.6	1028894.3	0.0	0.0	0.0	3284808.7
0.00	0.00	0.00	321657.0	268047.5	132147.4	0.0	2549131.9	198355.2	1825403.6	0.0	0.0	0.0	5294742.7
0.00	0.00	0.00	353400.3	198296.9	26308.7	0.0	1668835.0	45156.7	1549071.5	0.0	0.0	0.0	3841069.1
0.00	0.00	0.00	356470.0	131656.2	94108.1	0.0	525199.1	99811.6	370728.8	0.0	0.0	0.0	1577973.8
0.00	0.00	0.00	365932.1	93594.2	68823.4	0.0	425044.2	54889.8	267411.9	0.0	0.0	0.0	1275695.5
0.00	0.00	0.00	359867.7	141068.1	52720.6	0.0	645962.5	50381.5	476824.7	0.0	0.0	0.0	1726825.2
0.00	0.00	0.00	360177.4	138800.1	53323.8	0.0	626357.3	79941.8	389167.3	0.0	0.0	0.0	1647767.8
0.00	0.00	0.00	352926.5	156632.1	88567.7	0.0	988194.2	198311.1	520986.7	0.0	0.0	0.0	2305618.4
0.00	0.00	0.00	346380.1	196282.1	87419.7	0.0	1527371.4	127006.0	1080376.1	0.0	0.0	0.0	3364835.5
0.00	0.00	0.00	340409.5	200056.0	131712.3	0.0	853642.3	206864.2	552510.8	0.0	0.0	0.0	2285195.2
0.00	0.00	0.00	374060.2	64151.3	42549.3	0.0	564830.9	78552.6	307664.5	0.0	0.0	0.0	1431809.0
0.00	0.00	0.00	345230.9	133317.9	185102.5	0.0	2938135.7	715436.0	2056695.0	0.0	0.0	0.0	6373918.1
0.00	0.00	0.00	344421.3	204739.3	91845.7	0.0	3798201.2	193258.6	1756548.5	0.0	0.0	0.0	6389014.5
0.00	0.00	0.00	340607.6	186286.2	149343.3	0.0	461130.3	165063.7	343227.7	0.0	0.0	0.0	1645658.7
0.00	0.00	0.00	267859.5	193126.7	143304.8	0.0	254466.5	120536.8	182144.5	0.0	0.0	0.0	1161438.8
0.00	0.00	0.00	341388.1	211172.9	108024.9	0.0	543782.4	163378.6	363334.4	0.0	0.0	0.0	1731081.4
0.00	0.00	0.00	358357.4	142765.0	62885.9	0.0	910921.3	92479.3	538692.1	0.0	0.0	0.0	2106101.0
0.00	0.00	0.00	370430.3	100257.8	22145.3	0.0	926075.8	24963.8	474311.9	0.0	0.0	0.0	1918184.8
0.00	0.00	0.00	359440.0	121610.5	83509.9	0.0	2246500.0	129398.4	1084310.7	0.0	0.0	0.0	4024769.5
0.00	0.00	0.00	375900.5	50884.1	45841.5	0.0	1008513.4	60969.2	524885.4	0.0	0.0	0.0	2066994.1
0.00	0.00	0.00	371571.0	64596.2	62595.4	0.0	1148059.0	71456.0	620237.7	0.0	0.0	0.0	2338515.2
0.00	0.00	0.00	372051.9	61199.8	63356.7	0.0	1099979.5	81959.3	555381.8	0.0	0.0	0.0	2233928.9
0.00	0.00	0.00	371902.0	69027.3	53644.0	0.0	1515782.3	94102.5	709994.7	0.0	0.0	0.0	2814452.7
0.00	0.00	0.00	372987.4	64273.7	51285.8	0.0	1801662.4	69269.1	959110.5	0.0	0.0	0.0	3318588.8
0.00	0.00	0.00	362652.9	90277.4	100694.1	0.0	2029313.2	116511.9	787034.0	0.0	0.0	0.0	3486483.5
0.00	0.00	0.00	359407.9	108541.2	102071.8	0.0	3594.1	147357.2	359.4	0.0	0.0	0.0	721331.6
0.00	0.00	0.00	367883.6	67322.7	89395.7	0.0	367.9	103007.4	367.9	0.0	0.0	0.0	628345.2
0.00	0.00	0.00	368346.3	66039.2	87350.7	0.0	2631.0	110503.9	15786.3	0.0	0.0	0.0	650657.4
0.00	0.00	0.00	370871.8	39723.5	103218.6	0.0	69259.2	150136.1	93388.2	0.0	0.0	0.0	826597.4
0.00	0.00	0.00	369248.0	49233.1	103389.4	0.0	637568.3	353001.1	376140.7	0.0	0.0	0.0	1888580.6
0.00	0.00	0.00	367370.4	59217.9	105002.2	0.0	182040.3	45510.1	99244.9	0.0	0.0	0.0	858385.7
0.00	0.00	0.00	364228.1	76487.9	106918.6	0.0	143341.4	230286.1	128067.3	0.0	0.0	0.0	1049329.3
0.00	0.00	0.00	350591.1	140587.0	130419.9	0.0	108683.2	157766.0	119201.0	0.0	0.0	0.0	1007248.3
0.00	0.00	0.00	353391.6	131815.1	119446.4	0.0	95415.7	144890.6	91881.8	0.0	0.0	0.0	936841.1
0.00	0.00	0.00	355891.3	117147.5	119223.6	0.0	88972.8	142356.5	88972.8	0.0	0.0	0.0	912564.5
0.00	0.00	0.00	359897.7	96452.6	114927.3	0.0	45587.0	153556.3	59982.9	0.0	0.0	0.0	830403.9
0.00	0.00	0.00	359078.5	94839.0	123987.7	0.0	97162.4	173202.6	92938.0	0.0	0.0	0.0	941208.2
0.00	0.00	0.00	354709.6	113760.4	133776.2	0.0	182422.1	220426.7	129215.7	0.0	0.0	0.0	1134310.8
0.00	0.00	0.00	350963.6	148808.6	115818.0	0.0	94760.2	168462.5	84231.3	0.0	0.0	0.0	963044.2
0.00	0.00	0.00	355212.0	110115.7	134707.3	0.0	139352.4	226789.2	106563.6	0.0	0.0	0.0	1072740.2
0.00	0.00	0.00	362448.4	65724.0	136763.9	0.0	2107033.2	442187.0	947198.4	0.0	0.0	0.0	4061354.8
0.00	0.00	0.00	343928.9	103178.7	238104.6	0.0	1305166.0	939190.4	798091.4	0.0	0.0	0.0	3727659.9
0.00	0.00	0.00	344141.2	106069.2	232295.3	0.0	1696124.4	1272093.3	957450.0	0.0	0.0	0.0	4608173.4
0.00	0.00	0.00	342580.8	129279.2	212760.7	0.0	1200836.0	557144.6	694176.9	0.0	0.0	0.0	3136778.3
0.00	0.00	0.00	0.0	0.0	0.0	0.0	0.0	0.0	0.0	0.0	0.0	0.0	0.0
0.00	0.00	0.00	371863.7	100519.4	9877.6	0.0	31376.0	12782.8	40672.6	0.0	0.0	0.0	567092.1

100% Ir	100% Os	100% Ru	100% S	100% Ni	100% Cu	100% Rh	100% Pd	100% Au	100% Pt	100% Ir	100% Os	100% Ru	Total
0.00	0.00	0.00	292489.1	211242.1	149656.9	0.0	1317825.9	645101.0	961964.1	0.0	0.0	0.0	3578279.1
0.00	0.00	0.00	369705.9	84360.2	50414.4	0.0	23526.7	63858.3	336.1	0.0	0.0	0.0	592201.7
0.00	0.00	0.00	364406.7	99483.0	73245.7	0.0	32796.6	91101.7	25508.5	0.0	0.0	0.0	686542.2
0.00	0.00	0.00	367388.2	85064.5	68673.3	0.0	39564.9	87608.0	67825.5	0.0	0.0	0.0	716124.4
0.00	0.00	0.00	383113.3	30266.0	14813.7	0.0	3831.1	7662.3	127.7	0.0	0.0	0.0	439814.1
0.00	0.00	0.00	373197.1	75339.2	34054.2	0.0	6997.4	25657.3	233.2	0.0	0.0	0.0	515478.5
0.00	0.00	0.00	375001.5	59338.5	41470.8	0.0	22058.9	55147.3	220.6	0.0	0.0	0.0	553237.5
0.00	0.00	0.00	373231.4	41637.1	80947.6	0.0	773122.2	427034.9	330091.7	0.0	0.0	0.0	2026065.0
0.00	0.00	0.00	358472.6	52746.7	187942.1	0.0	387150.4	122392.8	328258.5	0.0	0.0	0.0	1436963.0
0.00	0.00	0.00	349487.0	117078.1	172496.8	0.0	716448.3	204699.5	247137.2	0.0	0.0	0.0	1807347.1
0.00	0.00	0.00	356203.7	72527.0	179091.3	0.0	723291.5	358182.6	440307.4	0.0	0.0	0.0	2129603.6
0.00	0.00	0.00	357532.6	56036.4	191142.4	0.0	1137916.1	488857.0	911020.4	0.0	0.0	0.0	3142504.9
0.00	0.00	0.00	373939.9	40547.7	76590.1	0.0	325507.9	173904.6	107451.4	0.0	0.0	0.0	1097941.6
0.00	0.00	0.00	371862.7	43384.0	89866.8	0.0	364819.9	184804.5	243401.1	0.0	0.0	0.0	1298139.0
0.00	0.00	0.00	355058.9	99790.2	150432.8	0.0	601731.3	366271.3	424201.9	0.0	0.0	0.0	1997486.4
0.00	0.00	0.00	385663.3	25710.9	17.0	0.0	277449.8	646026.7	336845.2	0.0	0.0	0.0	1671712.9
0.00	0.00	0.00	366412.9	55733.3	117830.7	0.0	493693.2	599760.1	242025.4	0.0	0.0	0.0	1875455.6
0.00	0.00	0.00	343388.3	103165.8	242611.3	0.0	346374.3	656916.7	424009.9	0.0	0.0	0.0	2116466.2
0.00	0.00	0.00	354089.0	71194.5	198515.9	0.0	228274.4	702527.6	323200.4	0.0	0.0	0.0	1877801.8
0.00	0.00	0.00	349101.3	96701.1	204224.3	0.0	210624.5	566707.8	301390.8	0.0	0.0	0.0	1728749.7
0.00	0.00	0.00	354186.0	107543.8	146826.2	0.0	141674.4	405704.0	270469.3	0.0	0.0	0.0	1426403.8
0.00	0.00	0.00	369792.2	52563.3	94209.0	0.0	170808.8	458718.5	284387.8	0.0	0.0	0.0	1430479.6
0.00	0.00	0.00	369895.0	63909.6	77472.5	0.0	90418.8	255844.0	86308.8	0.0	0.0	0.0	943848.7
0.00	0.00	0.00	362342.7	78507.6	119745.6	0.0	74194.0	381322.6	119055.5	0.0	0.0	0.0	1135168.0
0.00	0.00	0.00	354146.1	106834.1	148151.1	0.0	88536.5	534170.4	241999.9	0.0	0.0	0.0	1473838.1
0.00	0.00	0.00	356756.8	71971.8	175276.2	0.0	60493.5	491704.0	235769.7	0.0	0.0	0.0	1391972.0
0.00	0.00	0.00	362160.7	48367.5	163448.9	0.0	111745.6	676668.7	232783.6	0.0	0.0	0.0	1595175.0
0.00	0.00	0.00	361666.6	49833.3	165500.0	0.0	107833.3	673333.2	219166.6	0.0	0.0	0.0	1577332.9
0.00	0.00	0.00	363055.1	49140.8	154940.2	0.0	116434.3	671101.8	219116.6	0.0	0.0	0.0	1573788.8
0.00	0.00	0.00	361015.1	55540.8	162919.6	0.0	111081.6	698888.2	236048.3	0.0	0.0	0.0	1625493.6
0.00	0.00	0.00	361742.5	55454.9	156999.9	0.0	109257.3	670233.6	227695.8	0.0	0.0	0.0	1581384.0
0.00	0.00	0.00	361250.5	52612.9	165063.7	0.0	111154.0	679892.0	219529.2	0.0	0.0	0.0	1589502.2
0.00	0.00	0.00	360889.7	55821.1	163568.7	0.0	115277.0	664660.1	224582.4	0.0	0.0	0.0	1584799.0
0.00	0.00	0.00	361276.6	54348.6	162417.4	0.0	129745.4	785383.9	249123.8	0.0	0.0	0.0	1742295.6
0.00	0.00	0.00	356043.3	67347.9	187673.4	0.0	153141.5	855790.8	283118.8	0.0	0.0	0.0	1903115.8
0.00	0.00	0.00	362878.2	52024.9	152371.8	0.0	124785.7	781298.9	242535.9	0.0	0.0	0.0	1715895.4
0.00	0.00	0.00	362985.2	52528.2	150778.5	0.0	118144.7	643949.7	214649.9	0.0	0.0	0.0	1543036.2
0.00	0.00	0.00	357169.1	66407.0	179642.8	0.0	154244.1	801646.2	245520.7	0.0	0.0	0.0	1804629.9
0.00	0.00	0.00	351420.0	79689.7	208784.8	0.0	267699.4	598447.7	265632.2	0.0	0.0	0.0	1771673.8
0.00	0.00	0.00	348880.9	111641.9	185139.5	0.0	195373.3	737301.6	272127.1	0.0	0.0	0.0	1850464.2
0.00	0.00	0.00	344320.6	113281.5	220709.5	0.0	137728.2	457946.4	265126.9	0.0	0.0	0.0	1539113.1
0.00	0.00	0.00	352466.1	70078.6	213553.0	0.0	62199.9	661392.3	31100.0	0.0	0.0	0.0	1390789.9
0.00	0.00	0.00	369548.1	40755.9	112765.0	0.0	125857.5	559601.4	188786.3	0.0	0.0	0.0	1397314.1
0.00	0.00	0.00	362928.1	51089.1	153267.3	0.0	135120.9	636520.0	248187.0	0.0	0.0	0.0	1587112.5
0.00	0.00	0.00	362827.1	52898.2	151573.6	0.0	139705.4	671399.7	258387.1	0.0	0.0	0.0	1636791.0
0.00	0.00	0.00	356239.7	66271.1	187549.7	0.0	176024.3	893218.8	320877.7	0.0	0.0	0.0	2000181.4
0.00	0.00	0.00	361087.4	56246.3	161332.0	0.0	144203.5	747636.0	249983.6	0.0	0.0	0.0	1720488.7
0.00	0.00	0.00	364874.8	47008.4	142816.0	0.0	124012.7	615586.3	216014.8	0.0	0.0	0.0	1510312.9
0.00	0.00	0.00	369017.5	41294.8	116416.2	0.0	112462.5	467861.4	197687.9	0.0	0.0	0.0	1304740.4
0.00	0.00	0.00	356566.2	65859.9	185414.4	0.0	220651.6	807517.6	343981.5	0.0	0.0	0.0	1979991.3
0.00	0.00	0.00	350154.3	108547.8	178897.0	0.0	378803.3	620728.1	643010.7	0.0	0.0	0.0	2280141.3
0.00	0.00	0.00	352377.8	85852.0	192206.1	0.0	269088.5	767222.5	437268.8	0.0	0.0	0.0	2104015.7
0.00	0.00	0.00	370137.9	55903.6	86663.3	0.0	350992.8	656037.4	234846.1	0.0	0.0	0.0	1754581.1
0.00	0.00	0.00	359519.2	83669.9	135963.6	0.0	382397.7	457569.9	431423.0	0.0	0.0	0.0	1850543.4
0.00	0.00	0.00	356792.6	86522.2	154610.1	0.0	431124.4	603574.2	561948.4	0.0	0.0	0.0	2194572.1
0.00	0.00	0.00	369786.8	60528.3	83104.7	0.0	206302.1	346431.8	264689.5	0.0	0.0	0.0	1330843.1
0.00	0.00	0.00	367063.3	74100.9	86718.7	0.0	201884.8	484064.7	300533.1	0.0	0.0	0.0	1514365.4